Physiologically-based pharmacokinetic modelling and simulation of oral drug bioavailability: Focus on bariatric surgery patients and mechanism-based inhibition of gut wall metabolism

A thesis submitted to the University of Manchester for the degree of Doctor of Philosophy in the Faculty of Medical and Human Sciences

2013

Adam Saëd Darwich

Manchester Pharmacy School

Table of Contents

Word count: 50,422

List of Figures

List of Tables

List of Equations

Abstract

THE UNIVERSITY OF MANCHESTER,
Abstract of thesis submitted by Adam S. Darwich, for the degree of PhD and entitled: "Physiologically-based pharmacokinetic modelling and simulation of oral drug bioavailability: Focus on bariatric surgery patients and mechanism-based inhibition of gut wall metabolism"
Month and year of submission: November 2013.

Understanding the processes that govern pre-systemic drug absorption and elimination is of high importance in pharmaceutical research and development, and clinical pharmacotherapy, as the oral route remains the most frequently used route of drug administration. The emergence of systems pharmacology has enabled the utilisation of *in silico* physiologically-based pharmacokinetic (PBPK) modelling and simulation (M&S) coupled to *in vitro-in vivo* extrapolation in order to perform extrapolation and exploratory M&S in special populations and scenarios were concerns regarding alterations in oral drug exposure may arise, such as following gastrointestinal (GI) surgery or metabolic drug-drug interactions (DDIs).

Due to the multi-factorial physiological implications of bariatric surgery, resulting in the partial resection of the GI tract, the inability to rationalise and predict trends in oral drug bioavailability (F_{oral}) following surgery present considerable pharmacotherapeutical challenges. PBPK M&S is a highly implemented approach for the prediction of DDIs. Reoccurring issues have emerged with regards to predictions of the magnitude of mechanism-based inhibition (MBI) where overestimations of DDIs have repeatedly been reported for drugs exhibiting high intestinal extraction.

The aim of this thesis was to explore the interplay between oral drug absorption and metabolism occurring in the GI tract through the exploration of the impact of bariatric surgery on oral drug exposure and by theoretically examining the nesting and hierarchy of enterocyte and enzyme turnover and its impact on MBIs in the small intestine. This would be carried out by utilising a systems pharmacology PBPK M&S approach under a general model development framework of identification and characterisation of critical intrinsic factors and parameters, model implementation and validation.

Developed post bariatric surgery PBPK models allow a framework to theoretically explore physiological mechanisms associated with altered oral drug exposure pre to post surgery, which could be assigned to the interplay between dissolution, absorption and gut-wall metabolism, where dissolution and formulation properties emerged as the perhaps most important parameters in predicting the drug disposition following surgery. Model validation identified missing critical factors that are essential for additional model refinement. Developed post bariatric surgery PBPK models have the potential of aiding clinical pharmacotherapy and decision-making following surgery. A mechanistic PBPK model was developed to describe the hierarchical dependency of enzyme and enterocyte turnover in the small intestine. Predicted enzyme recovery using the nested enzyme-within-enterocyte turnover model may potentially account for reported overpredictions of mechanism-based inhibition. Developed models in this thesis showcase the advantage of PBPK M&S in the extrapolation of oral drug exposure to special population and the potential of a PBPK approach in understanding underlying the underlying mechanism governing F_{oral} and additionally highlight the need for generation of interdisciplinary data to support model development.

Declaration

No portion of the work referred to in this thesis has been submitted in support of an application for another degree or qualification of this or any other university or other institute of learning.

Copyright

i. The author of this thesis (including any appendices and/or schedules to this thesis) owns certain copyright or related rights in it (the "Copyright") and s/he has given The University of Manchester certain rights to use such Copyright, including for administrative purposes.

ii. Copies of this thesis, either in full or in extracts and whether in hard or electronic copy, may be made only in accordance with the Copyright, Designs and Patents Act 1988 (as amended) and regulations issued under it or, where appropriate, in accordance with licensing agreements which the University has from time to time. This page must form part of any such copies made.

iii. The ownership of certain Copyright, patents, designs, trade marks and other intellectual property (the "Intellectual Property") and any reproductions of copyright works in the thesis, for example graphs and tables ("Reproductions"), which may be described in this thesis, may not be owned by the author and may be owned by third parties. Such Intellectual Property and Reproductions cannot and must not be made available for use without the prior written permission of the owner(s) of the relevant Intellectual Property and/or Reproductions.

iv. Further information on the conditions under which disclosure, publication and commercialisation of this thesis, the Copyright and any Intellectual Property and/or Reproductions described in it may take place is available in the University IP Policy (see http://www.campus.manchester.ac.uk/medialibrary/policies/intellectual-property.pdf), in any relevant Thesis restriction declarations deposited in the University Library, The University Library's regulations (see http://www.manchester.ac.uk/library/aboutus/regulations) and in The University's policy on presentation of Theses.

List of abbreviations

A: Surface area

A_{CYP}: Abundance of Cytochrome P450

A_{diss}: Amount dissolved drug

$A_{Ent-n/0}$: Ratio of enzyme activity using the NEWE model compared to the conventional modelling approach

A_{Enz}: Amount of active enzyme

A_n: Amount of drug

A_{undis}: Amount undissolved drug

ACAT: Advanced compartmental absorption and transit

ACE: Angiotensin-converting-enzyme

ADAM: Advanced dissolution absorption and metabolism

ADME: Absorption, distribution, metabolism and elimination

AGBD: Adjustable gastric band

AGP: α-1 Acid Glycoprotein

AIDS: Acquired immunodeficiency syndrome

AUC: Area-under-curve

BCRP: Breast cancer resistance protein

BCS: Biopharmaceutics classification system

BDDCS: Biopharmaceutics drug disposition classification system

BMI: Body mass index

BPD: Biliopancreatic diversion

BPD-DS: Biliopancreatic diversion with duodenal switch

BSA: Body surface area

C: Concentration

C_{ent}: Enterocyte concentration

Caco-2: Colorectal adenocarcinoma-2 cells

CAT: Compartmental absorption and transit

CI: Confidence interval

CLogP: Calculated logP

C_{max}: Maximum concentration

C_{mic}: Concentration of microsomal protein in the assay

C_s: Solubility over the physiological pH range

CL: Clearance

CL_{int}: Intrinsic clearance

CLu_{int}: Intrinsic unbound clearance

CL_{PD}: Passive diffusion clearance

CNS: Central nervous system

CR: Controlled release

CV: Coefficient of variation

CYP: Cytochrome P450

D: Diffusion coefficient

Do: Dose number

DDI: Drug-drug interaction

DR: Dissolution rate

EC: Enteric-coated

ER: Extended release

f_a: Fraction of the absorbed dose that escapes gut wall metabolism

F_G: Fraction of the absorbed dose that escapes gut wall metabolism

F_H: fraction of the dose reaching the portal vein that escapes hepatic metabolism

F_{oral}: Oral drug bioavailability

FaSSIF: Fasted state simulated intestinal fluids

FeSSIF: Fed state simulated intestinal fluids

FDA: Food and drug administration

fu: Fraction of unbound substrate

fu_b: Fraction of unbound substrate in blood

fu_{Gut}: Fraction of unbound substrate in the gut

fu_{mic}: Fraction of unbound substrate in microsomes

fu_p: Fraction of unbound substrate in plasma

GI: Gastrointestinal

GFR: Glomerular filtration rate

GM: Geometric mean

GSD: Geometric standard deviation

GST: Glutathione S-transferases

h: Diffusion layer thickness

HA: Hepatic artery

HBA: Hydrogen-bond acceptors

HBD: Hydrogen-bond donors

HIV: Human immunodeficiency virus

HLM: Human liver microsomes

HSA: Human serum albumin

I: Inhibitor

IR: Immediate release

ISEF: Inter system expression factor

iv: Intravenous

IVIVC: *In vitro-in vivo* correlation

IVIVE: *In vitro-in vivo* extrapolation

J_{max}: Maximum flux

JIB: Jejunoileal bypass

k_a: Rate of absorption

k_{deg}: Rate of turnover

$k_{deg,CYP3A}$: Rate of CYP3A4 turnover

$k_{deg,Ent}$: Rate of enterocyte turnover

$k_{deg,Enz}$: Rate of enzyme turnover

$K_{I,u}$: Unbound dissociation constant

$K_{i,u}$: Unbound inhibition constant

k_{inact}: Maximum rate of enzyme inactivation

K_m: The concentration at which half of the maximum velocity is reached

K_{reabs}: Reabsorption rate

k_{sit}: Small intestinal transit

k_{st}: Gastric emptying rate

k_t: Transit rate

Kp: Tissue to plasma partition coefficient

Kpu: Unbound tissue to plasma partition coefficient

L: Length

LAGBD: Laparoscopic adjustable gastric band

LLC-PK_1: Lilly Laboratory Cells – Porcine Kidney Nr. 1

LogD: Logarithm of the distribution coefficient

LogP: Logarithm of the partitioning coefficient

M&S: Modelling and simulation

M_o: Highest dose level of a given drug

MBI: Mechanism-based inhibition

MDCK: Madin-Darby canine kidney cells

MDRD: Modification of diet in renal disease

MPPI: Microsomal protein per intestine

MPPGL: Microsomal protein per gram liver

MRC: Medical Research Council

MRP: Multidrug resistance-associated protein

MW: Molecular weight

NEWE: Nested enzyme-within-enterocyte

NHS: National Health Services

NSAID: Non-steroidal anti-inflammatory drug

OATP: Organic anion transporting polypeptide

ρ: Particle density

P-gp: P-glycoprotein

P_{app}: Apparent permeability

P_{eff}: Effective permeability

PAMPA: Parallel artificial membrane assay

PBPK: Physiologically-based pharmacokinetics

PEPT: Peptide transporter

PhysChem: Physicochemical

PK: Pharmacokinetics

po: per oral

PPI: Proton pump inhibitors

ppR: Post/pre surgery oral drug exposure ratio

PSA: Polar surface area

Q: Flow

Q_{sec}: Secretory flow

QSAR: Quantitative structure-activity relationships

r: Radius

R_{syn}: Rate of synthesis

R&D: Research and development

REF: Relative expression factor

RYGB: Roux-en-Y gastric bypass

S: Substrate

S/C: Subcutaneous

S_{diss}: Solubility of drug in bile micelle media

SD: Standard deviation

SFM: Segregated flow model

SG: Sleeve gastrectomy

SIT: Small intestinal transit

SSRI: Selective serotonin reuptake inhibitor

SULT: Sulfotransferase

t: Time

t½: Half-life

T_{lag}: Lag time

t_{max}: Time to reach maximum concentration

TCA: Tricyclic antidepressant

UGT: Uridine 5'-diphosphate-glucuronosyltransferase

V: Volume

V_{max}: Maximum velocity of reaction

V_o: Volume of co-administered fluid volume

V_{ss}: Volume of distribution at steady state following intravenous infusion

WHO: World Health Organisation

WX: Weighted combined geometric mean

Xd: Amount dissolved

Acknowledgements

I would like to acknowledge and express my deepest appreciation to:

My supervisors Professor Amin Rostami-Hodjegan and Professor Darren Ashcroft for their time, expertise, support and inspiration.

Professor Hege Christensen and Dr Anders Åsberg, University of Oslo, Dr Masoud Jamei, Dr Devendra Pade and Dr Karen Rowland-Yeo, Simcyp Ltd, Dr Nicola Ward, Mr Basel Ammori, Janet Whittam, Angela Burgin, NHS trust, and Kathryn Henderson and Umair Aslam, University of Manchester, for their contributions to the work that has gone in to this thesis for without whom this work would not have been.

Colleagues and friends in the CAPKR group. With a special thanks to Dr Oliver Hatley, Dr Henry Pertinez, Dr Kayode Ogungbenro, Dr Eleanor Howgate and Professor Leon Aarons for acting scientific sounding boards and showing great humour in times when needed.

Lesley Wright and Rhona Stephens for making any Kafkaesque administrative task seem so easy.

My wife, parents, family and friends for everything else.

Chapter 1: Introduction

Chapter 1: Introduction

Pharmacokinetics (PK) is defined as the processes that determine drug disposition in the body; these processes can conceptually be divided into absorption, distribution, metabolism and excretion (ADME) and will govern the exposure of a given drug at the site of measurement and effect (Rowland and Tozer, 1989).

The fundamental concept of the drug dose-effect relationship warrants the necessity to measure drug concentration *in vivo* over time in order quantify this relation. Utilising mathematical models drug specific PK parameters can be estimated for a given population, an approach referred to as compartmental PK modelling. In pharmaceutical research and development (R&D) it is however desirable to be able to extrapolate and predict drug disposition throughout R&D in order to inform decision making, this includes the prediction of PK in pre-clinical species and man from *in vitro* data, referred to as *in vitro-in vivo* extrapolation (IVIVE), extrapolation of PK from pre-clinical species to man, and the prediction of PK in special disease populations from healthy volunteers (Rowland and Tozer, 1989; Rowland *et al.*, 2011; Rostami-Hodjegan, 2012).

Physiologically-based pharmacokinetic (PBPK) modelling and simulation (M&S) assign physiological meaning to compartmental models from population specific systems parameters as well as drug specific parameters, such as permeability and metabolism, that may be informed via IVIVE and *in vitro-in vivo* correlation (IVIVC). This approach of coupling IVIVE to PBPK modelling is often referred to as systems pharmacology (Rowland *et al*., 2011; Rostami-Hodjegan, 2012).

Understanding the processes that determine pre-systemic drug absorption and elimination is a pivotal part of PBPK M&S and a constant focus of research as the oral route of drug administration remains the most frequently utilised due to its convenience and cost-efficiency (Bartholow, 2010; FDA, 2010).

The focus of the work in this thesis is on the PBPK M&S of the interplay between oral drug absorption and metabolism occurring in the gastrointestinal (GI) tract with a particular interest in special subpopulations, namely bariatric surgery patients and the theoretical

modelling of nested enzyme-within-enterocyte turnover, in order to improve the prediction of metabolic drug-drug interactions (DDIs) in the small intestine.

1.1 Oral drug bioavailability

Oral drug bioavailability (F_{oral}) is the product of three consecutive processes occurring following oral administration, the availability of the drug at each stage is defined as: The fraction of the administered dose that is absorbed into the gut wall (f_a), the fraction of the absorbed dose that escapes gut wall metabolism (F_G) and the fraction of the dose available to the portal vein that escapes hepatic metabolism (F_H) (Equation 1.1). The GI component ($f_a \cdot F_G$) of F_{oral} will be dependent upon a combination of systems, drug and formulation specific parameters.

$$F_{oral} = f_a \cdot F_G \cdot F_H$$

Equation 1.1: Components of F_{oral}.

Where F_{oral} can be determined experimentally in man as the ratio of the dose normalised area-under-curve (AUC) of a per oral (po) over that of the intravenous (iv) dose (Equation 1.2). The determination of human f_a and F_G will however typically rely on indirect methods of measure such as extrapolation from pre-clinical species to man, static or dynamic *in silico* modelling approaches (Rowland and Tozer, 1989; Yang *et al.*, 2007b).

$$F_{oral} = \frac{AUC_{po} \cdot Dose_{iv}}{AUC_{iv} \cdot Dose_{po}}$$

Equation 1.2: Experimental determination of F_{oral}.

1.1.1 Gastrointestinal systems parameters

The GI systems parameters that may influence F_{oral} comprise a number of intrinsic processes concerning the absorption of nutrients and the repulsion and metabolism of xenobiotics, including among others: Gastric emptying, intestinal motility and transit, luminal fluid dynamics, intestinal absorption area, abundances and regional distribution patterns of drug metabolising enzymes and transporters. Underneath follows an account of the most relevant factors and their impact on F_{oral}.

Gastric emptying and intestinal transit

Under normal conditions the gastric emptying half-life is approximately 0.24 hours following liquid intake with a coefficient of variation (CV) of 38%. A variety of factors may affect gastric emptying, including: the prandial state, composition and volume of the consumed meal or liquid, drugs (anticholinergics and opioid-analgesics amongst others), disease states and surgical procedures (diabetes, gastric ulceration, bariatric surgery and more) (Barowsky *et al.*, 1965; Horowitz *et al.*, 1982; Oberle *et al.*, 1990; Murphy *et al.*, 1997; Samsom *et al.*, 2003; Kamdem *et al.*, 2005; Hellmig *et al.*, 2006; Jamei *et al.*, 2009; Ogungbenro *et al.*, 2011). For highly permeable, highly soluble compounds gastric emptying becomes the rate-limiting step for absorption, thus potentially altering the time for the drug to reach the maximum systemic concentration (t_{max}), the maximum concentration (C_{max}) and f_a.

Small intestinal transit displays a mean of approximately 3.32 h, conforming to a logit-normal distribution pattern in the population (Yu *et al.*, 1996). A number of special disease subpopulations display altered small intestinal motility, including: Patients suffering from cystic fibrosis, AIDS, liver cirrhosis, portal hypertension and post bariatric surgery patients, amongst others (Sharpstone *et al.*, 1999; Karlsen *et al.*, 2012; Dirksen *et al.*, 2013). Small intestinal transit time may influence the absorption of solubility and permeability limited compounds or drugs given as extended-release formulation. Rapid transit through the small intestine may postpone the absorption process further distally and therefore limit the rate of absorption (k_a) and f_a (Rowland and Tozer, 1989).

The colonic transit time (~24 h) is considered to be of less significance for oral drug delivery as compared to the small intestine, where the colon displays a reduced capacity for absorption and dissolution. The colon is however a target for many controlled release formulations where the release may extend for up to 24 h (Hardy *et al.*, 1985; Schiller *et al.*, 2005; Tannergren *et al.*, 2009).

Gastrointestinal fluid volumes, composition and pH

GI fluid volumes, composition and pH are fundamental determinants for the amount of drug that will be dissolved, and consecutively absorbed, in the GI tract, especially for solubility limited compounds. Approximately seven litres of fluids are secreted daily from the GI tract in man in the form of saliva, gastric and pancreatic juices, bile and more (Valentin, 2002).

The amount of fluid available to dissolve a given drug will be determined by: Fluid intake, GI secretion, transit and reabsorption. Levels of measured fluid content under fasted condition amount to approximately 45 mL in the stomach with a standard deviation (SD) of 18 mL, 105 (±72) mL and 13 (±12) mL in the small intestine and colon respectively thus exhibiting considerable inter-individual variability (Schiller *et al.*, 2005; Sutton, 2009).

Bile micelle mediated solubilisation can act to greatly enhance the solubilisation and dissolution rate of highly lipophilic compounds. The extent at which bile mediated solubilisation occurs is related to concentration of bile salt in the small intestine, where bile is released at a rate of approximately 1.5-15.4 µL/min/kg in man (Sugano, 2009). Following secretion into the duodenum, the bile will be subject to dilution in luminal contents and reabsorption throughout the intestine, this results in a gradient where the bile salt concentration is reducing further distally along the small intestine. In the fasted state the bile salt concentration will be approximately 2 to 6.2 mM. Upon post-prandial triggered release the bile concentration can vary between 0.5 and 37 mM in man. Biliary secretion may act as a clearance route, eliminating drug from the system via the liver into the duodenum, mediated by active transport from the canicular membrane of the liver into the bile caniculus. Several transporters can act to mediate biliary secretion of drugs, including: P-glycoprotein (P-gp), multidrug resistance protein 2 (MRP2) and breast cancer resistance protein (BCRP) and a number of transporters involved in the biliary excretion of endogenous compounds (Funk, 2008; Holm *et al.*, 2013).

The GI pH varies widely across the stomach and small intestine, where the gastric pH sits between 1.7 and 5.0 in fasted and fed state respectively. The release of pancreatic juices by the gall bladder into the duodenum triggers an increase in the small intestinal pH, where it displays an increase distally from a pH of approximately 5-7 in the duodenum to 7.5 in the terminal ileum, pH is reduced in the caecum (pH 5.5-7.5), then increases further distally along the colon and in rectum (pH 6.1-7.5) (Kararli, 1995; Nugent *et al.*, 2001). Acid secretion and pH may vary in special disease populations, such as those suffering inflammatory bowel disease or following gastric resection thus potentially affecting oral drug absorption in these groups (Behrns *et al.*, 1994; Nugent *et al.*, 2001). pH plays a vital role in regulating the dissolution of orally administered compounds. Oral absorption of permeability limited drugs displaying a pKa within the range of the GI pH may be highly influenced by pH

fluctuations, where an acid compound may display an increase in solubility at a higher pH and an alkaline compound may display a reduced solubility as a result of an increase in pH (Rowland and Tozer, 1989).

The GI tract is populated by approximately 400-500 different bacterial species (Moore and Holdeman, 1975). The level of bacterial microflora is low in the stomach and proximal small intestine but increases considerably distally towards colon and rectum (Kararli, 1995). Bacterial microflora may facilitate presystemic clearance of orally administered drugs, thus reducing f_a, or can metabolise pro-drugs to active compounds and hydrolyse glucuronide conjugates excreted via biliary secretion thus facilitating enterohepatic circulation via reabsorption of parent compounds (Goldman, 1978; Pollack *et al.*, 1994; Chourasia and Jain, 2004).

Gastrointestinal hormones

A growing body of evidence has emerged over the last decade highlighting the importance of endogenous hormones in regulating gastrointestinal motility and behaviour in the prandial states. Gastric hormones, such as motilin and xenin, are released during the fasted state stimulating gastric emptying and potentially inhibiting gastric acid secretion, pancreatic secretion and intestinal motility. Food intake will trigger a cascade of post-prandial hormonal release, including GI hormones such as: ghrelin, gastrin, cholecystokinin, peptide YY and more, altering gastric emptying, acid secretion, intestinal fluid secretion and motility (Sanger and Lee, 2008). GI hormone responses have been reported to vary in special subpopulations, such as following bariatric surgery where the potential implications of these alterations may be crucial for determining oral nutrient and drug absorption in these populations (Savage *et al.*, 1987; Beckman *et al.*, 2011).

Absorption area

The absorption area of the small intestine directly affects f_a of orally administered drugs. The folding and villi structure of the small intestine helps to optimise the number of enterocytes that are exposed to the gut lumen and therefore can facilitate absorption. Several conditions do however reduce the absorption potential of oral nutrients and drugs due to a reduction in the length of the small intestine. These include: Short bowel syndrome and bariatric surgery.

Disease states can further alter the morphology of the villi, thus reducing the absorption area of the small intestine, such as the case for coeliac disease where a flattening of the villi structure is observed. A reduced absorption area may result in a reduced f_a of permeability limited drugs or delayed-release formulations (Parsons *et al.*, 1975; McFadden *et al.*, 1993; Bullen *et al.*, 2006; Padwal *et al.*, 2009).

Gut-wall metabolism

Small intestinal metabolism acts as a natural barrier for regulating F_{oral} of xenobiotics, despite the lower abundance of drug metabolising enzymes in the gut wall as compared to the liver, intestinal metabolism displays a metabolic capacity similar to the liver as a first line of exposure to orally administered drugs (Kolars *et al.*, 1994). Approximately 30% of orally administered drugs on the market display an F_G below 0.8, thus highlighting the relevance of appropriate models for describing gut wall metabolism (Varma *et al.*, 2010).

Similarly to the liver, Cytochrome P450 (CYP) 3A4 is the predominant drug metabolising enzyme in the small intestine, accounting for approximately 80% of the small intestinal CYP abundance, preceding CYP2C9, CYP2C19, CYP2J2, CYP2D6 and CYP3A5 (Peters *et al.*, 1989; Paine *et al.*, 1997; Fisher *et al.*, 2001; Paine *et al.*, 2006; Riches *et al.*, 2009). The regional abundance of CYP3A varies along the small intestine, where it is expressed at lower levels in the duodenum, increasing in the jejunum to then reduce further distally towards the ileum (Paine *et al.*, 1997). Inter-individual variation in abundance and polymorphism of enzyme expression (such as that for CYP2C9, 2D6 and 3A5) provide considerable variability in gut-wall metabolism and F_G of high affinity substrates (Ingelman-Sundberg, 2005; Sconce *et al.*, 2005; Barter *et al.*, 2010). In addition to the CYPs, the intestine is also abundant in sulfotransferases (SULTs) and uridine 5'-diphosphate-glucuronosyltransferases (UGTs) drug metabolising isoforms, some of which are exclusive for the small intestine (Radominska-Pandya *et al.*, 1998; Riches *et al.*, 2009).

Active transport

Numerous transporters are present in the gut facilitating both active uptake and efflux at the apical and basolateral side of the enterocytes. P-gp is the perhaps most extensively studied transporter. In the intestine, P-gp facilitates active efflux from the enterocyte into the gut

lumen of substrate drugs, displaying a relative expression distribution pattern increasing from the proximal to the distal small intestine (Mouly and Paine, 2003). Other active transporters present in the small intestine include (amongst others): efflux transporters (*e.g.* MRP2 and BCRP), apical uptake transporters (*e.g.* organic anion transporting polypeptide 1A2 (OATP1A2) and peptide transporter 1 (PEPT1)), and basolateral transporters (*e.g.* Organic cation transporter 1 (OCT1) and MRP3) (Fromm *et al.*, 2000; Maliepaard *et al.*, 2001; Ziegler *et al.*, 2002; Englund *et al.*, 2006; Glaeser *et al.*, 2007). Inter-individual variability in transporter expression can contribute to observed variability in F_{oral} of substrate drugs and have been proposed to affect F_G via interaction with drug metabolising enzymes. Utilising a PBPK M&S approach, Darwich and co-workers, assessed the impact of CYP3A4 and P-gp interplay on F_G where a reduction in F_G was observed as a consequence of active efflux resulting in enzyme de-saturation, this was however limited to a parameter space where the substrate in question displayed a high affinity to both CYP3A3 and P-gp (Benet and Cummins, 2001; Darwich *et al.*, 2010; Giacomini *et al.*, 2010).

1.2 IVIVE and IVIVC of drug specific parameters

Numerous drug specific parameters are known to influence f_a and F_G following oral dose administration. Over the last decades, pharmaceutical R&D has moved towards more mechanistic models for predicting F_{oral} based on compound characteristics, with advances originating from across pharmaceutical disciplines.

At the most fundamental level, solubility and permeability are the two key drug specific parameters contributing to f_a. Solubility and permeability are both related to the chemical structure and physicochemical (PhysChem) properties of a given compound. As a consequence of the emergence of combinatorial chemistry and high-throughput screening for lead compounds in pharmaceutical R&D, the need to quantify the relation between molecular descriptors and oral drug dissolution and absorption resulted in the definition of 'Lipinski's rule of five'. Lipinski, and co-workers, identified a number of PhysChem parameter criteria associated with a favourable F_{oral}, these include: molecular weight (MW < 500 g/mol), calculated octanol/water partitioning coefficient (CLogP < 5), number of hydrogen-bond donors (HBD < 5) and acceptors (HBA < 10). The 'Lipinski's rule of five' has been highly utilised in pharmaceutical R&D to screen for compounds with advantageous oral PK (Lipinski *et al.*, 2001).

Amidon, and co-workers (1995), developed the biopharmaceutics classification system (BCS) for assessing F_{oral} for immediate-release formulation drugs based on their solubility and permeability characteristics. According to the BCS, the *in vivo* solubility criterion is defined as a dimensionless dose number (Do) equal to the highest dose level of a given drug (M_o) in 250 mL of aqueous buffer (V_o), all divided by the drug solubility over a physiological pH range (C_s; Equation 1.3). According to the solubility criterion a drug is classed as solubility limited if Do ≥ 1 (i.e. if the dose amount one attempts to theoretically dissolve in 250 mL buffer is greater than that allowed by the solubility over a physiological pH range) (Amidon *et al*., 1995; FDA, 2000).

$$Do = \frac{M_o/V_o}{C_s}$$

Equation 1.3: Biopharmaceutics classification system: Dose number (Do) criterion.

A compound is defined as highly permeable if it has $f_a \geq 90\%$ in man or in pre-clinical species or via indirect measurement of f_a using *in vitro* assays. Combined with the solubility criterion this results in four classes of compounds (Amidon *et al*., 1995; FDA, 2000):

BCS class I:	High solubility, high permeability,
BCS class II:	Low solubility, high permeability,
BCS class III:	High solubility, low permeability
BCS class IV:	Low solubility, low permeability.

The BCS provides a rationale for the relation between solubility, permeability and f_a and potentially any additional parameters that may influence F_{oral}. A BCS class I drug may be subject to variability in absorption due to gastric emptying as this will be the rate limiting step for its dissolution and absorption. For a BCS class II drug the dissolution rate is highly relevant in determining F_{oral}, thus making the GI constituents, surfactants, GI pH fluctuations and processes that may alter compound solubility important for determining *in vivo* absorption. Further, class II compounds are the most likely to display efflux transporter effects due to their low solubility (which prevents saturation of transporters in the intestine). The effect of high-fat meals may be of importance in determining F_{oral} of class II drugs in the

case where micelle formation may enhance solubility, e.g. cyclosporine (Yu *et al.*, 2002; Wu and Benet, 2005).

In the case of a BCS class III drug, permeability is the rate limiting step in determining F_{oral}, which will be highly dependent upon GI transit, fluid dynamics and constituents, and the effective permeability. Class III compounds are the most likely to be sensitive to active uptake transporters in the GI tract due to the high level of drug available for uptake following dissolution in the small intestine (Yu *et al*., 2002; Wu and Benet, 2005).

Variability in absorption of BCS class IV drugs is inherently problematic due to the relative impact that minor alterations in dissolution and permeability may have on the overall F_{oral}; the low permeability and solubility makes it difficult to speculate on the impact of different factors on F_{oral} for this class (Wu and Benet, 2005).

As an extension to the BCS, Wu and Benet (2005) proposed the biopharmaceutics drug disposition classification system (BDDCS) replacing the permeability criteria with an elimination criteria, stating that a drug that exhibits ≥70% metabolism will be highly permeable. The criteria defining BDDCS classification imply that biliary excretion potentially plays an important role in the disposition of class III and IV drugs due to the low level of metabolic elimination and predominantly renal elimination (Wu and Benet, 2005).

The evolution of predictive models provides a good starting point in identifying drug specific key parameters influencing oral drug bioavailability: Solubility, permeability, affinity to drug metabolising enzymes and active transporters.

Solubility

Although possible, it is cumbersome to measure drug dissolution *in vivo*, whereas *in silico* models for prediction of *in vivo* solubility from PhysChem properties (including: LogP, melting point, PSA and quantitative structure-activity relationships [QSAR]) display a high level of uncertainty where no single model provide a universal tool for predicting aqueous solubility (Bonlokke *et al.*, 2001; Dearden, 2006; Dressman *et al.*, 2007; Hewitt *et al.*, 2009). This leaves *in vitro* measurement as the most common source of solubility data.

The most relevant measurements of *in vitro* solubility in pharmaceutical R&D include the kinetic and equilibrium solubility methods. The determination of kinetic solubility involves the measurement of the maximum solubility of a compound's fastest precipitating species and is performed early in the drug discovery phase. The method may however over-predict the true solubility. Equilibrium solubility is determined by measuring the saturation solubility of a drug in equilibrium in an aqueous buffer using *e.g.* the shake-flask method (Elder and Holm, 2013).

Due to the many physiological factors that may impact dissolution *in vivo*, such as: surfactants, viscosity, pH, bile, food and fluid dynamics, the intrinsic solubility (solubility of the non-ionised species) in aqueous media may underestimate true solubility in the GI tract (Dressman and Reppas, 2000). To overcome the limitations of *in vitro* solubility studies, biorelevant dissolution media such as FaSSIF and FeSSIF (fasted and fed state simulated intestinal media respectively) have been developed to mimic *in vivo* conditions, thus potentially improving solubility estimates for highly lipophilic drugs displaying poor solubility in aqueous buffer (Dressman *et al.*, 2007; Fagerberg *et al.*, 2010). Current biorelevant dissolution media does however not account for the full complexity of human intestinal fluids, where considerable discrepancies in the apparent solubility have been identified. The utilisation of IVIVC to improve the predictability has been explored with successful findings but does however require further validation (Clarysse *et al.*, 2011; Wuyts *et al.*, 2013). An integrated approach utilising solubility data coupled with PBPK modelling and simulation provides a successful formula for validating dissolution media (Otsuka *et al.*, 2013).

Dissolution and formulation specific parameters

The dissolution rate (DR) of a given drug is governed by the surface area of a drug (A), the diffusion coefficient (D), the diffusion layer thickness (h), the saturation concentration of the drug in the GI tract (C_s), the amount dissolved (Xd) and the volume of the dissolution medium (V) . The DR relation, originally developed by Noyes and Whitney (1897), and later refined by Nernst and Brunner in 1904, provides a theoretical framework for identifying formulation specific parameters, where Cs, A and h may be altered through changed formulation properties (Dokoumetzidis and Macheras, 2006). The most obvious formulation alterations include changes of particle size and wetting of a given drug to give an increase in

dissolution rate, through altering A (Noyes and Whitney, 1897; Dressman and Fleisher, 1986).

$$DR = \frac{A \cdot D}{h} \cdot \left(C_S - \frac{Xd}{V}\right)$$

Equation 1.4: Noyes-Whitney dissolution.

Numerous methods exist for enhancing solubilisation including the use of solutions, emulsions, microemulsions and micelles. Aqueous solutions can act to increase the solubility of hydrophobic drugs by utilising a pH buffer to increase the ionisation of weak acids and alkaline drugs or by the addition of a cosolvent or hydroxypropyl-β-cyclodextrins. Surfactants can be utilised to form a micelle forming emulsion, enhancing solubility by encapsulating the drug in micelles with a hydrophobic core and hydrophilic surface. Lipid microemulsions, such as cyclosporine Sandimmune Neoral (Sandoz), may improve solubilisation of a drug, reduce enzymatic hydrolysis and potentially improve permeability (Kovarik *et al.*, 1994; Constantinides, 1995; Narang *et al.*, 2007).

The design of a formulation is not always a consequence of poor solubility characteristics but can also be intended to provide an extended or controlled release (ER and CR respectively) in order to protect acid labile compounds (*e.g.* enteric-coating (EC)), or made to prolong the absorption phase of a given drug. The utilisation of ER formulations may have consequences on the f_a and F_G as absorption is delayed further distally to regions exhibiting a lower absorption capacity and abundance in drug metabolising enzymes (Sakr and Andheria, 2001; Wells and Losin, 2008).

Absorption

Following dissolution in the GI tract, an orally administered drug is subject to absorption. Permeability is highly relevant in determining the extent and rate of absorption of highly soluble low permeable (BCS class III) drugs. Human effective permeability ($P_{eff,human}$) has successfully been determined *in vivo* utilising jejunal perfusion (Loc-I-Gut) displaying excellent predictions of f_a in coupling with mechanistic modelling. The effective permeability represents the mass transfer of drug across the intestinal membrane as a function of perfusion

flow rate leaving the intestinal segment (Q_{out}), fluid-corrected concentrations entering and leaving the intestinal segment at steady state (C_{in} and C_{out}), and the surface area of the intestinal segment described as a cylinder (Lennernas *et al.*, 1992; Lennernas *et al.*, 1997).

$$P_{eff} = \frac{Q_{out} \cdot \left(\frac{C_{in} - C_{out}}{C_{out}}\right)}{2 \cdot \pi \cdot r \cdot L}$$

Equation 1.5: Determining P_{eff} *in vivo* utilising the jejunal perfusion technique (L=length, r=radius).

The Loc-I-Gut method is however difficult and costly to perform, thus leading to the utilisation of numerous different approaches to estimating permeability in human, including: *in vivo* animal models, *ex vivo* and *in situ* models in human and preclinical species, and *in vitro* methods coupled with IVIVC to obtain drug permeability parameters for human (Alqahtani *et al.*, 2013).

The Ussing chamber method utilises tissue samples from the intestine of preclinical species and human in order to determine apparent permeability (P_{app}) *ex vivo*. The method displays a good correlation with human f_a and allows the study of both passive and active transport across the epithelial membrane, thus allowing the study of transporter effects and regional differences in permeability. The method is however limited by its requirement for fresh tissue samples (Harwood *et al.*, 2013; Sjoberg *et al.*, 2013).

A number of *in vitro* assays are utilised to predict $P_{eff,human}$ which provide effective screening of drug specific permeability characteristics in pharmaceutical research. The most frequently utilised include: Caco-2 cell monolayers, Madin-Darby canine kidney (MDCK) cells and parallel artificial membrane assay (PAMPA).

The Caco-2 human colon adenocarcinoma cell line is highly utilised as a high-throughput screening method of intestinal drug permeability, allowing the study of passive transcellular, using for example transport inhibitors, and paracellular diffusion, and carrier-mediated transport across the epithelial membrane. The assay allows the determination of the effective or apparent permeability (P_{app}), as a flux per unit area over the cell monolayer based on the rate of drug appearance in the receiving compartment of the assay ($\Delta Q_R/\Delta t$), the area (A) and

the concentration of drug at time zero ($C_{D,0}$) (Equation 1.6) (Hidalgo *et al.*, 1989; Shah *et al.*, 2006; Sun *et al.*, 2008).

$$P_{app} = \frac{\Delta Q_R / \Delta t}{A \cdot C_{D,0}}$$

Equation 1.6: Apparent permeability (P_{app}).

This is based on a number of assumptions, including that the experiment is taking place under 'sink condition' and that accumulation of drug in the receiving compartment is proportional to time (Hidalgo *et al*., 1989; Shah *et al*., 2006; Sun *et al*., 2008). IVIVC can be utilised to estimate $P_{eff,human}$ from Caco-2 monolayers where correlations have been developed based on the Loc-I-Gut method using calibration compounds (Equation 1.7) (Sun *et al.*, 2002).

$$LogP_{eff,human} = 0.6532 \cdot LogP_{app,Caco-2} - 0.3036$$

Equation 1.7: IVIVC between $P_{app,Caco\text{-}2}$ (pH 6.5) and $P_{eff,human}$.

Some of the drawbacks with the Caco-2 assay include: that it requires a long time to culture (~20 days); that it underestimates paracellular transport due to the tighter tight junctions expressed in its cultured cell monolayer compared to those *in vivo*; that it has an inherently low expression of CYP3A and that it displays high variability between laboratories (Shah *et al*., 2006; Alqahtani *et al*., 2013).

MDCK cell lines require a shorter culturing time (3-5 days) and are better predictors of paracellular transport. One of the disadvantages with this system is however that they are derived from canine kidney cells. MDCK cells transfected with human P-gp or MRP2 are commonly utilised to study transporter effects *in vitro* (Tang *et al.*, 2002a; Tang *et al.*, 2002b; Shah *et al*., 2006). Similarly to Caco-2 cell lines, IVIVC has been developed for extrapolation to $P_{eff,human}$, where MDCK cell lines display good correlation with Caco-2 monolayers (Equation 1.8) (Irvine *et al.*, 1999; Gertz *et al.*, 2010).

$$LogP_{eff,human} = 0.829 \cdot LogP_{app,MDCK} - 1.30$$

Equation 1.8: IVIVC between $P_{app,MDCK\text{-}MDR1}$ and $P_{eff,human}$.

The PAMPA is a lipophilic artificial membrane allowing for rapid permeability screening without requiring cell culturing. The assay show good agreement of passive permeation and transcellular transport compared to Caco-2 monolayers and allows prediction of *in vivo* permeability using IVIVC (Equation 1.9) (Kansy *et al.*, 1998; Fujikawa *et al.*, 2005; Avdeef *et al.*, 2007; Gertz *et al.*, 2011).

$$LogP_{eff,human} = 0.6728 \cdot LogP_{app,PAMPA} - 0.0489$$

Equation 1.9: IVIVC between $P_{app,PAMPA}$ and $P_{eff,human}$.

Correlations have also been developed allowing the prediction of $P_{eff,human}$ from PhysChem descriptors such as the octanol/water distribution or partition coefficients (LogD or LogP) polar surface area (PSA) and HBD, where utilising LogD at a pH of 5.5 ($LogD_{5.5}$) together with PSA and HBD gave the best linear correlation (R^2=0.93). These models were however developed using a limited set of drugs (n drugs=13) (Winiwarter *et al.*, 1998).

$$LogP_{eff,human} = -2.883 - 0.010 \cdot PSA + 0.192 \cdot LogD_{5.5} - 0.239 \cdot HBD$$

Equation 1.10: Correlation between PhysChem descriptors and $P_{eff,human}$.

Metabolism

Drug specific affinities to metabolising enzymes, highly abundant in the small intestine and liver, play an important role in regulating F_{oral}. Numerous *in vitro* models are utilised in conjunction with IVIVE to determine drug metabolism in man, these include: primary hepatocytes, hepatoma cells, microsomes and precision-cut liver slice models; with human liver microsomes (HLM) being the most utilised system (Asha and Vidyavathi, 2010; Alqahtani *et al.*, 2013).

By measuring the rate of formation of metabolite or loss of substrate, enzyme kinetic analysis can be performed to determine the nonlinear saturable substrate concentration ([S]) dependent Michaelis-Menten kinetics of the metabolite formation, dependent on the parameters V_{max} (maximum velocity of the reaction) and K_m (the concentration that produces 50% of the maximal velocity). This provides an estimate of metabolic intrinsic clearance (Equation 1.11).

$$CL_{int} = \frac{V_{max} \cdot [S]}{K_m + [S]}$$

Equation 1.11: Michaelis-Menten elimination kinetics.

HLM are subcellular fractions prepared from human hepatocytes, and characteristically exhibit high levels of CYPs and UGTs. HLM can be utilised to identify and quantitatively assess metabolic pathways by introducing enzyme specific inhibitors. HLM have a number of advantages as being one of the most characterised *in vitro* systems to study metabolism and the possibility to study inter-individual variability (Asha and Vidyavathi, 2010; Alqahtani *et al*., 2013).

Linear and nonlinear clearance estimations of a given enzyme (CYP_j) using HLM can be scaled to human using IVIVE, accounting for the fraction unbound of substrate in microsomes ($fu_{mic,j}$), the abundance of enzyme *in vivo* ($A_{CYP,j}$) and the amount of microsomal protein (MP_i) per gram of liver (MPPGL) scaled to whole liver or microsomal protein per small intestine (MPPI) (Equation 1.2 and Equation 1.13) (Howgate *et al.*, 2006; Barter *et al*., 2010).

$$CLu_{int} = \left[\sum_{j=1}^{m}\left(\frac{CL_{int}}{fu_{mic,j}} \cdot A_{CYP,j}\right)\right] \cdot MP_i$$

Equation 1.12: IVIVE from CL_{int} in human liver microsomes to CLu_{int}.

$$CLu_{int} = \left[\sum_{j=1}^{n}\left(\frac{V_{\max(CYP_j)} \cdot A_{CYP,j}}{K_{m,u(CYP_j)}}\right)\right] \cdot MP_i$$

Equation 1.13: IVIVE of Michaelis-Menten saturable enzyme kinetics from human liver microsomes to CLu_{int}.

Recombinant *in vitro* metabolism systems, such as baculovirus insect cells expressing recombinatory CYP450 (rCYP), has the advantage of offering enhanced assay sensitivity through artificially high enzyme expression levels. Recombinant systems require the

utilisation of a system and enzyme specific inter system expression factor (ISEF) in order to account for differences in enzyme activity (Stringer *et al.*, 2009).

$$CLu_{int} = \left[\sum_{j=1}^{m}\left(ISEF_j \cdot \frac{CL_{int}}{fu_{mic,j}} \cdot A_{CYP,j}\right)\right] \cdot MP_i$$

Equation 1.14: IVIVE from CL_{int} in human liver microsomes to CLu_{int}.

$$CLu_{int} = \left[\sum_{j=1}^{n}\left(\frac{ISEF_j \cdot V_{\max(CYP_j)} \cdot A_{CYP,j}}{K_{m,u(CYP_j)}}\right)\right] \cdot MP_i$$

Equation 1.15: IVIVE of Michaelis-Menten saturable enzyme kinetics from recombinant P450 assays to CLu_{int}.

Hepatocytes offer the advantage of providing permeability limitation along with multi enzyme interactions as observed *in vivo* but used to require fresh liver tissue samples for preparation. Since the development of cryopreserved hepatocytes and cultured hepatocyte cell lines *in vitro* use of hepatocytes has gained new ground because of easier handling (Li, 2007).

Active transport

Depending on substrate specific affinity to intestinal transporters, a drug can be subject to altered bioavailability following oral administration; this can lead to either a reduction or increase in f_a depending on the transporters involved, and may give rise to nonlinear absorption kinetics depending on drug dissolution and permeability, as discussed above. As is the case for drug metabolising enzymes, active transport is a saturable process that can be described utilising Michaelis-Menten kinetics (Equation 1.16). Elucidating transporter kinetics does however require additional considerations as the drug is subject to passive diffusion clearance (CL_{PD}) across the membrane barrier (Harwood *et al.*, 2013).

$$CL_{int} = \frac{J_{max}}{K_m + C}$$

Equation 1.16: Michaelis-Menten transporter kinetics.

The determination of transporter kinetics *in vitro* and *ex vivo* uses many of the same methods utilised for permeability studies, namely: Caco-2, MDCK, Lilly Laboratory Cells – Porcine Kidney Nr. 1 (LLC-PK_1) assay and the Ussing chamber technique, where the transporter of interest may be expressed through transfection or be subjected to controlled inhibition in order to separate transporter effects from CL_{PD}. Transporter affinity can then be determined by measuring the bi-directional drug flux at a series of substrate concentrations. There are however issues regarding the IVIVE of transporter effects due to a number of disadvantages with current methods, including: the sparsity of quantitative absolute abundances of transporters *in vitro* and *in vivo* and the lack of transporter specific inhibitors. Due to this the extrapolation of transporter kinetics is done utilising relative expression factors (REF) based on the differences in expression utilising immunoblot densitometry *in vivo* compared to *in vitro* assays (Equation 1.17) (Harwood *et al*., 2013).

$$REF = \frac{In\ vivo\ expression}{In\ vitro\ expression}$$

Equation 1.17: Relative expression factor (REF).

1.3 Physiologically-based pharmacokinetic modelling of oral drug bioavailability

Due to the sheer number of physiological, drug and formulation specific parameters and interrelations that determine the bioavailability of an orally administered drug, PBPK modelling and simulation lends itself well to create a framework for the prediction and extrapolation of absorption processes (Chow and Pang, 2013).

1.3.1 Modelling oral drug bioavailability

A constant evolution of PBPK modelling of oral drug bioavailability has occurred over the last decades where conceptually three approaches to describing absorption processes have emerged, namely: The mixing-tank model, dispersion models and compartmental transit models (Dokoumetzidis *et al.*, 2007).

The mixing-tank model considers the small intestine as a single compartment where a drug is administered as a bolus dose, subject to Noyes-Whitney dissolution and subsequent absorption or removal via small intestinal transit. As a result, the amount of dissolved drug will depend upon the amount available for dissolution (A_{undis}), its aqueous solubility (C_s), diffusion coefficient (D), particle density (ρ) and radius (r_i), the volume of the small intestinal lumen (V_{lumen}), the rate of absorption (k_a) and small intestinal transit (Q_{sit}) (Figure 1.1 and Equation 1.18) (Dressman and Fleisher, 1986).

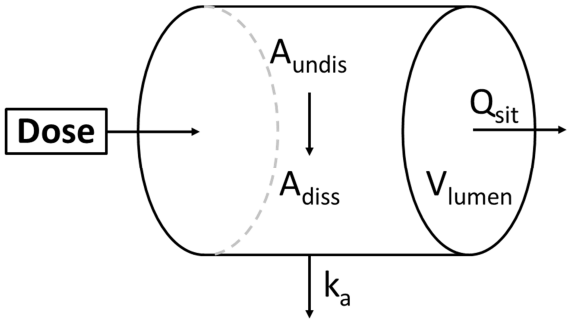

Figure 1.1. Schematics of the mixing tank model. A_{undis}=Amount undissolved drug, A_{diss}=Amount dissolved, k_a=Absorption rate constant, Q_{sit}=Small intestinal transit, V_{lumen}=Volume of small intestinal lumen. Adapted from Dressman and Fleisher (1986).

$$\frac{dA_{diss}}{dt} = \frac{3 \cdot D}{\rho \cdot h \cdot r_i} \cdot \left(Dose \cdot e^{-\frac{Q_{sit}(t)}{V_{lumen}}} \right)^{\frac{1}{3}} \cdot \left(C_s - \frac{A_{diss}}{V_{lumen}} \right) \cdot A_{undis}{}^{\frac{2}{3}} - k_a \cdot A_{diss} - \frac{Q_{sit} \cdot A_{diss}}{V_{lumen}}$$

Equation 1.18: Rate of change of amount dissolved described under the mixing tank model.

The dispersion model utilises partial differential equations to describe the intestine as a tube where drug concentration is described as a continuous profile over time subject to dispersion and transport along the small intestine. The model can be further refined to incorporate

spatial parameter variation to consider regional pH profiles, fluid dynamics, permeability and more, *e.g.* allowing the modelling of spatial luminal drug concentration (C_{lumen}) as a consequence of spatially varied transit (T_{SI}) and absorption (f_a), particle radius (r) and the length of the small intestine (L_{SI}) (Figure 1.2 and Equation 1.19) (Willmann *et al.*, 2003; Willmann *et al.*, 2004; Dokoumetzidis *et al.*, 2007).

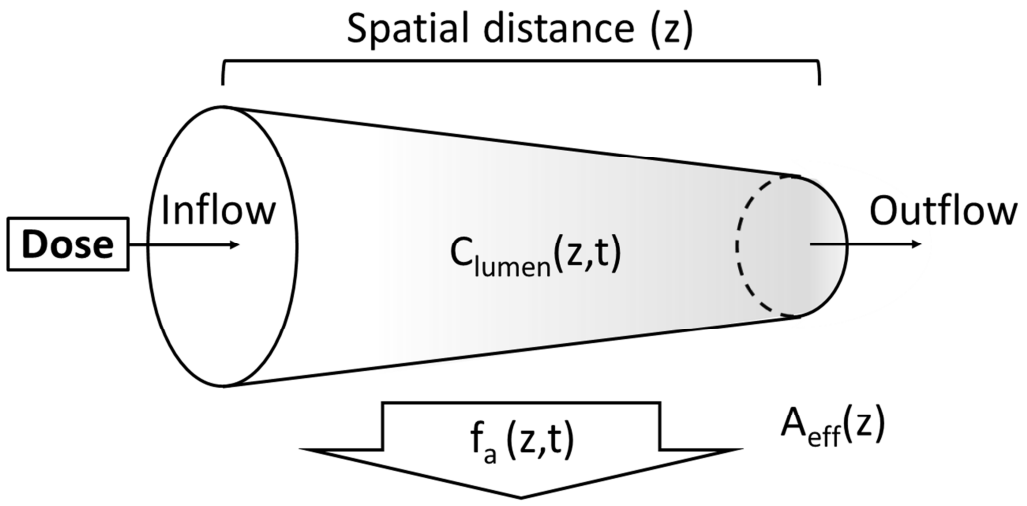

Figure 1.2. Conceptual schematic of the dispersion model of oral drug absorption. C_{lumen}=Spatially varied time dependent luminal drug concentration, f_a=absorption, A_{eff}=Effective permeability. Adapted from Willmann *et al.*, (2004) and Dokoumetzidis *et al.*, (2007).

$$\frac{\partial C_{lumen}(z,t)}{\partial t} = \frac{Dose \cdot [1 - f_a(z,t)]}{\pi \cdot r^2 \cdot L_{SI}} \cdot T_{SI}(z,t)$$

Equation 1.19: Conceptual partial differential equation for dispersion absorption model.

The compartmental absorption and transit (CAT) model, developed by Yu and Amidon (1999), utilises an equally divided seven compartment absorption model to describe the amount of drug (A_n) subject to small intestinal transit (k_{sit}) providing a flexible and more mechanistic description of the processes of intestinal transit as compared to the single-compartment absorption model and a reduced complexity of implementation compared to the dispersion model (Yu *et al.*, 1996; Yu and Amidon, 1999).

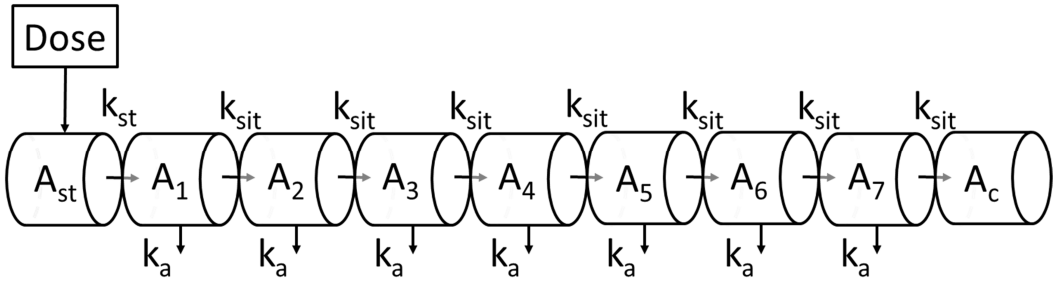

Figure 1.3. Schematic of the nine segment compartmental absorption model (CAT) model. A_{st}=Amount of drug in the stomach, A_n=Amount of drug in the nth small intestinal compartment, A_c=Amount of drug in the colon, k_{st}=Gastric emptying rate, k_{sit}=Small intestinal transit rate and k_a=Absorption rate constant. Adapted from Yu and Amidon (1999).

The CAT model serves as the basis for some of the most physiologically sophisticated PBPK models for oral drug bioavailability, including the implementations of the advanced compartmental absorption and transit (ACAT) and advanced dissolution absorption and metabolism (ADAM) models, incorporated into GastroPlus and the Simcyp Simulator respectively (Figure 1.4). These models further expand on the CAT model by adapting gastrointestinal compartments to conform to their physiological counter parts (*i.e.* the stomach, duodenum, jejunum, ileum and colon) with corresponding fluid volumes ($V_{lumen,n}$), transit times based on segment length (kt_n), regional distribution of enzymes and transporters, segmented segregated blood flows. The drug-related components of the model are refined to incorporate formulation subject to release, dissolution, supersaturation, and precipitation, absorption, active transport and metabolism in the enterocytes. In addition, the ADAM model incorporate inter-individual variability in physiological parameters (Agoram *et al.*, 2001; Jamei *et al.*, 2009).

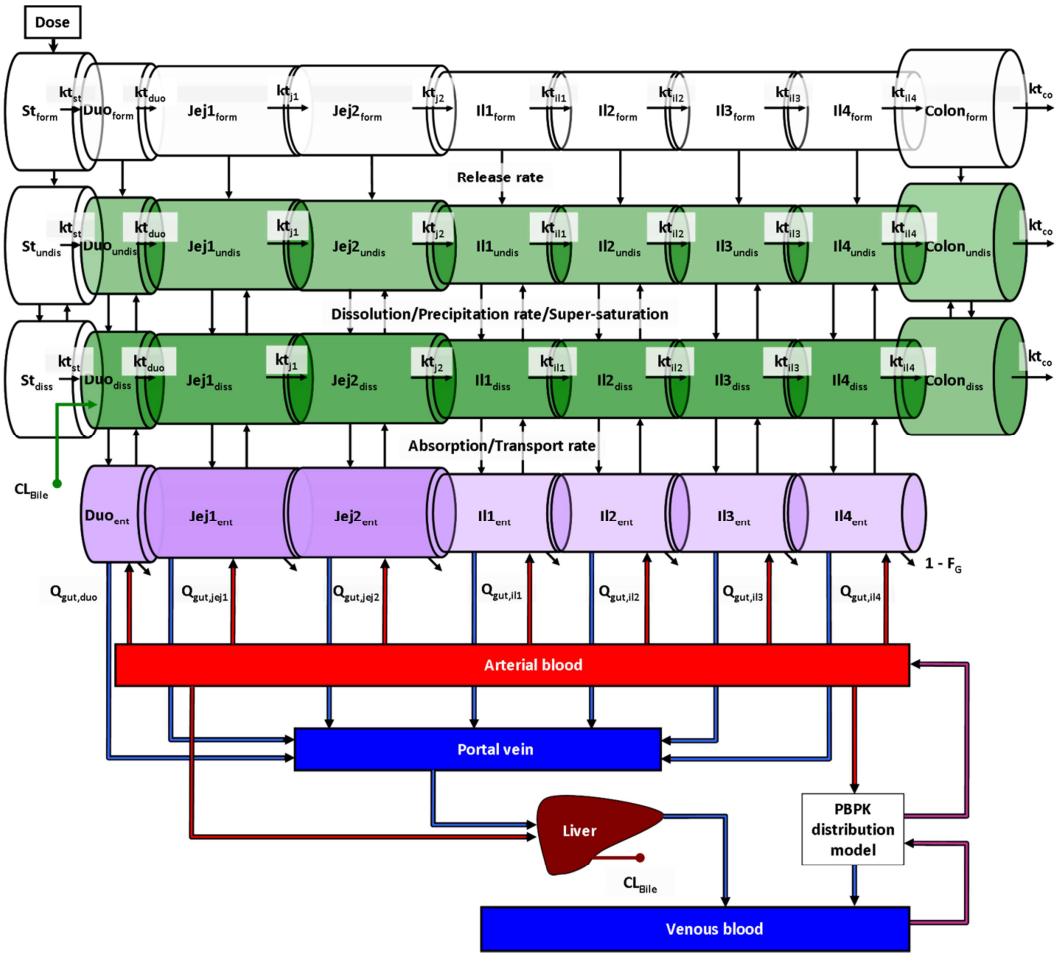

Figure 1.4. Depiction of the 9 segment ADAM model, consisting of following compartments: Stomach, Duodenum, Jejunum I, Jejunum II, Ileum I-IV, and Colon. Further describing: St=stomach, Jej1 & 2=jejunum, Il1-4=ileum, form=drug trapped in formulation, undiss=undissolved drug, diss= dissolved drug, ent=fraction absorbed drug in enterocytes, kt_n=transit rate, Q_n=gastrointestinal blood flow, F_G=fraction drug that escapes gut wall metabolism, CL_{bile}=biliary clearance. Compartment size and purple colour intensity (■) refers to segmental length and regional abundance of CYP3A4 respectively. Green colour scheme (■) indicates bile enhanced solubility. Adapted from Jamei, and co-workers (2009).

PBPK modelling of GI drug release and dissolution utilises a large set of models to describe the dissolution profile time course of amount dissolved, including: zero, first and second order models, Higuchi zero order and more. One of the most frequently utilised models is an adaptation of the empirical Weibull distribution allowing it to conform to most release and dissolution profiles by estimating scale and shape parameters α and β, and the lag time prior

to release (T_{lag}), giving the accumulated release (m) over time (t) (Equation 1.20) (Langenbucher, 1972; Costa and Sousa Lobo, 2001).

$$m = 1 - exp\left[\frac{-(t - T_{lag})^{\beta}}{\alpha}\right]$$

Equation 1.20: Weibull function for dissolution profiles.

Where dissolution profiles are lacking, the pH dependent solubility of a drug is obtained either through the Henderson-Hasselbalch equation or preferably using interpolation of experimentally derived solubility data at GI pH range (Bergstrom *et al.*, 2004). The solubility of a given drug in the GI tract is modelled utilising the diffusion layer models for solid dissolution developed by Noyes and Whitney (1897) or modified versions, such as the Nernst and Brunner equation which consider the dissolution from a planar surface (Dokoumetzidis and Macheras, 2006). Additional modifications of the diffusion layer model allow the modelling of dissolution of spherical mono-dispersed particles under sink and non-sink conditions, where equilibrium between the amount of dissolved ($A_{diss,n}$) and undissolved compound ($A_{undis,n}$) is dependent upon pH dependent solubility at the particle surface (Cs,n), the luminal volume ($V_{lumen,n}$), particle radius (r), density (ρ), diffusion coefficient (D) and diffusion layer thickness (h), as the drug is subject to transit (kt_n) through the GI tract and first order rate absorption of dissolved drug ($k_{a,n}$) (Equation 1.21 and Equation 1.22) (Wang and Flanagan, 1999; Wang and Flanagan, 2002; Jamei *et al*., 2009; Gertz *et al*., 2011).

$$\frac{dA_{undis,n}}{dt} = A_{undis,n-1} \cdot kt_{n-1} - A_{undis,n} \cdot kt_n - \frac{3 \cdot D}{\rho \cdot r \cdot h} \cdot A_{undis,n} \cdot \left(C_{S,n} - \frac{A_{dis,n}}{V_{lumen,n}}\right)$$

Equation 1.21: Rate of change of amount undissolved drug in the gut lumen.

$$\frac{dA_{diss,n}}{dt} = A_{diss,n-1} \cdot kt_{n-1} + \frac{3 \cdot D}{\rho \cdot r \cdot h} \cdot A_{undis,n} \cdot \left(C_{S,n} - \frac{A_{diss,n}}{V_{lumen,n}}\right) - A_{diss,n} \cdot kt_n - A_{diss,n} \cdot k_{a,n}$$

Equation 1.22: Rate of change of amount dissolved drug in the gut lumen.

The luminal volume in the stomach (V_{st}) and intestine ($V_{lumen,n}$) is either assumed to be a constant segmented volume, as in the ACAT model, or as a dynamic system based on physiological data on secretion of intestinal fluids in the stomach and small intestine ($Q_{sec,n}$) subject to reabsorption ($k_{reabs,n}$), gastric emptying ($k_{t,st}$) and transit ($k_{t,n}$) throughout the GI tract (Equation 1.23 and Equation 1.24) (Jamei *et al*., 2009; Sutton, 2009).

$$\frac{dV_{st}}{dt} = Q_{sec,s} - k_{t,st} \cdot V_{st}$$

Equation 1.23: Gastric fluid dynamics.

$$\frac{dV_{lumen,n}}{dt} = Q_{sec,n} - k_{reabs,n} \cdot V_{lumen.n} + k_{t,n-1} \cdot V_{lumen,n-1} - k_{t,n} \cdot V_{lumen,n}$$

Equation 1.24: Intestinal fluid dynamics.

The solubility of drug in bile micelle media (S_{diss}) can be modelled utilising the modified Henderson-Hasselbalch equation, as a function of the concentration of bile (C_{bile}) compared to water (C_{H20}), the drug specific micelle aqueous partition coefficient for the neutral drug ($K_{bm,0}$), K_{bm} for the ionised base or acid ($K_{bm,+}$ or $K_{bm,-}$), the hydrogen ion concentration [H^+] and the equilibrium constant for the ionisation (K_a); where K_{bm} can be derived from $LogP_{o:w}$ (Equation 1.25, Equation 1.26, Equation 1.27, Equation 1.28 and Equation 1.29) (Rippie *et al.*, 1964; Jinno *et al.*, 2000; Sugano, 2009).

$$S_{diss} = S_0 \cdot \left(1 + \frac{[H^+]}{K_a} + \frac{C_{bile}}{C_{H_20}} \cdot K_{bm,0} + \frac{[H^+]}{K_a} + \frac{C_{bile}}{C_{H_20}} \cdot K_{bm,+}\right)$$

Equation 1.25: Bile enhanced solubilisation of an alkaline compound.

$$S_{diss} = S_0 \cdot \left(1 + \frac{K_a}{[H^+]} + \frac{C_{bile}}{C_{H_20}} \cdot K_{bm,0} + \frac{K_a}{[H^+]} + \frac{C_{bile}}{C_{H_20}} \cdot K_{bm,-}\right)$$

Equation 1.26: Bile enhanced solubilisation of an acidic compound.

$$LogK_{bm,0} = 0.74 \cdot LogP_{o:w} + 2.29$$

Equation 1.27: Micelle aqueous partition coefficient for a neutral drug.

$$LogK_{bm,+} \approx LogK_{bm,o} - 1$$

Equation 1.28: Micelle aqueous partition coefficient for an ionised base.

$$LogK_{bm,-} \approx LogK_{bm,o} - 2$$

Equation 1.29: Micelle aqueous partition coefficient for an ionised acid.

Oral absorption

In the absence of active transport, absorption is modelled as a concentration dependent first order process, governed by a rate constant ($k_{a,n}$) proportional to the $P_{eff,human}$ considering the small intestinal radius ($r_{si,n}$) (Equation 1.30). Absorption from different segments of the intestine can be considered by changing $r_{si,n}$ to the corresponding physiological value (Sinko *et al.*, 1991; Yu and Amidon, 1999).

$$k_{a,n} = \frac{2 \cdot P_{eff}}{r_{si,n}}$$

Equation 1.30: Estimate of absorption rate constant from P_{eff}.

Gut-wall metabolism

Gut-wall metabolism can be incorporated into the model of the concentration of substrate in a well-stirred enterocyte compartment. The overall concentration of drug in the enterocytes ($C_{ent,n}$) will depend on $k_{a,n}$, the fraction unbound ($fu_{ent,n}$), the amount of active enzyme in the small intestine ($A_{Enz,n}$), the blood flow out of the enterocytes to the portal vein ($Q_{Gut,n}$), as well as the drug specific clearance parameters (V_{max} and K_m) giving rise to the net $CL_{u,int}$ (Equation 1.31) (Jamei *et al.*, 2009; Gertz *et al.*, 2011).

$$V_{ent,n} \cdot \frac{dC_{ent,n}}{dt} = k_{a,n} \cdot A_{diss,n} - \frac{V_{max} \cdot A_{Enz,n} \cdot fu_{ent,n} \cdot C_{ent,n}}{K_m + fu_{ent,n} \cdot C_{ent,n}} - fu_{ent,n} \cdot C_{ent,n} \cdot CLu_{int,GI} - Q_{Gut,n} \cdot C_{ent,n}$$

Equation 1.31: Model for rate of change of drug concentration in enterocytes, incorporating gut wall metabolism.

Nonlinear active efflux from the enterocytes to the intestinal lumen can be incorporated into the enterocyte model as well, described in a similar fashion to metabolic clearance utilising Michaelis-Menten kinetics where the outflow of the clearance term goes to dissolved drug in the intestinal lumen (Darwich *et al*., 2010).

Hepatic clearance

Hepatic first-pass elimination can be modelled using a well-stirred model for the liver compartment where the elimination of drug will depend on the unbound concentration of drug in liver ($fu_b \cdot C_{hep}$). Assuming a perfusion limited liver, the concentration of drug in the liver also depends on inflow of drug from the intestine ($Q_{gut,1:n}$) and the systemic influx via the hepatic artery (Q_{HA}) and an outflow equal to the sums of the inflow (Equation 1.32) (Rowland Yeo *et al.*, 2010; Pertinez *et al.*, 2013). Additional models for the liver exist in order to accommodate active hepatic uptake, such as the dispersion model (Roberts and Rowland, 1986; Yang *et al.*, 2007a).

$$V_{hep} \cdot \frac{dC_{hep}}{dt} = Q_{Gut,1:n} \cdot C_{ent,1:n} + Q_{HA} \cdot C_{Sys} - C_{hep} \cdot \left(fu_b \cdot CLu_{int,H} + Q_{Gut,1:n} + Q_{HA}\right)$$

Equation 1.32: The well-stirred perfusion-limited liver model.

Hepatobiliary elimination

Hepatobiliary clearance can be modelled either as a clearance from vascular liver compartment (CL_{bile}) to the duodenum or utilising Michaelis-Menten transporter kinetics to account for observed nonlinearity due to the transporter mediated clearance from the sinusoidal side of the liver. Because of the sequential nature of biliary secretion into the small intestine the utilisation of transit compartments or time-to-event modelling may be necessary to account for double peak phenomena (Bischoff *et al.*, 1971; Hofmann *et al.*, 1983).

1.3.2 Whole-body distribution

Distribution is defined as the reversible transfer of drug between different tissues of the body. The distribution of a drug can be modelled empirically by estimating inter-compartmental clearances and volumes of systemic blood or plasma and peripheral compartments (Rowland and Tozer, 1989).

A more mechanistic approach to modelling distribution is to describe drug concentrations in physiological tissues ($C_{T,n}$), compared to venous blood or plasma (C_v), resulting in the tissue to plasma partition coefficient ($Kp=C_{T,n}/C_v$). Direct measurements of Kp are often however lacking in man and rely instead on the utilisation of data from preclinical species or extrapolation from *in vitro* and PhysChem parameters. Utilising Kps, the plasma volume of distribution at steady state following iv infusion (V_{ss}) can be estimated from the volumes of individual tissues (V_t) and plasma (V_p) (Equation 1.33) (Graham *et al.*, 2012).

$$V_{ss} = \sum (Kp \cdot V_t) + V_p$$

Equation 1.33: Estimate of volume of distribution.

Mechanistic methods for estimating human Kp values from in vitro data to man include the equations developed by Poulin and Theil (2000), where Kp values can be estimated the olive oil buffer distribution coefficient at pH 7.4 ($K_{vo:w}$), tissue volumes (V), fractional tissue volumes of phospholipids (ph), neutral lipids (nl), water (w) in tissue (t) and plasma (p), the fraction unbound in plasma (fu_p) and tissue (fu_t) for estimates of Kp values in non-adipose (Kp_t) and adipose tissues (Kp_{adi}) (Equation 1.34 and Equation 1.35 respectively) (Poulin and Theil, 2000; Poulin and Theil, 2002b; Poulin and Theil, 2002a). Refined models based on the Poulin and Theil model have been developed to allow better predictions of highly lipophilic drugs (Berezhkovskiy, 2004; Poulin and Haddad, 2012).

$$Kp_t = \frac{\left[K_{vo:w} \cdot (V_{n,t} + 0.3 \cdot V_{ph,t})\right] \cdot \left[(V_{w,t} + 0.7 \cdot V_{ph,t})\right]}{\left[K_{vo:w} \cdot (V_{n,p} + 0.3 \cdot V_{ph,p})\right] \cdot \left[(V_{w,p} + 0.7 \cdot V_{ph,p})\right]} \cdot \frac{fu_p}{fu_t}$$

Equation 1.34: Poulin and Theil model for estimating Kp.

$$Kp_{adi} = \frac{\left[K^*_{vo:w} \cdot (V_{n,t} + 0.3 \cdot V_{ph,t})\right] \cdot \left[(V_{w,t} + 0.7 \cdot V_{ph,t})\right]}{\left[K^*_{vo:w} \cdot (V_{n,p} + 0.3 \cdot V_{ph,p})\right] \cdot \left[(V_{w,p} + 0.7 \cdot V_{ph,p})\right]} \cdot \frac{fu_p}{1}$$

Equation 1.35: Poulin and Theil model for estimating Kp_{adi}.

In addition to the Poulin and Theil derived models, an alternative model by Rodgers *et al.* (2005) has been proposed for the prediction of unbound Kp values ($Kpu=Kp/fu_p$). The

Rodgers and Rowland model separates intra- and extracellular volumes as fractions (f_{IW} and f_{EW}) and takes the ion species of the compound and pH dependent ionisation into account. One model is utilised for moderate to strong bases, requiring the association constant (Ka) with concentration of acidic phospholipid ($[AP^-]$) and P to predict Kpu values. A separate model is used for neutral, acid, weak alkaline and zwitterions, taking the concentration of binding protein in the tissue and plasma into account ($[PR]_T$ and $[PR]_P$ respectively) assuming only unionised unbound drug permeates into tissues, and specifying the permeation species (Y) dependent on the compound's acid-base nature (Rodgers *et al*., 2005; Rodgers and Rowland, 2006; Rodgers and Rowland, 2007).

$$Kpu = \left[f_{EW} + \left(\frac{1 + 10^{pKa - pH_{IW}}}{1 + 10^{pka - pH_p}} \cdot f_{IW} \right) + \left(\frac{Ka \cdot [AP^-]_T \cdot 10^{pKa - pH_{IW}}}{1 + 10^{pKa - pH_p}} \right) + \left(\frac{\left(P \cdot f_{NL} + \left((0.3 \cdot P + 0.7) \cdot f_{NP} \right) \right)}{1 + 10^{pKa - pH_p}} \right) \right]$$

Equation 1.36: Rodgers and Rowland model for estimating Kp's of moderate to strong bases.

$$Kpu = \frac{X \cdot f_{IW}}{Y} + f_{EW} + \left(\frac{P \cdot f_{NL} + (0.3 \cdot P + 0.7) \cdot f_{NP}}{Y} \right) + \left[\left(\frac{1}{fu} - 1 - \left(\frac{P \cdot f_{NL,P} + (0.3 \cdot P + 0.7) \cdot f_{NP,P}}{Y} \right) \right) \cdot \frac{[PR]_T}{[PR]_P} \right]$$

Equation 1.37: Rodgers and Rowland model for estimating Kp's of neutral, acid, weak alkaline and zwitterions compounds.

The Rodgers and Rowland model displays improved predictions for compounds compared to the Poulin and Theil method for specific different drug classes and tissues, whereas Poulin and Theil displays a higher accuracy for the prediction of V_{ss} (Graham *et al*., 2012).

Observed or predicted Kp values can be utilised in whole-body PBPK tissue distribution models to model and predict venous, arterial and tissue concentrations, where the tissue

concentration (C_T) in a well-perfused tissue will depend on the tissue specific blood flow (Q_T), volume (V_T) and Kp (Figure 1.5 and Equation 1.38) (Nestorov *et al.*, 1998).

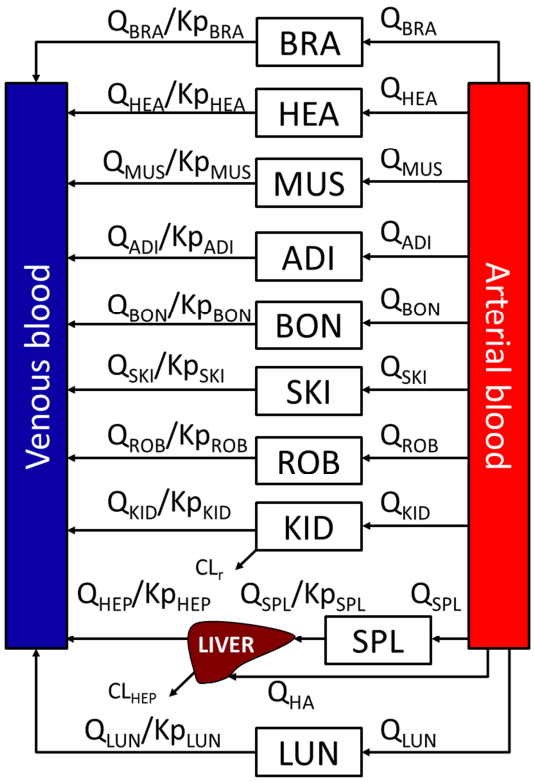

Figure 1.5. Whole-body distribution model describing the partitioning of drugs into tissues as compared to blood (Kp_n) dependent upon tissue specific blood flows (Q_n) and volumes (V_n). BRA=Brain, HEA=Heart, MUS=Muscle, ADI=Adipose, BON=Bone, SKI=Skin, ROB=Rest of body, KID=Kidney, SPL=Splanchnic organs, LUN=Lungs, CL_r=Renal clearance and CL_{HEP}=Hepatic clearance. Adapted from Nestorov *et al*., (1998).

$$\frac{dC_T}{dt} = \frac{Q_T}{V_T} \cdot C_{ART} - \frac{Q_T}{V_T \cdot K_P} \cdot C_T$$

Equation 1.38: Modelling tissue disposition in well-perfused non-eliminating tissues.

1.3.3 Modelling metabolic drug-drug interactions in the small intestine

PBPK M&S is a highly utilised approach for the implementing mechanistic prediction of metabolic enzyme DDIs, enabling the utilisation of drug specific inhibitory and induction parameters from *in vitro* assays, such as HLM and hepatocytes. In addition to the static models a PBPK M&S approach may show improved predictions as well as incorporate inter-individual variability to aid the prediction of DDIs (Fahmi *et al.*, 2009). The food and drug administration (FDA) has recognised the utilisation of PBPK modelling and simulation as a useful tool to quantitatively predict the impact of DDIs and assist the design of DDI studies (Rostami-Hodjegan, 2012).

The potency of a reversible enzyme inhibitor, including competitive and non-competitive inhibitors, can be established *in vitro* by determining the unbound inhibition constant ($K_{i,u}$), where the fold reduction in CLu_{int} following inhibition is dependent on the concentration of the inhibitor and $K_{i,u}$ (Equation 1.39) (Rostami-Hodjegan and Tucker, 2004).

$$Fold\ reduction\ in\ CLu_{int,GI} = \left(1 + \frac{[I]}{K_{i,u}}\right)$$

Equation 1.39: Impact on substrate clearance following reversible enzyme inhibition.

Mechanism-based inhibition (MBI) is characterised by the time-dependent inhibition of the level of active enzyme. Utilising *in vitro* metabolic assays the maximum rate of enzyme inactivation (k_{inact}) and unbound dissociation constant ($K_{I,u}$) can be determined and used to predict the level of enzyme inactivation over time. The net rate of inactivation will further depend on unbound inhibitor concentration in the gut ($fu_{Gut}\cdot[I]_{GI}$) and the baseline turnover of the enzyme ($k_{deg,GI}$) (Equation 1.40). Issues do however exist regarding the prediction of MBIs where over-predictions of the level of enzyme inhibition have been reported (Rostami-Hodjegan and Tucker, 2004; Obach *et al.*, 2007; Ohno *et al.*, 2008; Obach, 2013).

$$\frac{dA_{Enz,GI}}{dt} = R_{Syn-Enz,GI} - A_{Enz,GI} \cdot \left(k_{deg,GI} + \frac{k_{inact} \cdot fu_{Gut} \cdot [I]_{GI}}{K_{I,u} + fu_{Gut} \cdot [I]_{GI}}\right)$$

Equation 1.40: Amount of active enzyme in GI tract with over time following MBI - R_{syn}=base rate of synthesis.

Enzyme induction can be modelled utilising a Hill function, dependent on the maximum induction effect (E_{max}), 50% maximal induction effect ($EC_{50,I}$), the unbound inhibitor concentration in the enterocytes ($fu_{Gut} \cdot [I]_{GI}$) and enzyme turnover in the gut ($k_{deg,GI}$) (Equation 1.41) (Ohno *et al*., 2008; Guo *et al.*, 2013).

$$\frac{dA_{Enz,GI}}{dt} = R_{Syn-Enz,GI} \cdot \left(1 + \frac{E_{max} \cdot fu_{Gut} \cdot [I]_{GI}}{fu_{Gut} \cdot [I]_{GI} + EC_{50,I}}\right) - k_{deg,GI} \cdot A_{Enz,GI}$$

Equation 1.41: Amount of active enzyme in GI tract over time following induction.

Instances where induction is accompanied by MBI, such as for ritonavir, requires PBPK modelling and simulation due to the complexity of the interaction, which must combine the processes described in Equation 1.40 and Equation 1.41 in a single scheme (Fahmi *et al.*, 2008; Ohno *et al*., 2008).

1.3.4 Mechanistic modelling of special subpopulations

PBPK M&S and system pharmacology provides a framework for modelling drug exposure in special disease subpopulations due to its inherent ability to facilitate extrapolation by using physiology and anatomy to inform compartmental models. By utilising a systems pharmacology approach predictive models become attractive for special subpopulations that are not readily available for clinical research due to ethical or practical considerations. A number of special population PBPK models have been developed utilising this approach, including those for: Paediatrics, pregnancy, liver cirrhosis, renal failure, obesity as well as genetic differences in enzyme expression (Barter *et al*., 2010; Johnson *et al.*, 2010; Ghobadi *et al.*, 2011; Johnson and Rostami-Hodjegan, 2011; Rowland Yeo *et al.*, 2011; Ke *et al.*, 2012).

The utilisation of PBPK M&S together with IVIVE/C under the paradigm of systems pharmacology (together with the increased acceptance from the regulatory agencies for the utilisation of PBPK M&S in submission process and the emergence of individualised pharmacotherapy), in development of new mechanistic models for special subpopulation. The approach allows the assessment and prediction of (amongst others): study design issues and the powering of studies, the impact of enzyme ontogeny on metabolic clearance in

paediatrics, and the effect of expected variability in drug exposure in special populations (Zhao *et al.*, 2011; Rostami-Hodjegan, 2012).

The general method for the development of PBPK models for special subpopulations relies heavily on identification and extraction of multidisciplinary information relating to the alterations in physiological system specific parameters, coupled with statistical meta-analysis in order to estimate the variability of these system-specific parameters in the subpopulation in question. This specialised information regarding the physiological parameters of the subpopulation is needed in addition to an appropriate level of drug specific information in order carry out informative extrapolation within a general framework for PBPK modelling and model validation. The approach is very data intense and may therefore be limited in application to well-characterised subpopulations, with drugs which can be considered to show the greatest challenges in extrapolation between populations and for which there is knowledge of the impact of population covariates on drug disposition. An additional obstacle is the need for best practice guidelines in order to streamline the development process (Zhao *et al*., 2011).

1.3.5 Bariatric surgery subpopulation

The number of bariatric surgical procedures carried out in North America and the United Kingdom has increased dramatically in recent years. The rise in surgical procedures can be attributed to the increased prevalence of obesity and the proven clinical and cost effectiveness of surgical treatment of obesity and associated comorbidities (Picot *et al.*, 2009; Flegal *et al.*, 2010; OHE, 2010). Several bariatric surgical procedures exist in healthcare varying in degree of invasiveness. Procedures such as the sleeve gastrectomy are limited to restricting the capacity of the gastric pouch whereas procedures as the Roux-en-Y gastric bypass and biliopancreatic diversion with duodenal switch result in gastric resection, small intestinal bypass and delay in bile inlet. These surgical procedures will result in a number of GI anatomical and physiological alterations, where they for example may alter the gastric volume, pH, gastric emptying, GI fluid dynamics, absorption area, and exposure to gut-wall enzymes and transporters (Behrns *et al*., 1994; Buchwald and Oien, 2009).

Potential anatomical and physiological changes following bariatric surgery have clear implications on the exposure of orally administered drugs and consequently the

pharmacotherapy in a post bariatric surgery population. Clinical evidence suggests trends in oral drug exposure pre to post bariatric surgery to be highly variable, both drug and surgery dependent. This presents an apparent problem in the pharmacological treatment of post bariatric surgery patients where clinical data, and guidance on appropriate drug utilisation is lacking (Padwal *et al.*, 2009; Skottheim *et al.*, 2009; Skottheim *et al.*, 2010).

Due to the multi-factorial changes in the GI physiology and anatomy, a systems pharmacology PBPK approach may be particularly suitable approach for exploring the underlying processes resulting in alterations of oral drug exposure and may also inform clinical pharmacology in the treatment of post bariatric surgery patient populations.

1.4 Project aims and objectives

The aim of the work constituting this thesis was to examine the interplay between gastrointestinal systems parameters and their effects on oral drug bioavailability utilising physiologically-based pharmacokinetic modelling and simulation under a systems pharmacology approach.

The research would be carried out with the focus on PBPK M&S of trends in oral drug bioavailability in pre to post bariatric surgery subpopulation, resulting in the partial resection of the GI tract, in order to enable the theoretical examination of underlying physiological, drug and formulation specific factors accounting for observed changes in oral drug exposure pre to post surgery.

In order to establish the current knowledge around changes in oral drug exposure following bariatric surgery a systematic review of the topic would be performed together with surveying the clinical pharmacotherapeutical considerations at an NHS (National Health Services) hospital.

The review would be followed by characterisation of relevant systems parameters in a post bariatric surgery patient subpopulation in order to enable the PBPK model development and assessment utilising the Simcyp Simulator ADAM model. Developed models would then be subject to validation against observed clinical data.

The work in this thesis would also theoretically examine the nested turnover of CYP enzymes dependent on the turnover of the enterocytes and its impact on the prediction of mechanism-based enzyme inhibition in the small intestine. This would be carried out through characterising systems parameters relating to enterocyte and enzyme turnover that would be incorporated into a nested enzyme-within-enterocyte (NEWE) PBPK model. The discrepancies in the NEWE model predictions of mechanism-based inhibition would then be assessed against the conventional modelling approach only considering a lumped enzyme turnover in the gut.

The work would be carried out under the principles of the systems pharmacology approach, incorporating IVIVE, IVIVC, and statistical meta-analysis coupled with physiologically-based pharmacokinetic modelling and simulation in the development and assessment of mechanistic PBPK models for oral drug bioavailability.

1.5 List of manuscripts and author contribution statement

In accordance with University of Manchester guidelines for the alternative thesis format for doctor in philosophy, beneath follows a statement of the individual contributions of authors to published manuscripts and manuscripts in preparation. Please note that published manuscripts, Chapter 2-4, are available in their respective appendices.

Chapter 2:

Br J Clin Pharmacol. 2012,74(5):774-87

Trends in oral drug bioavailability following bariatric surgery: examining the variable extent of impact on exposure of different drug classes

A.S. Darwich: Literature search, data and statistical analysis, study design and lead coordination of clinical audit study design and execution, supervision of research carried out by K. Henderson, main preparation of manuscript.

K. Henderson: Literature search, data collection for clinical audit, preliminary data analysis. Preparation of manuscript, mainly clinical audit section. Please note that parts of the clinical audit sections in the published manuscript and as provided in this thesis is therefore available in the project report (titled: ‘An investigation into trends in altered bioavailability following

gastric bypass surgery') by K. Henderson, as supervised and edited by A.S. Darwich and A. Rostami-Hodjegan. The work was carried out as a part of Master of Pharmacy project report.
A. Burgin: Supervision of K. Henderson during clinical audit, coordination of data collection during the clinical audit and input on manuscript.
N. Ward: Expert opinion on clinical pharmacotherapy following bariatric surgery and input on manuscript.
J. Whittam: Expert opinion on clinical pharmacotherapy following bariatric surgery, input on clinical audit study design and manuscript.
B.J. Ammori: Expert opinion on bariatric surgical procedures, input on manuscript.
D.M. Ashcroft: Supervision of research, study design, preparation of manuscript.
A. Rostami-Hodjegan: Supervision of research, study design, input on data analysis, preparation of manuscript.

Chapter 3:

J Pharm Pharmacol. 2012, 64(7):1008-24

A mechanistic pharmacokinetic model to assess modified oral drug bioavailability post bariatric surgery in morbidly obese patients: interplay between CYP3A gut wall metabolism, permeability and dissolution

A.S. Darwich: Lead for study design, literature search and meta-analysis, modelling and simulation of post bariatric surgery models, data analysis and preparation of manuscript.
D. Pade: Input on model development and manuscript.
B.J. Ammori: Expert opinion on bariatric surgical procedures, input on surgical dimensions in models for post bariatric surgery populations and manuscript.
M. Jamei: Expert opinion and input on PBPK modelling, and input on manuscript.
D.M. Ashcroft: Supervision of research, study design and input on manuscript.
A. Rostami-Hodjegan: Supervision of research, study design, input on modelling and simulation of post bariatric surgery models and input on manuscript.

Chapter 4:

CPT Pharmacometrics and Syst Pharmacol. 2013, 2(e47):1-9

Evaluation of an *in silico* PBPK post-bariatric surgery model through simulating oral drug bioavailability of atorvastatin and cyclosporine

A.S. Darwich: Lead for study design, modelling and simulation utilising post bariatric surgery PBPK models, data analysis and preparation of manuscript.

D. Pade: Input on model development and simulation, and manuscript.

K. Rowland-Yeo: Input on modelling of atorvastatin acid and manuscript.

M. Jamei: Expert opinion and input on PBPK modelling, and input on manuscript.

A. Åsberg: Supply of atorvastatin data and input on PBPK modelling and manuscript.

H. Christensen: Supply of atorvastatin data and input on modelling and manuscript.

D.M. Ashcroft: Supervision of research, study design and input on manuscript.

A. Rostami-Hodjegan: Supervision of research, study design, input on PBPK modelling and simulation, and input on manuscript.

Chapter 5:

In preparation

Assessing the turnover of the intestinal epithelia in pre-clinical species and human

A.S. Darwich: Lead for literature search, study design, statistical meta-analysis, supervision of U. Aslam, and preparation of manuscript.

U. Aslam: Preliminary literature search on enterocyte turnover in pre-clinical species. The work was carried out as a part of Master of Pharmacy project report.

D.M. Ashcroft: Input on manuscript.

A. Rostami-Hodjegan: Supervision of research, study design, input on data analysis and manuscript preparation.

Chapter 6:

In preparation

Development and assessment of a nested enzyme-within-enterocyte turnover model for mechanism-based inhibition in the small intestine

A.S. Darwich: Lead for study design, literature search, PBPK modelling development and simulation and preparation of manuscript.

D.M. Ashcroft: Input on manuscript.

A. Rostami-Hodjegan: Supervision of research, input on PBPK modelling development and simulation, input on manuscript.

1.6 References

Agoram B, Woltosz WS, and Bolger MB (2001) Predicting the impact of physiological and biochemical processes on oral drug bioavailability. *Adv Drug Deliv Rev* **50 Suppl 1:**S41-67.

Alqahtani S, Mohamed LA, and Kaddoumi A (2013) Experimental models for predicting drug absorption and metabolism. *Expert Opin Drug Metab Toxicol* 9(10):1241-54.

Amidon GL, Lennernas H, Shah VP, and Crison JR (1995) A theoretical basis for a biopharmaceutic drug classification: the correlation of in vitro drug product dissolution and in vivo bioavailability. *Pharm Res* **12:**413-420.

Asha S and Vidyavathi M (2010) Role of human liver microsomes in in vitro metabolism of drugs-a review. *Applied biochemistry and biotechnology* **160:**1699-1722.

Avdeef A, Bendels S, Di L, Faller B, Kansy M, Sugano K, and Yamauchi Y (2007) PAMPA--critical factors for better predictions of absorption. *J Pharm Sci* **96:**2893-2909.

Barowsky H, Greene L, and Paulo D (1965) Cinegastroscopic Observations on the Effect of Anticholinergic and Related Drugs on Gastric and Pyloric Motor Activity. *Am J Dig Dis* **10:**506-513.

Barter ZE, Perrett HF, Yeo KR, Allorge D, Lennard MS, and Rostami-Hodjegan A (2010) Determination of a quantitative relationship between hepatic CYP3A5*1/*3 and CYP3A4 expression for use in the prediction of metabolic clearance in virtual populations. *Biopharm Drug Dispos* **31:**516-532.

Bartholow M (2010) Top 200 Prescription Drugs of 2009. *Pharmacy Times*, Intellisphere, LLC, New Jersey. Retrieved November 01, 2010, from: http://www.pharmacytimes.com/issue/pharmacy/2010/May2010/RxFocusTopDrugs-0510

Beckman LM, Beckman TR, Sibley SD, Thomas W, Ikramuddin S, Kellogg TA, Ghatei MA, Bloom SR, le Roux CW, and Earthman CP (2011) Changes in Gastrointestinal Hormones and Leptin After Roux-en-Y Gastric Bypass Surgery. *JPEN J Parenter Enteral Nutr* **35:**169-180.

Behrns KE, Smith CD, and Sarr MG (1994) Prospective evaluation of gastric acid secretion and cobalamin absorption following gastric bypass for clinically severe obesity. *Dig Dis Sci* **39:**315-320.

Benet LZ and Cummins CL (2001) The drug efflux-metabolism alliance: biochemical aspects. *Adv Drug Deliv Rev* **50 Suppl 1:**S3-11.

Berezhkovskiy LM (2004) Determination of volume of distribution at steady state with complete consideration of the kinetics of protein and tissue binding in linear pharmacokinetics. *J Pharm Sci* **93:**364-374.
Bergstrom CA, Luthman K, and Artursson P (2004) Accuracy of calculated pH-dependent aqueous drug solubility. *Eur J Pharm Sci* **22:**387-398.
Bischoff KB, Dedrick RL, Zaharko DS, and Longstreth JA (1971) Methotrexate pharmacokinetics. *J Pharm Sci* **60:**1128-1133.
Bonlokke L, Hovgaard L, Kristensen HG, Knutson L, and Lennernas H (2001) Direct estimation of the in vivo dissolution of spironolactone, in two particle size ranges, using the single-pass perfusion technique (Loc-I-Gut) in humans. *Eur J Pharm Sci* **12:**239-250.
Buchwald H and Oien DM (2009) Metabolic/bariatric surgery Worldwide 2008. *Obes Surg* **19:**1605-1611.
Bullen TF, Forrest S, Campbell F, Dodson AR, Hershman MJ, Pritchard DM, Turner JR, Montrose MH, and Watson AJ (2006) Characterization of epithelial cell shedding from human small intestine. *Lab Invest* **86:**1052-1063.
Chourasia MK and Jain SK (2004) Polysaccharides for colon targeted drug delivery. *Drug delivery* **11:**129-148.
Chow EC and Pang KS (2013) Why we need proper PBPK models to examine intestine and liver oral drug absorption. *Curr Drug Metab* **14:**57-79.
Clarysse S, Brouwers J, Tack J, Annaert P, and Augustijns P (2011) Intestinal drug solubility estimation based on simulated intestinal fluids: comparison with solubility in human intestinal fluids. *Eur J Pharm Sci* **43:**260-269.
Constantinides PP (1995) Lipid microemulsions for improving drug dissolution and oral absorption: physical and biopharmaceutical aspects. *Pharm Res* **12:**1561-1572.
Costa P and Sousa Lobo JM (2001) Modeling and comparison of dissolution profiles. *Eur J Pharm Sci* **13:**123-133.
Darwich AS, Neuhoff S, and Rostami-Hodjegan A (2010) Interplay of metabolism and transport in determining oral drug absorption and gut wall metabolism: a simulation assessment using the "advanced dissolution, absorption, metabolism (ADAM)" model. *Curr Drug Metab* **11:**716-729.
Dearden JC (2006) In silico prediction of aqueous solubility. *Expert opinion on drug discovery* **1:**31-52.
Dirksen C, Damgaard M, Bojsen-Moller KN, Jorgensen NB, Kielgast U, Jacobsen SH, Naver LS, Worm D, Holst JJ, Madsbad S, Hansen DL, and Madsen JL (2013) Fast pouch emptying, delayed small intestinal transit, and exaggerated gut hormone responses after Roux-en-Y gastric bypass. *Neurogastroenterol Motil.*
Dokoumetzidis A and Macheras P (2006) A century of dissolution research: from Noyes and Whitney to the biopharmaceutics classification system. *Int J Pharm* **321:**1-11.
Dokoumetzidis A, Valsami G, and Macheras P (2007) Modelling and simulation in drug absorption processes. *Xenobiotica* **37:**1052-1065.
Dressman JB and Fleisher D (1986) Mixing-tank model for predicting dissolution rate control or oral absorption. *J Pharm Sci* **75:**109-116.
Dressman JB and Reppas C (2000) In vitro-in vivo correlations for lipophilic, poorly water-soluble drugs. *Eur J Pharm Sci* **11 Suppl 2:**S73-80.
Dressman JB, Vertzoni M, Goumas K, and Reppas C (2007) Estimating drug solubility in the gastrointestinal tract. *Adv Drug Deliv Rev* **59:**591-602.
Elder D and Holm R (2013) Aqueous solubility: Simple predictive methods (in silico, in vitro and bio-relevant approaches). *Int J Pharm* **453:**3-11.

Englund G, Rorsman F, Ronnblom A, Karlbom U, Lazorova L, Grasjo J, Kindmark A, and Artursson P (2006) Regional levels of drug transporters along the human intestinal tract: co-expression of ABC and SLC transporters and comparison with Caco-2 cells. *Eur J Pharm Sci* **29:**269-277.

Fagerberg JH, Tsinman O, Sun N, Tsinman K, Avdeef A, and Bergstrom CA (2010) Dissolution rate and apparent solubility of poorly soluble drugs in biorelevant dissolution media. *Mol Pharm* **7:**1419-1430.

Fahmi OA, Hurst S, Plowchalk D, Cook J, Guo F, Youdim K, Dickins M, Phipps A, Darekar A, Hyland R, and Obach RS (2009) Comparison of different algorithms for predicting clinical drug-drug interactions, based on the use of CYP3A4 in vitro data: predictions of compounds as precipitants of interaction. *Drug Metab Dispos* **37:**1658-1666.

Fahmi OA, Maurer TS, Kish M, Cardenas E, Boldt S, and Nettleton D (2008) A combined model for predicting CYP3A4 clinical net drug-drug interaction based on CYP3A4 inhibition, inactivation, and induction determined in vitro. *Drug Metab Dispos* **36:**1698-1708.

FDA (2000) Guidance for Industry: Waiver of In Vivo Bioavailability and Bioequivalence Studies for Immediate-Release Solid Oral Dosage Forms Based on a Biopharmaceutics Classification System.

FDA (2010) Drugs@FDA: FDA Approved Drug Products, FDA, Retrieved November 01, 2010, from: http://www.accessdata.fda.gov/scripts/cder/drugsatfda/index.cfm

Fisher MB, Paine MF, Strelevitz TJ, and Wrighton SA (2001) The role of hepatic and extrahepatic UDP-glucuronosyltransferases in human drug metabolism. *Drug Metab Rev* **33:**273-297.

Flegal KM, Carroll MD, Ogden CL, and Curtin LR (2010) Prevalence and trends in obesity among US adults, 1999-2008. *JAMA* **303:**235-241.

Fromm MF, Kauffmann HM, Fritz P, Burk O, Kroemer HK, Warzok RW, Eichelbaum M, Siegmund W, and Schrenk D (2000) The effect of rifampin treatment on intestinal expression of human MRP transporters. *Am J Pathol* **157:**1575-1580.

Fujikawa M, Ano R, Nakao K, Shimizu R, and Akamatsu M (2005) Relationships between structure and high-throughput screening permeability of diverse drugs with artificial membranes: application to prediction of Caco-2 cell permeability. *Bioorganic & medicinal chemistry* **13:**4721-4732.

Funk C (2008) The role of hepatic transporters in drug elimination. *Expert Opin Drug Metab Toxicol* **4:**363-379.

Gertz M, Harrison A, Houston JB, and Galetin A (2010) Prediction of human intestinal first-pass metabolism of 25 CYP3A substrates from in vitro clearance and permeability data. *Drug Metab Dispos* **38:**1147-1158.

Gertz M, Houston JB, and Galetin A (2011) Physiologically based pharmacokinetic modeling of intestinal first-pass metabolism of CYP3A substrates with high intestinal extraction. *Drug Metab Dispos* **39:**1633-1642.

Ghobadi C, Johnson TN, Aarabi M, Almond LM, Allabi AC, Rowland-Yeo K, Jamei M, and Rostami-Hodjegan A (2011) Application of a systems approach to the bottom-up assessment of pharmacokinetics in obese patients: expected variations in clearance. *Clin Pharmacokinet* **50:**809-822.

Giacomini KM, Huang SM, Tweedie DJ, Benet LZ, Brouwer KL, Chu X, Dahlin A, Evers R, Fischer V, Hillgren KM, Hoffmaster KA, Ishikawa T, Keppler D, Kim RB, Lee CA, Niemi M, Polli JW, Sugiyama Y, Swaan PW, Ware JA, Wright SH, Yee SW, Zamek-Gliszczynski MJ, and Zhang L (2010) Membrane transporters in drug development. *Nat Rev Drug Discov* **9:**215-236.

Glaeser H, Bailey DG, Dresser GK, Gregor JC, Schwarz UI, McGrath JS, Jolicoeur E, Lee W, Leake BF, Tirona RG, and Kim RB (2007) Intestinal drug transporter expression and the impact of grapefruit juice in humans. *Clin Pharmacol Ther* **81:**362-370.

Goldman P (1978) Biochemical pharmacology of the intestinal flora. *Annual review of pharmacology and toxicology* **18:**523-539.

Graham H, Walker M, Jones O, Yates J, Galetin A, and Aarons L (2012) Comparison of in-vivo and in-silico methods used for prediction of tissue: plasma partition coefficients in rat. *J Pharm Pharmacol* **64:**383-396.

Guo H, Liu C, Li J, Zhang M, Hu M, Xu P, Liu L, and Liu X (2013) A mechanistic physiologically based pharmacokinetic-enzyme turnover model involving both intestine and liver to predict CYP3A induction-mediated drug-drug interactions. *J Pharm Sci* **102:**2819-2836.

Hardy JG, Wilson CG, and Wood E (1985) Drug delivery to the proximal colon. *J Pharm Pharmacol* **37:**874-877.

Harwood MD, Neuhoff S, Carlson GL, Warhurst G, and Rostami-Hodjegan A (2013) Absolute abundance and function of intestinal drug transporters: a prerequisite for fully mechanistic in vitro-in vivo extrapolation of oral drug absorption. *Biopharm Drug Dispos* **34:**2-28.

Hellmig S, Von Schoning F, Gadow C, Katsoulis S, Hedderich J, Folsch UR, and Stuber E (2006) Gastric emptying time of fluids and solids in healthy subjects determined by 13C breath tests: influence of age, sex and body mass index. *J Gastroenterol Hepatol* **21:**1832-1838.

Hewitt M, Cronin MT, Enoch SJ, Madden JC, Roberts DW, and Dearden JC (2009) In silico prediction of aqueous solubility: the solubility challenge. *J Chem Inf Model* **49:**2572-2587.

Hidalgo IJ, Raub TJ, and Borchardt RT (1989) Characterization of the human colon carcinoma cell line (Caco-2) as a model system for intestinal epithelial permeability. *Gastroenterology* **96:**736-749.

Hofmann AF, Molino G, Milanese M, and Belforte G (1983) Description and simulation of a physiological pharmacokinetic model for the metabolism and enterohepatic circulation of bile acids in man. Cholic acid in healthy man. *J Clin Invest* **71:**1003-1022.

Holm R, Müllertz A, and Mu H (2013) Bile salts and their importance for drug absorption. *Int J Pharm* **453:**44-55.

Horowitz M, Cook DJ, Collins PJ, Harding PE, Hooper MJ, Walsh JF, and Shearman DJ (1982) Measurement of gastric emptying after gastric bypass surgery using radionuclides. *Br J Surg* **69:**655-657.

Howgate EM, Rowland Yeo K, Proctor NJ, Tucker GT, and Rostami-Hodjegan A (2006) Prediction of in vivo drug clearance from in vitro data. I: impact of inter-individual variability. *Xenobiotica* **36:**473-497.

Ingelman-Sundberg M (2005) Genetic polymorphisms of cytochrome P450 2D6 (CYP2D6): clinical consequences, evolutionary aspects and functional diversity. *Pharmacogenomics J* **5:**6-13.

Irvine JD, Takahashi L, Lockhart K, Cheong J, Tolan JW, Selick HE, and Grove JR (1999) MDCK (Madin-Darby canine kidney) cells: A tool for membrane permeability screening. *J Pharm Sci* **88:**28-33.

Jamei M, Turner D, Yang J, Neuhoff S, Polak S, Rostami-Hodjegan A, and Tucker G (2009) Population-based mechanistic prediction of oral drug absorption. *AAPS J* **11:**225-237.

Jinno J, Oh D, Crison JR, and Amidon GL (2000) Dissolution of ionizable water-insoluble drugs: the combined effect of pH and surfactant. *J Pharm Sci* **89:**268-274.

Johnson TN, Boussery K, Rowland-Yeo K, Tucker GT, and Rostami-Hodjegan A (2010) A semi-mechanistic model to predict the effects of liver cirrhosis on drug clearance. *Clin Pharmacokinet* **49:**189-206.

Johnson TN and Rostami-Hodjegan A (2011) Resurgence in the use of physiologically based pharmacokinetic models in pediatric clinical pharmacology: parallel shift in incorporating the knowledge of biological elements and increased applicability to drug development and clinical practice. *Paediatric anaesthesia* **21:**291-301.

Kamdem LK, Streit F, Zanger UM, Brockmoller J, Oellerich M, Armstrong VW, and Wojnowski L (2005) Contribution of CYP3A5 to the in vitro hepatic clearance of tacrolimus. *Clin Chem* **51:**1374-1381.

Kansy M, Senner F, and Gubernator K (1998) Physicochemical high throughput screening: parallel artificial membrane permeation assay in the description of passive absorption processes. *J Med Chem* **41:**1007-1010.

Kararli TT (1995) Comparison of the gastrointestinal anatomy, physiology, and biochemistry of humans and commonly used laboratory animals. *Biopharm Drug Dispos* **16:**351-380.

Karlsen S, Fynne L, Gronbaek H, and Krogh K (2012) Small intestinal transit in patients with liver cirrhosis and portal hypertension: a descriptive study. *BMC gastroenterology* **12:**176.

Ke AB, Nallani SC, Zhao P, Rostami-Hodjegan A, and Unadkat JD (2012) A PBPK Model to Predict Disposition of CYP3A-Metabolized Drugs in Pregnant Women: Verification and Discerning the Site of CYP3A Induction. *CPT: pharmacometrics & systems pharmacology* **1:**e3.

Kolars JC, Lown KS, Schmiedlin-Ren P, Ghosh M, Fang C, Wrighton SA, Merion RM, and Watkins PB (1994) CYP3A gene expression in human gut epithelium. *Pharmacogenetics* **4:**247-259.

Kovarik JM, Mueller EA, van Bree JB, Tetzloff W, and Kutz K (1994) Reduced inter- and intraindividual variability in cyclosporine pharmacokinetics from a microemulsion formulation. *J Pharm Sci* **83:**444-446.

Langenbucher F (1972) Linearization of dissolution rate curves by the Weibull distribution. *J Pharm Pharmacol* **24:**979-981.

Lennernas H, Ahrenstedt O, Hallgren R, Knutson L, Ryde M, and Paalzow LK (1992) Regional jejunal perfusion, a new in vivo approach to study oral drug absorption in man. *Pharm Res* **9:**1243-1251.

Lennernas H, Lee ID, Fagerholm U, and Amidon GL (1997) A residence-time distribution analysis of the hydrodynamics within the intestine in man during a regional single-pass perfusion with Loc-I-Gut: in-vivo permeability estimation. *J Pharm Pharmacol* **49:**682-686.

Li AP (2007) Human hepatocytes: isolation, cryopreservation and applications in drug development. *Chemico-biological interactions* **168:**16-29.

Lipinski CA, Lombardo F, Dominy BW, and Feeney PJ (2001) Experimental and computational approaches to estimate solubility and permeability in drug discovery and development settings. *Adv Drug Deliv Rev* **46:**3-26.

Maliepaard M, Scheffer GL, Faneyte IF, van Gastelen MA, Pijnenborg AC, Schinkel AH, van De Vijver MJ, Scheper RJ, and Schellens JH (2001) Subcellular localization and distribution of the breast cancer resistance protein transporter in normal human tissues. *Cancer Res* **61:**3458-3464.

McFadden MA, DeLegge MH, and Kirby DF (1993) Medication delivery in the short-bowel syndrome. *JPEN J Parenter Enteral Nutr* **17:**180-186.

Moore WEC and Holdeman LV (1975) Discussion of Current Bacteriological Investigations of the Relationships between Intestinal Flora, Diet, and Colon Cancer. *Cancer Res* **35:**3418-3420.
Mouly S and Paine MF (2003) P-glycoprotein increases from proximal to distal regions of human small intestine. *Pharm Res* **20:**1595-1599.
Murphy DB, Sutton JA, Prescott LF, and Murphy MB (1997) Opioid-induced delay in gastric emptying: a peripheral mechanism in humans. *Anesthesiology* **87:**765-770.
Narang AS, Delmarre D, and Gao D (2007) Stable drug encapsulation in micelles and microemulsions. *Int J Pharm* **345:**9-25.
Nestorov IA, Aarons LJ, Arundel PA, and Rowland M (1998) Lumping of whole-body physiologically based pharmacokinetic models. *J Pharmacokinet Biopharm* **26:**21-46.
Noyes AA and Whitney WR (1897) The rate of solution of solid substances in their own solutions. *J Am Chem Soc* **19:**930-934.
Nugent SG, Kumar D, Rampton DS, and Evans DF (2001) Intestinal luminal pH in inflammatory bowel disease: possible determinants and implications for therapy with aminosalicylates and other drugs. *Gut* **48:**571-577.
Obach RS (2013) Time-dependent inhibition of cytochrome P450 is important in drug-drug interactions - recent advances to meet the challenges, in: *DDI 2013 - 4th International Workshop on Regulatory Requirements and Current Scientific Aspects on the Preclinical and Clinical Investigation of Drug-Drug Interaction*, Marbach Castle, Germany.
Obach RS, Walsky RL, and Venkatakrishnan K (2007) Mechanism-based inactivation of human cytochrome p450 enzymes and the prediction of drug-drug interactions. *Drug Metab Dispos* **35:**246-255.
Oberle RL, Chen TS, Lloyd C, Barnett JL, Owyang C, Meyer J, and Amidon GL (1990) The influence of the interdigestive migrating myoelectric complex on the gastric emptying of liquids. *Gastroenterology* **99:**1275-1282.
Ogungbenro K, Vasist L, Maclaren R, Dukes G, Young M, and Aarons L (2011) A semi-mechanistic gastric emptying model for the population pharmacokinetic analysis of orally administered acetaminophen in critically ill patients. *Pharm Res* **28:**394-404.
OHE (2010) Office of Health Economics, UK. Shedding the Pounds: Obesity management, NICE guidance and bariatric surgery in England.
Ohno Y, Hisaka A, Ueno M, and Suzuki H (2008) General framework for the prediction of oral drug interactions caused by CYP3A4 induction from in vivo information. *Clin Pharmacokinet* **47:**669-680.
Otsuka K, Shono Y, and Dressman J (2013) Coupling biorelevant dissolution methods with physiologically based pharmacokinetic modelling to forecast in-vivo performance of solid oral dosage forms. *J Pharm Pharmacol* **65:**937-952.
Padwal R, Brocks D, and Sharma AM (2009) A systematic review of drug absorption following bariatric surgery and its theoretical implications. *Obes Rev* **11:**41-50.
Paine MF, Hart HL, Ludington SS, Haining RL, Rettie AE, and Zeldin DC (2006) The human intestinal cytochrome P450 "pie". *Drug Metab Dispos* **34:**880-886.
Paine MF, Khalighi M, Fisher JM, Shen DD, Kunze KL, Marsh CL, Perkins JD, and Thummel KE (1997) Characterization of interintestinal and intraintestinal variations in human CYP3A-dependent metabolism. *J Pharmacol Exp Ther* **283:**1552-1562.
Parsons RL, Hossack G, and Paddock G (1975) The absorption of antibiotics in adult patients with coeliac disease. *J Antimicrob Chemother* **1:**39-50.
Pertinez H, Chenel M, and Aarons L (2013) A physiologically based pharmacokinetic model for strontium exposure in rat. *Pharm Res* **30:**1536-1552.

Peters WH, Roelofs HM, Nagengast FM, and van Tongeren JH (1989) Human intestinal glutathione S-transferases. *Biochem J* **257:**471-476.

Picot J, Jones J, Colquitt JL, Gospodarevskaya E, Loveman E, Baxter L, and Clegg AJ (2009) The clinical effectiveness and cost-effectiveness of bariatric (weight loss) surgery for obesity: a systematic review and economic evaluation. *Health Technol Assess* **13:**1-190, 215-357, iii-iv.

Pollack GM, Spencer AP, Horton TL, and Brouwer KL (1994) Site-dependent intestinal hydrolysis of valproate and morphine glucuronide in the developing rat. *Drug Metab Dispos* **22:**120-123.

Poulin P and Haddad S (2012) Advancing prediction of tissue distribution and volume of distribution of highly lipophilic compounds from a simplified tissue-composition-based model as a mechanistic animal alternative method. *J Pharm Sci* **101:**2250-2261.

Poulin P and Theil FP (2000) A priori prediction of tissue:plasma partition coefficients of drugs to facilitate the use of physiologically-based pharmacokinetic models in drug discovery. *J Pharm Sci* **89:**16-35.

Poulin P and Theil FP (2002a) Prediction of pharmacokinetics prior to in vivo studies. 1. Mechanism-based prediction of volume of distribution. *J Pharm Sci* **91:**129-156.

Poulin P and Theil FP (2002b) Prediction of pharmacokinetics prior to in vivo studies. II. Generic physiologically based pharmacokinetic models of drug disposition. *J Pharm Sci* **91:**1358-1370.

Radominska-Pandya A, Little JM, Pandya JT, Tephly TR, King CD, Barone GW, and Raufman JP (1998) UDP-glucuronosyltransferases in human intestinal mucosa. *Biochimica et biophysica acta* **1394:**199-208.

Riches Z, Stanley EL, Bloomer JC, and Coughtrie MW (2009) Quantitative evaluation of the expression and activity of five major sulfotransferases (SULTs) in human tissues: the SULT "pie". *Drug Metab Dispos* **37:**2255-2261.

Rippie EG, Lamb DJ, and Romig PW (1964) Solubilization of Weakly Acidic and Basic Drugs by Aqueous Solutions of Polysorbate 80. *J Pharm Sci* **53:**1346-1348.

Roberts MS and Rowland M (1986) A dispersion model of hepatic elimination: 1. Formulation of the model and bolus considerations. *J Pharmacokinet Biopharm* **14:**227-260.

Rodgers T, Leahy D, and Rowland M (2005) Physiologically based pharmacokinetic modeling 1: predicting the tissue distribution of moderate-to-strong bases. *J Pharm Sci* **94:**1259-1276.

Rodgers T and Rowland M (2006) Physiologically based pharmacokinetic modelling 2: predicting the tissue distribution of acids, very weak bases, neutrals and zwitterions. *J Pharm Sci* **95:**1238-1257.

Rodgers T and Rowland M (2007) Mechanistic approaches to volume of distribution predictions: understanding the processes. *Pharm Res* **24:**918-933.

Rostami-Hodjegan A (2012) Physiologically Based Pharmacokinetics Joined With In Vitro-In Vivo Extrapolation of ADME: A Marriage Under the Arch of Systems Pharmacology. *Clin Pharmacol Ther* **92:**50-61.

Rostami-Hodjegan A and Tucker G (2004) 'In silico' simulations to assess the 'in vivo' consequences of 'in vitro' metabolic drug-drug interactions. *Drug Discov Today: Technol* **1:**441-448.

Rowland M, Peck C, and Tucker G (2011) Physiologically-based pharmacokinetics in drug development and regulatory science. *Annual review of pharmacology and toxicology* **51:**45-73.

Rowland M and Tozer TN (1989) *Clinical Pharmacokinetics: Concepts and Applications*. Lea & Febiger, Philadelphia.

Rowland Yeo K, Aarabi M, Jamei M, and Rostami-Hodjegan A (2011) Modeling and predicting drug pharmacokinetics in patients with renal impairment. *Expert review of clinical pharmacology* **4:**261-274.

Rowland Yeo K, Jamei M, Yang J, Tucker GT, and Rostami-Hodjegan A (2010) Physiologically based mechanistic modelling to predict complex drug-drug interactions involving simultaneous competitive and time-dependent enzyme inhibition by parent compound and its metabolite in both liver and gut - the effect of diltiazem on the time-course of exposure to triazolam. *Eur J Pharm Sci* **39:**298-309.

Sakr A and Andheria M (2001) Pharmacokinetics of buspirone extended-release tablets: a single-dose study. *J Clin Pharmacol* **41:**783-789.

Samsom M, Vermeijden JR, Smout AJ, Van Doorn E, Roelofs J, Van Dam PS, Martens EP, Eelkman-Rooda SJ, and Van Berge-Henegouwen GP (2003) Prevalence of delayed gastric emptying in diabetic patients and relationship to dyspeptic symptoms: a prospective study in unselected diabetic patients. *Diabetes Care* **26:**3116-3122.

Sanger GJ and Lee K (2008) Hormones of the gut-brain axis as targets for the treatment of upper gastrointestinal disorders. *Nature Reviews Drug Discovery* **7:**241-254.

Savage AP, Adrian TE, Carolan G, Chatterjee VK, and Bloom SR (1987) Effects of peptide YY (PYY) on mouth to caecum intestinal transit time and on the rate of gastric emptying in healthy volunteers. *Gut* **28:**166-170.

Schiller C, Frohlich CP, Giessmann T, Siegmund W, Monnikes H, Hosten N, and Weitschies W (2005) Intestinal fluid volumes and transit of dosage forms as assessed by magnetic resonance imaging. *Aliment Pharmacol Ther* **22:**971-979.

Sconce EA, Khan TI, Wynne HA, Avery P, Monkhouse L, King BP, Wood P, Kesteven P, Daly AK, and Kamali F (2005) The impact of CYP2C9 and VKORC1 genetic polymorphism and patient characteristics upon warfarin dose requirements: proposal for a new dosing regimen. *Blood* **106:**2329-2333.

Shah P, Jogani V, Bagchi T, and Misra A (2006) Role of Caco-2 cell monolayers in prediction of intestinal drug absorption. *Biotechnology progress* **22:**186-198.

Sharpstone D, Neild P, Crane R, Taylor C, Hodgson C, Sherwood R, Gazzard B, and Bjarnason I (1999) Small intestinal transit, absorption, and permeability in patients with AIDS with and without diarrhoea. *Gut* **45:**70-76.

Sinko PJ, Leesman GD, and Amidon GL (1991) Predicting fraction dose absorbed in humans using a macroscopic mass balance approach. *Pharm Res* **8:**979-988.

Sjoberg A, Lutz M, Tannergren C, Wingolf C, Borde A, and Ungell AL (2013) Comprehensive study on regional human intestinal permeability and prediction of fraction absorbed of drugs using the Ussing chamber technique. *Eur J Pharm Sci* **48:**166-180.

Skottheim IB, Jakobsen GS, Stormark K, Christensen H, Hjelmesaeth J, Jenssen T, Asberg A, and Sandbu R (2010) Significant increase in systemic exposure of atorvastatin after biliopancreatic diversion with duodenal switch. *Clin Pharmacol Ther* **87:**699-705.

Skottheim IB, Stormark K, Christensen H, Jakobsen GS, Hjelmesaeth J, Jenssen T, Reubsaet JL, Sandbu R, and Asberg A (2009) Significantly altered systemic exposure to atorvastatin acid following gastric bypass surgery in morbidly obese patients. *Clin Pharmacol Ther* **86:**311-318.

Stringer RA, Strain-Damerell C, Nicklin P, and Houston JB (2009) Evaluation of recombinant cytochrome P450 enzymes as an in vitro system for metabolic clearance predictions. *Drug Metab Dispos* **37:**1025-1034.

Sugano K (2009) Computational oral absorption simulation for low-solubility compounds. *Chem Biodivers* **6:**2014-2029.

Sun D, Lennernas H, Welage LS, Barnett JL, Landowski CP, Foster D, Fleisher D, Lee KD, and Amidon GL (2002) Comparison of human duodenum and Caco-2 gene expression profiles for 12,000 gene sequences tags and correlation with permeability of 26 drugs. *Pharm Res* **19:**1400-1416.

Sun H, Chow EC, Liu S, Du Y, and Pang KS (2008) The Caco-2 cell monolayer: usefulness and limitations. *Expert Opin Drug Metab Toxicol* **4:**395-411.

Sutton SC (2009) Role of physiological intestinal water in oral absorption. *AAPS J* **11:**277-285.

Tang F, Horie K, and Borchardt RT (2002a) Are MDCK cells transfected with the human MDR1 gene a good model of the human intestinal mucosa? *Pharm Res* **19:**765-772.

Tang F, Horie K, and Borchardt RT (2002b) Are MDCK cells transfected with the human MRP2 gene a good model of the human intestinal mucosa? *Pharm Res* **19:**773-779.

Tannergren C, Bergendal A, Lennernas H, and Abrahamsson B (2009) Toward an increased understanding of the barriers to colonic drug absorption in humans: implications for early controlled release candidate assessment. *Mol Pharm* **6:**60-73.

Valentin J (2002) Pages 38-40 from *Basic Anatomical and Physiological Data for Use in Radiological Protection: Reference Values*. The International Comission on Radiological Protection, Pergamon.

Varma MV, Obach RS, Rotter C, Miller HR, Chang G, Steyn SJ, El-Kattan A, and Troutman MD (2010) Physicochemical space for optimum oral bioavailability: contribution of human intestinal absorption and first-pass elimination. *J Med Chem* **53:**1098-1108.

Wang J and Flanagan DR (1999) General solution for diffusion-controlled dissolution of spherical particles. 1. Theory. *J Pharm Sci* **88:**731-738.

Wang J and Flanagan DR (2002) General solution for diffusion-controlled dissolution of spherical particles. 2. Evaluation of experimental data. *J Pharm Sci* **91:**534-542.

Wells KA and Losin WG (2008) In vitro stability, potency, and dissolution of duloxetine enteric-coated pellets after exposure to applesauce, apple juice, and chocolate pudding. *Clin Ther* **30:**1300-1308.

Willmann S, Schmitt W, Keldenich J, and Dressman JB (2003) A physiologic model for simulating gastrointestinal flow and drug absorption in rats. *Pharm Res* **20:**1766-1771.

Willmann S, Schmitt W, Keldenich J, Lippert J, and Dressman JB (2004) A physiological model for the estimation of the fraction dose absorbed in humans. *J Med Chem* **47:**4022-4031.

Winiwarter S, Bonham NM, Ax F, Hallberg A, Lennernas H, and Karlen A (1998) Correlation of human jejunal permeability (in vivo) of drugs with experimentally and theoretically derived parameters. A multivariate data analysis approach. *J Med Chem* **41:**4939-4949.

Wu CY and Benet LZ (2005) Predicting drug disposition via application of BCS: transport/absorption/ elimination interplay and development of a biopharmaceutics drug disposition classification system. *Pharm Res* **22:**11-23.

Wuyts B, Brouwers J, Mols R, Tack J, Annaert P, and Augustijns P (2013) Solubility Profiling of HIV Protease Inhibitors in Human Intestinal Fluids. *J Pharm Sci.*

Yang J, Jamei M, Yeo KR, Rostami-Hodjegan A, and Tucker GT (2007a) Misuse of the well-stirred model of hepatic drug clearance. *Drug Metab Dispos* **35:**501-502.

Yang J, Jamei M, Yeo KR, Tucker GT, and Rostami-Hodjegan A (2007b) Prediction of intestinal first-pass drug metabolism. *Curr Drug Metab* **8:**676-684.

Yu LX and Amidon GL (1999) A compartmental absorption and transit model for estimating oral drug absorption. *Int J Pharm* **186:**119-125.

Yu LX, Amidon GL, Polli JE, Zhao H, Mehta MU, Conner DP, Shah VP, Lesko LJ, Chen ML, Lee VH, and Hussain AS (2002) Biopharmaceutics classification system: the scientific basis for biowaiver extensions. *Pharm Res* **19:**921-925.

Yu LX, Crison JR, and Amidon GL (1996) Compartmental transit and dispersion model analysis of small intestinal transit flow in humans. *Int J Pharm* **140:**111-118.

Zhao P, Zhang L, Grillo JA, Liu Q, Bullock JM, Moon YJ, Song P, Brar SS, Madabushi R, Wu TC, Booth BP, Rahman NA, Reynolds KS, Gil Berglund E, Lesko LJ, and Huang SM (2011) Applications of physiologically based pharmacokinetic (PBPK) modeling and simulation during regulatory review. *Clin Pharmacol Ther* **89:**259-267.

Ziegler TR, Fernandez-Estivariz C, Gu LH, Bazargan N, Umeakunne K, Wallace TM, Diaz EE, Rosado KE, Pascal RR, Galloway JR, Wilcox JN, and Leader LM (2002) Distribution of the H+/peptide transporter PepT1 in human intestine: up-regulated expression in the colonic mucosa of patients with short-bowel syndrome. *Am J Clin Nutr* **75:**922-930.

Chapter 2: Trends in oral drug bioavailability following bariatric surgery: examining the variable extent of impact on exposure of different drug classes

Chapter 2: Trends in oral drug bioavailability following bariatric surgery: examining the variable extent of impact on exposure of different drug classes

A.S. Darwich, K. Henderson, A. Burgin, N. Ward, J. Whittam, B.J. Ammori, D.M. Ashcroft and A. Rostami-Hodjegan

Br J Clin Pharmacol. 2012,74(5):774-87

2.1 Abstract

2.1.1 Aims

To identify the most commonly prescribed drugs in a bariatric surgery population and to assess existing evidence regarding trends in oral drug bioavailability post bariatric surgery.

2.1.2 Methods

A retrospective audit was undertaken to document commonly prescribed drugs amongst patients undergoing bariatric surgery in an NHS hospital in the UK and to assess practice for drug administration following bariatric surgery. The available literature was examined for trends relating to drug permeability and solubility with regards to the Biopharmaceutics Classification System (BCS) and main route of elimination.

2.1.3 Results

No significant difference in the 'post/pre surgery oral drug exposure ratio' (ppR) was apparent between BCS class I to IV drugs, with regards to dose number (Do) or main route of elimination. Drugs classified as 'solubility limited' displayed an overall reduction as compared with 'freely soluble' compounds, as well as an unaltered and increased ppR.

2.1.4 Conclusion

Clinical studies establishing guidelines for commonly prescribed drugs, and the monitoring of drugs exhibiting a narrow therapeutic window or without a readily

assessed clinical endpoint, are warranted. Using mechanistically based pharmacokinetic modelling for simulating the multivariate nature of changes in drug exposure may serve as a useful tool in the further understanding of postoperative trends in oral drug exposure and in developing practical clinical guidance.

2.2 Summary

2.2.1 What is already known about this subject

Changes to oral drug bioavailability have been observed post bariatric surgery. However, the magnitude and the direction of changes have not been assessed systematically to provide insights into the parameters governing the observed trends. Understanding these can help with dose adjustments.

2.2.2 What this study adds

Analysis of drug characteristics based on a biopharmaceutical classification system is not adequate to explain observed trends in altered oral drug bioavailability following bariatric surgery, although the findings suggest solubility to play an important role.

2.3 Introduction

Obesity is generally defined by the body mass index (BMI = Body Weight (kg) / Height $(m)^2$). The classification is somewhat arbitrary such that 'overweight' means a BMI $\geq$ 25 but <30 $kg \cdot m^{-2}$, 'obesity' refers to BMI $\geq$ 30 but <40 $kg \cdot m^{-2}$ and 'morbid obesity' is a BMI $\geq$ 40 $kg \cdot m^{-2}$ (this may also refer to being obese and suffering from related co-morbid conditions) (WHO, 2006; Picot *et al.*, 2009).

Over the last decade the prevalence of obesity has increased dramatically in the USA and Europe. In the USA 32.2% of the male and 35.5% of the female population over the age of 20 years were characterised as obese in 2007-2008 (Flegal *et al.*, 2010). The United Kingdom has the highest reported obesity rate in Europe (OECD, 2011). In England, 24.1% of the male and 24.9% of the female population over the age of 16 years were classified as obese in 2008 (OHE, 2010). Bariatric surgery has proven to be successful in treating morbid obesity. In the USA and Canada approximately 200,000

bariatric surgeries were performed in 2008 (Buchwald and Oien, 2009). In England 4,221 surgeries were performed in 2008/09, an increase of over 100% since 2006/07 (Picot *et al.*, 2009; The NHS Information Centre, 2010). Several bariatric surgical methods currently coexist in healthcare. These include the adjustable gastric band (AGBD), sleeve gastrectomy (SG), biliopancreatic diversion (BPD), biliopancreatic diversion with duodenal switch (BPD-DS) and Roux-en-Y gastric bypass (RYGB) (National Institutes of Health, 2010). Other procedures, such as jejunoileal bypass (JIB), have been gradually phased out due to a higher likelihood of adverse events (Griffen *et al.*, 1977; Elder and Wolfe, 2007; Singh *et al.*, 2009).

Bariatric surgical procedures have been well described in the literature (Schneider and Mun, 2005; Elder and Wolfe, 2007), where they are generally characterised as being restrictive, in terms of physiologically reducing dietary intake, malabsorptive, through reducing the ability of the gastrointestinal (GI) tract to absorb nutrients or a combination of both. Restrictive procedures such as AGBD and SG result in a reduced gastric capacity to 15-20 mL and 60-80 mL respectively (Schneider and Mun, 2005; Lee *et al.*, 2007). The JIB, considered a malabsorptive procedure, results in a 90-95% bypass of the small intestine, retaining the duodenum, proximal jejunum and terminal ileum (Griffen *et al.*, 1977; Elder and Wolfe, 2007; Singh *et al.*, 2009). The BPD-DS, primarily a malabsorptive procedure, results in a reduced gastric volume (100-175 mL) and bypass of larger parts of the small intestine, forming a biliopancreatic canal transporting the bile juices to the distal ileum (Hess and Hess, 1998; Spak *et al.*, 2010). The RYGB, combining restriction and malabsorption, results in the restriction of the stomach to 15-30 mL, and bypass of the proximal small intestine (Wittgrove and Clark, 2000; DeMaria *et al.*, 2002; Spak *et al.*, 2010).

Bariatric surgery imposes a number of physiological alterations known to affect the bioavailability of orally administered drugs (F_{oral}), dependent on the fraction of drug that is absorbed in the intestinal gut wall (f_a), the fraction that escapes gut wall metabolism (F_G), and the fraction that escapes hepatic metabolism (F_H) (Equation 1.1).

$$F_{oral} = f_a \cdot F_G \cdot F_H$$

Equation 1.1: Components of Foral.

f_a and F_G are highly influenced by drug specific properties, such as permeability and solubility, and the GI physiology such as gastric emptying time, GI pH profiles, small intestinal transit time, GI drug metabolising enzymes and GI efflux transporters (Rowland and Tozer, 1989; Jamei *et al.*, 2009). Gastric emptying time can serve as the rate limiting step for highly permeable and highly soluble drugs as the absorption from the stomach is low (Higaki *et al.*, 2008). The gastrointestinal pH may affect drug dissolution of permeability-limited drugs displaying a pKa within the range of the GI pH fluctuations. Small intestinal transit time can influence the drug absorption of poorly soluble or extended release drug formulations (Rowland and Tozer, 1989).

Metabolism in the gut acts to regulate oral bioavailability of drugs and other xenobiotics, and is an important determinant in the metabolism of substrate drugs (Kolars *et al.*, 1994). CYP3A4 is the most abundant drug metabolising enzyme in the GI tract, preceding CYP2C9/19 amongst others in order of appearance (Peters *et al.*, 1989; Fisher *et al.*, 2001; Paine *et al.*, 2006; Riches *et al.*, 2009). CYP3A4 and CYP3A5 are both present along the GI tract, where CYP3A4 expression rises towards the jejunum to decrease towards the ileum (Kolars *et al.*, 1994; Paine *et al.*, 1997). GI transporters may influence the absorption of orally administered drugs and potentially also the extent of metabolism in the gut through active substrate efflux (Benet and Cummins, 2001). Numerous transporters are present in the gut, where P-glycoprotein (P-gp) is perhaps the most extensively studied of the GI transporters. The relative expression pattern of P-gp in the small intestine increases from the proximal to the distal parts of the small intestine (Mouly and Paine, 2003).

The Biopharmaceutics Classification System (BCS) classifies drugs in accordance to solubility and permeability. Solubility takes on the form of a dose number (Do), given by dividing highest dose strength in mg (M_O) by a volume of 250 mL (V_O) divided by the aqueous solubility of the drug ($mg \cdot mL^{-1}$) over a pH range of 1.0-7.5 at 37°C (C_S) (FDA, 2000). Defining $Do \leq 1$ as highly soluble and an $f_a \geq 90\%$ as a highly permeable drug, drugs are classified as class I (high solubility-high permeability), class II (poor solubility-high permeability), class III (high solubility-poor permeability) and class IV (poor solubility-poor permeability) (Amidon *et al.*, 1995).

The aims of this study were to identify the most commonly prescribed drugs in a bariatric surgery population and to assess existing evidence with respect to altered oral drug bioavailability post bariatric surgery. This would be carried out through methodologically reviewing the current literature, evaluating drug specific pharmacokinetic characteristics relating to solubility, permeability and main route of elimination.

2.4 Methods

2.4.1 Evaluation of drug utilisation following gastric bypass

A retrospective audit of drug utilisation by bariatric surgery patients was performed at Salford Royal NHS Foundation Trust, Salford, UK. Data collection was performed using the hospitals electronic patient record (EPR) system, iSOFT clinical manager 1.4, which incorporates the medication prescription and administration records. A search of the EPR system was carried out for all patients under the care of a consultant bariatric surgeon. The search consisted of patients that had undergone surgery in the previous 5 months, from the 21st March 2011. The medical history of patients was initially searched to identify those having undergone laparoscopic RYGB. Patients who had a colostomy, gastric banding and reversal of gastric banding were excluded.

Data extraction was performed utilising an anonymous data collection form, maintaining patient confidentiality. Information extracted consisted of type of bariatric surgical procedure, pre surgery prescribed drug therapy and associated co-morbidities, post surgery medication including formulation changes and documented reasons behind alterations. Pre surgery medications were compared to the patients' medical charts on discharge, generally 2-3 days post-surgery. Statistical analysis of trends in prescribed drugs observed during the retrospective audit was conducted using McNemar's non-parametric test ($P \leq 0.05$) in R v 2.12 (the R Foundation for Statistical Computing).

2.4.2 Review and analysis of oral drug bioavailability following gastric bypass

Embase (1980-2010) and PubMed (1977-2010) were searched using the following combinations of key words: 'oral administration or bioavailability', 'absorption',

'bioavailability', 'gastric bypass', 'jejunoileal bypass', 'bariatric surgery'. In addition, references of related articles were systematically investigated for relevant publications.

Initial screening of titles and abstracts was carried out to identify those compliant with pre specified criteria of reporting observational trends in bioavailability/oral drug exposure of pharmaceutical agents following bariatric surgery or the identification of adverse events related to oral drug exposure following surgery. Studies excluded consisted of gastric surgical procedures not related to obesity, reports on nutrients or supplementation post bariatric surgery, publications written in a language other than English. Screening was carried out to determine inclusion or exclusion criteria. Information extracted included study characteristics: surgical procedure, study design, number of participants, year of publication, country of origin and time since procedure; study population characteristics: sex, average age, average BMI and co-morbidities. The principle measurement of bioavailability in the analysis was area under the curve (AUC), bioavailability, steady-state plasma or serum concentration.

Observed trends in oral drug exposure were assumed to follow a log normal distribution. Quantitative analysis was carried out through estimating the mean effect size of response ratios and their variance following random-effect model. Statistical analysis was carried out with a two-tailed t-test of the standard normal cumulative distribution (Borenstein *et al.*, 2009). Statistical analysis between subgroups were carried out utilising Welch's t-test ($P \leq 0.05$) of log-transformed weighted means and SDs with *post hoc* Dunn-Šidák correction ($P \leq 0.05$) using Microsoft® Excel 2003 and Matlab 2010 (the Mathworks Inc).

2.5 Results

2.5.1 Evaluation of clinical drug utilisation following gastric bypass

The search of iSOFT identified 63 patients under the care of the bariatric surgeon and 38 patients (26 female) with a mean age of 45 (range 23-64) years were eligible for data extraction after fulfilling the pre-specified criteria. The surgical procedures performed included laparoscopic RYGB (n=34), laparoscopic RYGB with abdominal wall hernia repair (n=3) and conversion of AGBD to RYGB (n=1). Commonly treated

comorbidities amongst the study population included hypertension (n=12), type 2 diabetes (n=15), depression/anxiety (n=11), hypothyroidism (n=5), osteoarthritis (n=11), hypercholesterolemia (n=10) and asthma (n=9).

The most commonly prescribed drugs prior to surgery included statins (n=13), ACE inhibitors (n=10), proton pump inhibitors (PPIs)/H_2-receptor antagonists (n=10) and metformin (n=10). Comparing pre to post surgery, a significant increase in the prescription of paracetamol, opioids, PPIs/H_2 receptor antagonists, heparin and antimicrobials was observed ($P<0.05$) as well as an overall reduction in the number of patients treated for type 2 diabetes ($P<0.05$). The most common drugs prescribed following surgery included heparin (n=38), PPIs/H_2 receptor antagonists (n=38) and paracetamol (n=34). The number of patients prescribed cardiovascular agents remained constant postoperatively, whereas prescriptions of statins displayed a non-significant reduction of 31% ($P>0.05$). The postoperative formulation of choice for diuretics was liquid (n=4), whereas the remaining cardiovascular agents were tablets that were being crushed postoperatively (n=28) (Figure 2.1).

All patients receiving antidepressants remained on the same antidepressant post surgery, with all but one receiving a different formulation. Of the 11 patients prescribed antidepressants, 50% were switched on to liquid formulations, whereas the remaining 50% were advised to crush their tablets post surgery (Figure 2.1). All patients with a prior diagnosis of diabetes underwent a diabetic review during their stay in hospital. The review resulted in a significant reduction in post-surgical prescriptions of anti-diabetic medications by 67% ($P<0.05$). Patients who no longer required diabetic medication were alternatively switched to manual monitoring of blood glucose concentrations. Metformin was the only agent continued postoperatively and in 60% of cases continued at a reduced dose of up to a third of the pre-surgical dose level. All but one patient were converted to liquid preparations (Figure 2.1). Standard postoperative treatment consisted of 1-2 weeks low molecular weight heparin injection, PPIs (lansoprazole FasTab) and liquid formulation pain-killers (codeine and paracetamol) being prescribed for all patients. This patient group also displayed a significant increase in the prescription of PPIs/H_2 receptor antagonists, opioids, paracetamol and heparin ($P<0.05$). One patient with a history of deep vein thrombosis remained on tinzaparin for 4 weeks.

Lansoprazole was given at a dose of 30 mg twice daily as a orodispersible formulation. The prophylactic therapy was to continue for at least 6 months postoperatively, before reducing the dose to once daily for a further 18 months. Approximately 2 weeks after surgery the sublingual formulation was switched to the solid tablet or capsule formulation.

Antimicrobials were given to 7 patients post-operatively for the eradication of *Helicobacter pylori* (n=5) that was detected from an intra-operative gastric mucosal biopsy, development of hospital-acquired pneumonia (n=1) and anastomotic leakage (n=1). All patients were given liquid preparations.

In total 17 patients were taking analgesics on regular basis prior to surgery, increasing to 38 patients postoperatively. Analgesic products included paracetamol (n=2, $P<0.05$), aspirin (n=5), opioids (n=9, $P<0.05$) and non-steroidal anti-inflammatory drugs (NSAIDs) (n=3). Patients taking NSAIDs prior to surgery (n=3) were advised to stop taking these postoperatively due to an increased risk of developing gastro-jejunal anastomotic ulceration.

As stated in the patients 'plan' for postoperative care, a review of the nutritional progress usually occurred approximately 2 weeks post surgery. Patients were therefore advised to cease taking any non-essential vitamins and minerals immediately after surgery until the nutritional review had been completed. On discharge patients were informed that they would require taking lifelong dietary supplementation.

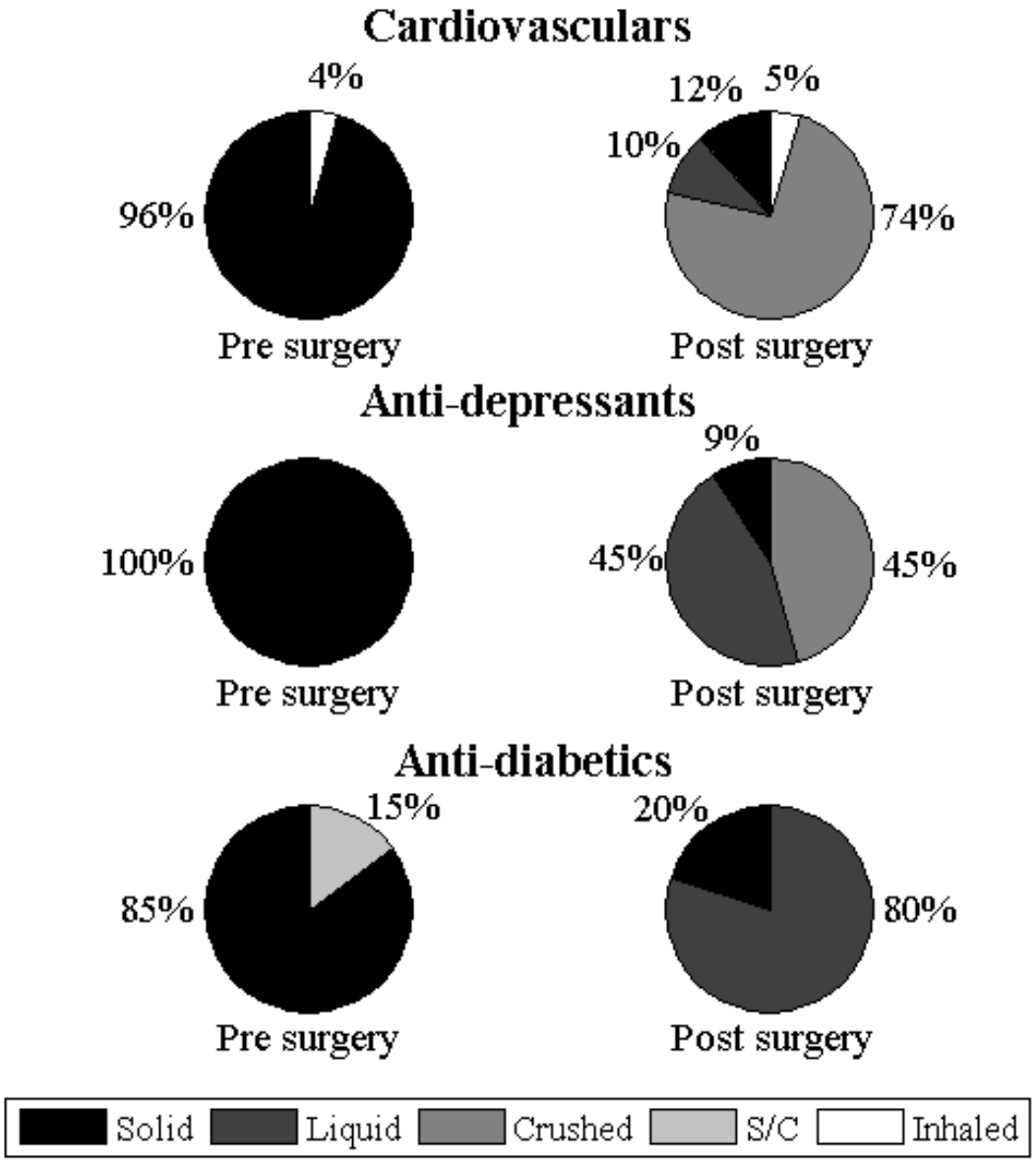

Figure 2.1. Pharmacotherapeutic alterations in formulation properties post bariatric surgery (Solid=solid tablets, Liquid=liquid formulation, S/C=subcutaneous, Crushed=patients instructed to crush tablets, Inhaled=inhalation formulation) of prescribed cardiovascular drugs, anti-depressants and anti-diabetics as compared to prior to surgery observed in 38 evaluated patients.

2.5.2 Oral drug bioavailability following bariatric surgery

The initial search of Embase and PubMed identified 311 potentially relevant publications based on search terms. After screening of abstracts, 66 articles were identified of which 22 matched the pre-specified criteria following full text screening.

Overall, the literature search included 41 articles (20 controlled trials, 18 case reports and three case series) published between 1974 and 2011 that were suitable for further evaluation and data extraction.

Articles relating to JIB mainly appeared between 1974 and 1985. An increase of published data on RYGB was identified between 2000 and 2011, following the trend of RYGB being the most widely used bariatric surgical procedure at the present time (Picot *et al.*, 2009).

Surgical techniques identified included RYGB (n=14), JIB (n=19), reversal of jejunoileal bypass (JIB R) (n=4), BPD-DS (n=2) BPD (n=3), GBP (n=1) and AGBD (n=1) (Table 2.1). The 41 identified publications originated from the USA (58%), followed by the UK (10%), Italy (5%), Norway (5%) and Canada (5%).

A total of 230 participants were studied in the identified publications. The time point for post surgical examination of oral drug exposure ranged from 0.1 to 88.9 months (Fuller *et al.*, 1986; Rogers *et al.*, 2008). In total 38 drugs were identified. These were categorically divided based on therapeutic indication. The studied drugs consisted of antimicrobials (n=12 drugs), cardiovascular drugs (n=2), immunosuppressants (n=4), antiepileptics (n=3), analgesics (n=2), oral contraceptives (n=4), anti-ulcer drugs (n=1), statins (n=1), thyroid hormones (n=1), anti-depressants (n=2), anti-cancer drugs (n=2), anti-diabetics (n=1) and HIV medication (n=1). Postoperative trends in drug bioavailability based on geometric mean drug exposure ranged from a 10.43 fold increase with a 95% confidence interval (CI) ranging from 0.10 to 1058 (n=32) (Terry *et al.*, 1982) to a 5.88 fold reduction (n=1) (Liu and Artz; Marcus *et al.*, 1977; Gerson *et al.*, 1980; Adami *et al.*, 1991; Cossu *et al.*, 1999; Skottheim *et al.*, 2009; Skottheim *et al.*). The overall post/pre surgical oral drug exposure ratio ('ppR') obtained from meta-analysis significantly diverged from pre-surgery with a mean ppR of 0.80 with a 95% confidence interval (CI) of 0.67 to 0.94 ($P<0.01$), when analysing quantitative data providing mean and variance of exposure pre and post bariatric surgery.

Table 2.1. Controlled trials examining the trend in oral drug exposure following bariatric surgery.

	Drug	Surgery	Pre to post surgery oral drug exposure ratio (X, 95% CI)	Patients (n)	References
▲	Phenoxymethyl penicillin 1,000 mg	JIB	**10.43 (0.10, 1058)***	3	(Terry *et al.*, 1982)
	Atorvastatin acid 20-80 mg	BPD-DS	**1.85 (0.81, 4.27)†**	10	(Skottheim *et al.*, 2010)
▬	Ranitidine 300 mg	BPD	**1.43 (1.12, 1.81)***	11	(Cossu *et al.*, 1999)
	Metformin 1,000 mg	RYGB	**1.20 (0.91, 1.58)†**	16	(Padwal *et al.*)
	Propylthiouracil 400 mg	JIB	**1.09 (0.84, 1.42)†**	6	(Kampmann *et al.*, 1984)
	Phenazone 15 mg/kg	JIB	**1.06 (0.81, 1.38)‡**	17	(Andreasen *et al.*, 1977)
	Atorvastatin acid 20-80 mg	RYGB	**1.00 (0.29, 3.46)†**	12	(Skottheim *et al.*, 2009)
	Paracetamol 1,500 mg	JIB	**1.00 (0.647, 1.54)***	3	(Terry *et al.*, 1982)
	Digoxin 0.5 mg daily (First day: 1 mg)	JIB	**0.89 (0.70, 1.14)†**	7	(Marcus *et al.*, 1977)
	Erythromycin 250 mg	GBP	**0.61 (0.38, 0.99)†**	7	(Prince *et al.*, 1984)
▼	Sulfisoxazole 1,000 mg	JIB	**0.84 (0.74, 0.94)***	3	(Garrett *et al.*, 1981)
	Norethisterone 3 mg	JIB	**0.80 (0.39, 1.63)‡**	6	(Victor *et al.*, 1987)
	Digoxin 0.5 mg	JIB	**0.76 (0.59, 0.97)†**	9	(Gerson *et al.*, 1980)
	MMF 2·1,000 mg	RYGB	**0.66 (0.21, 2.06)***	2	(Rogers *et al.*, 2008; Genentech, 2010)
	Levonorgestrel 0.25 mg	JIB	**0.55 (0.34, 0.90) ‡**	6	(Victor *et al.*, 1987)
	Sirolimus 8 mg	RYGB	**0.54 (0.25, 1.17)***	4	(Brattstrom *et al.*, 2000; Mathew *et al.*, 2006; Rogers *et al.*, 2008)
	Hydrochlorothiazide 75 mg	JIB	**0.46 (0.33, 0.65)***	4	(Beermann and Groschinsky-Grind, 1977; Backman *et al.*, 1979)
	Sertraline 100 mg	RYGB	**0.40 (0.19, 0.84)†**	5	(Roerig *et al.*)
	Ampicillin (pivampicillin 750 mg)	JIB	**0.37 (0.16, 0.89)†**	5	(Kampmann *et al.*, 1984)
	Phenytoin 200 mg	JIB	**0.32 (0.17, 0.58)†**	7	(Kennedy and Wade, 1979)

▲ = Indicating a significant increase in oral drug exposure (AUC, F_{oral} or steady state concentration) following surgery. ▬ = No statistical significant change in oral drug exposure. ▼ = Significant reduction in oral drug exposure. X=mean ratio change based on geometric mean, CI=95% confidence interval. GBP=Gastric Bypass (gastroplasty and Roux-en-Y gastric bypass), JIB=Jejunoileal Bypass, BPD=Biliopancreatic Diversion, BPDDS=Biliopancreatic Diversion with a Duodenal Switch, RYGB=Roux-en-Y Gastric Bypass, MMF=mycophenolate mofetil. *t-test performed at 5% significance level. †Statistical outcome as reported in publication. ‡Welch's t-test at a 5% significance level.

2.5.3 Analysis in accordance to the biopharmaceutics classification system

Classifying drugs into BCS classification, class I (high solubility, high permeability), class II (low solubility, high permeability), class III (high solubility, low permeability) and class IV (low solubility, low permeability), identified eight drugs as BCS class I (n=66 patients), three drugs as BCS class II (n=7), eleven drugs as BCS class III (n=53) and three drugs as BCS class IV (n=8). A total of eight drugs were found to be inconclusive (n=40). Information was lacking in the literature with regards to the BCS classification of pivampicillin, para-aminosalicylic acid and lopinavir/ritonavir.

Of the eight drugs identified as BCS class I, four drugs displayed a reduction in exposure following surgery, four drugs remained unaltered and one drug displayed an increase in drug exposure. Out of eleven mapped BCS class III drugs, five displayed a reduction in drug exposure following surgery. An additional five drugs displayed unaltered drug exposure, whereas one drug displayed an increase. All BCS class II and IV drugs (total of six) displayed a reduction in drug exposure following surgery (Figure 2.2).

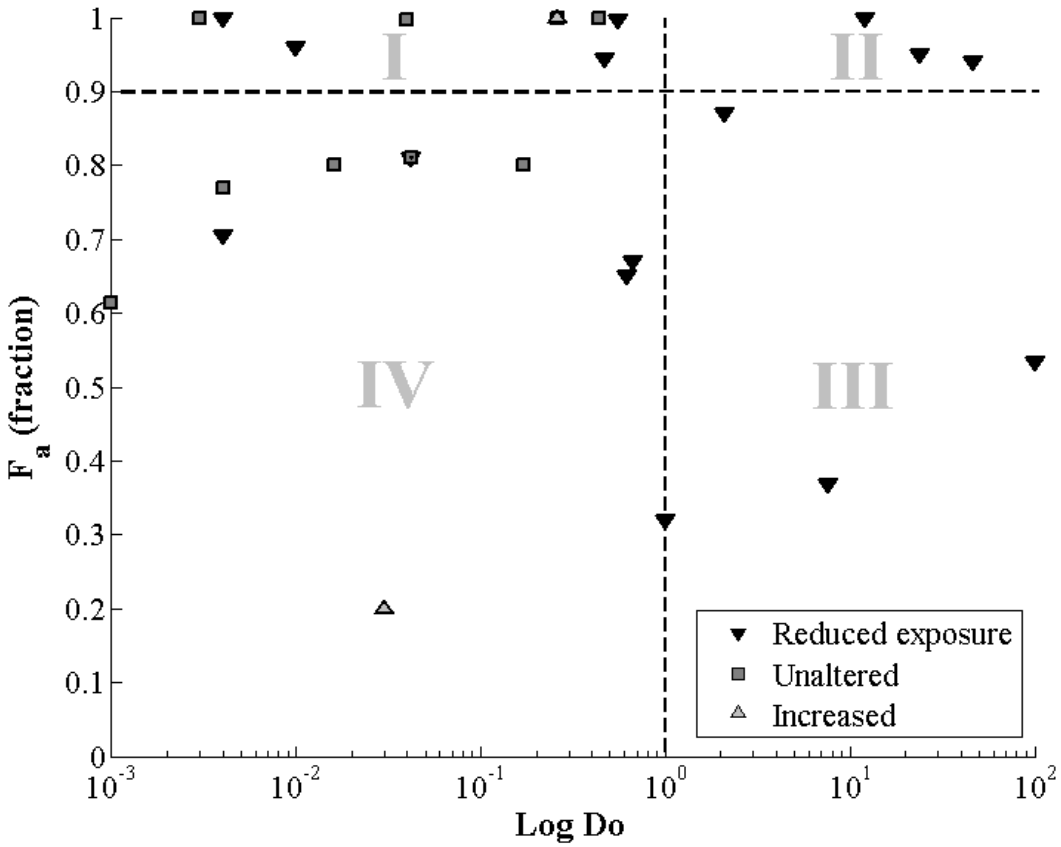

Figure 2.2. Categorical trends in oral drug exposure in relation to f_a (fraction of orally administered dose absorbed) and Do (dose number) in accordance to the BCS dividing drugs into BCS class I-IV). Reduced exposure (▼); Unaltered (□); Increased (△) (Kaplan *et al.*, 1972; Kampmann and Skovsted, 1974; Patel *et al.*, 1975; Wenzel and Kirschsieper, 1977; Nelson *et al.*, 1982; Oie *et al.*, 1982; Dressman *et al.*, 1985; Kearney *et al.*, 1993; Stewart *et al.*, 1995; Crowe and Lemaire, 1998; Peloquin *et al.*, 1999; Tavelin *et al.*, 1999; Lennernas *et al.*, 2002; Tamura *et al.*, 2002; Bock *et al.*, 2003; Garekani *et al.*, 2003; Lennernas, 2003; Yalkowsky and He, 2003; Bolton *et al.*, 2004; Kasim *et al.*, 2004; Lindenberg *et al.*, 2004; Wu and Benet, 2005; Song *et al.*, 2006; Ashiru *et al.*, 2008; Becker *et al.*, 2008; Ni *et al.*, 2008; Petan *et al.*, 2008; Chemical, 2010; FDA, 2010; BNF, 2011; NCBI, 2011).

Analysing BCS classified drugs where studies provided quantifiable measurements of drug exposure (*i.e.* AUC, F_{oral} and plasma or serum concentration levels), combining weighted means and variance of pre/post drug exposure ratio, BCS class I (n=5 drugs, n=108 population) displayed a weighted mean ppR of 0.94 (CI 0.66, 1.34). BCS class II

(n=2 drugs, n=5 population) displayed a weighted mean ppR of 0.80 (CI 0.48, 1.36), BCS class III (n=8 drugs, n=111 population) showed a weighted mean ppR of 0.86 (CI 0.68, 1.10), whereas BCS class IV (n=2 drugs, n=17 population) displayed a weighted mean ppR of 0.51 (CI 0.22, 1.17). Statistical analysis did not reveal any significant differences from pre-surgical ratio of 1 between BCS subgroups (P>0.05) (Figure 2.3).

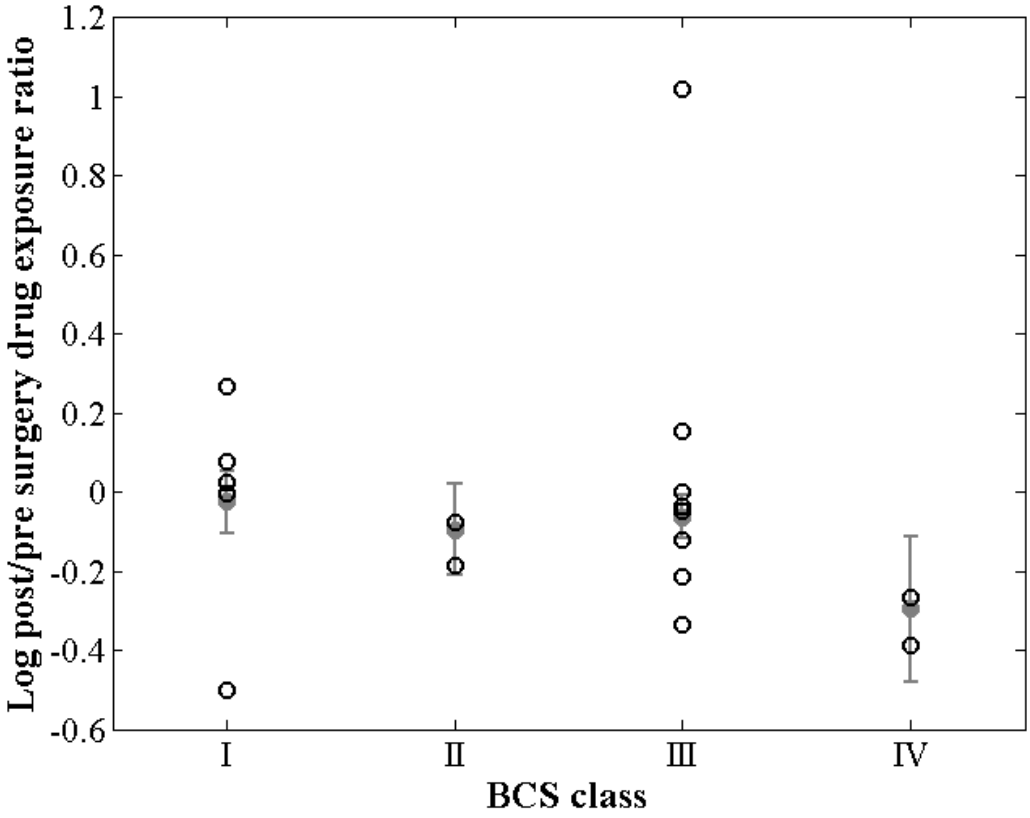

Figure 2.3. Log mean post/pre surgery drug exposure ratio of BCS class I-IV drugs. ○ log mean drug ratio, ● combined log mean ratio and standard deviation of subgroup.

Drugs where studies provided quantifiable measurements of drug exposure were further statistically analysed with regards to Do≤1, BCS class I and III (n=16 drugs, n=262 population) vs. BCS class II and IV (n=4 drugs, n=48 patients). Do≤1 drugs displayed a weighted mean ppR of 0.83 (0.69-1.00), whereas Do>1 drugs displayed a ratio of 0.70 (95% CI 0.45, 1.10). Statistical analysis revealed no statistical significance from a pre surgical ratio of 1 or between subgroups (P>0.05) (Figure 2.4).

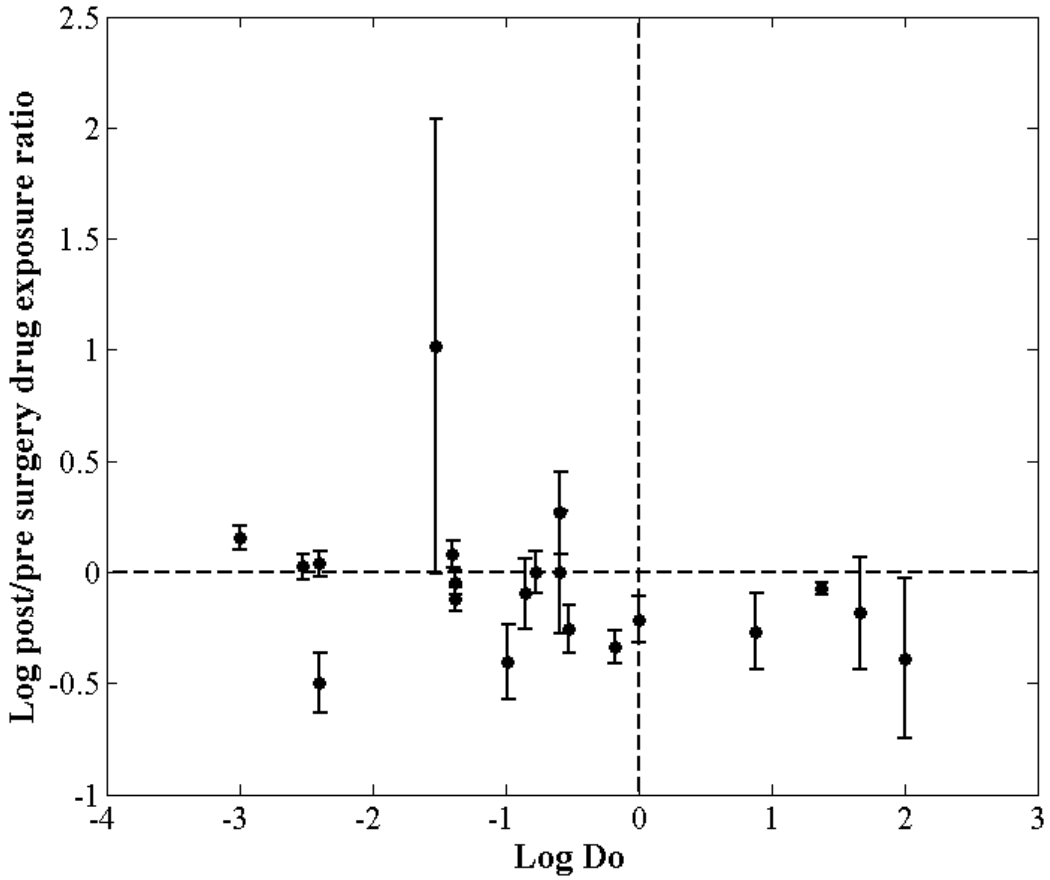

Figure 2.4. Mean post/pre surgery drug exposure ratio and standard deviation in relation to quantitative Do (dose number).

2.5.4 Analysis in accordance to main route of elimination

Examining drugs in accordance to the main route of elimination produced a weighted mean ppR in oral drug exposure of 0.83 (95% CI 0.59, 1.17) for CYP3A4/5 substrates (n=7 drugs, n=99 patients), 0.32 (95% CI 0.14, 0.72) for CYP2C substrates (n=1 drug, n=16 population), 0.90 (95% CI 0.68, 1.18) for mainly renally-cleared drugs (n=5 drugs, n=103 population) and 0.76 (95% CI 0.57, 1.01) for the remaining drugs (n=8 drugs, n=92 population). Statistical analysis revealed no difference in ppR between the subgroups ($P>0.05$), whereas the CYP2C subgroup significantly differed from the pre-surgical ratio of 1 ($P<0.001$).

2.6 Discussion

2.6.1 Evaluation of drug utilisation following gastric bypass

The observed practice of altering formulation properties to liquid preparations are considered necessary in healthcare due to the postoperative condition of the patient rather than as a proactive measure against altered pharmacokinetics due to changes in GI physiology. Patients are advised to remain on liquid formulations for approximately 2-3 weeks, varying nationally to 3 months to lifelong, post bariatric surgery to prevent any unnecessary strain on the gastric and jejunal transection lines and the gastrojejunal anastomosis and therefore to allow time for healing. As an unintentional consequence changing to liquid preparations may result in an increase in oral bioavailability for solubility limited drugs.

Pharmacotherapeutic treatment of type 2 diabetes was ceased in 67% of patients following surgery. The prescription of metformin remained unaltered following surgery, albeit being observed to be significantly reduced 12 months postoperatively, by Malone and Alger-Mayer, following 114 patients up to 24 months post surgery (Malone and Alger-Mayer, 2005).

Antidepressants, TCAs and SSRIs were continued immediately postoperatively in all cases. This was consistent with the report by Malone and Alger-Mayer, indicating prescriptions of TCAs and SSRIs remained statistically unaltered 12 months post surgery.

Vitamin and mineral deficiencies are likely to occur indefinitely in the bariatric patient, resulting in the need for lifelong supplementation (Ponsky *et al.*, 2005). Deficiencies are most likely to occur with fat-soluble vitamins (A, D, E and K), calcium and iron. Calcium and iron absorption is highly influenced by the reduction of hydrochloric acid production within the stomach after bariatric surgery (Ponsky *et al.*, 2005).

Medication reviews have been performed observing modifications to patient dosing and formulation after bariatric surgery. Currently no consensus guidelines are available regarding considerations of pharmacotherapy post bariatric surgery. Evidence based

national guidelines are warranted as bariatric surgery is becoming a more popular method for the treatment of obesity (Buchwald and Williams, 2004).

2.6.2 Oral drug exposure following bariatric surgery

Reviewing current data on changes in drug exposure prior to, and post bariatric surgery reveals many uncertainties regarding the prediction of post bariatric surgery drug bioavailability and the mechanisms behind these changes. BCS did not prove to be enough to explain the observed trend.

Post-bariatric surgery imposed restrictions on gastric volume (*e.g.* SG and RYGB) has been observed to reduce the gastric emptying time of liquids (Horowitz *et al.*, 1982; Braghetto *et al.*, 2009) and may further lead to an increase in gastric pH (Smith *et al.*, 1993; Behrns *et al.*, 1994). This together with a reduced fluid intake may impact the solubility of orally administered drugs.

Statistical analysis did not present any significant trends when examining BCS class I-IV, Do or elimination subgroups. None of the Do>1 classified drugs displayed an increase in bioavailability postoperatively, whereas the Do≤1 group exhibited a larger variability in post/pre surgery drug exposure outcome. This may be due to solubility issues of the Do>1 group, resulting in an overall reduction in oral drug exposure following surgery. The impact is however unclear due to a low number of drugs falling into the Do>1 category, where further clinical data is necessary to establish the case. Due to the restriction of the gastric volume following certain types of bariatric surgery (e.g. RYGB and BPD-DS) the default concomitant fluid intake of 250 mL in the BCS may no longer be valid. This will have implications for shifting the boundaries between BCS class I/III and II/IV, such that some freely soluble drugs may become solubility limited dependent on the administered dose. This is further complicated by a potentially altered gastric pH (Smith *et al.*, 1993; Behrns *et al.*, 1994; FDA, 2000; Schneider and Mun, 2005; Elder and Wolfe, 2007).

A small intestinal bypass will reduce the absorption area and may also alter the regional distribution and abundances of drug metabolising enzymes and transporters thus altering exposure of substrate drugs. When examining drugs with respect to main route

of elimination, no significant difference was observed between CYP3A, CYP2C, renal and other drugs. These results were also associated with a high degree of uncertainty due to scarcity of data, albeit a higher ppR of CYP3A may be expected due to the GI abundance of CYP enzymes were CYP3A4 is the most highly abundant. The bypass of highly abundant regions of CYP3A4 may lead to an increase in oral bioavailability while such an effect may become less relevant for substrates due to decreasingly abundant CYP2C9/19 and CYP2D6. Such a hypothesis may be supported by the observed trend in AUC of atorvastatin acid, mainly metabolised by CYP3A4 (Lennernas and Fager, 1997), thus potentially displaying an increase in bioavailability post malabsorptive bariatric surgery due to the bypass of significant segments GI regions highly abundant of CYP3A4 (Paine *et al.*, 1997), whereas this effect may be counteracted by a reduced absorption area. Following BPD-DS a significant increase in AUC of atorvastatin acid (2-fold) was observed, whereas no significant change was observed following RYGB, thus potentially increasing the risk of adverse effects, such as myopathy, following BPD-DS (Omar *et al.*, 2001; Skottheim *et al.*, 2009; Skottheim *et al.*, 2010).

The lack of quantifiable drug exposure data means that drugs displaying a low F_G or limited absorption prior to surgery are likely to be wrongly classified when trying to generalise over a wide variety of drugs, such as metformin and phenoxymethylpenicillin.

Metformin, a highly soluble and permeability limited basic compound (van de Merbel *et al.*, 1998; Kasim *et al.*, 2004) has been suggested to be subject to saturable transporter uptake to an extent by organic cation transporters in the intestine although not fully understood, thus resulting in a dose-dependent absorption that is mainly renally-cleared (Tucker *et al.*, 1981; Proctor *et al.*, 2008). The observed increase in postoperative bioavailability (Padwal *et al.*) might be due to altered small intestinal transit; reductions in gastric emptying time and small intestinal motility would in theory lead to a longer exposure time to enterocytic influx transporters. A further reason could be a post-surgical alteration in transporter distribution patterns. Phenoxymethylpenicillin, considered a highly soluble and permeable compound (Kasim *et al.*, 2004), displayed a significant increase in AUC post-JIB, possibly due to a reduced intestinal degradation by bacterial β-lactamase due to a major small intestinal restriction (Cole *et al.*, 1973).

The different surgical implications on GI physiology may result in variable trends in post-surgery drug exposure across the range of bariatric procedures, as is the case with atorvastatin acid displaying a significant increase in AUC following BPD-DS procedure as compared to no significant change following the less malabsorptive RYGB procedure (Skottheim *et al.*, 2009; Skottheim *et al.*, 2010). Also the case for cyclosporine, implicated to display a reduction in drug exposure following JIB, an exclusively malabsorptive procedure, as compared to remaining unaltered following the restrictive AGBD (Knight *et al.*, 1988; Ablassmaier *et al.*, 2002; Chenhsu *et al.*, 2003).

The outcomes of oral drug exposure of many commonly prescribed drugs in bariatric surgery populations are still unknown, such as many antidepressants and analgesics. Current available clinical data is very valuable. Going forward it is important that further clinical studies are designed taking into the consideration the potential alterations in concentration-time profiles, relating to pharmacokinetic parameters such as t_{max}. Drugs exhibiting narrow therapeutic range or displaying less readily measurable clinical endpoints will require more stringent monitoring after bariatric surgery, such as immunosuppressants and CNS active drugs.

Due to the multiple physiological factors altered in bariatric surgery (*i.e.* gastric volume, absorption area, CYP-abundance and regional distribution), and the fact that various drugs might be affected to different degrees by each of these changes, physiologically-based pharmacokinetic (PBPK) modelling may help in elucidating the impact of various bariatric surgeries on different drugs given at different doses (Schneider and Mun, 2005; Elder and Wolfe, 2007). Such investigation was outside the scope of the current research however initial attempts on this approach are addressed in another report (Darwich *et al.*, 2012) where the complex nature of interplays were manifested.

In conclusion, based on current findings, analysis of general pharmacokinetic parameters alone (*i.e.* solubility, permeability and main route of elimination) is not enough to explain observed trends in oral drug bioavailability following bariatric surgery, although the findings of this study suggest solubility to potentially play an important role.

These implications support the hypothesis that there are several physiologic and drug-specific parameters which govern the observed changes in drug exposure, thus calling for a more mechanistic approach, integrating all known parameters.

To the authors' knowledge this is the first publication quantitatively examining oral drug bioavailability in relation to a set of pharmacokinetic, biopharmaceutic and other drug-specific parameters and also in the context of pharmacotherapeutic practice following bariatric surgery. Along with further clinical studies, PBPK modelling may provide essential insights into the significance of individual pharmacokinetic parameters and generate important clinical guidance for a constantly growing post bariatric surgery population. Currently, there seems to be no simple algorithm or decision tree that predicts the variable changes to drug bioavailability following bariatric surgery.

2.7 Acknowledgements

There are no competing interests to declare.

2.8 References

Ablassmaier B, Klaua S, Jacobi CA, and Muller JM (2002) Laparoscopic gastric banding after heart transplantation. *Obes Surg* **12:**412-415.

Adami GF, Gandolfo P, Esposito M, and Scopinaro N (1991) Orally-administered Serum Ranitidine Concentration after Biliopancreatic Diversion for Obesity. *Obes Surg* **1:**293-294.

Amidon GL, Lennernas H, Shah VP, and Crison JR (1995) A theoretical basis for a biopharmaceutic drug classification: the correlation of in vitro drug product dissolution and in vivo bioavailability. *Pharm Res* **12:**413-420.

Andreasen PB, Dano P, Kirk H, and Greisen G (1977) Drug absorption and hepatic drug metabolism in patients with different types of intestinal shunt operation for obesity. A study with phenazone. *Scand J Gastroenterol* **12:**531-535.

Ashiru DA, Patel R, and Basit AW (2008) Polyethylene glycol 400 enhances the bioavailability of a BCS class III drug (ranitidine) in male subjects but not females. *Pharm Res* **25:**2327-2333.

Backman L, Beerman B, Groschinsky-Grind M, and Hallberg D (1979) Malabsorption of hydrochlorothiazide following intestinal shunt surgery. *Clin Pharmacokinet* **4:**63-68.

Becker C, Dressman JB, Amidon GL, Junginger HE, Kopp S, Midha KK, Shah VP, Stavchansky S, and Barends DM (2008) Biowaiver monographs for immediate release solid oral dosage forms: ethambutol dihydrochloride. *J Pharm Sci* **97:**1350-1360.

Beermann B and Groschinsky-Grind M (1977) Pharmacokinetics of hydrochlorothiazide in man. *Eur J Clin Pharmacol* **12:**297-303.

Behrns KE, Smith CD, and Sarr MG (1994) Prospective evaluation of gastric acid secretion and cobalamin absorption following gastric bypass for clinically severe obesity. *Dig Dis Sci* **39:**315-320.

Benet LZ and Cummins CL (2001) The drug efflux-metabolism alliance: biochemical aspects. *Adv Drug Deliv Rev* **50 Suppl 1:**S3-11.

BNF (2011) British National Formulary.

Bock U, Kottke T, Gindorf C, and Haltner E (2003) Validation of the Caco-2 cell monolayer system for determining the permeability of drug substances according to the Biopharmaceutics Classification System (BCS). *Across Barriers* **July**:1-7.

Bolton AE, Peng B, Hubert M, Krebs-Brown A, Capdeville R, Keller U, and Seiberling M (2004) Effect of rifampicin on the pharmacokinetics of imatinib mesylate (Gleevec, STI571) in healthy subjects. *Cancer Chemother Pharmacol* **53:**102-106.

Borenstein M, Hedges LV, Higgins JPT, and Rothstein HR (2009). Pages 33-39 In *Introduction to Meta-Analysis*. John Wiley & Sons, Ltd, Chichester.

Braghetto I, Davanzo C, Korn O, Csendes A, Valladares H, Herrera E, Gonzalez P, and Papapietro K (2009) Scintigraphic evaluation of gastric emptying in obese patients submitted to sleeve gastrectomy compared to normal subjects. *Obes Surg* **19:**1515-1521.

Brattstrom C, Sawe J, Jansson B, Lonnebo A, Nordin J, Zimmerman JJ, Burke JT, and Groth CG (2000) Pharmacokinetics and safety of single oral doses of sirolimus (rapamycin) in healthy male volunteers. *Ther Drug Monit* **22:**537-544.

Buchwald H and Oien DM (2009) Metabolic/bariatric surgery Worldwide 2008. *Obes Surg* **19:**1605-1611.

Buchwald H and Williams SE (2004) Bariatric surgery worldwide 2003. *Obes Surg* **14:**1157-1164.

Chemical C (2010) Product information - Imatinib (mesylate), Cayman Chemical Company, Ann Arbor, USA.

Chenhsu RY, Wu Y, Katz D, and Rayhill S (2003) Dose-adjusted cyclosporine c2 in a patient with jejunoileal bypass as compared to seven other liver transplant recipients. *Ther Drug Monit* **25:**665-670.

Cole M, Kenig MD, and Hewitt VA (1973) Metabolism of penicillins to penicilloic acids and 6-aminopenicillanic acid in man and its significance in assessing penicillin absorption. *Antimicrob Agents Chemother* **3:**463-468.

Cossu ML, Caccia S, Coppola M, Fais E, Ruggiu M, Fracasso C, Nacca A, and Noya G (1999) Orally administered ranitidine plasma concentrations before and after biliopancreatic diversion in morbidly obese patients. *Obes Surg* **9:**36-39.

Crowe A and Lemaire M (1998) In vitro and in situ absorption of SDZ-RAD using a human intestinal cell line (Caco-2) and a single pass perfusion model in rats: comparison with rapamycin. *Pharm Res* **15:**1666-1672.

Darwich AS, Pade D, Ammori BJ, Jamei M, Ashcroft DM, and Rostami-Hodjegan A (2012) A mechanistic pharmacokinetic model to assess modified oral drug bioavailability post bariatric surgery in morbidly obese patients: interplay between CYP3A gut wall metabolism, permeability and dissolution. *J Pharm Pharmacol* **64:**1008-1024.

DeMaria EJ, Sugerman HJ, Kellum JM, Meador JG, and Wolfe LG (2002) Results of 281 consecutive total laparoscopic Roux-en-Y gastric bypasses to treat morbid obesity. *Ann Surg* **235:**640-645; discussion 645-647.

Dressman JB, Amidon GL, and Fleisher D (1985) Absorption potential: estimating the fraction absorbed for orally administered compounds. *J Pharm Sci* **74:**588-589.
Elder KA and Wolfe BM (2007) Bariatric surgery: a review of procedures and outcomes. *Gastroenterology* **132:**2253-2271.
FDA (2000) Guidance for Industry: Waiver of In Vivo Bioavailability and Bioequivalence Studies for Immediate-Release Solid Oral Dosage Forms Based on a Biopharmaceutics Classification System.
FDA (2010) Drugs@FDA: FDA Approved Drug Products, FDA, Retrieved November 01, 2010, from: http://www.accessdata.fda.gov/scripts/cder/drugsatfda/index.cfm
Fisher MB, Paine MF, Strelevitz TJ, and Wrighton SA (2001) The role of hepatic and extrahepatic UDP-glucuronosyltransferases in human drug metabolism. *Drug Metab Rev* **33:**273-297.
Flegal KM, Carroll MD, Ogden CL, and Curtin LR (2010) Prevalence and trends in obesity among US adults, 1999-2008. *JAMA* **303:**235-241.
Fuller AK, Tingle D, DeVane CL, Scott JA, and Stewart RB (1986) Haloperidol pharmacokinetics following gastric bypass surgery. *J Clin Psychopharmacol* **6:**376-378.
Garekani HA, Sadeghi F, and Ghazi A (2003) Increasing the aqueous solubility of acetaminophen in the presence of polyvinylpyrrolidone and investigation of the mechanisms involved. *Drug Dev Ind Pharm* **29:**173-179.
Garrett ER, Suverkrup RS, Eberst K, Yost RL, and O'Leary JP (1981) Surgically affected sulfisoxazole pharmacokinetics in the morbidly obese. *Biopharm Drug Dispos* **2:**329-365.
Genentech (2010) Cellcept prescribing information, Genentech USA Inc, San Fransisco.
Gerson CD, Lowe EH, and Lindenbaum J (1980) Bioavailability of digoxin tablets in patients with gastrointestinal dysfunction. *Am J Med* **69:**43-49.
Griffen WO, Jr., Young VL, and Stevenson CC (1977) A prospective comparison of gastric and jejunoileal bypass procedures for morbid obesity. *Ann Surg* **186:**500-509.
Hess DS and Hess DW (1998) Biliopancreatic diversion with a duodenal switch. *Obes Surg* **8:**267-282.
Higaki K, Choe SY, Lobenberg R, Welage LS, and Amidon GL (2008) Mechanistic understanding of time-dependent oral absorption based on gastric motor activity in humans. *Eur J Pharm Biopharm* **70:**313-325.
Horowitz M, Cook DJ, Collins PJ, Harding PE, Hooper MJ, Walsh JF, and Shearman DJ (1982) Measurement of gastric emptying after gastric bypass surgery using radionuclides. *Br J Surg* **69:**655-657.
Jamei M, Turner D, Yang J, Neuhoff S, Polak S, Rostami-Hodjegan A, and Tucker G (2009) Population-based mechanistic prediction of oral drug absorption. *AAPS J* **11:**225-237.
Kampmann J and Skovsted L (1974) The pharmacokinetics of propylthiouracil. *Acta Pharmacol Toxicol (Copenh)* **35:**361-369.
Kampmann JP, Klein H, Lumholtz B, and Molholm Hansen JE (1984) Ampicillin and propylthiouracil pharmacokinetics in intestinal bypass patients followed up to a year after operation. *Clin Pharmacokinet* **9:**168-176.
Kaplan SA, Weinfeld RE, Abruzzo CW, and Lewis M (1972) Pharmacokinetic profile of sulfisoxazole following intravenous, intramuscular, and oral administration to man. *J Pharm Sci* **61:**773-778.
Kasim NA, Whitehouse M, Ramachandran C, Bermejo M, Lennernas H, Hussain AS, Junginger HE, Stavchansky SA, Midha KK, Shah VP, and Amidon GL (2004)

Molecular properties of WHO essential drugs and provisional biopharmaceutical classification. *Mol Pharm* **1:**85-96.
Kearney AS, Crawford LF, Mehta SC, and Radebaugh GW (1993) The interconversion kinetics, equilibrium, and solubilities of the lactone and hydroxyacid forms of the HMG-CoA reductase inhibitor, CI-981. *Pharm Res* **10:**1461-1465.
Kennedy MC and Wade DN (1979) Phenytoin absorption in patients with ileojejunal bypass. *Br J Clin Pharmacol* **7:**515-518.
Knight GC, Macris MP, Peric M, Duncan JM, Frazier OH, and Cooley DA (1988) Cyclosporine A pharmacokinetics in a cardiac allograft recipient with a jejuno-ileal bypass. *Transplant Proc* **20:**351-355.
Kolars JC, Lown KS, Schmiedlin-Ren P, Ghosh M, Fang C, Wrighton SA, Merion RM, and Watkins PB (1994) CYP3A gene expression in human gut epithelium. *Pharmacogenetics* **4:**247-259.
Lee CM, Cirangle PT, and Jossart GH (2007) Vertical gastrectomy for morbid obesity in 216 patients: report of two-year results. *Surg Endosc* **21:**1810-1816.
Lennernas H (2003) Clinical pharmacokinetics of atorvastatin. *Clin Pharmacokinet* **42:**1141-1160.
Lennernas H and Fager G (1997) Pharmacodynamics and pharmacokinetics of the HMG-CoA reductase inhibitors. Similarities and differences. *Clin Pharmacokinet* **32:**403-425.
Lennernas H, Gjellan K, Hallgren R, and Graffner C (2002) The influence of caprate on rectal absorption of phenoxymethylpenicillin: experience from an in-vivo perfusion in humans. *J Pharm Pharmacol* **54:**499-508.
Lindenberg M, Kopp S, and Dressman JB (2004) Classification of orally administered drugs on the World Health Organization Model list of Essential Medicines according to the biopharmaceutics classification system. *Eur J Pharm Biopharm* **58:**265-278.
Liu H and Artz AS Reduction of imatinib absorption after gastric bypass surgery. *Leuk Lymphoma* **52:**310-313.
Malone M and Alger-Mayer SA (2005) Medication use patterns after gastric bypass surgery for weight management. *Ann Pharmacother* **39:**637-642.
Marcus FI, Quinn EJ, Horton H, Jacobs S, Pippin S, Stafford M, and Zukoski C (1977) The effect of jejunoileal bypass on the pharmacokinetics of digoxin in man. *Circulation* **55:**537-541.
Mathew TH, Van Buren C, Kahan BD, Butt K, Hariharan S, and Zimmerman JJ (2006) A comparative study of sirolimus tablet versus oral solution for prophylaxis of acute renal allograft rejection. *J Clin Pharmacol* **46:**76-87.
Mouly S and Paine MF (2003) P-glycoprotein increases from proximal to distal regions of human small intestine. *Pharm Res* **20:**1595-1599.
National Institutes of Health U (2010) Bariatric Surgery for Severe Obesity.
NCBI (2011) PubChem Public Chemical Database, National Center of Biotechnology Information, USA.
Nelson E, Powell JR, Conrad K, Likes K, Byers J, Baker S, and Perrier D (1982) Phenobarbital pharmacokinetics and bioavailability in adults. *J Clin Pharmacol* **22:**141-148.
Ni J, Ouyang H, Aiello M, Seto C, Borbridge L, Sakuma T, Ellis R, Welty D, and Acheampong A (2008) Microdosing assessment to evaluate pharmacokinetics and drug metabolism in rats using liquid chromatography-tandem mass spectrometry. *Pharm Res* **25:**1572-1582.
OECD (2011) Obesity and the Economics of Prevention: Fit not Fat - United Kingdom (England) Key Facts, OECD.

OHE (2010) Office of Health Economics, UK. Shedding the Pounds: Obesity management, NICE guidance and bariatric surgery in England.

Oie S, Gambertoglio JG, and Fleckenstein L (1982) Comparison of the disposition of total and unbound sulfisoxazole after single and multiple dosing. *J Pharmacokinet Biopharm* **10:**157-172.

Omar MA, Wilson JP, and Cox TS (2001) Rhabdomyolysis and HMG-CoA reductase inhibitors. *Ann Pharmacother* **35:**1096-1107.

Padwal RS, Gabr RQ, Sharma AM, Langkaas LA, Birch DW, Karmali S, and Brocks DR (2011) Effect of gastric bypass surgery on the absorption and bioavailability of metformin. *Diabetes Care* **34:**1295-1300.

Paine MF, Hart HL, Ludington SS, Haining RL, Rettie AE, and Zeldin DC (2006) The human intestinal cytochrome P450 "pie". *Drug Metab Dispos* **34:**880-886.

Paine MF, Khalighi M, Fisher JM, Shen DD, Kunze KL, Marsh CL, Perkins JD, and Thummel KE (1997) Characterization of interintestinal and intraintestinal variations in human CYP3A-dependent metabolism. *J Pharmacol Exp Ther* **283:**1552-1562.

Patel IH, Levy RH, and Bauer TG (1975) Pharmacokinetic properties of ethosuximide in monkeys. I. Single-dose intravenous and oral administration. *Epilepsia* **16:**705-716.

Peloquin CA, Namdar R, Singleton MD, and Nix DE (1999) Pharmacokinetics of rifampin under fasting conditions, with food, and with antacids. *Chest* **115:**12-18.

Petan JA, Undre N, First MR, Saito K, Ohara T, Iwabe O, Mimura H, Suzuki M, and Kitamura S (2008) Physiochemical properties of generic formulations of tacrolimus in Mexico. *Transplant Proc* **40:**1439-1442.

Peters WH, Roelofs HM, Nagengast FM, and van Tongeren JH (1989) Human intestinal glutathione S-transferases. *Biochem J* **257:**471-476.

Picot J, Jones J, Colquitt JL, Gospodarevskaya E, Loveman E, Baxter L, and Clegg AJ (2009) The clinical effectiveness and cost-effectiveness of bariatric (weight loss) surgery for obesity: a systematic review and economic evaluation. *Health Technol Assess* **13:**1-190, 215-357, iii-iv.

Ponsky TA, Brody F, and Pucci E (2005) Alterations in gastrointestinal physiology after Roux-en-Y gastric bypass. *J Am Coll Surg* **201:**125-131.

Prince RA, Pincheira JC, Mason EE, and Printen KJ (1984) Influence of bariatric surgery on erythromycin absorption. *J Clin Pharmacol* **24:**523-527.

Proctor WR, Bourdet DL, and Thakker DR (2008) Mechanisms underlying saturable intestinal absorption of metformin. *Drug Metab Dispos* **36:**1650-1658.

Riches Z, Stanley EL, Bloomer JC, and Coughtrie MW (2009) Quantitative evaluation of the expression and activity of five major sulfotransferases (SULTs) in human tissues: the SULT "pie". *Drug Metab Dispos* **37:**2255-2261.

Roerig JL, Steffen K, Zimmerman C, Mitchell JE, Crosby RD, and Cao L (2012) Preliminary comparison of sertraline levels in postbariatric surgery patients versus matched nonsurgical cohort. *Surg Obes Relat Dis* **8:**62-66.

Rogers CC, Alloway RR, Alexander JW, Cardi M, Trofe J, and Vinks AA (2008) Pharmacokinetics of mycophenolic acid, tacrolimus and sirolimus after gastric bypass surgery in end-stage renal disease and transplant patients: a pilot study. *Clin Transplant* **22:**281-291.

Rowland M and Tozer TN (1989) *Clinical Pharmacokinetics: Concepts and Applications*. Lea & Febiger, Philadelphia.

Schneider BE and Mun EC (2005) Surgical management of morbid obesity. *Diabetes Care* **28:**475-480.

Singh D, Laya AS, Clarkston WK, and Allen MJ (2009) Jejunoileal bypass: a surgery of the past and a review of its complications. *World J Gastroenterol* **15:**2277-2279.

Skottheim IB, Jakobsen GS, Stormark K, Christensen H, Hjelmesaeth J, Jenssen T, Asberg A, and Sandbu R (2010) Significant increase in systemic exposure of atorvastatin after biliopancreatic diversion with duodenal switch. *Clin Pharmacol Ther* **87:**699-705.

Skottheim IB, Stormark K, Christensen H, Jakobsen GS, Hjelmesaeth J, Jenssen T, Reubsaet JL, Sandbu R, and Asberg A (2009) Significantly altered systemic exposure to atorvastatin acid following gastric bypass surgery in morbidly obese patients. *Clin Pharmacol Ther* **86:**311-318.

Smith CD, Herkes SB, Behrns KE, Fairbanks VF, Kelly KA, and Sarr MG (1993) Gastric acid secretion and vitamin B12 absorption after vertical Roux-en-Y gastric bypass for morbid obesity. *Ann Surg* **218:**91-96.

Song NN, Li QS, and Liu CX (2006) Intestinal permeability of metformin using single-pass intestinal perfusion in rats. *World J Gastroenterol* **12:**4064-4070.

Spak E, Bjorklund P, Helander HF, Vieth M, Olbers T, Casselbrant A, Lonroth H, and Fandriks L (2010) Changes in the mucosa of the Roux-limb after gastric bypass surgery. *Histopathology* **57:**680-688.

Stewart BH, Chan OH, Lu RH, Reyner EL, Schmid HL, Hamilton HW, Steinbaugh BA, and Taylor MD (1995) Comparison of intestinal permeabilities determined in multiple in vitro and in situ models: relationship to absorption in humans. *Pharm Res* **12:**693-699.

Tamura S, Ohike A, Ibuki R, Amidon GL, and Yamashita S (2002) Tacrolimus is a class II low-solubility high-permeability drug: the effect of P-glycoprotein efflux on regional permeability of tacrolimus in rats. *J Pharm Sci* **91:**719-729.

Tavelin S, Milovic V, Ocklind G, Olsson S, and Artursson P (1999) A conditionally immortalized epithelial cell line for studies of intestinal drug transport. *J Pharmacol Exp Ther* **290:**1212-1221.

Terry SI, Gould JC, McManus JP, and Prescott LF (1982) Absorption of penicillin and paracetamol after small intestinal bypass surgery. *Eur J Clin Pharmacol* **23:**245-248.

The NHS Information Centre LS (2010) Statistics on obesity, physical activity and diet: England, 2010.

Tucker GT, Casey C, Phillips PJ, Connor H, Ward JD, and Woods HF (1981) Metformin kinetics in healthy subjects and in patients with diabetes mellitus. *Br J Clin Pharmacol* **12:**235-246.

van de Merbel NC, Wilkens G, Fowles S, Oosterhuis B, and Jonkman JHG (1998) LC Phases Improve, But Not All Assays Do: Metformin Bioanalysis Revisited. *Chromatographia* **47:**542-546.

Victor A, Odlind V, and Kral JG (1987) Oral contraceptive absorption and sex hormone binding globulins in obese women: effects of jejunoileal bypass. *Gastroenterol Clin North Am* **16:**483-491.

Wenzel KW and Kirschsieper HE (1977) Aspects of the absorption of oral L-thyroxine in normal man. *Metabolism* **26:**1-8.

WHO (2006) WHO. Obesity and Overweight, fact sheet 311.

Wittgrove AC and Clark GW (2000) Laparoscopic gastric bypass, Roux-en-Y- 500 patients: technique and results, with 3-60 month follow-up. *Obes Surg* **10:**233-239.

Wu CY and Benet LZ (2005) Predicting drug disposition via application of BCS: transport/absorption/ elimination interplay and development of a biopharmaceutics drug disposition classification system. *Pharm Res* **22:**11-23.

Yalkowsky SH and He Y (2003) *Handbook of aqueous solubility data*. CRC Press, Boca Raton, Fla.

Chapter 3: A mechanistic pharmacokinetic model to assess modified oral drug bioavailability post bariatric surgery in morbidly obese patients: interplay between CYP3A gut wall metabolism, permeability and dissolution

Chapter 3: A mechanistic pharmacokinetic model to assess modified oral drug bioavailability post bariatric surgery in morbidly obese patients: interplay between CYP3A gut wall metabolism, permeability and dissolution

A.S. Darwich, D. Pade, B.J. Ammori, M. Jamei, D.M. Ashcroft, A. Rostami-Hodjegan

J Pharm Pharmacol. 2012, 64(7):1008-24

3.1 Abstract

3.1.1 Objectives

Due to the multi-factorial physiological implications of bariatric surgery, attempts to explain trends in oral bioavailability following bariatric surgery using singular attributes of drugs or simplified categorisations such as the biopharmaceutics classification system have been unsuccessful.

3.1.2 Methods

Pharmacokinetic post bariatric surgery models were created for Roux-en-Y gastric bypass, biliopancreatic diversion with duodenal switch, sleeve gastrectomy and jejunoileal bypass, through altering the 'Advanced Dissolution Absorption and Metabolism' (ADAM) model incorporated into the Simcyp® Simulator. Post to pre surgical simulations were carried out for five drugs with varying characteristics regarding their gut wall metabolism, dissolution and permeability (simvastatin, omeprazole, diclofenac, fluconazole and ciprofloxacin).

3.1.3 Key findings

The trends in oral drug bioavailability pre to post surgery were found to be dependent on a combination of drug parameters, including solubility, permeability and gastrointestinal metabolism as well as the surgical procedure carried out.

3.1.4 Conclusions

In the absence of clinical studies, the ability to project the direction and the magnitude of changes in bioavailability of drug therapy, using evidence-based mechanistic pharmacokinetic *in silico* models would be of significant value in guiding prescribers to make the necessary adjustments to dosage regimens for an increasing population of patients who are undergoing bariatric surgery.

3.2 Introduction

The prevalence of obesity has increased dramatically in the USA and Europe over the last decade (Elder and Wolfe, 2007; Flegal *et al.*, 2010; OECD, 2011; Ammori, 2012). Bariatric surgery has proven to be successful in treating morbid obesity. In 2008, approximately 220,000 bariatric surgeries were performed in the USA and Canada, whereas over 66,000 operations were carried out in Europe (Buchwald and Oien, 2009; Picot *et al.*, 2009).

Several bariatric surgical procedures currently coexist in healthcare, being characterised as either restrictive, in terms of reducing gastric capacity, malabsorptive, with regard to restricting the small intestine and/or delaying the bile inlet, or a combination of both (Schneider and Mun, 2005; Lee *et al.*, 2007). These procedures include: adjustable gastric band (AGB), sleeve gastrectomy (SG), biliopancreatic diversion (BPD), biliopancreatic diversion with a duodenal switch (BPD-DS) and Roux-en-Y gastric bypass (RYGB) (National Institutes of Health, 2010). Other procedures have been gradually phased out due to a higher likelihood of adverse events, such as jejunoileal bypass (JIB) (Figure 3.1) (Griffen *et al.*, 1977; Elder and Wolfe, 2007; Singh *et al.*, 2009).

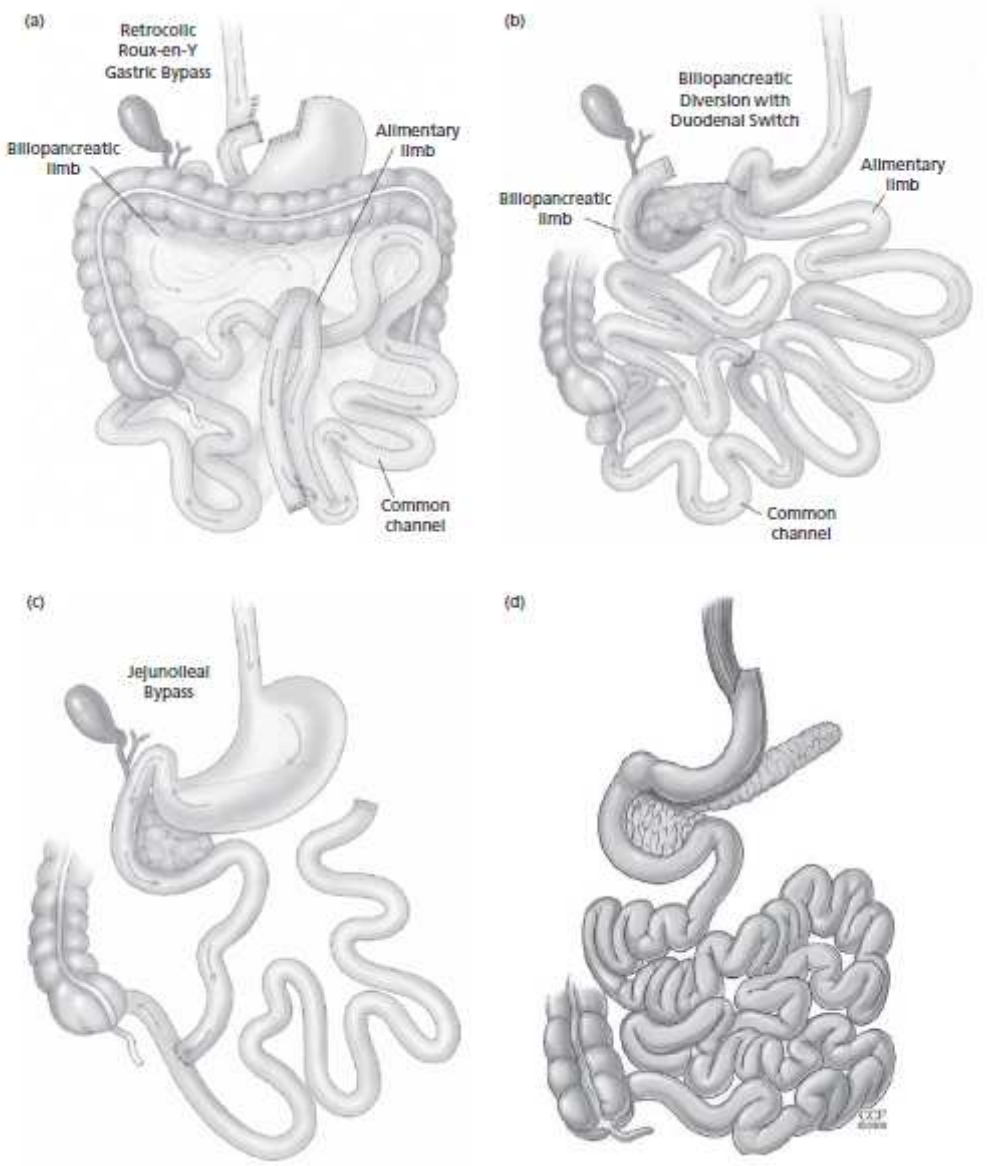

Figure 3.1. Schematic illustrations of a selected bariatric surgical procedures imposing restrictions to the gastrointestinal tract. **A:** Roux-en-Y gastric bypass, **B:** biliopancreatic diversion with duodenal switch, **C:** jejunoileal bypass, obtained from (Elder and Wolfe, 2007), **D:** sleeve gastrectomy, obtained from (Ammori, 2012).

Different types of bariatric surgery will impose a number of physiological changes varying in extent depending on the invasiveness of the procedure. Many of these alterations are known to affect the bioavailability of orally administered drugs, although studies investigating alterations in oral drug exposure pre to post operatively have been limited (Darwich *et al.*, 2012).

Oral bioavailability (F_{oral}) is dependent on the fraction of drug that is absorbed in the intestinal gut wall (f_a), the fraction that escapes gut wall metabolism (F_G), and the fraction that escapes hepatic metabolism (F_H) (Equation 1.1).

$$F_{oral} = f_a \cdot F_G \cdot F_H$$

Equation 1.1: Components of Foral.

f_a and F_G are highly influenced by drug and formulation properties, such as disintegration, dissolution, permeability, solubility, and the susceptibility to being metabolised by certain enzymes (*e.g.* certain cytochrome P450 families [CYP3A] or UDP-Glucuronsyltransferases [UGT]). Gastrointestinal (GI) physiology such as gastric emptying time, pH profiles, small intestinal transit time, abundance and genotype of gut wall drug metabolising enzymes and transporters can also affect f_a and F_G (Rowland and Tozer, 1989; Jamei *et al.*, 2009b).

Gastric emptying time can serve as the rate limiting step for highly permeable and highly soluble drugs as the absorption from the stomach is inevitably low (Higaki *et al.*, 2008). The gastrointestinal pH may affect drug dissolution for drugs displaying a pKa within the range of the GI pH fluctuations (Blum *et al.*, 1991; Avdeef, 2007). Furthermore, small intestinal transit time may influence the drug absorption of poorly soluble or extended release drug formulations as it is the main site of absorption (Koch *et al.*, 1993). Metabolism in the gut acts to regulate the oral bioavailability of drugs and other xenobiotics, an important determinant in the metabolism of substrate drugs (Kolars *et al.*, 1994). Cytochrome P450 (CYP), UDP-Glucuronsyltransferases, sulfotransferases (SULTs) and glutathione S-transferases (GST) drug metabolising enzymes are present in the enterocytes along the GI tract. CYP3A4 is the most abundant drug metabolising enzyme in the GI tract, preceding CYP2C9, CYP2C19, CYP2J2 and CYP2D6 in order of abundance (Peters *et al.*, 1989; Fisher *et al.*, 2001; Paine *et al.*, 2006; Riches *et al.*, 2009). CYP3A4 and CYP3A5 are both present along the whole GI tract, where CYP3A4 is expressed at lower levels in the duodenum, rising in the jejunum and decreasing towards the ileum (Kolars *et al.*, 1994; Paine *et al.*, 1997).

GI transporters may influence the absorption of orally administered drugs and potentially also the extent of metabolism in the gut through active substrate efflux (Benet and Cummins, 2001; Darwich *et al.*, 2010). Numerous transporters are present in the gut, such as the multidrug resistance transporter 1 (MDR1), also referred to as P-glycoprotein (P-gp), multidrug resistance associated protein 2 (MRP2) and breast cancer related protein (BCRP) (Fromm *et al.*, 2000; Maliepaard *et al.*, 2001). P-gp is the most extensively studied of the GI transporters and the relative expression pattern of P-gp in the small intestine increases from the proximal to the distal parts of the small intestine (Mouly and Paine, 2003).

The ADAM (Advanced Dissolution Absorption and Metabolism) model is a mechanistic representation of the GI tract which is implemented in the Simcyp® Simulator (Jamei *et al.*, 2009a). It is a successive development of the Advanced Compartmental Absorption and Transit (ACAT) model (Agoram *et al.*, 2001; Huang *et al.*, 2009), and includes distinct parameters which reflect the physiology better with regards to handling of fluid dynamics (no constant volume in each segment), anatomical mirroring of the GI anatomy and biology for different segments (un-equal segments with relative abundance of enzymes), and dissolution models (avoiding assumptions of a flat surface in Noyes-Whitney). The model defines the amount of drug in 'formulation', 'released but undissolved', 'dissolved' and 'enterocytes' as separate compartment structures and further adds hepato-biliary circulation and bile mediated solubility (Figure 1.4). The model also incorporates fluid dynamics along the GI tract flowing at the rate of gastric emptying and small intestinal transit time and rates of fluid absorption, secretion and reabsorption along the GI tract as opposed to a static volume in each segment (Jamei *et al.*, 2009b).

Furthermore, the ADAM model incorporates the abundance and distribution of GI enzymes and inter-individual variability as well as the distribution of the GI transporter P-gp (Jamei *et al.*, 2009b). The model attributes can be modified to reflect changes following bariatric surgery in a morbidly obese patient population and to investigate the validity of predicting the influence of surgery on oral bioavailability of drugs (Ghobadi *et al.*, 2011).

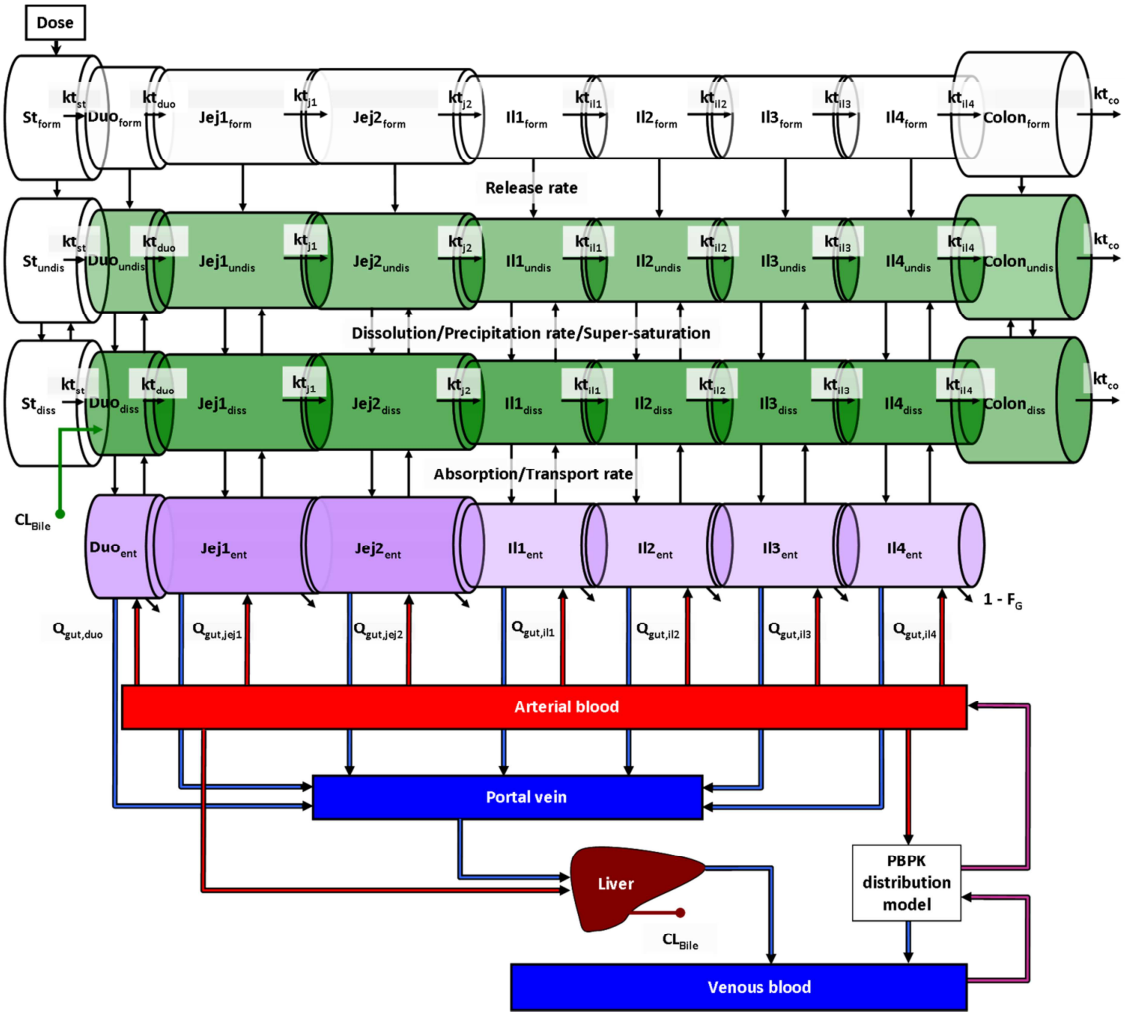

Figure 1.4. Depiction of the 9 segment ADAM model, consisting of following compartments: Stomach, Duodenum, Jejunum I, Jejunum II, Ileum I-IV, and Colon. Further describing: St=stomach, Jej1 & 2=jejunum, Il1-4=ileum, form=drug trapped in formulation, undiss=undissolved drug, diss= dissolved drug, ent=fraction absorbed drug in enterocytes, kt_n=transit rate, Q_n=gastrointestinal blood flow, F_G=fraction drug that escapes gut wall metabolism, CL_{bile}=biliary clearance. Compartment size and purple colour intensity (■) refers to segmental length and regional abundance of CYP3A4 respectively. Green colour scheme (■) indicates bile enhanced solubility. Adapted from Jamei, and co-workers (2009b).

Due to the multi-factorial physiological implications of bariatric surgery, attempts to explain trends in changes to oral bioavailability following bariatric surgery using single

attributes of drugs or simplified categorisations such as the biopharmaceutics classification system (BCS) have been unsuccessful (Darwich *et al.*, 2012).

In the absence of clinical studies showing direction and magnitude of changes in bioavailability of various drugs, evidence-based mechanistic pharmacokinetic *in silico* models which define such alterations would be of value in determining appropriate dosage regimens for an increasing patient population who are undergoing bariatric surgery. The current study, to our knowledge, is the first to develop such a model.

3.3 Methods

3.3.1 Characterisation of post bariatric surgery population

A set of gastrointestinal and 'whole body' physiological parameters were identified based on factors influencing oral drug bioavailability post bariatric surgery, these included: gastric volume and gastric emptying rate, gastrointestinal pH, post surgical small intestinal dimensions, small intestinal motility and transit time and bile properties. Whole body physiological factors known to influence oral drug exposure were also identified, such as: renal function and serum protein levels as a function of post surgical weight loss.

An extensive literature search of identified parameters in relation to bariatric surgery was performed utilising PubMed (1966-2011). The gastrointestinal and physiological parameters were analysed in accordance to appropriate functions. Weighted means (WX) and standard deviations (overall SD) of results were calculated from the reported means (x) and standard deviations (SD), dependent on the number of observations in the i^{th} study (n) (Equation 3.1, Equation 3.2 and Equation 3.3), and where applicable analysed using Welch's t test at a significance level of 0.05 assuming parameter data to be normally distributed and taking unequal variance (s) into account, where X is the sample mean and N is the sample size (Equation 3.4).

$$WX = \frac{\sum_{i=1}^{n} n_i \cdot x_i}{\sum_{i=1}^{n} n_i}$$

Equation 3.1. Calculating weighted mean.

$$OverallSD = \sqrt{\frac{Overall\ sum of\ squares}{N}}$$

Equation 3.2. Overall standard deviation.

$$Overall\ sum\ of\ squares = \sum_{i=1}^{n} \left[\left\{ (SD_i)^2 + (x_i)^2 \right\} \cdot n_i \right] - N \cdot WX^2$$

Equation 3.3. Overall sum of squares.

$$t = \frac{X_1 - X_2}{\sqrt{\frac{s_1^2}{N_1} + \frac{s_2^2}{N_2}}}$$

Equation 3.4. Welch's t test.

3.3.2 Adapting the ADAM model to mimic post bariatric surgery conditions

The Simcyp® Simulator v10 (Simcyp Ltd, Sheffield, UK) population template for Morbidly Obese based on a Northern European Caucasian population was used. Validation of this model with respect to prediction of clearance has recently been published by Ghobadi and co-workers (2011). We re-evaluated and analysed model performance against the identified post bariatric surgery model. Whenever applicable, we altered necessary population parameters to conform to post bariatric surgery conditions, applying reported data of weighted means and coefficient of variation (CV %) (Table 3.1).

Table 3.1. Pre- to post-surgery intrinsic factors.

Gastric emptying of liquids (minutes)
Gastric emptying of solids (minutes)
Post operative gastric volume (mL)
Secretion in stomach (Q_{sec}; L/h)
Initial volume of stomach fluid (mL)
Small intestinal bypass (cm)
Small intestinal bile delay (cm)
Small intestinal bile concentrations at fasted and fed state (nM)
Gastrointestinal pH at fasted and fed state
GI CYP3A4 abundance (nmol/total gut)
GI CYP3A5 abundance (nmol/total gut)
Small intestinal transit time (hours)
Renal function (GFR; mL/min)
Human Serum Albumin levels (HSA; g/L)
α-1 Acid Glycoprotein levels (AGP; g/L)
Hepatic function (enzymatic activity)

GI=Gastrointestinal.

GFR=Glomerular filtration rate.

Post bariatric surgery gastrointestinal physiological parameters based on population/surgical data or physiologically rational assumptions were implemented to the ADAM model, creating 'Post sleeve gastrectomy', 'Post Roux-en-Y gastric bypass', 'Post biliopancreatic diversion with duodenal switch' and 'Post jejunoileal bypass' population templates (so called "population files" within Simcyp).

Post surgical basal steady state gastric fluid volumes at fasted state were estimated through one compartmental simulations of gastric fluid dynamics (Equation 3.5) in Matlab® R2010a (MathWorks, Natick, MA, USA) utilising reported post surgical gastric emptying and assuming a linear relationship with regards to the excretion of gastric juices (0.08 L/h) as a function of gastric capacity, utilising an average gastric volume of 230±13 mL as reported in 134 individuals. Saliva production was kept constant at 0.05 L/h (Valentin, 2002; Delgado-Aros *et al.*, 2004; Jamei *et al.*, 2009b).

$$\frac{dV_{st}}{dt} = Q_{\text{sec},s} - k_{t,st}V_{st}$$

Equation 3.5. Gastric fluid dynamics model.

Population implementations of small intestinal bypass and delay in bile inlet were dimensionally estimated as a function of body surface area utilising Equation 3.6 and Equation 3.7, as implemented in the Simcyp® Simulator ADAM model. Further, the human effective permeability (P_{eff}) was set to close to zero in segments corresponding to the small intestinal bypass in the drug template (Turner, 2008).

$$Length\ of\ duodenum = 0.205 \cdot BSA^{0.550}$$

Equation 3.6. Length of the duodenum.

$$Length\ of\ jejunum\ and\ ileum = 5.231 \cdot BSA^{0.414}$$

Equation 3.7. Length of the distal small intestine.

Post surgical estimations of small intestinal transit time were implemented into the ADAM model utilising the incorporated Weibull distribution fitted to describe a log normal distribution through altering the scale factor (β) of small intestinal transit time keeping the shape factor (α) constant, altering β thus retaining the log normal distribution assumption (Equation 3.8) (Turner, 2008).

$$f(x) = \frac{\alpha}{\beta}\left(\frac{x}{\beta}\right)^{\alpha-1} e^{-(x/\beta)^{\alpha}}$$

Equation 3.8. Weibull distribution of variance in small intestinal transit.

Following the dimensional alterations to the post-operative surgical GI anatomy the bariatric surgical team at Salford Royal Foundation NHS Hospital Trust (Salford, UK) was consulted in order to establish consensus on physiological dimension reflecting a realistic patient population. The parameters subject to a consensus discussion included: Post surgical gastric volume and capacity, small intestinal bypass and delay in bile inlet.

3.3.3 Virtual study of bioavailability 'post bariatric surgery'

An identified set of compounds in the Simcyp® Simulator were simulated utilising 'Post Sleeve Gastrectomy in Morbidly Obese', 'Post Roux-en-Y Gastric Bypass in Morbidly Obese', 'Post Biliopancreatic Diversion with Duodenal Switch in Morbidly Obese' and 'Post Jejunoileal Bypass in Morbidly Obese' population templates in a total of 100 subjects per group, displaying an age range of 20 to 50 years and 0.50 proportion of females, varying the mean small intestinal transit time to account for any ambiguity in reported data following surgery.

The selected drugs (simvastatin, omeprazole, diclofenac, fluconazole and ciprofloxacin) had a wide range of physicochemical and metabolic attributes and were commonly used in patients undergoing bariatric surgery (Darwich *et al.*, 2012). Oral drug exposure was simulated for a low, medium and high therapeutic dose in accordance with the British National Formulary (BNF), which included: Simvastatin immediate release (IR; 10, 20 and 80 mg), diclofenac enteric-coated (EC; 25, 50 and 75 mg), omeprazole EC (10, 20 and 40 mg), fluconazole IR (50, 200, 400 mg) and ciprofloxacin IR (250, 500 and 750 mg). Drugs simulated in post bariatric surgery population templates were compared to simulations carried out in the Morbidly Obese population template, examining trends in oral drug bioavailability, f_a and F_G (Equation 1.1), and related surrogate biomarkers: $AUC_{0\text{-}24h}$, C_{max} and t_{max} where simulated data were analysed in MATLAB® R2010a.

3.4 Results

3.4.1 Characterisation and validation of virtual populations

Roux-en-Y gastric bypass (RYGB)

Post RYGB stomach volume:

A reduced gastric volume was implemented in the 'Morbidly Obese' population template through limiting concomitant fluid intake from the default value of 250 mL to 30 mL based on surgical restriction in accordance to Wittgrove and Clark (2000). The initial volume of stomach fluid at fasted state was estimated to be 9.9 mL (CV: 30%) utilising simulations at steady state as per Equation 3.5.

Gastric acid secretion and pH:

Two studies were identified measuring gastric acid production in a total of 18 post RYGB patients, with an approximate gastric volume of 10 mL, as compared to pre surgery or controls (Smith *et al.*, 1993; Behrns *et al.*, 1994). Combining weighted means and variance displayed a mean basal gastric acid excretion of 0.08 (±0.008) mEq/h, and a weighted mean peak acid excretion of 0.048 (±0.048) mEq/30 minutes post surgery, as compared to a basal and peak acid excretion of 9.1±3.6 mEq/h (P<0.05) and 12.8±1.8 mEq/30 minutes (P<0.05) respectively in pre surgery patients (n=8) and a basal and peak acid secretion of 5.0±0.7 (P<0.05) and 12.1±1.3 (P<0.05) respectively in healthy volunteers (n=15) (Figure 3.2) (Smith *et al.*, 1993; Behrns *et al.*, 1994). Implementation into the Simcyp® Simulator Morbidly Obese population template was based on assuming a gastric pH of 6.4 at fasted state.

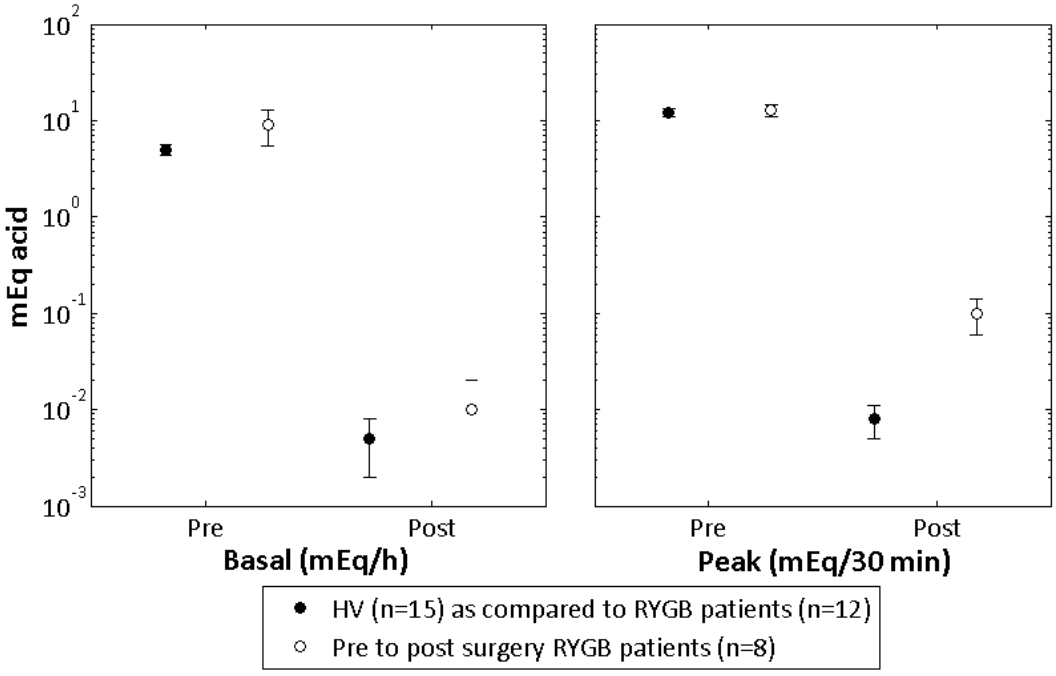

Figure 3.2. Mean acid secretion and standard deviation, mEq HCl, over time at basal and peak level. Acid secretion in 12 post Roux-en-Y Gastric Bypass (RYGB) patients as compared to 15 healthy volunteers not subject to surgery (HV) (Smith *et al.*, 1993). Acid secretion in 8 RYGB patients, pre and post surgery (Behrns *et al.*, 1994).

Gastric emptying time:

Following RYGB surgery a significant reduction in t½ gastric emptying time has been observed for liquids, whereas available data on gastric emptying of solids display a considerably increased variability (Figure 3.3 and Figure 3.4). Four studies measuring gastric emptying time following gastrectomy surgery were identified (RYGB, SG, Billroth gastrectomy with Roux-en-Y gastrectomy and partial gastrectomy) . Combining weighted means and variance in a total of 68 post surgery patients resulted in a mean t½ gastric emptying of 8.48 (±9.12) minutes, as compared to 24.33 (±23.71) minutes in controls (n=39; P<0.05) (Figure 3.3).(Horowitz *et al.*, 1982; Hinder *et al.*, 1988; Rieu *et al.*, 1989; Braghetto *et al.*, 2009)

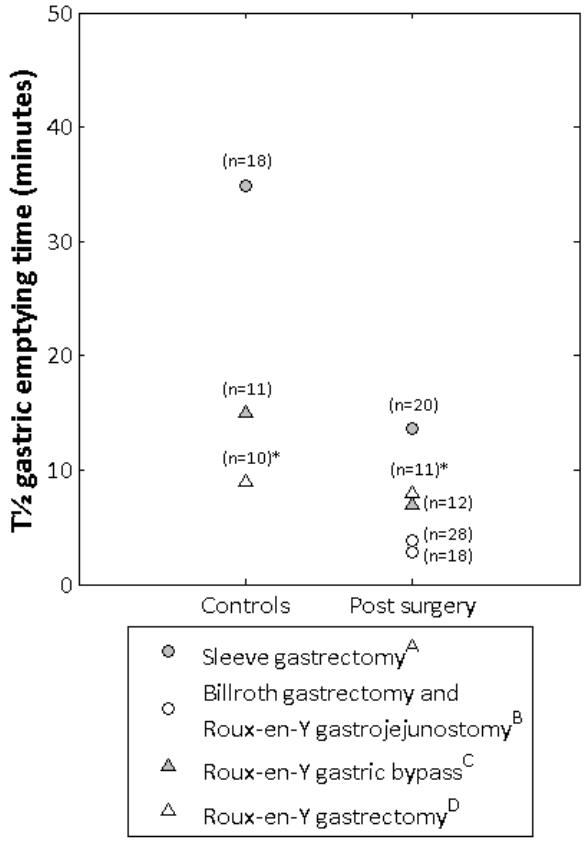

Figure 3.3. Reported mean (*****median) t½ gastric emptying time of liquids in post gastric surgery patients subject to various surgeries resulting in a reduced gastric volume as compared to controls (pre surgery or healthy volunteers not subject to surgery). A: Sleeve gastrectomy, B: Billroth gastrectomy and Roux-en-Y gastrojejunostomy, C: Roux-en-Y gastric bypass and D: Roux-en-Y gastrectomy (Horowitz *et al.*, 1982; Hinder *et al.*, 1988; Rieu *et al.*, 1989; Braghetto *et al.*, 2009).

Identified publications examining gastric emptying time of solids post gastric surgery resulting in a reduced gastric volume (RYGB, SG and Billroth gastrectomy with Roux-en-Y gastrectomy) displayed an observable increase in variability following surgery as compared to controls: reported observations ranging from 4 minutes to over 200 minutes post surgery (Figure 3.4) (Shah *et al.,* 2010; Horowitz *et al.,* 1982; Hinder *et al.,* 1988; Rieu *et al.,* 1989; Petrakis *et al.,* 1998; Bernstine *et al.,* 2009; Braghetto *et al.,* 2009).

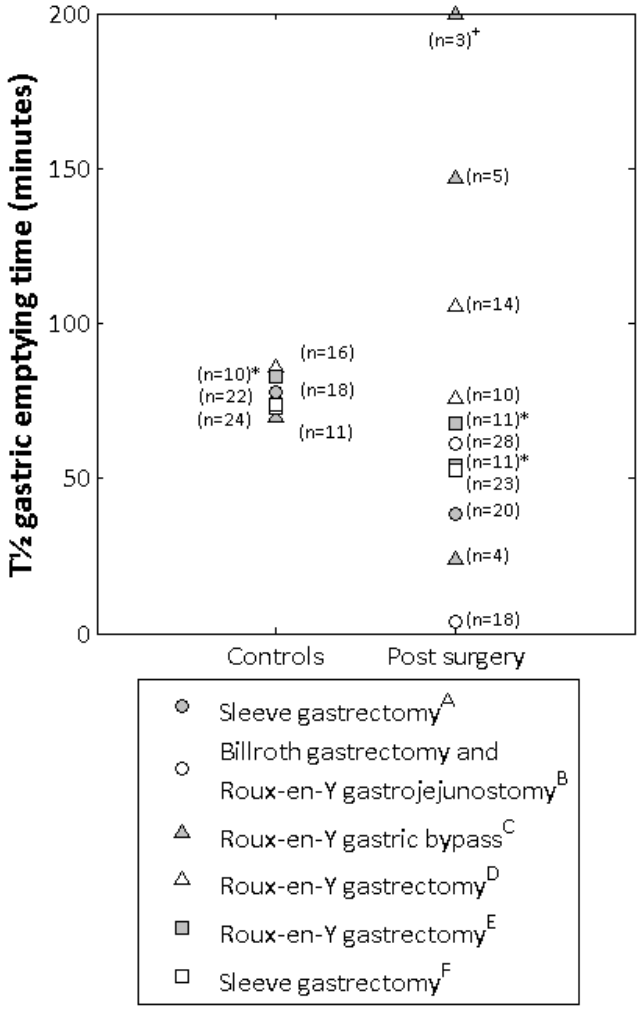

Figure 3.4. Reported mean (*median) t½ gastric emptying time of solids in post gastric surgery patients subject to various gastrointestinal surgeries, as described in publication, resulting in a reduced gastric volume as compared to controls. A: Sleeve gastrectomy, B: Billroth gastrectomy and Roux-en-Y gastrectomy, C: Roux-en-Y gastric bypass, D: Roux-en-Y gastrectomy, E: Roux-en-Y gastrectomy, F: sleeve gastrectomy (Shah *et al.,* 2010; Horowitz *et al.,* 1982; Hinder *et al.,* 1988; Rieu *et al.,* 1989; Petrakis *et al.,* 1998; Bernstine *et al.,* 2009; Braghetto *et al.,* 2009).

Following RYGB, the gastric emptying half-life of liquids was measured to be 7 (±3) minutes after liquid intake in 12 post gastric bypass patients 12 months post surgery with a newly formed stomach pouch of size of 60-80 mL and a gastrojejunal anastomosis of 12-20 mm in diameter, as compared to 11 healthy volunteers displaying a gastric emptying half-life of 15 (±2) minutes (Figure 3.3) (Horowitz *et al.*, 1982).

Gastric emptying half-life of a solid meal was highly variable in the post RYGB patient population, where 4 patients displayed a t½ of 24 (±10) minutes, exhibiting an initial rapid gastric emptying followed by a linear emptying, whereas five patients displayed an initial lag time followed by linear emptying. Three patients displayed a prolonged lag time followed by slow gastric emptying, with a reported gastric emptying half time of over 200 minutes. The control group displayed a t½ of 70 (±7) minutes (Figure 3.4). Alteration to the gastric emptying was implemented based on post surgical gastric emptying time for liquids of 7 (CV: 45%) minutes in a fasted state (Horowitz *et al.*, 1982).

Small intestinal bypass and regional abundances of CYP3A:
Approximately 75-100 cm's of the proximal small intestine is bypassed following RYGB surgery, bypassing the duodenum and proximal jejunum (Wittgrove and Clark, 2000; DeMaria *et al.*, 2002; Schneider and Mun, 2005; Elder and Wolfe, 2007; Skottheim *et al.*, 2009; Spak *et al.*, 2010). In accordance with the small intestinal bypass, the duodenum and proximal jejunum were bypassed through setting transit time close to zero in the duodenum and reducing small intestinal transit time in jejunum I by 38%, thus creating an approximate bypass of 87.5 cm in the ADAM model based on BSA (Equation 3.6 and Equation 3.7).

Small intestinal motility and transit time:
Studies in humans examining small intestinal transit and motility in patients subject to total gastrectomy were reviewed, as compared to a partial gastrectomy in the treatment of obesity (Pellegrini *et al.*, 1986; Haglund *et al.*, 1989; Le Blanc-Louvry *et al.*, 1999; Wittgrove and Clark, 2000).

The data suggested changes in small intestinal motility after a Roux-en-Y reconstruction (van der Mijle *et al.*, 1993; Le Blanc-Louvry *et al.*, 2000). In ten patients subject to Roux-en-Y with a total gastrectomy (cancer being the main indication), a mean small intestinal transit for solids of 293 (±37) minutes was observed as compared to 187 (±37) minutes in five controls ($P<0.02$), thus suggesting the small intestinal transit to be increased post Roux-en-Y gastric bypass (Pellegrini *et al.*, 1986). Animal models of Roux-en-Y gastric bypass surgery suggested a similar impact of surgery as that observed in man, with disturbed small intestinal motility reported in rat and dog (Woodward *et al.*, 1993; Le Blanc-Louvry *et al.*, 1999; Suzuki *et al.*, 2005).

Two scenarios were created with regards to small intestinal transit time. In the first scenario the transit time was assumed to be 5.0 hours based on a reduced motility as reported by Pellegrini and co-workers (1986); whereas, in the second scenario the small intestinal motility was assumed to remain unaltered thus reducing small intestinal transit to 3.0 hours as a function of the small intestinal bypass (Pellegrini *et al.*, 1986).

Regional abundances of CYP3A metabolising enzymes were set to close to zero in the bypassed segments of the small intestine. Mean total enzyme abundances of CYP3A4 and CYP3A5 were recalculated to account for the small intestinal bypass of the duodenum, resulting in a reduction from 66.2 to 50.2 nmol/total gut and from 24.6 to 18.7 nmol/total gut respectively (Turner, 2008).

Bile and pancreatic fluids

Following RYGB surgery, the inlet of bile and pancreatic fluids is delayed to the common channel approximately 75-150 cm distally of the newly formed stomach pouch (Wittgrove and Clark, 2000; DeMaria *et al.*, 2002; Spak *et al.*, 2010). A delayed bile inlet was implemented into the ADAM model through setting bile concentrations in the fasted and fed state to zero in the gastrointestinal regions of the stomach, duodenum and jejunum corresponding to approximately 90 cm.

Biliopancreatic diversion with duodenal switch (BPD-DS)

Stomach volume

In accordance to the surgical procedure the gastric volume following biliopancreatic diversion with duodenal switch was effectively restricted to 150 mL, through limiting concomitant fluid intake with oral administration to 150 mL. Due to lack of data gastric emptying and gastric pH was assumed to remain unaltered (Smith *et al.*, 1993; Behrns *et al.*, 1994; Wittgrove and Clark, 2000; DeMaria *et al.*, 2002; Schneider and Mun, 2005; Elder and Wolfe, 2007; Spak *et al.*, 2010).

Small intestinal bypass and regional abundances of CYP3A:

Segments Jej1 and 2 were bypassed corresponding to approximately 294 cm (Wittgrove and Clark, 2000); recalculating gastrointestinal abundances of CYP3A4 and CYP3A5 accordingly to 30.0 and 11.2 nmol/total gut respectively (Turner, 2008).

Small intestinal motility and transit time:

In the first scenario the transit time was assumed to be 3.7 hours in accordance to the reduced motility observed post total gastrectomy with Roux-en-Y jejunostomy corrected for the small intestinal length following BPD-DS (Pellegrini *et al.*, 1986); whereas, in the second scenario the small intestinal motility was assumed to be 2.2 hours thus reducing as a function of the small intestinal bypass.

Bile and pancreatic fluids

In accordance with the surgical procedure the bile inlet was delayed to ileum III corresponding to 252 cm (Wittgrove and Clark, 2000; Schneider and Mun, 2005; Elder and Wolfe, 2007).

Sleeve gastrectomy (SG)

Stomach volume:

Sleeve gastrectomy surgery is limited to the restriction of the dimension of the gastric pouch (to approximately 60-80 mL), preserving the pyloric sphincter (Baltasar *et al.*, 2005; Lee *et al.*, 2007). Albeit not being as invasive as malabsorptive procedures, the reduction in gastric volume has been reported to affect the gastric emptying time of liquids and solids (Figure 3.2 and Figure 3.3) (Braghetto *et al.*, 2009; Shah *et al.*, 2010). This was implemented through setting concomitant fluid intake to 80 mL and initial

volume of stomach fluid to 24.2 mL (CV: 30%) in the fasted state in accordance with simulated steady state gastric volumes.

Gastric emptying time

One study was identified examining gastric emptying of liquids following sleeve gastrectomy, observing a significantly reduced t½ gastric emptying time of 13.6 (±11.9) minutes in 20 post surgery patients as compared to 34.9 (±24.6) minutes in 18 controls (Figure 3.3) (Braghetto *et al.,* 2009). Thus, gastric emptying was set to 13.6 (CV: 53%) in the post sleeve gastrectomy population template.

Results from combining weighted means and variance of identified studies examining gastric emptying of solids resulted in a significant reduction post operatively ($P<0.05$), with an observed mean gastric emptying time of 46.1 (±17.7) minutes in 43 post surgery patients as compared to 74.6 (±26.2) minutes in 64 controls (Figure 3.4) (Braghetto *et al.,* 2009; Shah *et al.,* 2010)

Gastric acid secretion and pH:

There is a lack of published data on the impact of sleeve gastrectomy on gastric acid secretion or gastric pH measurements pre to post surgery. Given this, gastric pH was assumed to remain unaltered following sleeve gastrectomy.

Jejunoileal bypass (JIB)

Small intestinal bypass and regional abundance of CYP3A:

In accordance with the surgical procedure a small intestinal bypass was created retaining the duodenum segment, 20% of the proximal jejunum I and 23% of the terminal ileum IV approximately, bypassing the remainder of the small intestine (Scott *et al.,* 1971; Scott *et al.,* 1973; Griffen *et al.,* 1977). Accordingly the abundances of CYP3A4 and CYP3A5 were set to zero in jejunum II to Ileum III and recalculated to 32.3 and 12.1 nmol per total gut respectively.

Small intestinal motility and transit time:

In the first scenario the transit time was assumed to be 0.7 hours in accordance to the reduced motility observed post total gastrectomy with Roux-en-Y jejunostomy corrected for the small intestinal length post JIB; whereas, in the second scenario the

small intestinal motility was assumed to be 0.4 hours thus reducing as a function of the small intestinal bypass (Pellegrini *et al.*, 1986).

Bariatric surgery – Whole body physiological parameters

Renal function:

Comparing observed data on renal function, in terms of Glomerular Filtration Rate (GFR), in relation to BMI following bariatric surgery induced weight loss, estimates made utilising Cockcroft-Gault and Modification of Diet in renal Disease (MDRD; Equation 3.9) equations, concluded a better prediction by MDRD equation (Chagnac *et al.*, 2003; Navarro-Diaz *et al.*, 2006; Serra *et al.*, 2006; Saliba *et al.*, 2010). The Cockcroft-Gault equation estimates the creatinine clearance the MDRD equation estimates the GFR corrected for body surface area (Michels *et al.*, 2010). Simulating age and sex matched populations over a range of BMI, utilising the Simcyp® Simulator incorporating inter-individual variability, observed data was within 95% confidence interval of simulated estimations utilising the MDRD equation, whereas, Cockcroft Gault over predicted GFR at a higher BMI in agreement with previous publications examining predicted versus observed GFR in Morbidly Obese and Obese populations (Figure 3.5) (Michels *et al.*, 2010; Ghobadi *et al.*, 2011). Based on these findings the MDRD equation was utilised to estimate GFR in the Simcyp® Simulator.

$$GFR(mL/min/1.73m^2) = 186 \cdot Serumcreatinine^{-1.154} \cdot age^{-0.203} \cdot (0.742\ for\ females)$$

Equation 3.9. Modification of Diet in renal disease (MDRD) equation for estimating glomerular filtration rate (GFR).

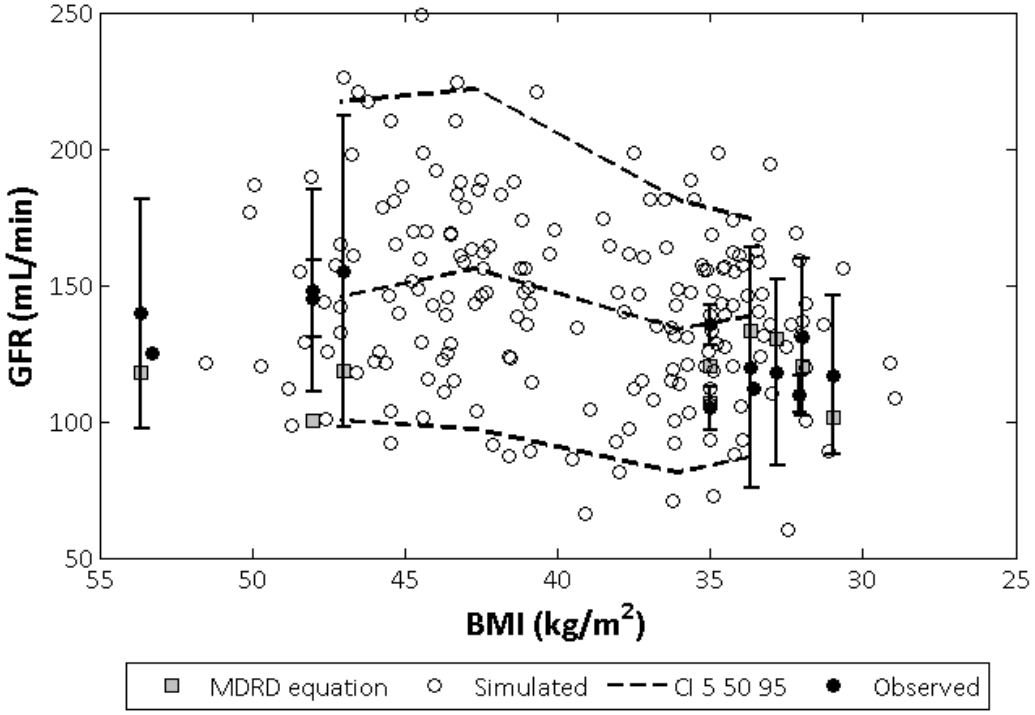

Figure 3.5. Observed Glomerular Filtration Rate (GFR) following bariatric surgery induced weight loss, as compared to calculated GFR utilising the Modification of Diet in Renal Disease (MDRD) equation and simulated age and gender matched GFR with 5, 50 and 95% confidence intervals (CI) utilising the Simcyp® Simulator (MDRD) with inter-individual variability (Chagnac *et al.*, 2003; Navarro-Diaz *et al.*, 2006; Serra *et al.*, 2006; Saliba *et al.*, 2010).

Serum protein levels:

Prior to and following bariatric surgery induced weight loss, Human Serum Albumin (HSA) levels remained consistent with the normal reported range (at a total of 322 data points; n=163) evaluated utilising sex and age matched simulations in the Simcyp® Simulator, predicting HSA within the 95% confidence interval (Figure 3.6) (Benedek *et al.*, 1984; Mattar *et al.*, 2005; Stratopoulos *et al.*, 2005; Barker *et al.*, 2006). Levels of α-1 Acid Glycoprotein (AGP) was significantly reduced following bariatric surgery induced weight loss (at a total of 170 data points; n=50), regressing towards ranges observed in normal weight controls, where simulations in Simcyp® Simulator overestimated the levels of AGP at lower BMI ranges (Figure 3.7) (Benedek *et al.*, 1984; van Dielen *et al.*, 2004).

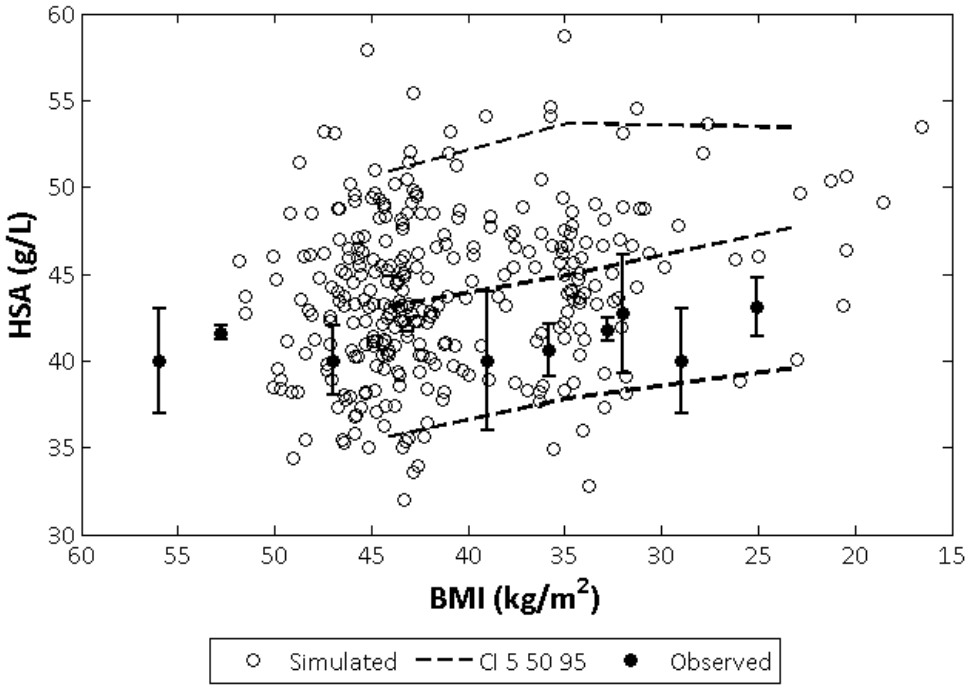

Figure 3.6. Observed mean and standard deviation of serum concentrations of Human Serum Albumin (HSA) in morbidly obese patients subject to bariatric surgery induced weight loss as compared to simulated HSA levels with 5, 50 and 95% confidence intervals (CI) based on Simcyp® demographics characteristics (Benedek *et al.*, 1984; Mattar *et al.*, 2005; Stratopoulos *et al.*, 2005; Barker *et al.*, 2006).

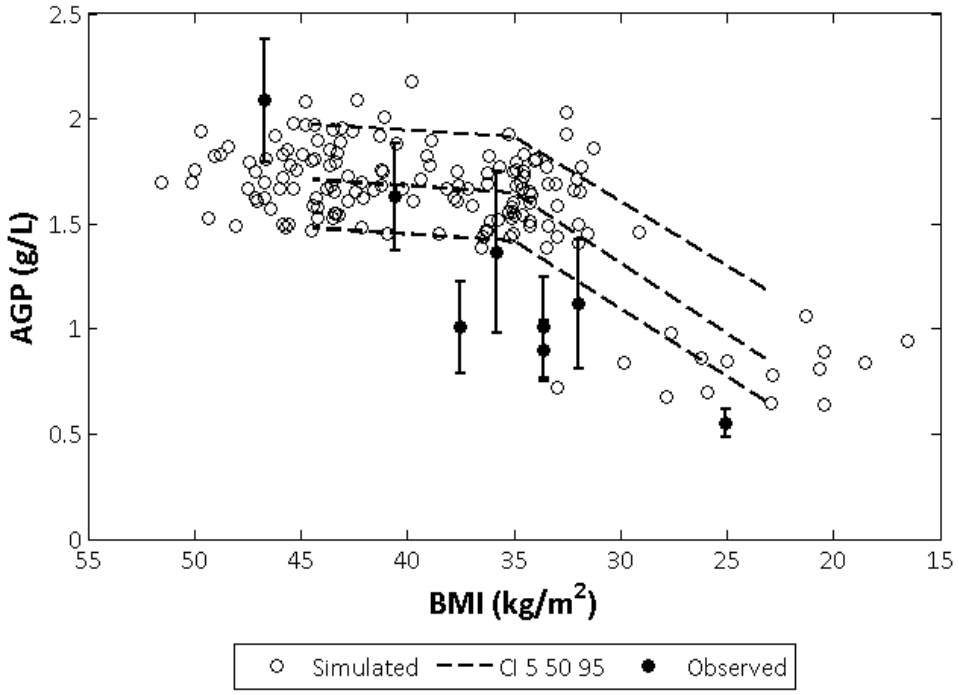

Figure 3.7. Observed mean and standard deviation of serum concentrations of α-1 Acid Glycoprotein (AGP) in morbidly obese patients subject to bariatric surgery induced weight loss as compared to simulated AGP levels with 5, 50 and 95% confidence intervals (CI) based on Simcyp® Simulator demographics characteristics (Benedek *et al.*, 1984; Mattar *et al.*, 2005; Stratopoulos *et al.*, 2005; Barker *et al.*, 2006).

Hepatic function:

The reduction in liver volume following bariatric surgery induced weight loss was assumed to be a function of the reduction in Body Surface Area (BSA) as observed in a general population, where the equation incorporated into the Simcyp® Simulator corrects for the observed under prediction in liver volume at a BMI≥40 kg/m^2 utilising a correction factor of 1.25 (Johnson *et al.*, 2005; Ghobadi *et al.*, 2011). Tissue blood perfusions were obtained as a function of cardiac output estimated from BSA as incorporated into the Simcyp® Simulator (Howgate *et al.*, 2006).

Table 3.2. Summary of physiological parameters alterations following bariatric surgery for input into Simcyp® Simulator.

Physiological parameters	RYGB	BPD-DS	JIB	SG	References
Population alterations					
Stomach					
Gastric emptying time (h)	7.0 (CV 45%)	Unaltered	Unaltered	13.6 (CV 53%)	(Horowitz *et al.*, 1982; Braghetto *et al.*, 2009)
Initial fluid volume (mL)	9.9 (CV 30%)	Unaltered	Unaltered	24.2 (CV 30%)	
Gastric pH	6.4 (CV 38%)	1.5 (CV 38%)	1.5 (CV 38%)	1.5 (CV 38%)	(Smith *et al.*, 1993; Behrns *et al.*, 1994)
Small intestine					
Bypass (segments)	Duo, jej I†	Jej I, jej II	Jej II-Il III	Unaltered	(Scott *et al.*, 1971; Scott *et al.*, 1973; Wittgrove and Clark, 2000; DeMaria *et al.*, 2002; Chagnac *et al.*, 2003; Baltasar *et al.*, 2005; Schneider and Mun, 2005; Navarro-Diaz *et al.*, 2006; Serra *et al.*, 2006; Elder and Wolfe, 2007; Lee *et al.*, 2007; Skottheim *et al.*, 2009; Saliba *et al.*, 2010; Spak *et al.*, 2010)
Bile delay (segments)	Duo-jej I†	Duo-il II	Unaltered	Unaltered	
SIT: Scenario 1 (h)	3.0	2.2	0.4	3.3	
Weibull β*	3.6	2.6	0.5	4.0	
SIT: Scenario 2	5.0	3.7	0.7	-	
Weibull β*	6.0	4.4	0.8	-	
GI metabolism					
CYP3A bypass (segments)	Duo, jej I†	Jej I, jej II	Jej II-Il III	Unaltered	
CYP3A4 abundance	50.2 (CV 60%)	30.0 (CV 60%)	32.3 (CV 60%)	66.2 (CV 60%)	
CYP3A5 abundance	18.7 (CV 60%)	11.2 (CV 60%)	12.1 (CV 60%)	24.2 (CV 60%)	
Whole-body physiology					
GFR prediction	MDRD	MDRD	MDRD	MDRD	
Study design alterations					
Fluid intake with dose	30 (CV 60%)	150 (CV 60%)	250 (CV 60%	80 (CV 60%)	

RYGB=Roux-en-Y gastric bypass, BPD-DS=biliopancreatic diversion with duodenal switch, JIB=jejunoileal bypass, SG=sleeve gastrectomy, SIT=small intestinal transit, GI=gastrointestinal, duo=duodenum, jej=jejunum, IL=ileum, GFR=glomerular filtration rate, MDRD=modification of diet in renal disease. *Weibull function (α=2.92; Equation 3.8). †Partial small intestinal bypass.

3.4.2 Virtual studies

Roux-en-Y gastric bypass:

Simulated simvastatin IR 10 mg oral drug exposure post RYGB (SIT=3.0h) displayed an unaltered oral bioavailability with a mean post/pre surgery AUC ratio of 1.14±0.18 due to a mean increase in F_G from 0.24 (±0.10) to 0.27 (±0.11) counteracted by a reduction in f_a from 0.90 (±0.11) to 0.87 (±0.12) (Figure 3.8). At a high therapeutic dose (80 mg) the mean post/pre surgery ratio became less apparent (1.07±0.19) due to a more apparent reduction in f_a from 0.88±0.12 to 0.82±0.14 (Figure 3.9). Assuming a reduction in small intestinal motility post RYGB (SIT=5.0h) simvastatin displayed a mean ratio of 1.22 (±0.19) to 1.17 (±0.20) over the therapeutic dose range due to reduced post operative impact on f_a. This was apparent over the whole range of studied drugs, where the increased small intestinal transit time influenced f_a positively (data not shown).

Oral drug exposure of omeprazole remained unaltered following RYGB (SIT=3.0h), although displaying a reduction in t_{max} from approximately 1.24 (±0.41) to 0.97 (±0.23) hours over the therapeutic dose range. Diclofenac post/pre surgery AUC ratio displayed a minor reduction following RYGB (SIT=3.0h). This became more apparent at a high therapeutic dose, displaying an AUC ratio of 0.99 (±0.14), due to a reduction in f_a 0.88 (±0.13) to 0.84 (±0.13), counteracted by a minor increase in F_G from 0.95 (±0.04) to 0.96 (±0.03); whereas t_{max} displayed a reduction from 1.44 (±0.54) to 1.28 (±0.51) hours. Ciprofloxacin displayed a minor reduction in AUC post RYGB (SIT=3.0h), displaying a ratio of 0.96 (±0.02) over the therapeutic dose range due to a reduction in f_a from 0.77 (±0.15) to 0.74 (±0.15). Fluconazole remained unaltered over the dose range.

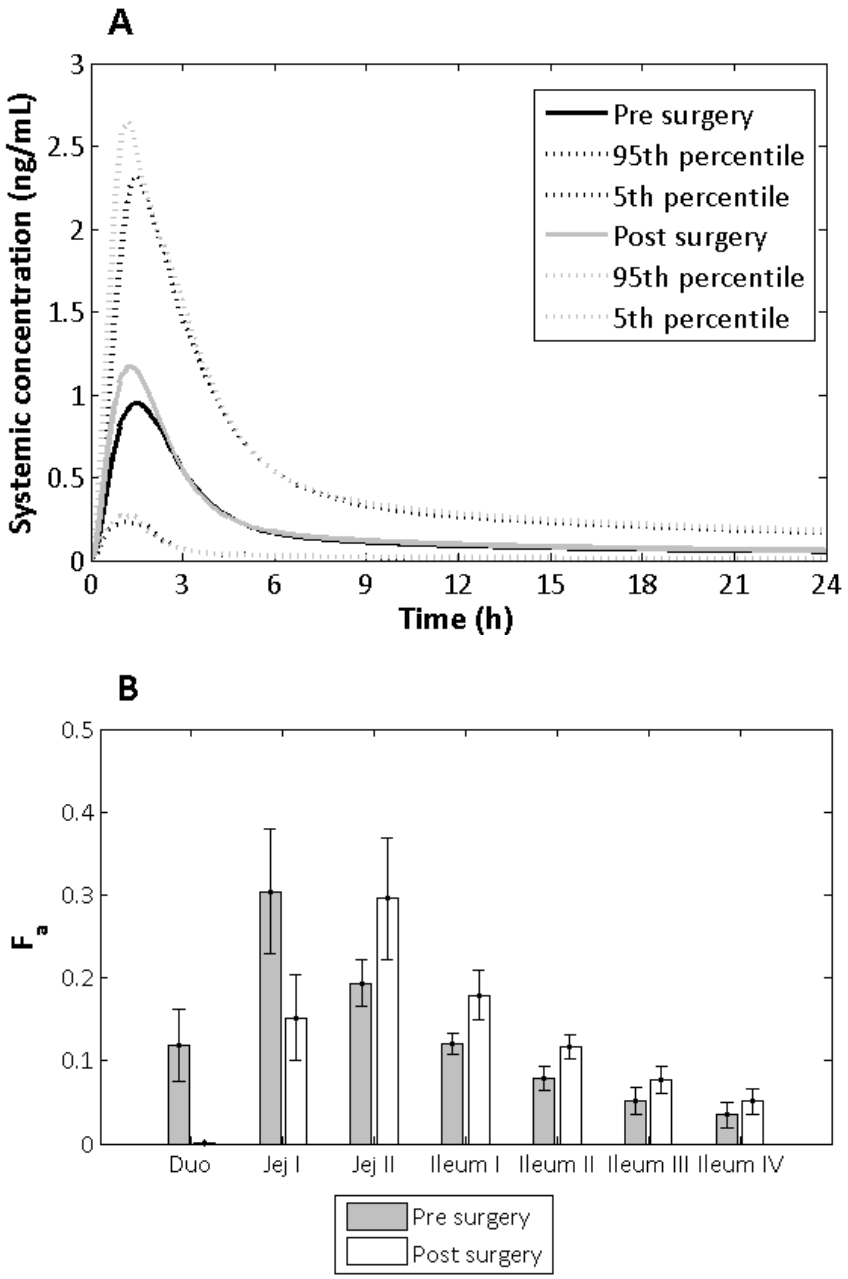
A
Systemic concentration (ng/mL)
Time (h)
Pre surgery
95th percentile
5th percentile
Post surgery
95th percentile
5th percentile
B
F a
Duo
Jej I
Jej II
Ileum I
Ileum II
Ileum III
Ileum IV
Pre surgery
Post surgery

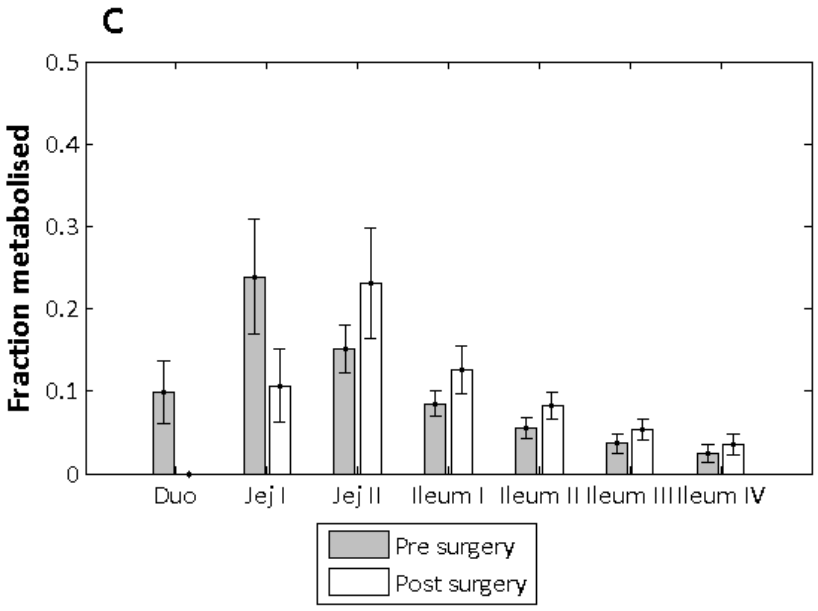

Figure 3.8. Simulated simvastatin immediate release (IR) 10 mg (low therapeutic dose) in morbidly obese (n=100) and post Roux-en-Y gastric bypass surgery (n=100; small intestinal transit=3.0h) **A:** Mean, 95th and 5th percentile plasma concentration time profile over 24 hours, **B:** Mean and standard deviation of segmental fraction of dose absorbed along the small intestine (f_a), **C:** Mean and standard deviation of segmental fraction of dose metabolised in the gut wall ($1-F_G$). Duo=duodenum, Jej=jejunum.

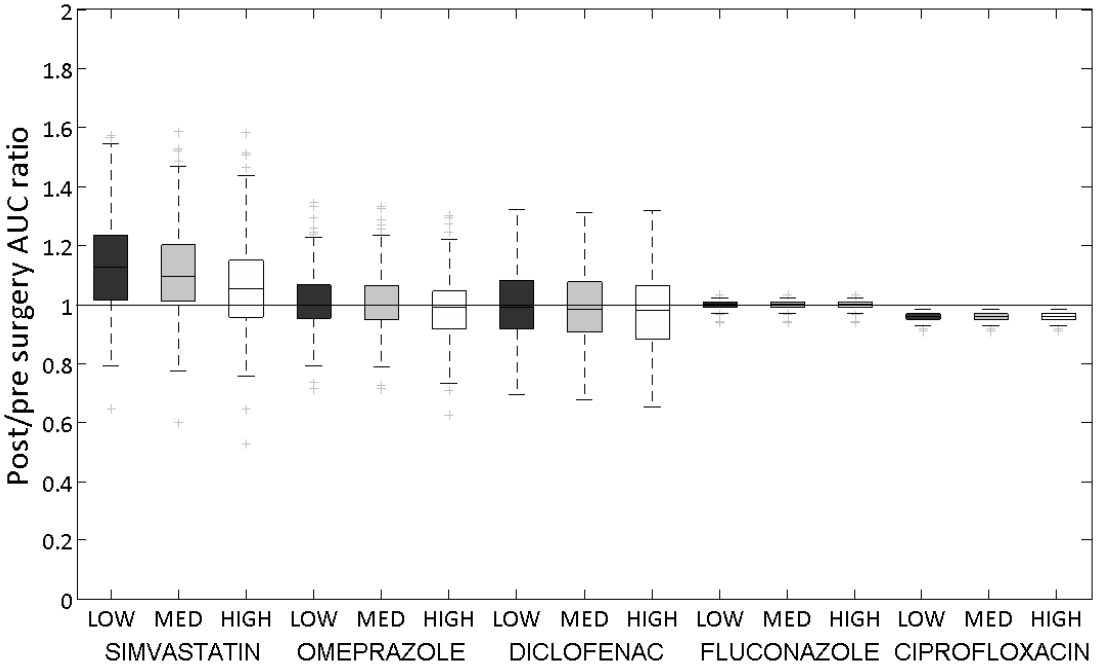

Figure 3.9. Simulated post/pre Roux-en-Y gastric bypass surgery (small intestinal transit=3.0h) AUC ratio over a range of selected drugs at a low (LOW), medium (MED) and high (HIGH) therapeutic dose: Simvastatin immediate release (IR; 10, 20 and 80 mg), omeprazole enteric coated (EC; 10, 20 and 40 mg), diclofenac EC (25, 50 75 mg), fluconazole IR (50, 200, 400 mg) and ciprofloxacin IR (250, 500 and 750 mg).

Biliopancreatic diversion with duodenal switch:

Following BPD-DS (SIT=2.2 h), simvastatin displayed a reduction in AUC, with an observed post/pre surgical AUC ratio ranging from 0.89 (±0.15) to 0.65 (±0.22) as a result of a more extensive reduction in f_a as compared to following RYGB; whereas assuming a higher SIT of 3.7 h simvastatin displayed an increase in AUC, displaying a ratio of 1.05 (±0.08) at a low therapeutic dose level ranging to a reduction, with a simulated ratio of 0.83 (±0.22) at the highest therapeutic dose. This was observed for the whole range of simulated drugs.

Omeprazole displayed a post/pre BPD-DS AUC ratio of 0.88 (±0.10) at a low therapeutic dose due to a reduction in f_a from 0.94 (±0.09) to 0.83 (±0.14) (Figure 3.10), whereas a minor increase in F_G was observed from 0.96 (±0.02) to 0.97 (±0.02). T_{max} displayed an increase from 1.22 (±0.38) to 1.50 (±0.54) hours, whereas C_{max} displayed a reduction by approximately 19%. At a high therapeutic dose, omeprazole displayed a

post/pre surgery AUC ratio of 0.77 (±0.15), due to a more extensive reduction in f_a; whereas t_{max} was increased from 1.42 (±0.50) to 2.26 (±0.63) hours. The reduction became less apparent assuming a small intestinal transit time of 3.7 h.

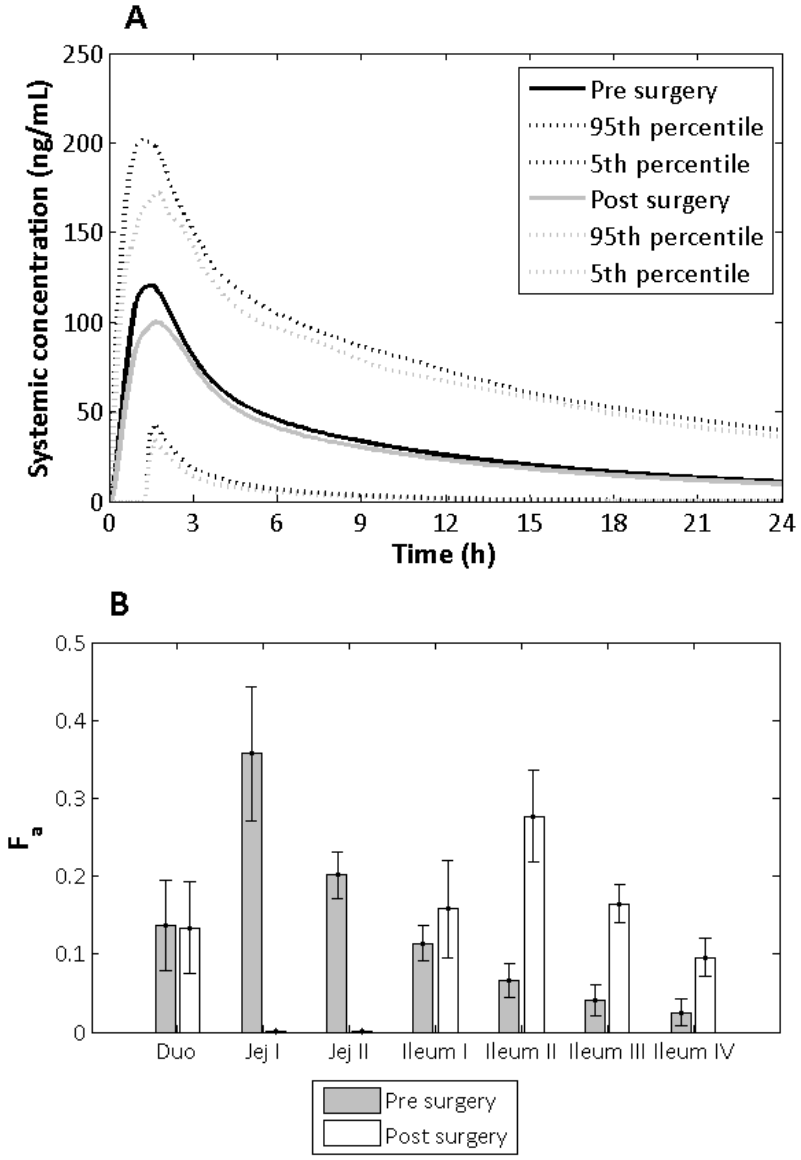

Figure 3.10. Simulated omeprazole enteric coated (EC) 10 mg (low therapeutic dose) in morbidly obese (n=100) and post biliopancreatic diversion with duodenal switch (n=100; small intestinal transit=2.2h) **A:** Mean, 95th and 5th percentile plasma concentration time profile over 24 hours, **B:** Mean and standard deviation of segmental fraction of dose absorbed along the small intestine (f_a). Duo=duodenum, Jej=jejunum.

Diclofenac displayed an AUC ratio of 0.87 (±0.09) following BPD-DS (SIT=2.2 h) at a low therapeutic dose due to a reduction in f_a from 0.89 (±0.12) to 0.75 (±0.15), whereas F_G displayed an increase from 0.91 (±0.06) to 0.94 (±0.04). At a high therapeutic dose diclofenac displayed a more apparent reduction due to a higher post surgical impact on f_a. Again the reduction was less apparent assuming a small intestinal transit time of 3.7 h (Figure 3.11).

Fluconazole displayed an AUC ratio of approximately 0.95 (±0.05) over the dose range. Ciprofloxacin displayed an AUC ratio of 0.80 (±0.06) following BPD-DS (SIT=2.2 h) at a low therapeutic dose, reflected by a reduction in f_a. Following BPD-DS (SIT=3.7 h), Ciprofloxacin displayed no significant alteration, with an AUC ratio of 1.01 (±0.01) at a low therapeutic dose ranging to 0.98(±0.01) at a high therapeutic dose (Figure 3.11).

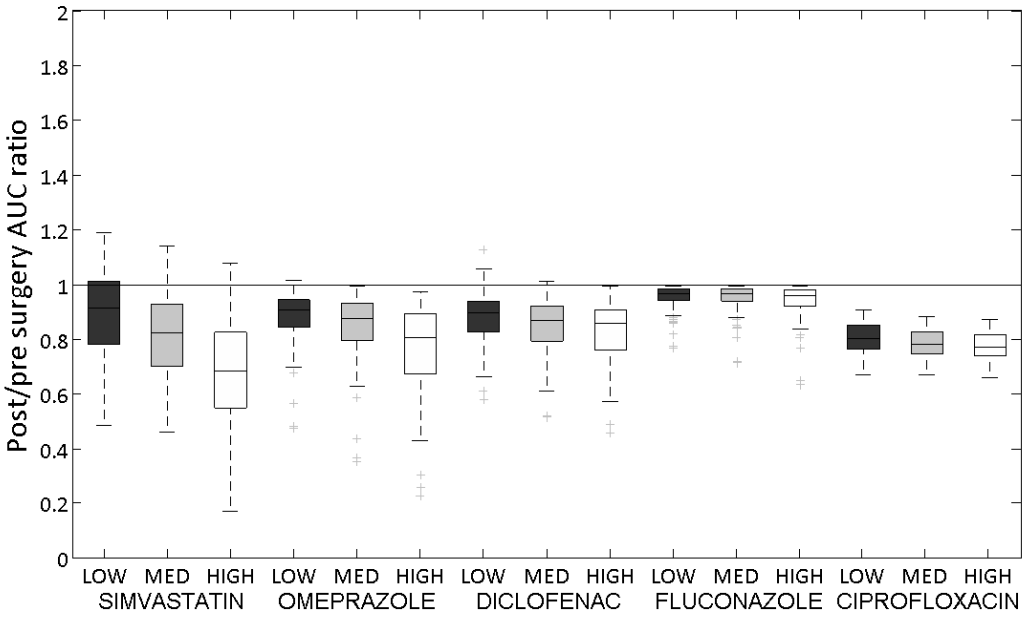

Figure 3.11. Simulated post/pre biliopancreatic diversion with duodenal switch (small intestinal transit=2.2h) AUC ratio over a range of selected drugs at a low (LOW), medium (MED) and high (HIGH) therapeutic dose: Simvastatin immediate release (IR; 10, 20 and 80 mg), omeprazole enteric coated (EC; 10, 20 and 40 mg), diclofenac EC (25, 50 75 mg), fluconazole IR (50, 200, 400 mg) and ciprofloxacin IR (250, 500 and 750 mg).

Jejunoileal bypass:

Following JIB the whole range of studied drugs displayed an extensive reduction in AUC due to a more apparent reduction in f_a as compared to RYGB and BPD-DS where fluconazole displayed the least apparent reduction, with a post/pre surgery AUC ratio of 0.47 (±0.12) at a low therapeutic dose whereas displaying an AUC ratio 0.44 (±0.13) at a high dose level due to a more extensive reduction in f_a from 0.97 (±0.07) to 0.45 (±0.13) (Figure 3.12 and Figure 3.13).

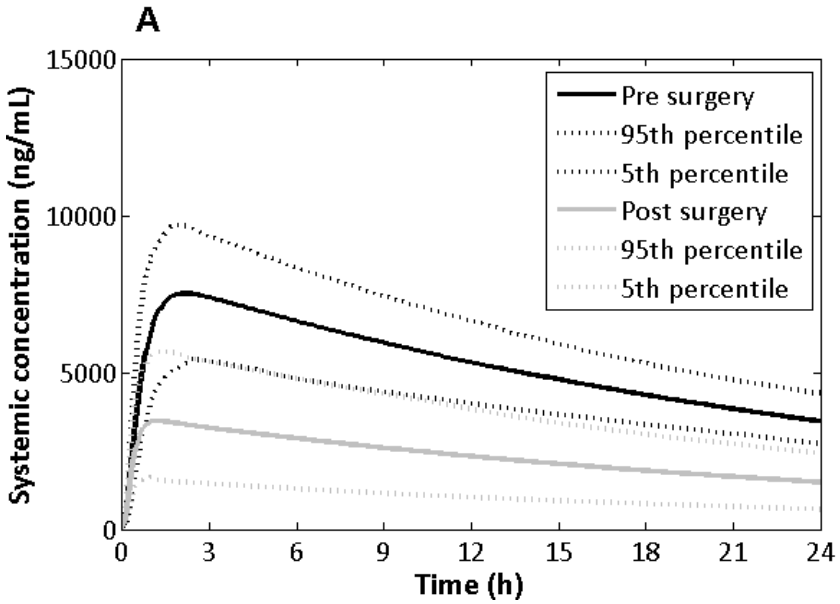

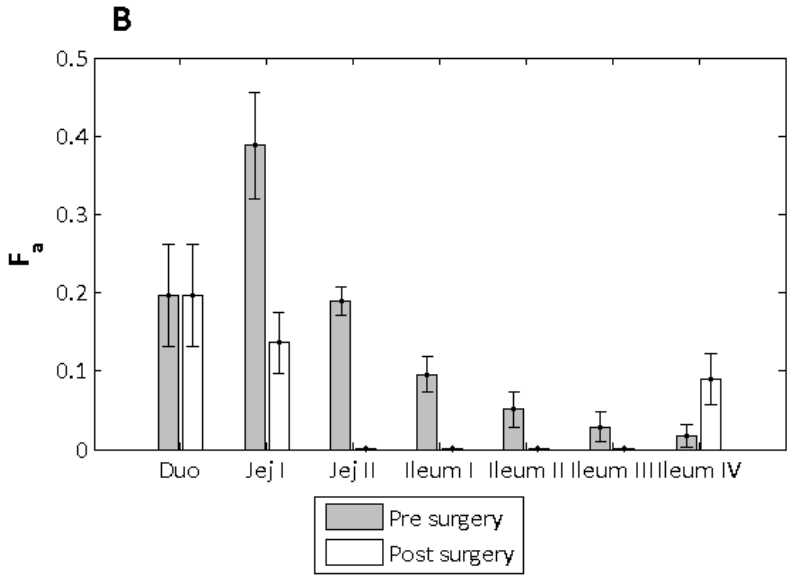

Figure 3.12. Simulated fluconazole immediate release (IR) 400 mg (high therapeutic dose) in morbidly obese (n=100) and post jejunoileal bypass (n=100; small intestinal transit=0.4h) **A:** Mean, 95th and 5th percentile plasma concentration time profile over 24 hours, **B:** Mean and standard deviation of segmental fraction of dose absorbed along the small intestine (f_a). Duo=duodenum, Jej=jejunum.

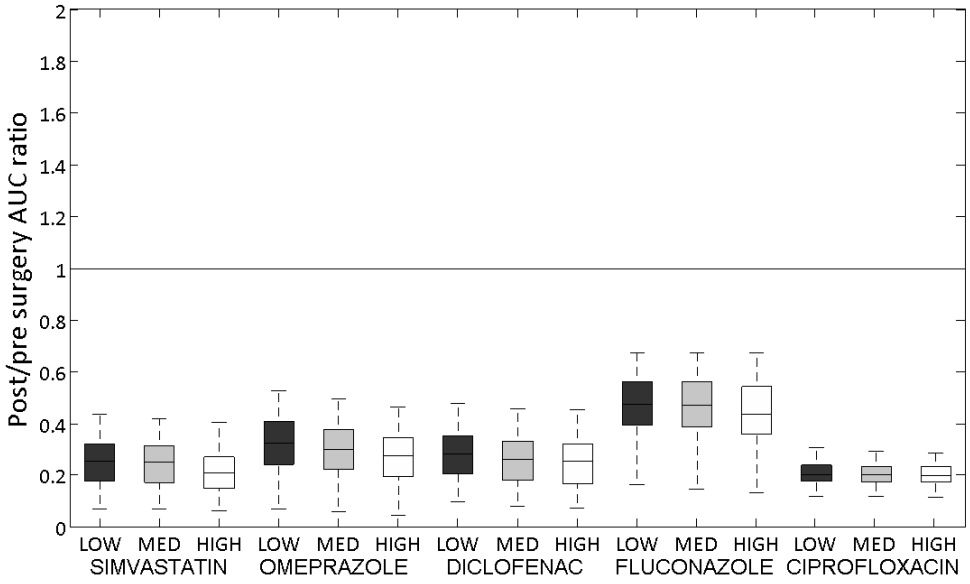

Figure 3.13. Simulated post/pre jejunoileal bypass (small intestinal transit=0.4h) AUC ratio over a range of selected drugs at a low (LOW), medium (MED) and high (HIGH) therapeutic dose: Simvastatin immediate release (IR; 10, 20 and 80 mg), omeprazole enteric coated (EC; 10, 20 and 40 mg), diclofenac EC (25, 50 75 mg), fluconazole IR (50, 200, 400 mg) and ciprofloxacin IR (250, 500 and 750 mg).

Sleeve gastrectomy:

Simulated post sleeve gastrectomy applied to Morbidly Obese did not significantly alter the pre to post surgery drug exposure for the range of studied drugs over low to high therapeutic dose ranges (data not shown).

3.5 Discussion

3.5.1 Simulating oral drug exposure following bariatric surgery:

Simulating oral drug bioavailability following bariatric surgery identified a number of potential pharmacokinetic parameters suggested to influence bioavailability following bariatric surgery.

Simvastatin is characterised as a BCS class IV, and further classified as a BDDCS (Biopharmaceutics Drug Disposition Classification System) class II compound (Darwich *et al.*, 2010; Benet *et al.*, 2011). The drug is considered a low soluble compound at therapeutic dose, displaying an aqueous solubility 0.03 mg/mL (Kasim *et al.*, 2004; BNF, 2011). The drug is administered in its lactone form and undergoes pH and temperature dependent interconversion to its hydroxyacid form at a pH below 6, whereas the lactone form mainly is formed at pH's over the equilibrium (Kearney *et al.*, 1993). Approximately 85% of the administered dose is absorbed, being further exposed to extensive metabolism by CYP3A4 in the small intestine and liver, and CYP3A5 to lesser extent (Lennernas and Fager, 1997; Prueksaritanont *et al.*, 1997).

The simulated increase in drug exposure of simvastatin in the post RYGB (SIT=3.0h) population was due to an increase in F_G post surgery. These findings suggest intestinal gut wall metabolism plays an important role in the observed trend in drug bioavailability pre to post surgery for compounds subject to a high small intestinal metabolic extraction ratio, such as atorvastatin and simvastatin, where simulated post/pre surgical AUC ratio following RYGB was similar to that observed of atorvastatin, displaying a median AUC ratio of 1.20 (0.3-2.3) (Skottheim *et al.*, 2009). Simulated compound characteristics of simvastatin did not incorporate the pH dependent interconversion of the lactone and acid form, but treated this as a part of the CYP3A4 clearance term through fitting to observed data, thus not taking into account

the increased gastric pH following RYGB surgery and its impact on the interconversion (Kearney *et al.*, 1993).

Omeprazole (BCS class II and BDDCS class I ampholyte, pKa=8.7, pKb=3.79), is a sparingly soluble highly lipophilic compound with stability issues at a lower pH levels, thus motivating enteric coated formulation (EC) protecting the drug from degradation caused by the gastric pH (Brandstrom *et al.*, 1985; El-Badry *et al.*, 2009; Darwich *et al.*, 2010; Benet *et al.*, 2011). The drug displays a highly variable absorption and further mainly undergoes hepatic metabolism and clearance by CYP3A4 and 2C19 (Shimamoto *et al.*, 2000). Only a minor alteration in F_G was observed following simulations post BPD-DS, where an increase was observed, overall. The biggest impact was observed on f_a, potentially due to the reduction in absorption area.

Diclofenac (BCS class II; BDDCS class I) is mainly metabolised by CYP2C9 (Shimamoto *et al.*, 2000; Darwich *et al.*, 2010; Benet *et al.*, 2011). The drug undergoes extensive first-pass metabolism, displaying an oral bioavailability of approximately 54% (Willis *et al.*, 1979). Following RYGB and BPD-DS a minor increase in F_G was observed due to the bypass of intestinal regions abundant of CYP2C9, however this was counteracted by a reduction in f_a.

Fluconazole (BCS class I; BDDCS class III) is soluble at a therapeutic dose and displays a bioavailability over 90% in healthy volunteers, further being mainly renally cleared (Brammer *et al.*, 1990; Darwich *et al.*, 2010; Benet *et al.*, 2011). Following bariatric surgery simulated oral drug exposure of fluconazole only displayed minor changes in AUC with the exception following JIB. These results are consistent with observations in AIDS patients, frequently displaying gastrointestinal disturbances, and a case report in a patient subject to gastrointestinal restriction of the gastric antrum, duodenum and ileum following peptic ulcer disease, displaying no altered bioavailability or a comparable bioavailability as compared to healthy volunteers (DeMuria *et al.*, 1993; Joe *et al.*, 1994).

Ciprofloxacin (BCS class III; BDDCS class IV) is sparingly soluble at the therapeutic dose range, further having a reported oral bioavailability ranging from approximately 60 to 80% in healthy volunteers and is mainly renally cleared (Hoffken *et al.*, 1985;

Lettieri *et al.*, 1992; Darwich *et al.*, 2010; Benet *et al.*, 2011). The simulated reduction in AUC following bariatric surgery is therefore most likely an effect of a reduction in absorption area and a product of post-operative solubility issues.

The major issue following SG would be potential solubility issues due to a reduced concomitant fluid volume with the administered dose although this was not a major issue for any of the studied drugs.

3.5.2 Post bariatric surgery ADAM model limitations:

Conclusions drawn from this study are limited by a number of "known unknowns" relating to gastrointestinal physiology post bariatric surgery, where data relating to gastrointestinal pH, small intestinal transit and post surgical gastrointestinal physiological adaptation and whole body physiological alterations, such as hepatic activity and bile secretion and it's GI levels, is sparse or nonexistent.

Following RYGB, gastric pH was estimated to increase based on measuring acid secretion in the gastric pouch (mEq/time). Albeit, examining the relationship between pH and gastric acid output the relationship is not straightforward. Pratha, and co-workers (2006), examined the effect of proton pump inhibitors (PPI) on gastric acid output and pH and concluded the relation between pH and gastric acid output to be highly ambiguous. At a gastric acid output of ≤1 mEq/30 min a pH 0.9 to 7.7 was observed, whereas a pH of 2.5 and upwards was rendered at minimal gastric acid output, thus rendering a high degree of uncertainty in the implications of mEq/time post Roux-en-Y gastric bypass (Pratha *et al.*, 2006).

Small intestinal transit time estimation following bariatric surgery was limited to one study examining small intestinal transit time of solids in 10 patients subject to total gastrectomy with Roux-en-Y reconstruction (Pellegrini *et al.*, 1986) or estimations based on the extent of small intestinal bypass. As the procedure differs in terms of the extent of gastrectomy as compared to RYGB for the treatment of obesity such an assumption may not necessarily hold true.

Following gastric restrictive surgery, *i.e.* RYGB and SG, gastric emptying of liquid displayed an overall significant reduction, whereas gastric emptying of solids displayed an increase in variability following RYGB. The impact of RYGB surgery on gastric emptying of solids may be due to post surgical state of stasis due to a reduced nervous stimulus (Horowitz *et al.*, 1982; Woodward *et al.*, 1993).

The methodology of how the ADAM model was adapted to mimic post bariatric surgery conditions is subject to a number of limitations due to the limited nature of how the ADAM model could be adjusted through the Simcyp® Simulator through the existing interface. Rather than bypassing the proximal small intestinal compartments, the transit time through these compartments were reduced close to zero. As a consequence the modelling and simulations of drug concentration in the bilio limb could not be conducted, thus limiting the predictability of drugs subject to biliary elimination. A further concern was the fluid dynamics within the ADAM model which is governed by secretion and reabsorption of GI fluids taking place throughout the gastrointestinal tract compartments (Valentin, 2002; Jamei *et al.*, 2009b). As a consequence of such parameter alterations not being possible through the Simcyp user-interface an overestimation of GI fluid volumes and consequential underestimation of potential drug specific solubility issues following surgery are possible.

3.6 Conclusions

Trends in pre and post Roux-en-Y gastric bypass bioavailability seem to be highly dependent on drug specific parameters such as affinity to CYP3A4, solubility and permeability issues based on simulated outcome, albeit yet to be confirmed with regards to clinical data. A mechanistic modelling approach has the potential of examining the impact of drug specific parameters on trend of pre to post surgery and to serve as a useful tool in examining the impact of physiological alterations on oral drug bioavailability in the absence of clinical data.

Current limitations in estimating and simulating the impact of oral drug bioavailability following bariatric surgery include the sparsity in clinical data for further model validation and the lack of data on resultant physiological changes post surgery.

3.7 Acknowledgements

The authors wish to thank the bariatric surgery team at Salford Royal Hospital NHS Foundation Trust for discussions on bariatric surgical dimensions and Dr David Turner at Simcyp Limited and Mr James Kay at Simcyp Limited for his assistance with the preparation of the manuscript. Prof Amin Rostami, Dr Devendra Pade and Dr Masoud Jamei are employees and/or shareholders in Simcyp Limited. Simcyp® Simulator is freely available, following completion of the model-based drug development workshop, to approved members of academic institutions and other non-for-profit organisations for research and teaching purposes.

3.8 References

Agoram B, Woltosz WS, and Bolger MB (2001) Predicting the impact of physiological and biochemical processes on oral drug bioavailability. *Adv Drug Deliv Rev* **50 Suppl 1:**S41-67.

Ammori BJ (2012) Laparoscopic Sleeve Gastrectomy Manchester UK: Professor Basil Ammori-Laparoscopic Obesity Surgery - Manchester, Manchester.

Avdeef A (2007) Solubility of sparingly-soluble ionizable drugs. *Adv Drug Deliv Rev* **59:**568-590.

Baltasar A, Serra C, Perez N, Bou R, Bengochea M, and Ferri L (2005) Laparoscopic sleeve gastrectomy: a multi-purpose bariatric operation. *Obes Surg* **15:**1124-1128.

Barker KB, Palekar NA, Bowers SP, Goldberg JE, Pulcini JP, and Harrison SA (2006) Non-alcoholic steatohepatitis: effect of Roux-en-Y gastric bypass surgery. *Am J Gastroenterol* **101:**368-373.

Behrns KE, Smith CD, and Sarr MG (1994) Prospective evaluation of gastric acid secretion and cobalamin absorption following gastric bypass for clinically severe obesity. *Dig Dis Sci* **39:**315-320.

Benedek IH, Blouin RA, and McNamara PJ (1984) Serum protein binding and the role of increased alpha 1-acid glycoprotein in moderately obese male subjects. *Br J Clin Pharmacol* **18:**941-946.

Benet LZ, Broccatelli F, and Oprea TI (2011) BDDCS Applied to Over 900 Drugs. *AAPS J* **13:**519-547.

Benet LZ and Cummins CL (2001) The drug efflux-metabolism alliance: biochemical aspects. *Adv Drug Deliv Rev* **50 Suppl 1:**S3-11.

Bernstine H, Tzioni-Yehoshua R, Groshar D, Beglaibter N, Shikora S, Rosenthal RJ, and Rubin M (2009) Gastric emptying is not affected by sleeve gastrectomy--scintigraphic evaluation of gastric emptying after sleeve gastrectomy without removal of the gastric antrum. *Obes Surg* **19:**293-298.

Blum RA, D'Andrea DT, Florentino BM, Wilton JH, Hilligoss DM, Gardner MJ, Henry EB, Goldstein H, and Schentag JJ (1991) Increased gastric pH and the bioavailability of fluconazole and ketoconazole. *Ann Intern Med* **114:**755-757.

BNF (2011) British National Formulary.

Braghetto I, Davanzo C, Korn O, Csendes A, Valladares H, Herrera E, Gonzalez P, and Papapietro K (2009) Scintigraphic evaluation of gastric emptying in obese

patients submitted to sleeve gastrectomy compared to normal subjects. *Obes Surg* **19:**1515-1521.

Brammer KW, Farrow PR, and Faulkner JK (1990) Pharmacokinetics and tissue penetration of fluconazole in humans. *Rev Infect Dis* **12 Suppl 3:**S318-326.

Brandstrom A, Lindberg P, and Junggren U (1985) Structure activity relationships of substituted benzimidazoles. *Scand J Gastroenterol Suppl* **108:**15-22.

Buchwald H and Oien DM (2009) Metabolic/bariatric surgery Worldwide 2008. *Obes Surg* **19:**1605-1611.

Chagnac A, Weinstein T, Herman M, Hirsh J, Gafter U, and Ori Y (2003) The effects of weight loss on renal function in patients with severe obesity. *J Am Soc Nephrol* **14:**1480-1486.

Darwich AS, Henderson K, Burgin A, Ward N, Whittam J, Ammori BJ, Ashcroft DM, and Rostami-Hodjegan A (2012) Trends in oral drug bioavailability following bariatric surgery: Examining the variable extent of impact on exposure of different drug classes. *Br J Clin Pharmacol* **74:**774-787.

Darwich AS, Neuhoff S, and Rostami-Hodjegan A (2010) Interplay of metabolism and transport in determining oral drug absorption and gut wall metabolism: a simulation assessment using the "advanced dissolution, absorption, metabolism (ADAM)" model. *Curr Drug Metab* **11:**716-729.

Delgado-Aros S, Cremonini F, Castillo JE, Chial HJ, Burton DD, Ferber I, and Camilleri M (2004) Independent influences of body mass and gastric volumes on satiation in humans. *Gastroenterology* **126:**432-440.

DeMaria EJ, Sugerman HJ, Kellum JM, Meador JG, and Wolfe LG (2002) Results of 281 consecutive total laparoscopic Roux-en-Y gastric bypasses to treat morbid obesity. *Ann Surg* **235:**640-645; discussion 645-647.

DeMuria D, Forrest A, Rich J, Scavone JM, Cohen LG, and Kazanjian PH (1993) Pharmacokinetics and bioavailability of fluconazole in patients with AIDS. *Antimicrob Agents Chemother* **37:**2187-2192.

El-Badry M, Taha EI, Alanazi FK, and Alsarra IA (2009) Study of omperazole stability in aqueous solution: influence of cyclodextrins. *J Drug Del Sci Tech* **19:**347-351.

Elder KA and Wolfe BM (2007) Bariatric surgery: a review of procedures and outcomes. *Gastroenterology* **132:**2253-2271.

Fisher MB, Paine MF, Strelevitz TJ, and Wrighton SA (2001) The role of hepatic and extrahepatic UDP-glucuronosyltransferases in human drug metabolism. *Drug Metab Rev* **33:**273-297.

Flegal KM, Carroll MD, Ogden CL, and Curtin LR (2010) Prevalence and trends in obesity among US adults, 1999-2008. *JAMA* **303:**235-241.

Fromm MF, Kauffmann HM, Fritz P, Burk O, Kroemer HK, Warzok RW, Eichelbaum M, Siegmund W, and Schrenk D (2000) The effect of rifampin treatment on intestinal expression of human MRP transporters. *Am J Pathol* **157:**1575-1580.

Ghobadi C, Johnson TN, Aarabi M, Almond LM, Allabi AC, Rowland-Yeo K, Jamei M, and Rostami-Hodjegan A (2011) Application of a systems approach to the bottom-up assessment of pharmacokinetics in obese patients: expected variations in clearance. *Clin Pharmacokinet* **50:**809-822.

Griffen WO, Jr., Young VL, and Stevenson CC (1977) A prospective comparison of gastric and jejunoileal bypass procedures for morbid obesity. *Ann Surg* **186:**500-509.

Haglund U, Fork FT, Hogstrom H, and Lilja B (1989) Esophageal and jejunal motor function after total gastrectomy and Roux-Y esophagojejunostomy. *Am J Surg* **157:**308-311.

Higaki K, Choe SY, Lobenberg R, Welage LS, and Amidon GL (2008) Mechanistic understanding of time-dependent oral absorption based on gastric motor activity in humans. *Eur J Pharm Biopharm* **70:**313-325.

Hinder RA, Esser J, and DeMeester TR (1988) Management of gastric emptying disorders following the Roux-en-Y procedure. *Surgery* **104:**765-772.

Hoffken G, Lode H, Prinzing C, Borner K, and Koeppe P (1985) Pharmacokinetics of ciprofloxacin after oral and parenteral administration. *Antimicrob Agents Chemother* **27:**375-379.

Horowitz M, Cook DJ, Collins PJ, Harding PE, Hooper MJ, Walsh JF, and Shearman DJ (1982) Measurement of gastric emptying after gastric bypass surgery using radionuclides. *Br J Surg* **69:**655-657.

Howgate EM, Rowland Yeo K, Proctor NJ, Tucker GT, and Rostami-Hodjegan A (2006) Prediction of in vivo drug clearance from in vitro data. I: impact of inter-individual variability. *Xenobiotica* **36:**473-497.

Huang W, Lee SL, and Yu LX (2009) Mechanistic approaches to predicting oral drug absorption. *AAPS J* **11:**217-224.

Jamei M, Marciniak S, Feng K, Barnett A, Tucker G, and Rostami-Hodjegan A (2009a) The Simcyp population-based ADME simulator. *Expert Opin Drug Metab Toxicol* **5:**211-223.

Jamei M, Turner D, Yang J, Neuhoff S, Polak S, Rostami-Hodjegan A, and Tucker G (2009b) Population-based mechanistic prediction of oral drug absorption. *AAPS J* **11:**225-237.

Joe LA, Jacobs RA, and Guglielmo BJ (1994) Systemic absorption of oral fluconazole after gastrointestinal resection. *J Antimicrob Chemother* **33:**1070.

Johnson TN, Tucker GT, Tanner MS, and Rostami-Hodjegan A (2005) Changes in liver volume from birth to adulthood: a meta-analysis. *Liver Transpl* **11:**1481-1493.

Kasim NA, Whitehouse M, Ramachandran C, Bermejo M, Lennernas H, Hussain AS, Junginger HE, Stavchansky SA, Midha KK, Shah VP, and Amidon GL (2004) Molecular properties of WHO essential drugs and provisional biopharmaceutical classification. *Mol Pharm* **1:**85-96.

Kearney AS, Crawford LF, Mehta SC, and Radebaugh GW (1993) The interconversion kinetics, equilibrium, and solubilities of the lactone and hydroxyacid forms of the HMG-CoA reductase inhibitor, CI-981. *Pharm Res* **10:**1461-1465.

Koch KM, Parr AF, Tomlinson JJ, Sandefer EP, Digenis GA, Donn KH, and Powell JR (1993) Effect of sodium acid pyrophosphate on ranitidine bioavailability and gastrointestinal transit time. *Pharm Res* **10:**1027-1030.

Kolars JC, Lown KS, Schmiedlin-Ren P, Ghosh M, Fang C, Wrighton SA, Merion RM, and Watkins PB (1994) CYP3A gene expression in human gut epithelium. *Pharmacogenetics* **4:**247-259.

Le Blanc-Louvry I, Ducrotte P, Lemeland JF, Metayer J, Denis P, and Teniere P (1999) Motility in the Roux-Y limb after distal gastrectomy: relation to the length of the limb and the afferent duodenojejunal segment--an experimental study. *Neurogastroenterol Motil* **11:**365-374.

Le Blanc-Louvry I, Ducrotte P, Peillon C, Michel P, Chiron A, and Denis P (2000) Roux-en-Y limb motility after total or distal gastrectomy in symptomatic and asymptomatic patients. *J Am Coll Surg* **190:**408-417.

Lee CM, Cirangle PT, and Jossart GH (2007) Vertical gastrectomy for morbid obesity in 216 patients: report of two-year results. *Surg Endosc* **21:**1810-1816.

Lennernas H and Fager G (1997) Pharmacodynamics and pharmacokinetics of the HMG-CoA reductase inhibitors. Similarities and differences. *Clin Pharmacokinet* **32:**403-425.

Lettieri JT, Rogge MC, Kaiser L, Echols RM, and Heller AH (1992) Pharmacokinetic profiles of ciprofloxacin after single intravenous and oral doses. *Antimicrob Agents Chemother* **36:**993-996.

Maliepaard M, Scheffer GL, Faneyte IF, van Gastelen MA, Pijnenborg AC, Schinkel AH, van De Vijver MJ, Scheper RJ, and Schellens JH (2001) Subcellular localization and distribution of the breast cancer resistance protein transporter in normal human tissues. *Cancer Res* **61:**3458-3464.

Mattar SG, Velcu LM, Rabinovitz M, Demetris AJ, Krasinskas AM, Barinas-Mitchell E, Eid GM, Ramanathan R, Taylor DS, and Schauer PR (2005) Surgically-induced weight loss significantly improves nonalcoholic fatty liver disease and the metabolic syndrome. *Ann Surg* **242:**610-617; discussion 618-620.

Michels WM, Grootendorst DC, Verduijn M, Elliott EG, Dekker FW, and Krediet RT (2010) Performance of the Cockcroft-Gault, MDRD, and new CKD-EPI formulas in relation to GFR, age, and body size. *Clin J Am Soc Nephrol* **5:**1003-1009.

Mouly S and Paine MF (2003) P-glycoprotein increases from proximal to distal regions of human small intestine. *Pharm Res* **20:**1595-1599.

National Institutes of Health U (2010) Bariatric Surgery for Severe Obesity.

Navarro-Diaz M, Serra A, Romero R, Bonet J, Bayes B, Homs M, Perez N, and Bonal J (2006) Effect of drastic weight loss after bariatric surgery on renal parameters in extremely obese patients: long-term follow-up. *J Am Soc Nephrol* **17:**S213-217.

OECD (2011) Obesity and the Economics of Prevention: Fit not Fat - United Kingdom (England) Key Facts, OECD.

Paine MF, Hart HL, Ludington SS, Haining RL, Rettie AE, and Zeldin DC (2006) The human intestinal cytochrome P450 "pie". *Drug Metab Dispos* **34:**880-886.

Paine MF, Khalighi M, Fisher JM, Shen DD, Kunze KL, Marsh CL, Perkins JD, and Thummel KE (1997) Characterization of interintestinal and intraintestinal variations in human CYP3A-dependent metabolism. *J Pharmacol Exp Ther* **283:**1552-1562.

Pellegrini CA, Deveney CW, Patti MG, Lewin M, and Way LW (1986) Intestinal transit of food after total gastrectomy and Roux-Y esophagojejunostomy. *Am J Surg* **151:**117-125.

Peters WH, Roelofs HM, Nagengast FM, and van Tongeren JH (1989) Human intestinal glutathione S-transferases. *Biochem J* **257:**471-476.

Petrakis J, Vassilakis JS, Karkavitsas N, Tzovaras G, Epanomeritakis E, Tsiaoussis J, and Xynos E (1998) Enhancement of gastric emptying of solids by erythromycin in patients with Roux-en-Y gastrojejunostomy. *Arch Surg* **133:**709-714.

Picot J, Jones J, Colquitt JL, Gospodarevskaya E, Loveman E, Baxter L, and Clegg AJ (2009) The clinical effectiveness and cost-effectiveness of bariatric (weight loss) surgery for obesity: a systematic review and economic evaluation. *Health Technol Assess* **13:**1-190, 215-357, iii-iv.

Pratha VS, Hogan DL, Lane JR, Williams PJ, Burton MS, Lynn RB, and Karlstadt RG (2006) Inhibition of pentagastrin-stimulated gastric acid secretion by pantoprazole and omeprazole in healthy adults. *Dig Dis Sci* **51:**123-131.

Prueksaritanont T, Gorham LM, Ma B, Liu L, Yu X, Zhao JJ, Slaughter DE, Arison BH, and Vyas KP (1997) In vitro metabolism of simvastatin in humans [SBT]identification of metabolizing enzymes and effect of the drug on hepatic P450s. *Drug Metab Dispos* **25:**1191-1199.

Riches Z, Stanley EL, Bloomer JC, and Coughtrie MW (2009) Quantitative evaluation of the expression and activity of five major sulfotransferases (SULTs) in human tissues: the SULT "pie". *Drug Metab Dispos* **37:**2255-2261.

Rieu PN, Van Kroonenburgh MJ, Jansen JB, Joosten HJ, and Lamers CB (1989) Gastric emptying after partial gastrectomy without vagotomy with primary Roux-en-Y or Billroth II anastomosis. *Nucl Med Commun* **10:**715-722.

Rowland M and Tozer TN (1989) *Clinical Pharmacokinetics: Concepts and Applications*. Lea & Febiger, Philadelphia.

Saliba J, Kasim NR, Tamboli RA, Isbell JM, Marks P, Feurer ID, Ikizler A, and Abumrad NN (2010) Roux-en-Y gastric bypass reverses renal glomerular but not tubular abnormalities in excessively obese diabetics. *Surgery* **147:**282-287.

Schneider BE and Mun EC (2005) Surgical management of morbid obesity. *Diabetes Care* **28:**475-480.

Scott HW, Jr., Dean R, Shull HJ, Abram HS, Webb W, Younger RK, and Brill AB (1973) Considerations in use of jejunoileal bypass in patients with morbid obesity. *Ann Surg* **177:**723-735.

Scott HW, Jr., Sandstead HH, Brill AB, Burko H, and Younger RK (1971) Experience with a new technic of intestinal bypass in the treatment of morbid obesity. *Ann Surg* **174:**560-572.

Serra A, Granada ML, Romero R, Bayes B, Canton A, Bonet J, Rull M, Alastrue A, and Formiguera X (2006) The effect of bariatric surgery on adipocytokines, renal parameters and other cardiovascular risk factors in severe and very severe obesity: 1-year follow-up. *Clin Nutr* **25:**400-408.

Shah S, Shah P, Todkar J, Gagner M, Sonar S, and Solav S (2010) Prospective controlled study of effect of laparoscopic sleeve gastrectomy on small bowel transit time and gastric emptying half-time in morbidly obese patients with type 2 diabetes mellitus. *Surg Obes Relat Dis* **6:**152-157.

Shimamoto J, Ieiri I, Urae A, Kimura M, Irie S, Kubota T, Chiba K, Ishizaki T, Otsubo K, and Higuchi S (2000) Lack of differences in diclofenac (a substrate for CYP2C9) pharmacokinetics in healthy volunteers with respect to the single CYP2C9*3 allele. *Eur J Clin Pharmacol* **56:**65-68.

Singh D, Laya AS, Clarkston WK, and Allen MJ (2009) Jejunoileal bypass: a surgery of the past and a review of its complications. *World J Gastroenterol* **15:**2277-2279.

Skottheim IB, Stormark K, Christensen H, Jakobsen GS, Hjelmesaeth J, Jenssen T, Reubsaet JL, Sandbu R, and Asberg A (2009) Significantly altered systemic exposure to atorvastatin acid following gastric bypass surgery in morbidly obese patients. *Clin Pharmacol Ther* **86:**311-318.

Smith CD, Herkes SB, Behrns KE, Fairbanks VF, Kelly KA, and Sarr MG (1993) Gastric acid secretion and vitamin B12 absorption after vertical Roux-en-Y gastric bypass for morbid obesity. *Ann Surg* **218:**91-96.

Spak E, Bjorklund P, Helander HF, Vieth M, Olbers T, Casselbrant A, Lonroth H, and Fandriks L (2010) Changes in the mucosa of the Roux-limb after gastric bypass surgery. *Histopathology* **57:**680-688.

Stratopoulos C, Papakonstantinou A, Terzis I, Spiliadi C, Dimitriades G, Komesidou V, Kitsanta P, Argyrakos T, and Hadjiyannakis E (2005) Changes in liver histology accompanying massive weight loss after gastroplasty for morbid obesity. *Obes Surg* **15:**1154-1160.

Suzuki S, Ramos EJ, Goncalves CG, Chen C, and Meguid MM (2005) Changes in GI hormones and their effect on gastric emptying and transit times after Roux-en-Y gastric bypass in rat model. *Surgery* **138:**283-290.

Turner D (2008) Simcyp User Manual Version 8.

Valentin J (2002) Pages 37-39 from *Basic Anatomical and Physiological Data for Use in Radiological Protection: Reference Values*. The International Comission on Radiological Protection, Pergamon.

van der Mijle HC, Kleibeuker JH, Limburg AJ, Bleichrodt RP, Beekhuis H, and van Schilfgaarde R (1993) Manometric and scintigraphic studies of the relation between motility disturbances in the Roux limb and the Roux-en-Y syndrome. *Am J Surg* **166:**11-17.

van Dielen FM, Buurman WA, Hadfoune M, Nijhuis J, and Greve JW (2004) Macrophage inhibitory factor, plasminogen activator inhibitor-1, other acute phase proteins, and inflammatory mediators normalize as a result of weight loss in morbidly obese subjects treated with gastric restrictive surgery. *J Clin Endocrinol Metab* **89:**4062-4068.

Willis JV, Kendall MJ, Flinn RM, Thornhill DP, and Welling PG (1979) The pharmacokinetics of diclofenac sodium following intravenous and oral administration. *Eur J Clin Pharmacol* **16:**405-410.

Wittgrove AC and Clark GW (2000) Laparoscopic gastric bypass, Roux-en-Y- 500 patients: technique and results, with 3-60 month follow-up. *Obes Surg* **10:**233-239.

Woodward A, Sillin LF, Wojtowycz AR, and Bortoff A (1993) Gastric stasis of solids after Roux gastrectomy: is the jejunal transection important? *J Surg Res* **55:**317-322.

Chapter 4: Evaluation of an *in silico* PBPK post-bariatric surgery model through simulating oral drug bioavailability of atorvastatin and cyclosporine

Chapter 4: Evaluation of an *in silico* PBPK post-bariatric surgery model through simulating oral drug bioavailability of atorvastatin and cyclosporine

A.S. Darwich, D. Pade, K. Rowland-Yeo, M. Jamei, A. Åsberg, H. Christensen, D.M. Ashcroft, A. Rostami-Hodjegan

CPT Pharmacometrics and Syst Pharmacol. 2013, 2(e47):1-9

4.1 Abstract

An increasing prevalence of morbid obesity has led to dramatic increases in the number of bariatric surgeries performed. Altered gastrointestinal physiology following surgery can be associated with modified oral drug bioavailability (F_{oral}). In the absence of clinical data, an indication of changes to F_{oral} via systems pharmacology models would be of value in adjusting dose levels after surgery. A previously developed virtual "post-bariatric surgery" population was evaluated through mimicking clinical investigations on cyclosporine and atorvastatin after bariatric surgery. Cyclosporine simulations displayed a reduced fraction absorbed through gut wall (f_a) and F_{oral} after surgery, consistent with reported observations. Simulated atorvastatin F_{oral} post surgery was broadly reflective of observed data with indications of counteracting interplay between reduced f_a and an increased fraction escaping gut wall metabolism (F_G). Inability to fully recover observed atorvastatin exposure after biliopancreatic diversion with duodenal switch highlights the current gap regarding the knowledge of associated biological changes.

4.2 Introduction

The prevalence of obesity has increased dramatically in the USA and Europe over the last decade (Flegal *et al.*, 2010; OECD, 2011). Bariatric surgery has proven to be successful in treating morbid obesity with over 220,000 surgeries performed in the USA and Canada in 2008 (Buchwald and Oien, 2009). Several bariatric surgical methods coexist in healthcare, where Roux-en-Y gastric bypass (RYGB) is considered gold-standard (Picot *et al.*, 2009). RYGB results in a reduced gastric volume, complete bypass of the pylorus, partial bypass of the duodenum and proximal jejunum and a delay in bile inflow to the distal jejunum. The more invasive biliopancreatic diversion

with duodenal switch (BPD-DS) results in a partial resection of the stomach with the pylorus retained, bypass of jejunum and proximal ileum, and an approximate 250 cm delay of the bile inlet. Jejunoileal bypass (JIB) is considered the most invasive procedure, retaining only the stomach (with pylorus) and distal ileum (Darwich *et al.*, 2012a; Darwich *et al.*, 2012b).

As a consequence of bariatric surgery, a number of physiological parameters influencing oral drug bioavailability (F_{oral}) are altered, including: a reduced gastric capacity and emptying time, altered gastrointestinal (GI) pH, reduced absorption area, altered bile flow and small intestinal transit, altered substrate exposure to drug metabolising enzymes and active efflux transporters (Jamei *et al.*, 2009b; Ghobadi *et al.*, 2011; Darwich *et al.*, 2012a). Patients undergoing bariatric surgery continue to receive various therapeutic drugs without dose adjustments for altered bioavailability which can potentially lead to no therapeutic effect or higher than required systemic exposure. There are a very limited number of studies that have investigated oral drug exposure post bariatric surgery (Malone and Alger-Mayer, 2005; Darwich *et al.*, 2012a).

The direction and magnitude of impact on F_{oral} following surgery may depend on the characteristics and invasiveness of the surgical procedure, where the extent of the small intestinal bypass may influence the fraction of dose absorbed through the gut wall (f_a) (Skottheim *et al.*, 2009; Skottheim *et al.*, 2010). Bypassing regions highly abundant in drug metabolising enzymes can affect the fraction of absorbed drug escaping gut wall metabolism (F_G) (Darwich *et al.*, 2012b). F_H, the fraction that escapes hepatic first-pass metabolism, may be assumed to remain unaltered (Equation 1.1) (Jamei *et al.*, 2009b; Ghobadi *et al.*, 2011; Darwich *et al.*, 2012a).

$$F_{oral} = f_a \cdot F_G \cdot F_H$$

Equation 1.1: Components of Foral.

A level of uncertainty remains regarding the small intestinal transit (SIT) post surgery where a reduction in motility has been observed, albeit well powered clinical studies of small intestinal transit in man are lacking (Pellegrini *et al.*, 1986; Suzuki *et al.*, 2005; Darwich *et al.*, 2012b).

The post surgical physiology is further complicated by the possibility of small intestinal trauma or adaptation, where an enhanced permeability due to impairment of the mucosa or long-term villi elongation has been observed in rat BPD-DS models (Gaggiotti *et al.*, 1995; Mendieta-Zeron *et al.*, 2011). Alterations in levels of gastric hormones (including: peptide YY, ghrelin and Glucagon-Like Peptide 1) may lead to redistribution of intestinal blood flow to the submucosa, as observed in dog models. Post surgical hormonal levels have been observed to vary depending on the bariatric surgical procedure (Savage *et al.*, 1987; Buell and Harding, 1989; Suzuki *et al.*, 2005; Garcia-Fuentes *et al.*, 2008).

Due to these multi-factorial changes, physiologically-based pharmacokinetic (PBPK) modelling enables one to predict *in silico*, the effects of various bariatric surgeries in a morbidly obese population (Darwich *et al.*, 2012b). The Advanced Dissolution Absorption and Metabolism (ADAM) model describes the variability in F_{oral} through a physiologically-based seven segment model of the small intestine, including: duodenum, jejunum I and II, and ileum I-IV. The model describes drug release from formulation, dissolution, precipitation, degradation, absorption, active transport and metabolism as the drug transits through the small intestine, allowing the incorporation of saturation effects and population variability. The ADAM model has been well described and utilised in previous literature (Jamei *et al.*, 2009b).

In our previous work, a virtual ‘post bariatric surgery’ population was created utilising the ADAM model within a PBPK system containing characteristics of a morbidly obese population. Developed models for RYGB, BPD-DS and JIB included specific anatomical and physiological parameters that are altered following surgery, namely: Gastric capacity and fluid dynamics, gastric emptying time, small intestinal bypass, GI pH, bile flow and alterations to regional abundance of drug metabolising enzymes (*e.g.* CYP3A) and efflux transporter P-glycoprotein. The model further incorporated whole body physiological changes, such as post surgical recovery of renal function as a function of weight loss (Darwich *et al.*, 2012b).

Simulations predicted change in oral bioavailability of various drugs pre to post bariatric surgery revealing the magnitude and direction of the effect to be surgery dependent, due to altered GI system parameters, and influenced by a complex interplay between drug characteristics, including: solubility, permeability, dissolution, gut wall metabolism and dose level. However, no comparison so far has been made between the results of these simulations and existing clinical data (Darwich *et al.*, 2012b).

In the current study, we report on the evaluation of previously developed post bariatric surgery models by comparing the observed versus predicted impact of bariatric surgery on oral exposure of cyclosporine and atorvastatin acid using virtual simulations.

4.3 Methods

4.3.1 Bariatric surgery model

Sex, age, height and weight matched simulations were carried out corresponding to identified clinical studies (Marterre *et al.*, 1996; Chenhsu *et al.*, 2003; Skottheim *et al.*, 2009; Skottheim *et al.*, 2010) utilising the ADAM model coupled to a full PBPK distribution model, incorporated into the Simcyp® Simulator (Simcyp Ltd., Sheffield, UK) (Equation 4.1, Equation 4.2 and Equation 4.3) (Jamei *et al.*, 2009a; Jamei *et al.*, 2009b). Detailed specification for the demographics and physiological parameters of the morbidly obese population have been published previously. Similarly, surgical changes to the anatomy and physiology of gastrointestinal tract following bariatric surgeries, including: RYGB, BPD-DS and JIB, are defined in an earlier publication. Study population specific surgical alterations are summarised in (Table 4.1).

$$Height = C0 + C1 \cdot Age + C2 \cdot Age^2$$

Equation 4.1: Height equation.

$$Weight = e^{(C0 + C1 \cdot Height)}$$

Equation 4.2: Weight equation.

$$BSA = Weight^{Weight\ exponent} \cdot Height^{Height\ exponent}$$

Equation 4.3: Body surface area equation.

Table 4.1. Summary of alterations to population template in order to mimic and simulate post surgical conditions.

Parameters	Bariatric surgical procedures			References
	JIB	RYGB	BPD-DS	
Gastric emptying: Liquids (minutes)	24[A] CV: 38%	7 CV: 45%	24[A] CV: 38%	(Horowitz *et al.*, 1982; Hedberg *et al.*, 2011a; Darwich *et al.*, 2012b)
Gastric capacity (mL)	250[A]	30	150	(Wittgrove and Clark, 2000; Darwich *et al.*, 2012b)
Q_{sec} stomach (L/h)	0.108	0.059	0.295	
Initial volume of stomach fluid (mL)	50[A]	9.9	32.6	
Gastric pH	1.5[A]	6.5	1.5[A]	(Smith *et al.*, 1993; Behrns *et al.*, 1994; Hedberg *et al.*, 2011b; Darwich *et al.*, 2012b)
Small intestinal bypass (centimeters and/or segments)	Retaining the duodenum, 20% of jejunum I and 23% of ileum IV.[B]	100 cm (duodenum and jejunum I)[B]	Retaining 2.5 cm of duodenum and 250 cm of the distal ileum[C]	(Wittgrove and Clark, 2000; Darwich *et al.*, 2012b)
Bile exclusion (centimeters and segments)	Not applicable (jej II – ileum III)	110 cm (stomach – jejunum I)	252 cm (stomach – ileum III)	
CYP3A4 abundance (nmol/total gut)	32.3 CV: 60%	48.3 CV: 60%	12.6[D] CV: 38%	
CYP3A5 abundance (mmol/total gut)	12.1 CV: 60%	18.0 CV: 60%	10.1[D] CV: 38%	
Mean small intestinal transit time (hours) – Scenario 1	0.4 α = 0.5 β = 0.4	3.0 α = 2.6 β = 3.7	1.2 α = 1.3 β = 1.9	
Mean small intestinal transit time (hours) – Scenario 2	0.7 α = 0.6 β = 0.4	5.0 α = 4.0 β = 5.3	4.2[E] α = 3.7 β = 5.0	(Pellegrini *et al.*, 1986; Savage *et al.*, 1987; Suzuki *et al.*, 2005; Darwich *et al.*, 2012b)
Renal equation	MDRD	MDRD	MDRD	{Chagnac, 2003 #78; Darwich, 2012 #521; Navarro-Diaz, 2006 #79; Saliba, 2010 #76; Serra, 2006 #80 (6, 37-40)

JIB=Jejunoileal bypass, RYGB=Roux-en-Y gastric bypass, BPD-DS=Biliopancreatic diversion with duodenal switch. Q_{sec}=Secretion flow.
[A]Unaltered parameter as compared to morbidly obese controls.
[B]Setting human effective permeability (P_{eff}) of compounds close to zero in bypassed segments.
[C]Altering small intestinal parameters in the ADAM model to conform to remaining segments.
[D]Based on intestinal biopsy in the study population (11).
[E]Derived based on a pre to post surgical peptide YY level of 413% utilising linear relation between peptide YY and small intestinal transit time as reported by Savage, and co-workers (16, 18).
α & β = Weibull scaling factors utilising assuming a variance of 1.8h.
MDRD=Modification of Diet Renal Disease equation.

Cyclosporine

The cyclosporine compound file, available in the Simcyp® Simulator compound library, was adapted to account for formulation properties corresponding to Sandimmune® solution and Sandimmune® Neoral® microemulsion (Novartis), using an aqueous solubility of 0.01 mg/mL and particle sizes of 3.73 μm and 0.03 μm respectively, further allowing Neoral® to supersaturate freely without precipitation assuming a linear dose-concentration relationship (Mueller *et al.*, 1994). A full PBPK model was utilised to describe the cyclosporine distribution, where tissue to plasma partition coefficients (Kp's) were obtained from tissue to plasma concentrations at steady state following intravenous infusion were obtained from rat (Bernareggi and Rowland, 1991).

Atorvastatin acid

Physicochemical parameters for atorvastatin acid were taken from the publication by Lennernas (Lennernas, 2003). Metabolic data were obtained from the *in vitro* study reported by Jacobsen, and co-workers (Jacobsen *et al.*, 2000); CYP3A4 was found to be the main enzyme involved in the formation of the two primary metabolites ortho- and para-hydroxyatorvastatin acid with a minor contribution from CYP2C8. Intersystem extrapolation factors (ISEFs), which correct for differences in intrinsic activity per unit CYP enzyme relative to its native environment were applied to the kinetic data for recombinantly expressed CYP3A4 and CYP2C8, respectively. Acyl glucuronidation of atorvastatin acid to the lactone and UDPGA-dependent metabolism of atorvastatin acid mainly via UGT1A1 to a minor ether glucuronide was also considered (Prueksaritanont *et al.*, 2002; Goosen *et al.*, 2007). The resultant intrinsic clearance data were scaled to whole organ values according to Equation 4.4 and Equation 4.5 (Howgate *et al.*, 2006). The uptake of atorvastatin acid has been demonstrated in an OATP1B1-transfected cell system (HEK293 cells) (Lau *et al.*, 2007; Amundsen *et al.*, 2010). While these *in vitro* data support the involvement of OATP1B1 in the hepatic uptake of atorvastatin acid, it was found that when used in combination with the metabolic data, the clearance was significantly under-predicted. In order to recover the plasma concentration time profile of atorvastatin acid prior to BPD-DS, $J_{max,OATP1B1}$ and Kp_{muscle} were re-estimated to 532.4 pmol/min/million cells and 4.0, utilising weighted least square Nelder-Mead minimisation method in the parameter estimation toolbox within the Simcyp® Simulator (Skottheim *et al.*, 2010).

$$CLu_{H,\text{int}} = \frac{ISEF \cdot V_{\max-rhCYP} \cdot Abundance \cdot MPPGL \cdot LiverWeight}{K_{m,u}}$$

Equation 4.4: IVIVE of $CLu_{H,int}$ from rCYP.

$$CLu_{G,\text{int}} = \frac{ISEF \cdot V_{\max-rhCYP} \cdot Abundance}{K_{m,u}}$$

Equation 4.5: IVIVE of $CLu_{G,int}$ from rCYP.

Sensitivity analysis was carried out with regards to potential gastrointestinal physiological parameters subject to potential alterations following surgery due to hormonal alterations, including: small intestinal transit time, villous blood flow (Q_{villi}), gastric emptying, small intestinal bile concentration, the enterocyte volume in the remaining small intestine (V_{ent}), post-surgical abundance of gastrointestinal CYP3A (GI CYP3A) and small intestinal effective permeability (P_{eff}).

Analysis

Simulated data was visually inspected against observed data. In addition, the potential mechanism of changes to oral drug absorption was examined through the simulations in terms of assessing the effects on plasma drug concentration time profile, maximum plasma drug concentration (C_{max}), time of maximum plasma drug concentration (t_{max}), f_a and F_G.

4.4 Results

Changes in oral drug bioavailability post bariatric surgery were demonstrated for cyclosporine and atorvastatin acid following Roux-en-Y gastric bypass (RYGB), biliopancreatic diversion with duodenal switch (BPD-DS) and jejunoileal bypass (JIB) (Marterre *et al.*, 1996; Chenhsu *et al.*, 2003; Skottheim *et al.*, 2009; Skottheim *et al.*, 2010). Sex, age, height and weight matched simulations were carried out based on corresponding clinical studies utilising post bariatric surgery models coupled to a full

PBPK distribution model into the Simcyp® Simulator. The results from the comparison of observed versus simulation studies are as follows:

4.4.1 Cyclosporine

Roux-en-Y gastric bypass

Following RYGB, Marterre and co-workers (Marterre *et al.*, 1996) reported a 194% increase in the daily dose per kg body weight in kidney transplant patients (n=3) of cyclosporine A (CsA) Sandimmune® solution. CsA trough blood levels were monitored from 6 months prior to RYGB up to 12 months postoperatively, using a TDx immunoassay. The observed reduction in exposure prompted an increase in the oral dose from 1.8 (±0.5) to 3.5 (±1.1) mg/kg/day in order to maintain pre-RYGB CsA trough levels (Figure 8.1 A-D) (Marterre *et al.*, 1996). Due to the reported over prediction of the TDx immunoassay, observed and simulated data were normalised for trough levels immediately before RYGB surgery, indicated by the time of 0 months (Figure 8.1 B and C) (Steimer, 1999).

In an age, sex, and weight matched virtual population, oral drug exposure of Sandimmune® CsA solution was simulated in 10 randomised trials consisting of 3 individuals in each trial (n=10·3). Cyclosporine displayed a reduction in f_a from 0.40 (5-95% confidence interval [CI95]: 0.24-0.59) to 0.19 (0.10-0.32) following RYGB, at a simulated small intestinal transit (SIT) time of 3.0h; whereas F_G remained unaltered at 0.86 (0.74-0.87). A 194% increase in dose level, resulted in a trough level ratio of 0.96 (0.58-1.44) as compared to the pre operative exposure at 0 months. Assuming a post surgical small intestinal transit time of 5.0h, cyclosporine displayed reduction in f_a to 0.26 (0.14-0.41), F_G remained unaltered. A 194% increase in the dose level resulted in an over prediction in post RYGB CsA trough levels, with a simulated post/pre surgical ratio of 1.45 (0.85-2.19) as compared to pre operative exposure at 0 months (Figure 8.1 A-D).

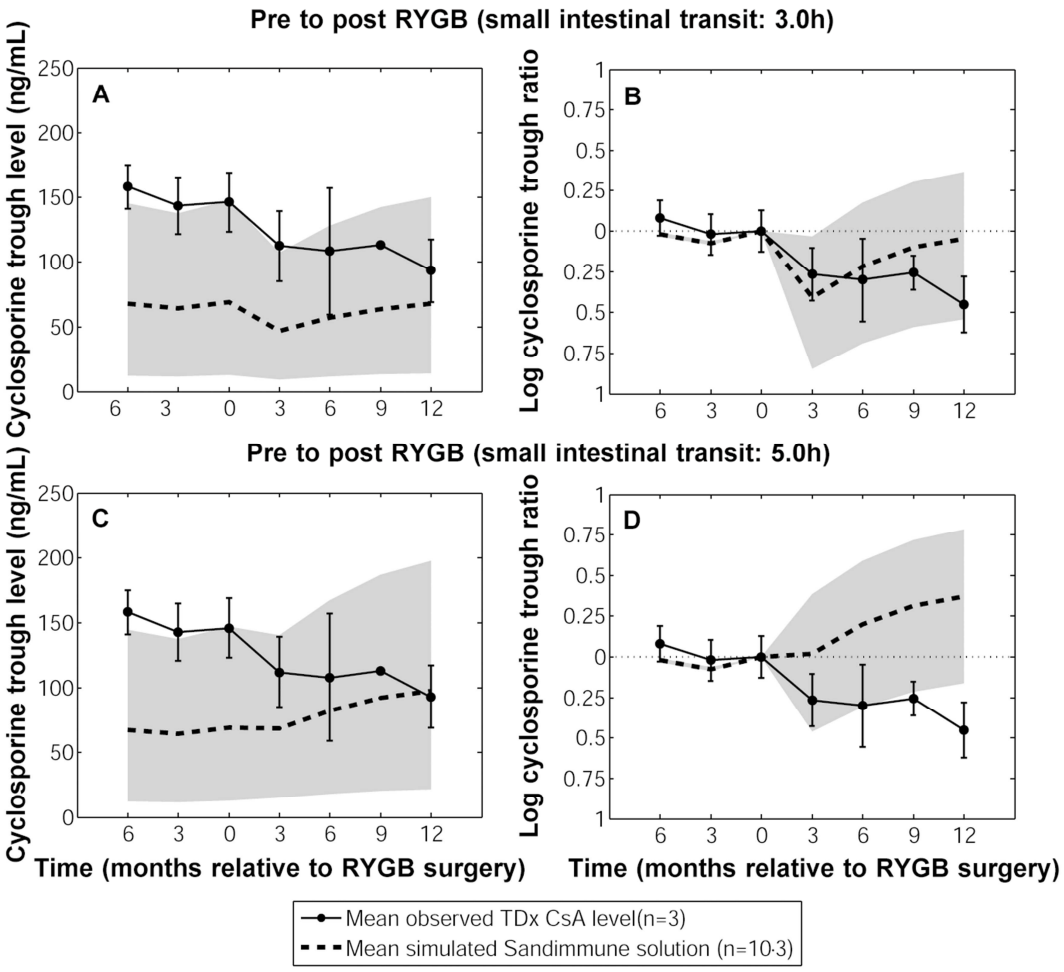

Figure 4.1. Mean and standard deviation of observed cyclosporine (CsA) TDx trough levels at steady state pre to post Roux-en-Y gastric bypass (RYGB) at -6, -3, 0, 3, 6, 9 and 12 months relative to RYGB surgical event (0 months). Time points from -6 to 12 months correspond to dose levels of: 1.7, 1.7, 1.8, 2.4, 2.8, 3.2, 3.5 mg/kg/day respectively (n patients=3) administered twice daily. Observed data is compared to simulated 50, 95 and 5% prediction interval, indicated by grey area, of cyclosporine Sandimmune® trough levels (n patients=10·3), A: Simulated post RYGB at a small intestinal transit time (SIT) of 3.0h, B: Log normalised simulated CsA trough ratio as compared to 0 months (RYGB SIT=3.0h), C: Simulated CsA trough levels at RYGB SIT of 5.0h, D: Log normalised simulated CsA trough ratio as compared to 0 months (RYGB SIT=5.0h) (Marterre *et al.*, 1996).

Simulations of the theoretical impact of RYGB on the solubilisation enhanced cyclosporine Neoral® microemulsion, at a post surgical SIT of 3.0h, produced an AUC ratio of 1.84 (1.26-2.37) at 12 months post surgery as compared to levels at 0 months

relative to RYGB surgery. The observed increase in oral exposure of Neoral® was due to a 194% dose increase, where f_a displayed an increase from 0.72 (0.47-0.92) to 0.82 (0.57-0.94); whereas F_G increased from 0.90 (0.81-0.96) to 0.94 (0.90-0.98) (Appendices 8.3).

Jejunoileal bypass

In a case study by Chenhsu, and co-workers (2003), CsA blood levels at 2 hours post administration at steady state (C2) administered as Neoral® microemulsion in controls (n=7) and post JIB (n=1), displayed a reduced exposure when comparing the mean C2 concentration over the administered dose range, reporting a reduction in C2 levels of approximately 59% (Chenhsu *et al.*, 2003).

Simulating demographically matched morbidly obese controls (n=10·7) and post JIB patients (SIT=0.4h; n=10·1), cyclosporine displayed a reduction in C2 levels from 452 (153-776) to 357 (103-650) ng/mL at a dose level of 4 mg/kg/day and from 2,528 (388-6089) to 1,632 (571-2,811) ng/mL, at a dose of 12 mg/kg/day. Simulated levels corresponded well with the linear regression of observed data as compare to the 5-95% prediction interval. The simulated reduction in oral drug exposure in the post JIB population as compared to controls was due to a reduction in f_a from 0.61 (0.35-0.86) to 0.12 (0.04-0.19); whereas F_G displayed a minor reduction from 0.90 (0.79-97) to 0.88 (0.75-0.96) at a therapeutic dose of 2 mg/kg/day. At a dose of 12 mg/kg/day a major reduction in f_a was observed from 0.34 (0.16-0.53) to 0.08 (0.01-0.18) whereas F_G was reduced from 0.91 (0.81-0.93) to 0.90 (0.80-0.97) (Figure 4.2).

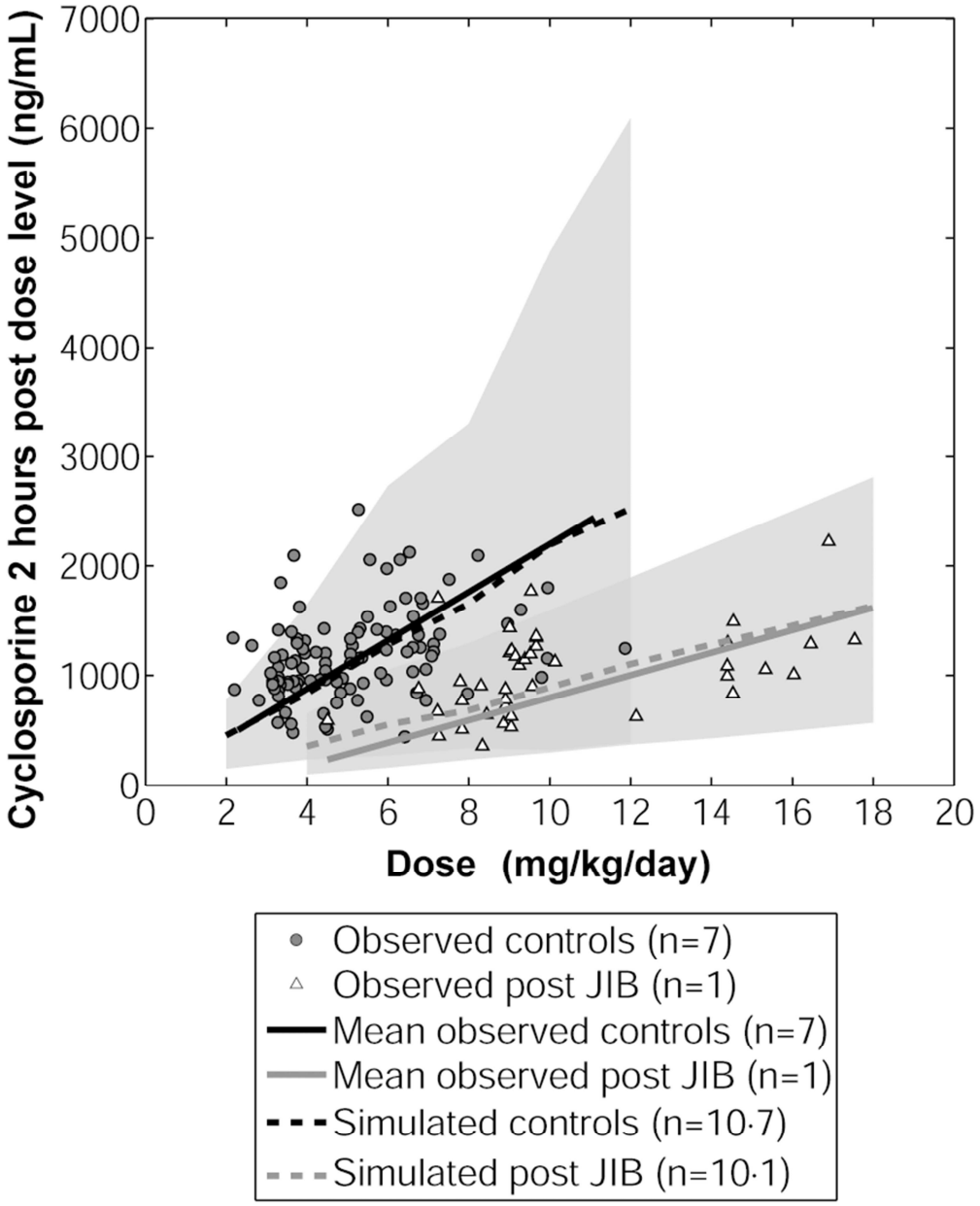

Figure 4.2. Observed mean blood concentration of cyclosporine microemulsion (Sandimmune® Neoral®, Novartis) at steady state 2 hours post dosing in controls (n =7) and one patient (n=1) post jejunoileal bypass (JIB)as compared to simulated sex and age matched controls (n=300) and post JIB (n patients=800)at a small intestinal transit time of 0.4 hours over dose range of 300 to 1,000 mg, where 5, 50 and 95% prediction intervals are indicated by grey areas (Chenhsu *et al.*, 2003).

Assuming a SIT of 0.7h post JIB, cyclosporine displayed a less apparent reduction in C2 levels due to a less apparent reduction in f_a to 0.19 (0.05-0.30) and 0.13 (0.02-0.26)

at corresponding dose levels of 2 and 12 mg/kg/day respectively. Post JIB (SIT=0.7h), F_G was altered to 0.89 (0.79-0.96) and 0.92 (0.84-0.98) at a therapeutic dose level of 2 and 12 mg/kg/day respectively (Appendices 8.3).

4.4.2 Atorvastatin

Roux-en-Y gastric bypass

In a clinical trial carried out on 12 morbidly obese patients, atorvastatin was administered as an immediate release (IR) tablet of 20-80 mg in fasted state where patients were allowed to eat two hours post administration. Plasma concentration profiles were obtained from 0-8 hours after drug administration pre and three to six weeks post RYGB. The pre to post surgical trend in oral exposure displayed a high variability where the overall reported trend displayed a median post/pre surgery AUC ratio of 1.12 (range: 0.34-2.33), albeit being statistically insignificant (Skottheim *et al.*, 2009).

Virtual simulations for oral drug exposure of atorvastatin acid pre to post RYGB were conducted in 10 randomised trials, each consisting of 12 age, sex and BMI matched individuals (n=10·12). Assuming a reduction in small intestinal transit as function of the small intestinal bypass (SIT=3.0h), resulted in an overall increase in AUC with a simulated median post/pre surgical AUC ratio of 1.13, capturing 100% of observed data within the simulated 95% prediction interval of 0.27-3.80 (Figure 4.3). Alternatively, with an increase in small intestinal transit time post RYGB (SIT=5.0h), atorvastatin acid displayed a median post/pre surgical AUC ratio of 1.42 (0.34-4.91) (Appendices 8.3).

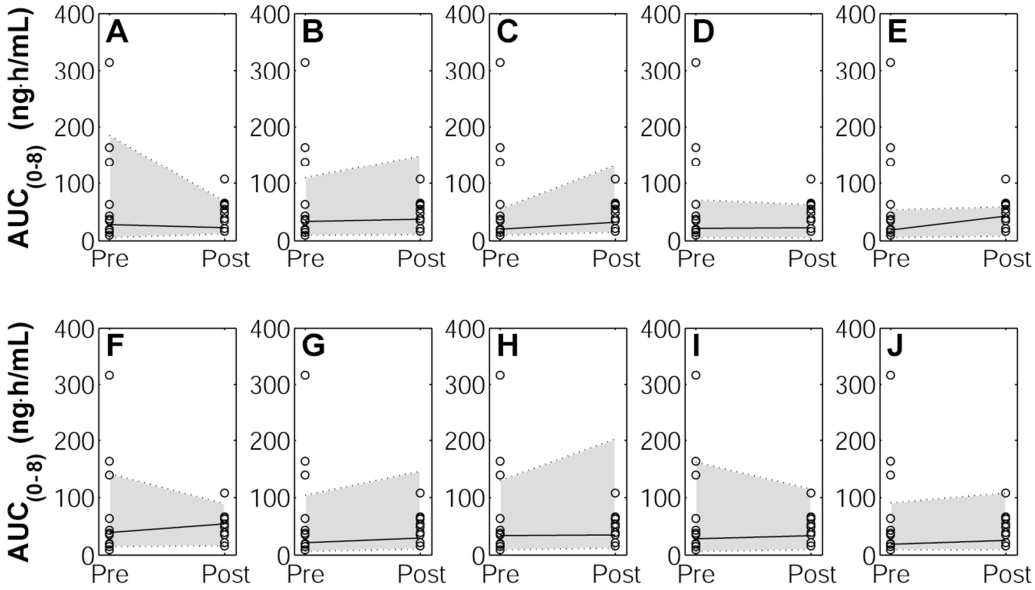

Figure 4.3. Simulated 50, 95 and 5% prediction interval (indicated by grey areas) of oral drug exposure of atorvastatin acid in randomised trials of age, sex, dose and BMI (Body Mass Index) matched patients pre to post Roux-en-Y gastric bypass surgery (small intestinal transit=3.0h) as compared to observed data A-J: Ten randomised simulated trials consisting of 10 individuals in each trial (n individuals=10·12), as compared to observed (n=12; ○) (Skottheim *et al.*, 2009).

Simulated increase in exposure of atorvastatin following RYGB (SIT=3.0h) was due to a reduction in f_a from 0.58 (0.33-0.77) to 0.54 (0.29-0.74) counteracted by an increase in F_G from 0.69 (0.48-0.86) to 0.73 (0.53-0.88) (Figure 4.4). Assuming a reduced small intestinal motility (RYGB SIT=5.0h), the more apparent increase in AUC was the result of an extensive increase in f_a.

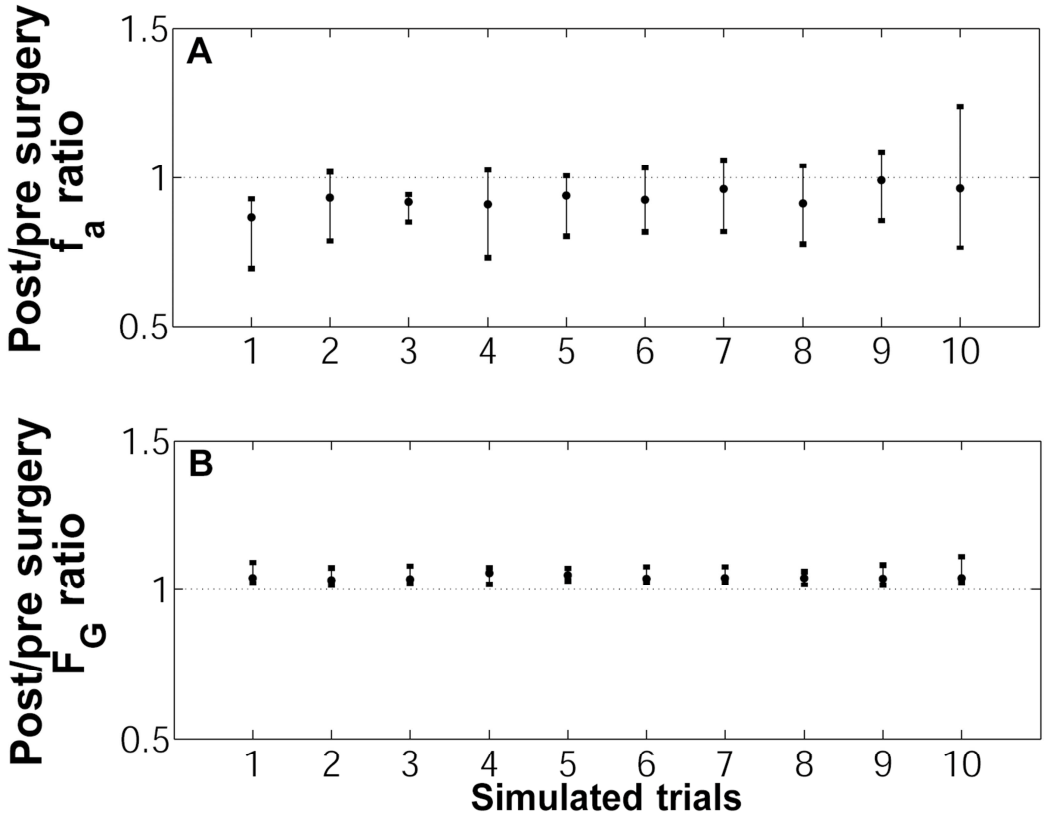

Figure 4.4. Simulated 50, 95% and 5% prediction intervals of the ratio of A: fraction of dose absorbed in the intestine (f_a), and B: fraction escaping gut wall metabolism (F_G)of atorvastatin acid pre to post Roux-en-Y gastric bypass surgery (small intestinal transit=3.0h) in ten individually simulated randomised trials (1-10) consisting of ten individuals in each pre and post surgery (n individuals=10·10) (Skottheim *et al.*, 2009).

Biliopancreatic diversion with duodenal switch

Atorvastatin IR tablet 20-80 mg administered in the fasted state, allowing feeding at 2 hours, displayed a significant increase in oral drug exposure following BPD-DS in 10 morbidly obese patients, with an observed mean AUC ratio of 2.0 (±1.0) and observed increase in the C_{max} from 20.0 ng/mL (±24.9) to 28.0 (±22.5), whereas t_{max} increased from 1.2h (±0.8) to 2.3h (±1.0) post BPD-DS (Skottheim *et al.*, 2010).

Predicted plasma concentration-time profiles of atorvastatin acid were consistent with observed data prior to surgery in a morbidly obese population (Appendices 8.3).

However, simulated plasma concentration-time profiles following BPD-DS (SIT=1.2h) were unable to capture the observed increase in oral drug exposure. The predicted AUC ratio of 0.90 (0.16-2.24), was lower than expected due to a reduction in f_a from 0.61 (0.34-0.79) to 0.39 (0.06-0.72) which was counteracted by an increase in F_G from 0.69 (0.59-0.79) to 0.72 (0.63-0.81). C_{max} displayed a minor increase, with a post/pre BPD-DS C_{max} ratio of 1.32 (0.31-2.38), whereas t_{max} displayed a post/pre BPD-DS ratio of 0.62 (0.31-1.00). The simulated pre to post BPD-DS alterations in AUC, C_{max} and t_{max} correspond to the central points of Figure 4.5A, B and C respectively.

Sensitivity analysis was performed to assess the impact of potential physiological alterations post surgery on the plasma exposure of atorvastatin acid, including the impact of: SIT, gastric emptying time, bile concentration in the terminal ileum, small intestinal enterocyte volume (V_{ent}), gastrointestinal CYP3A content (GI CYP3A) and small intestinal permeability (P_{eff}). The AUC was insensitive to changes in the post surgical bile concentration and V_{ent}. Following BPD-DS (SIT=1.2h) a five-fold increase in P_{eff} led to a post/pre surgical AUC ratio of 1.93 (0.60-5.53), whereas C_{max} displayed a post/pre surgical ratio of 4.36 (1.23-9.68). A five-fold increase in Q_{villi} resulted in a minor increase in AUC with a simulated post/pre AUC BPD-DS ratio of 1.24 (0.22-3.24) and a C_{max} ratio of 1.86 (0.47-4.19). A reduction in GI CYP3A by 5-fold, gave a post/pre BPD-DS AUC ratio of 1.13 (0.19-3.06) (Figure 4.5).

Pre to post BPD-DS (SIT=4.2h) displayed an AUC ratio of 1.71 (0.74-5.79), C_{max} ratio of 1.56 (0.69-3.39) and a t_{max} ratio of 0.87 (0.51-1.31). In the sensitivity analysis a two-fold increase in Q_{villi} resulted in a post/pre surgery AUC ratio of 2.07 (0.86-6.96) and a C_{max} ratio of 1.91 (0.84-4.22), whereas t_{max} remained unaltered. A two-fold increase in P_{eff} displayed a post/pre BPD-DS AUC ratio of 2.11 (0.90-6.91), a C_{max} ratio of 2.64 (1.17-5.66) and a minor reduction in t_{max}. A two-fold reduction in GI CYP3A gave a post/pre surgery AUC ratio of 1.99 (0.83-6.76), whereas C_{max} saw a minor increase, displaying an AUC ratio of 1.80 (0.79-4.00). Gastric emptying had the most apparent impact on t_{max}, where a five-fold increase resulted in a post/pre BPD-DS ratio of 1.78 (1.11-2.58) (Figure 4.5).

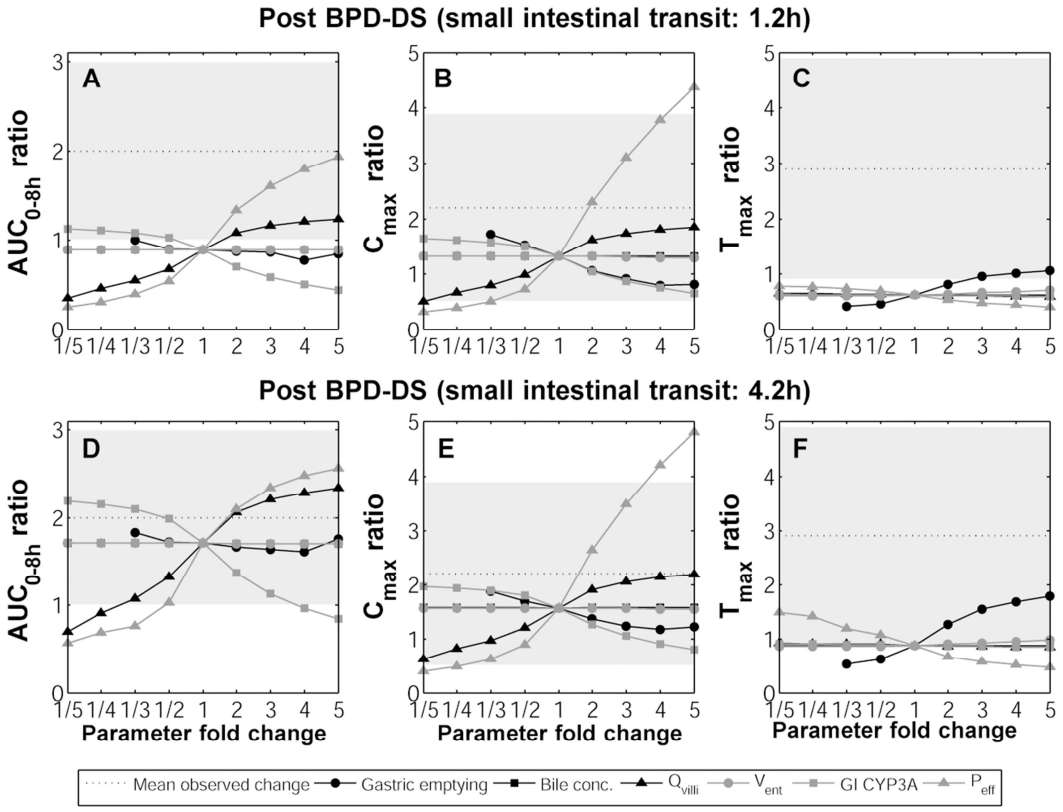

Figure 4.5. Spider plot of sensitivity analysis of simulated post/pre biliopancreatic diversion with duodenal switch (BPD-DS) at a small intestinal transit time (SIT) of 1.2h A: $AUC_{0\text{-}8h}$, B: C_{max} and C: t_{max} ratio, BPD-DS (SIT=4.2h) D: $AUC_{0\text{-}8h}$, E: C_{max} and F: t_{max} ratio, examining the impact of the fold change in physiological parameters: gastric emptying, ileal bile concentration (bile conc.), villous blood flow (Q_{villi}), enterocytic volume (V_{ent}) in the remaining post surgical small intestine, post BPD-DS gastrointestinal CYP3A content, small intestinal permeability (P_{eff}), as compared to mean observed ratio pre to post BPD-DS.

4.5 Discussion

4.5.1 Cyclosporine

The immunosuppressant cyclosporine (molecular weight 1202.61 g/mol) displays poor aqueous solubility and a relatively low permeability due to its lipophilic and bulky character making the compound dependent on bile mediated solubility to facilitate absorption (Venkataramanan *et al.*, 1985; Mehta *et al.*, 1988). The drug is mainly metabolised by CYP3A4 in the intestine and liver and is subject to P-glycoprotein

efflux (Lown *et al.*, 1997; Wojcikowski *et al.*, 2003). The oral bioavailability displays a high interindividual variability, ranging from 5-89% for Sandimmune® formulation, whereas Neoral® displays improved absorption properties and an oral bioavailability of 21-73% (Paine *et al.*, 2000).

The simulated underprediction of Sandimmune® TDx trough levels prior to RYGB surgery was expected and is most likely due to the unspecificity of the immunoassay displaying a high cross-reactivity between the parent compound and metabolites resulting in a significantly higher variability in the trough levels as compared to peak concentrations (Marterre *et al.*, 1996; Steimer, 1999).

Normalising simulated cyclosporine trough levels to pre RYGB levels produced a reduction in exposure comparable to observed data. Further, a simulated 194% increase in Sandimmune® dose levels recovered pre surgical trough levels as stated in the publication (Marterre *et al.*, 1996).

In the simulation study of cyclosporine Neoral® microemulsion pre to post JIB, observed data of the control population was well described within the 95% prediction interval of the simulated data; whereas the observed exposure post JIB was well described within the 95% prediction interval of simulated data assuming a reduction in small intestinal transit time equivalent to the bypass (SIT=0.4h). An alternative 'what-if' scenario simulating a longer transit time (SIT=0.7h) over predicted the observed mean blood concentration post JIB as reported by Chenhsu, and co-workers (Figure 4.2). The overprediction could suggest small intestinal motility to remain unaltered following JIB or be a result of a small post surgical study population (n=1), displaying a low study power, albeit the simulated magnitude of reduction in C2 levels post JIB (SIT=0.4h) closely matched the estimated reduction in cyclosporine exposure following JIB in another case study where a patient was subject to a surgical reversal of the procedure. The reversed JIB produced an observed 2.78-fold increase in exposure in the case study (Knight *et al.*, 1988; Chenhsu *et al.*, 2003).

The simulated discrepancy in oral drug exposure of Sandimmune® and Neoral® pre to post RYGB, where bariatric surgery had the highest effect on the oral bioavailability of Sandimmune®, highlights the importance of formulation characteristics and its impact

on oral drug bioavailability pre to post bariatric surgery. The choice of a solubilised biopharmaceutical formulation such as a self-micro-emulsifying drug delivery system, solution or dispersible tablet may be considered as a first hand choice for patients undergoing bariatric surgery and are treated with limited solubility drugs with a narrow therapeutic index. This suggestion supports earlier observations in clinical practice, where alterations in pharmacotherapy post bariatric surgery aim at switching to formulations displaying improved dissolution properties (Darwich *et al.*, 2012a).

Atorvastatin

The HMG-CoA reductase inhibitor atorvastatin, which is administered in the acid form, displays a high solubility and permeability. The compound is extensively metabolised in the small intestine and liver, namely by CYP3A4 but also via the UGT1A1 and UGT1A3 route. Atorvastatin acid and the lactone metabolite are also subject to inter-conversion by the UGTs and another minor chemical pathway. Atorvastatin acid is a substrate of P-glycoprotein efflux and OATP1B1 mediated active hepatic uptake (Lennernas, 2003).

Trends in simulated oral drug exposure of atorvastatin pre to post RYGB were consistent with observed data, where simulated trends in f_a and F_G suggested that an interplay between reduced absorption area and bypass of regions highly abundant in CYP3A is of high importance when considering the overall effect on oral bioavailability. Simulated RYGB (SIT=3.0h) produced the closest agreement with observed data of atorvastatin exposure following RYGB, again suggesting a reduction in small intestinal transit time to be the most likely consequence of surgery (Skottheim *et al.*, 2009).

The inability to recover the observed 2-fold increase in atorvastatin AUC pre to post BPD-DS at a simulated SIT of 1.2h, may suggest additional post surgical physiological parameters to be governing the trend in oral drug bioavailability post BPD-DS. The exploratory sensitivity analysis identified a number of potential parameters leading to a comparable increase in oral drug exposure pre to post BPD-DS. An increase in small intestinal transit following BPD-DS, corresponding to the linear regression relationship between mouth to caecum transit time and plasma levels of peptide YY, resulted in an AUC ratio of 1.71 (0.74-5.79). Further, a simulated two-fold increase in P_{eff} and Q_{villi}, or

a two-fold reduction in the gastrointestinal content of CYP3A post BPD-DS (SIT=4.2h) recovered the observed AUC of atorvastatin. The reoccurring under prediction of t_{max} following surgery may be explained by an altered postprandial response causing a delayed absorption.

These findings suggest that additional physiological parameters, such as impairment in permeability or redistribution of intestinal blood flow, may play an important role in governing trends in oral drug exposure pre to immediately post BPD-DS. The results highlight the surgery specific trends observed post bariatric surgery due to the intricate interplay between fluid dynamics, absorption area, transporters, metabolism and gastrointestinal physiology.

Current limitations in simulating the impact of oral drug bioavailability following bariatric surgery include the lack of clinical and post surgical physiological data. Nonetheless, the models integrate all available knowledge on changes known to occur in the GI tract following bariatric surgery and can assist with dosage recommendation when there is an absence of clinical observations.

4.6 Conclusions

In this work we demonstrated the potential of a physiologically-based pharmacokinetic modelling and simulation to predict oral drug bioavailability post bariatric surgery by evaluating earlier developed models using observed data for cyclosporine and atorvastatin. Trends in oral drug exposure of atorvastatin and cyclosporine were predicted well within the 95% prediction interval following Roux-en-Y gastric bypass utilising the previously developed model at a small intestinal transit time of 3.0 hours. The results suggest a reduction in small intestinal transit time to be the most likely scenario following RYGB. The observed increase in atorvastatin exposure following biliopancreatic diversion with a duodenal switch could not be captured utilising the developed BPD-DS model incorporating all known physiological alterations.

A mechanistic PBPK modelling approach has the potential to serve as a tool in examining the impact of physiological alterations on oral drug bioavailability in the

absence of clinical data. The demonstrated approach may allow a framework for optimisation of oral drug therapy post bariatric surgery.

4.7 Acknowledgements

The authors wish to thank Prof. Basil Ammori, Salford Royal Hospital NHS Foundation Trust and Dr. David Turner, Simcyp (a Certara company) for discussions leading up to this work; and Mr James Kay for his assistance with the manuscript.

4.8 Conflict of interest

The authors reported no conflicts of interest.

4.9 Study highlights

4.9.1 What is the current knowledge?

Patients undergoing bariatric surgery receive various therapeutic drugs. A limited number of studies have investigated oral drug exposure postoperatively. Bariatric surgery models were previously developed using the ADAM model within the PBPK simulator, Simcyp.

4.9.2 What question this study addressed?

We report on the evaluation of previously developed bariatric surgery PBPK models by comparing observed vs. predicted impact of surgery on oral exposure of cyclosporine and atorvastatin.

4.9.3 What this study adds to our knowledge

Trends in oral exposure of atorvastatin and cyclosporine were well predicted following RYGB. Observed increase in atorvastatin exposure following BPD-DS could not be captured using the current model.

4.9.4 How this might change clinical pharmacology and therapeutics

The potential of a PBPK modelling approach was demonstrated, allowing a framework for optimizing oral drug therapy post-bariatric surgery. Developed models integrated available knowledge on physiological changes. The study highlights areas of further research, where models are not predictive due to the lack of information on systems parameters.

4.10 References

Amundsen R, Christensen H, Zabihyan B, and Asberg A (2010) Cyclosporine A, but not tacrolimus, shows relevant inhibition of organic anion-transporting protein 1B1-mediated transport of atorvastatin. *Drug Metab Dispos* **38:**1499-1504.

Behrns KE, Smith CD, and Sarr MG (1994) Prospective evaluation of gastric acid secretion and cobalamin absorption following gastric bypass for clinically severe obesity. *Dig Dis Sci* **39:**315-320.

Bernareggi A and Rowland M (1991) Physiologic modeling of cyclosporin kinetics in rat and man. *J Pharmacokinet Biopharm* **19:**21-50.

Buchwald H and Oien DM (2009) Metabolic/bariatric surgery Worldwide 2008. *Obes Surg* **19:**1605-1611.

Buell MG and Harding RK (1989) Effects of peptide YY on intestinal blood flow distribution and motility in the dog. *Regul Pept* **24:**195-208.

Chenhsu RY, Wu Y, Katz D, and Rayhill S (2003) Dose-adjusted cyclosporine c2 in a patient with jejunoileal bypass as compared to seven other liver transplant recipients. *Ther Drug Monit* **25:**665-670.

Darwich AS, Henderson K, Burgin A, Ward N, Whittam J, Ammori BJ, Ashcroft DM, and Rostami-Hodjegan A (2012a) Trends in oral drug bioavailability following bariatric surgery: Examining the variable extent of impact on exposure of different drug classes. *Br J Clin Pharmacol* **74:**774-787.

Darwich AS, Pade D, Ammori BJ, Jamei M, Ashcroft DM, and Rostami-Hodjegan A (2012b) A mechanistic pharmacokinetic model to assess modified oral drug bioavailability post bariatric surgery in morbidly obese patients: interplay between CYP3A gut wall metabolism, permeability and dissolution. *J Pharm Pharmacol* **64:**1008-1024.

Flegal KM, Carroll MD, Ogden CL, and Curtin LR (2010) Prevalence and trends in obesity among US adults, 1999-2008. *JAMA* **303:**235-241.

Gaggiotti G, Catassi C, Sgattoni C, Bonucci A, Ricci S, Spazzafumo L, and Coppa GV (1995) Modifications of Intestinal Permeability Test Induced by Biliopancreatic Diversion: Preliminary Results. *Obes Surg* **5:**424-426.

Garcia-Fuentes E, Garrido-Sanchez L, Garcia-Almeida JM, Garcia-Arnes J, Gallego-Perales JL, Rivas-Marin J, Morcillo S, Cardona I, and Soriguer F (2008) Different effect of laparoscopic Roux-en-Y gastric bypass and open biliopancreatic diversion of Scopinaro on serum PYY and ghrelin levels. *Obes Surg* **18:**1424-1429.

Ghobadi C, Johnson TN, Aarabi M, Almond LM, Allabi AC, Rowland-Yeo K, Jamei M, and Rostami-Hodjegan A (2011) Application of a systems approach to the

bottom-up assessment of pharmacokinetics in obese patients: expected variations in clearance. *Clin Pharmacokinet* **50:**809-822.

Goosen TC, Bauman JN, Davis JA, Yu C, Hurst SI, Williams JA, and Loi CM (2007) Atorvastatin glucuronidation is minimally and nonselectively inhibited by the fibrates gemfibrozil, fenofibrate, and fenofibric acid. *Drug Metab Dispos* **35:**1315-1324.

Hedberg J, Hedenstrom H, Karlsson FA, Eden-Engstrom B, and Sundbom M (2011a) Gastric emptying and postprandial PYY response after biliopancreatic diversion with duodenal switch. *Obes Surg* **21:**609-615.

Hedberg J, Hedenstrom H, and Sundbom M (2011b) Wireless pH-metry at the gastrojejunostomy after Roux-en-Y gastric bypass: a novel use of the BRAVO system. *Surg Endosc* **25:**2302-2307.

Horowitz M, Cook DJ, Collins PJ, Harding PE, Hooper MJ, Walsh JF, and Shearman DJ (1982) Measurement of gastric emptying after gastric bypass surgery using radionuclides. *Br J Surg* **69:**655-657.

Howgate EM, Rowland Yeo K, Proctor NJ, Tucker GT, and Rostami-Hodjegan A (2006) Prediction of in vivo drug clearance from in vitro data. I: impact of inter-individual variability. *Xenobiotica* **36:**473-497.

Jacobsen W, Kuhn B, Soldner A, Kirchner G, Sewing KF, Kollman PA, Benet LZ, and Christians U (2000) Lactonization is the critical first step in the disposition of the 3-hydroxy-3-methylglutaryl-CoA reductase inhibitor atorvastatin. *Drug Metab Dispos* **28:**1369-1378.

Jamei M, Marciniak S, Feng K, Barnett A, Tucker G, and Rostami-Hodjegan A (2009a) The Simcyp population-based ADME simulator. *Expert Opin Drug Metab Toxicol* **5:**211-223.

Jamei M, Turner D, Yang J, Neuhoff S, Polak S, Rostami-Hodjegan A, and Tucker G (2009b) Population-based mechanistic prediction of oral drug absorption. *AAPS J* **11:**225-237.

Knight GC, Macris MP, Peric M, Duncan JM, Frazier OH, and Cooley DA (1988) Cyclosporine A pharmacokinetics in a cardiac allograft recipient with a jejuno-ileal bypass. *Transplant Proc* **20:**351-355.

Lau YY, Huang Y, Frassetto L, and Benet LZ (2007) effect of OATP1B transporter inhibition on the pharmacokinetics of atorvastatin in healthy volunteers. *Clin Pharmacol Ther* **81:**194-204.

Lennernas H (2003) Clinical pharmacokinetics of atorvastatin. *Clin Pharmacokinet* **42:**1141-1160.

Lown KS, Mayo RR, Leichtman AB, Hsiao HL, Turgeon DK, Schmiedlin-Ren P, Brown MB, Guo W, Rossi SJ, Benet LZ, and Watkins PB (1997) Role of intestinal P-glycoprotein (mdr1) in interpatient variation in the oral bioavailability of cyclosporine. *Clin Pharmacol Ther* **62:**248-260.

Malone M and Alger-Mayer SA (2005) Medication use patterns after gastric bypass surgery for weight management. *Ann Pharmacother* **39:**637-642.

Marterre WF, Hariharan S, First MR, and Alexander JW (1996) Gastric bypass in morbidly obese kidney transplant recipients. *Clin Transplant* **10:**414-419.

Mehta MU, Venkataramanan R, Burckart GJ, Ptachcinski RJ, Delamos B, Stachak S, Van Thiel DH, Iwatsuki S, and Starzl TE (1988) Effect of bile on cyclosporin absorption in liver transplant patients. *Br J Clin Pharmacol* **25:**579-584.

Mendieta-Zeron H, Larrad-Jimenez A, Burrell MA, Rodriguez MM, Da Boit K, Fruhbeck G, and Dieguez C (2011) Biliopancreatic diversion induces villi elongation and cholecystokinin and ghrelin increase. *Diabetes Metab Syndr* **5:**66-70.

Mueller EA, Kovarik JM, van Bree JB, Tetzloff W, Grevel J, and Kutz K (1994) Improved dose linearity of cyclosporine pharmacokinetics from a microemulsion formulation. *Pharm Res* **11:**301-304.

OECD (2011) Obesity and the Economics of Prevention: Fit not Fat - United Kingdom (England) Key Facts, OECD.

Paine MF, Davis CL, Shen DD, Marsh CL, Raisys VA, and Thummel KE (2000) Can oral midazolam predict oral cyclosporine disposition? *Eur J Pharm Sci* **12:**51-62.

Pellegrini CA, Deveney CW, Patti MG, Lewin M, and Way LW (1986) Intestinal transit of food after total gastrectomy and Roux-Y esophagojejunostomy. *Am J Surg* **151:**117-125.

Picot J, Jones J, Colquitt JL, Gospodarevskaya E, Loveman E, Baxter L, and Clegg AJ (2009) The clinical effectiveness and cost-effectiveness of bariatric (weight loss) surgery for obesity: a systematic review and economic evaluation. *Health Technol Assess* **13:**1-190, 215-357, iii-iv.

Prueksaritanont T, Tang C, Qiu Y, Mu L, Subramanian R, and Lin JH (2002) Effects of fibrates on metabolism of statins in human hepatocytes. *Drug Metab Dispos* **30:**1280-1287.

Savage AP, Adrian TE, Carolan G, Chatterjee VK, and Bloom SR (1987) Effects of peptide YY (PYY) on mouth to caecum intestinal transit time and on the rate of gastric emptying in healthy volunteers. *Gut* **28:**166-170.

Skottheim IB, Jakobsen GS, Stormark K, Christensen H, Hjelmesaeth J, Jenssen T, Asberg A, and Sandbu R (2010) Significant increase in systemic exposure of atorvastatin after biliopancreatic diversion with duodenal switch. *Clin Pharmacol Ther* **87:**699-705.

Skottheim IB, Stormark K, Christensen H, Jakobsen GS, Hjelmesaeth J, Jenssen T, Reubsaet JL, Sandbu R, and Asberg A (2009) Significantly altered systemic exposure to atorvastatin acid following gastric bypass surgery in morbidly obese patients. *Clin Pharmacol Ther* **86:**311-318.

Smith CD, Herkes SB, Behrns KE, Fairbanks VF, Kelly KA, and Sarr MG (1993) Gastric acid secretion and vitamin B12 absorption after vertical Roux-en-Y gastric bypass for morbid obesity. *Ann Surg* **218:**91-96.

Steimer W (1999) Performance and specificity of monoclonal immunoassays for cyclosporine monitoring: how specific is specific? *Clin Chem* **45:**371-381.

Suzuki S, Ramos EJ, Goncalves CG, Chen C, and Meguid MM (2005) Changes in GI hormones and their effect on gastric emptying and transit times after Roux-en-Y gastric bypass in rat model. *Surgery* **138:**283-290.

Venkataramanan R, Starzl TE, Yang S, Burckart GJ, Ptachcinski RJ, Shaw BW, Iwatsuki S, Van Thiel DH, Sanghvi A, and Seltman H (1985) Biliary Excretion of Cyclosporine in Liver Transplant Patients. *Transplant Proc* **17:**286-289.

Wittgrove AC and Clark GW (2000) Laparoscopic gastric bypass, Roux-en-Y- 500 patients: technique and results, with 3-60 month follow-up. *Obes Surg* **10:**233-239.

Wojcikowski J, Pichard-Garcia L, Maurel P, and Daniel WA (2003) Contribution of human cytochrome p-450 isoforms to the metabolism of the simplest phenothiazine neuroleptic promazine. *Br J Pharmacol* **138:**1465-1474.

Chapter 5: Assessing the turnover of the intestinal epithelia in pre-clinical species and humans

Chapter 5: Assessing the turnover of the intestinal epithelia in pre-clinical species and humans

A.S. Darwich, U. Aslam, D.M. Ashcroft, A. Rostami-Hodjegan

In preparation

5.1 Abstract

Due to the rapid turnover of the small intestinal epithelia, the rate at which enterocyte renewal occurs plays an important role in determining the level drug-metabolising enzymes in the gut wall. Current physiologically-based pharmacokinetic (PBPK) models consider enzyme and enterocyte recovery as a lumped first-order rate. An assessment of the enterocyte turnover would allow enzyme and enterocyte renewal to be modelled more mechanistically. A comprehensive literature search together with statistical analysis was employed in order to establish the enterocyte turnover (or lifespan) in human and pre-clinical species. A total of 54 studies were identified reporting enterocyte turnover in 929 subjects in six species (mouse, rat, guinea pig, hamster, pig and human). In the mouse, the weighted combined geometric mean (WX) enterocyte turnover was 2.78 (±1.06, n=113) days. In the rat, the weighted arithmetic mean enterocyte turnover was determined to be 2.01 days (n=287). Combined human enterocyte turnover data (n=265) exhibited a WX turnover of 3.48 (±1.55) days for the gastrointestinal epithelia, thus displaying comparable turnover to that of Cytochrome P450 enzymes as determined *in vitro* (0.96-4.33 days). Statistical analysis indicated that humans display a longer enterocyte turnover time as compared to pre-clinical species. Human data was too sparse to support regional differences in small intestinal enterocyte turnover despite being indicated in mouse. The utilisation of enterocyte turnover data, together with *in vitro* enzyme turnover, in PBPK modelling may be of assistance in improving predictions of drug-drug interactions and gastrointestinal metabolism in special populations where enterocyte turnover may be altered.

5.2 Introduction

Physiologically-based pharmacokinetic (PBPK) models of oral drug absorption and gut-wall metabolism may be implemented at a varying degree of complexity from simple first-order rate of absorption into the enterocytes to more sophisticated segmented models of the intestinal tract, such as the advanced compartmental absorption and transit (ACAT) model, advanced dissolution absorption and metabolism (ADAM) model and the segregated flow model (SFM); allowing the incorporation of segmentally segregated blood flows and regional variations in permeability, mucosal volumes and metabolic capacity (Agoram *et al.*, 2001; Pang, 2003; Darwich *et al.*, 2010). PBPK modelling of the oral component of drug bioavailability allows the estimation of the gut-wall extraction and further implementation to accommodate mechanistic prediction of drug-drug interactions (DDIs) in the small intestine, including: Reversible inhibition, mechanism-based inhibition (MBI) and enzyme induction (Fahmi *et al.*, 2009; Rowland Yeo *et al.*, 2010).

Furthermore, the utilisation of PBPK modelling and simulation of oral drug absorption processes enables the extrapolation of gastrointestinal drug disposition to special disease populations allowing the investigation drug-disease interactions where the metabolic capacity may be altered, such as post bariatric surgery or untreated coeliac disease (Johnson *et al.*, 2001; Darwich *et al.*, 2012; Darwich *et al.*, 2013).

Dynamic modelling of intestinal metabolism requires knowledge of the level of enzyme in the gut-wall where the amount of active enzyme at steady state is a product of rate of synthesis and degradation, a process generally referred to as turnover. Enzyme turnover plays an important role in the pharmacokinetic outcome and model-based prediction of MBIs and enzyme induction in the small intestine, where the reliance upon small intestinal enzyme turnover becomes especially apparent for drugs exhibiting high small intestinal metabolism and for substrates of cytochrome P450 (CYP) 3A, being the most abundant enzyme in the gut (Yang *et al.*, 2008).

Current PBPK models do not account for the nesting of enzyme turnover and enterocyte turnover and instead utilises a lumped first-order enzyme turnover rate informed via indirect measures, such as clinical MBI studies. Accounting for the nesting of enzyme turnover within the enterocytes may provide a framework for improved predictions of

mechanism-based inhibition, enzyme induction, and special subpopulations where the turnover may potentially be altered. The utilisation of enterocyte turnover does however require the data to inform such parameters. Where earlier research has characterised the indirect and *in vitro* enzyme turnover utilising meta-analysis no similar efforts have been made to establish enterocyte turnover (Yang *et al.*, 2008).

Physiologically, the enterocytes are produced through cell division of progenitor stem cells in the crypt at the base of the villi in the intestinal tissue. These progenitor cells are subject to proliferation into enterocytes and other functional cells through cell division. Mature enterocytes will migrate up the crypt-villous axis where the turnover will be governed by apoptosis and shedding into the gut lumen at the tip of the villi. The time from enterocyte generation to shedding will occur within days after proliferation (Wilson and Potten, 2004; Malato *et al.*, 2011).

The aim of the current study was to assess the enterocyte turnover in pre-clinical species and human and to identify the most commonly utilised methods for determining enterocyte turnover.

5.3 Methods

A comprehensive literature search was performed in order to identify published data on direct determination of full small intestinal (duodenum, jejunum and ileum) enterocyte turnover, lifespan, cell cycle or migration rate in healthy adults in preclinical species (including: rat, mouse, pig, dog, guinea pig, rabbit and hamster) as well as methods utilised to determine the turnover, using PubMed (1950-2013). For human data the literature was extended to include gastric, colonic and rectal epithelial cells and patient populations due to the sparsity of data. Additional sources were identified through publication citations for all species.

Collated data was analysed using descriptive statistics, calculating weighted arithmetic means (WX) utilising reported means (x_i) and sample size (n_i) of individual studies (Equation 5.1). Studies reporting mean data only where n_j was not clearly stated were penalised assuming $n_j = 1$; whereas for studies where the mean and standard deviation were reported without clearly stating n_j were assigned $n_j = 3$. The combined standard

deviation (overall SD) was obtained through calculating the total sum of squares (overall SS) (Equation 5.2 and Equation 5.3). When data allowed, the geometric mean (GM) and geometric standard deviation (GSD) of the enterocyte turnover were calculated by calculating σ (lnSD; Equation 5.4 and Equation 5.5), using the reported mean and variance and μ (lnGM; Equation 5.6 and Equation 5.7). Statistical analysis was carried out to test for regional and interspecies differences in enterocyte turnover using Welch's t test (P<0.05) with post-hoc Dunn-Šidák correction in Matlab® R2010a (Mathworks, Natick, USA) using sample means (X), size (n) and standard deviations (s^2) where data allowed (Equation 5.8).

$$WX = \frac{\sum_{i=1}^{n} n_1 \cdot X_i}{\sum_{i=1}^{n} n_i}$$

Equation 5.1. Weighted mean.

$$Overall\ SS = \sum_{i=1}^{n} [(SD_i^2 + X_i^2) + n_i] - N \cdot WX^2$$

Equation 5.2. Overall sum of squares.

$$Overall\ SD = \sqrt{\frac{Overall\ SS}{N}}$$

Equation 5.3. Overall standard deviation.

$$\sigma = \sqrt{\ln\left(\frac{variance}{X^2} + 1\right)}$$

Equation 5.4. logarithmic standard deviation.

$$GSD = e^{\sigma}$$

Equation 5.5. Geometric standard deviation.

$$\mu = lnX - \frac{1}{2} \cdot ln\left(\frac{1}{2} \cdot \sigma^2\right)$$

Equation 5.6. Logarithmic mean.

$$GM = e^{\mu}$$

Equation 5.7. Geometric mean.

$$t = \frac{X_1 - X_2}{\sqrt{\frac{s_1^2}{N_1} - \frac{s_2^2}{N_2}}}$$

Equation 5.8. Welch's t test.

5.4 Results

Overall, a total of 54 studies where identified reporting enterocyte turnover in 954 subjects in 6 species. In a majority of the studies determination of enterocyte turnover was carried out using isotope labelling utilising ^{3}H-thymidine or BrdUrd (81%), the remainder were carried out using techniques such as mitotic arrest methods with colchine and vincristine, and turnover determination in biopsy samples. Underneath follows an account for some of the most common methods for determining enterocyte turnover.

5.4.1 Methods for determining the turnover of enterocytes

Various *in vivo* and *in vitro* methods exist for determining the turnover of the enterocytes where many of these remain consistent across different tissues. The small intestinal epithelia differ from other physiological cell lines in the sense that it is a highly organised tissue allowing the study of cell migration within the tissue (Wilson and Potten, 2004).

Isotope labelling methods

The most commonly used method for measuring enterocyte turnover is the 'pulse-chase' method, where the DNA of a population of cells is labelled with an isotopic nucleoside, such as ^{3}H-thymidine, or a synthetic isotopic analogue such as bromodeoxyuridine (BrdUrd). Following administration of the isotopic nucleotide the

label will incorporate into the DNA during the synthetic phase (S-phase). The cell line can be monitored post labelling using autoradiography as cells are progressing through their life cycles, thus allowing quantitative determination of the time span of these different phases (Figure 5.1) (Quastler and Sherman, 1959; Creamer, 1967; Scragg and Johnson, 1980).

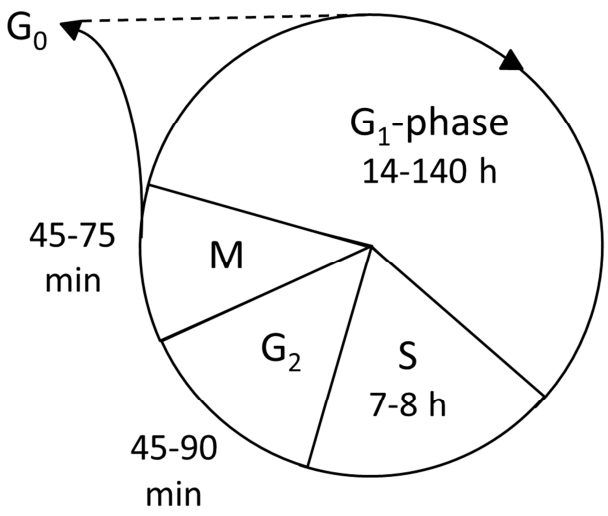

Figure 5.1. Schematic of the phases of the enterocyte cell cycle, characterised by: The time between mitosis and DNA synthesis (G_1: 14-140 h), DNA synthesis (S: 7-8 h), time between DNA synthesis and mitosis (G_2: 45-90 min) and mitosis (M: 45-74 min). Adapted from Scragg and Johnson, 1980 (Scragg and Johnson, 1980).

With knowledge of the duration of the S-phase (T_S) and the labelling index of the cell population (LI), the turnover of a cell line can be determined *in vitro* or *in vivo*, where the turnover time (T_{ot}) is equal to the ratio (reported as a percentage) of the T_S and LI (Equation 5.9 and Figure 5.2) (Scragg and Johnson, 1980).

$$T_{ot} = \frac{T_s}{LI} \cdot 100$$

Equation 5.9. Determination of turnover time.

Due to the high organisation of the intestinal tissue, the turnover of the enterocytes can be determined by estimating the migration time of cells from the villous-crypt junction

to the tip of the villous if the height of the villous is determined. The migration time will be equal to the enterocyte lifespan and thus the turnover of the small intestinal epithelia (Leblond and Stevens, 1948).

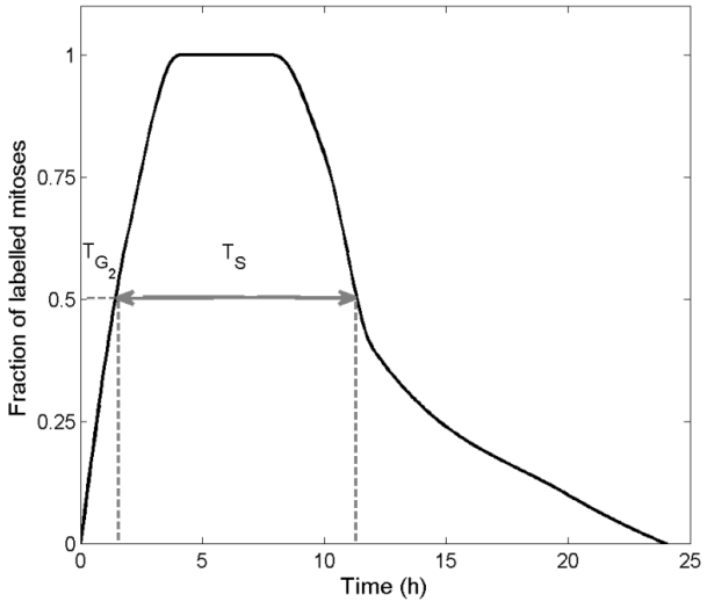

Figure 5.2. Conceptual figure of the fraction of labelled mitoses against time following the isotope labelling, indicating the length of the G_2 and S-phase (T_{G2} and T_S), thus allowing the determination of cell turnover time. Adapted from Scragg and Johnson 1980 (Scragg and Johnson, 1980).

Mitotic arrest methods

The mitotic arrest methods involve stathmokinetic agents (such as: colchine, colcemid, vinblastine or vincristine) arresting cells in the metaphase entering mitosis. This will result in an accumulation of the mitotic figures, allowing the determination of the number of cells in metaphases by histological examination. The mitotic arrest technique can be used *in vitro*, or *in vivo* by administering the blocking agent via intravenous or intraperitoneal injection (Scragg and Johnson, 1980).

Cell production rate can be determined from the relation between the number of cells in metaphase against time. The relation can be used to estimate the cell cycle times as the inverse relation of the rate of cells entering mitosis (Equation 5.10) (MI_s/t).

$$T_C = \frac{1}{MI_s/t}$$

Equation 5.10. Cell production rate.

Additionally, the villous transit time can be determined as a ratio between the villous population and the cell influx per villous (Equation 5.11) (Al-Nafussi and Wright, 1982).

$$Transit\ time = \frac{Villous\ population}{Cell\ influx/villous}$$

Equation 5.11. Enterocyte transit time.

Cytophotometric methods

Cytophotometric methods involve the staining of the cell line DNA using dyes, such as ethidium bromide, which bind specifically to DNA and fluoresce with intensity proportional to the amount of bound DNA. This allows the distinguishment between cell cycle states and the proliferative index of a population, percentage in D G2 and M phase (Scragg and Johnson, 1980).

5.5 Results

Overall, a total of 53 studies where identified reporting enterocyte turnover in 929 subjects in 6 species. In a majority of the studies determination of enterocyte turnover was carried out with isotope labelling utilising ^{3}H-thymidine or BrdUrd (83%), where other techniques included mitotic arrest methods with colchine and vincristine, and turnover determination using biopsy samples. The outcome of the data analysis of enterocyte turnover follows below.

5.5.1 Enterocyte turnover in pre-clinical species

The literature search of enterocyte turnover in healthy adult subjects of pre-clinical species identified a total of 36 studies, consisting of approximately 664 subjects based on sample size assumptions given in the Methods section. In the rat, 14 studies

consisting of 262 subjects were identified, where the weighted arithmetic mean full small intestinal enterocyte turnover (*i.e.* lifespan) was determined to be 2.01 days. Values for segmental turnover of the small intestinal epithelia were within close proximity of each other with weighted averages of 1.89, 2.11 and 1.91 days, in the duodenum, jejunum and ileum respectively. Estimates of variability were limited to two radiographic studies of the duodenum and jejunum reporting standard deviations of the mean turnover. The weighted geometric mean and standard deviation of these reports resulted in an enterocyte turnover corresponding to 2.76 (±1.68) days (n rats=14). Due to the limited reported variance statistical verification of regional differences was restricted, albeit reported turnover in the duodenum (1.20±0.20 days, n=4) and jejunum (3.95±0.54 days, n=10) displayed a statistically significant difference ($P<0.05$) (Figure 5.3) (Leblond and Stevens, 1948; Bertalanffy, 1960; Loran and Althausen, 1960; Bertalanffy and Lau, 1962; Koldovsky *et al.*, 1966; Altmann and Enesco, 1967; Shambaugh *et al.*, 1967; Menge *et al.*, 1982; Holt *et al.*, 1983; King *et al.*, 1983; Cheeseman, 1986; Nsi-Emvo *et al.*, 1994; Thomson *et al.*, 1994; Gomes and Alvares, 1998; Macallan *et al.*, 1998; Qi *et al.*, 2009).

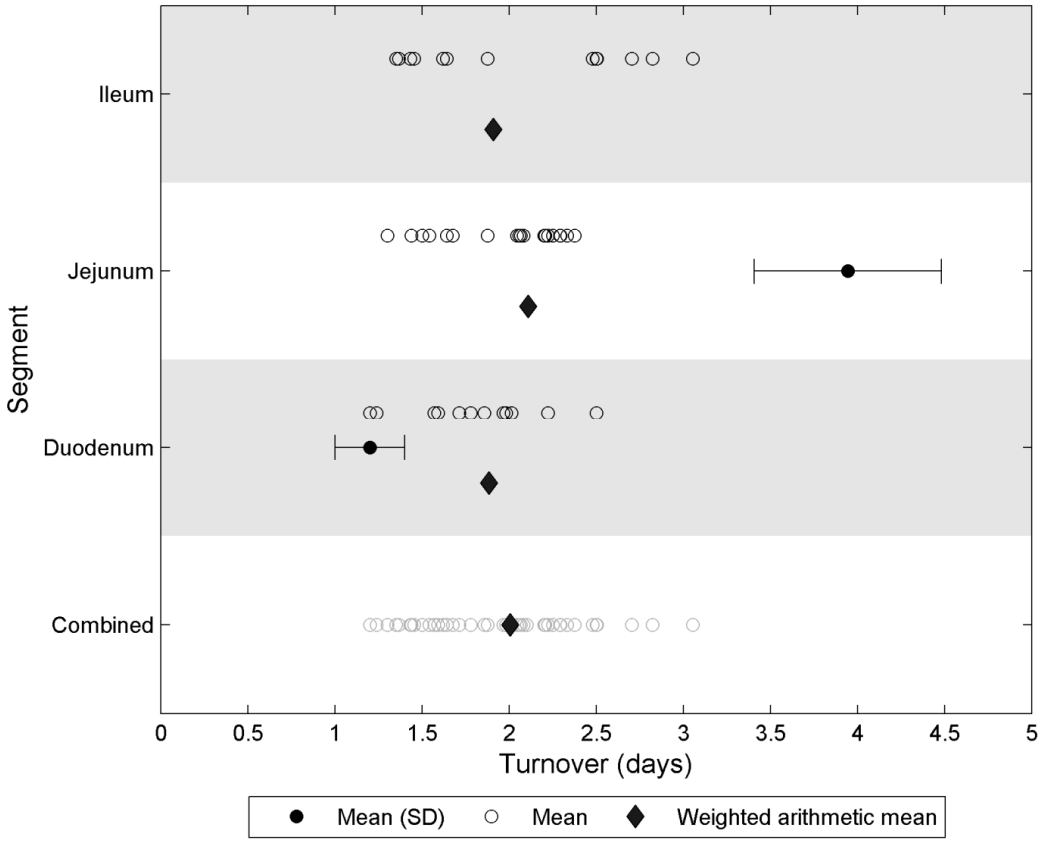

Figure 5.3. Reported means and standard deviations (SD; n rats=14) and mean only data (n=248) of small intestinal enterocyte turnover in rat and the combined weighted geometric mean and SD (GSD) based on dataset of mean and SD.

In the mouse, a total of 15 studies consisting of 373 healthy adult mice were identified reporting the enterocyte turnover in the small intestinal epithelia. The weighted combined geometric mean full enterocyte turnover for the whole small intestine was 2.78 (±1.06 n=113 mice) days. The duodenum, jejunum and ileum displayed an enterocyte turnover of 2.83 (±1.06, n=40), 2.97 (±1.05, n=35) and 2.56 (±1.05, n=35) days respectively. All intestinal segments differed at a statistically significant level using post-hoc analysis (P<0.05) (Figure 5.4) (Leblond and Messier, 1958; Walker and Leblond, 1958; Quastler and Sherman, 1959; Fry *et al.*, 1961; Lesher *et al.*, 1961; Fry *et al.*, 1962; Grey, 1968; Merzel and Leblond, 1969; Cheng and Leblond, 1974; Tsubouchi, 1981; Cheng and Bjerknes, 1983; Smith *et al.*, 1984; Thompson *et al.*, 1990; Ferraris *et al.*, 1992).

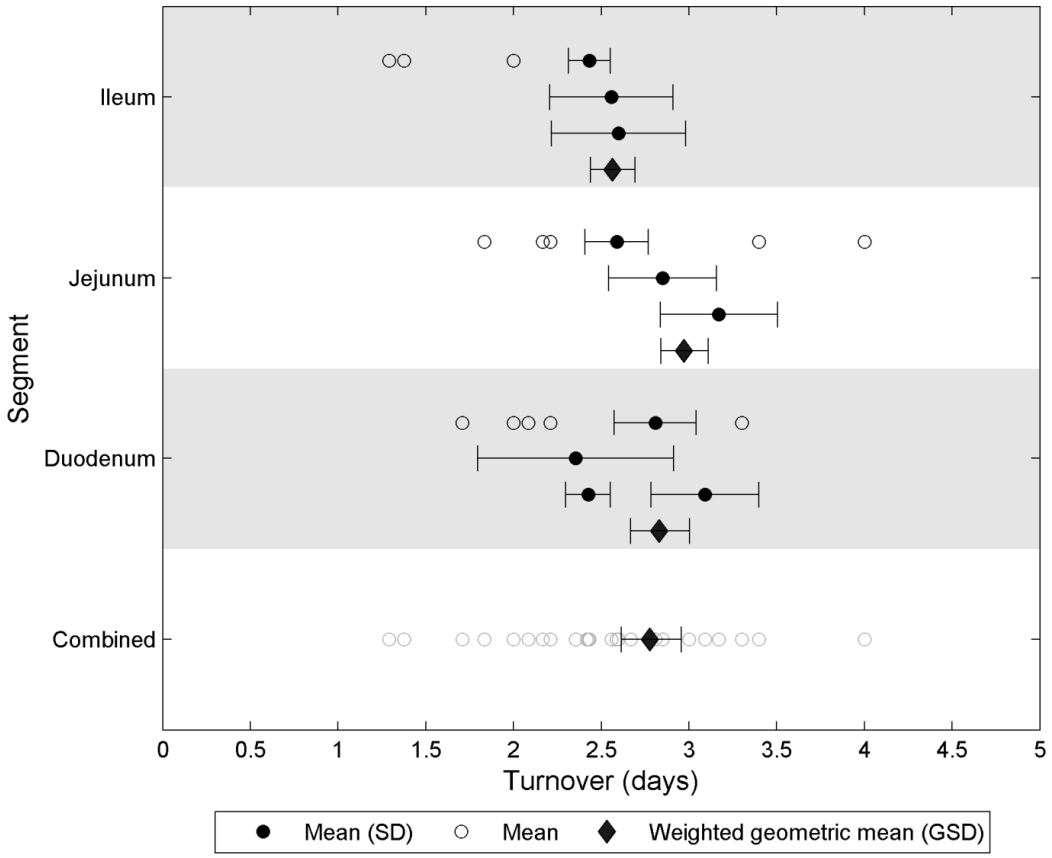

Figure 5.4. Reported means and standard deviations (SD; n=113 mice) and mean only data (n=260) of small intestinal enterocyte turnover in the mouse and the combined weighted geometric mean and SD (GSD) based on dataset of mean and SD.

5.5.2 Enterocyte turnover in human

The literature search of human enterocyte turnover data identified 17 studies, with a total sample size of n=265, reporting the turnover of human gastrointestinal epithelial cells in the form of mean and standard deviation (n=86), mean only (n=153) and ranges (n=26). The majority of turnover values were from colonic, rectal (n=157), duodenal (n=60) and gastric epithelial cells (n=36), whereas jejunum and ileum was limited to a sample size of n=3 and n=9 respectively. A weighted geometric mean turnover of 3.48 (±1.55) days was obtained for the gastrointestinal epithelia, limiting analysis to data reporting the mean and standard deviation. Analysis of individual gastrointestinal segments identified a weighted mean turnover of 1.50 (±2.90, n=3) days for the duodenum, 2.83 (±1.60, n=30) days for the stomach and 4.12 (±1.32, n=53) days for the colorectal region, where the stomach displayed a statistically faster turnover as

compared to the colorectal region utilising post-hoc test (P<0.05) (Figure 5.5) (Bertalanffy and Nagy, 1961; Cole and Mc, 1961; Deschner *et al.*, 1963; Lipkin *et al.*, 1963a; Lipkin *et al.*, 1963b; Macdonald *et al.*, 1964; Shorter *et al.*, 1964; Shorter *et al.*, 1966; Bell *et al.*, 1967; Lipkin, 1969; Bleiberg *et al.*, 1970; Weinstein, 1974; Bleiberg and Galand, 1976; Wright *et al.*, 1977; Potten *et al.*, 1992; Patel *et al.*, 1993; Bullen *et al.*, 2006).

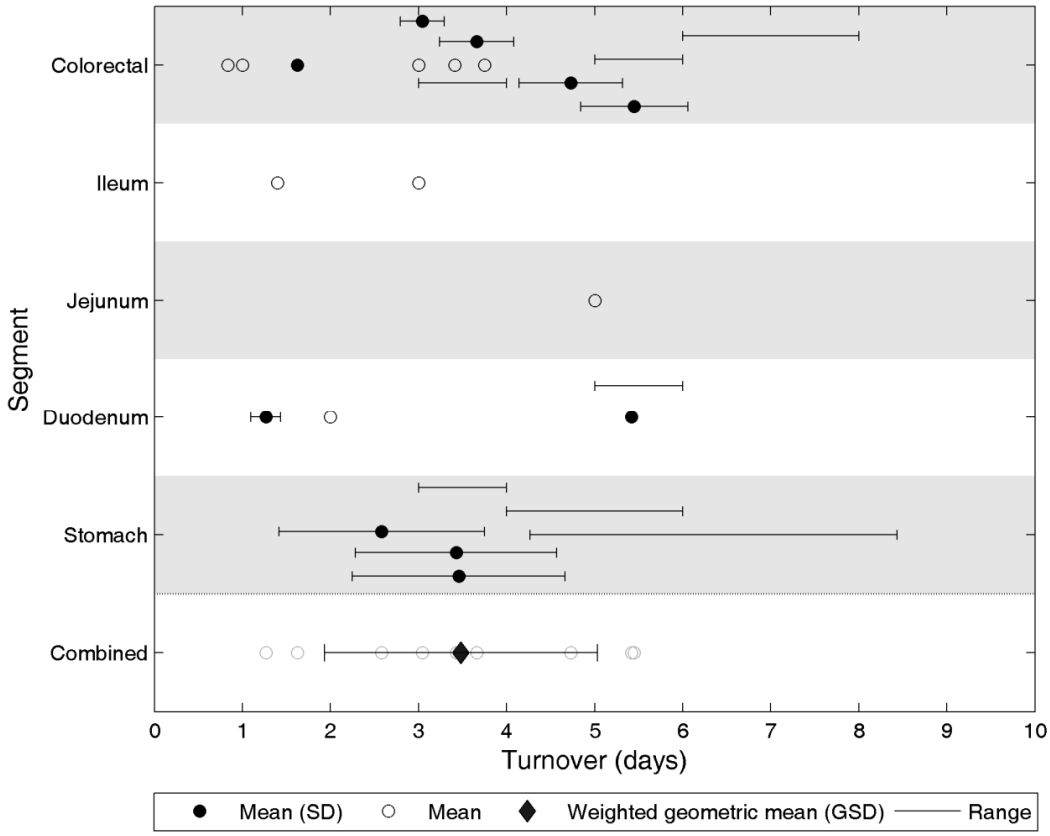

Figure 5.5. Reported means and standard deviations (SD; n individuals=86), mean only data (n=153), and ranges (n=26) of human gastrointestinal epithelial turnover and the combined weighted geometric mean and geometric SD (GSD; n=86) based on dataset of mean and SD.

5.5.3 Summary results on enterocyte turnover

In addition to human, rat and mouse, data on small intestinal enterocyte turnover was identified for healthy adult rabbits, guinea pigs and hamsters, albeit being sparse. The arithmetic mean enterocyte turnover in rabbit, guinea pig and hamster corresponded to 3.40 (n=20 rabbits), 3.38 (n=Not clear) and 1.67 (n=8) days respectively. Statistical analysis of enterocyte turnover in human, mouse and rat identified human and mouse enterocyte turnover to differ statistically significantly (P<0.05) (Figure 5.6) (Cremaschi *et al.*, 1982; Cremaschi *et al.*, 1984; Smith *et al.*, 1984).

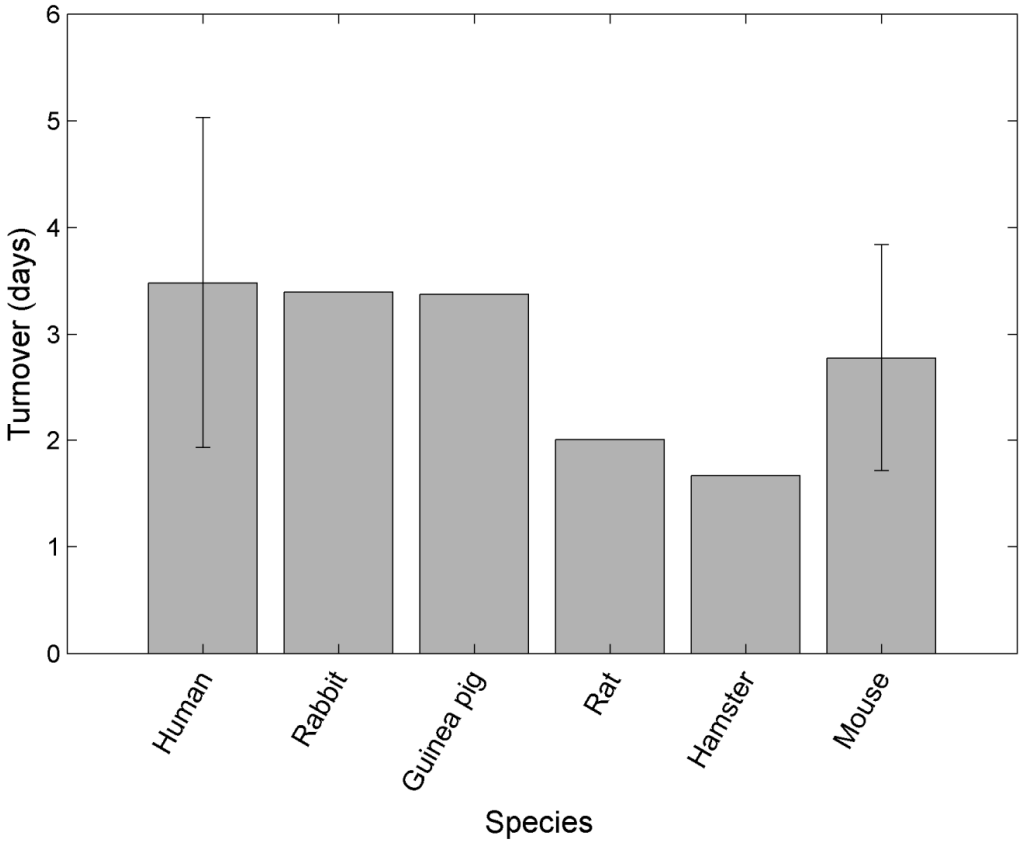

Figure 5.6. Reported enterocyte turnover in days across species, ranked approximately according to body weight, in: Human (n individuals=86), rabbit (n =20), guinea pig (n=Not clear), rat (n=262), hamster (n=8) and mouse (n=131).

5.6 Discussion and conclusions

Turnover of the gastrointestinal epithelia was established based on large sample size in rats, mice and human and based on sparse samples in rabbits, guinea pig and hamster. Statistical analysis indicated a shorter enterocyte turnover in preclinical species as compared to human, where the mouse displayed a significantly shorter turnover, albeit the limitation of data did not allow a conclusive analysis for the remaining species. It should further be noted that human data included gastric and colorectal epithelial turnover data due to the sparse dataset from the small intestinal region.

Statistical analysis of regional differences in enterocyte turnover indicated the ileum to display the fastest turnover, followed by the duodenum and ileum in mouse. A similar trend was indicated in rat although a majority of the data lacked variance and could therefore not be determined statistically. Human data on gastrointestinal epithelial turnover identified the colorectal cell renewal to be slower as compared to the stomach, whereas data from the small intestinal regions were too sparse in order to observe any regional differences. Additional indications of regional differences in enterocyte turnover include observations from neonatal pig, where the distal small intestine displayed a slower turnover (10.2±1.5 days, n=16) as compared to the proximal region (4.7±0.4 days, n=16) (Fan *et al.*, 2001). In summary, evidence for regional differences in enterocyte turnover in man is inconclusive which would favour the utilisation of a single parameter value of 3.48 (±1.55) days for the intestine.

Several factors have been identified to alter the turnover of the enterocytes, and may therefore account for variability seen in the data set, these factors include the age of the subjects, where several reports have reported slower enterocyte turnover in neonatal or infant pigs, guinea pigs, rats, mice and hamsters (Creamer *et al.*, 1961; Koldovsky *et al.*, 1966; Grey, 1968; Rundell and Lecce, 1972; Al-Nafussi and Wright, 1982; Holt *et al.*, 1983; Cremaschi *et al.*, 1986; Fan *et al.*, 2001; Leaphart *et al.*, 2008). In addition, an altered enterocyte turnover has been reported in rats subject to numerous environmental changes and disease states, including: Small intestinal resection, dietary changes, diabetes and irradiation (Menge *et al.*, 1982; Menge *et al.*, 1983; Cheeseman, 1986; Thomson *et al.*, 1994). It can therefore be concluded that the enterocyte turnover is highly sensitive to numerous environmental factors.

The quality of data posed the perhaps most significant limitation in this study, with a large number of studies only reporting mean data or ranges of enterocyte turnover, this was especially true for the human data where labelling studies tend to be performed in colorectal cancer patients, this may further influence the turnover. A majority of human data therefore originated from the colorectal and gastric region, which should be taken into consideration when interpreting interspecies differences in enterocyte turnover as reported in this study.

The enterocyte turnover, as determined in this analysis (approximately 3.48 days), suggests the gastrointestinal epithelia to display a comparable rate of renewal to that of the CYP enzymes as determined *in vitro*, where Yang, and co-workers, found reported CYP turnover vary between 0.96 and 4.33 days. The individual impact of these two hierarchically dependent processes on enzyme recovery following DDIs is however not completely straightforward to compare as the rate of turnover of the enzymes will follow a first-order rate following mechanism-based inhibition whereas the enterocytes can be assumed to be renewed at a zero-order rate as steady-state levels of the enterocyte population remain undisrupted following inhibition. Exploring the impact of nesting enzyme and enterocyte turnover for the prediction of DDIs and MBI may be considered particularly suitable using a PBPK modelling and simulation approach (Bell *et al.*, 1967; Yang *et al.*, 2008; van Leeuwen *et al.*, 2009).

This is the most extensive analysis of enterocyte turnover in multiple species, including human, to the authors' knowledge. The incorporation of enterocyte turnover data in PBPK modelling and simulation may be of assistance in improving the predictions of DDIs where substrates are subject to small intestinal metabolism through the incorporation of independent enterocyte and enzyme turnover in the gut wall, thus allowing a more mechanistic description of the recovery of enzyme following MBI or induction or disease states where enzyme or enterocyte turnover are altered independently.

5.7 Acknowledgements

The Authors declare no conflict of interest.

5.8 References

Agoram B, Woltosz WS, and Bolger MB (2001) Predicting the impact of physiological and biochemical processes on oral drug bioavailability. *Adv Drug Deliv Rev* **50 Suppl 1:**S41-67.

Al-Nafussi AI and Wright NA (1982) Cell kinetics in the mouse small intestine during immediate postnatal life. *Virchows Archiv B, Cell pathology including molecular pathology* **40:**51-62.

Altmann GG and Enesco M (1967) Cell number as a measure of distribution and renewal of epithelial cells in the small intestine of growing and adult rats. *Am J Anat* **121:**319-336.

Bell B, Almy TP, and Lipkin M (1967) Cell proliferation kinetics in the gastrointestinal tract of man. 3. Cell renewal in esophagus, stomach, and jejunum of a patient with treated pernicious anemia. *Journal of the National Cancer Institute* **38:**615-628.

Bertalanffy FD (1960) Mitotic rates and renewal times of the digestive tract epithelia in the rat. *Acta anatomica* **40:**130-148.

Bertalanffy FD and Lau C (1962) Cell Renewal. *International Journal of Cytology* **13:**357-366.

Bertalanffy FD and Nagy KP (1961) Mitotic activity and renewal rate of the epithelial cells of human duodenum. *Acta anatomica* **45:**362-370.

Bleiberg H and Galand P (1976) In vitro autoradiographic determination of cell kinetic parameters in adenocarcinomas and adjacent healthy mucosa of the human colon and rectum. *Cancer Res* **36:**325-328.

Bleiberg H, Mainguet P, Galand P, Chretien J, and Dupont-Mairesse N (1970) Cell renewal in the human rectum. In vitro autoradiographic study on active ulcerative colitis. *Gastroenterology* **58:**851-855.

Bullen TF, Forrest S, Campbell F, Dodson AR, Hershman MJ, Pritchard DM, Turner JR, Montrose MH, and Watson AJ (2006) Characterization of epithelial cell shedding from human small intestine. *Lab Invest* **86:**1052-1063.

Cheeseman CI (1986) Expression of amino acid and peptide transport systems in rat small intestine. *Am J Physiol* **251:**G636-641.

Cheng H and Bjerknes M (1983) Cell production in mouse intestinal epithelium measured by stathmokinetic flow cytometry and Coulter particle counting. *Anat Rec* **207:**427-434.

Cheng H and Leblond CP (1974) Origin, differentiation and renewal of the four main epithelial cell types in the mouse small intestine. V. Unitarian Theory of the origin of the four epithelial cell types. *Am J Anat* **141:**537-561.

Cole JW and Mc KA (1961) Observations of cell renewal in human rectal mucosa in vivo with thymidine-H3. *Gastroenterology* **41:**122-125.

Creamer B (1967) The turnover of the epithelium of the small intestine. *British medical bulletin* **23:**226-230.

Creamer B, Shorter RG, and Bamforth J (1961) The turnover and shedding of epithelial cells. I. The turnover in the gastro-intestinal tract. *Gut* **2:**110-118.

Cremaschi D, James PS, Meyer G, Peacock MA, and Smith MW (1982) Membrane potentials of differentiating enterocytes. *Biochimica et biophysica acta* **688:**271-274.

Cremaschi D, James PS, Meyer G, Rossetti C, and Smith MW (1986) Intracellular potassium as a possible inducer of amino acid transport across hamster jejunal enterocytes. *J Physiol* **375:**107-119.

Cremaschi D, James PS, Meyer G, and Smith MW (1984) Positional dependence of enterocyte membrane potential in hamster and rabbit enterocytes. *Comparative biochemistry and physiology A, Comparative physiology* **78:**661-666.

Darwich AS, Neuhoff S, and Rostami-Hodjegan A (2010) Interplay of metabolism and transport in determining oral drug absorption and gut wall metabolism: a simulation assessment using the "advanced dissolution, absorption, metabolism (ADAM)" model. *Curr Drug Metab* **11:**716-729.

Darwich AS, Pade D, Ammori BJ, Jamei M, Ashcroft DM, and Rostami-Hodjegan A (2012) A mechanistic pharmacokinetic model to assess modified oral drug bioavailability post bariatric surgery in morbidly obese patients: interplay between CYP3A gut wall metabolism, permeability and dissolution. *J Pharm Pharmacol* **64:**1008-1024.

Darwich AS, Pade D, Rowland-Yeo K, Jamei M, Asberg A, Christensen H, Ashcroft DM, and Rostami-Hodjegan A (2013) Evaluation of an In Silico PBPK Post-Bariatric Surgery Model through Simulating Oral Drug Bioavailability of Atorvastatin and Cyclosporine. *CPT: pharmacometrics & systems pharmacology* **2:**e47.

Deschner E, Lewis CM, and Lipkin M (1963) In Vitro Study of Human Rectal Epithelial Cells. I. Atypical Zone of H3 Thymidine Incorporation in Mucosa of Multiple Polyposis. *J Clin Invest* **42:**1922-1928.

Fahmi OA, Hurst S, Plowchalk D, Cook J, Guo F, Youdim K, Dickins M, Phipps A, Darekar A, Hyland R, and Obach RS (2009) Comparison of different algorithms for predicting clinical drug-drug interactions, based on the use of CYP3A4 in vitro data: predictions of compounds as precipitants of interaction. *Drug Metab Dispos* **37:**1658-1666.

Fan MZ, Stoll B, Jiang R, and Burrin DG (2001) Enterocyte digestive enzyme activity along the crypt-villus and longitudinal axes in the neonatal pig small intestine. *Journal of animal science* **79:**371-381.

Ferraris RP, Villenas SA, and Diamond J (1992) Regulation of brush-border enzyme activities and enterocyte migration rates in mouse small intestine. *Am J Physiol* **262:**G1047-1059.

Fry RJ, Lesher S, and Kohn HI (1961) Age effect on cell-transit time in mouse jejunal epithelium. *Am J Physiol* **201:**213-216.

Fry RJ, Lesher S, and Kohn HI (1962) Influence of age on the transit time of cells of the mouse intestinal epithelium. III. Ileum. *Lab Invest* **11:**289-293.

Gomes JR and Alvares EP (1998) Cell proliferation and migration in the jejunum of suckling rats submitted to progressive fasting. *Braz J Med Biol Res* **31:**281-288.

Grey RD (1968) Epithelial cell migration in the intestine of the young mouse. *Developmental biology* **18:**501-504.

Holt PR, Kotler DP, and Pascal RR (1983) A simple method for determining epithelial cell turnover in small intestine. Studies in young and aging rat gut. *Gastroenterology* **84:**69-74.

Johnson TN, Tanner MS, Taylor CJ, and Tucker GT (2001) Enterocytic CYP3A4 in a paediatric population: developmental changes and the effect of coeliac disease and cystic fibrosis. *Br J Clin Pharmacol* **51:**451-460.

King IS, Paterson JY, Peacock MA, Smith MW, and Syme G (1983) Effect of diet upon enterocyte differentiation in the rat jejunum. *J Physiol* **344:**465-481.

Koldovsky O, Sunshine P, and Kretchmer N (1966) Cellular migration of intestinal epithelia in suckling and weaned rats. *Nature* **212:**1389-1390.

Leaphart CL, Dai S, Gribar SC, Richardson W, Ozolek J, Shi XH, Bruns JR, Branca M, Li J, Weisz OA, Sodhi C, and Hackam DJ (2008) Interferon-gamma inhibits

enterocyte migration by reversibly displacing connexin43 from lipid rafts. *American journal of physiology Gastrointestinal and liver physiology* **295:**G559-569.

Leblond CP and Messier B (1958) Renewal of chief cells and goblet cells in the small intestine as shown by radioautography after injection of thymidine-H3 into mice. *Anat Rec* **132:**247-259.

Leblond CP and Stevens CE (1948) The constant renewal of the intestinal epithelium in the albino rat. *Anat Rec* **100:**357-377.

Lesher S, Fry RJ, and Kohn HI (1961) Influence of age on transit time of cells of mouse intestinal epithelium. I. Duodenum. *Lab Invest* **10:**291-300.

Lipkin M (1969) Cell proliferation in gastrointestinal disease. *National Cancer Institute monograph* **30:**199-207.

Lipkin M, Bell B, and Sherlock P (1963a) Cell Proliferation Kinetics in the Gastrointestinal Tract of Man. I. Cell Renewal in Colon and Rectum. *J Clin Invest* **42:**767-776.

Lipkin M, Sherlock P, and Bell B (1963b) Cell Proliferation Kinetics in the Gastrointestinal Tract of Man. II. Cell Renewal in Stomach, Ileum, Colon, and Rectum. *Gastroenterology* **45:**721-729.

Loran MR and Althausen TL (1960) Cellular proliferation of intestinal epithelia in the rat two months after partial resection of the ileum. *The Journal of biophysical and biochemical cytology* **7:**667-672.

Macallan DC, Fullerton CA, Neese RA, Haddock K, Park SS, and Hellerstein MK (1998) Measurement of cell proliferation by labeling of DNA with stable isotope-labeled glucose: studies in vitro, in animals, and in humans. *Proc Natl Acad Sci U S A* **95:**708-713.

Macdonald WC, Trier JS, and Everett NB (1964) Cell Proliferation and Migration in the Stomach, Duodenum, and Rectum of Man: Radioautographic Studies. *Gastroenterology* **46:**405-417.

Malato Y, Naqvi S, Schurmann N, Ng R, Wang B, Zape J, Kay MA, Grimm D, and Willenbring H (2011) Fate tracing of mature hepatocytes in mouse liver homeostasis and regeneration. *J Clin Invest* **121:**4850-4860.

Menge H, Hopert R, Alexopoulos T, and Riecken EO (1982) Three-dimensional structure and cell kinetics at different sites of rat intestinal remnants during the early adaptive response to resection. *Research in experimental medicine Zeitschrift fur die gesamte experimentelle Medizin einschliesslich experimenteller Chirurgie* **181:**77-94.

Menge H, Sepulveda FV, and Smith MW (1983) Cellular adaptation of amino acid transport following intestinal resection in the rat. *J Physiol* **334:**213-223.

Merzel J and Leblond CP (1969) Origin and renewal of goblet cells in the epithelium of the mouse small intestine. *Am J Anat* **124:**281-305.

Nsi-Emvo E, Foltzer-Jourdainne C, Raul F, Gosse F, Duluc I, Koch B, and Freund JN (1994) Precocious and reversible expression of sucrase-isomaltase unrelated to intestinal cell turnover. *Am J Physiol* **266:**G568-575.

Pang KS (2003) Modeling of intestinal drug absorption: roles of transporters and metabolic enzymes (for the Gillette Review Series). *Drug Metab Dispos* **31:**1507-1519.

Patel S, Rew DA, Taylor I, Potten CS, Owen C, and Roberts SA (1993) Study of the proliferation in human gastric mucosa after in vivo bromodeoxyuridine labelling. *Gut* **34:**893-896.

Potten CS, Kellett M, Rew DA, and Roberts SA (1992) Proliferation in human gastrointestinal epithelium using bromodeoxyuridine in vivo: data for different sites, proximity to a tumour, and polyposis coli. *Gut* **33:**524-529.

Qi WM, Yamamoto K, Yokoo Y, Miyata H, Inamoto T, Udayanga KG, Kawano J, Yokoyama T, Hoshi N, and Kitagawa H (2009) Histoplanimetrical study on the relationship between the cell kinetics of villous columnar epithelial cells and the proliferation of indigenous bacteria in rat small intestine. *The Journal of veterinary medical science / the Japanese Society of Veterinary Science* **71:**463-470.

Quastler H and Sherman FG (1959) Cell population kinetics in the intestinal epithelium of the mouse. *Experimental cell research* **17:**420-438.

Rowland Yeo K, Jamei M, Yang J, Tucker GT, and Rostami-Hodjegan A (2010) Physiologically based mechanistic modelling to predict complex drug-drug interactions involving simultaneous competitive and time-dependent enzyme inhibition by parent compound and its metabolite in both liver and gut - the effect of diltiazem on the time-course of exposure to triazolam. *Eur J Pharm Sci* **39:**298-309.

Rundell JO and Lecce JG (1972) Independence of intestinal epithelial cell turnover from cessation of absorption of macromolecules (closure) in the neonatal mouse, rabbit, hamster and guinea pig. *Biology of the neonate* **20:**51-57.

Scragg MA and Johnson NW (1980) Epithelial cell kinetics--A review of methods of study and their application to oral mucosa in health and disease. Part A. Methods for studying cell proliferation and some sources of variation. *Journal of oral pathology* **9:**309-341.

Shambaugh GE, MacNair DS, and Beisel WR (1967) Small-bowel epithelial migration during a generalized nonenteric infection in the rat. *Am J Dig Dis* **12:**403-408.

Shorter RG, Moertel CG, Titus JL, and Reitemeier RJ (1964) Cell Kinetics in the Jejunum and Rectum of Man. *Am J Dig Dis* **9:**760-763.

Shorter RG, Spencer RJ, and Hallenbeck GA (1966) Kinetic studies of the epithelial cells of the rectal mucosa in normal subjects and patients with ulcerative colitis. *Gut* **7:**593-596.

Smith MW, Patterson JY, and Peacock MA (1984) A comprehensive description of brush border membrane development applying to enterocytes taken from a wide variety of mammalian species. *Comparative biochemistry and physiology A, Comparative physiology* **77:**655-662.

Thompson EM, Price YE, and Wright NA (1990) Kinetics of enteroendocrine cells with implications for their origin: a study of the cholecystokinin and gastrin subpopulations combining tritiated thymidine labelling with immunocytochemistry in the mouse. *Gut* **31:**406-411.

Thomson AB, Cheeseman CI, Keelan M, Fedorak R, and Clandinin MT (1994) Crypt cell production rate, enterocyte turnover time and appearance of transport along the jejunal villus of the rat. *Biochimica et biophysica acta* **1191:**197-204.

Tsubouchi S (1981) Kinetic analysis of epithelial cell migration in the mouse descending colon. *Am J Anat* **161:**239-246.

van Leeuwen IM, Mirams GR, Walter A, Fletcher A, Murray P, Osborne J, Varma S, Young SJ, Cooper J, Doyle B, Pitt-Francis J, Momtahan L, Pathmanathan P, Whiteley JP, Chapman SJ, Gavaghan DJ, Jensen OE, King JR, Maini PK, Waters SL, and Byrne HM (2009) An integrative computational model for intestinal tissue renewal. *Cell Prolif* **42:**617-636.

Walker BE and Leblond CP (1958) Sites of nucleic acid synthesis in the mouse visualized by radioautography after administration of C14-labelled adenine and thymidine. *Experimental cell research* **14:**510-531.

Weinstein WM (1974) Epithelial cell renewal of the small intestinal mucosa. *The Medical clinics of North America* **58:**1375-1386.

Wilson JW and Potten CS (2004) Cell turnover: Intestine and other tissues, in: *When cells die II a comprehensive evaluation of apoptosis and programmed cell death* (Lockshin RA and Zakeri Z eds), pp 201-240, John Wiley & Sons, Inc., Hoboken, New Jersey.

Wright NA, Britton DC, Bone G, and Appleton DR (1977) An in vivo stathmokinetic study of cell proliferation in human gastric carcinoma and gastric mucosa. *Cell and tissue kinetics* **10:**429-436.

Yang J, Liao M, Shou M, Jamei M, Yeo KR, Tucker GT, and Rostami-Hodjegan A (2008) Cytochrome p450 turnover: regulation of synthesis and degradation, methods for determining rates, and implications for the prediction of drug interactions. *Curr Drug Metab* **9:**384-394.

Chapter 6: Development and assessment of a nested enzyme-within-enterocyte turnover model for mechanism-based inhibition in the small intestine

Chapter 6: Development and assessment of a nested enzyme-within-enterocyte turnover model for mechanism-based inhibition in the small intestine

A.S. Darwich, D.M. Ashcroft, A. Rostami-Hodjegan

6.1 Abstract

The extent of mechanism-based inhibition (MBI) of gut wall metabolism depends upon the degradation and synthesis of drug metabolising enzymes ($k_{deg,Enz}$) as well as the turnover rate of the enterocytes ($k_{deg,Ent}$). Current models do not consider the hybrid function determining $k_{deg,Enz}$ and instead utilise surrogate markers. Considering the complexity of the hybrid function would potentially improve the prediction of MBIs in the gut wall.

A 'nested enzyme-within-enterocyte' (NEWE) model describing Cytochrome P450 (CYP) 3A4 dynamics in the gut wall was developed using Matlab® R2010a (Mathworks, Natick, USA). A sensitivity analysis was carried out, exploring the impact of realistic ranges of MBI parameters on the extent of interaction, including: The maximal rate of enzyme inactivation (k_{inact}), unbound inhibitor concentration producing half of the maximal rate of inactivation ($K_{I,u}$), the turnover rate of the enterocytes ($k_{deg,Ent}$) and CYP3A4 ($k_{deg,CYP3A}$).

The conventional modelling approach ($k_{deg,Ent}$=0 h^{-1}) led to a higher level of inhibition of small intestinal CYP3A4 activity following MBI as compared to the NEWE model. The lower range of $K_{I,u}$'s or a higher k_{inact} were more likely to be associated with a higher predicted interaction following MBI when using the conventional model as compared to the NEWE model after single dose of inhibitor. Following multiple dose, a low k_{inact} and medium $K_{I,u}$ produced the highest discrepancy between the two models. The NEWE model may partly explain the commonly reported overpredictions of small intestinal inhibition seen for MBI when utilising the conventional modelling approach and may further improve the prediction of moderate to high MBIs. Parameter estimations of $k_{deg,CYP3A}$ based on clinical studies involving CYP3A4 MBI may be inaccurate without considering the $k_{deg,Ent}$.

6.2 Introduction

Intestinal metabolism plays an important role in the first-pass of orally administered drugs. The small intestine has been shown to exhibit comparable metabolic capability to the liver, where cytochrome P450 3A4 (CYP3A4) is the most abundant drug metabolising enzyme (Thelen and Dressman, 2009).

In physiologically-based pharmacokinetic (PBPK) modelling of intestinal first-pass, metabolism is treated as the net intrinsic unbound clearance ($CL_{u,int,G}$) often occurring inside a "well-stirred" gut model or the Q_{gut} model, where the flow from the enterocyte is treated as a hybrid term of permeability and villous blood flow (Yang *et al.*, 2007). More mechanistic models describing oral drug bioavailability generally include a series of intestinal gut wall compartments to accommodate the regional variation in enzyme abundances and segmental segregated villous blood flows, examples of these models include: The advanced compartmental absorption and transit (ACAT) and advanced dissolution absorption and metabolism (ADAM) models (Agoram *et al.*, 2001; Yang *et al.*, 2007; Jamei *et al.*, 2009; Gertz *et al.*, 2011).

Prediction of drug-drug interactions (DDIs), such as mechanism-based inhibition (MBI), through the utilisation *in vitro-in vivo* extrapolation (IVIVE) is an essential application of PBPK modelling and simulation. In order to predict MBI, PBPK models rely on a set of inhibitor and systems specific parameters, where the level of active enzyme over time in the small intestine ($A_{Enz\text{-}GI}$) will depend upon the unbound inhibitor concentration in the enterocytes ($fu_{Ent} \cdot I_{Ent}$), its maximal rate of enzyme inactivation (k_{inact}) and the inhibitor concentration that produces half of the maximal rate of inactivation ($K_{I,u}$). The level of interaction will further be determined by the level of active enzyme at steady state ($A_{Enz\text{-}GI,SS}$) and the effective enzyme degradation rate ($k_{deg,Enz}$) (Equation 6.1) (Rowland Yeo *et al.*, 2010).

$$\frac{dA_{CYP-GI}}{dt} = k_{\mathrm{deg},Enz} \cdot A_{Enz-GI,SS} - A_{Enz-GI} \cdot \left(k_{\mathrm{deg},Enz} \cdot \frac{k_{inact} \cdot fu_{Ent} \cdot I_{Ent}}{K_{I,u} + fu_{Ent} \cdot I_{Ent}} \right)$$

Equation 6.1. Mechanistic model of mechanism-based inhibition.

The systems parameter $k_{deg,Enz}$, a surrogate parameter of the combined turnover rate of the enterocyte and enzyme, is crucial in determining the timeframe and extent at which the MBI will occur (Equation 6.2) (Yang *et al.*, 2008).

$$R_{syn} = A_{CYP-GI,SS} \cdot k_{deg-CYP}$$

Equation 6.2. Enzyme turnover.

Due to the rapid turnover of the gastrointestinal epithelium compared to other tissues the enzyme turnover in the intestine will highly depend on the enterocyte lifespan (between 1-7 days in man), as opposed other cell tissues with metabolic capabilities, such as the hepatocytes (approximately 200-400 days in rat and mouse) (Malato *et al.*, 2011).

In vivo methods for determining $k_{deg-Enz}$ through measuring the recovery time of enzyme activity following enzyme the MBI are confounded by the turnover of the enterocytes; whereas *in vitro* data of enzyme degradation are sparse (Yang *et al.*, 2008).

Techniques for measuring cell turnover often rely on the incorporation of a label into the intracellular DNA. Non-radioactive labeling techniques where label compounds, such as bromodeoxyuridine and iododeoxyuridine, are administered as a single pulse label together with flow cytometry have enabled the examination of cell kinetics to a wider extent both *in vivo* and *in vitro* (Rew and Wilson, 2000).

A reoccurring problem exists in the prediction of the magnitude of mechanism-based inhibition (MBI) where overestimations of DDIs have been reported repeatedly, in particular for drugs exhibiting high intestinal extraction. Despite the improved predictions of DDIs using more mechanistic approaches, several examples of over-predictions exist, including fluoxetine and mibefradil (Obach *et al.*, 2007; Galetin *et al.*, 2008; Fahmi *et al.*, 2009; Burt *et al.*, 2012).

A systems pharmacology modelling approach to nesting enzyme-within-enterocyte turnover would provide a more mechanistic framework for modelling the physiological factors involved in the recovery of enzyme activity over time following MBI by taking

enzyme and enterocyte turnover into account and thus has the potential to improve the predictions of MBI in the gut wall.

The aim was to theoretically examine the nesting and hierarchy of enterocyte and CYP3A4 enzyme turnover and its impact on MBIs in the small intestine using a systems pharmacology approach. This would be carried out through the development and assessment of a nested enzyme-within-enterocyte (NEWE) model.

6.3 Materials and Methods

A nested enzyme-within-enterocyte (NEWE) turnover model describing CYP3A4 activity in the gastrointestinal tract was developed using Matlab® R2010a combined with the C programming language.

Realistic parameter estimates and ranges of $k_{deg\text{-}Ent}$, the degradation rate of small intestinal CYP3A4 ($k_{deg\text{-}CYP3A}$), K_{inact} and $K_{I,u}$, where explored through a simulation based exploratory sensitivity analysis utilising the developed NEWE model. The range of the explored parameter space of $k_{deg\text{-}CYP3A}$ was based on CYP3A4 turnover data extracted from the review by Yang, and co-workers, 2007 (Yang *et al.*, 2007). Ranges of explored K_{inact} and K_I values were extracted from the review of MBIs by Zhou, and co-workers, 2005 (Zhou *et al.*, 2005). $K_{I,u}$ was estimated from the fraction of unbound drug in the inhibitory assay (fu_{mic}), this was estimated from drug dependent chemical descriptors (logP and logD) and microsomal assay protein concentrations (C_{mic}) obtained from relevant studies. If no information regarding C_{mic} was given a value of 0.1 mg/mL was assumed (Equation 6.3) (Austin *et al.*, 2002).

$$fu_{mic} = \frac{1}{C_{mic} \cdot 10^{0.56 \cdot \log P/D - 1.41} + 1}$$

Equation 6.3. Estimation of fu_{mic}.

An additional set of simulations were carried out for identified geometric mean values of $k_{deg,Ent}$, based on literature search carried out by Darwich, and co-workers, and $k_{deg,CYP3A}$, based on *in vitro* data, using the NEWE model as compared to the surrogate $k_{deg,CYP3A}$ ($k_{deg,Ent}$=0 h^{-1}) (Yang *et al.*, 2008).

The dose level was determined based on the average dose of the 17th World Health Organisation (WHO) Model List of Essential Medicines (n drugs=135). Absorption rate (k_a) was based on the average of readily available reported k_a values from published population pharmacokinetic studies in human for drugs included in the 17th WHO model list of Essential Medicines (n drugs=74) (see supplementary material) (WHO, 2011).

The simulated outcome of the sensitivity analysis was examined by comparing the ratio of relative activity of CYP3A4 following MBI using the NEWE model as compared to corresponding $k_{deg,CYP3A}$ using the conventional model ($k_{deg,Ent}$=0 h^{-1}) up to 240 hours ($A_{Ent\text{-}n/0,0\text{-}t}$ [%]; Equation 6.4).

$$A_{Ent-n\,/\,0,0-t} = \frac{A_{CYP3A4,0-t}\ k_{\mathrm{deg},Ent-n}}{A_{CYP3A4,0-t}\ k_{\mathrm{deg},Ent-0}}$$

Equation 6.4. Ratio of relative enzyme activity.

6.4 Results

A nested enzyme-within-enterocyte model was developed and utilised to explore the impact of $k_{deg\text{-}Ent}$ and $k_{deg\text{-}CYP3A}$ on mechanism-based inhibitor specific parameters k_{inact} and $K_{I,u}$ through sensitivity analysis. The results follow below.

6.4.1 Model specification

The time dependent amount of active CYP3A4 in the small intestine ($A_{CYP3A\text{-}GI}$) as a consequence of MBI was described in accordance to Equation 6.1 where the level of active enzyme ($A_{CYP3A\text{-}GI}$) will depend on the unbound inhibitor concentration in the enterocytes ($fu_{Ent}\cdot I_{Ent}$), its maximal rate of enzyme inactivation ($k_{inact\text{-}CYP3A}$) and the inhibitor concentration that produces half of the maximal rate of inactivation ($K_{I,u\text{-}CYP3A}$). The level of interaction is further dependent on the level of active enzyme at steady state ($A_{CYP\text{-}GI,SS}$), the effective CYP degradation rate ($k_{deg\text{-}CYP}$), which in the proposed model is a product of enzyme degradation alone (Equation 6.5).

$$\frac{dA_{CYP3A-GI}}{dt} = k_{\deg-CYP} \cdot A_{CYP3A-GI,SS} - \frac{\sum_{i=1}^{N} A_{CYP-GI,i}}{N} \cdot \left(k_{\deg-CYP} \cdot \frac{k_{inact-CYP3A} \cdot fu_{Ent} \cdot I_{Ent}}{K_{Iu-CYP3A} + fu_{Ent} \cdot I_{Ent}} \right)$$

Equation 6.5. NEWE model (1): Level of active enzyme.

The progression of the enterocyte lifecycle was described utilising a zero order growth rate ($k_{deg,ent}$) equal to the rate of enterocyte turnover ($T_{tot,ent}$) where a lifespan of one was assumed (Equation 6.6).

$$k_{deg,ent} = \frac{1}{T_{tot,ent}}$$

Equation 6.6. Definition of enterocyte zero-rate turnover.

The initial starting point of the enterocyte lifespan at time zero was determined by a pseudorandom generation between zero and one from a uniform distribution at the initially simulated time point ($A(0)_{Ent\text{-}Lifespan}$) (Equation 6.7).

$$\frac{dA_{Ent-Lifespan}}{dt} = A(0)_{Ent-Lifespan} + k_{\deg-Ent}$$

Equation 6.7. NEWE model (2): Enterocyte lifespan.

The time dependent turnover of enterocytes was modelled using an event algorithm, where the amount of active CYP3A4 one enterocyte ($A_{CYP3A\text{-}GI,j}$) was dependent on its enterocyte life progression ($A_{Ent\text{-}Lifespan,j}$) increasing at a zero order rate equal to $k_{deg,ent}$. An $A_{Ent\text{-}LIfespan,j}$ equal to one equated cell apoptosis or shedding. The enterocyte was replaced by a new enterocyte starting at a life progression of zero and an amount of CYP3A4 equal to its steady state abundance. Thus governing the lifespan of the total population of enterocytes ($A_{Ent\text{-}Lifespan,N}$) and consequently the total amount of CYP3A4 in the small intestine ($A_{Ent\text{-}Lifespan,N}$). It was assumed that the level of CYP3A4 was immediately restored to steady state levels at renewal. The system allowed a scaling of the resolution of the enterocyte compartment, where the number of enterocytes could be altered based on *e.g.* computational time (Equation 6.8 and Figure 6.1).

$$f(t, A_{Ent-Lifespan,N}, A_{CYP3A-GI,N}) = \begin{cases} A_{Ent-Lifespan,i} = 0,\ A_{CYP3A-GI,i} = A_{CYP3A-GI,SS} & if\ A_{Ent-Lifespan,i} \geq 1 \\ A_{Ent-Lifespan,i}(t), A_{CYP3A-GI,i}(t) & else \end{cases}$$

Equation 6.8. NEWE model (3): Time to event function.

The developed NEWE model was further coupled to a minimal PBPK absorption model, describing the amount of inhibitor as it was administered into the gut lumen ($A_{I,lumen}$), the rate of absorption into the enterocytes (k_a) and the rate of elimination via small intestinal transit (k_{sit}), where the cumulative elimination was equal to 1 - f_a (the fraction of administered drug that is absorbed through the gut wall) (Equation 6.9 and Figure 6.1).

$$\frac{dI_{lumen}}{dt} = -A_{I,lumen} \cdot (k_a + k_{sit})$$

Equation 6.9. NEWE model (4): Inhibitor concentration in gut lumen.

The inhibitory concentration in the enterocyte (I_{ent}) was dependent on the volume of the enterocyte tissue (V_{ent}), rate of absorption from the small intestine ($k_a \cdot A_{I,lumen}$) and further clearance through the villous blood flow (Q_{villi}) and an unbound inhibitory clearance ($CLu_{int,gut}$) dependent on the fraction of unbound inhibitor in the enterocytes (fu_{gut}) (Equation 6.10).

$$V_{ent} \cdot \frac{dI_{ent}}{dt} = A_{I,lumen} \cdot k_a - I_{ent} \cdot (Q_{villi} + CLu_{int,gut} \cdot fu_{gut})$$

Equation 6.10. NEWE model (5): Inhibitor concentration in the enterocytes.

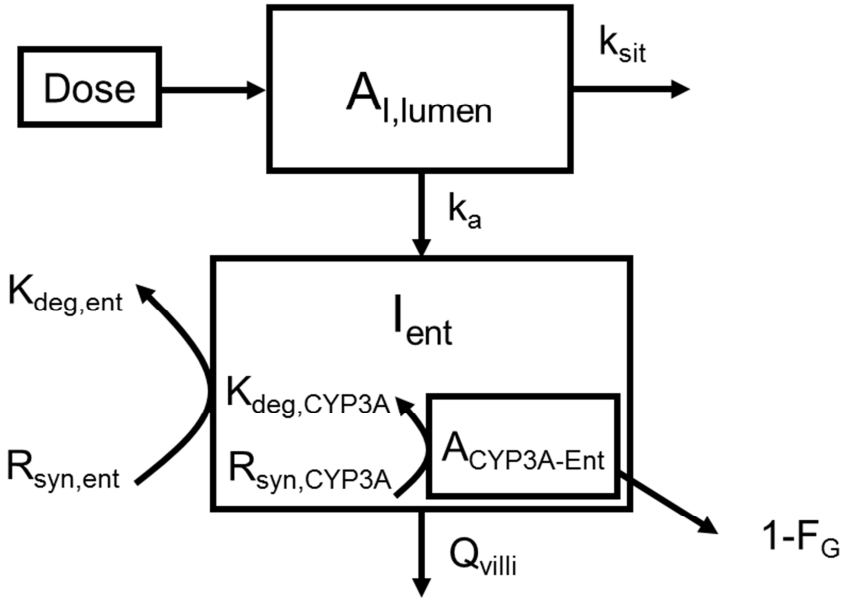

Figure 6.1. Model schematics of the nested enzyme-within-enterocyte model, Amount of inhibitor in the gut lumen ($A_{I,lumen}$) and concentration of inhibitor in the enterocytes (I_{ent}). Indicated rates and blood flows include: absorption rate constant (k_a) and small intestinal transit rate (k_{sit}), villous blood flow (Q_{villi}), portal vein blood flow (Q_{pv}), hepatic artery blood flow (Q_{ha}), and hepatic blood flow (Q_{hep}). $R_{syn,ent}$ and $k_{deg,ent}$ are the production and degradation rate of the enterocytes respectively. $R_{syn,CYP3A}$ $K_{deg,CYP3A}$ indicate the synthesis and degradation rate of CYP3A4 in the small intestine.

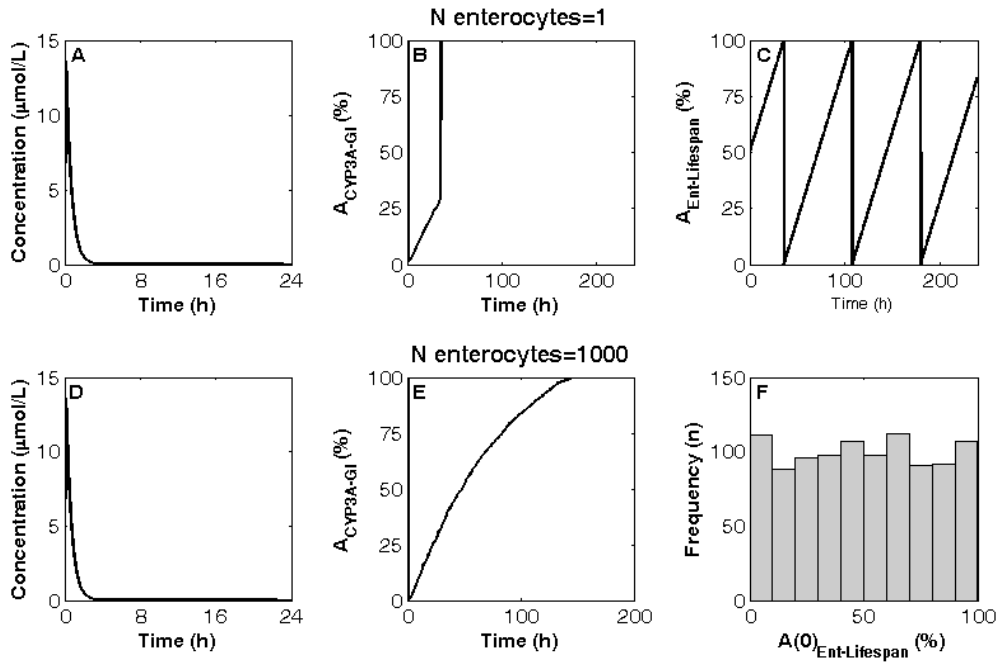

Figure 6.2. Conceptual simulation of an enterocyte (n=1) utilising the proposed model, displaying **A:** Inhibitor concentration in the enterocyte tissue, **B:** Relative activity of CYP3A4 in the small intestine ($A_{CYP3A-GI}$) over time following mechanism-based inhibition, **C:** Enterocyte life progression and regeneration over time. Conceptual simulations of n=1000 enterocytes **D:** Inhibitor concentration in the enterocyte tissue, **E:** $A_{CYP3A-GI}$ following mechanism-based inhibition, **F:** Distribution of initial starting points of the enterocyte population life progression ($A(t=0)_{Ent-Lifespan}$).

6.4.2 Exploratory sensitivity analysis - study design

Parameter ranges utilised for the simulation-based exploratory sensitivity analysis were based on observed data, where the inhibitor specific parameters were based on 37 compounds, displaying a geometric mean $K_{I,u}$ of 5.15 and a 95% confidence interval (CI95) of 0.14-119.50 µM, ranging from 0.06 to 1640 µM. K_{inact} displayed a geometric mean of 7.18 h^{-1} (CI95: 1.61-34.26, range: 1.02-120). Gastrointestinal $k_{deg,ent-CYP3A4}$ was based on data from 13 studies (n samples=121), ranging from 0.005-0.069 h^{-1} (Figure 6.3) (Zhou *et al.*, 2005; Yang *et al.*, 2008). Static parameters k_a and dose were set to 1.5 h^{-1} and 200 µmol respectively based on the 17th WHO model list of Essential Medicines (n drugs=74; see Appendix 8.5) (WHO, 2011).

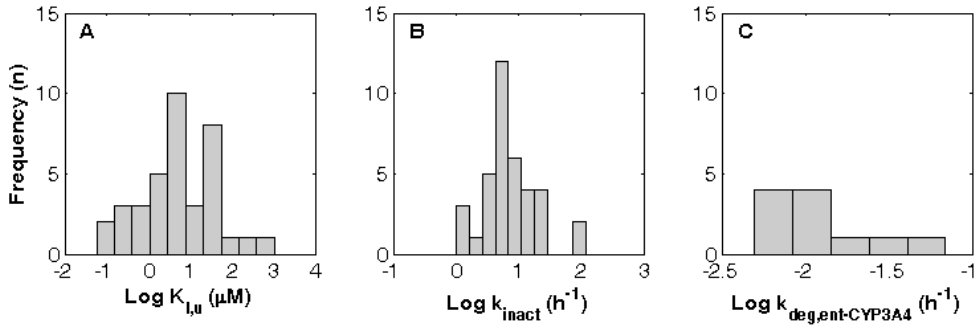

Figure 6.3. Observed distribution of the frequency of the reported inhibitor specific parameters, including: The concentration that produces half the maximal rate of inactivation ($K_{I,u}$ [µM]) maximal rate of inactivation (k_{inact} [h^{-1}]) and turnover rate of small intestinal CYP3A4 ($k_{deg,Ent-CYP3A4}$ [h^{-1}]).

The sensitivity analysis study design included six values of $k_{deg,Ent}$ (0.083, 0.042, 0.014, 0.007 0.006 and 0.003 h^{-1}), six values of $k_{deg,CYP3A}$ (0.001, 0.003, 0.007, 0.01, 0.03 and 0.07 h^{-1}), five values of $K_{I,u}$ (0.01, 0.1, 5, 100 and 2000 µM) and three values of k_{inact} (1, 10 and 150 h^{-1}) resulting in a total of 630 simulations (Figure 6.4).

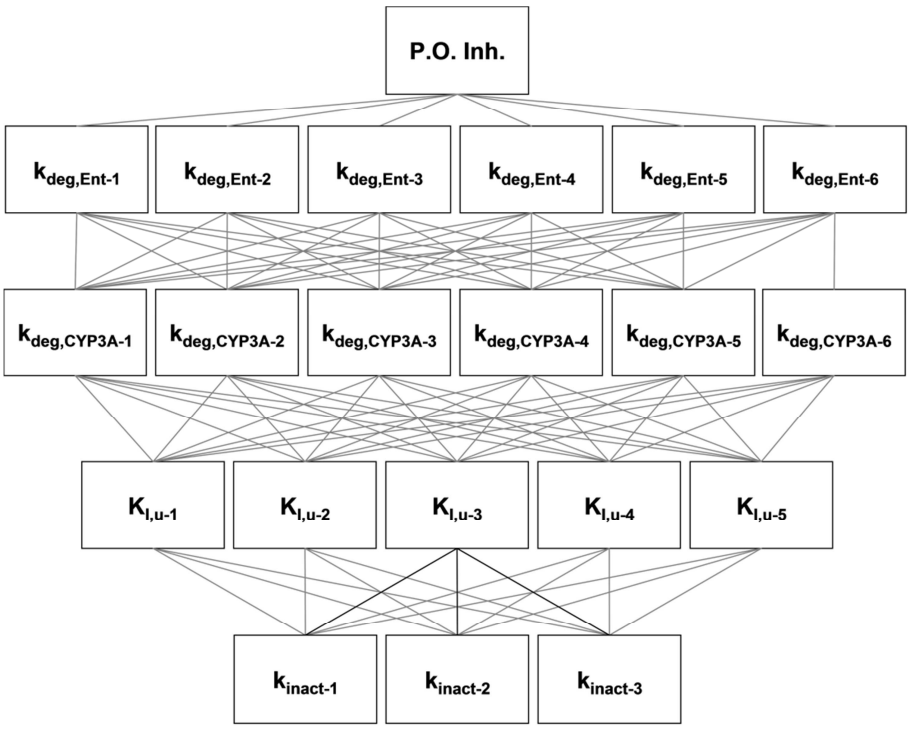

Figure 6.4. Study design of exploratory simulation assessment of an orally administered single dose of a mechanism-based inhibitor (p.o. Inh.), introducing systematic variation to four parameter levels, including: Life progression rate of enterocytes ($k_{deg\text{-}Ent\text{-}(1\text{-}7)}$), degradation rate of enterocytic CYP3A4 ($k_{deg,CYP3A\text{-}(1\text{-}6)}$), ($K_{I,u\text{-}(1\text{-}5)}$) and ($k_{inact\text{-}(1\text{-}3)}$) resulting in a total of 630 simulations using a resolution of n=1,000 enterocytes.

6.4.3 Exploratory sensitivity analysis - results

Examining the simulated relative activity of CYP3A4 in the gastrointestinal tract over 24h following MBI relative to the standard model scenario only taking changes to $k_{deg,CYP3A}$ into account ($A_{Ent\text{-}n/0,0\text{-}24h}$ [%]; $k_{deg,Ent}$=0 h^{-1}), the CYP3A4 activity was either increased or unaltered using the NEWE model in the majority simulated scenarios. Considering $A_{Ent\text{-}n/0,0\text{-}24h}$ as a function of $k_{deg,Ent}$ and $k_{deg,CYP3A4}$ the most extensive increase in $A_{CYP3A4,0\text{-}24h}$ was observed at a maximum $k_{deg,Ent}$ and $k_{deg,CYP3A4}$ of 0.08 and 0.07 h^{-1} respectively, displaying a $A_{Ent\text{-}n/0,0\text{-}24h}$ ranging from 100.0 to 7,295% dependent on the inhibitor specific parameters ($K_{I,u}$ and k_{inact}; Figure 6.5).

Increasing inhibitor specific $K_{I,u}$ generally resulted in a reduction in $A_{Ent\text{-}n/0,0\text{-}24h}$, where the increase in relative CYP3A4 activity following MBI varied from 100 to 156.4% at a

midrange $K_{I,u}$ (5 µM) and a low k_{inact} (1 h^{-1}). A reduction in $K_{I,u}$ to 0.1 µM led to an increase in relative CYP3A4 activity, where $A_{Ent\text{-}n/0,0\text{-}24h}$ varied between 100 and 1,063.6%. Discrepancies in CYP3A4 activity between the two models were less sensitive to alterations in $k_{deg,Ent}$ and $k_{deg,CYP3A}$ at a $K_{I,u}$ of 2000 µM, displaying $A_{Ent\text{-}n/0,0\text{-}24h}$ between 100-100.3% (Figure 6.5).

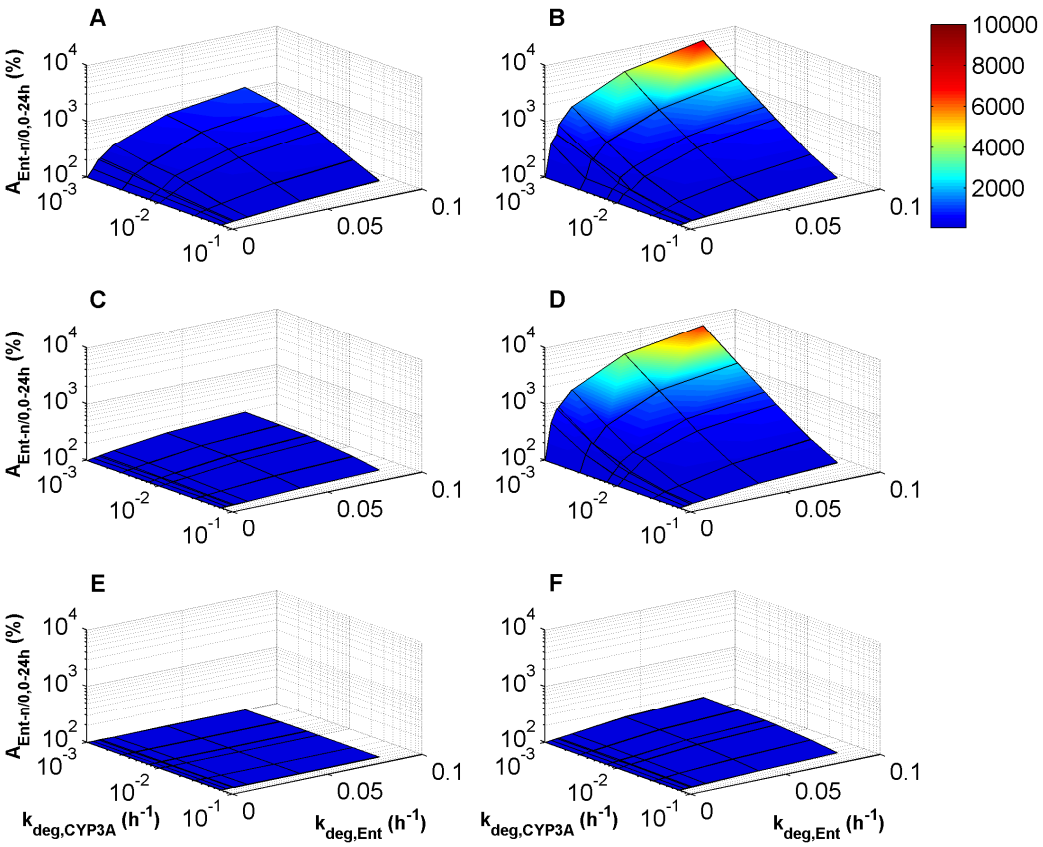

Figure 6.5. Simulated relative activity of CYP3A4 in the gastrointestinal tract over 24h following mechanism-based inhibition relative to the standard model scenario only taking changes to CYP3A4 degradation rate ($k_{deg,CYP3A}$) into account (enterocyte degradation rate [$k_{deg,Ent}$]=0 h^{-1}; $A_{CYP3A4,0\text{-}24h}$ $k_{deg,Ent\text{-}n/0}$ [%]) in relation to $k_{deg,CYP3A}$ (h^{-1}) and $k_{deg,Ent\text{-}0}$ (h^{-1}), varying the maximal rate of enzyme inactivation (k_{inact} [h^{-1}]) and the inhibitor concentration that produces half of the maximal rate of inactivation ($K_{I,u}$ [µM]) **A:** $K_{I,u}$=0.01 µM and k_{inact}=1 h^{-1}, **B:** $K_{I,u}$=0.01 µM and k_{inact}=150 h^{-1}, **C:** $K_{I,u}$=5 µM and k_{inact}=1 h^{-1}, **D:** $K_{I,u}$=5 µM and k_{inact}=150 h^{-1}, **E:** $K_{I,u}$=2000 µM and k_{inact}=1h^{-1}, and **F:** $K_{I,u}$=2000 µM and k_{inact}=150 h^{-1}.

An increase in k_{inact} generally lead to an increase $A_{Ent\text{-}n/0,0\text{-}24h}$. At a high k_{inact} (150 h^{-1}) the increase in $A_{Ent\text{-}n/0,0\text{-}24h}$ became more apparent, resulting in an increase in the relative CYP3A4 activity from 100.0 to 7,295% at a low $K_{I,u}$ (0.1 µM), whereas $A_{Ent\text{-}n/0,0\text{-}24h}$ ranged between 100 and 169% at a high $K_{I,u}$ (2000 µM) (Figure 6.5).

Examining the simulated relative activity of CYP3A4 in the gastrointestinal tract over 240 h following MBI as compared to impact of MBI on A_{CYP3A4} using the conventional model predictions, $A_{Ent\text{-}n/0,0\text{-}24h}$, resulted in a less pronounced sensitivity to alterations in $k_{deg,Ent}$ and $k_{deg,CYP3A4}$ as compared to the activity up to 24h, displaying a maximum simulated $A_{Ent\text{-}n/0,0\text{-}24h}$ of 903% following MBI up to 240h at a $K_{I,u}$ of 0.01 µM, k_{inact} 150 h^{-1}, $k_{deg,Ent}$ of 0.003 h^{-1} and $k_{deg,CYP3A}$ of 0.001 h^{-1} (Figure 6.6).

Considering the activity of small intestinal CYP3A4 following MBI, relative to activity at a $k_{deg,Ent}$ of zero, as a function of $K_{I,u}$ and $k_{deg,CYP3A}$ and varying $k_{deg,Ent}$ and k_{inact}, $A_{Ent\text{-}n/0,0\text{-}24h}$ displayed an apparent non-linear relationship in the lower range of $K_{I,u}$'s and a low to medium k_{inact} (1-10 h^{-1}). Further, the $A_{Ent\text{-}n/0,0\text{-}24h}$ in general displayed lower sensitivity to $K_{I,u}$ at a high $k_{deg,CYP3A}$. $A_{Ent\text{-}n/0,0\text{-}24h}$ varied from 100 to 1,064% at a high $k_{deg,Ent}$ (0.083 h^{-1}), whereas a low $k_{deg,Ent}$ (0.006 h^{-1}), resulted in a lower sensitivity to $K_{I,u}$ with a $A_{Ent\text{-}n/0,0\text{-}24h}$ ranging from 101 to 7295% (Figure 6.7 A, B, D, E, G and H).

At a high k_{inact} (150 h^{-1}) $A_{Ent\text{-}n/0,0\text{-}24h}$ displayed a more linear relation to $K_{I,u}$ with a less apparent sensitivity to $K_{I,u}$ at a high $k_{deg,CYP3A}$. $A_{Ent\text{-}n/0,0\text{-}24h}$ displayed less sensitivity to $k_{deg,CYP3A}$ and $K_{I,u}$ at a high $k_{deg,Ent}$ (0.083 h^{-1}) ranging from 103 to 903% at a low $k_{deg,Ent}$ (0.006 h^{-1}) and 100 to 382% at a high $k_{deg,Ent}$ (0.083 h^{-1}) (Figure 6.7 C, F and I).

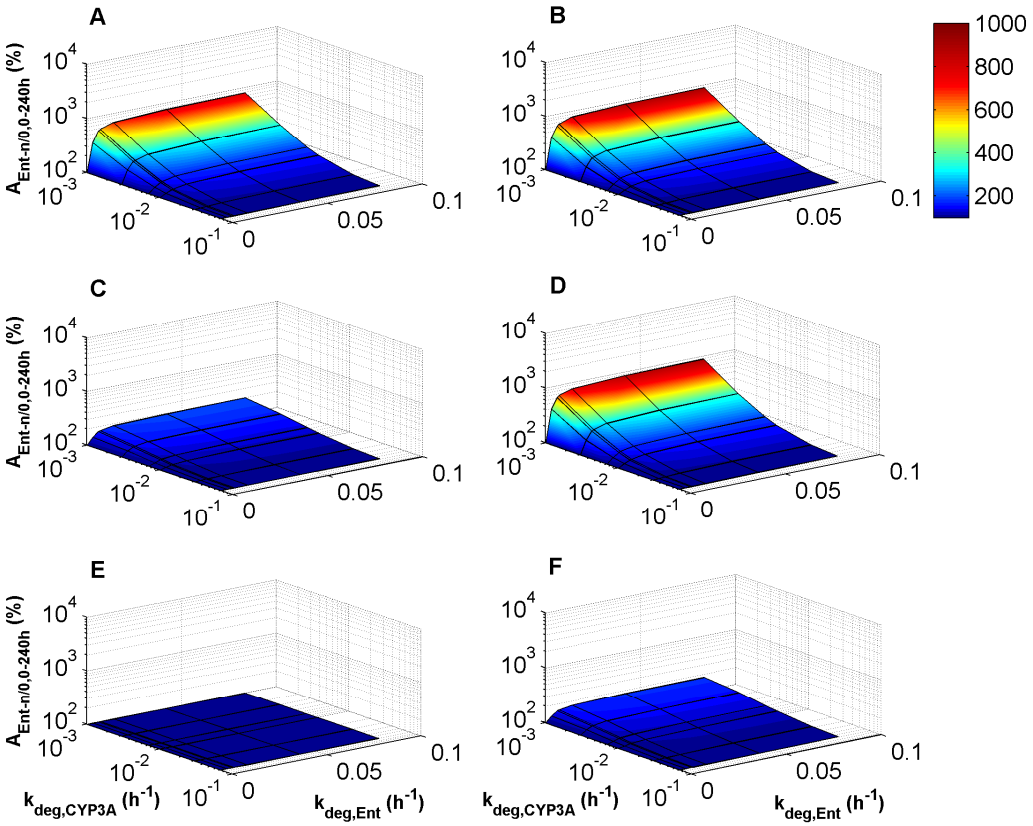

Figure 6.6. Simulated activity of CYP3A4 in the gastrointestinal tract over 240h following mechanism-based inhibition relative to the standard model scenario only taking changes to CYP3A4 degradation rate ($k_{deg,CYP3A}$) into account (enterocyte degradation rate [$k_{deg,Ent}$]=0 h^{-1}; $A_{Ent-n/0,0-24h}$ [%]) in relation to $k_{deg,CYP3A}$ (h^{-1}) and $k_{deg,Ent}$ (h^{-1}), varying the maximal rate of enzyme inactivation (k_{inact} [h^{-1}]) and the inhibitor concentration that produces half of the maximal rate of inactivation ($K_{I,u}$ [µM]) **A:** $K_{I,u}$=0.01 µM and k_{inact}=1 h^{-1}, **B:** $K_{I,u}$=0.01 µM and k_{inact}=150 h^{-1}, **C:** $K_{I,u}$=5 µM and k_{inact}=1 h^{-1}, **D:** $K_{I,u}$=5 µM and k_{inact}=150 h^{-1}, **E:** $K_{I,u}$=2000 µM and k_{inact}=1h^{-1}, and **F:** $K_{I,u}$=2000 µM and k_{inact}=150 h^{-1}.

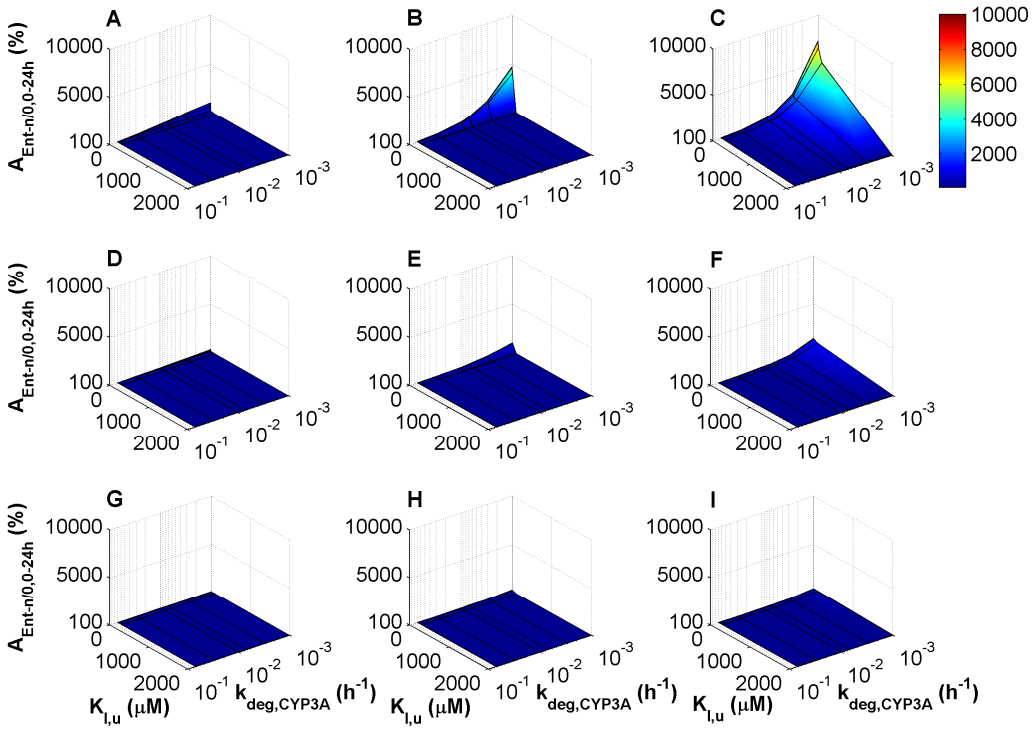

Figure 6.7. Simulated activity of CYP3A4 in the gastrointestinal tract over 24h following mechanism-based inhibition relative to the standard model scenario only taking changes to CYP3A4 degradation rate ($k_{deg,CYP3A}$) into account (enterocyte degradation rate [$k_{deg,Ent}$]=0 h^{-1}; $A_{Ent-n/0,0-240h}$ [%]) in relation to $K_{I,u}$ (the inhibitor concentration that produces half of the maximal rate of inactivation [μM]) and $k_{deg,CYP3A}$ (h^{-1}), varying $k_{deg,Ent}$ and k_{inact} (maximal rate of enzyme inactivation) **A:** $k_{deg,Ent}$ =0.083 h^{-1} and k_{inact}=1 h^{-1}, **B:** $k_{deg,Ent}$ =0.007 h^{-1} and k_{inact}=10 h^{-1}, **C:** $k_{deg,Ent}$ =0.006 h^{-1} and k_{inact}=150 h^{-1}, **D:** $k_{deg,Ent}$ =0.083 h^{-1} and k_{inact}=1 h^{-1}, **E:** $k_{deg,Ent}$ =0.007 h^{-1} and k_{inact}=10 h^{-1}, **F:** $k_{deg,Ent}$ =0.006 h^{-1} and k_{inact}=50 h^{-1}, **G:** $k_{deg,Ent}$ =0.083 h^{-1} and k_{inact}=1 h^{-1}, **H:** $k_{deg,Ent}$ =0.007 h^{-1} and k_{inact}=10 h^{-1}, and **I:** $k_{deg,Ent}$ =0.006 h^{-1} and k_{inact}=150 h^{-1}.

Considering $A_{Ent-n/0,0-24h}$ as a function of $K_{I,u}$ and k_{inact}, varying $k_{deg,Ent}$ and $k_{deg,CYP3A}$, $A_{Ent-n/0,0-240h}$ displayed an apparent low sensitivity to $K_{I,u}$ and k_{inact}. At a low $k_{deg,CYP3A}$ (0.001 h^{-1}), with a $A_{Ent-n/0,0-24h}$ varying from 135.5 to 999% at a $k_{deg,Ent}$ varying from 0.014 to 0.003 h^{-1}. At a high $k_{deg,CYP3A}$ (0.07 h^{-1}) $A_{Ent-n/0,0-24h}$ displayed a low sensitivity varying from 101.46 to 113.43 % at a $k_{deg,Ent}$ varying from 0.014 to 0.003 h^{-1} (Figure 6.8).

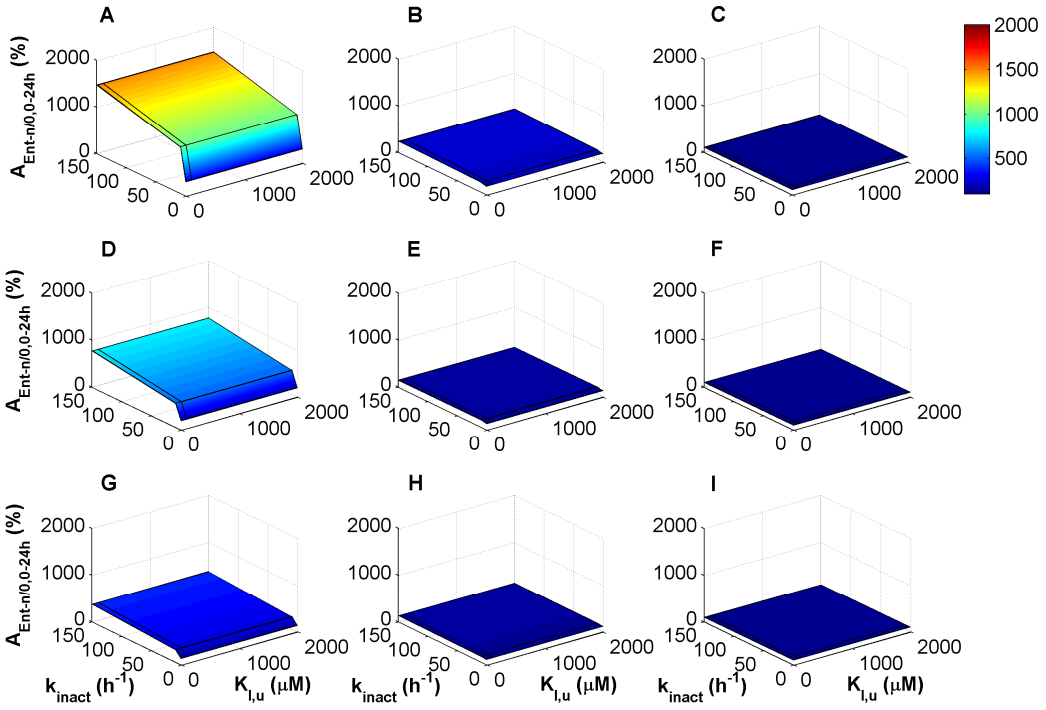

Figure 6.8. Simulated relative activity of CYP3A4 in the gastrointestinal tract over 240h following mechanism-based inhibition relative to the standard model scenario only taking changes to CYP3A4 degradation rate ($k_{deg,CYP3A}$) into account (enterocyte degradation rate [$k_{deg,Ent}$]=0 h^{-1}; $A_{Ent-n/0,0-240h}$ [%]) in relation to $K_{I,u}$ (the inhibitor concentration that produces half of the maximal rate of inactivation [μM]) and k_{inact} (the maximal rate of enzyme inactivation [h^{-1}]), varying $k_{deg,Ent}$ and $k_{deg,CYP3A}$ **A:** $k_{deg,Ent}$=0.0139 h^{-1} and $k_{deg,CYP3A}$=0.001 h^{-1}, **B:** $k_{deg,Ent}$=0.0139 h^{-1} and $k_{deg,CYP3A}$=0.01 h^{-1}, **C:** $k_{deg,Ent}$=0.0139 h^{-1} and $k_{deg,CYP3A}$=0.07 h^{-1}, **D:** $k_{deg,Ent}$=0.007 h^{-1} and $k_{deg,CYP3A}$=0.001 h^{-1}, **E:** $k_{deg,Ent}$=0.007 h^{-1} and $k_{deg,CYP3A}$=0.01 h^{-1}, **F:** $k_{deg,Ent}$=0.007 h^{-1} and $k_{deg,CYP3A}$=0.07 h^{-1}, **G:** $k_{deg,Ent}$=0.003 h^{-1} and $k_{deg,CYP3A}$=0.001 h^{-1}, **H:** $k_{deg,Ent}$=0.003 h^{-1} and $k_{deg,CYP3A}$=0.01 h^{-1}, **I:** $k_{deg,Ent}$=0.003 h^{-1} and $k_{deg,CYP3A}$=0.07 h^{-1}.

Simulations utilising the NEWE model at $k_{deg,Ent}$ of 0.013 h^{-1}, based on current study, and $k_{deg,CYP3A}$ of 0.027 h^{-1} (t½=26 h) based *in vitro* data estimated by Yang, and co-workers (2008), was compared to the conventional model ($k_{deg,Ent}$=0 h^{-1}) using a $k_{deg,CYP3A}$ of 0.03 h^{-1} based on the recovery time of intestinal CYP3A4 estimated by Yang, and co-workers (Yang *et al.*, 2008).

In agreement with the sensitivity analysis, a higher activity of CYP3A was displayed utilising the NEWE model for inhibitors exhibiting a high k_{inact} and a low $K_{I,u}$, with a $A_{Ent\text{-}n/0,0\text{-}240h}$ varying from 100.04% at a $K_{I,u}$ of 2,000 µM and k_{inact} of 1 h^{-1}, to 647.26% at $K_{I,u}$ of 0.01 µM and a k_{inact} of 150 h^{-1} (Figure 6.9).

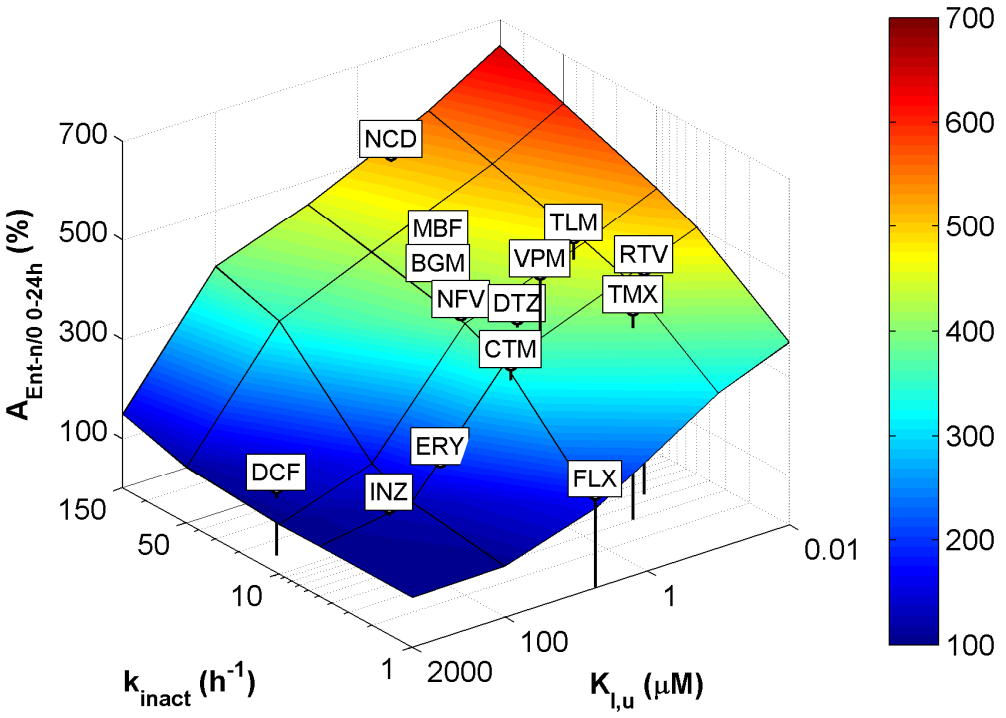

Figure 6.9. Simulated relative activity of CYP3A4 in the gastrointestinal tract over 24h following single dose mechanism-based inhibition using the nested enzyme-within-enterocyte (NEWE) model relative to the conventional model scenario ($A_{Ent\text{-}n/0,0\text{-}24h}$ [%]) in relation to $K_{I,u}$ (the inhibitor concentration that produces half of the maximal rate of inactivation [µM]) and k_{inact} (the maximal rate of enzyme inactivation [h^{-1}]). FLX=fluoxetine, TMX=tamoxifen, CTM=clarithromycin, RTV=ritonavir, ERM=erythromycin, INZ=isoniazid, VPM=verapamil, DTZ=diltiazem, TLM=troleandomycin, NFV=nelfinavir, DCF=diclofenac, BGM=bergamottin, MBF=mibefradil and NCD=nicardipine.

Comparing simulations of multiple dose inhibition, once daily for three days, using the NEWE model and conventional modelling approach the NEWE model displayed higher CYP3A activity as compared to the conventional modelling approach, albeit to a lesser extent as compared to single dose simulations. $A_{Ent\text{-}n/0,48\text{-}72h}$ varied from 100%, at a $K_{I,u}$

of 2000 µM and a k_{inact} of 1 h^{-1}, to 209% at a $K_{I,u}$ of 0.1 µM and a k_{inact} of 1 h^{-1} (Figure 6.10).

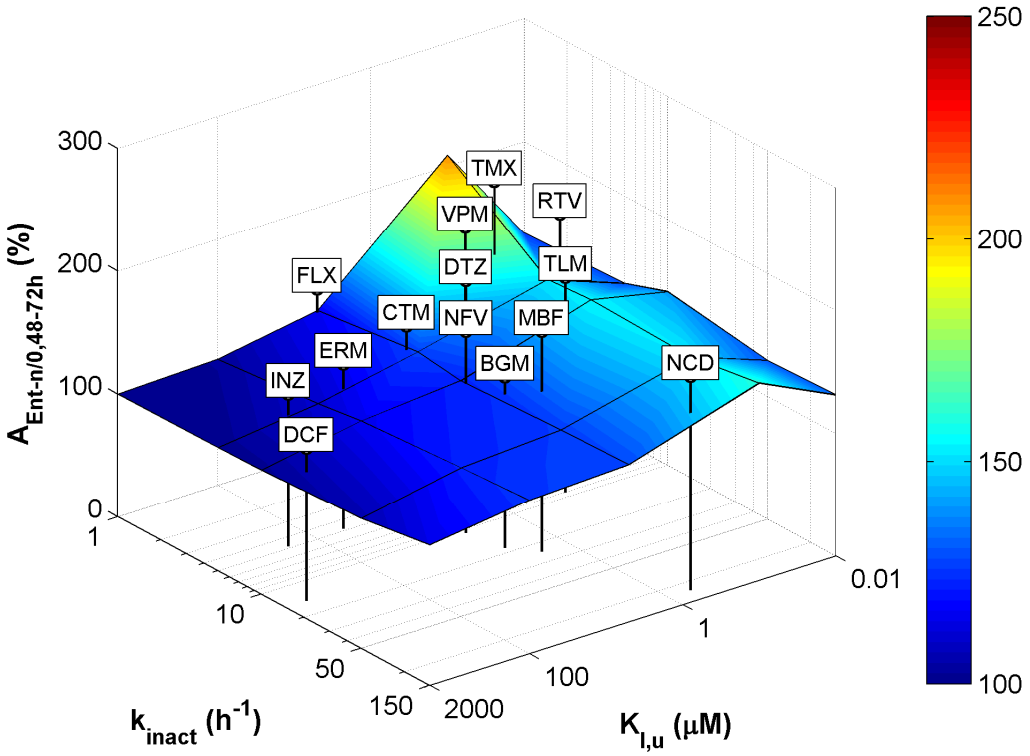

Figure 6.10. Simulated relative activity of CYP3A4 in the gastrointestinal tract over 24h following multiple dosing mechanism-based inhibition using the nested enzyme-within-enterocyte (NEWE) model relative to the conventional model scenario ($A_{Ent-n/0,48-72h}$ [%]) in relation to $K_{I,u}$ (the inhibitor concentration that produces half of the maximal rate of inactivation [µM]) and k_{inact} (the maximal rate of enzyme inactivation [h^{-1}]). FLX=fluoxetine, TMX=tamoxifen, CTM=clarithromycin, RTV=ritonavir, ERM=erythromycin, INZ=isoniazid, VPM=verapamil, DTZ=diltiazem, TLM=troleandomycin, NFV=nelfinavir, DCF=diclofenac, BGM=bergamottin, MBF=mibefradil and NCD=nicardipine.

6.5 Discussion

Overall, the developed NEWE model produced a higher small intestinal CYP3A4 activity following mechanism-based inhibition as compared to the conventional PBPK modelling approach ($k_{deg,Ent}$=0 h^{-1}). The NEWE model displayed a higher level of CYP3A4 activity following MBI as a consequence of an increase in $k_{deg,Ent}$ and $k_{deg,CYP3A}$. Inhibitors displaying a low $K_{I,u}$ or high k_{inact} were more likely to give rise to a lower level of inhibition, where a combination of a low $K_{I,u}$ and a high k_{inact} led to the lowest level of inhibition, using the NEWE model as compared to the conventional model (Figure 6.5-6.10).

Comparing the outcome of the NEWE model on intestinal CYP3A4 activity using observed data of $k_{deg,Ent}$ and $k_{deg,CYP3A}$ as compared to the hybrid parameter $k_{deg,CYP3A}$ in the conventional model, indicated the NEWE model to display a lower degree of inhibition for a number of mechanism-based inhibitors. The increase in intestinal CYP3A4 activity was further apparent for inhibitors where over-predictions have been observed utilising a conventional modelling approach, including fluoxetine ($K_{I,u}$=5.19 µM, k_{inact}=1.02 h^{-1}) and mibefradil ($K_{I,u}$=2.23 µM, k_{inact}=24 h^{-1}), displaying approximately 13% and 31% higher activity of intestinal CYP3A4 respectively following MBI (Figure 6.9).

The data utilised for observed values of $k_{deg,Ent}$ and $k_{deg,CYP3A}$ and the surrogate parameter of $k_{deg,CYP3A}$ were however suffering from a high degree of uncertainty where lack of variance in reported data limited the simulation to the use of arithmetic mean values. The enzyme turnover data was based on human *in vitro* hepatocyte assays, where it is questionable how this translates into small intestinal CYP3A4 turnover *in vivo* (Yang *et al.*, 2008). The surrogate parameter of $k_{deg,Ent}$ and $k_{deg,CYP3A}$ was based on the rate of recovery of grapefruit juice studies in man, known to display a high variability in the level of inhibition depending on the volume grapefruit juice consumed and its concentration of inhibitory constituents, displaying a large variability between batches. It has further been observed *in vivo* that the inhibitory constituents are both mechanism-based and reversible inhibitors, thus leading to a potential overestimation in $k_{deg,CYP3A}$ based on grapefruit juice data (Paine *et al.*, 2004; Uesawa *et al.*, 2011). Further, the estimate of $k_{deg,Ent}$ was subject to limitations in sample size, where a the majority of the data was based on colorectal and gastric epithelium turnover data.

Method limitations for measuring $k_{deg,Ent}$ also limited the human data to mainly consist of cancer patients where discrepancies may exist as compared to a healthy population.

In conventional PBPK approaches to modelling MBI the enzyme turnover rate is modelled as a first-order rate (Rowland Yeo *et al.*, 2010); whereas the gastrointestinal epithelial cell population conforms to a uniform distribution where the turnover is most likely to follow a zero-order rate or be of a sequential nature, where for example the distribution of DNA synthesising cells in the small intestine has been indicated to conform to a random or asynchronous distribution (Bell *et al.*, 1967; van Leeuwen *et al.*, 2009). As a consequence the NEWE model may improve the prediction of not only the extent and timeframe of MBI but also describing the time profile at which recovery of active enzyme occurs in the small intestine.

A more physiological modelling approach may further allow the prediction of DDIs in special subpopulations where small intestinal mucosal structure, enzyme or enterocyte turnover are altered. Alteration to the renewal of the small intestinal epithelium has been observed for a number of disease conditions in man, including: Coeliac disease patients, patients subject to small intestinal resection, patients subject to radiation therapy and untreated patients with pernicious anaemia or vitamin B_{12} and folate deficiency (Winawer *et al.*, 1965; Trier and Browning, 1966; Foroozan and Trier, 1967; Weinstein *et al.*, 1969). Certain drugs may also affect the turnover of the enterocytes, where altered small intestinal epithelial cell renewal has been observed following treatment with antibiotics, cancer chemotherapy, colchicine and methotrexate (Trier, 1962; Race *et al.*, 1970; Weinstein, 1974).

In addition to alterations of the enterocyte renewal in disease populations, pre-clinical data imply alterations in the turnover as a consequence of age e.g., in lambs and piglets, an increase in epithelial cell turnover time was observed as a consequence of postnatal adaptation of the small intestine following birth (Attaix and Meslin, 1991).

Contrasting evidence exist regarding the regional difference in enterocyte turnover along the small intestine. In neonatal pig the distal small intestine displayed a slower turnover as compared to the proximal small intestine using bromodeoxyuridine labeling assay; whereas regional differences in enterocyte turnover between the small intestine

and colon have been observed in rat, although differences between duodenum, jejunum and ileum were minimal (Bertalanffy and Lau, 1962; Fan *et al.*, 2001). In the previous study, analysis of human data on gastrointestinal epithelial turnover identified the colorectal cell renewal to be slower as compared to the stomach, whereas data from the small intestinal regions were too sparse in order to capture any regional differences (Figure 5.5).

The development of the NEWE model was subject to a number of assumptions where the modelling approach did not consider the maturation of enterocytes, metabolic and absorptive capability or any regional differences in turnover, albeit the collated information of $k_{deg,Ent}$ did not support this. The sensitivity analysis was limited to altering a restricted number of drug specific parameters, where k_a, dose and the clearance of the inhibitor was kept at a constant level which only satisfies hypothetical scenarios of MBI. The developed model therefore requires validation against clinical MBI data in order to determine if improvements are made in the prediction of DDIs. Due to the sparse data on enzyme and enterocyte turnover the level at which the small intestinal activity of CYP3A4 differs may differ in reality due to the uncertainty in the estimates of $k_{deg,Ent}$ and $k_{deg,CYP3A}$, although the discrepancy between the two models should remain as indicated by the sensitivity analysis where the overall trend was that the NEWE model produced equal or higher level of intestinal CYP3A4 activity.

The developed NEWE model is, to our knowledge, the first PBPK model to consider the nesting and hierarchy of the enzyme and enterocyte turnover in the small intestine. The model has the potential to improve on predictions of mechanism-based inhibition where overpredictions have been observed. The utilisation of a more physiological description of small intestinal enzyme and cell dynamics following DDIs has the potential for further application on a number of subpopulations and disease states where the enzyme or enterocyte turnover may be altered.

6.6 Acknowledgements

Authors wish to thank Mr Michael Croucher (University of Manchester), for his assistance with optimising the model code in Matlab and C programming language.

6.7 References

Agoram B, Woltosz WS, and Bolger MB (2001) Predicting the impact of physiological and biochemical processes on oral drug bioavailability. *Adv Drug Deliv Rev* **50 Suppl 1:**S41-67.

Attaix D and Meslin JC (1991) Changes in small intestinal mucosa morphology and cell renewal in suckling, prolonged-suckling, and weaned lambs. *Am J Physiol* **261:**R811-818.

Austin RP, Barton P, Cockroft SL, Wenlock MC, and Riley RJ (2002) The influence of nonspecific microsomal binding on apparent intrinsic clearance, and its prediction from physicochemical properties. *Drug Metab Dispos* **30:**1497-1503.

Bell B, Almy TP, and Lipkin M (1967) Cell proliferation kinetics in the gastrointestinal tract of man. 3. Cell renewal in esophagus, stomach, and jejunum of a patient with treated pernicious anemia. *Journal of the National Cancer Institute* **38:**615-628.

Bertalanffy FD and Lau C (1962) Cell Renewal. *International Journal of Cytology* **13:**357-366.

Burt HJ, Pertinez H, Sall C, Collins C, Hyland R, Houston JB, and Galetin A (2012) Progress curve mechanistic modeling approach for assessing time-dependent inhibition of CYP3A4. *Drug Metab Dispos* **40:**1658-1667.

Fahmi OA, Hurst S, Plowchalk D, Cook J, Guo F, Youdim K, Dickins M, Phipps A, Darekar A, Hyland R, and Obach RS (2009) Comparison of different algorithms for predicting clinical drug-drug interactions, based on the use of CYP3A4 in vitro data: predictions of compounds as precipitants of interaction. *Drug Metab Dispos* **37:**1658-1666.

Fan MZ, Stoll B, Jiang R, and Burrin DG (2001) Enterocyte digestive enzyme activity along the crypt-villus and longitudinal axes in the neonatal pig small intestine. *Journal of animal science* **79:**371-381.

Foroozan P and Trier JS (1967) Mucosa of the small intestine in pernicious anemia. *The New England journal of medicine* **277:**553-559.

Galetin A, Gertz M, and Houston JB (2008) Potential role of intestinal first-pass metabolism in the prediction of drug-drug interactions. *Expert Opin Drug Metab Toxicol* **4:**909-922.

Gertz M, Houston JB, and Galetin A (2011) Physiologically based pharmacokinetic modeling of intestinal first-pass metabolism of CYP3A substrates with high intestinal extraction. *Drug Metab Dispos* **39:**1633-1642.

Jamei M, Turner D, Yang J, Neuhoff S, Polak S, Rostami-Hodjegan A, and Tucker G (2009) Population-based mechanistic prediction of oral drug absorption. *AAPS J* **11:**225-237.

Malato Y, Naqvi S, Schurmann N, Ng R, Wang B, Zape J, Kay MA, Grimm D, and Willenbring H (2011) Fate tracing of mature hepatocytes in mouse liver homeostasis and regeneration. *J Clin Invest* **121:**4850-4860.

Obach RS, Walsky RL, and Venkatakrishnan K (2007) Mechanism-based inactivation of human cytochrome p450 enzymes and the prediction of drug-drug interactions. *Drug Metab Dispos* **35:**246-255.

Paine MF, Criss AB, and Watkins PB (2004) Two major grapefruit juice components differ in intestinal CYP3A4 inhibition kinetic and binding properties. *Drug Metab Dispos* **32:**1146-1153.

Race TF, Paes IC, and Faloon WW (1970) Intestinal malabsorption induced by oral colchicine. Comparison with neomycin and cathartic agents. *The American journal of the medical sciences* **259:**32-41.

Rew DA and Wilson GD (2000) Cell production rates in human tissues and tumours and their significance. Part 1: an introduction to the techniques of measurement and their limitations. *European journal of surgical oncology : the journal of the European Society of Surgical Oncology and the British Association of Surgical Oncology* **26:**227-238.

Rowland Yeo K, Jamei M, Yang J, Tucker GT, and Rostami-Hodjegan A (2010) Physiologically based mechanistic modelling to predict complex drug-drug interactions involving simultaneous competitive and time-dependent enzyme inhibition by parent compound and its metabolite in both liver and gut - the effect of diltiazem on the time-course of exposure to triazolam. *Eur J Pharm Sci* **39:**298-309.

Thelen K and Dressman JB (2009) Cytochrome P450-mediated metabolism in the human gut wall. *J Pharm Pharmacol* **61:**541-558.

Trier JS (1962) Morphologic alterations induced by methotrexate in the mucosa of human proximal intestine. II. Electron microscopic observations. *Gastroenterology* **43:**407-424.

Trier JS and Browning TH (1966) Morphologic response of the mucosa of human small intestine to x-ray exposure. *J Clin Invest* **45:**194-204.

Uesawa Y, Abe M, Fukuda E, Baba M, Okada Y, and Mohri K (2011) Construction of a model to estimate the CYP3A inhibitory effect of grapefruit juice. *Die Pharmazie* **66:**525-528.

van Leeuwen IM, Mirams GR, Walter A, Fletcher A, Murray P, Osborne J, Varma S, Young SJ, Cooper J, Doyle B, Pitt-Francis J, Momtahan L, Pathmanathan P, Whiteley JP, Chapman SJ, Gavaghan DJ, Jensen OE, King JR, Maini PK, Waters SL, and Byrne HM (2009) An integrative computational model for intestinal tissue renewal. *Cell Prolif* **42:**617-636.

Weinstein LD, Shoemaker CP, Hersh T, and Wright HK (1969) Enhanced intestinal absorption after small bowel resection in man. *Arch Surg* **99:**560-562.

Weinstein WM (1974) Epithelial cell renewal of the small intestinal mucosa. *The Medical clinics of North America* **58:**1375-1386.

WHO (2011) WHO Model List of Esssential Medicines, 17th Edition, WHO.

Winawer SJ, Sullivan LW, Herbert V, and Zamcheck N (1965) The Jejunal Mucosa in Patients with Nutritional Folate Deficiency and Megaloblastic Anemia. *The New England journal of medicine* **272:**892-895.

Yang J, Jamei M, Yeo KR, Tucker GT, and Rostami-Hodjegan A (2007) Prediction of intestinal first-pass drug metabolism. *Curr Drug Metab* **8:**676-684.

Yang J, Liao M, Shou M, Jamei M, Yeo KR, Tucker GT, and Rostami-Hodjegan A (2008) Cytochrome p450 turnover: regulation of synthesis and degradation, methods for determining rates, and implications for the prediction of drug interactions. *Curr Drug Metab* **9:**384-394.

Zhou S, Chan E, Li X, and Huang M (2005) Clinical outcomes and management of mechanism-based inhibition of cytochrome P450 3A4. *Ther Clin Risk Manag* **1:**3-13.

Chapter 7: Discussion and conclusions

Chapter 7: Discussion and conclusions

In this thesis, a systems pharmacology approach utilising physiologically-based pharmacokinetic modelling and simulation coupled to *in vitro-in vivo* extrapolation was utilised to model oral drug bioavailability with a particular interest in the gastrointestinal component. Two cases were investigated were $f_a \cdot F_G$ plays a potentially important role in the prediction of systemic exposure, thus allowing the exploration of the interplay between oral drug absorption and metabolism in the gut-wall. Examined cases were PBPK M&S of trends in oral drug exposure in a morbidly obese patient population subject to bariatric surgery and the development and assessment of a nested enzyme-within-enterocyte model in order to improve the mechanistic description of mechanism-based inhibition of gut wall metabolism facilitated by CYP3A.

7.1 PBPK M&S of oral drug bioavailability post bariatric surgery

Post bariatric surgery PBPK models were developed through a systematic approach including the identification of population dependent intrinsic factors, characterisation of systems parameters, model development and implementation based on the mechanistic model for oral drug bioavailability, the ADAM model. Assessment of the perturbed model was carried out using sensitivity analysis and validation against clinical data.

The outcome of the validation exercise of post bariatric surgery PBPK models was to some extent reflective how well characterised the systems parameters of intrinsic factors were, where the most well-characterised post bariatric surgery model, post Roux-en-Y gastric bypass, was highly predictive of clinical outcomes of oral drug exposure of atorvastatin acid and cyclosporine, whereas oral drug exposure of atorvastatin acid following BPD-DS was underpredicted using the standard model including all known physiological changes. Additional validation occurred prospectively through generation of clinical data of omeprazole and midazolam pre to post RYGB by Tandra, and co-workers. The study found omeprazole to display a minimal discrepancy post RYGB as compared to controls, whereas midazolam displayed a minor increase in exposure post RYGB as compared to controls. This was consistent with simulations carried out during the model assessment and application (Figure 3.9, Figure 7.1 and Figure 8.6) (Darwich *et al.*, 2012b; Tandra *et al.*, 2013).

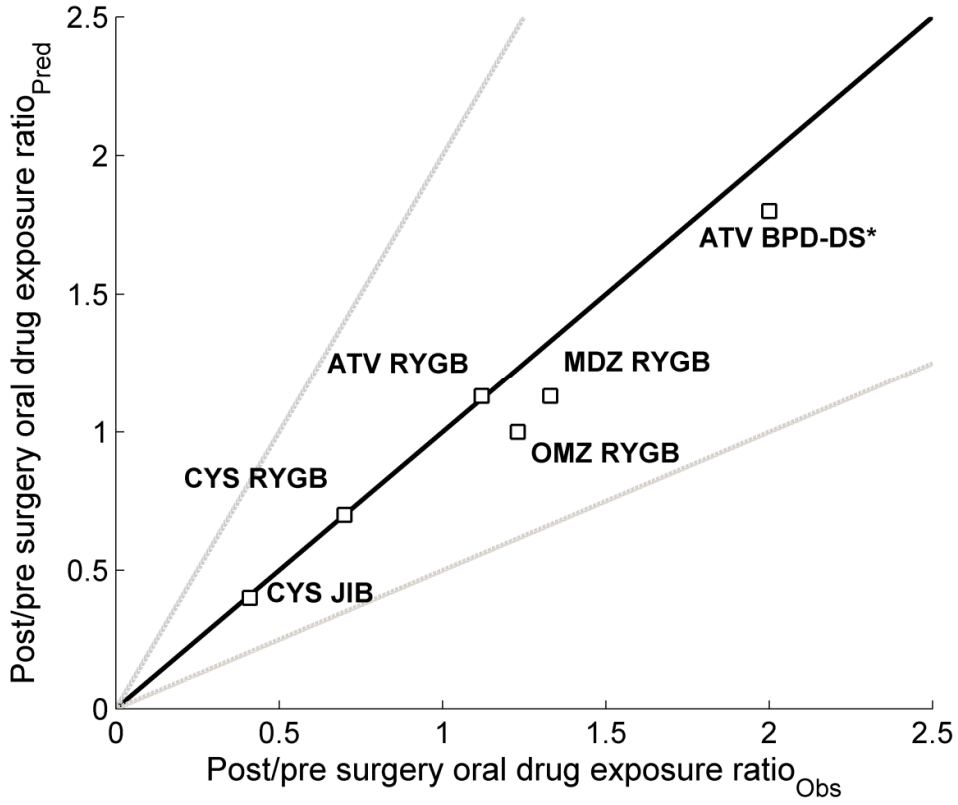

Figure 7.1. Mean predicted (Pred) versus observed (Obs) post/pre surgery AUC ratios for cyclosporine (CYS), atorvastatin acid (ATV), omeprazole (OMZ) and midazolam (MDZ) following Roux-en-Y gastric bypass (RYGB) at a small intestinal transit (SIT) time of 3.0 h, jejunoileal bypass (JIB SIT=0.4 h) and biliopancreatic diversion with duodenal switch (BPD-DS* SIT=4.2 h) in relation to the line of unity and two-fold within observed data (Chenhsu *et al.*, 2003; Skottheim *et al.*, 2009; Skottheim *et al.*, 2010; Darwich *et al.*, 2012b; Tandra *et al.*, 2013; Darwich *et al.*, 2013).

The discrepancy between observed and simulated exposure of atorvastatin acid pre to post BPD-DS could be anticipated as the BPD-DS model was populated with relatively uninformative systems parameters of small intestinal transit and biliary excretion, it was further speculated that the surgical procedure may produce unanticipated physiological outcomes due to its relative invasiveness as compared to RYGB and SG. The PBPK M&S approach did however have the advantage of allowing exploratory sensitivity analysis, where a prediction of small intestinal transit based on peptide YY-mouth-to-

caecum transit recovered the observed exposure albeit underpredicting observed C_{max} and t_{max}, the same was true for altering villous blood flow.

Hendriks highlighted that for the publication of negative results in M&S to be justified necessary considerations have to be made regarding a model's credibility where evaluation of a model's credibility becomes increasingly difficult as PBPK models become more complex. This holds true for both positive and negative prediction outcomes. Hendriks further argued that necessary steps should be taken to articulate how the negative finding may inform scientific and hypotheses generation (Hendriks, 2013).

The utilised ADAM model and its predecessors have been applied extensively in the past (Jamei *et al.*, 2009). In the publication by Darwich, and co-workers, it was however made clear that physiological data was lacking for crucial systems parameters following BPD-DS (Darwich *et al.*, 2013). The sensitivity analysis of atorvastatin acid exposure following BPD-DS provided a potential scientific rationale for the observed increase in oral drug exposure following surgery and highlighted potentially important intrinsic factors that require further research in order to understand the post-surgical physiology. This would not have been made apparent had the results been published utilising only optimised systems parameters. It can therefore be argued that the aim of PBPK M&S within a systems pharmacology framework should not only be limited to the ability of predicting retrospective clinical data but it is of equal importance as a scientific framework for hypothesis generation.

An emerging body of evidence has been published supporting the impact of gastrointestinal hormones on physiological function, this can become crucial in fully unravelling the impact of bariatric surgery on oral first-pass effects as several hormones have been confirmed to affect intestinal physiological parameters whereas the quantitative data concerning the relationship between gastric hormone levels and systems parameters are at its best limited (Savage *et al.*, 1987; Sanger and Lee, 2008). The Medical Research Council (MRC) has identified bariatric surgery as a research tool for understanding the mechanisms of obesity and related diseases and the neuroscience of obesity. The developed PBPK models for bariatric surgery that are presented in this

thesis may provide a framework for linking physiological and hormonal data to oral drug delivery to potentially assist future research efforts (MRC, 2013).

Developed post bariatric surgery PBPK models provide a framework for theoretical exploration of physiological mechanisms associated with altered oral drug exposure pre to post surgery, which could be assigned to the interplay between dissolution, absorption and gut-wall metabolism, where dissolution and formulation properties emerged as the perhaps most important parameters in predicting the exposure following surgery.

At its full potential, post bariatric surgery models can be utilised for optimisation of pharmacotherapy, facilitating clinical decision making, and drug regulation. It may be postulated that this would be an area of particular relevance for the prediction of oral exposure of antidepressants as emerging clinical evidence suggest this drug class to display a reduced oral drug exposure following RYGB whereas they remain clinically relevant following surgery (Malone and Alger-Mayer, 2005; Darwich *et al.*, 2012a; Roerig *et al.*, 2012; Roerig *et al.*, 2013).

The utilisation of bariatric surgery PBPK models in clinical pharmacotherapy could partly be made possible due to user interface improvements in population-based PBPK software such as the Simcyp® Simulator, albeit usage may be restricted due to the required expertise to carry out M&S of novel compounds. The systems pharmacology approach does however provide complimentary advantages in addition to population pharmacokinetic approaches that have been used for clinical dose optimisation, such as the RightDose™ software developed at the University of Southern California Laboratory of Applied Pharmacokinetics, by allowing mechanistic-based extrapolation along with estimates of population variability (Hope *et al.*, 2013).

In conclusion developed post bariatric surgery models provide a framework for studying mechanisms involved in the alteration of oral drug exposure and potentially provides a framework for pharmacotherapeutic drug optimisation. The relative success in modelling of oral drug exposure in post bariatric surgery patient populations further serves as a validation of the utilised template model, ADAM, incorporated into the

Simcyp® Simulator, through the successful prediction of oral drug exposure in a perturbed model system (Jamei *et al.*, 2009; Tsamandouras *et al.*, 2013).

7.2 Development of a nested enzyme-within-enterocyte model for predicting MBIs

A mechanistic model was developed to describe the hierarchical interdependency between enterocyte and enzyme turnover in the small intestine and its impact on the prediction of enzyme recovery following mechanism-based inhibition as compared to the conventional PBPK approach to modelling MBIs where enzyme and enterocyte turnover are lumped into a single rate of renewal as determined via indirect data in the form of clinical MBI studies.

The developed nested enzyme-within-enterocyte (NEWE) model is to the authors' knowledge the first model to differentiate between the first-order renewal of CYP enzyme activity and the zero-order turnover of the enterocytes in the small intestine following mechanism-based inhibition, thus avoiding the misspecification resulting from the lumping of these two physiological processes into a first-order rate.

Utilising the developed NEWE model, a lower level of inhibition of CYP3A following MBI was predicted during simulations as had been postulated. The predicted enzyme recovery using the NEWE model may potentially account for reported overpredictions in the level of mechanism-based inhibition as seen utilising static and dynamic modelling approaches coupled to IVIVE (Obach *et al.*, 2007; Fahmi *et al.*, 2009; Obach, 2013).

Uncertainties emerged regarding the parameter estimates of enzyme turnover as these were limited to *in vitro* data from cultured hepatocytes and human liver microsomes. It was further unclear what the consequences of enzyme inhibition would be on the substrate specific metabolic extraction in the gut wall where nonlinearity between enzyme activity and F_G may exist. This may be addressed through further model assessment and application, exploring the impact of NEWE model predictions subject to substrate specific metabolism.

Regardless, the model provides a more mechanistic description of enzyme recovery following mechanism-based enzyme inhibition in the small intestine where systems parameters are derived utilising a systems pharmacology approach rather than parameter estimation informed via indirect clinical data. The model can be utilised to predict the extent of gut wall metabolism and DDIs for orally administered drugs in special disease populations where enzyme or enterocyte turnover may be altered.

7.3 Principles and concepts of physiologically-based pharmacokinetic modelling and simulation

In this thesis, it was demonstrated that the systems pharmacology approach provides a potentially useful tool in the extrapolation and mechanistic exploration of the gastrointestinal component of F_{oral} in special subpopulations and theoretical modelling scenarios, such as the NEWE model development.

More mechanistic and highly specialised PBPK models have emerged in recent years to address scientific queries regarding special subpopulations and disease modelling. This has been made possible due to interdisciplinary efforts in the areas of systems biology, pharmacology and PBPK modelling, with the result of PBPK models with increasing levels of complexity *e.g.* type II diabetes, cardiac safety, hormonal responses, enterocyte maturation and more (Gadkar *et al.*, 2007; Shoda *et al.*, 2010; Machavaram *et al.*, 2013; Polak, 2013; Chen *et al.*, 2014). Implemented modelling approaches throughout this thesis clearly conform to this trend and motivates the discussion of some of the underlying principles that make up PBPK M&S and systems pharmacology, and where PBPK will be heading in future.

'Top-down' versus 'bottom-up' and meeting in the middle

The utilisation of PBPK M&S under the principles of systems pharmacology is often referred to as a 'bottom-up' approach, where model specification and parameterisation is based on physiological data, IVIVE and IVIVC. The 'bottom-up' approach may, philosophically and in principle, be considered the flip-side of the empirical compartmental modelling approach, referred to as the 'top-down' approach.

These two approaches do however serve distinct purposes in PK M&S, where 'bottom-up' has the inherent advantages of allowing mechanistic interpretation and facilitating extrapolation, including: IVIVE, interspecies and between population extrapolation, such as the case of bariatric surgery and DDIs as exemplified in this thesis where clinical data may be sparse. The 'bottom-up' approach is however extremely 'data hungry', requiring data from interdisciplinary sciences in order to populate and give confidence to systems parameters, there has however been an easement over the last decades due to the development and refinement of IVIVE, IVIVC and *in silico* methods for parameter predictions based on PhysChem data.

Utilising a 'top-down' approach an empirical model can be derived solely based on clinical data, producing estimates of population parameters and their variability. The success of the approach is however highly dependent on the clinical data and does not enable extrapolation to other study populations. The 'top-down' approach is highly advantageous in clinical research where it may be utilised for optimal design of late-stage clinical trials and covariate analysis.

The perhaps more pragmatic and viable approach is to utilise a data driven modelling approach where the angle from which the problem is tackled may be chosen based on available data and the aim of the modelling exercise. Depending on available data, model parameters may be derived using a physiologically-based approach or parameter estimation methods inferred from clinical data, this approach is often referred to as the 'middle-out' approach. One of the main challenges of utilising such a 'middle-out' approach is the issue of structural identifiability, where a complex PBPK model structure may not enable the unique identification of a single 'true' parameter value, or global optima. Further, complex PBPK models may not be sensitive to specific parameter estimates due to the intrinsic sensitivity of the structural model or design of associated clinical data. An important consideration when estimating parameters in a PBPK model is the correlation between parameters, where for example a substrate's affinity to a particular enzyme should not differ in different tissues. These issues may be overcome to a varying extent by altering the structural model or through reparameterisation, designing experiments to inform the model or the usage of prior knowledge to inform model parameters thus restricting parameters within plausible ranges (Yates, 2006; Tsamandouras *et al.*, 2013).

To examining the PBPK M&S cases in this thesis it was prerequisite to utilise a 'bottom-up' approach as the modelling tasks were concerned with the extrapolation of drug disposition between populations and exploratory M&S albeit some elements of 'middle-out' approach were implemented due to the utilisation of parameter estimation concerning transporter activity. Due to the complexity of the model concerns regarding the structural identifiability of estimated parameters may be justified as is the general concern when estimating parameters of a full PBPK model. Estimated parameters concerning transporter activity were not possible to scale using IVIVE due to the lack of absolute transporter abundance data in man. Estimations could however be considered to lie within plausible ranges.

External versus internal tools

The research carried out in this thesis further showcase the utilisation and respective benefits of external and internal tools in PBPK M&S. External tools can in short be described as externally developed M&S platforms consisting of a set of predefined models that may be utilised and perturbed to varying extent, *e.g.* Simcyp® Simulator and GastroPlus™. Internal tools provide a more general modelling environment for custom model development and usually involve the utilisation of a high-level programming language, such as Matlab and R, but may also provide model development through a graphical user interface, such as the case for SAAM 2. This is not to be confused with commercial versus open-source software platforms as toolsets may exist in both forms (Vicini *et al.*, 2013).

External and internal PBPK M&S tools have their distinct advantages and disadvantages. External tools provide several advantages, including the provision of a general framework for PBPK M&S consisting of widely recognised modelling approaches and procedures. In general, external models are also populated with parameters from rich datasets, thus providing more reliable estimates of systems parameters and their variability. This enables modellers, reviewers and regulatory bodies with ease of interpretation of model development and outcomes, and reproducing results. As external tools generally provide user-friendly interfaces the toolset are more readily available for non-modellers, this is of particular importance in PBPK where the

discipline relies on the generation of parameter data from interdisciplinary sciences (Vicini *et al.*, 2013).

One of the main disadvantages with the utilising of external tools is that these in general provide highly specific frameworks for modelling which may be considered a 'black box' if the user is not adequately trained in utilising provided models and tools (Vicini *et al.*, 2013).

The use of an external toolset was of particular benefit in the development of post bariatric surgery PBPK models as these were all developed through the perturbation of a highly complex absorption model, it was therefore essential for the models to be populated by well-characterised systems parameters in order to estimate population variability. The user-friendly interface may further be an advantage if the models are to be implemented by non-modellers in a clinical setting. The main limitation was the lack of flexibility that the external tool provided where certain aspects of alterations in fluid dynamics (altered luminal secretion and reabsorption) could not be tested.

The most apparent advantage of utilising an internal PBPK M&S toolset is the inherent flexibility in model development and customisation. This may be particularly suitable for testing novel modelling concepts and ideas, such as the case of the NEWE model described above, or performing modelling tasks outside the general framework of PBPK. Providing that a published model is adequately described reproduction may be considered a non-issue, this does however require adequate expertise in utilising the programming language of an internal toolset and may therefore make interpretation and reviewing more difficult. An additional disadvantage of internal tools is the lack of the volume of data and analysis that has gone into populating the parameters of an external tool. As external M&S tools are developing into more flexible working environments the distinction between the two toolsets is becoming less apparent where both toolsets may for example facilitate a 'middle-out' model development approach, as exemplified in this thesis where parameters for the tissue disposition of atorvastatin acid could be estimated in order to infer missing data (Vicini *et al.*, 2013).

General framework and the regulatory view on PBPK M&S

In recent years there has been a significant increase in the usage of PBPK models by regulatory bodies and pharmaceutical industry to support regulatory submissions and prescribing information for dose optimisation, DDI predictions and extrapolation to special populations. PBPK M&S has now for the first time been utilised in drug labelling to singlehandedly inform outcomes following DDIs. Due to cost and practical issues with recruitment not all physiological conditions where several physiological factors vary from the norm can be investigated through clinical studies to inform drug labelling. This extends to post bariatric surgery patient populations where patient numbers are increasing rapidly whereas patient recruitment can be cumbersome. FDA highlighted some of the issues that need to be overcome in order for PBPK M&S to reach its full potential, this includes: a better understanding of off target effects and drug disposition, integration of 'bottom-up' and 'top-down' modelling approaches, education and training, sharing of data between academia industry and government, better procedures for model evaluation, and the development and utilisation of general frameworks and best practices in PBPK M&S (Huang *et al.*, 2013; Pharmacyclics, 2013).

In 2011 FDA published a general scheme for PBPK model development based on lessons learned from earlier reviewed submissions of new drug applications and investigational new drugs. The general framework for PBPK subsequent fashion included: identification and quantification of clearance pathways, incorporation of drug dependent parameters into a PBPK model, comparison of concentration-time profiles to clinical data and finally the utilisation of refined PBPK model to predict drug disposition (Zhao *et al.*, 2011).

FDA also highlighted the increasing availability of PBPK models for special population due progress made in systems biology and pharmacology. Model development of special population models requires the identification of population specific extrinsic and intrinsic factors in order identify and characterise systems parameters, this will be followed by a general model development framework, incorporating systems and drug-specific parameters into a PBPK model followed by stages of predictions, learning and confirmation (Zhao *et al.*, 2011).

A similar framework was drawn up by the WHO in an attempt to harmonise the development of PBPK models for risk assessment. The postulated workflow put particular emphasis on problem evaluation and the need for purpose specific validation and evaluation (WHO, 2011).

The development of post bariatric surgery PBPK models took on a very similar approach, where the identification of the modelling aim was followed by problem evaluation in the form of a literature review and statistical meta-analysis, the identification of relevant intrinsic factors and their characterisation, model development, assessment and validation. In the case of bariatric surgery it is of particular interest to note its potential usage in identifying 'known unknown' intrinsic factors. As more data emerges further model refinements will be made possible. The systems pharmacology approach should be subject to constant review and revision of both models and parameter values in order to remain current as a tool for exploration and extrapolation.

Further, it should be emphasised that the model development for special populations should not be considered a problem constrained to population specific systems parameters. It is also critical to identify and characterise relevant drug and formulation-specific parameters that may interact with the altered systems parameters in order to answer the purpose specific questions, e.g. In order to draw well-founded conclusions regarding changes in F_G following bariatric surgery necessary metabolic assay *in vitro* data is required.

7.4 Final conclusions

A systems pharmacology approach was used in order to explore the GI component making up oral drug delivery. The impact of f_a and F_G on F_{oral} was explored through the successful implementation of PBPK models for a morbidly obese patient population subject to bariatric surgery and a mechanistic model describing the recovery of enzyme activity following mechanism-based inhibition using a nested enzyme-within-enterocyte turnover model of the small intestine. Developed models showcase the advantage of PBPK M&S in the extrapolation of oral drug exposure to special population and potential of the approach in understanding underlying the underlying mechanism governing oral drug delivery.

7.5 Future work

During the development and application of post bariatric surgery PBPK models a number of potential areas of further research presented themselves, these included: The quantitative modelling of gastric hormones and their effect on gastrointestinal systems parameters relevant to drug disposition and model application on the predicted oral exposure of antidepressants. Further, it would be of great interest to explore the potential of implementing a PBPK M&S framework in a clinical setting to optimise clinical pharmacotherapy.

Although assessment of the NEWE model suggested its potential for improving the prediction of enzyme recovery in the gut wall following mechanism-based inhibition further work is required to determine the predicted impact on substrate specific extraction in the gut wall and its ability to reproduce clinical outcomes. This should be done through model further model assessment exploring substrate specific F_G and validation against clinical MBI data.

In addition, the exploratory assessment of developed PBPK models identified areas of where our current understanding is lacking that may therefore require further research. Data is currently very limited with regards to the mechanistic and quantitative relation between gastric hormones, gastrointestinal physiology and how altered hormonal levels will affect the post bariatric surgery physiology short and long-term. Areas of interest for further research would also include: intestinal transit and fluid dynamics following bariatric surgery, the long-term adaptation of the gastrointestinal tract following bariatric surgery, and the characterisation of enzyme turnover in the small intestine independent from enterocyte turnover.

7.6 References

Chen EP, Tai G, and Ellens H (2014) The importance of villous physiology and morphology in mechanistic physiologically-based pharmacokinetic models. *Pharm Res* **31:**305-321.

Chenhsu RY, Wu Y, Katz D, and Rayhill S (2003) Dose-adjusted cyclosporine c2 in a patient with jejunoileal bypass as compared to seven other liver transplant recipients. *Ther Drug Monit* **25:**665-670.

Darwich AS, Henderson K, Burgin A, Ward N, Whittam J, Ammori BJ, Ashcroft DM, and Rostami-Hodjegan A (2012a) Trends in oral drug bioavailability following bariatric surgery: Examining the variable extent of impact on exposure of different drug classes. *Br J Clin Pharmacol* **74:**774-787.

Darwich AS, Pade D, Ammori BJ, Jamei M, Ashcroft DM, and Rostami-Hodjegan A (2012b) A mechanistic pharmacokinetic model to assess modified oral drug bioavailability post bariatric surgery in morbidly obese patients: interplay between CYP3A gut wall metabolism, permeability and dissolution. *J Pharm Pharmacol* **64:**1008-1024.

Darwich AS, Pade D, Rowland-Yeo K, Jamei M, Asberg A, Christensen H, Ashcroft DM, and Rostami-Hodjegan A (2013) Evaluation of an In Silico PBPK Post-Bariatric Surgery Model through Simulating Oral Drug Bioavailability of Atorvastatin and Cyclosporine. *CPT: pharmacometrics & systems pharmacology* **2:**e47.

Fahmi OA, Hurst S, Plowchalk D, Cook J, Guo F, Youdim K, Dickins M, Phipps A, Darekar A, Hyland R, and Obach RS (2009) Comparison of different algorithms for predicting clinical drug-drug interactions, based on the use of CYP3A4 in vitro data: predictions of compounds as precipitants of interaction. *Drug Metab Dispos* **37:**1658-1666.

Gadkar KG, Shoda LK, Kreuwel HT, Ramanujan S, Zheng Y, Whiting CC, and Young DL (2007) Dosing and timing effects of anti-CD40L therapy: predictions from a mathematical model of type 1 diabetes. *Annals of the New York Academy of Sciences* **1103:**63-68.

Hendriks B (2013) Negative modeling results: A dime a dozen or a stepping stone of scientific discovery? *CPT: pharmacometrics & systems pharmacology* **2:**1-2.

Hope WW, Vanguilder M, Donnelly JP, Blijlevens NM, Bruggemann RJ, Jelliffe RW, and Neely MN (2013) Software for dosage individualization of voriconazole for immunocompromised patients. *Antimicrob Agents Chemother* **57:**1888-1894.

Huang SM, Abernethy DR, Wang Y, Zhao P, and Zineh I (2013) The utility of modeling and simulation in drug development and regulatory review. *J Pharm Sci* **102:**2912-2923.

Jamei M, Turner D, Yang J, Neuhoff S, Polak S, Rostami-Hodjegan A, and Tucker G (2009) Population-based mechanistic prediction of oral drug absorption. *AAPS J* **11:**225-237.

Machavaram KK, Almond LM, Rostami-Hodjegan A, Gardner I, Jamei M, Tay S, Wong S, Joshi A, and Kenny JR (2013) A Physiologically Based Pharmacokinetic Modeling Approach to Predict Disease-Drug Interactions: Suppression of CYP3A by IL-6. *Clin Pharmacol Ther* **94:**260-268.

Malone M and Alger-Mayer SA (2005) Medication use patterns after gastric bypass surgery for weight management. *Ann Pharmacother* **39:**637-642.

MRC (2013) MRC Obesity research, Medical Research Council, Retrieved September 5, 2013, from: http://www.mrc.ac.uk/Ourresearch/Priorities/Obesityresearch/Fundedresearch/index.htm.

Obach RS (2013) Time-dependent inhibition of cytochrome P450 is important in drug-drug interactions - recent advances to meet the challenges, in: *DDI 2013 - 4th International Workshop on Regulatory Requirements and Current Scientific Aspects on the Preclinical and Clinical Investigation of Drug-Drug Interaction*, Marbach Castle, Germany.

Obach RS, Walsky RL, and Venkatakrishnan K (2007) Mechanism-based inactivation of human cytochrome p450 enzymes and the prediction of drug-drug interactions. *Drug Metab Dispos* **35:**246-255.

Pharmacyclics (2013) Highlights of prescribing information of IMBRUVICA (ibrutinib) capsules, for oral use.

Polak S (2013) In vitro to human in vivo translation - pharmacokinetics and pharmacodynamics of quinidine. *Altex* **30:**309-318.

Roerig JL, Steffen K, Zimmerman C, Mitchell JE, Crosby RD, and Cao L (2012) Preliminary comparison of sertraline levels in postbariatric surgery patients versus matched nonsurgical cohort. *Surg Obes Relat Dis* **8:**62-66.

Roerig JL, Steffen KJ, Zimmerman C, Mitchell JE, Crosby RD, and Cao L (2013) A comparison of duloxetine plasma levels in postbariatric surgery patients versus matched nonsurgical control subjects. *J Clin Psychopharmacol* **33:**479-484.

Sanger GJ and Lee K (2008) Hormones of the gut-brain axis as targets for the treatment of upper gastrointestinal disorders. *Nature Reviews Drug Discovery* **7:**241-254.

Savage AP, Adrian TE, Carolan G, Chatterjee VK, and Bloom SR (1987) Effects of peptide YY (PYY) on mouth to caecum intestinal transit time and on the rate of gastric emptying in healthy volunteers. *Gut* **28:**166-170.

Shoda L, Kreuwel H, Gadkar K, Zheng Y, Whiting C, Atkinson M, Bluestone J, Mathis D, Young D, and Ramanujan S (2010) The Type 1 Diabetes PhysioLab Platform: a validated physiologically based mathematical model of pathogenesis in the non-obese diabetic mouse. *Clinical and experimental immunology* **161:**250-267.

Skottheim IB, Jakobsen GS, Stormark K, Christensen H, Hjelmesaeth J, Jenssen T, Asberg A, and Sandbu R (2010) Significant increase in systemic exposure of atorvastatin after biliopancreatic diversion with duodenal switch. *Clin Pharmacol Ther* **87:**699-705.

Skottheim IB, Stormark K, Christensen H, Jakobsen GS, Hjelmesaeth J, Jenssen T, Reubsaet JL, Sandbu R, and Asberg A (2009) Significantly altered systemic exposure to atorvastatin acid following gastric bypass surgery in morbidly obese patients. *Clin Pharmacol Ther* **86:**311-318.

Tandra S, Chalasani N, Jones DR, Mattar S, Hall SD, and Vuppalanchi R (2013) Pharmacokinetic and Pharmacodynamic Alterations in the Roux-en-Y Gastric Bypass Recipients. *Ann Surg* **258**:262-269

Tsamandouras N, Rostami-Hodjegan A, and Aarons L (2013) Combining the "bottom-up" and "top-down" approaches in pharmacokinetic modelling: Fitting PBPK models to observed clinical data. *Br J Clin Pharmacol*.

Vicini P, Friberg LE, van der Graaf PH, and Rostami-Hodjegan A (2013) Pharmacometrics and Systems Pharmacology Software Tutorials and Use: Comments and Guidelines for PSP Contributions. *CPT: Pharmcometrics & Systems Pharmacology* **2:**1-3.

WHO (2011) Characterization and application of physiologically based pharmacokinetic models in risk assessment (Organisation WH ed, World Health Organisation, Geneva, Switzerland.

Yates JW (2006) Structural identifiability of physiologically based pharmacokinetic models. *J Pharmacokinet Pharmacodyn* **33:**421-439.

Zhao P, Zhang L, Grillo JA, Liu Q, Bullock JM, Moon YJ, Song P, Brar SS, Madabushi R, Wu TC, Booth BP, Rahman NA, Reynolds KS, Gil Berglund E, Lesko LJ, and Huang SM (2011) Applications of physiologically based pharmacokinetic (PBPK) modeling and simulation during regulatory review. *Clin Pharmacol Ther* **89:**259-267.

Chapter 8: Appendices

Chapter 8: Appendices

8.1 Trends in oral drug bioavailability following bariatric surgery: examining the variable extent of impact on exposure of different drug classes

8.1.1 Publication in British Journal of Clinical Pharmacology (2012) 74:774-787

BJCP British Journal of Clinical Pharmacology

DOI:10.1111/j.1365-2125.2012.04284.x

Trends in oral drug bioavailability following bariatric surgery: examining the variable extent of impact on exposure of different drug classes

Adam S. Darwich,[1] Kathryn Henderson,[1] Angela Burgin,[2,3] Nicola Ward,[4] Janet Whittam,[2,3] Basil J. Ammori,[3,5] Darren M. Ashcroft[2] & Amin Rostami-Hodjegan[1,6]

[1]Centre of Applied Pharmacokinetic Research, School of Pharmacy and Pharmaceutical Sciences, [2]School of Pharmacy and Pharmaceutical Sciences, University of Manchester, Manchester, [3]Salford Royal NHS Foundation Trust, Salford, [4]Leicester Royal Infirmary, University Hospitals of Leicester NHS Foundation Trust, Leicester, [5]School of Biomedicine, University of Manchester, Manchester and [6]Simcyp Ltd, Blades Enterprise Centre, Sheffield, UK

Correspondence
Professor Amin Rostami-Hodjegan, School of Pharmacy and Pharmaceutical Sciences, Faculty of Medical and Human Sciences, University of Manchester, Stopford Building, Oxford Road, Manchester M13 9PT UK.
Tel.: +44 161 306 0634
Fax: +44 161 275 2358
E-mail: amin.rostami@manchester.ac.uk

Keywords
bariatric surgery, biopharmaceutics classification system, CYP2C, CYP2D6, CYP3A, oral bioavailability

Received
9 November 2011

Accepted
23 March 2012

Accepted Article Published Online
30 March 2012

WHAT IS ALREADY KNOWN ABOUT THIS SUBJECT

- Changes to oral drug bioavailability have been observed post bariatric surgery. However, the magnitude and the direction of changes have not been assessed systematically to provide insights into the parameters governing the observed trends. Understanding these can help with dose adjustments.

WHAT THIS STUDY ADDS

- Analysis of drug characteristics based on a biopharmaceutical classification system is not adequate to explain observed trends in altered oral drug bioavailability following bariatric surgery, although the findings suggest solubility to play an important role.

AIMS

To identify the most commonly prescribed drugs in a bariatric surgery population and to assess existing evidence regarding trends in oral drug bioavailability post bariatric surgery.

METHODS

A retrospective audit was undertaken to document commonly prescribed drugs amongst patients undergoing bariatric surgery in an NHS hospital in the UK and to assess practice for drug administration following bariatric surgery. The available literature was examined for trends relating to drug permeability and solubility with regards to the Biopharmaceutics Classification System (BCS) and main route of elimination.

RESULTS

No significant difference in the 'post/pre surgery oral drug exposure ratio' (ppR) was apparent between BCS class I to IV drugs, with regards to dose number (Do) or main route of elimination. Drugs classified as 'solubility limited' displayed an overall reduction as compared with 'freely soluble' compounds, as well as an unaltered and increased ppR.

CONCLUSION

Clinical studies establishing guidelines for commonly prescribed drugs, and the monitoring of drugs exhibiting a narrow therapeutic window or without a readily assessed clinical endpoint, are warranted. Using mechanistically based pharmacokinetic modelling for simulating the multivariate nature of changes in drug exposure may serve as a useful tool in the further understanding of postoperative trends in oral drug exposure and in developing practical clinical guidance.

Introduction

Obesity is generally defined by the body mass index (BMI = body weight (kg)/height (m)^2). The classification is somewhat arbitrary such that 'overweight' means a BMI $\geq$ 25 but <30 kg m^{-2}, 'obesity' refers to BMI $\geq$ 30 but <40 kg m^{-2} and 'morbid obesity' is a BMI $\geq$ 40 kg m^{-2} (this may also refer to being obese and suffering from related co-morbid conditions) [1, 2]. Over the last decade the prevalence of obesity has increased dramatically in the USA and Europe. In the USA 32.2% of the male and 35.5% of the female population over the age of 20 years were characterized as obese in 2007–2008 [3]. The United Kingdom has the highest reported obesity rate in Europe [4]. In England, 24.1% of the male and 24.9% of the female population over the age of 16 years were classified as obese in 2008 [5]. Bariatric surgery has proven to be successful in treating morbid obesity. In the USA and Canada approximately 200 000 bariatric surgeries were performed in 2008 [6]. In England 4221 surgeries were performed in 2008/09, an increase of over 100% since 2006/07 [1, 7]. Several bariatric surgical methods currently coexist in healthcare. These include the adjustable gastric band (AGBD), sleeve gastrectomy (SG), biliopancreatic diversion (BPD), biliopancreatic diversion with duodenal switch (BPD-DS) and Roux-en-Y gastric bypass (RYGB) [8]. Other procedures, such as jejunoileal bypass (JIB), have been gradually phased out due to a higher likelihood of adverse events [9–11].

Bariatric surgical procedures have been well described in the literature [11, 12], where they are generally characterized as being restrictive, in terms of physiologically reducing dietary intake, malabsorptive, through reducing the ability of the gastrointestinal (GI) tract to absorb nutrients or a combination of both.

Restrictive procedures such as AGBD and SG result in a reduced gastric capacity to 15–20 ml and 60–80 ml respectively [12, 13]. The JIB, considered a malabsorptive procedure, results in a 90–95% bypass of the small intestine, retaining the duodenum, proximal jejunum and terminal ileum [9–11]. The BPD-DS, primarily a malabsorptive procedure, results in a reduced gastric volume (100–175 ml) and bypass of larger parts of the small intestine, forming a biliopancreatic canal transporting the bile juices to the distal ileum [14, 15]. The RYGB, combining restriction and malabsorption, results in the restriction of the stomach to 15–30 ml and bypass of the proximal small intestine [15–17].

Bariatric surgery imposes a number of physiological alterations known to affect the bioavailability of orally administered drugs (F_{oral}), dependent on the fraction of drug that is absorbed in the intestinal gut wall (f_a), the fraction that escapes gut wall metabolism (f_G), and the fraction that escapes hepatic metabolism (f_H) (Equation 1).

$$F_{oral} = f_a \cdot f_G \cdot f_H \quad (1)$$

f_a and f_G are highly influenced by drug specific properties, such as permeability and solubility, and the GI physiology such as gastric emptying time, GI pH profiles, small intestinal transit time, GI drug metabolizing enzymes and GI efflux transporters [18, 19]. Gastric emptying time can serve as the rate limiting step for highly permeable and highly soluble drugs as the absorption from the stomach is low [20]. The gastrointestinal pH may affect drug dissolution of permeability-limited drugs displaying a pKa within the range of the GI pH fluctuations. Small intestinal transit time can influence the drug absorption of poorly soluble or extended release drug formulations [18].

Metabolism in the gut acts to regulate oral bioavailability of drugs and other xenobiotics, and is an important determinant in the metabolism of substrate drugs [21]. CYP3A4 is the most abundant drug metabolizing enzyme in the GI tract, preceding CYP2C9/19 amongst others in order of appearance [22–25]. CYP3A4 and CYP3A5 are both present along the GI tract, where CYP3A4 expression rises towards the jejunum to decrease towards the ileum [21, 26]. GI transporters may influence the absorption of orally administered drugs and potentially also the extent of metabolism in the gut through active substrate efflux [27]. Numerous transporters are present in the gut, where P-glycoprotein (P-gp) is perhaps the most extensively studied of the GI transporters. The relative expression pattern of P-gp in the small intestine increases from the proximal to the distal parts of the small intestine [28].

The Biopharmaceutics Classification System (BCS) classifies drugs in accordance with their solubility and permeability. Solubility takes on the form of a dose number (Do), given by dividing highest dose strength in mg (M_O) by a volume of 250 ml (V_O) divided by the aqueous solubility of the drug (mg ml^{-1}) over a pH range of 1.0–7.5 at 37°C (C_S) [29]. Defining Do $\leq$ 1 as highly soluble and an $f_a \geq$ 90% as a highly permeable drug, drugs are classified as Class I (high solubility-high permeability), class II (poor solubility-high permeability), class III (high solubility-poor permeability) and class IV (poor solubility-poor permeability) [30].

The aims of this study were to identify the most commonly prescribed drugs in a bariatric surgery population and to assess existing evidence with respect to altered oral drug bioavailability post bariatric surgery. This would be carried out through methodologically reviewing the current literature, evaluating drug specific pharmacokinetic characteristics relating to solubility, permeability and main route of elimination.

Methods

Evaluation of drug utilization following gastric bypass

A retrospective audit of drug utilization by bariatric surgery patients was performed at Salford Royal NHS

Foundation Trust, Salford, UK. Data collection was performed using the hospitals electronic patient record (EPR) system, iSOFT clinical manager 1.4, which incorporates the medication prescription and administration records. A search of the EPR system was carried out for all patients under the care of a consultant bariatric surgeon. The search consisted of patients who had undergone surgery in the previous 5 months, from the 21 March 2011. The medical history of patients was initially searched to identify those having undergone laparoscopic RYGB. Patients who had a colostomy, gastric banding and reversal of gastric banding were excluded.

Data extraction was performed utilizsing an anonymous data collection form, maintaining patient confidentiality. Information extracted consisted of type of bariatric surgical procedure, pre surgery prescribed drug therapy and associated co-morbidities, post surgery medication including formulation changes and documented reasons behind alterations. Pre surgery medications were compared with the patients' medical charts on discharge, generally 2–3 days post surgery. Statistical analysis of trends in prescribed drugs observed during the retrospective audit was conducted using McNemar's non-parametric test ($P \leq 0.05$) in R v 2.12 (the R Foundation for Statistical Computing).

Review and analysis of oral drug bioavailability following gastric bypass

Embase (1980–2010) and PubMed (1977–2010) were searched using the following combinations of keywords: 'oral administration or bioavailability', 'absorption', 'bioavailability', 'gastric bypass', 'jejunoileal bypass', 'bariatric surgery'. In addition, references of related articles were systematically investigated for relevant publications.

Initial screening of titles and abstracts was carried out to identify those compliant with pre specified criteria of reporting observational trends in bioavailability/oral drug exposure of pharmaceutical agents following bariatric surgery or the identification of adverse events related to oral drug exposure following surgery. Studies excluded consisted of gastric surgical procedures not related to obesity, reports on nutrients or supplementation post bariatric surgery and publications written in a language other than English. Screening was carried out to determine inclusion or exclusion criteria. Information extracted included study characteristics (surgical procedure, study design, number of participants, year of publication, country of origin and time since procedure) and study population characteristics (gender, average age, average body mass index (BMI) and co-morbidities). The principle measurement of bioavailability in the analysis was area under the curve (AUC), bioavailability and steady-state plasma or serum concentration.

Observed trends in oral drug exposure were assumed to follow a log normal distribution. Quantitative analysis was carried out through estimating the mean effect size of response ratios and their variance following a random-effect model. Statistical analysis was carried out with a two-tailed *t*-test of the standard normal cumulative distribution [31]. Statistical analysis between subgroups were carried out utilizing Welch's *t*-test ($P \leq 0.05$) of log-transformed weighted means and SDs with *post hoc* Dunn-Šidák correction ($P \leq 0.05$) using Microsoft® Excel 2003 and Matlab 2010 (the Mathworks Inc).

Results

Evaluation of clinical drug utilization following gastric bypass

The search of iSOFT identified 63 patients under the care of the bariatric surgeon and 38 patients (26 female) with a mean age of 45 (range 23–64) years were eligible for data extraction after fulfilling the pre-specified criteria. The surgical procedures performed included laparoscopic RYGB ($n = 34$), laparoscopic RYGB with abdominal wall hernia repair ($n = 3$) and conversion of AGBD to RYGB ($n = 1$). Commonly treated comorbidities amongst the study population included hypertension ($n = 12$), type 2 diabetes ($n = 15$), depression/anxiety ($n = 11$), hypothyroidism ($n = 5$), osteoarthritis ($n = 11$), hypercholesterolaemia ($n = 10$) and asthma ($n = 9$).

The most commonly prescribed drugs prior to surgery included statins ($n = 13$), ACE inhibitors ($n = 10$), proton pump inhibitors (PPIs)/histamine H_2-receptor antagonists ($n = 10$) and metformin ($n = 10$). Comparing pre to post surgery, a significant increase in the prescription of paracetamol, opioids, PPIs/histamine H_2-receptor antagonists, heparin and antimicrobials was observed ($P < 0.05$) as well as an overall reduction in the number of patients treated for type 2 diabetes ($P < 0.05$). The most common drugs prescribed following surgery included heparin ($n = 38$), PPIs/histamine H_2-receptor antagonists ($n = 38$) and paracetamol ($n = 34$). The number of patients prescribed cardiovascular agents remained constant postoperatively, whereas prescriptions of statins displayed a non-significant reduction of 31% ($P > 0.05$). The postoperative formulation of choice for diuretics was liquid ($n = 4$), whereas the remaining cardiovascular agents were tablets that were being crushed postoperatively ($n = 28$) (Figure 1).

All patients receiving antidepressants remained on the same antidepressant post surgery, with all but one receiving a different formulation. Of the 11 patients prescribed antidepressants, 50%were switched on to liquid formulations, whereas the remaining 50% were advised to crush their tablets post surgery (Figure 1). All patients with a prior diagnosis of diabetes underwent a diabetic review during their stay in hospital. The review resulted in a significant reduction in post-surgical prescriptions of anti-diabetic medications by 67% ($P < 0.05$). Patients who no longer required diabetic medication were alternatively switched to manual monitoring of blood glucose concen-

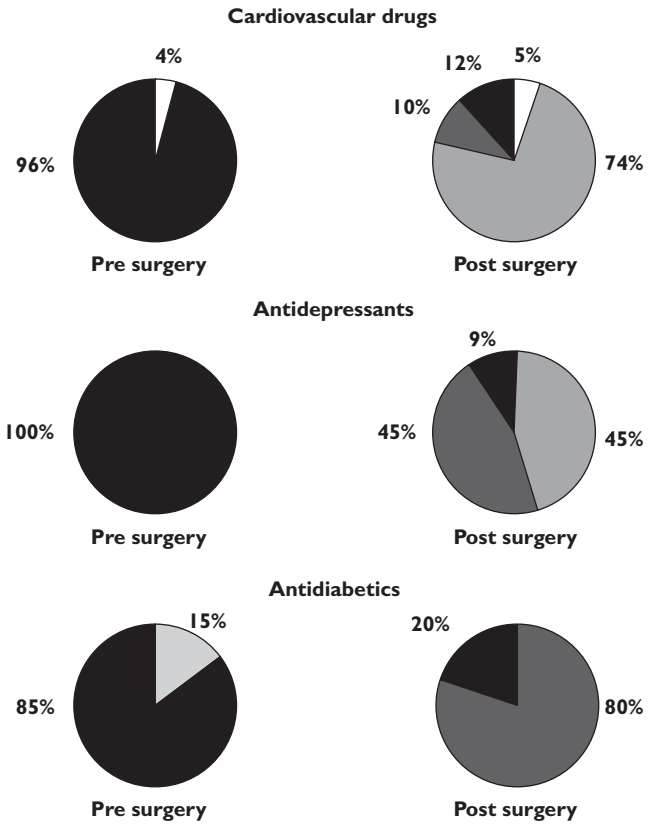

Figure 1

Pharmacotherapeutic alterations in formulation properties (Solid = solid tablets, Liquid = liquid formulation, S/C = subcutaneous, Crushed = patients instructed to crush tablets, Inhaled = inhalation formulation) post bariatric surgery of prescribed cardiovascular drugs, antidepressants and antidiabetics as compared with prior to surgery observed in 38 evaluated patients. Solid (■); Liquid (■); Crushed (■); S/C (□); Inhaled (□)

trations. Metformin was the only agent continued postoperatively and in 60% of cases continued at a reduced dose of up to a third of the pre-surgical dose level. All but one patient were converted to liquid preparations (Figure 1). Standard postoperative treatment consisted of 1–2 weeks low molecular weight heparin injection, PPIs (lansoprazole FasTab) and liquid formulation pain-killers (codeine and paracetamol) being prescribed for all patients. This patient group also displayed a significant increase in the prescription of PPIs/histamine H_2 receptor antagonists, opioids, paracetamol and heparin ($P < 0.05$). One patient with a history of deep vein thrombosis remained on tinzaparin for 4 weeks.

Lansoprazole was given at a dose of 30 mg twice daily as a orodispersible formulation. The prophylactic therapy was to continue for at least 6 months postoperatively, before reducing the dose to once daily for a further 18 months. Approximately 2 weeks after surgery the sublingual formulation was switched to the solid tablet or capsule formulation.

Antimicrobials were given to seven patients postoperatively for the eradication of *Helicobacter pylori* ($n = 5$) that was detected from an intra-operative gastric mucosal biopsy, development of hospital-acquired pneumonia ($n = 1$) and anastomotic leakage ($n = 1$). All patients were given liquid preparations.

In total 17 patients were taking analgesics on a regular basis prior to surgery, increasing to 38 patients postoperatively. Analgesic products included paracetamol ($n = 2$, $P < 0.05$), aspirin ($n = 5$), opioids ($n = 9$, $P < 0.05$) and non-steroidal anti-inflammatory drugs (NSAIDs) ($n = 3$). Patients taking NSAIDs prior to surgery ($n = 3$) were advised to stop taking these postoperatively due to an increased risk of developing gastro-jejunal anastomotic ulceration.

As stated in the patients 'plan' for postoperative care, a review of the nutritional progress usually occurred approximately 2 weeks post surgery. Patients were therefore advised to cease taking any non-essential vitamins and minerals immediately after surgery until the nutritional review has been completed. On discharge patients were informed that they would require taking lifelong dietary supplementation.

Oral drug bioavailability following bariatric surgery

The initial search of Embase and PubMed identified 311 potentially relevant publications based on search terms. After screening of abstracts, 66 articles were identified of which 22 matched the pre-specified criteria following full text screening. Overall, the literature search included 41 articles (20 controlled trials, 18 case reports and three case series) published between 1974 and 2011 that were suitable for further evaluation and data extraction.

Articles relating to JIB mainly appeared between 1974 and 1985. An increase of published data on RYGB was identified between 2000 and 2011, following the trend of RYGB being the most widely used bariatric surgical procedure at the present time [1].

Surgical techniques identified included RYGB ($n = 14$), JIB ($n = 19$), reversal of jejunoileal bypass (JIB R) ($n = 4$), BPD-DS ($n = 2$) BPD ($n = 3$), GBP ($n = 1$) and AGB ($n = 1$) (Table 1). The 41 identified publications originated from the USA (58%), followed by the UK (10%), Italy (5%), Norway (5%) and Canada (5%).

A total of 230 participants were studied in the identified publications. The time point for post surgical examination of oral drug exposure ranged from 0.1 to 88.9 months [32, 33]. In total 38 drugs were identified. These were categorically divided based on therapeutic indication. The studied drugs consisted of antimicrobials ($n = 12$ drugs), cardiovascular drugs ($n = 2$), immunosuppressants ($n = 4$), antiepileptics ($n = 3$), analgesics ($n = 2$), oral contraceptives ($n = 4$), anti-ulcer drugs ($n = 1$), statins ($n = 1$), thyroid hormones ($n = 1$), antidepressants ($n = 2$), anti-cancer drugs ($n = 2$), anti-diabetics ($n = 1$) and HIV medication ($n = 1$). Postoperative trends in drug bioavailability based on

Table 1

Controlled trials examining the trend in oral drug exposure following bariatric surgery.

	Drug	Surgery	Pre to post surgery oral drug exposure ratio (X, 95% CI))	Patients (*n*)	References
▲	Phenoxymethyl penicillin 1000 mg	JIB	**10.43 (0.10, 1058)***	3	[34]
	Atorvastatin acid 20–80 mg	BPD-DS	**1.85 (0.81, 4.27)**†	10	[36]
—	Ranitidine 300 mg	BPD	**1.43 (1.12, 1.81)***	11	[40]
	Metformin 1000 mg	RYGB	**1.20 (0.91, 1.58)**†	16	[55]
	Propylthiouracil 400 mg	JIB	**1.09 (0.84, 1.42)**†	6	[90]
	Phenazone 15 mg kg^{-1}	JIB	**1.06 (0.81, 1.38)**‡	17	[91]
	Atorvastatin acid 20–80 mg	RYGB	**1.00 (0.29, 3.46)**†	12	[37]
	Paracetamol 1500 mg	JIB	**1.00 (0.647, 1.54)***	3	[34]
	Digoxin 0.5 mg daily (First day: 1 mg)	JIB	**0.89 (0.70, 1.14)**†	7	[39]
	Erythromycin 250 mg	GBP	**0.61 (0.38, 0.99)**†	7	[92]
▼	Sulfisoxazole 1000 mg	JIB	**0.84 (0.74, 0.94)***	3	[93]
	Norethisterone 3 mg	JIB	**0.80 (0.39, 1.63)**‡	6	[94]
	Digoxin 0.5 mg	JIB	**0.76 (0.59, 0.97)**†	9	[38]
	MMF 2·1000 mg	RYGB	**0.66 (0.21, 2.06)***	2	[33, 95]
	Levonorgestrel 0.25 mg	JIB	**0.55 (0.34, 0.90)**‡	6	[94]
	Sirolimus 8 mg	RYGB	**0.54 (0.25, 1.17)***	4	[33, 96, 97]
	Hydrochlorothiazide 75 mg	JIB	**0.46 (0.33, 0.65)***	4	[98, 99]
	Sertraline 100 mg	RYGB	**0.40 (0.19, 0.84)**†	5	[100]
	Ampicillin (pivampicillin 750 mg)	JIB	**0.37 (0.16, 0.89)**†	5	[90]
	Phenytoin 200 mg	JIB	**0.32 (0.17, 0.58)**†	7	[101]

▲ = Indicating a significant increase in oral drug exposure (AUC, F_{oral} or steady-state concentration) following surgery. — = No statistical significant change in oral drug exposure. ▼ = Significant reduction in oral drug exposure. X = mean ratio change based on geometric mean, GBP, Gastric bypass (gastroplasty and Roux-en-Y gastric bypass); JIB, Jejunoileal bypass; BPD, Biliopancreatic diversion; BPDDS, Biliopancreatic dDiversion with a duodenal switch; RYGB, Roux-en-Y gastric bypass; MMF, mycophenolate mofetil. **t*-test performed at 5% significance level. †Statistical outcome as reported in publication. ‡Welch's *t*-test at a 5% significance level.

geometric mean drug exposure ranged from a 10.43 fold increase with a 95% confidence interval (CI) ranging from 0.10 to 1058 ($n = 32$) [34] to a 5.88 fold reduction ($n = 1$) [35] (Table 1) [36–41]. The overall post/pre surgical oral drug exposure ratio (ppR) obtained from meta-analysis significantly diverged from pre surgery with a mean ppR of 0.80 with a 95% CI of 0.67, 0.94 (z value = –2.65, $P < 0.01$), when analyzing quantitative data providing mean and variance of exposure pre and post bariatric surgery.

Analysis in accordance to the Biopharmaceutics Classification System Classifying drugs into BCS classification, class I (high solubility, high permeability), class II (low solubility, high permeability), class III (high solubility, low permeability) and class IV (low solubility, low permeability), identified eight drugs as BCS class I ($n = 66$ patients), three drugs as BCS class II ($n = 7$), eleven drugs as BCS class III ($n = 53$) and three drugs as BCS class IV ($n = 8$). A total of eight drugs were found to be inconclusive ($n = 40$). Information was lacking in the literature with regards to the BCS classification of pivampicillin, para-aminosalicylic acid and lopinavir/ritonavir.

Of the eight drugs identified as BCS class I, four drugs displayed a reduction in exposure following surgery, four drugs remained unaltered and one drug displayed an increase in drug exposure. Out of eleven mapped BCS class III drugs, five displayed a reduction in drug exposure following surgery. An additional five drugs displayed unaltered drug exposure, whereas one drug displayed an increase. All BCS class II and IV drugs (total of six) displayed a reduction in drug exposure following surgery (Figure 2).

Analyzing BCS classified drugs where studies provided quantifiable measurements of drug exposure (*i.e.* AUC, F_{oral} and plasma or serum concentrations), combining weighted means and variance of pre/post drug exposure ratio, BCS class I ($n = 5$ drugs, $n = 108$ population) displayed a weighted mean ppR of 0.94 (95% CI 0.66, 1.34). BCS class II ($n = 2$ drugs, $n = 5$ population) displayed a weighted mean ppR of 0.80 (95% CI 0.48, 1.36), BCS class III ($n = 8$ drugs, $n = 111$ population) showed a weighted mean ppR of 0.86 (95% CI 0.68, 1.10), whereas BCS class IV ($n = 2$ drugs, $n = 17$ population) displayed a weighted mean ppR of 0.51 (95% CI 0.22, 1.17). Statistical analysis did not reveal any significant differences from pre surgical ratio of 1 between BCS subgroups ($P > 0.05$) (Figure 3).

Drugs where studies provided quantifiable measurements of drug exposure were further statistically analyzed with regards to Do ≤ 1, BCS class I and III ($n = 16$ drugs, $n = 262$ population) *vs*. BCS class II and IV ($n = 4$ drugs, $n = 48$ patients). Do ≤ 1 drugs displayed a weighted mean ppR of 0.83 (0.69–1.00), whereas Do > 1 drugs displayed a ratio of 0.70 (95% CI 0.45, 1.10). Statistical analysis revealed no statistical significance from a pre surgical ratio of 1 or between subgroups ($P > 0.05$) (Figure 4).

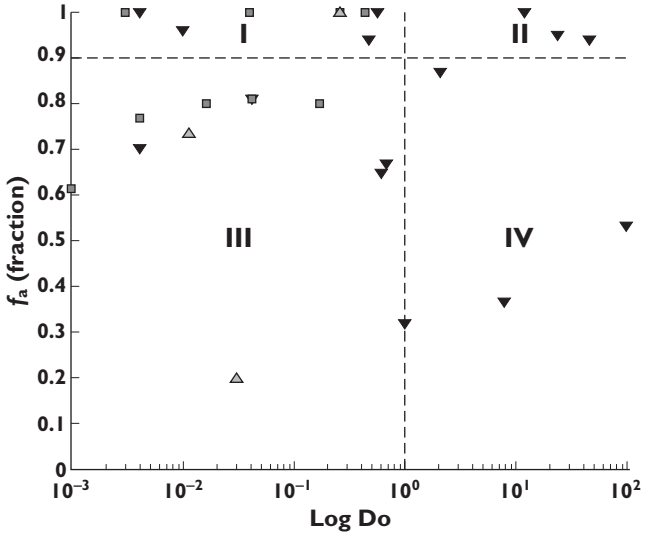

Figure 2

Categorical trends (reduced, unaltered and increased) in oral drug exposure in relation to f_a (fraction of orally administered dose absorbed) and Do (dose number) in accordance with the BCS dividing drugs into BCS class I–IV [52, 60–89]. Reduced exposure (▼); Unaltered (□); Increased (△).

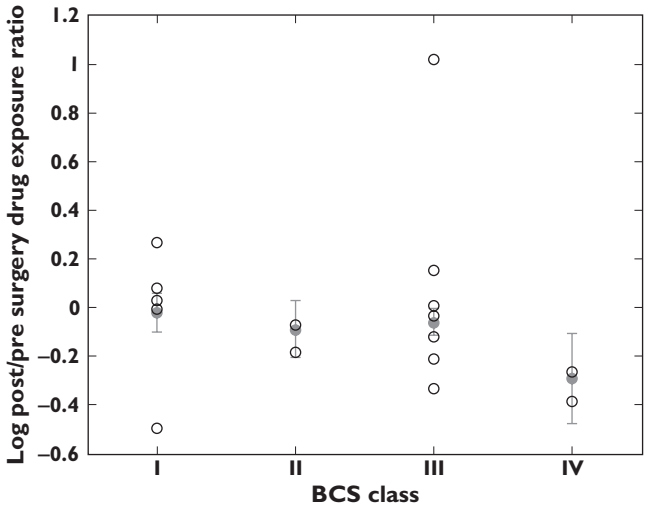

Figure 3

Log mean post/pre surgery drug exposure ratio of BCS I-IV classified drugs. ○ log mean drug ratio, ● combined log mean ratio and standard deviation of subgroup

Analysis in accordance to main route of elimination

Examining drugs in accordance with the main route of elimination produced a weighted mean ppR in oral drug exposure of 0.83 (95% CI 0.59, 1.17) for CYP3A4/5 substrates ($n = 7$ drugs, $n = 99$ patients), 0.32 (95% CI 0.14, 0.72) for CYP2C substrates ($n = 1$ drug, $n = 16$ population), 0.90 (95% CI 0.68, 1.18) for mainly renally-cleared drugs ($n = 5$ drugs, $n = 103$ population) and 0.76 (95% CI 0.57, 1.01) for the remaining drugs ($n = 8$ drugs, $n = 92$ population). Statistical analysis revealed no difference in ppR between the subgroups ($P > 0.05$), whereas the CYP2C subgroup significantly differed from the pre-surgical ratio of 1, displaying a z-value of −2.72 and $P < 0.001$.

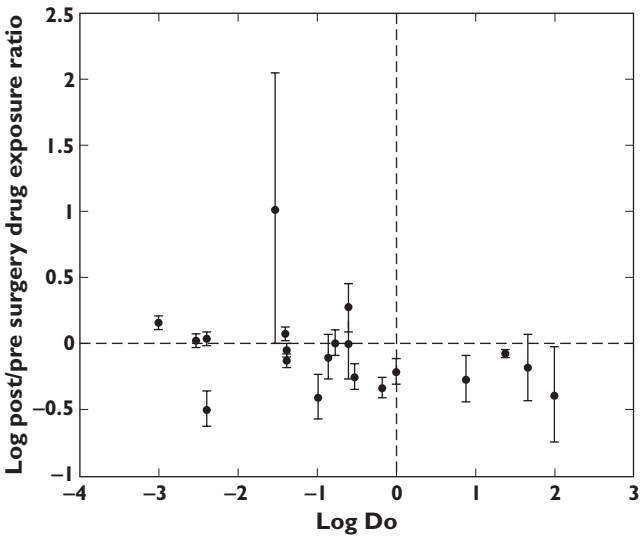

Figure 4

Mean post/pre surgery drug exposure ratio and standard deviation in relation to quantitative Do (dose number)

Discussion

Evaluation of drug utilization following gastric bypass

The observed practice of altering formulation properties to liquid preparations is considered necessary in healthcare due to the postoperative condition of the patient rather than as a proactive measure against altered pharmacokinetics due to changes in GI physiology. Patients are advised to remain on liquid formulations for approximately 2–3 weeks, varying nationally to 3 months to lifelong, post bariatric surgery to prevent any unnecessary strain on the gastric and jejunal transection lines and the gastrojejunal anastomosis and therefore to allow time for healing. As an unintentional consequence changing to liquid preparations may result in an increase in oral bioavailability for solubility limited drugs.

Pharmacotherapeutic treatment of type 2 diabetes was ceased in 67% of patients following surgery. The prescription of metformin remained unaltered following surgery, albeit being observed to be significantly reduced 12 months postoperatively, by Malone & Alger-Mayer, following 114 patients up to 24 months post surgery [42].

Antidepressants, TCAs and SSRIs were continued immediately postoperatively in all cases. This was consistent with

the report by Malone & Alger-Mayer, indicating prescriptions of TCAs and SSRIs remained statistically unaltered 12 months post surgery. Vitamin and mineral deficiencies are likely to occur indefinitely in the bariatric patient, resulting in the need for lifelong supplementation [43]. Deficiencies are most likely to occur with fat soluble vitamins (A, D, E and K), calcium and iron. Calcium and iron absorption is highly influenced by the reduction of hydrochloric acid production within the stomach after bariatric surgery [43].

Medication reviews have been performed observing modifications to patient dosing and formulation after bariatric surgery. Currently no consensus guidelines are available regarding considerations of pharmacotherapy post bariatric surgery. Evidence based national guidelines are warranted as bariatric surgery is becoming a more popular method for the treatment of obesity [44].

Oral drug exposure following bariatric surgery

Reviewing current data on changes in drug exposure prior to and post bariatric surgery reveals many uncertainties regarding the prediction of post bariatric surgery drug bioavailability and the mechanisms behind these changes. BCS did not prove to be enough to explain the observed trend.

Post bariatric surgery imposed restrictions on gastric volume (e.g. SG and RYGB) has been observed to reduce the gastric emptying time of liquids [45, 46] and may further lead to an increase in gastric pH [47, 48]. This together with a reduced fluid intake may impact on the solubility of orally administered drugs.

Statistical analysis did not present any significant trends when examining BCS class I-IV, Do or elimination subgroups. None of the Do > 1 classified drugs displayed an increase in bioavailability postoperatively, whereas the Do $\leq$ 1 group exhibited a larger variability in pre/post surgery drug exposure outcome. This may be due to solubility issues of the Do > 1 group, resulting in an overall reduction in oral drug exposure following surgery. The impact is however unclear due to a low number of drugs falling into the Do > 1 category, where further clinical data are necessary to establish the case.

Due to the restriction of the gastric volume following certain types of bariatric surgery (e.g. RYGB and BPD-DS) the default concomitant fluid intake of 250 ml in the BCS may no longer be valid. This will have implications for shifting the boundaries between BCS class I/III and II/IV, such that some freely soluble drugs may become solubility limited dependent on the administered dose. This is further complicated by a potentially altered gastric pH [11, 12, 29, 47, 48].

A small intestinal bypass will reduce the absorption area and may also alter the regional distribution and abundance of drug metabolizing enzymes and transporters thus altering exposure of substrate drugs. When examining drugs with respect to the main route of elimination, no significant difference was observed between CYP3A, CYP2C, renal and other drugs. These results were also associated with a high degree of uncertainty due to scarcity of data, albeit a higher ppR of CYP3A may be expected due to the GI abundance of CYP enzymes where CYP3A4 is the most highly abundant. The bypass of highly abundant regions of CYP3A4 may lead to an increase in oral bioavailability while such an effect may become less relevant for substrates due to decreasingly abundant CYP2C9/19 and CYP2D6. Such a hypothesis may be supported by the observed trend in AUC of atorvastatin acid, mainly metabolized by CYP3A4 [49], thus potentially displaying an increase in bioavailability post malabsorptive bariatric surgery due to the bypass of significant segments of GI regions highly abundant in CYP3A4 [26], whereas this effect may be counteracted by a reduced absorption area. Following BPD-DS a significant increase in AUC of atorvastatin acid (two-fold) was observed, whereas no significant change was observed following RYGB, thus potentially increasing the risk of adverse effects, such as myopathy, following BPD-DS [36, 37, 50].

The lack of quantifiable drug exposure data means that drugs displaying a low f_G or limited absorption prior to surgery are likely to be wrongly classified when trying to generalize over a wide variety of drugs, such as metformin and phenoxymethylpenicillin.

Metformin, a highly soluble and permeability limited basic compound [51, 52], has been suggested to be subject to saturable transporter uptake to some extent by organic cation transporters in the intestine although this is not fully understood, thus resulting in a dose-dependent absorption that is mainly renally-cleared [53, 54]. The observed increase in postoperative bioavailability [55] might be due to altered small intestinal transit; reductions in gastric emptying time and small intestinal motility would in theory lead to a longer exposure time to enterocytic influx transporters. A further reason could be a post surgical alteration in transporter distribution patterns.

Phenoxymethylpenicillin, considered a highly soluble and permeable compound [52], displayed a significant increase in AUC post JIB, possibly due to a reduced intestinal degradation by bacterial β-lactamase due to a major small intestinal restriction [56].

The different surgical implications on GI physiology may result in variable trends in post surgery drug exposure across the range of bariatric procedures, as is the case with atorvastatin acid displaying a significant increase in AUC following the BPD-DS procedure as compared with no significant change following the less malabsorptive RYGB procedure [36, 37]. Also ciclosporin, there was a reduction in drug exposure following JIB, an exclusively malabsorptive procedure [57, 58], as compared with remaining unaltered following the restrictive AGB [59].

The outcomes of oral drug exposure of many commonly prescribed drugs in bariatric surgery populations are still unknown, such as many antidepressants and analgesics. Current available clinical data are very valuable.

Going forward it is important that further clinical studies are designed taking into consideration the potential alterations in concentration–time profiles, relating to pharmacokinetic parameters such as t_{max}. Drugs exhibiting a narrow therapeutic range or displaying less readily measurable clinical endpoints will require more stringent monitoring after bariatric surgery, such as immunosuppressant agents and CNS active drugs.

Due to the multiple physiological factors altered in bariatric surgery (i.e. gastric volume, absorption area, CYP-abundance and regional distribution) [11, 12], and the fact that various drugs might be affected to different degrees by each of these changes, physiologically-based pharmacokinetic (PBPK) modelling may help in elucidating the impact of various bariatric surgeries on different drugs given at different doses. Such an investigation was outside the scope of the current research. However initial attempts on this approach are addressed in another report (Darwich *et al*. submitted and under review) where the complex nature of interplays were manifested.

In conclusion, based on current findings, analysis of general pharmacokinetic parameters alone (i.e. solubility, permeability and main route of elimination) is not enough to explain observed trends in oral drug bioavailability following bariatric surgery, although the findings of this study suggest solubility to potentially play an important role.

These implications support the hypothesis that there are several physiologic and drug-specific parameters which govern the observed changes in drug exposure, thus calling for a more mechanistic approach, integrating all known parameters.

To the authors' knowledge this is the first publication quantitatively examining oral drug bioavailability in relation to a set of pharmacokinetic, biopharmaceutic and other drug-specific parameters and also in the context of pharmacotherapeutic practice following bariatric surgery. Along with further clinical studies, PBPK modelling may provide essential insights into the significance of individual pharmacokinetic parameters and generate important clinical guidance for a constantly growing post bariatric surgery population. Currently, there seems to be no simple algorithm or decision tree that predicts the variable changes to drug bioavailability following bariatric surgery.

Competing Interests

There are no competing interests to declare.

Appendix

Table A1

Controlled trials examining oral drug bioavailability following bariatric surgery

Drug	Surgical procedure	Post/pre surgery drug exposure ratio (mean (95% CI))	Additional information	References
Antimicrobials				
Erythromycin 250 mg	GBP	**AUC: 0.61 (0.38, 0.99)** ($P > 0.05$)*	Controlled prospective study (*n* patients = 7)	[92]
Ampicillin (pivampicillin 750 mg)	JIB	**F_{oral}0.37 (0.16, 0.89)** ($P < 0.05$)*	Controlled prospective study (*n* patients = 6)	[90]
Sulfisoxazole 1000 mg	JIB	**F_{oral}: 0.84 (0.74, 0.94)** ($P < 0.05$)†	Controlled prospective study (*n* patients = 3)	[93]
Phenoxymethyl penicillin 1000 mg	JIB	**AUC: 10.43 (0.10, 1058)** ($P < 0.05$)†	Controlled prospective study (*n* patients = 3)	[34]
Cardiovascular drugs				
Digoxin 0.5 mg	JIB	**AUC: 0.76 (0.59, 0.97)** ($P < 0.05$)*	Controlled study (*n* patients = 9, *n* controls = 16)	[38]
Digoxin 0.5 mg daily (First day 1 mg)	JIB	**AUC: 0.89 (0.70, 1.14)** ($P > 0.05$)*	Controlled prospective study (*n* pre patients = 5, *n* post patients = 6)	[39]
Hydrochlorothiazide 75 mg	JIB	**AUC: 0.46 (0.33, 0.65)** ($P < 0.05$)‡	Controlled study as compared to literature data (*n* patients = 4, *n* healthy volunteers = 7)	[98, 99]
Immunosuppressants				
Mycophenolic acid (MPA) 2·1000 mg Sirolimus 6 mg Tacrolimus 2·4 mg	RYGB‡	**AUC: 0.66 (0.21, 2.06)*** **AUC: 0.54 (0.25, 1.17)*** **AUC:** 'Reduced'	Pilot study as compared to literature data (*n* patients = 2, 4, 1, *n* controls =)	[33, 102]
Antiepileptics				
Phenytoin 200 mg	JIB	**AUC: 0.32 (0.17, 0.58)** ($P < 0.05$)*	Controlled study (*n* patients = 7, *n* controls = 9)	[101]
Analgesics				
Paracetamol 1500 mg	JIB	**AUC: 1.00 (0.647, 1.54)** ($P > 0.05$)†	Controlled prospective study (*n* patients = 3 at 2.7–3.9 months, 5 at 6.4–34 months)	[34]
Phenazone 15 mg kg^{-1}	JIB	**AUC§: 1.06 (0.81, 1.38)** ($P > 0.05$)¶	Controlled study (*n* patients = 17, *n* controls = 11)	[91]
Oral contraceptives				
Norethisterone 3 mg Levonorgestrel 0.25 mg	JIB	**AUC§: 0.80 (0.39, 1.63)** ($P < 0.05$)¶ **AUC§: 0.55 (0.34, 0.90)** ($P < 0.05$)¶	Controlled study (*n* patients = 6, *n* controls = 5)	[94]
Estradiol 4 mg Levonorgestrel 0.125 mg	JIB	**'Unaltered'** **'Unaltered'**	Controlled study (*n* patients = 12)	[103]
'Contraceptives'	BPD	'Reduced'	Observed increase in levels of sex-hormone-binding globulin and reduced levels of dehydroepiandrosterone sulphate. Controlled prospective study (*n* patients = 40)	[104]
Anti-ulceratives				
Ranitidine 300 mg	BPD	**AUC: 1.43 (1.12, 1.81)** ($P < 0.05$)†	Controlled study (*n* patients = 11, *n* controls = 10)	[40]
Ranitidine 150 and 300 mg	BPD	'Unaltered'	Controlled study as compared to literature data (*n* patients = 7)	[41]
Statins				
Atorvastatin acid 20–80 mg	BPD-DS	**AUC: 1.85 (0.81, 4.27)** ($P < 0.05$)*	Controlled prospective study C_{max} ratio: 2.2 ± 1.7, t_{max} ratio: 2.3 ± 1.3 (*n* patients = 10)	[36]
Atorvastatin acid 20–80 mg	RYGB	**AUC: 1.43 (1.12, 1.81)** ($P > 0.05$)*	Controlled prospective study C_{max} ratio: 1.1, t_{max} ratio: 0.5 (*n* patients = 12)	[37]
Anti-diabetics				
Metformin 1000 mg	RYGB	**AUC: 1.20 (0.91, 1.58)** ($P > 0.05$)*	Controlled study (*n* patients = 16, *n* controls = 16)	[55]
Antidepressants				
Sertraline 100 mg	RYGB	**AUC: 0.40 (0.19, 0.84)** ($P < 0.05$)*	Controlled study (n patients = 5, n controls = 5)	[100]
Thyroid blockers				
Propylthiouracil 400 mg	JIB	**F_{oral}: 1.09 (0.84, 1.42)** ($P > 0.05$)*	Controlled prospective study (*n* patients = 9)	Kampmann 1984

SD, Standard deviation; GBP, Gastric bypass (gastroplasty and Roux-en-Y gastric bypass); JIB, Jejunoileal bypass; BPD, Biliopancreatic diversion; BPD-DS, Biliopancreatic diversion with a duodenal switch; RYGB, Roux-en-Y gastric bypass; AUC, area under curve; *F*, bioavailability; SS, mean concentration at steady-state; C_{max}, maximum concentration; t_{max}, time at maximum concentration. *Statistical outcome as reported in publication. †*t*-test performed at 5% significance level. ‡Pre (sirolimus) and post (tacrolimus and MPA) renal transplant patients. §Welch's *t*-test at a 5% significance level. ¶Calculated estimate of AUC from report.

Table A2

Case reports (*n* patients = 1) on oral drug bioavailability following bariatric surgery

Drug	Surgical procedure	Post/pre surgery drug exposure ratio	Additional information	References
Antimicrobials				
Rifampicin	JIB	**Reduced**	Following JIB, the rifampicin dose was increased from 600 to 1200 mg in order to reach necessary serum concentrations.	[105]
Isoniazid		**Unaltered**		
Ethambutol		**Unaltered**		
Rifampicin	JIB	**Reduced**	Patient 1: Isoniazid 300 mg – Serum concentration of 3.6 μg ml^{-1} at 2 h as compared with reference value of 4–6 μg ml^{-1}. Patient 2: Isoniazid 300 mg – Serum concentration of 8.4 μg ml^{-1} at 2 h. Ethambutol 2400 mg – Serum concentration under 1 μg ml^{-1}. Rifampicin 600 mg – Serum concentration of 4 μg ml^{-1} at 4 h as compared with reference value of 8 μg ml^{-1}.	[106]
Isoniazid		**Inconclusive**		
Ethambutol		**Unaltered**		
Rifampicin	JIB	**Reduced**	Four female patients out of one hundred patients undergoing JIB developed tuberculosis. Blood concentrations were obtained from two patients, displaying a reduced concentration of rifampicin, whereas isoniazid and ethambutol remained within therapeutic range (*n* patients = 4).	[107]
Isoniazid		**Unaltered**		
Ethambutol		**Unaltere**		
Isoniazid	JIB	**Unaltered**	Isoniazid and ethambutol blood concentration reported to be within the normal range.	[108]
Ethambutol		**Unaltered**		
Isoniazid	JIB	**Reduced**	Drugs excreted in faeces as unaltered tablets after oral administration.	[109]
Ethambutol		**Reduced**		
Para-aminosalicylic acid		Reduced		
Isoniazid	JIB	**Unaltered**	Serum concentrations equivalent to that observed in healthy volunteers.	[110]
Ethambutol		**Unaltered**		
Nitrofurantoin	RYGB	**Reduced**	Intravenous antibiotics administered due to failure of oral drug therapy failed.	[111]
Amoxicillin		Reduced		
Immunosuppressants				
Tacrolimus	JIB R	**AUC:** 0.53	After JIB R a 1.90-fold increase in AUC was observed.	[112]
Ciclosporin	JIB	**SS concentration:** 0.41	*n* patients = 1, as compared with *n* controls = 6	[57]
Ciclosporin	JIB R	F_{oral}**:** 0.36	2.78-fold Increase in drug exposure following JIB R.	[58]
Ciclosporin	LAGBD	**Unaltered**	Standard cyclosporine therapy was successful in the treatment of a post LAGB surgery patient subject to heart transplant.	[59]
Anticonvulsants				
Phenytoin	RYGB	Reduced	Dose strength up to 500 mg did not achieve therapeutic effect (<3 mg l^{-1} as compared with a normal range of 10–20 mg l^{-1}).	[113]
Phenobarbitone	RYGB	**Reduced**	At a dose of 60 mg bid, serum levels were reduced (9.9 mg l^{-1}) as compared with normal range (15–41 mg l^{-1}).	
Phenytoin	JIB	**Reduced**	Dose increased from 300 to 500 mg in order to achieve therapeutic effect.	[114]
Ethosuximide	JIB	**Reduced**	Dose doubled in order to achieve therapeutic effect.	
Phenytoin	JIB R	**SS concentration:** 0.48	JIB R resulted in an increase in SS concentration.	[115]
Antipsychotics				
Haloperidol	RYGB	Unaltered	Dose doubled immediate post surgery to thereafter be lower to pre surgery dose with effective treatment.	[32]
Anti-cancer drugs				
Imatinib mesylate	BPD-DS	**SS concentration:** 0.17	Plasma concentration of imatinib 400 mg at steady-state reduced from 965 to 166 ng ml^{-1}.	[35]
Tamoxifen	RYGB	**Reduced**	3 case reports (n patients = 3).	[116]
Temozolomide	RYGB	**AUC:** 1.02	Unaltered drug exposure following surgery at a dose of 190 mg as compared with literature.	[117]
Anti-HIV drugs				
Lopinavir/ritonavir	RYGB*	Increased	An observed increase in plasma concentration in comparison with control patients.	[118]
Thyroid hormones				
Thyroxine	JIB	Reduced	Dose increase required from 0.2 mg to 0.8 mg daily to produce sufficient response.	[119]
Thyroxine	JIB	Reduced	C_{max} ratio: 0.31. JIB R restored to pre surgery drug exposure.	[120]
Thyroxine	JIB R	Reduced	Dose increase required from 0.3 mg to 0.6 mg daily to reach SS sufficient concentration.	[121]

JIB, Jejunoileal bypass; JIB R, Jejunoileal bypass reversal; BPD, Biliopancreatic diversion; BPD-DS, Biliopancreatic diversion with a duodenal switch; RYGB, Roux-en-Y gastric bypass; LAGBD, Laporoscopic adjustable gastric banding; AUC, area under curve; *F*, bioavailability; SS concentration, mean concentration at steady-state; C_{max}, maximum concentration; t_{max}, time at maximum concentration. *Total gastrectomy followed by an oesophagojejunostomy with a Roux-en-Y reconstruction.

REFERENCES

1 Picot J, Jones J, Colquitt JL, Gospodarevskaya E, Loveman E, Baxter L, Clegg AJ. The clinical effectiveness and cost effectiveness of bariatric (weight loss) surgery for obesity: a systematic review and economic evaluation. Health Technol Assess 2009; 13: 1–358.

2 Obesity and Overweight. Fact Sheet 311. Geneva: World Health Organisation, 2006. Available at http://www.who.int/mediacentre/factsheets/fs311/en/ (last accessed 8 November 2011).

3 Flegal KM, Carroll MD, Ogden CL, Curtin LR. Prevalence and trends in obesity among US adults, 1999-2008. JAMA 2010; 303: 235–41.

4 Sassi F. Obesity and the Economics of Prevention: Fit Not Fat – United Kingdom (England) Key Facts. Paris: Organisation for Economic Co-operation and Development, London, 2011.

5 O'Neill P. Office of Health Economics, UK. Shedding the Pounds: Obesity Management, NICE Guidance and Bariatric Surgery in England. London: Office of Health Economics, 2010.

6 Buchwald H, Oien DM. Metabolic/bariatric surgery Worldwide 2008. Obes Surg 2009; 19: 1605–11.

7 The NHS Information Centre. Lifestyle Statistics. Statistics on Obesity, Physical Activity and Diet: England, 2010, First Edition. Leeds: The Health and Social Care Information Centre, 2010.

8 National Institute of Diabetes and Digestive and Kidney Diseases. Bariatric Surgery for Severe Obesity. Bethesda, MD: National Institute of Health, 2010.

9 Singh D, Laya AS, Clarkston WK, Allen MJ. Jejunoileal bypass: a surgery of the past and a review of its complications. World J Gastroenterol 2009; 15: 2277–9.

10 Griffen WO Jr, Young VL, Stevenson CC. A prospective comparison of gastric and jejunoileal bypass procedures for morbid obesity. Ann Surg 1977; 186: 500–9.

11 Elder KA, Wolfe BM. Bariatric surgery: a review of procedures and outcomes. Gastroenterology 2007; 132: 2253–71.

12 Schneider BE, Mun EC. Surgical management of morbid obesity. Diabetes Care 2005; 28: 475–80.

13 Lee CM, Cirangle PT, Jossart GH. Vertical gastrectomy for morbid obesity in 216 patients: report of two-year results. Surg Endosc 2007; 21: 1810–6.

14 Hess DS, Hess DW. Biliopancreatic diversion with a duodenal switch. Obes Surg 1998; 8: 267–82.

15 Spak E, Bjorklund P, Helander HF, Vieth M, Olbers T, Casselbrant A, Lonroth H, Fandriks L. Changes in the mucosa of the Roux-limb after gastric bypass surgery. Histopathology 2010; 57: 680–8.

16 DeMaria EJ, Sugerman HJ, Kellum JM, Meador JG, Wolfe LG. Results of 281 consecutive total laparoscopic Roux-en-Y gastric bypasses to treat morbid obesity. Ann Surg 2002; 235: 640–5. discussion 45–7.

17 Wittgrove AC, Clark GW. Laparoscopic gastric bypass, Roux-en-Y- 500 patients: technique and results, with 3-60 month follow-up. Obes Surg 2000; 10: 233–9.

18 Rowland M, Tozer TN. In: Clinical Pharmacokinetics: Concepts and Applications, 2nd edn. Philadelphia, PA: Lea & Febiger, 1989.

19 Jamei M, Turner D, Yang J, Neuhoff S, Polak S, Rostami-Hodjegan A, Tucker G. Population-based mechanistic prediction of oral drug absorption. AAPS J 2009; 11: 225–37.

20 Higaki K, Choe SY, Lobenberg R, Welage LS, Amidon GL. Mechanistic understanding of time-dependent oral absorption based on gastric motor activity in humans. Eur J Pharm Biopharm 2008; 70: 313–25.

21 Kolars JC, Lown KS, Schmiedlin-Ren P, Ghosh M, Fang C, Wrighton SA, Merion RM, Watkins PB. CYP3A gene expression in human gut epithelium. Pharmacogenetics 1994; 4: 247–59.

22 Paine MF, Hart HL, Ludington SS, Haining RL, Rettie AE, Zeldin DC. The human intestinal cytochrome P450 'pie'. Drug Metab Dispos 2006; 34: 880–6.

23 Fisher MB, Paine MF, Strelevitz TJ, Wrighton SA. The role of hepatic and extrahepatic UDP-glucuronosyltransferases in human drug metabolism. Drug Metab Rev 2001; 33: 273–97.

24 Riches Z, Stanley EL, Bloomer JC, Coughtrie MW. Quantitative evaluation of the expression and activity of five major sulfotransferases (SULTs) in human tissues: the SULT 'pie'. Drug Metab Dispos 2009; 37: 2255–61.

25 Peters WH, Roelofs HM, Nagengast FM, van Tongeren JH. Human intestinal glutathione S-transferases. Biochem J 1989; 257: 471–6.

26 Paine MF, Khalighi M, Fisher JM, Shen DD, Kunze KL, Marsh CL, Perkins JD, Thummel KE. Characterization of interintestinal and intraintestinal variations in human CYP3A-dependent metabolism. J Pharmacol Exp Ther 1997; 283: 1552–62.

27 Benet LZ, Cummins CL. The drug efflux-metabolism alliance: biochemical aspects. Adv Drug Deliv Rev 2001; 50: (Suppl. 1): S3–11.

28 Mouly S, Paine MF. P-glycoprotein increases from proximal to distal regions of human small intestine. Pharm Res 2003; 20: 1595–9.

29 FDA, Center for Drug Evaluation and Research. Guidance for Industry: Waiver of In Vivo Bioavailability and Bioequivalence Studies for Immediate-Release Solid Oral Dosage Forms Based on A Biopharmaceutics Classification System. Rockville, MD: U.S. Department of Health and Human Services, 2000.

30 Amidon GL, Lennernas H, Shah VP, Crison JR. A theoretical basis for a biopharmaceutic drug classification: the correlation of *in vitro* drug product dissolution and *in vivo* bioavailability. Pharm Res 1995; 12: 413–20.

31 Borenstein M, Hedges LV, Higgins JPT, Rothstein HR. Introduction to Meta-Analysis. Chichester: John Wiley & Sons, Ltd, 2009.

32 Fuller AK, Tingle D, DeVane CL, Scott JA, Stewart RB. Haloperidol pharmacokinetics following gastric bypass surgery. J Clin Psychopharmacol 1986; 6: 376–8.

33 Rogers CC, Alloway RR, Alexander JW, Cardi M, Trofe J, Vinks AA. Pharmacokinetics of mycophenolic acid, tacrolimus and sirolimus after gastric bypass surgery in end-stage renal disease and transplant patients: a pilot study. Clin Transplant 2008; 22: 281–91.

34 Terry SI, Gould JC, McManus JP, Prescott LF. Absorption of penicillin and paracetamol after small intestinal bypass surgery. Eur J Clin Pharmacol 1982; 23: 245–8.

35 Liu H, Artz AS. Reduction of imatinib absorption after gastric bypass surgery. Leuk Lymphoma 2011; 52: 310–3.

36 Skottheim IB, Jakobsen GS, Stormark K, Christensen H, Hjelmesaeth J, Jenssen T, Asberg A, Sandbu R. Significant increase in systemic exposure of atorvastatin after biliopancreatic diversion with duodenal switch. Clin Pharmacol Ther 2010; 87: 699–705.

37 Skottheim IB, Stormark K, Christensen H, Jakobsen GS, Hjelmesaeth J, Jenssen T, Reubsaet JL, Sandbu R, Asberg A. Significantly altered systemic exposure to atorvastatin acid following gastric bypass surgery in morbidly obese patients. Clin Pharmacol Ther 2009; 86: 311–8.

38 Gerson CD, Lowe EH, Lindenbaum J. Bioavailability of digoxin tablets in patients with gastrointestinal dysfunction. Am J Med 1980; 69: 43–9.

39 Marcus FI, Quinn EJ, Horton H, Jacobs S, Pippin S, Stafford M, Zukoski C. The effect of jejunoileal bypass on the pharmacokinetics of digoxin in man. Circulation 1977; 55: 537–41.

40 Cossu ML, Caccia S, Coppola M, Fais E, Ruggiu M, Fracasso C, Nacca A, Noya G. Orally administered ranitidine plasma concentrations before and after biliopancreatic diversion in morbidly obese patients. Obes Surg 1999; 9: 36–9.

41 Adami GF, Gandolfo P, Esposito M, Scopinaro N. Orally-administered serum ranitidine concentration after biliopancreatic diversion for obesity. Obes Surg 1991; 1: 293–94.

42 Malone M, Alger-Mayer SA. Medication use patterns after gastric bypass surgery for weight management. Ann Pharmacother 2005; 39: 637–42.

43 Ponsky TA, Brody F, Pucci E. Alterations in gastrointestinal physiology after Roux-en-Y gastric bypass. J Am Coll Surg 2005; 201: 125–31.

44 Buchwald H, Williams SE. Bariatric surgery worldwide 2003. Obes Surg 2004; 14: 1157–64.

45 Horowitz M, Cook DJ, Collins PJ, Harding PE, Hooper MJ, Walsh JF, Shearman DJ. Measurement of gastric emptying after gastric bypass surgery using radionuclides. Br J Surg 1982; 69: 655–7.

46 Braghetto I, Davanzo C, Korn O, Csendes A, Valladares H, Herrera E, Gonzalez P, Papapietro K. Scintigraphic evaluation of gastric emptying in obese patients submitted to sleeve gastrectomy compared to normal subjects. Obes Surg 2009; 19: 1515–21.

47 Smith CD, Herkes SB, Behrns KE, Fairbanks VF, Kelly KA, Sarr MG. Gastric acid secretion and vitamin B12 absorption after vertical Roux-en-Y gastric bypass for morbid obesity. Ann Surg 1993; 218: 91–6.

48 Behrns KE, Smith CD, Sarr MG. Prospective evaluation of gastric acid secretion and cobalamin absorption following gastric bypass for clinically severe obesity. Dig Dis Sci 1994; 39: 315–20.

49 Lennernas H, Fager G. Pharmacodynamics and pharmacokinetics of the HMG-CoA reductase inhibitors. Similarities and differences. Clin Pharmacokinet 1997; 32: 403–25.

50 Omar MA, Wilson JP, Cox TS. Rhabdomyolysis and HMG-CoA reductase inhibitors. Ann Pharmacother 2001; 35: 1096–107.

51 van de Merbel NC, Wilkens G, Fowles S, Oosterhuis B, Jonkman JHG. LC phases improve, but not all assays do: metformin bioanalysis revisited. Chromatographia 1998; 47: 542–46.

52 Kasim NA, Whitehouse M, Ramachandran C, Bermejo M, Lennernas H, Hussain AS, Junginger HE, Stavchansky SA, Midha KK, Shah VP, Amidon GL. Molecular properties of WHO essential drugs and provisional biopharmaceutical classification. Mol Pharm 2004; 1: 85–96.

53 Tucker GT, Casey C, Phillips PJ, Connor H, Ward JD, Woods HF. Metformin kinetics in healthy subjects and in patients with diabetes mellitus. Br J Clin Pharmacol 1981; 12: 235–46.

54 Proctor WR, Bourdet DL, Thakker DR. Mechanisms underlying saturable intestinal absorption of metformin. Drug Metab Dispos 2008; 36: 1650–8.

55 Padwal RS, Gabr RQ, Sharma AM, Langkaas LA, Birch DW, Karmali S, Brocks DR. Effect of gastric bypass surgery on the absorption and bioavailability of metformin. Diabetes Care 2011; 34: 1295–300.

56 Cole M, Kenig MD, Hewitt VA. Metabolism of penicillins to penicilloic acids and 6-aminopenicillanic acid in man and its significance in assessing penicillin absorption. Antimicrob Agents Chemother 1973; 3: 463–8.

57 Chenhsu RY, Wu Y, Katz D, Rayhill S. Dose-adjusted cyclosporine c2 in a patient with jejunoileal bypass as compared to seven other liver transplant recipients. Ther Drug Monit 2003; 25: 665–70.

58 Knight GC, Macris MP, Peric M, Duncan JM, Frazier OH, Cooley DA. Cyclosporine A pharmacokinetics in a cardiac allograft recipient with a jejuno-ileal bypass. Transplant Proc 1988; 20: 351–5.

59 Ablassmaier B, Klaua S, Jacobi CA, Muller JM. Laparoscopic gastric banding after heart transplantation. Obes Surg 2002; 12: 412–5.

60 Chemical C. Product Information – Imatinib (Mesylate). Ann Arbor, MI: Cayman Chemical Company, 2010.

61 FDA. Drugs@FDA: FDA Approved Drug Products. Rockville, MD: U.S. Department of Health and Human Services, 2010.

62 Ni J, Ouyang H, Aiello M, Seto C, Borbridge L, Sakuma T, Ellis R, Welty D, Acheampong A. Microdosing assessment to evaluate pharmacokinetics and drug metabolism in rats using liquid chromatography-tandem mass spectrometry. Pharm Res 2008; 25: 1572–82.

63 Ashiru DA, Patel R, Basit AW. Polyethylene glycol 400 enhances the bioavailability of a BCS class III drug (ranitidine) in male subjects but not females. Pharm Res 2008; 25: 2327–33.

64 Lindenberg M, Kopp S, Dressman JB. Classification of orally administered drugs on the World Health Organization Model list of Essential Medicines according to the biopharmaceutics classification system. Eur J Pharm Biopharm 2004; 58: 265–78.

65 Wu CY, Benet LZ. Predicting drug disposition via application of BCS: transport/absorption/ elimination interplay and development of a biopharmaceutics drug disposition classification system. Pharm Res 2005; 22: 11–23.

66 Oie S, Gambertoglio JG, Fleckenstein L. Comparison of the disposition of total and unbound sulfisoxazole after single and multiple dosing. J Pharmacokinet Biopharm 1982; 10: 157–72.

67 Kaplan SA, Weinfeld RE, Abruzzo CW, Lewis M. Pharmacokinetic profile of sulfisoxazole following intravenous, intramuscular, and oral administration to man. J Pharm Sci 1972; 61: 773–8.

68 Yalkowsky SH, He Y. Handbook of Aqueous Solubility Data. Boca Raton, FL: CRC Press, 2003.

69 Lennernas H, Gjellan K, Hallgren R, Graffner C. The influence of caprate on rectal absorption of phenoxymethylpenicillin: experience from an in-vivo perfusion in humans. J Pharm Pharmacol 2002; 54: 499–508.

70 Stewart BH, Chan OH, Lu RH, Reyner EL, Schmid HL, Hamilton HW, Steinbaugh BA, Taylor MD. Comparison of intestinal permeabilities determined in multiple *in vitro* and *in situ* models: relationship to absorption in humans. Pharm Res 1995; 12: 693–9.

71 Bock U, Kottke T, Gindorf C, Haltner E. Validation of the Caco-2 cell monolayer system for determining the permeability of drug substances according to the Biopharmaceutics Classification System (BCS). Saarbrucken: Across Barriers, 2003: 1–7. Available at http://www.acrossbarriers.de/uploads/media/FCT02-I-0305_BCS_01.pdf (last accessed 8 November 2011).

72 Dressman JB, Amidon GL, Fleisher D. Absorption potential: estimating the fraction absorbed for orally administered compounds. J Pharm Sci 1985; 74: 588–9.

73 Garekani HA, Sadeghi F, Ghazi A. Increasing the aqueous solubility of acetaminophen in the presence of polyvinylpyrrolidone and investigation of the mechanisms involved. Drug Dev Ind Pharm 2003; 29: 173–9.

74 Joint Formulary Committee. British National Formulary, Sixty-Second edn. London: BMJ Group and Pharmaceutical Press, 2011.

75 Crowe A, Lemaire M. *In vitro* and *in situ* absorption of SDZ-RAD using a human intestinal cell line (Caco-2) and a single pass perfusion model in rats: comparison with rapamycin. Pharm Res 1998; 15: 1666–72.

76 Tamura S, Ohike A, Ibuki R, Amidon GL, Yamashita S. Tacrolimus is a class II low-solubility high-permeability drug: the effect of P-glycoprotein efflux on regional permeability of tacrolimus in rats. J Pharm Sci 2002; 91: 719–29.

77 Tavelin S, Milovic V, Ocklind G, Olsson S, Artursson P. A conditionally immortalized epithelial cell line for studies of intestinal drug transport. J Pharmacol Exp Ther 1999; 290: 1212–21.

78 Petan JA, Undre N, First MR, Saito K, Ohara T, Iwabe O, Mimura H, Suzuki M, Kitamura S. Physiochemical properties of generic formulations of tacrolimus in Mexico. Transplant Proc 2008; 40: 1439–42.

79 Kearney AS, Crawford LF, Mehta SC, Radebaugh GW. The interconversion kinetics, equilibrium, and solubilities of the lactone and hydroxyacid forms of the HMG-CoA reductase inhibitor, CI-981. Pharm Res 1993; 10: 1461–5.

80 Lennernas H. Clinical pharmacokinetics of atorvastatin. Clin Pharmacokinet 2003; 42: 1141–60.

81 Song NN, Li QS, Liu CX. Intestinal permeability of metformin using single-pass intestinal perfusion in rats. World J Gastroenterol 2006; 12: 4064–70.

82 Kampmann J, Skovsted L. The pharmacokinetics of propylthiouracil. Acta Pharmacol Toxicol (Copenh) 1974; 35: 361–9.

83 Peloquin CA, Namdar R, Singleton MD, Nix DE. Pharmacokinetics of rifampin under fasting conditions, with food, and with antacids. Chest 1999; 115: 12–8.

84 Becker C, Dressman JB, Amidon GL, Junginger HE, Kopp S, Midha KK, Shah VP, Stavchansky S, Barends DM. Biowaiver monographs for immediate release solid oral dosage forms: ethambutol dihydrochloride. J Pharm Sci 2008; 97: 1350–60.

85 Nelson E, Powell JR, Conrad K, Likes K, Byers J, Baker S, Perrier D. Phenobarbital pharmacokinetics and bioavailability in adults. J Clin Pharmacol 1982; 22: 141–8.

86 Patel IH, Levy RH, Bauer TG. Pharmacokinetic properties of ethosuximide in monkeys. I. Single-dose intravenous and oral administration. Epilepsia 1975; 16: 705–16.

87 Bolton AE, Peng B, Hubert M, Krebs-Brown A, Capdeville R, Keller U, Seiberling M. Effect of rifampicin on the pharmacokinetics of imatinib mesylate (Gleevec, STI571) in healthy subjects. Cancer Chemother Pharmacol 2004; 53: 102–6.

88 Wenzel KW, Kirschsieper HE. Aspects of the absorption of oral L-thyroxine in normal man. Metabolism 1977; 26: 1–8.

89 NCBI PubChem Public Chemical Database. National Center of Biotechnology Information. Bethesda, MD: National Institute of Health, 2011. Available at http://www.ncbi.nlm.nih.gov/pubmed/ (last accessed 8 November 2011).

90 Kampmann JP, Klein H, Lumholtz B, Molholm Hansen JE. Ampicillin and propylthiouracil pharmacokinetics in intestinal bypass patients followed up to a year after operation. Clin Pharmacokinet 1984; 9: 168–76.

91 Andreasen PB, Dano P, Kirk H, Greisen G. Drug absorption and hepatic drug metabolism in patients with different types of intestinal shunt operation for obesity. A study with phenazone. Scand J Gastroenterol 1977; 12: 531–5.

92 Prince RA, Pincheira JC, Mason EE, Printen KJ. Influence of bariatric surgery on erythromycin absorption. J Clin Pharmacol 1984; 24: 523–7.

93 Garrett ER, Suverkrup RS, Eberst K, Yost RL, O'Leary JP. Surgically affected sulfisoxazole pharmacokinetics in the morbidly obese. Biopharm Drug Dispos 1981; 2: 329–65.

94 Victor A, Odlind V, Kral JG. Oral contraceptive absorption and sex hormone binding globulins in obese women: effects of jejunoileal bypass. Gastroenterol Clin North Am 1987; 16: 483–91.

95 Genentech. Cellcept Prescribing Information. San Fransisco, CA: Genentech USA Inc, 2010.

96 Mathew TH, Van Buren C, Kahan BD, Butt K, Hariharan S, Zimmerman JJ. A comparative study of sirolimus tablet versus oral solution for prophylaxis of acute renal allograft rejection. J Clin Pharmacol 2006; 46: 76–87.

97 Brattstrom C, Sawe J, Jansson B, Lonnebo A, Nordin J, Zimmerman JJ, Burke JT, Groth CG. Pharmacokinetics and safety of single oral doses of sirolimus (rapamycin) in healthy male volunteers. Ther Drug Monit 2000; 22: 537–44.

98 Backman L, Beerman B, Groschinsky-Grind M, Hallberg D. Malabsorption of hydrochlorothiazide following intestinal shunt surgery. Clin Pharmacokinet 1979; 4: 63–8.

99 Beermann B, Groschinsky-Grind M. Pharmacokinetics of hydrochlorothiazide in man. Eur J Clin Pharmacol 1977; 12: 297–303.

100 Roerig JL, Steffen K, Zimmerman C, Mitchell JE, Crosby RD, Cao L. Preliminary comparison of sertraline levels in postbariatric surgery patients versus matched nonsurgical cohort. Surg Obes Relat Dis 2012; 8: 62–6.

101 Kennedy MC, Wade DN. Phenytoin absorption in patients with ileojejunal bypass. Br J Clin Pharmacol 1979; 7: 515–8.

102 Dowell JA, Stogniew M, Krause D, Henkel T, Damle B. Lack of pharmacokinetic interaction between anidulafungin and tacrolimus. J Clin Pharmacol 2007; 47: 305–14.

103 Andersen AN, Lebech PE, Sorensen TI, Borggaard B. Sex hormone levels and intestinal absorption of estradiol and D-norgestrel in women following bypass surgery for morbid obesity. Int J Obes 1982; 6: 91–6.

104 Gerrits EG, Ceulemans R, van Hee R, Hendrickx L, Totte E. Contraceptive treatment after biliopancreatic diversion needs consensus. Obes Surg 2003; 13: 378–82.

105 Griffiths TM, Thomas P, Campbell IA. Antituberculosis drug levels after jejunoileal bypass. Br J Dis Chest 1982; 76: 286–9.

106 Harris JO, Wasson KR. Tuberculosis after intestinal bypass operation for obesity. Ann Intern Med 1977; 86: 115–6.

107 Bruce RM, Wise L. Tuberculosis after jejunoileal bypass for obesity. Ann Intern Med 1977; 87: 574–6.

108 Pickleman JR, Evans LS, Kane JM, Freeark RJ. Tuberculosis after jejunoileal bypass for obesity. JAMA 1975; 234: 744.

109 Werbin N. Tuberculosis after jejuno-ileal bypass for morbid obesity. Postgrad Med J 1981; 57: 252–3.

110 Polk RE, Tenenbaum M, Kline B. Isoniazid and ethambutol absorption with jejunoileal bypass. Ann Intern Med 1978; 89: 430–1.

111 Magee SR, Shih G, Hume A. Malabsorption of oral antibiotics in pregnancy after gastric bypass surgery. J Am Board Fam Med 2007; 20: 310–3.

112 Kelley M, Jain A, Kashyap R, Orloff M, Abt P, Wrobble K, Venkataramanan R, Bozorgzadeh A. Change in oral absorption of tacrolimus in a liver transplant recipient after reversal of jejunoileal bypass: case report. Transplant Proc 2005; 37: 3165–7.

113 Pournaras DJ, Footitt D, Mahon D, Welbourn R. Reduced phenytoin levels in an epileptic patient following Roux-En-Y gastric bypass for obesity. Obes Surg 2011; 21: 684–5.

114 Peterson DI, Zweig RW. Absorption of anticonvulsants after jejunoileal bypass. Bull Los Angeles Neurol Soc 1974; 39: 51–5.

115 Peterson DI. Phenytoin absorption following jejunoileal bypass. Bull Clin Neurosci 1983; 48: 148–9.

116 Wills SM, Zekman R, Bestul D, Kuwajerwala N, Decker D. Tamoxifen malabsorption after Roux-en-Y gastric bypass surgery: case series and review of the literature. Pharmacotherapy 2011; 30: 217.

117 Park DM, Shah DD, Egorin MJ, Beumer JH. Disposition of temozolomide in a patient with glioblastoma multiforme after gastric bypass surgery. J Neurooncol 2009; 93: 279–83.

118 Boffito M, Lucchini A, Maiello A, Dal Conte I, Hoggard PG, Back DJ, Di Perri G. Lopinavir/ritonavir absorption in a gastrectomized patient. AIDS 2003; 17: 136–7.

119 Topliss DJ, Wright JA, Volpe R. Increased requirement for thyroid hormone after a jejunoileal bypass operation. Can Med Assoc J 1980; 123: 765–6.

120 Azizi F, Belur R, Albano J. Malabsorption of thyroid hormones after jejunoileal bypass for obesity. Ann Intern Med 1979; 90: 941–2.

121 Bevan JS, Munro JF. Thyroxine malabsorption following intestinal bypass surgery. Int J Obes 1986; 10: 245–6.

8.1.2 Investigating changes in pharmacotherapy post bariatric surgery: Study protocol and data collection form

Introduction:

The prevalence of obesity has dramatically increased over the last decade. In the USA, where the highest reported obesity rate in the world has been observed, approximately 32.2% of the male and 35.5% of the female population aged 20 years or older were characterised as obese in 2007-2008 (Flegal *et al.*, 2010).

Obesity corresponds with an increased risk for comorbidities, such as cardiovascular diseases and diabetes; subsequently new clinical treatment methods of obesity have therefore emerged during the last decades as the prevalence of obesity has increased. Bariatric surgery, resulting in the removing of parts of the GI tract, has proven to be a clinically and cost effective method of reducing obesity (Picot *et al.*, 2009). These new surgical methods impose new challenges in terms of estimating the pharmacokinetics of orally administered drugs (WHO, 2006; OHE, 2010).

Aim:

This study aims to perform a service evaluation of clinical pharmaceutical practice regarding gastric bypass patient pharmacotherapy pre and post bariatric surgery in an attempt to identify drugs that impose formulation and dose adjustment challenges in post bariatric surgery patients, and additionally identify the required pharmacotherapeutic interventions to meet the patient group's specific treatment needs. This service evaluation is a continuation of a systematic review examining trends in drug absorption after bariatric surgery. In the long term these findings will serve as a substratum for research into predicting and extracting clinical guidance for drug therapy of post bariatric surgery patients.

Personnel:

Personnel that are going to carry out research through the NHS' electronic chart system are undertaking the Master of Science programme in pharmacy at University of Manchester. Additionally personnel have undertaken and passed a Criminal Records

Bureau (CRB) check in accordance with NHS policy. In hospital training will be provided at the IT department at the Royal Salford Hospital in order to be able to utilise and search through the electronic clinical chart system.

Data collection procedure:

The data will be collected through observing the pharmaceutical interventions carried out by clinical pharmacists in practice at a daily basis. The extraction and documentation of information will be done in accordance to the data collection form.

Data analysis:

Acquired data will be analysed through the comparison drug therapy post surgery as compared to pre surgery to identify the most commonly prescribed drugs in bariatric surgery patient groups and to identify systematic changes in. Observed changes will be analysed statistically. The implications of these changes in terms of relations to physiological changes and the impact of change in treatment would further be evaluated.

Data collection form

Salford Royal Hospital, Salford, UK.

Date of data extraction (DD/MM/YYYY): ____/____/_____

Study subject number: | | | |

Type of surgery: _____
_____

Pre surgery drug therapy
Date (DD/MM/YYYY): _____
Days pre bariatric surgery: _____

Table 1. Pre surgery drug therapy.

Drug	Administration form	Dosing (mg·times daily)

Comments regarding pharmacotherapy: (underlying comorbidities)

Post surgery (Page 2 of 2)
Date (DD/MM/YYYY): ____/____/_____
Days since bariatric surgery: _____

Table 1. Post surgery drug therapy.

Drug	Administration form	Dosing (mg·times daily)

Reasoning behind drug therapy interventions: (changes in dose, administration form, eventual time period until drug is changed back to original administration form, reason for changes in pharmacotherapy)

8.1.3 Supplementary data on oral drug exposure post bariatric surgery

Table 8.1. Controlled trials examining oral drug exposure following bariatric surgery.

Drug	Surgical procedure	Post/pre surgery drug exposure ratio (mean (CI))	Additional information	References
Antimicrobial drugs				
Erythromycin 250 mg	GBP	**AUC: 0.61 (0.38-0.99)** (P>0.05)[A]	Controlled prospective study (n patients=7)	(Prince *et al.*, 1984)
Ampicillin (pivampicillin 750 mg)	JIB	**F_{oral}0.37 (0.16-0.89)** (P<0.05)[A]	Controlled prospective study (n patients=6)	(Kampmann *et al.*, 1984)
Sulfisoxazole 1,000 mg	JIB	**F_{oral}: 0.84 (0.74-0.94)** (P<0.05)[B]	Controlled prospective study (n patients=3)	(Garrett *et al.*, 1981)
Phenoxymethyl penicillin 1,000 mg	JIB	**AUC: 10.43 (0.10-1058)** (P<0.05)[B]	Controlled prospective study (n patients=3)	(Terry *et al.*, 1982)
Cardiovascular drugs				
Digoxin 0.5 mg	JIB	**AUC: 0.76 (0.59-0.97)** (P<0.05)[A]	Controlled study (n patients=9, n controls=16)	(Gerson *et al.*, 1980)
Digoxin 0.5 mg daily (First day: 1 mg)	JIB	**AUC: 0.89 (0.70-1.14)** (P>0.05)[A]	Controlled prospective study (n pre patients=5, n post patients=6)	(Marcus *et al.*, 1977)
Hydrochlorothiazide 75 mg	JIB	**AUC: 0.46 (0.33-0.65)** (P<0.05)[C]	Controlled study as compared to literature data (n patients=4, n healthy volunteers=7)	(Beermann and Groschinsky-Grind, 1977; Backman *et al.*, 1979)
Immunosuppressants				
Mycophenolic acid (MPA) 2·1,000 mg	RYGB[C]	**AUC: 0.66 (0.21-2.06)**[A]	Pilot study as compared to literature data (n patients=2, 4, 1, n controls=)	(Dowell *et al.*, 2007; Rogers *et al.*, 2008)
Sirolimus 6 mg		**AUC: 0.54 (0.25-1.17)**[A]		
Tacrolimus 2·4 mg		**AUC:** 'Reduced'		
Antiepileptic drugs				
Phenytoin 200 mg	JIB	**AUC: 0.32 (0.17-0.58)** (P<0.05)[A]	Controlled study (n patients=7, n controls=9)	(Kennedy and Wade, 1979)

SD=Standard deviation, GBP=Gastric Bypass (gastroplasty and Roux-en-Y gastric bypass), JIB=Jejunoileal Bypass, BPD=Biliopancreatic Diversion, BPD-DS=Biliopancreatic Diversion with a Duodenal Switch, RYGB=Roux-en-Y Gastric Bypass, AUC=Area Under Curve, F=Bioavailability, SS=Mean concentration at steady state, C_{max}=Maximum concentration, t_{max}=Time at maximum concentration. [A]Statistical outcome as reported in publication. [B]t-test performed at 5% significance level. [C]Pre (sirolimus) and post (tacrolimus and MPA) renal transplant patients. [F]Calculated estimate of AUC from report. [E]Welch's t-test at a 5% significance level.

Table 8.1. (Continued) Controlled trials examining oral drug exposure following bariatric surgery.

Drug	Surgical procedure	Post/pre surgery drug exposure ratio (mean (CI))	Additional information	References
Analgesics				
Paracetamol 1,500 mg	JIB	**AUC: 1.00 (0.647-1.54)** (P>0.05)[B]	Controlled prospective study (n patients=3 at 2.7-3.9 months, 5 at 6.4-34 months)	(Terry *et al.*, 1982)
Phenazone 15 mg/kg	JIB	**AUC[E]: 1.06 (0.81-1.38)** (P>0.05)[F]	Controlled study (n patients=17, n controls=11)	(Andreasen *et al.*, 1977)
Oral contraceptives				
Norethisterone 3 mg	JIB	**AUC[E]: 0.80 (0.39-1.63)** (P<0.05)[F]	Controlled study (n patients=6, n controls=5)	(Victor *et al.*, 1987)
Levonorgestrel 0.25 mg		**AUC[E]: 0.55 (0.34-0.90)** (P<0.05)[F]		
Estradiol 4 mg	JIB	**'Unaltered'**	Controlled study (n patients=12)	(Andersen *et al.*, 1982)
Levonorgestrel 0.125 mg		**'Unaltered'**		
'Contraceptives'	BPD	**'Reduced'**	Observed increase in levels of sex-hormone-binding globulin and reduced levels of dehydroepiandrosterone sulphate. Controlled prospective study (n patients=40)	(Gerrits *et al.*, 2003)
Anti-ulcerative drugs				
Ranitidine 300 mg	BPD	**AUC: 1.43 (1.12-1.81)** (P<0.05)[B]	Controlled study (n patients=11, n controls=10)	(Cossu *et al.*, 1999)
Ranitidine 150 and 300 mg	BPD	**'Unaltered'**	Controlled study as compared to literature data (n patients=7)	(Adami *et al.*, 1991)
HMG-CoA reductase inhibitors				
Atorvastatin acid 20-80 mg	BPD-DS	**AUC: 1.85 (0.81-4.27)** (P<0.05)[A]	Controlled prospective study C_{max} ratio: 2.2±1.7, t_{max} ratio: 2.3±1.3 (n patients=10)	(Skottheim *et al.*, 2010)
Atorvastatin acid 20-80 mg	RYGB	**AUC: 1.43 (1.12-1.81)** (P>0.05)[A]	Controlled prospective study C_{max} ratio: 1.1, t_{max} ratio: 0.5 (n patients=12)	(Skottheim *et al.*, 2009)
Anti-diabetic drugs				
Metformin 1,000 mg	RYGB	**AUC: 1.20 (0.91-1.58)** (P>0.05)[A]	Controlled study (n patients=16, n controls=16)	(Padwal *et al.*, 2011)
Antidepressants				
Sertraline 100 mg	RYGB	**AUC: 0.40 (0.19-0.84)** (P<0.05)[A]	Controlled study (n patients=5, n controls=5)	(Roerig *et al.*, 2012)
Thyroid blockers				
Propylthiouracil 400 mg	JIB	**F_{oral}: 1.09 (0.84-1.42)** (P>0.05)[A]	Controlled prospective study (n patients=9)	(Kampmann *et al.*, 1984)

SD=Standard deviation, GBP=Gastric Bypass (gastroplasty and Roux-en-Y gastric bypass), JIB=Jejunoileal Bypass, BPD=Biliopancreatic Diversion, BPD-DS=Biliopancreatic Diversion with a Duodenal Switch, RYGB=Roux-en-Y Gastric Bypass, AUC=Area Under Curve, F=Bioavailability, SS=Mean concentration at steady state, C_{max}=Maximum concentration, t_{max}=Time at maximum concentration. [A]Statistical outcome as reported in publication. [B]t-test performed at 5% significance level. [C]Pre (sirolimus) and post (tacrolimus and MPA) renal transplant patients. [F]Calculated estimate of AUC from report. [E]Welch's t-test at a 5% significance level.

Table 8.2. Case reports (n patients=1) on oral drug exposure following bariatric surgery.

Drug	Surgical procedure	Post/pre surgery drug exposure ratio	Additional information	References
Antimicrobial drugs				
Rifampicin Isoniazid Ethambutol	JIB	**'Reduced'** **'Unaltered'** **'Unaltered'**	Following JIB, the rifampicin dose was increased from 600 to 1,200 mg in order to reach necessary serum levels.	(Griffiths *et al.*, 1982)
Rifampicin Isoniazid Ethambutol	JIB	**'Reduced'** **'Inconclusive'** **'Unaltered'**	Patient 1: Isoniazid 300 mg – Serum concentration of 3.6 µg/mL at 2 hours as compared to reference value of 4-6 µg/mL. Patient 2: Isoniazid 300 mg – Serum concentration of 8.4 µg/mL at 2 hours. Ethambutol 2,400 mg - Serum concentration under 1 µg/mL. Rifampicin 600 mg – Serum concentration of 4 µg/mL at 4 hours as compared to reference value of 8 µg/mL.	(Harris and Wasson, 1977)
Rifampicin Isoniazid Ethambutol	JIB	**'Reduced'** **'Unaltered'** **'Unaltered'**	Four female patients out of one hundred patients undergoing JIB developed tuberculosis. Blood levels were obtained from two patients, displaying a reduced level of rifampicin, whereas isoniazid and ethambutol remained within therapeutic range (n patients=4).	(Bruce and Wise, 1977)
Isoniazid Ethambutol	JIB	**'Unaltered'** **'Unaltered'**	Isoniazid and ethambutol blood levels reported to be within normal range.	(Pickleman *et al.*, 1975)
Isoniazid Ethambutol Para-aminosalicylic acid	JIB	**'Reduced'** **'Reduced'** **'Reduced'**	Drugs excreted in faeces as unaltered tablets after oral administration.	(Werbin, 1981)
Isoniazid Ethambutol	JIB	**'Unaltered'** **'Unaltered'**	Serum levels equivalent to that observed in healthy volunteers.	(Polk *et al.*, 1978)
Nitrofurantoin Amoxicillin	RYGB	**'Reduced'** **'Reduced'**	Intravenous antibiotics administered due to failure of oral drug therapy failed.	(Magee *et al.*, 2007)
Immunosuppressants				
Tacrolimus	JIB R	**AUC:** 0.53	After JIB R a 1.90-fold increase in AUC was observed.	(Kelley *et al.*, 2005)
Cyclosporine	JIB	**SS conc:** 0.41	n patients=1, as compared to n controls=6	(Chenhsu *et al.*, 2003)
Cyclosporine	JIB R	**F_{oral}:** 0.36	2.78-fold Increase in drug exposure following JIB R.	(Knight *et al.*, 1988)
Cyclosporine	LAGBD	**'Unaltered'**	Standard cyclosporine therapy was successful in the treatment of a post LAGB surgery patient subject to heart transplant.	(Ablassmaier *et al.*, 2002)

JIB=Jejunoileal Bypass, JIB R=Jejunoileal Bypass Reversal, BPD=Biliopancreatic Diversion, BPD-DS=Biliopancreatic Diversion with a Duodenal Switch, RYGB=Roux-en-Y Gastric Bypass, LAGBD=Laparoscopic Adjustable Gastric Banding, AUC=Area Under Curve, F=Bioavailability, SS Conc=Mean concentration at steady state, C_{max}=Maximum concentration, t_{max}=Time at maximum concentration. [A] Total gastrectomy followed by an oesophagojejunostomy with a Roux-en-y reconstruction.

Table 8.2. (Continued) Case reports (n patients=1) on oral drug exposure following bariatric surgery.

Drug	Surgical procedure	Post/pre surgery drug exposure ratio	Additional information	References
Anticonvulsants				
Phenytoin	RYGB	**'Reduced'**	Dose strength up to 500 mg did not achieve therapeutic effect (<3 mg/l as compared to a normal range of 10-20 mg/l).	(Pournaras *et al.*)
Phenobarbitone	RYGB	**'Reduced'**	At a dose of 60 mg bid, serum levels were reduced (9.9 mg/l) as compared to normal range (15-41 mg/l).	
Phenytoin	JIB	**'Reduced'**	Dose increased from 300 to 500 mg in order to achieve therapeutic effect.	(Peterson and Zweig, 1974)
Ethosuximide	JIB	**'Reduced'**	Dose doubled in order to achieve therapeutic effect.	
Phenytoin	JIB R	**SS conc:** 0.48	JIB R resulted in an increase in SS conc.	(Peterson, 1983)
Antipsychotic drugs				
Haloperidol	RYGB	**'Unaltered'**	Dose doubled immediate post surgery to thereafter be lower to pre-surgery dose with effective treatment.	(Fuller *et al.*, 1986)
Anti-cancer drugs				
Imatinib mesylate	BPD-DS	**SS conc:** 0.17	Plasma concentration of imatinib 400 mg at steady state reduced from 965 to 166 ng/mL.	(Liu and Artz)
Tamoxifen	RYGB	**'Reduced'**	3 case reports (n patients=3).	(Wills *et al.*)
Temozolomide	RYGB	**AUC:** 1.02	Unaltered drug exposure following surgery at a dose of 190 mg as compared to literature.	(Park *et al.*, 2009)
Anti-HIV drugs				
Lopinavir/ritonavir	RYGB[A]	**'Increased'**	An observed increase in plasma concentration in comparison to control patients.	(Boffito *et al.*, 2003)
Thyroid hormones				
Thyroxin	JIB	**'Reduced'**	Dose increase required from 0.2 mg to 0.8 mg daily to produce sufficient response.	(Topliss *et al.*, 1980)
Thyroxin	JIB	**'Reduced'**	C_{max} ratio: 0.31. JIB R restored to pre surgery drug exposure.	(Azizi *et al.*, 1979)
Thyroxin	JIB R	**'Reduced'**	Dose increase required from 0.3 mg to 0.6 mg daily to reach SS sufficient concentration.	(Bevan and Munro, 1986)

JIB=Jejunoileal Bypass, JIB R=Jejunoileal Bypass Reversal, BPD=Biliopancreatic Diversion, BPD-DS=Biliopancreatic Diversion with a Duodenal Switch, RYGB=Roux-en-Y Gastric Bypass, LAGBD=Laparoscopic Adjustable Gastric Banding, AUC=Area Under Curve, F=Bioavailability, SS Conc=Mean concentration at steady state, C_{max}=Maximum concentration, t_{max}=Time at maximum concentration. [A] Total gastrectomy followed by an oesophagojejunostomy with a Roux-en-y reconstruction.

8.1.4 Statistical data analysis

The combined standard deviation (S_{pooled}) was computed utilising Equation 8.1, where S_n denotes the sample standard deviation and n represents the sample size.

$$S_{pooled} = \sqrt{\frac{(n_1 - 1) \cdot S_1^2 + (n_2 - 1) \cdot S_2^2}{n_1 + n_2 - 2}}$$

Equation 8.1: Pooled variance.

The natural logarithmic ratio (lnR) was computed from sample means (X_n; Equation 8.2):

$$\ln R = \ln(\overline{X}_1) - \ln(\overline{X}_2)$$

Equation 8.2: logarithmic ratio.

The variance of the log response ratio (V_{lnR}) was obtained through Equation 8.3:

$$V_{\ln R} = S_{pooled}^2 \left(\frac{1}{n_1 \cdot (\overline{X}_1)^2} + \frac{1}{n_2 \cdot (\overline{X}_2)^2} \right)$$

Equation 8.3: Variance of ratio.

The standard error of the log response ratio (SE_{lnR}; Equation 8.4) was calculated from the variance:

$$SE_{\ln R} = \sqrt{V_{\ln R}}$$

Equation 8.4: Standard error of ratio.

The log ratio was converted to the geometric mean ratio (R), upper and lower 95th Percentiles (UL_R and LL_R respectively) utilising the exponent (e) utilising Equation 8.5, Equation 8.6 and Equation 8.7:

$$R = e^{lnR}$$

Equation 8.5: Geometric mean ratio.

$$LL_R = e^{LL_{lnR}}$$

Equation 8.6: Lower percentile of geometric mean ratio.

$$UL_R = e^{UL_{lnR}}$$

Equation 8.7: Upper percentile of geometric mean ratio.

The weighted mean (WX) was calculated based on averages (xj) and sample sizes (nj) from literature data (Equation 8.8) (Ghobadi *et al.*, 2011):

$$WX = \frac{\sum_{j=1}^{n} nj \cdot xj}{\sum_{j=1}^{n} nj}$$

Equation 8.8: Weighted mean.

Overall sum of squares (SS) was obtained based on standard deviations (SD_j) from literature data, xj, nj, overall sample size (N) and WX (Equation 8.9):

$$SS = \sum \left[\left\{ SD_j^2 + xj^2 \right\} \cdot nj \right] - N \cdot WX^2$$

Equation 8.9: Overall sum of squares.

Overall SD was obtained from SS and N (Equation 8.10):

$$SD = \sqrt{\frac{SS}{N}}$$

Equation 8.10: Overall standard deviation.

The coefficient of variance (CV) was obtained based on SD and WX (Equation 8.11):

$$CV = \frac{SD}{WX}$$

Equation 8.11: Coefficient of variation.

Overall σ was obtained from the log-transformed CV (Equation 8.12):

$$\sigma = \sqrt{\ln(1 + CV^2)}$$

Equation 8.12: Log-transformed coefficient of variation.

The overall μ was obtained from WX and σ (Equation 8.13):

$$\mu = \ln(WX) - (0.5 \cdot \sigma^2)$$

Equation 8.13: Log-transformed mean ratio.

The overall geometrical mean (GM) was obtained from the exponent of μ (Equation 8.14):

$$GM = e^{\mu}$$

Equation 8.14: Geometric mean.

The overall geometrical standard deviation (GSD) was obtained from the exponent of σ (Equation 8.15):

$$GSD = e^{\sigma}$$

Equation 8.15: Geometric standard deviation.

8.1.5 References

Ablassmaier B, Klaua S, Jacobi CA, and Muller JM (2002) Laparoscopic gastric banding after heart transplantation. *Obes Surg* **12**:412-415.

Adami GF, Gandolfo P, Esposito M, and Scopinaro N (1991) Orally-administered Serum Ranitidine Concentration after Biliopancreatic Diversion for Obesity. *Obes Surg* **1**:293-294.

Andersen AN, Lebech PE, Sorensen TI, and Borggaard B (1982) Sex hormone levels and intestinal absorption of estradiol and D-norgestrel in women following bypass surgery for morbid obesity. *Int J Obes* **6**:91-96.

Andreasen PB, Dano P, Kirk H, and Greisen G (1977) Drug absorption and hepatic drug metabolism in patients with different types of intestinal shunt operation for obesity. A study with phenazone. *Scand J Gastroenterol* **12**:531-535.

Azizi F, Belur R, and Albano J (1979) Malabsorption of thyroid hormones after jejunoileal bypass for obesity. *Ann Intern Med* **90**:941-942.

Backman L, Beerman B, Groschinsky-Grind M, and Hallberg D (1979) Malabsorption of hydrochlorothiazide following intestinal shunt surgery. *Clin Pharmacokinet* **4**:63-68.

Beermann B and Groschinsky-Grind M (1977) Pharmacokinetics of hydrochlorothiazide in man. *Eur J Clin Pharmacol* **12**:297-303.

Bevan JS and Munro JF (1986) Thyroxine malabsorption following intestinal bypass surgery. *Int J Obes* **10**:245-246.

Boffito M, Lucchini A, Maiello A, Dal Conte I, Hoggard PG, Back DJ, and Di Perri G (2003) Lopinavir/ritonavir absorption in a gastrectomized patient. *AIDS* **17**:136-137.

Bruce RM and Wise L (1977) Tuberculosis after jejunoileal bypass for obesity. *Ann Intern Med* **87**:574-576.

Chenhsu RY, Wu Y, Katz D, and Rayhill S (2003) Dose-adjusted cyclosporine c2 in a patient with jejunoileal bypass as compared to seven other liver transplant recipients. *Ther Drug Monit* **25**:665-670.

Cossu ML, Caccia S, Coppola M, Fais E, Ruggiu M, Fracasso C, Nacca A, and Noya G (1999) Orally administered ranitidine plasma concentrations before and after biliopancreatic diversion in morbidly obese patients. *Obes Surg* **9**:36-39.

Dowell JA, Stogniew M, Krause D, Henkel T, and Damle B (2007) Lack of pharmacokinetic interaction between anidulafungin and tacrolimus. *J Clin Pharmacol* **47**:305-314.

Flegal KM, Carroll MD, Ogden CL, and Curtin LR (2010) Prevalence and trends in obesity among US adults, 1999-2008. *JAMA* **303**:235-241.

Fuller AK, Tingle D, DeVane CL, Scott JA, and Stewart RB (1986) Haloperidol pharmacokinetics following gastric bypass surgery. *J Clin Psychopharmacol* **6**:376-378.

Garrett ER, Suverkrup RS, Eberst K, Yost RL, and O'Leary JP (1981) Surgically affected sulfisoxazole pharmacokinetics in the morbidly obese. *Biopharm Drug Dispos* **2**:329-365.

Gerrits EG, Ceulemans R, van Hee R, Hendrickx L, and Totte E (2003) Contraceptive treatment after biliopancreatic diversion needs consensus. *Obes Surg* **13**:378-382.

Gerson CD, Lowe EH, and Lindenbaum J (1980) Bioavailability of digoxin tablets in patients with gastrointestinal dysfunction. *Am J Med* **69**:43-49.

Ghobadi C, Johnson TN, Aarabi M, Almond LM, Allabi AC, Rowland-Yeo K, Jamei M, and Rostami-Hodjegan A (2011) Application of a systems approach to the

bottom-up assessment of pharmacokinetics in obese patients: expected variations in clearance. *Clin Pharmacokinet* **50**:809-822.
Griffiths TM, Thomas P, and Campbell IA (1982) Antituberculosis drug levels after jejunoileal bypass. *Br J Dis Chest* **76**:286-289.
Harris JO and Wasson KR (1977) Tuberculosis after intestinal bypass operation for obesity. *Ann Intern Med* **86**:115-116.
Kampmann JP, Klein H, Lumholtz B, and Molholm Hansen JE (1984) Ampicillin and propylthiouracil pharmacokinetics in intestinal bypass patients followed up to a year after operation. *Clin Pharmacokinet* **9**:168-176.
Kelley M, Jain A, Kashyap R, Orloff M, Abt P, Wrobble K, Venkataramanan R, and Bozorgzadeh A (2005) Change in oral absorption of tacrolimus in a liver transplant recipient after reversal of jejunoileal bypass: case report. *Transplant Proc* **37**:3165-3167.
Kennedy MC and Wade DN (1979) Phenytoin absorption in patients with ileojejunal bypass. *Br J Clin Pharmacol* **7**:515-518.
Knight GC, Macris MP, Peric M, Duncan JM, Frazier OH, and Cooley DA (1988) Cyclosporine A pharmacokinetics in a cardiac allograft recipient with a jejuno-ileal bypass. *Transplant Proc* **20**:351-355.
Liu H and Artz AS Reduction of imatinib absorption after gastric bypass surgery. *Leuk Lymphoma* **52**:310-313.
Magee SR, Shih G, and Hume A (2007) Malabsorption of oral antibiotics in pregnancy after gastric bypass surgery. *J Am Board Fam Med* **20**:310-313.
Marcus FI, Quinn EJ, Horton H, Jacobs S, Pippin S, Stafford M, and Zukoski C (1977) The effect of jejunoileal bypass on the pharmacokinetics of digoxin in man. *Circulation* **55**:537-541.
OHE (2010) Office of Health Economics, UK. Shedding the Pounds: Obesity management, NICE guidance and bariatric surgery in England.
Padwal RS, Gabr RQ, Sharma AM, Langkaas LA, Birch DW, Karmali S, and Brocks DR (2011) Effect of gastric bypass surgery on the absorption and bioavailability of metformin. *Diabetes Care* **34**:1295-1300.
Park DM, Shah DD, Egorin MJ, and Beumer JH (2009) Disposition of temozolomide in a patient with glioblastoma multiforme after gastric bypass surgery. *J Neurooncol* **93**:279-283.
Peterson DI (1983) Phenytoin absorption following jejunoileal bypass. *Bull Clin Neurosci* **48**:148-149.
Peterson DI and Zweig RW (1974) Absorption of anticonvulsants after jejunoileal bypass. *Bull Los Angeles Neurol Soc* **39**:51-55.
Pickleman JR, Evans LS, Kane JM, and Freeark RJ (1975) Tuberculosis after jejunoileal bypass for obesity. *JAMA* **234**:744.
Picot J, Jones J, Colquitt JL, Gospodarevskaya E, Loveman E, Baxter L, and Clegg AJ (2009) The clinical effectiveness and cost-effectiveness of bariatric (weight loss) surgery for obesity: a systematic review and economic evaluation. *Health Technol Assess* **13**:1-190, 215-357, iii-iv.
Polk RE, Tenenbaum M, and Kline B (1978) Isoniazid and ethambutol absorption with jejunoileal bypass. *Ann Intern Med* **89**:430-431.
Pournaras DJ, Footitt D, Mahon D, and Welbourn R Reduced phenytoin levels in an epileptic patient following Roux-En-Y gastric bypass for obesity. *Obes Surg* **21**:684-685.
Prince RA, Pincheira JC, Mason EE, and Printen KJ (1984) Influence of bariatric surgery on erythromycin absorption. *J Clin Pharmacol* **24**:523-527.

Roerig JL, Steffen K, Zimmerman C, Mitchell JE, Crosby RD, and Cao L (2012) Preliminary comparison of sertraline levels in postbariatric surgery patients versus matched nonsurgical cohort. *Surg Obes Relat Dis* **8**:62-66.

Rogers CC, Alloway RR, Alexander JW, Cardi M, Trofe J, and Vinks AA (2008) Pharmacokinetics of mycophenolic acid, tacrolimus and sirolimus after gastric bypass surgery in end-stage renal disease and transplant patients: a pilot study. *Clin Transplant* **22**:281-291.

Skottheim IB, Jakobsen GS, Stormark K, Christensen H, Hjelmesaeth J, Jenssen T, Asberg A, and Sandbu R (2010) Significant increase in systemic exposure of atorvastatin after biliopancreatic diversion with duodenal switch. *Clin Pharmacol Ther* **87**:699-705.

Skottheim IB, Stormark K, Christensen H, Jakobsen GS, Hjelmesaeth J, Jenssen T, Reubsaet JL, Sandbu R, and Asberg A (2009) Significantly altered systemic exposure to atorvastatin acid following gastric bypass surgery in morbidly obese patients. *Clin Pharmacol Ther* **86**:311-318.

Terry SI, Gould JC, McManus JP, and Prescott LF (1982) Absorption of penicillin and paracetamol after small intestinal bypass surgery. *Eur J Clin Pharmacol* **23**:245-248.

Topliss DJ, Wright JA, and Volpe R (1980) Increased requirement for thyroid hormone after a jejunoileal bypass operation. *Can Med Assoc J* **123**:765-766.

Victor A, Odlind V, and Kral JG (1987) Oral contraceptive absorption and sex hormone binding globulins in obese women: effects of jejunoileal bypass. *Gastroenterol Clin North Am* **16**:483-491.

Werbin N (1981) Tuberculosis after jejuno-ileal bypass for morbid obesity. *Postgrad Med J* **57**:252-253.

WHO (2006) WHO. Obesity and Overweight, fact sheet 311.

Wills SM, Zekman R, Bestul D, Kuwajerwala N, and Decker D Tamoxifen malabsorption after Roux-en-Y gastric bypass surgery: case series and review of the literature. *Pharmacotherapy* **30**:217.

8.2 A mechanistic pharmacokinetic model to assess modified oral drug bioavailability post bariatric surgery in morbidly obese patients: interplay between CYP3A gut wall metabolism, permeability and dissolution

8.2.1 Publication in Journal of Pharmacy and Pharmacology (2012) 64(7):1008-1024

JPP JOURNAL OF Pharmacy and Pharmacology
ROYAL PHARMACEUTICAL SOCIETY
JPP Journal of Pharmacy And Pharmacology
Research Paper

A mechanistic pharmacokinetic model to assess modified oral drug bioavailability post bariatric surgery in morbidly obese patients: interplay between CYP3A gut wall metabolism, permeability and dissolution

Adam S. Darwich[a], Devendra Pade[c], Basil J. Ammori[b,d], Masoud Jamei[c], Darren M. Ashcroft[a] and Amin Rostami-Hodjegan[a,c]

[a]Centre of Applied Pharmacokinetic Research, School of Pharmacy and Pharmaceutical Sciences, [b]School of Biomedicine, University of Manchester, Manchester, [c]Simcyp Limited (a Certara Company), Blades Enterprise Centre, Sheffield, [d]Salford Royal Hospital, Salford, UK

Keywords
ADAM model; bariatric surgery; obesity; oral drug bioavailability; pharmacokinetic modelling

Correspondence
Amin Rostami-Hodjegan, School of Pharmacy and Pharmaceutical Sciences, Faculty of Medical and Human Sciences, University of Manchester, Stopford Building, Oxford Road, Manchester M13 9PT, UK.
E-mail: amin.rostami@manchester.ac.uk

Received December 16, 2011
Accepted April 19, 2012

doi: 10.1111/j.2042-7158.2012.01538.x

Abstract

Objectives Due to the multi-factorial physiological implications of bariatric surgery, attempts to explain trends in oral bioavailability following bariatric surgery using singular attributes of drugs or simplified categorisations such as the biopharmaceutics classification system have been unsuccessful. So we have attempted to use mechanistic models to assess changes to bioavailability of model drugs.

Methods Pharmacokinetic post bariatric surgery models were created for Roux-en-Y gastric bypass, biliopancreatic diversion with duodenal switch, sleeve gastrectomy and jejunoileal bypass, through altering the 'Advanced Dissolution Absorption and Metabolism' (ADAM) model incorporated into the Simcyp® Simulator. Post to pre surgical simulations were carried out for five drugs with varying characteristics regarding their gut wall metabolism, dissolution and permeability (simvastatin, omeprazole, diclofenac, fluconazole and ciprofloxacin).

Key findings The trends in oral bioavailability pre to post surgery were found to be dependent on a combination of drug parameters, including solubility, permeability and gastrointestinal metabolism as well as the surgical procedure carried out.

Conclusions In the absence of clinical studies, the ability to project the direction and the magnitude of changes in bioavailability of drug therapy, using evidence-based mechanistic pharmacokinetic *in silico* models would be of significant value in guiding prescribers to make the necessary adjustments to dosage regimens for an increasing population of patients who are undergoing bariatric surgery.

Introduction

The prevalence of obesity has increased dramatically in the USA and Europe over the last decade.[1–4] Bariatric surgery has proven to be successful in treating morbid obesity. In 2008, approximately 220 000 bariatric surgeries were performed in the USA and Canada, and over 66 000 operations were carried out in Europe.[5,6]

Several bariatric surgical procedures currently coexist in healthcare, being characterised as either restrictive, in terms of reducing gastric capacity, malabsorptive, with regard to restricting the small intestine and/or delaying the bile inlet, or a combination of both.[7,8] These procedures include: adjustable gastric band, sleeve gastrectomy, biliopancreatic diversion (BPD), biliopancreatic diversion with a duodenal switch (BPD-DS) and Roux-en-Y gastric bypass (RYGB).[9] Other procedures, such as jejunoileal bypass, have been gradually phased out due to a higher likelihood of adverse events (Figure 1).[4,10,11]

Different types of bariatric surgery will impose a number of physiological changes varying in extent depending on the invasiveness of the procedure. Many of these alterations are known to affect the bioavailability of orally administered drugs, although studies investigating alterations in oral drug exposure pre- to postoperatively have been limited.[12]

Oral bioavailability (F_{oral}) is dependent on the fraction of drug that is absorbed in the intestinal gut wall (f_a), the fraction that escapes gut wall metabolism (F_G) and the fraction that escapes hepatic metabolism (F_H) (Equation 1).

$$F_{oral} = f_a \cdot F_G \cdot F_H \quad (1)$$

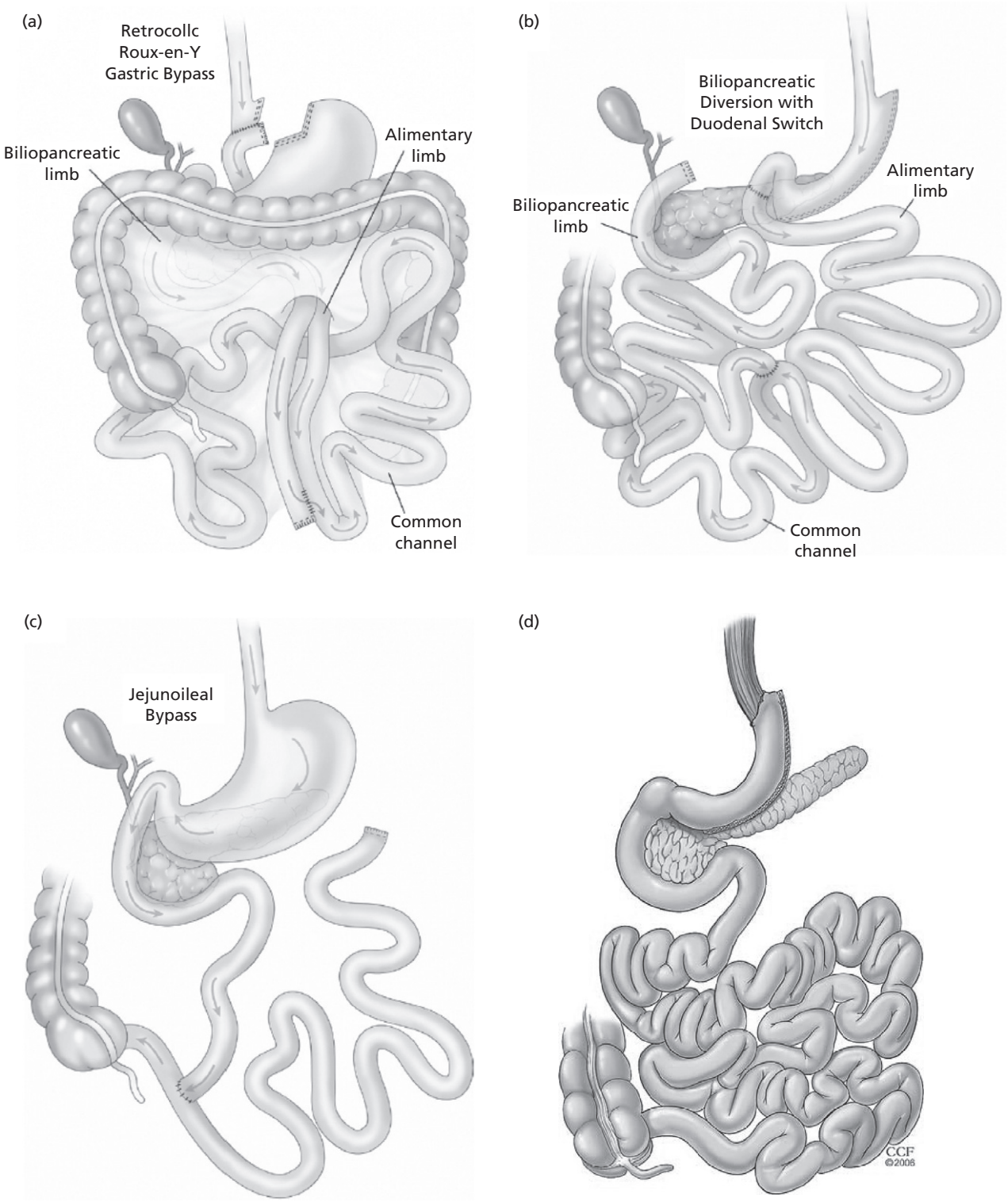

Figure 1 Schematic illustrations of selected bariatric surgical procedures imposing restrictions to the gastrointestinal tract. (a) Roux-en-Y gastric bypass. (b) Biliopancreatic diversion with duodenal switch. (c) Jejunoileal bypass.[4] (d) Sleeve gastrectomy.[3]

Both f_a and F_G are highly influenced by drug and formulation properties, such as disintegration, dissolution, permeability, solubility, and the susceptibility to being metabolised by certain enzymes (e.g. certain cytochrome P450 families (CYP3A) or UDP-glucuronsyltransferases). Gastrointestinal (GI) physiology such as gastric emptying time, pH profile, small intestinal transit time, abundance and genotype of gut wall drug metabolising enzymes and transporters can also affect f_a and F_G.[13,14]

Gastric emptying time can serve as the rate limiting step for highly permeable and highly soluble drugs as the absorption from the stomach is inevitably low.[15] The gastrointestinal pH may affect drug dissolution for drugs displaying a pKa within the range of GI pH fluctuations.[16,17] Furthermore, small intestinal transit time may influence the drug absorption of poorly soluble or extended release drug formulations as it is the main site of absorption.[18] Metabolism in the gut acts to regulate the oral bioavailability of drugs and other xenobiotics, an important determinant in the metabolism of substrate drugs.[19] Cytochrome P450 (CYP), UDP-glucuronsyltransferases, sulfotransferases and glutathione *S*-transferases drug metabolising enzymes are present in the enterocytes along the GI tract. CYP3A4 is the most abundant drug metabolising enzyme in the GI tract, preceding CYP2C9, CYP2C19, CYP2J2 and CYP2D6 in order of abundance.[20–23] CYP3A4 and CYP3A5 are both present along the whole GI tract, where CYP3A4 is expressed at lower levels in the duodenum, rising in the jejunum and decreasing towards the ileum.[19,24]

GI transporters may influence the absorption of orally administered drugs and potentially also the extent of metabolism in the gut through active substrate efflux.[25,26] Numerous transporters are present in the gut, such as the multidrug resistance transporter 1, also referred to as P-glycoprotein (P-gp), multidrug resistance associated protein 2 and breast cancer related protein.[27,28] P-gp is the most extensively studied of the GI transporters and the relative expression pattern of P-gp in the small intestine increases from the proximal to the distal parts of the small intestine.[29]

The advanced dissolution absorption and metabolism (ADAM) model is a mechanistic representation of the GI tract which is implemented into the Simcyp Simulator.[30] It is a successive development of the advanced compartmental absorption and transit model,[31,32] and includes distinct parameters that better reflect the physiology with regards to handling of fluid dynamics (no constant volume in each segment), anatomical mirroring of the GI anatomy and biology for different segments (unequal segments with relative abundance of enzymes), and dissolution models (avoiding assumptions of a flat surface in Noyes-Whitney). The model defines the amount of drug in 'formulation', 'released but undissolved', 'dissolved' and 'enterocytes' as separate compartment structures and further adds hepatobiliary circulation and bile mediated solubility (Figure 2). The model also incorporates fluid dynamics along the GI tract flowing at the rate of gastric emptying and small intestinal transit time, and rates of fluid absorption, secretion and reabsorption along the GI tract as opposed to a static volume in each segment.[14]

Furthermore, the ADAM model incorporates the abundance and distribution of GI enzymes and inter-individual variability as well as the distribution of the GI transporter P-gp.[14] The model attributes can be modified to reflect changes following bariatric surgery in a morbidly obese patient population[33] and to investigate the validity of predicting the influence of surgery on oral bioavailability of drugs.

Due to the multifactorial physiological implications of bariatric surgery, attempts to explain trends in changes to oral bioavailability following bariatric surgery using single attributes of drugs or simplified categorisations such as the biopharmaceutics classification system (BCS) have been unsuccessful.[12]

In the absence of clinical studies showing the direction and magnitude of changes in bioavailability of various drugs, evidence-based mechanistic pharmacokinetic in-silico models that define such alterations would be of value in determining appropriate dosage regimens for an increasing patient population undergoing bariatric surgery. The current study, to our knowledge, is the first to develop such a model.

Methods

Characterisation of post bariatric surgery population

A set of gastrointestinal and whole-body physiological parameters were identified based on factors influencing oral drug bioavailability post bariatric surgery. These included: gastric volume and gastric emptying rate, gastrointestinal pH, post surgical small intestinal dimensions, small intestinal motility and transit time, and bile properties. Whole-body physiological factors known to influence oral drug exposure were also identified, such as renal function and serum protein levels as a function of post surgical weight loss.

An extensive literature search of identified parameters in relation to bariatric surgery was performed utilising PubMed (1966–2011). The gastrointestinal and physiological parameters were analysed in accordance with appropriate functions. Weighted means (WX) and standard deviations (overall SD) of results were calculated from the reported means (x) and standard deviations (SD), dependent on the number of observations in the i^{th} study (n) (Equations 2, 3 and 4), and where applicable were analysed using Welch's t-test at a significance level of 0.05 assuming parameter data to be normally distributed and taking unequal variance (s) into

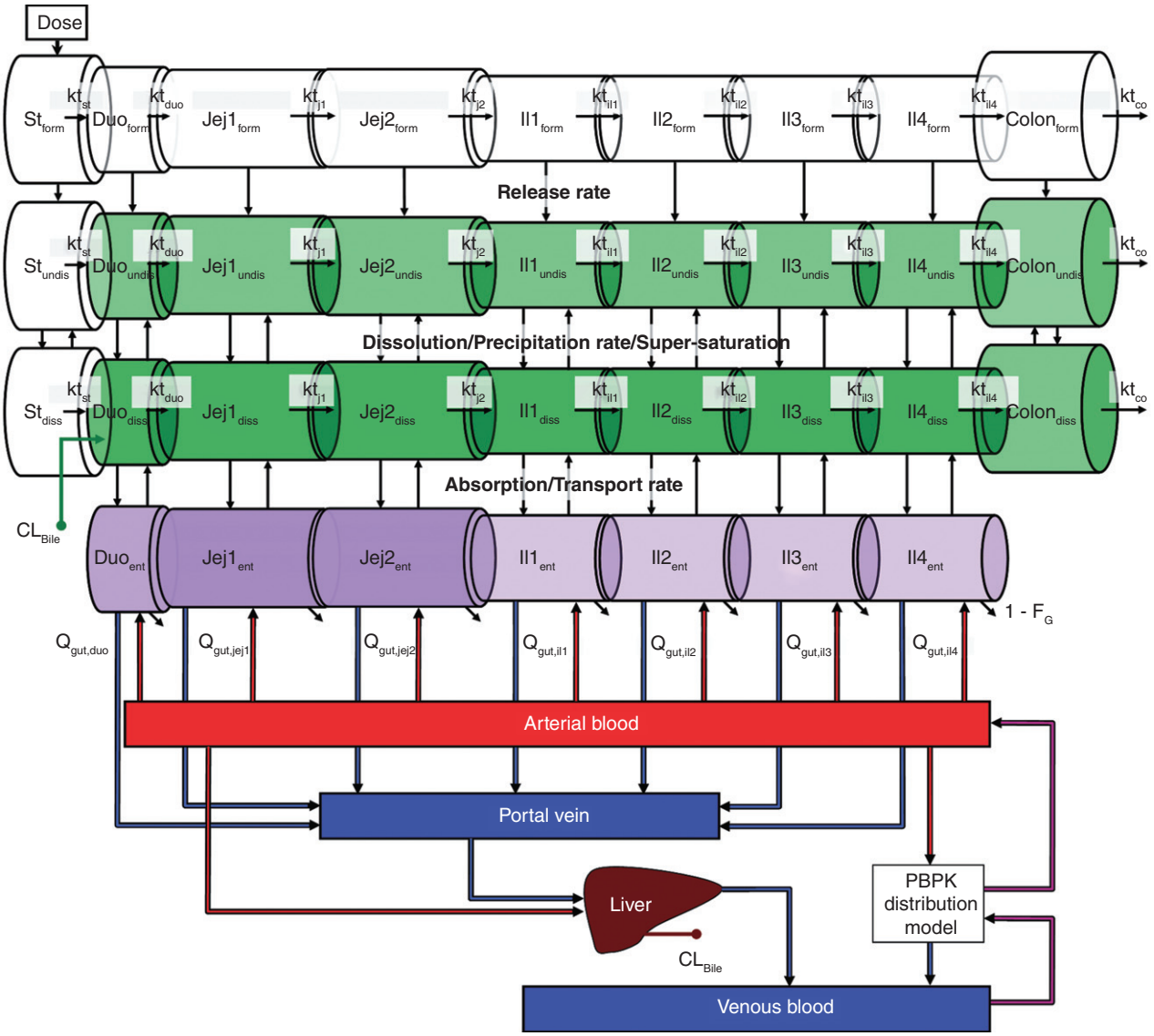

Figure 2 Depiction of the 9-segment ADAM model consisting of the following compartments: stomach, duodenum, jejunum I, jejunum II, ileum I–IV and colon. St, stomach; Jej1 and 2, jejunum; Il1-4, ileum; form, drug trapped in formulation; undiss, undissolved drug; diss, dissolved drug; ent, fraction absorbed drug in enterocytes; kt_n, transit rate; Q_n, gastrointestinal blood flow; F_G, fraction drug that escapes gut wall metabolism; CL_{bile}, biliary clearance. Compartment size and purple colour intensity refers to segmental length and regional abundance of CYP3A4 respectively. Green colour scheme indicates bile enhanced solubility. Adapted from Jamei *et al*.[14]

account, where X is the sample mean and N is the sample size (Equation 5).

$$WX = \frac{\sum_{i=1}^{n} n_i \cdot x_i}{\sum_{i=1}^{n} n_i} \quad (2)$$

$$Overall\ SD = \sqrt{\frac{Overall\ sum\ of\ squares}{N}} \quad (3)$$

$$Overall\ sum\ of\ squares = \sum_{i=1}^{n}\left[\left\{(SD_i)^2 + (x_i)^2\right\} \cdot n_i\right] - N \cdot WX^2 \quad (4)$$

$$t = \frac{X_1 - X_2}{\sqrt{\frac{s_1^2}{N_1} + \frac{s_2^2}{N_2}}} \quad (5)$$

Adapting the ADAM model to mimic post bariatric surgery conditions

The Simcyp Simulator v10 (Simcyp Limited, Sheffield, UK) population template for the morbidly obese based on a northern European Caucasian population was used. Validation of this model with respect to prediction of clearance has recently been published by Ghobadi *et al*.[33] We re-evaluated and analysed model performance against the identified post bariatric surgery model. Whenever applicable, we altered necessary population parameters to conform to post bariatric surgery conditions, applying reported data of weighted means and coefficient of variation (CV %) (Table 1).

Post bariatric surgery gastrointestinal physiological parameters based on population/surgical data or physiologically rational assumptions were implemented into the ADAM model, creating 'post sleeve gastrectomy', 'post Roux-en-Y gastric bypass', 'post biliopancreatic diversion with duodenal switch' and 'post jejunoileal bypass' population templates (so called population files within Simcyp).

Post surgical basal steady state gastric fluid volumes at fasted state were estimated through one-compartmental simulations of gastric fluid dynamics (Equation 6) in Matlab R2010a (MathWorks, Natick, MA, USA) utilising reported post surgical gastric emptying and assuming a linear relationship with regards to the excretion of gastric juices (0.08 l/h) as a function of gastric capacity, utilising an average gastric volume of 230 ± 13 ml as reported in 134 individuals. Saliva production was kept constant at 0.05 l/h.[14,34,35] Where V_{st} is the volume of fluids in the stomach, $Q_{sec,s}$ is the secretion of fluids into the stomach, and $k_{t,st}$ is the rate at which the stomach is emptied.

$$\frac{dV_{st}}{dt} = Q_{\text{sec},s} - k_{t,st} V_{st} \tag{6}$$

Table 1 Pre to post surgery physiological parameters evaluated

Gastric emptying of liquids (min)
Gastric emptying of solids (min)
Postoperative gastric volume (ml)
Secretion in stomach (Q_{sec}; l/h)
Initial volume of stomach fluid (ml)
Small intestinal bypass (cm)
Small intestinal bile delay (cm)
Small intestinal bile concentrations at fasted and fed state (nM)
Gastrointestinal pH at fasted and fed state
Gastrointestinal CYP3A4 abundance (nmol/total gut)
Gastrointestinal CYP3A5 abundance (nmol/total gut)
Small intestinal transit time (h)
Renal function (glomerular filtration rate; ml/min)
Human serum albumin levels (g/l)
α-1 Acid glycoprotein levels (g/l)
Hepatic function (enzymatic activity)

Population implementations of small intestinal bypass and delay in bile inlet were dimensionally estimated as a function of body surface area (BSA) utilising Equations 7 and 8 as implemented into the Simcyp Simulator ADAM model. Further, the human effective permeability (P_{eff}) was set to close to zero in segments corresponding to the small intestinal bypass in the drug template.[36]

$$Length\ of\ duodenum = 0.205 \cdot BSA^{0.550} \tag{7}$$

$$Length\ of\ jejunum\ and\ ileum = 5.231 \cdot BSA^{0.414} \tag{8}$$

Post surgical estimations of small intestinal transit time were implemented into the ADAM model utilising the incorporated Weibull distribution fitted to describe a log normal distribution through altering the scale factor (β) of small intestinal transit time, keeping the shape factor (α) constant, altering β thus retaining the log normal distribution assumption (Equation 9).[36]

$$f(x) = \frac{\alpha}{\beta}\left(\frac{x}{\beta}\right)^{\alpha-1} e^{-(x/\beta)^{\alpha}} \tag{9}$$

Following the dimensional alterations to the postoperative surgical GI anatomy, the bariatric surgical team at Salford Royal Foundation NHS Hospital Trust (Salford, UK) was consulted in order to establish consensus on physiological dimensions reflecting a realistic patient population. The parameters subject to a consensus discussion included: post surgical gastric volume and capacity, small intestinal bypass and delay in bile inlet.

Virtual study of bioavailability post bariatric surgery

An identified set of compounds in the Simcyp Simulator were simulated utilising 'post sleeve gastrectomy in morbidly obese', 'post Roux-en-Y gastric bypass in morbidly obese', 'post biliopancreatic diversion with duodenal switch in morbidly obese' and 'post jejunoileal bypass in morbidly obese' population templates in a total of 100 subjects per group, with an age range of 20 to 50 years and 0.50 proportion of females, varying the mean small intestinal transit time to account for any ambiguity in reported data following surgery.

The selected drugs (simvastatin, omeprazole, diclofenac, fluconazole and ciprofloxacin) had a wide range of physicochemical and metabolic attributes and were commonly used in patients undergoing bariatric surgery.[12] Oral drug exposure was simulated for a low, medium and high therapeutic dose in accordance with the British National Formulary, which included: simvastatin immediate release (10, 20 and 80 mg), diclofenac enteric coated (25, 50 and 75 mg),

omeprazole enteric coated (10, 20 and 40 mg), fluconazole immediate release (50, 200, 400 mg) and ciprofloxacin immediate release (250, 500 and 750 mg). Drugs simulated in post bariatric surgery population templates were compared with simulations carried out in the 'morbidly obese' population template, examining trends in oral drug bioavailability, f_a and F_G (Equation 1), and related surrogate biomarkers: $AUC_{0-24\,h}$, C_{max} and t_{max} where simulated data were processed utilising Matlab R2010a.

Results

Characterisation and validation of virtual populations

Roux-en-Y gastric bypass

Post RYGB stomach volume

A reduced gastric volume was implemented into the 'morbidly obese' population template through limiting concomitant fluid intake from the default value of 250 ml to 30 ml based on surgical restriction in accordance to Wittgrove & Clark.[37] The initial volume of stomach fluid in the fasted state was estimated to be 9.9 ml (CV 30%) utilising simulations at steady state as per Equation 6.

Gastric acid secretion and pH

Two studies were identified measuring gastric acid production in a total of 18 post RYGB patients, with an approximate gastric volume of 10 ml, as compared with pre surgery or controls.[38,39] Combining weighted means and variance displayed a mean basal gastric acid excretion of 0.08 ± 0.008 mEq/h, and a weighted mean peak acid excretion of 0.048 ± 0.048 mEq/30 min post surgery, as compared with a basal and peak acid excretion of 9.1 ± 3.6 mEq/h ($P < 0.05$) and 12.8 ± 1.8 mEq/30 min ($P < 0.05$), respectively, in pre surgery patients ($n = 8$), and a basal and peak acid secretion of 5.0 ± 0.7 ($P < 0.05$) and 12.1 ± 1.3 ($P < 0.05$), respectively, in healthy volunteers ($n = 15$)[38,39] (Figure 3). Implementation into the Simcyp Simulator 'morbidly obese' population template was based on the assumption of gastric pH of 6.4 in the fasted state.

Gastric emptying time

Following RYGB surgery a significant reduction in $t^1/_2$ gastric emptying time has been observed for liquids, whereas available data on gastric emptying of solids display a considerably increased variability (Figures 4 and 5). Four studies measuring gastric emptying time following gastrectomy surgery were identified (RYGB, sleeve gastrectomy, Billroth gastrectomy with Roux-en-Y gastrectomy and partial gastrectomy). Combining weighted means and variance in a total of 68 post surgery patients resulted in a mean $t^1/_2$ gastric emptying of 8.48 ± 9.12 min, as compared with 24.33 ± 23.71 min in controls ($n = 39$; $P < 0.05$) (Figure 4).[40–43]

Identified publications examining gastric emptying time of solids post gastric surgery resulting in a reduced gastric volume (RYGB, sleeve gastrectomy and Billroth gastrectomy with Roux-en-Y gastrectomy) displayed an observable increase in variability following surgery as compared with controls, with reported observations ranging from 4 min to over 200 min post surgery (Figure 5).[40–46]

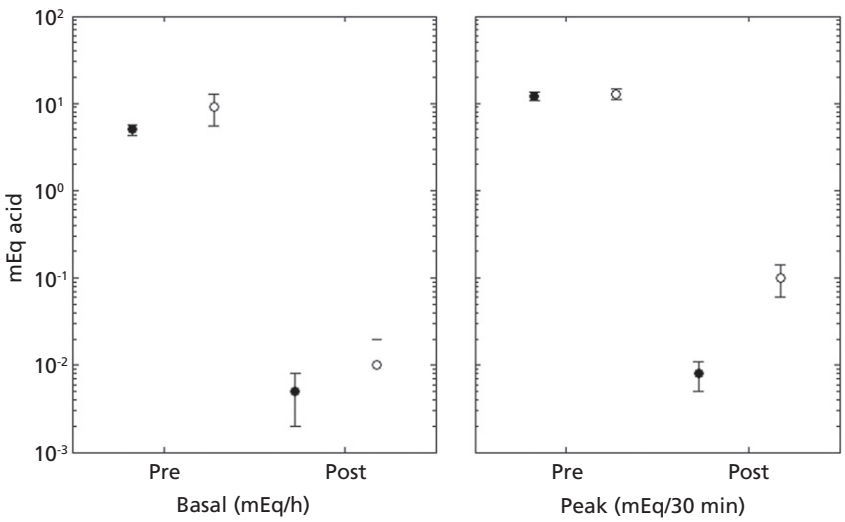

Figure 3 Acid secretion over time at basal and peak levels. Acid secretion (mean ± SD, mEq HCl) in 12 post Roux-en-Y gastric bypass patients as compared with 15 healthy volunteers not subject to surgery (●).[38] Acid secretion in eight Roux-en-Y gastric bypass patients, pre and post surgery (○).[39]

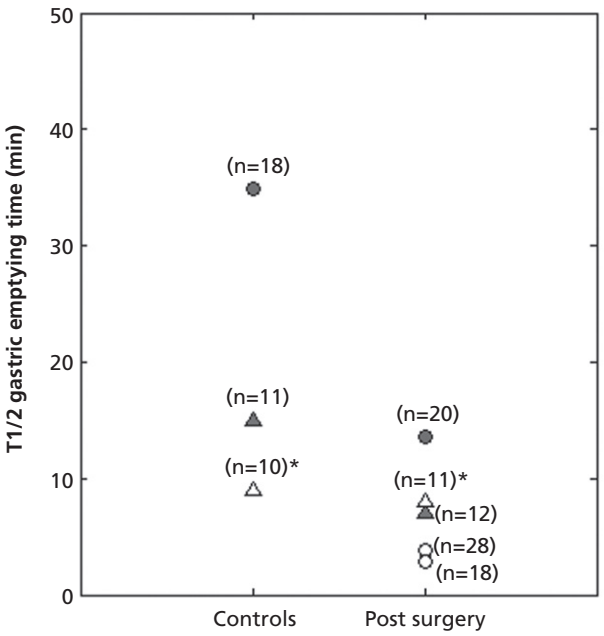

Figure 4 Reported mean (*median) $t^1/_2$ gastric emptying time of liquids in post gastric surgery patients subject to various surgeries resulting in a reduced gastric volume as compared with controls (pre surgery or healthy volunteers not subject to surgery). (●) Sleeve gastrectomy, (○) Billroth gastrectomy and Roux-en-Y gastrojejunostomy, (▲) Roux-en-Y gastric bypass and (△) Roux-en-Y gastrectomy.[40–43]

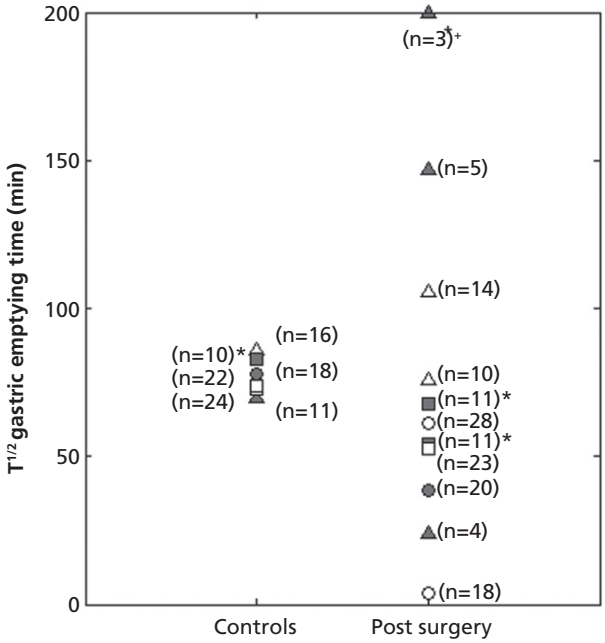

Figure 5 Reported mean (*median) $t^1/_2$ gastric emptying time of solids in post gastric surgery patients subject to various gastrointestinal surgeries, as described in publication, resulting in a reduced gastric volume as compared to controls. (●) Sleeve gastrectomy, (○) Billroth gastrectomy and Roux-en-Y gastrectomy, (▲) Roux-en-Y gastric bypass, (△) Roux-en-Y gastrectomy, (■) Roux-en-Y gastrectomy, (□) sleeve gastrectomy.[40–46]

Following RYGB, the gastric emptying half life of liquids was measured to be 7 ± 3 min after liquid intake in 12 post gastric bypass patients 12 months post surgery with a newly formed stomach pouch size of 60–80 ml and a gastrojejunal anastomosis of 12–20 mm in diameter, as compared with 11 healthy volunteers displaying a gastric emptying half life of 15 ± 2 min (Figure 5).[42]

Gastric emptying half life of a solid meal was highly variable in the post RYGB patient population, where four patients displayed a $t^1/_2$ of 24 ± 10 min, exhibiting an initial rapid gastric emptying followed by a linear emptying, whereas five patients displayed an initial lag time followed by linear emptying. Three patients displayed a prolonged lag time followed by slow gastric emptying, with a reported gastric emptying half time of over 200 min. The control group displayed a $t^1/_2$ of 70 ± 7 min (Figure 5).[42] Alteration of the gastric emptying was implemented based on post surgical gastric emptying time for liquids of 7 min (CV 45%) in the fasted state.[42]

Small intestinal bypass and regional abundance of CYP3A

Approximately 75–100 cm of the proximal small intestine is bypassed following RYGB surgery, bypassing the duodenum and proximal jejunum.[4,7,37,47–49] In accordance with the small intestinal bypass, the duodenum and proximal jejunum were bypassed through setting transit time close to zero in the duodenum and reducing small intestinal transit time in jejunum I by 38%, thus creating an approximate bypass of 87.5 cm in the ADAM model based on body surface area (Equations 7 and 8).

Small intestinal motility and transit time

Studies in humans examining small intestinal transit and motility in patients subject to total gastrectomy[50,51,52] were reviewed as compared with a partial gastrectomy in the treatment of obesity.[37]

The data suggested changes in small intestinal motility after a Roux-en-Y reconstruction.[52,53] In ten patients subject to Roux-en-Y with a total gastrectomy (cancer being the main indication), a mean small intestinal transit for solids of 293 ± 37 min was observed as compared with 187 ± 37 min in five controls ($P < 0.02$), thus suggesting the small intestinal transit to be increased post RYGB.[50] Animal models of RYGB surgery suggested a similar impact of surgery as that observed in man, with disturbed small intestinal motility reported in rat and dog.[54–56]

Two scenarios were created with regards to small intestinal transit time. In the first scenario the transit time was assumed

to be 5.0 h based on a reduced motility as reported by Pellegrini *et al*;[50] whereas, in the second scenario the small intestinal motility was assumed to remain unaltered, thus reducing small intestinal transit to 3.0 h as a function of the small intestinal bypass.

Regional abundance of CYP3A metabolising enzymes was set to close to zero in the bypassed segments of the small intestine. Mean total enzyme abundance of CYP3A4 and CYP3A5 was recalculated to account for the small intestinal bypass of the duodenum, resulting in a reduction from 66.2 to 50.2 nmol/total gut and from 24.6 to 18.7 nmol/total gut, respectively.[36]

Bile and pancreatic fluids

Following RYGB surgery, the inlet of bile and pancreatic fluids is delayed to the common channel approximately 75–150 cm distally of the newly formed stomach pouch.[37,47,48] A delayed bile inlet was implemented into the ADAM model through setting bile concentrations in the fasted and fed state to zero in the gastrointestinal regions of the stomach, duodenum and jejunum corresponding to approximately 90 cm.

Biliopancreatic diversion with duodenal switch

Stomach volume

In accordance with the surgical procedure the gastric volume following biliopancreatic diversion with duodenal switch was effectively restricted to 150 ml through limiting concomitant fluid intake with oral administration to 150 ml. Due to lack of data, gastric emptying and gastric pH was assumed to remain unaltered.[4,7,37–39,47,48]

Small intestinal bypass and regional abundance of CYP3A

Jejunum segments Jej1 and 2 were bypassed corresponding to approximately 294 cm,[37] recalculating gastrointestinal abundance of CYP3A4 and CYP3A5 accordingly to 30.0 and 11.2 nmol/total gut respectively.[36]

Small intestinal motility and transit time

In the first scenario the transit time was assumed to be 3.7 h in accordance with the reduced motility observed post total gastrectomy with Roux-en-Y jejunostomy corrected for the small intestinal length following BPD-DS.[50] In the second scenario the small intestinal motility was assumed to be 2.2 h, thus reducing as a function of the small intestinal bypass.

Bile and pancreatic fluids

In accordance with the surgical procedure the bile inlet was delayed to ileum III corresponding to 252 cm.[4,7,37]

Sleeve gastrectomy

Stomach volume

Sleeve gastrectomy surgery is limited to restriction of the dimension of the gastric pouch (to approx. 60–80 ml), preserving the pyloric sphincter.[8,57] Although not as invasive as malabsorptive procedures, the reduction in gastric volume has been reported to affect the gastric emptying time of liquids and solids (Figures 4 and 5).[40,44] This was implemented through setting concomitant fluid intake to 80 ml and initial volume of stomach fluid to 24.2 ml (CV: 30%) in the fasted state in accordance with simulated steady state gastric volumes.

Gastric emptying time

One study was identified examining gastric emptying of liquids following sleeve gastrectomy, observing a significantly reduced $t^1/_2$ gastric emptying time of 13.6 ± 11.9 min in 20 post surgery patients as compared with 34. ± 24.6 min in 18 controls (Figure 4).[40] Thus, gastric emptying was set to 13.6 (CV: 53%) in the post sleeve gastrectomy population template.

Results from combining weighted means and variance of identified studies examining gastric emptying of solids resulted in a significant reduction postoperatively ($P < 0.05$), with an observed mean gastric emptying time of 46.1 ±17.7 min in 43 post surgery patients as compared with 74.6 ± 26.2 min in 64 controls (Figure 5).[40, 44]

Gastric acid secretion and pH

There is a lack of published data on the impact of sleeve gastrectomy on gastric acid secretion or gastric pH measurements pre to post surgery. Given this, gastric pH was assumed to remain unaltered following sleeve gastrectomy.

Jejunoileal bypass

Small intestinal bypass and regional abundance of CYP3A

In accordance with the surgical procedure a small intestinal bypass was created retaining the duodenum segment, approximately 20% of the proximal jejunum I and 23% of the terminal ileum IV, bypassing the remainder of the small intestine.[10,58,59] Accordingly, the abundance of CYP3A4 and CYP3A5 was set to zero in jejunum II to ileum III and recalculated to 32.3 and 12.1 nmol/total gut, respectively.

Small intestinal motility and transit time

In the first scenario the transit time was assumed to be 0.7 h in accordance with the reduced motility observed post total gastrectomy with Roux-en-Y jejunostomy corrected for the small intestinal length post jejunoileal bypass.[50] In the second scenario the small intestinal motility was assumed to be 0.4 h, thus reducing as a function of the small intestinal bypass.

Bariatric surgery: whole-body physiological parameters

Renal function

Comparing observed data on renal function, in terms of glomerular filtration rate (GFR), in relation to body mass index (BMI) following bariatric surgery induced weight loss, estimates made utilising Cockcroft-Gault and modification of diet in renal disease (MDRD; Equation 10) equations, concluded a better prediction by the MDRD equation.[60–63] The Cockcroft-Gault equation estimates the creatinine clearance, while the MDRD equation estimates the GFR corrected for body surface area.[64] Simulating age and sex matched populations over a range of BMI, utilising the Simcyp Simulator incorporating inter-individual variability, observed data was within 95% confidence interval of simulated estimations utilising the MDRD equation, whereas, the Cockcroft-Gault equation over-predicted GFR at a higher BMI in agreement with previous publications examining predicted versus observed GFR in 'morbidly obese' and 'obese' populations.[33,63] Based on these findings the MDRD equation was utilised to estimate GFR in the Simcyp Simulator (Figure 6).

$$GFR\left(mL/\min/1.73m^2\right) = 186 \cdot Serum\ creatinine\left(mg/dL\right)^{-1.154} \cdot age^{-0.203} \cdot (0.742\ for\ females) \quad (10)$$

Serum protein levels

Prior to and following bariatric surgery induced weight loss, human serum albumin levels remained consistent with the normal reported range (at a total of 322 data points; $n = 163$) evaluated utilising sex- and age-matched simulations in the Simcyp Simulator, predicting human serum albumin within the 95% confidence interval (Figure 7).[65–68] Levels of α-1 acid glycoprotein were significantly reduced following bariatric surgery induced weight loss (at a total of 170 data points; $n = 50$), regressing towards ranges observed in normal weight controls, where simulations in the Simcyp Simulator overestimated the levels of α-1 acid glycoprotein at lower BMI ranges (Figure 8).[65,69]

Hepatic function

The reduction in liver volume following bariatric surgery induced weight loss was assumed to be a function of the reduction in body surface area as observed in a general population,[70] where the equation incorporated into the Simcyp Simulator corrects for the observed under-prediction in liver volume at a BMI $\geq$ 40 kg/m^2 utilising a correction factor of 1.25.[33] Tissue blood perfusions were obtained as a function of cardiac output estimated from body surface area as incorporated into the Simcyp Simulator. A summary of altered physiological parameters are provided in Table 2.[71]

Virtual studies

Roux-en-Y gastric bypass

Simulated simvastatin immediate release 10 mg oral drug exposure post RYGB (small intestinal transit time 3.0 h) displayed an unaltered oral bioavailability with a mean post/pre surgery AUC ratio of 1.14 $\pm$ 0.18 due to a mean increase in F_G from 0.24 $\pm$ 0.10 to 0.27 $\pm$ 0.11 counteracted by a reduction

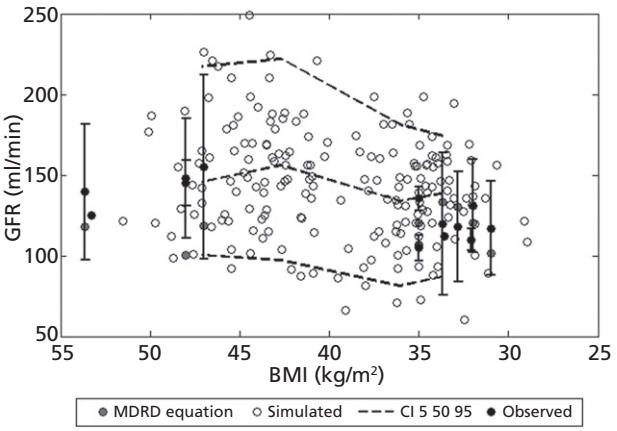

Figure 6 Observed glomerular filtration rate (GFR) following bariatric surgery induced weight loss as compared with calculated GFR utilising the modification of diet in renal disease (MDRD) equation and simulated age- and gender-matched GFR with 5, 50 95% confidence intervals (CI) utilising the Simcyp Simulator (MDRD) with inter-individual variability. BMI, body mass index.[60–63]

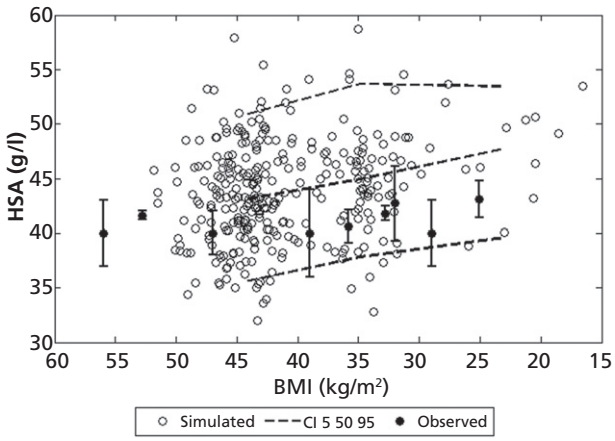

Figure 7 Observed serum concentrations human serum albumin (HSA) in morbidly obese patients subject to bariatric surgery induced weight loss as compared with simulated HSA levels with 5, 50 95% confidence intervals (CI) based on Simcyp demographics characteristics. BMI, body mass index.[65–68]

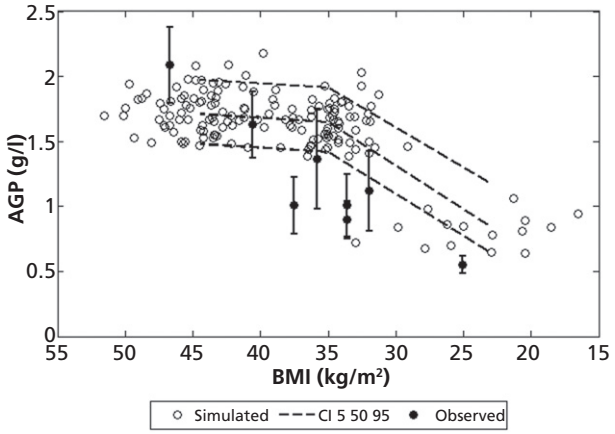

Figure 8 Observed serum concentrations (mean ± SD) of α-1 acid glycoprotein (AGP) in morbidly obese patients subject to bariatric surgery induced weight loss as compared with simulated AGP levels with 5, 50 95% confidence intervals (CI) based on Simcyp Simulator demographics characteristics. BMI, body mass index.[65,69]

in f_a from 0.90 ± 0.11 to 0.87 ± 0.12 (Figure 9). At a high therapeutic dose (80 mg) the mean post/pre surgery ratio became less apparent (1.07 ± 0.19) due to a more apparent reduction in f_a from 0.88 ± 0.12 to 0.82 ± 0.14 (Figure 10). Assuming a reduction in small intestinal motility post RYGB (small intestinal transit time 5.0 h) simvastatin displayed a mean ratio of 1.22 ± 0.19 to 1.17 ± 0.20 over the therapeutic dose range due to reduced postoperative impact on f_a. This was apparent over the whole range of studied drugs, where the increased small intestinal transit time positively influenced f_a (data not shown).

Oral drug exposure of omeprazole remained unaltered following RYGB (small intestinal transit time 3.0 h), although displaying a reduction in t_{max} from approximately 1.24 ± 0.41 to 0.97 ± 0.23 h over the therapeutic dose range. Diclofenac post/pre surgery AUC ratio displayed a minor reduction following RYGB (small intestinal transit time 3.0 h). This became more apparent at a high therapeutic dose, displaying an AUC ratio of 0.99 ± 0.14, due to a reduction in f_a from 0.88 ± 0.13 to 0.84 ± 0.13, counteracted by a minor increase in F_G from 0.95 ± 0.04 to 0.96 ± 0.03; whereas t_{max} displayed a reduction from 1.44 ± 0.54 to 1.28 ± 0.51 h. Ciprofloxacin displayed a minor reduction in AUC post RYGB (small intestinal transit time 3.0 h), displaying a ratio of 0.96 ± 0.02 over the therapeutic dose range due to a reduction in f_a from 0.77 ± 0.15 to 0.74 ± 0.15. Fluconazole remained unaltered over the dose range.

Biliopancreatic diversion with duodenal switch

Following BPD-DS (small intestinal transit time 2.2 h), simvastatin displayed a reduction in AUC, with an observed post/pre surgical AUC ratio ranging from 0.89 ± 0.15 to

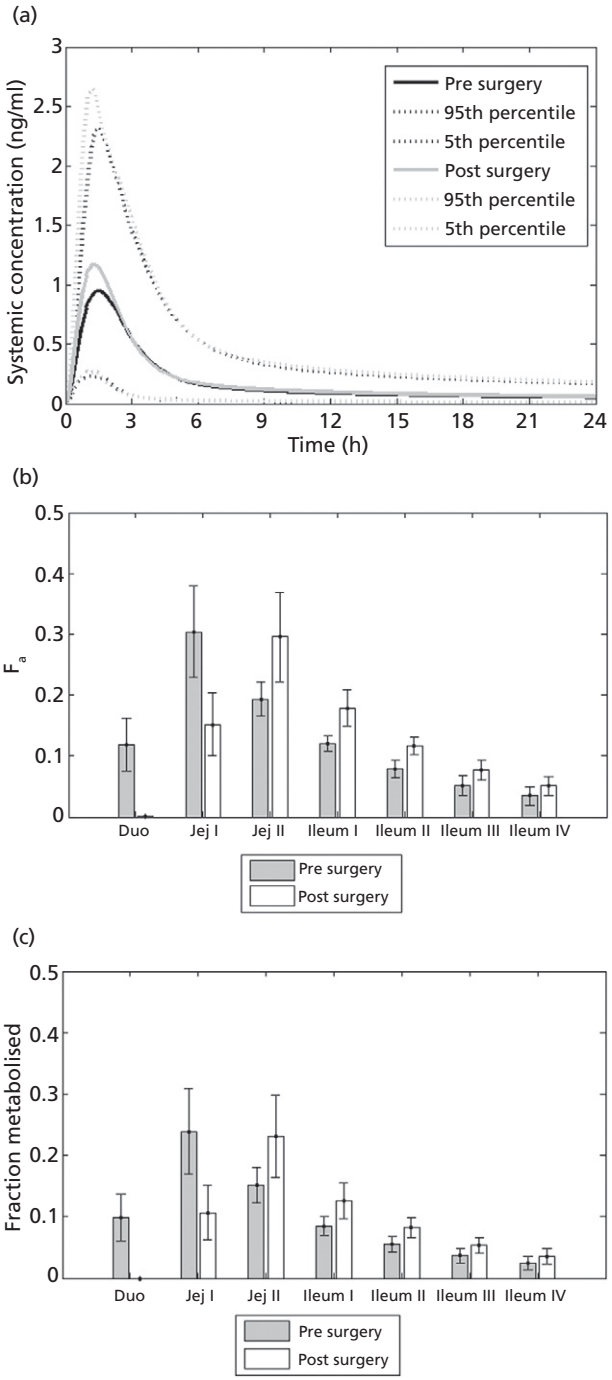

Figure 9 Simulated simvastatin immediate release 10 mg (low therapeutic dose) in morbidly obese (n = 100) and post Roux-en-Y gastric bypass surgery (n = 100; small intestinal transit = 3.0 h). (a) Mean, 95th and 5th percentile plasma concentration time profile over 24 h. (b) Mean ± SD of segmental fraction of dose absorbed along the small intestine (f_a). (c) Mean ± SD of segmental fraction of dose metabolised in the gut wall ($1 - F_G$). Duo, duodenum; Jej, jejunum.

Table 2 Summary of physiological parameter alterations following bariatric surgery for input into the Simcyp Simulator

Physiological parameters	RYGB	BPD-DS	JIB	SG	References
Population alterations					
Stomach					
Gastric emptying time (min)	7 (CV 45%)	Unaltered	Unaltered	13.6 (CV 53%)	[40,42]
Initial fluid volume (ml)	9.9 (CV 30%)	Unaltered	Unaltered	24.2 (CV 30%)	
Gastric pH	6.4 (CV 38%)	1.5 (CV 38%)	1.5 (CV 38%)	1.5 (CV 38%)	[38,39]
Small intestine					
Bypass (segments)	Duo, jej I[b]	Jej I, jej II	Jej II-IL III	Unaltered	[4,7,8,37,47–49,57–59]
Bile delay (segments)	Duo-jej II	Duo-il II		Unaltered	
SIT: scenario 1 (h)	3.0	2.2	0.4	3.3	
Weibull β[a]	3.6	2.6	0.5	4.0	
SIT: scenario 2 (h)	5.0	3.7	0.7	–	
Weibull β[a]	6.0	4.4	0.8	–	
GI metabolism					
CYP3A bypass (segments)	Duo, jej I[b]	Jej I, jej II	Jej II-IL III	Unaltered	[4,7,8,14,37,47–49,57–59]
CYP3A4 abundance (nmol/total gut)	50.2 (CV 60%)	30.0 (CV 60%)	32.3 (CV 60%)	66.2 (CV 60%)	
CYP3A5 abundance (nmol/total gut)	18.7 (CV 60%)	11.2 (CV 60%)	12.1 (CV 60%)	24.2 (CV 60%)	
Whole-body physiological alterations					
GFR prediction	MDRD	MDRD	MDRD	MDRD	[60–63]
Study design alterations					
Concomitant fluid intake with administered dose (ml)	30 (CV 60%)	150 (CV 60%)	250 (CV 60%)	80 (CV 60%)	[4,7,8,14,37,47–49,57–59]

BPD-DS, biliopancreatic diversion with duodenal switch; duo, duodenum; GFR, glomerular filtration rate; GI, gastrointestinal; IL, ileum; jej, jejunum; JIB, jejunoileal bypass; MDRD, modification of diet in renal disease equation; RYGB, Roux-en-Y gastric bypass; SG, sleeve gastrectomy; SIT, small intestinal transit. [a]Weibull distribution function ($\alpha = 2.92$; Equation 9). [b]Partial small intestinal bypass.

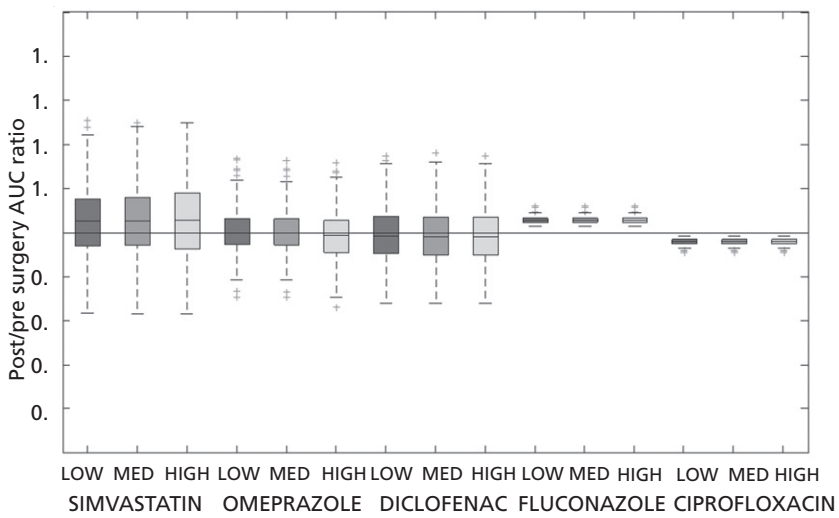

Figure 10 Simulated post/pre Roux-en-Y gastric bypass surgery (small intestinal transit = 3.0 h) AUC ratio over a range of selected drugs at a low, medium (MED) and high therapeutic dose: simvastatin immediate release (10, 20 and 80 mg), omeprazole enteric coated (10, 20 and 40 mg), diclofenac enteric coated (25, 50 75 mg), fluconazole immediate release (50, 200, 400 mg) and ciprofloxacin immediate release (250, 500 and 750 mg).

0.65 ± 0.22 as a result of a more extensive reduction in f_a as compared with following RYGB; assuming a higher small intestinal transit time of 3.7 h, simvastatin displayed an increase in AUC, displaying a ratio of 1.05 ± 0.08 at a low therapeutic dose level ranging to a reduction with a simulated ratio of 0.83 ± 0.22 at the highest therapeutic dose. This was observed for the whole range of simulated drugs.

Omeprazole displayed a post/pre BPD-DS AUC ratio of 0.88 ± 0.10 at a low therapeutic dose due to a reduction in f_a from 0.94 ± 0.09 to 0.83 ± 0.14 (Figure 11), whereas a minor increase in F_G was observed from 0.96 ± 0.02 to 0.97 ± 0.02. T_{max} displayed an increase from 1.22 ± 0.38 to 1.50 ± 0.54 h, whereas C_{max} displayed a reduction by approximately 19%. At a high therapeutic dose, omeprazole

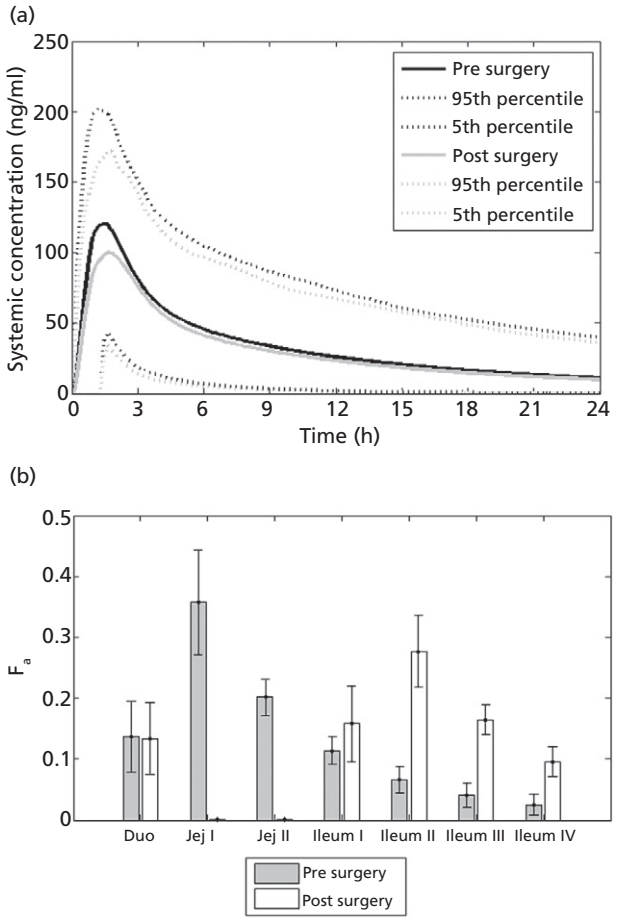

Figure 11 Simulated omeprazole enteric coated 10 mg (low therapeutic dose) in morbidly obese (n = 100) and post biliopancreatic diversion with duodenal switch (n = 100; small intestinal transit = 2.2 h). (a) Mean, 95th and 5th percentile plasma concentration time profile over 24 h. (b) Mean ± SD of segmental fraction of dose absorbed along the small intestine (f_a). Duo, duodenum; Jej, jejunum.

displayed a post/pre surgery AUC ratio of 0.77 ± 0.15, due to a more extensive reduction in f_a, whereas t_{max} was increased from 1.42 ± 0.50 to 2.26 ± 0.63 h. The reduction became less apparent assuming a small intestinal transit time of 3.7 h.

Diclofenac displayed an AUC ratio of 0.87 ± 0.09 following BPD-DS (small intestinal transit time 2.2 h) at a low therapeutic dose due to a reduction in f_a from 0.89 ± 0.12 to 0.75 ± 0.15, whereas F_G displayed an increase from 0.91 ± 0.06 to 0.94 ± 0.04. At a high therapeutic dose, diclofenac displayed a more apparent reduction due to a higher post surgical impact on f_a. Again the reduction was less apparent assuming a small intestinal transit time of 3.7 h.

Fluconazole displayed an AUC ratio of approximately 0.95 ± 0.05 over the dose range. Ciproflocaxin displayed an AUC ratio of 0.80 ± 0.06 following BPD-DS (small intestinal transit time 2.2 h) at a low therapeutic dose, reflected by a reduction in f_a. Following BPD-DS (small intestinal transit time 3.7 h), Ciprofloxacin displayed no significant alteration, with an AUC ratio of 1.01 ± 0.01 at a low therapeutic dose ranging to 0.98 ± 0.01 at a high therapeutic dose (Figure 12).

Jejunoileal bypass

Following jejunoileal bypass the whole range of studied drugs displayed an extensive reduction in AUC due to a more apparent reduction in f_a as compared with RYGB and BPD-DS where fluconazole displayed the least apparent reduction, with a post/pre surgery AUC ratio of 0.47 ± 0.12 at a low therapeutic dose, whereas an AUC ratio of 0.44 ± 0.13 was displayed at a high dose level due to a more extensive reduction in f_a from 0.97 ± 0.07 to 0.45 ± 0.13 (Figures 13 and 14).

Sleeve gastrectomy

Simulated post sleeve gastrectomy applied to the 'morbidly obese' population did not significantly alter the pre to post surgery drug exposure for the range of studied drugs over low to high therapeutic dose ranges (data not shown).

Discussion

Simulating oral drug exposure following bariatric surgery

Simulating oral drug bioavailability following bariatric surgery identified a number of potential pharmacokinetic parameters suggested to influence bioavailability following bariatric surgery.

Simvastatin is characterised as a BCS class IV drug, and further classified as a Biopharmaceutics Drug Disposition Classification System (BDDCS) class II compound.[26,72] The drug is considered a low soluble compound at the therapeutic dose, displaying an aqueous solubility 0.03 mg/ml.[73,74] The drug is administered in its lactone form and undergoes pH- and temperature-dependent interconversion to its hydroxyacid form at a pH below 6, whereas the lactone form is mainly formed at pH values over the equilibrium.[75] Approximately 85% of the administered dose is absorbed, being further exposed to extensive metabolism by CYP3A4 in the small intestine and liver, and CYP3A5 to lesser extent.[76,77]

The simulated increase in drug exposure of simvastatin in the post RYGB (small intestinal transit time 3.0 h) population was due to an increase in F_G post surgery. These findings suggest intestinal gut wall metabolism plays an important role in the observed trend in drug bioavailability pre to post surgery for compounds subject to a high small intestinal metabolic extraction ratio, such as atorvastatin and simvastatin, where the simulated post/pre surgical AUC ratio following RYGB was similar to that observed for atorvastatin, displaying a median AUC ratio of 1.20 (0.3–2.3).[49] Simulated

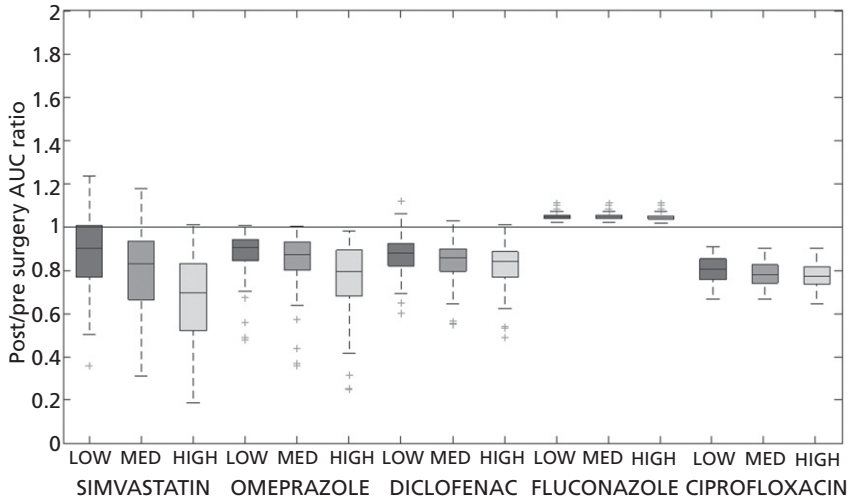

Figure 12 Simulated post/pre biliopancreatic diversion with duodenal switch (small intestinal transit = 2.2 h) AUC ratio over a range of selected drugs at a low, medium (MED) and high therapeutic dose: simvastatin immediate release (10, 20 and 80 mg), omeprazole enteric coated (10, 20 and 40 mg), diclofenac enteric coated (25, 50 75 mg), fluconazole immediate release (50, 200, 400 mg) and ciprofloxacin immediate release (250, 500 and 750 mg).

compound characteristics of simvastatin did not incorporate the pH-dependent interconversion of the lactone and acid form,[75] but treated this as a part of the CYP3A4 clearance term through fitting to observed data, thus not taking into account the increased gastric pH following RYGB surgery and its impact on the interconversion.

Omeprazole (BCS class II and BDDCS class I ampholyte, pKa = 8.7, pKb = 3.79) is a sparingly soluble highly lipophilic compound with stability issues at a lower pH levels, thus motivating the enteric coated formulation to protect the drug from degradation caused by the gastric pH.[26,72,78,79] The drug displays a highly variable absorption and further mainly undergoes hepatic metabolism and clearance by CYP3A4 and 2C19.[80] Only a minor alteration in F_G was observed following simulations post BPD-DS, where an overall increase was observed. The biggest impact was observed on f_a, potentially due to the reduction in absorption area.

Diclofenac (BCS class II, BDDCS class I) is mainly metabolised by CYP2C9.[26,71,79] The drug undergoes extensive first-pass metabolism, displaying an oral bioavailability of approximately 54%.[80,81] Following RYGB and BPD-DS, a minor increase in F_G was observed due to the bypass of intestinal regions abundance of CYP2C9, however this was counteracted by a reduction in f_a.

Fluconazole (BCS class I, BDDCS class III) is soluble at the therapeutic dose and displays a bioavailability of over 90% in healthy volunteers, and further is mainly renally cleared.[26,72,82] Following bariatric surgery simulated oral drug exposure of fluconazole only displayed minor changes in AUC, with the exception following jejunoileal bypass. These results are consistent with observations in AIDS patients, frequently displaying gastrointestinal disturbances, and a case report in a patient subject to gastrointestinal restriction of the gastric antrum, duodenum and ileum following peptic ulcer disease, displaying no altered bioavailability or a comparable bioavailability as compared with healthy volunteers.[83,84]

Ciprofloxacin (BCS class III, BDDCS class IV) is sparingly soluble at the therapeutic dose range, further having a reported oral bioavailability ranging from approximately 60% to 80% in healthy volunteers, and is mainly renally cleared.[26,72,85,86] The simulated reduction in AUC following bariatric surgery is therefore most likely an effect of a reduction in absorption area and a product of postoperative solubility issues.

The major issue following sleeve gastrectomy would be potential solubility issues due to a reduced concomitant fluid volume with the administered dose, although this was not a major issue for any of the studied drugs.

Post bariatric surgery ADAM model limitations

Conclusions drawn from this study are limited by a number of 'known unknowns' relating to gastrointestinal physiology post bariatric surgery, where data relating to gastrointestinal pH, small intestinal transit and post surgical gastrointestinal physiological adaptation and whole-body physiological alterations, such as hepatic activity and bile secretion and its GI levels, is sparse or nonexistent.

Following RYGB, gastric pH was estimated to increase based on measuring acid secretion in the gastric pouch (mEq/time). However, examining the relationship between pH and gastric acid output is not straightforward. Pratha

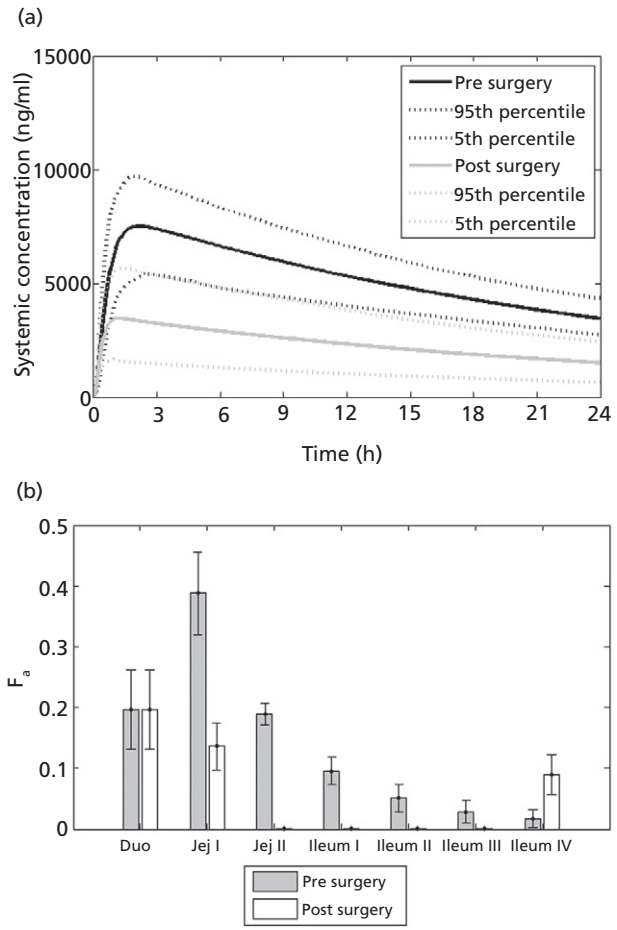

Figure 13 Simulated fluconazole immediate release 400 mg (high therapeutic dose) in morbidly obese (n = 100) and post jejunolieal bypass (n = 100; small intestinal transit = 0.4 h). (a) Mean, 95th and 5th percentile plasma concentration time profile over 24 h. (b) Mean ± SD of segmental fraction of dose absorbed along the small intestine (f_a). Duo, duodenum; Jej, jejunum.

et al.[87] examined the effect of proton pump inhibitors on gastric acid output and pH and concluded the relationship between pH and gastric acid output to be highly ambiguous. At a gastric acid output of ≤1 mEq/30 min a pH of 0.9–7.7 was observed, whereas a pH of 2.5 and upwards was rendered at minimal gastric acid output,[87] thus rendering a high degree of uncertainty in the implications of mEq/time post RYGB.

Small intestinal transit time estimation following bariatric surgery was limited to one study examining small intestinal transit time of solids in 10 patients subject to total gastrectomy with Roux-en-Y reconstruction[50] or estimations based on the extent of small intestinal bypass. As the procedure differs in terms of the extent of gastrectomy as compared with RYGB for the treatment of obesity, such an assumption may not necessarily hold true.

Following gastric restrictive surgery (RYGB and sleeve gastrectomy), gastric emptying of liquid displayed an overall significant reduction, whereas gastric emptying of solids displayed an increase in variability following RYGB. The impact of RYGB surgery on gastric emptying of solids may be due to a postsurgical state of stasis due to a reduced nervous stimulus.[42,54]

The methodology of how the ADAM model was adapted to mimic post bariatric surgery conditions is subject to a number of limitations due to the limited nature of how the ADAM model could be adjusted through the Simcyp Simulator through the existing interface. Rather than bypassing the proximal small intestinal compartments, the transit times through these compartments were reduced to close to zero. As a consequence the modelling and simulations of drug concentration in the bilio limb could not be conducted, thus limiting the predictability of drugs subject to biliary elimination. A further concern was the fluid dynamics within the ADAM model which is governed by secretion and reabsorption of GI fluids taking place throughout the GI compartments.[14,35] As a result of such parameter alterations not being possible through the Simcyp user interface, an overestimation of GI fluid volumes and consequential underestimation of potential drug specific solubility issues following surgery are possible.

Conclusions

Trends in pre and post RYGB bioavailability seem to be highly dependent on drug-specific parameters such as affinity to CYP3A4, solubility and permeability issues based on simulated outcomes, although this has yet to be confirmed with regards to clinical data. A mechanistic modelling approach has the potential of examining the impact of drug-specific parameters on trends pre to post surgery and to serve as a useful tool in examining the impact of physiological alterations on oral drug bioavailability in the absence of clinical data.

Current limitations in estimating and simulating the impact of oral drug bioavailability following bariatric surgery include the sparsity of clinical data for further model validation and the lack of data on resultant physiological changes post surgery.

Declarations

Conflict of interest

Amin Rostami, Devendra Pade and Masoud Jamei are employees and/or shareholders in Simcyp Limited.

Funding

This research received no specific grant from any funding agency in the public, commercial or not-for-profit sectors.

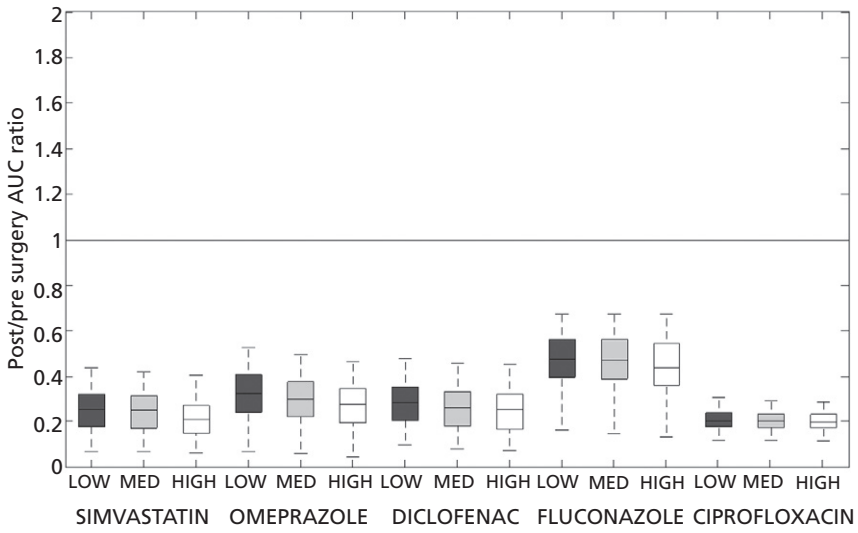

Figure 14 Simulated post/pre jejunoileal bypass (small intestinal transit = 0.4 h) AUC ratio over a range of selected drugs at a low, medium (MED) and high therapeutic dose: simvastatin immediate release (10, 20 and 80 mg), omeprazole enteric coated (10, 20 and 40 mg), diclofenac enteric coated (25, 50 75 mg), fluconazole immediate release (50, 200, 400 mg) and ciprofloxacin immediate release (250, 500 and 750 mg).

Acknowledgements

The authors wish to thank the bariatric surgery team at Salford Royal Hospital NHS Foundation Trust for discussions on bariatric surgical dimensions and Dr David Turner (Simcyp Limited) and Mr James Kay (Simcyp Limited) for assistance with the preparation of the manuscript.

References

1. Flegal KM *et al*. Prevalence and trends in obesity among US adults, 1999–2008. *JAMA* 2010; 303: 235–241.
2. Organisation for Economic Co-operation and Development *Obesity and the Economics of Prevention: Fit Not Fat – United Kingdom (England) Key Facts*. Paris: Organisation for Economic Co-operation and Development, 2011. http://www.oecd.org/document/58/0,3746,en_2649_33929_46039034_1_1_1_1,00.html#Further_Reading (accessed January 17 2012).
3. Ammori BJ. *Laparoscopic Sleeve Gastrectomy*. Manchester: Laparoscopic Obesity Surgery Experts, 2012. http://www.obesitysurgeryexperts.co.uk/Laparoscopic_Sleeve_Gastrectomy_Manchester#top (accessed April 2 2012).
4. Elder KA, Wolfe BM. Bariatric surgery: a review of procedures and outcomes. *Gastroenterology* 2007; 132: 2253–2271.
5. Buchwald H, Oien DM. Metabolic/bariatric surgery worldwide 2008. *Obes Surg* 2009; 19: 1605–1611.
6. Picot J *et al*. The clinical effectiveness and cost effectiveness of bariatric (weight loss) surgery for obesity: a systematic review and economic evaluation. *Health Technol Assess* 2009; 13: 23–77.
7. Schneider BE, Mun EC. Surgical management of morbid obesity. *Diabetes Care* 2005; 28: 475–480.
8. Lee CM *et al*. Vertical gastrectomy for morbid obesity in 216 patients: report of two-year results. *Surg Endosc* 2007; 21: 1810–1816.
9. National Institute of Diabetes and Digestive and Kidney Diseases. *Bariatric Surgery for Severe Obesity*. Bethesda, MD: National Institutes of Health, 2010: http://win.niddk.nih.gov/publications/gastric.htm#rygastric (accessed November 9 2012).
10. Griffen WO Jr *et al*. A prospective comparison of gastric and jejunoileal bypass procedures for morbid obesity. *Ann Surg* 1977; 186: 500–509.
11. Singh D *et al*. Jejunoileal bypass: a surgery of the past and a review of its complications. *World J Gastroenterol* 2009; 15: 2277–2279.
12. Darwich AS *et al*. Trends in oral drug bioavailability following bariatric surgery: examining the variable extent of impact on exposure of different drug classes. *Br J Clin Pharmacol* 2012. [Epub ahead of print]
13. Rowland M, Tozer TN. *Clinical Pharmacokinetics: Concepts and Applications*, 2nd edn. Philadelphia: Lea & Febiger, 1989.
14. Jamei M *et al*. Population-based mechanistic prediction of oral drug absorption. *AAPS J* 2009; 11: 225–237.
15. Higaki K *et al*. Mechanistic understanding of time-dependent oral absorption based on gastric motor activity in humans. *Eur J Pharm Biopharm* 2008; 70: 313–325.

16. Blum RA *et al.* Increased gastric pH and the bioavailability of fluconazole and ketoconazole. *Ann Intern Med* 1991; 114: 755–757.
17. Avdeef A. Solubility of sparingly-soluble ionizable drugs. *Adv Drug Deliv Rev* 2007; 59: 568–590.
18. Koch KM *et al.* Effect of sodium acid pyrophosphate on ranitidine bioavailability and gastrointestinal transit time. *Pharm Res* 1993; 10: 1027–1030.
19. Kolars JC *et al.* CYP3A gene expression in human gut epithelium. *Pharmacogenetics* 1994; 4: 247–259.
20. Peters WH *et al.* Human intestinal glutathione S-transferases. *Biochem J* 1989; 257: 471–476.
21. Fisher MB *et al.* The role of hepatic and extrahepatic UDP-glucuronosyltransferases in human drug metabolism. *Drug Metab Rev* 2001; 33: 273–297.
22. Paine MF *et al.* The human intestinal cytochrome P450 'pie'. *Drug Metab Dispos* 2006; 34: 880–886.
23. Riches Z *et al.* Quantitative evaluation of the expression and activity of five major sulfotransferases (SULTs) in human tissues: the SULT 'pie'. *Drug Metab Dispos* 2009; 37: 2255–2261.
24. Paine MF *et al.* Characterization of interintestinal and intraintestinal variations in human CYP3A-dependent metabolism. *J Pharmacol Exp Ther* 1997; 283: 1552–1562.
25. Benet LZ, Cummins CL. The drug efflux-metabolism alliance: biochemical aspects. *Adv Drug Deliv Rev* 2001; 50(Suppl.): 1S3–111.
26. Darwich AS *et al.* Interplay of metabolism and transport in determining oral drug absorption and gut wall metabolism: a simulation assessment using the 'advanced dissolution, absorption, metabolism (ADAM)' model. *Curr Drug Metab* 2010; 11: 716–729.
27. Fromm MF *et al.* The effect of rifampin treatment on intestinal expression of human MRP transporters. *Am J Pathol* 2000; 157: 1575–1580.
28. Maliepaard M *et al.* Subcellular localization and distribution of the breast cancer resistance protein transporter in normal human tissues. *Cancer Res* 2001; 61: 3458–3464.
29. Mouly S, Paine MF. P-glycoprotein increases from proximal to distal regions of human small intestine. *Pharm Res* 2003; 20: 1595–1599.
30. Jamei M *et al.* The Simcyp population-based ADME simulator. *Expert Opin Drug Metab Toxicol* 2009; 5: 211–223.
31. Huang W *et al.* Mechanistic approaches to predicting oral drug absorption. *AAPS J* 2009; 11: 217–224.
32. Agoram B *et al.* Predicting the impact of physiological and biochemical processes on oral drug bioavailability. *Adv Drug Deliv Rev* 2001; 50(Suppl. 1): S41–S67.
33. Ghobadi C *et al.* Application of a systems approach to the bottom-up assessment of pharmacokinetics in obese patients: expected variations in clearance. *Clin Pharmacokinet* 2011; 50: 809–822.
34. Delgado-Aros S *et al.* Independent influences of body mass and gastric volumes on satiation in humans. *Gastroenterology* 2004; 126: 432–440.
35. Valentin J. *Basic Anatomical and Physiological Data for Use in Radiological Protection: Reference Values*. ICRP Publication, 89, Oxford: International Commission on Radiological Protection, Pergamon, 2002.
36. Turner D. *Simcyp User Manual Version 8*, 8 edn. Sheffield: Simcyp Limited, 2008.
37. Wittgrove AC, Clark GW. Laparoscopic gastric bypass, Roux-en-Y- 500 patients: technique and results, with 3–60 month follow-up. *Obes Surg* 2000; 10: 233–239.
38. Smith CD *et al.* Gastric acid secretion and vitamin B12 absorption after vertical Roux-en-Y gastric bypass for morbid obesity. *Ann Surg* 1993; 218: 91–96.
39. Behrns KE *et al.* Prospective evaluation of gastric acid secretion and cobalamin absorption following gastric bypass for clinically severe obesity. *Dig Dis Sci* 1994; 39: 315–320.
40. Braghetto I *et al.* Scintigraphic evaluation of gastric emptying in obese patients submitted to sleeve gastrectomy compared to normal subjects. *Obes Surg* 2009; 19: 1515–1521.
41. Hinder RA *et al.* Management of gastric emptying disorders following the Roux-en-Y procedure. *Surgery* 1988; 104: 765–772.
42. Horowitz M *et al.* Measurement of gastric emptying after gastric bypass surgery using radionuclides. *Br J Surg* 1982; 69: 655–657.
43. Rieu PN *et al.* Gastric emptying after partial gastrectomy without vagotomy with primary Roux-en-Y or Billroth II anastomosis. *Nucl Med Commun* 1989; 10: 715–722.
44. Shah S *et al.* Prospective controlled study of effect of laparoscopic sleeve gastrectomy on small bowel transit time and gastric emptying half-time in morbidly obese patients with type 2 diabetes mellitus. *Surg Obes Relat Dis* 2010; 6: 152–157.
45. Petrakis J *et al.* Enhancement of gastric emptying of solids by erythromycin in patients with Roux-en-Y gastrojejunostomy. *Arch Surg* 1998; 133: 709–714.
46. Bernstine H *et al.* Gastric emptying is not affected by sleeve gastrectomy – scintigraphic evaluation of gastric emptying after sleeve gastrectomy without removal of the gastric antrum. *Obes Surg* 2009; 19: 293–298.
47. Spak E *et al.* Changes in the mucosa of the Roux-limb after gastric bypass surgery. *Histopathology* 2010; 57: 680–688.
48. Demaria EJ *et al.* Results of 281 consecutive total laparoscopic Roux-en-Y gastric bypasses to treat morbid obesity. *Ann Surg* 2002; 235: 640–645. discussion 645–647.
49. Skottheim IB *et al.* Significantly altered systemic exposure to atorvastatin acid following gastric bypass surgery in morbidly obese patients. *Clin Pharmacol Ther* 2009; 86: 311–318.
50. Pellegrini CA *et al.* Intestinal transit of food after total gastrectomy and Roux-Y esophagojejunostomy. *Am J Surg* 1986; 151: 117–125.
51. Haglund U *et al.* Esophageal and jejunal motor function after total gastrectomy and Roux-Y esophagojejunostomy. *Am J Surg* 1989; 157: 308–311.
52. Le Blanc-Louvry I *et al.* Roux-en-Y limb motility after total or distal gastrectomy in symptomatic and asymptomatic patients. *J Am Coll Surg* 2000; 190: 408–417.

53. Van Der Mijle HC *et al*. Manometric and scintigraphic studies of the relation between motility disturbances in the Roux limb and the Roux-en-Y syndrome. *Am J Surg* 1993; 166: 11–17.
54. Woodward A *et al*. Gastric stasis of solids after Roux gastrectomy: is the jejunal transection important? *J Surg Res* 1993; 55: 317–322.
55. Le Blanc-Louvry I *et al*. Motility in the Roux-Y limb after distal gastrectomy: relation to the length of the limb and the afferent duodenojejunal segment – an experimental study. *Neurogastroenterol Motil* 1999; 11: 365–374.
56. Suzuki S *et al*. Changes in GI hormones and their effect on gastric emptying and transit times after Roux-en-Y gastric bypass in rat model. *Surgery* 2005; 138: 283–290.
57. Baltasar A *et al*. Laparoscopic sleeve gastrectomy: a multi-purpose bariatric operation. *Obes Surg* 2005; 15: 1124–1128.
58. Scott HW Jr *et al*. Considerations in use of jejunoileal bypass in patients with morbid obesity. *Ann Surg* 1973; 177: 723–735.
59. Scott HW Jr *et al*. Experience with a new technic of intestinal bypass in the treatment of morbid obesity. *Ann Surg* 1971; 174: 560–572.
60. Saliba J *et al*. Roux-en-Y gastric bypass reverses renal glomerular but not tubular abnormalities in excessively obese diabetics. *Surgery* 2010; 147: 282–287.
61. Chagnac A *et al*. The effects of weight loss on renal function in patients with severe obesity. *J Am Soc Nephrol* 2003; 14: 1480–1486.
62. Navarro-Diaz M *et al*. Effect of drastic weight loss after bariatric surgery on renal parameters in extremely obese patients: long-term follow-up. *J Am Soc Nephrol* 2006; 17(Suppl. 3): S213–S217.
63. Serra A *et al*. The effect of bariatric surgery on adipocytokines, renal parameters and other cardiovascular risk factors in severe and very severe obesity: 1-year follow-up. *Clin Nutr* 2006; 25: 400–408.
64. Michels WM *et al*. Performance of the Cockcroft-Gault, MDRD, and new CKD-EPI formulas in relation to GFR, age, and body size. *Clin J Am Soc Nephrol* 2010; 5: 1003–1009.
65. Benedek IH *et al*. Serum protein binding and the role of increased alpha 1-acid glycoprotein in moderately obese male subjects. *Br J Clin Pharmacol* 1984; 18: 941–946.
66. Mattar SG *et al*. Surgically-induced weight loss significantly improves nonalcoholic fatty liver disease and the metabolic syndrome. *Ann Surg* 2005; 242: 610–617. discussion 618–620.
67. Stratopoulos C *et al*. Changes in liver histology accompanying massive weight loss after gastroplasty for morbid obesity. *Obes Surg* 2005; 15: 1154–1160.
68. Barker KB *et al*. Non-alcoholic steatohepatitis: effect of Roux-en-Y gastric bypass surgery. *Am J Gastroenterol* 2006; 101: 368–373.
69. Van Dielen FM *et al*. Macrophage inhibitory factor, plasminogen activator inhibitor-1, other acute phase proteins, and inflammatory mediators normalize as a result of weight loss in morbidly obese subjects treated with gastric restrictive surgery. *J Clin Endocrinol Metab* 2004; 89: 4062–4068.
70. Johnson TN *et al*. Changes in liver volume from birth to adulthood: a meta-analysis. *Liver Transpl* 2005; 11: 1481–1493.
71. Howgate EM *et al*. Prediction of in vivo drug clearance from in vitro data. I: impact of inter-individual variability. *Xenobiotica* 2006; 36: 473–497.
72. Benet LZ *et al*. BDDCS applied to over 900 drugs. *AAPS J* 2011; 13: 519–547.
73. Kasim NA *et al*. Molecular properties of WHO essential drugs and provisional biopharmaceutical classification. *Mol Pharm* 2004; 1: 85–96.
74. Joint Formulary Committee. *British National Formulary*. Vol. 62**,** London: Pharmaceutical Press, 2011.
75. Kearney AS *et al*. The interconversion kinetics, equilibrium, and solubilities of the lactone and hydroxyacid forms of the HMG-CoA reductase inhibitor, CI-981. *Pharm Res* 1993; 10: 1461–1465.
76. Lennernas H, Fager G. Pharmacodynamics and pharmacokinetics of the HMG-CoA reductase inhibitors. Similarities and differences. *Clin Pharmacokinet* 1997; 32: 403–425.
77. Prueksaritanont T *et al*. In vitro metabolism of simvastatin in humans [SBT]identification of metabolizing enzymes and effect of the drug on hepatic P450s. *Drug Metab Dispos* 1997; 25: 1191–1199.
78. Brandstrom A *et al*. Structure activity relationships of substituted benzimidazoles. *Scand J Gastroenterol Suppl* 1985; 108: 15–22.
79. El-Badry M *et al*. Study of omperazole stability in aqueous solution: influence of cyclodextrins. *J Drug Deliv Sci Tech* 2009; 19: 347–351.
80. Shimamoto J *et al*. Lack of differences in diclofenac (a substrate for CYP2C9) pharmacokinetics in healthy volunteers with respect to the single CYP2C9*3 allele. *Eur J Clin Pharmacol* 2000; 56: 65–68.
81. Willis JV *et al*. The pharmacokinetics of diclofenac sodium following intravenous and oral administration. *Eur J Clin Pharmacol* 1979; 16: 405–410.
82. Brammer KW *et al*. Pharmacokinetics and tissue penetration of fluconazole in humans. *Rev Infect Dis* 1990; 12(Suppl. 3): S318–S326.
83. Demuria D *et al*. Pharmacokinetics and bioavailability of fluconazole in patients with AIDS. *Antimicrob Agents Chemother* 1993; 37: 2187–2192.
84. Joe LA *et al*. Systemic absorption of oral fluconazole after gastrointestinal resection. *J Antimicrob Chemother* 1994; 33: 1070.
85. Hoffken G *et al*. Pharmacokinetics of ciprofloxacin after oral and parenteral administration. *Antimicrob Agents Chemother* 1985; 27: 375–379.
86. Lettieri JT *et al*. Pharmacokinetic profiles of ciprofloxacin after single intravenous and oral doses. *Antimicrob Agents Chemother* 1992; 36: 993–996.
87. Pratha VS *et al*. Inhibition of pentagastrin-stimulated gastric acid secretion by pantoprazole and omeprazole in healthy adults. *Dig Dis Sci* 2006; 51: 123–131.

8.2.2 Compound Simcyp Simulator template input properties

Table 8.3. Drug specific parameters as incorporated into Simcyp® Simulator.

	Drugs				
Parameters	**CPF**	**DCF**	**FCZ**	**OMZ**	**SIM**
PhysChem					
MW (g/mol)	331.4	296.2	306.3	345.4	418.6
$LogP_{o:w}$	0.3	4.5	0.2	2.23	4.68
Acid-base nature	Ampholyte	Acid	Base	Ampholyte	Neutral
pKa	5.88	4.01	1.76	8.7	NA
pKb	8.74			4.4	
Blood binding					
BP	0.75	0.61	1	0.59	1
fu_p	0.79	0.003	0.89	0.043	0.011
Dissolution					
Formulation	IR	EC	IR	EC	IR
Solubility input	Predicted	Predicted	Predicted	Predicted	Predicted
S_0 (mg/mL)	26.324	0.001	30.630	0.322	0.001
Absorption					
IVIVC method	PSA PSA: 72.9 HBD: 2	PSA PSA: 49.3 HBD: 2	Caco-2, pH6.5:7.4 P_{app}: 29.8·10^{-6} cm/s	MDCK: P_{app}: 59·10^{-6} cm/s	PSA PSA: 72.83 HBD: 1
$P_{eff,man}$ (10^{-4} cm/s)	1.25	2.27	4.27	3.25	2.37
Distribution					
Model	1-comp.	1-comp.	1-comp.	1-comp.	1-comp.
Estimation method	$V_{ss,iv}$	$V_{ss,iv}$	$V_{ss,iv}$	$V_{ss,iv}$	$V_{ss,iv}$
V_{ss} (L/kg)	2.48	0.195	0.748	0.35	2.13
Elimination					
Metabolism	NA	*CYP2C9* V_{max}: 8.28[A] $K_{m,u}$: 0.71[B] *UGT2B7* V_{max}: 2800[C] $K_{m,u}$: 2.45[B]	CL_{iv}: 1.01 L/h	*CYP2C19* V_{max}: 6.47[A] $K_{m,u}$: 1.28[B] *CYP3A4* V_{max}: 2.3[A] $K_{m,u}$: 58.5[B] *CYP3A4* V_{max}: 12.2[A] $K_{m,u}$: 137[B]	*CYP3A4* CL_{int}: 2597[D]
CL_R (L/h)	23.7	1.05	0.7	0.037	NA

References: (Turner, 2008)

CPF=Ciprofloxacin, DCF=Diclofenac, FCZ=Fluconazole, OMZ=Omeprazole, SIM=Simvastatin, MW=Molecular weight, $LogP_{o:w}$=Octanol:Water partitioning coefficient, BP=Blood to plasma ratio, fu_p=fraction unbound in plasma, S0=intrinsic aqueous solubility, IVIVC=*In vitro-in vivo* correlation, $P_{eff,man}$=Estimated human permeability, CYP=Cytochrome P450, CL_R=Typical renal clearance in healthy volunteers, Vss=Volume of distribution at steady state, iv=Intravenous infusion, NA=Not applicable.

[A]pmol/min/mg microsomal protein

[B]µM

[C]pmol/min/mg protein

[D]µL/min/mg microsomal protein

8.3 Evaluation of an *in silico* PBPK post-bariatric surgery model through simulating oral drug bioavailability of atorvastatin and cyclosporine

8.3.1 Publication in Clinical Pharmacology and Therapeutics: Pharmacometrics and Systems Pharmacology (2013) 2(e47):1-9

Citation: CPT: Pharmacometrics & Systems Pharmacology (2013) 2, e47; doi:10.1038/psp.2013.23

www.nature.com/psp

ORIGINAL ARTICLE

Evaluation of an *In Silico* PBPK Post-Bariatric Surgery Model through Simulating Oral Drug Bioavailability of Atorvastatin and Cyclosporine

AS Darwich[1], D Pade[2], K Rowland-Yeo[2], M Jamei[2], A Åsberg[3], H Christensen[3], DM Ashcroft[1] and A Rostami-Hodjegan[1,2]

An increasing prevalence of morbid obesity has led to dramatic increases in the number of bariatric surgeries performed. Altered gastrointestinal physiology following surgery can be associated with modified oral drug bioavailability (F_{oral}). In the absence of clinical data, an indication of changes to F_{oral} via systems pharmacology models would be of value in adjusting dose levels after surgery. A previously developed virtual "post-bariatric surgery" population was evaluated through mimicking clinical investigations on cyclosporine and atorvastatin after bariatric surgery. Cyclosporine simulations displayed a reduced fraction absorbed through gut wall (f_a) and F_{oral} after surgery, consistent with reported observations. Simulated atorvastatin F_{oral} postsurgery was broadly reflective of observed data with indications of counteracting interplay between reduced f_a and an increased fraction escaping gut wall metabolism (F_G). Inability to fully recover observed atorvastatin exposure after biliopancreatic diversion with duodenal switch highlights the current gap regarding the knowledge of associated biological changes.
CPT: Pharmacometrics & Systems Pharmacology (2013) **2**, e47; doi:10.1038/psp.2013.23; advance online publication 12 June 2013

The prevalence of obesity has increased dramatically in the USA and Europe over the past decade.[1,2] Bariatric surgery has proven to be successful in treating morbid obesity with over 220,000 surgeries performed in the USA and Canada in 2008.[3] Several bariatric surgical methods coexist in healthcare, where Roux-en-Y gastric bypass (RYGB) is considered the gold standard.[4] RYGB results in a reduced gastric volume, complete bypass of the pylorus, partial bypass of the duodenum and proximal jejunum, and a delay in bile inflow to the distal jejunum. The more invasive biliopancreatic diversion with duodenal switch (BPD-DS) results in a partial resection of the stomach with the pylorus retained, bypass of jejunum and proximal ileum, and an approximately 250 cm delay of the bile inlet. Jejunoileal bypass (JIB) is considered to be the most invasive procedure, retaining only the stomach (with pylorus) and distal ileum.[5,6]

As a consequence of bariatric surgery, a number of physiological parameters influencing oral drug bioavailability (F_{oral}) are altered, including: a reduced gastric capacity and emptying time, altered gastrointestinal (GI) pH, reduced absorption area, altered bile flow and small intestinal transit (SIT), altered substrate exposure to drug-metabolizing enzymes, and active efflux transporters.[5,7,8] Patients undergoing bariatric surgery continue to receive various therapeutic drugs without dose adjustments for altered bioavailability, which can potentially lead to no therapeutic effect or higher than required systemic exposure. There are a very limited number of studies that have investigated oral drug exposure post-bariatric surgery.[5,9]

The direction and magnitude of impact on F_{oral} following surgery may depend on the characteristics and invasiveness of the surgical procedure,[10,11] where the extent of the small intestinal bypass may influence the fraction of dose absorbed through the gut wall (f_a). Bypassing regions highly abundant in drug-metabolizing enzymes can affect the fraction of absorbed drug F_G.[6] F_H, the fraction that escapes hepatic first-pass metabolism, may be assumed to remain unaltered (Eq. 1).[5,7,8]

$$F_{oral} = f_a \cdot F_G \cdot F_H \quad (1)$$

A level of uncertainty remains regarding the SIT postsurgery, where a reduction in motility has been observed, albeit well-powered clinical studies of SIT in man are lacking.[6,12,13]

The postsurgical physiology is further complicated by the possibility of small intestinal trauma or adaptation, where an enhanced permeability due to impairment of the mucosa or long-term villi elongation has been observed in rat BPD-DS models.[14,15] Alterations in the levels of gastric hormones (including: peptide YY, ghrelin, and Glucagon-Like Peptide 1) may lead to redistribution of intestinal blood flow to the submucosa, as observed in dog models. Postsurgical hormonal levels have been observed to vary depending on the bariatric surgical procedure.[13,16–18]

Due to these multifactorial changes, physiologically based pharmacokinetic (PBPK) modeling enables one to predict, *in silico*, the effects of various bariatric surgeries in a morbidly obese population.[6] The Advanced Dissolution Absorption and Metabolism (ADAM) model describes the variability in F_{oral} through a physiologically based seven-segment model of the small intestine, including: duodenum, jejunum I and II, and ileum I–IV. The model describes drug release from formulation, dissolution, precipitation,

[1]Centre for Applied Pharmacokinetic Research, School of Pharmacy and Pharmaceutical Sciences, University of Manchester, Manchester, UK; [2]Simcyp Ltd, Blades Enterprise Centre, Sheffield, UK; [3]Department of Pharmaceutical Biosciences, School of Pharmacy, University of Oslo, Oslo, Norway. Correspondence: A Rostami-Hodjegan (amin.rostami@manchester.ac.uk)
Received 30 January 2013; accepted 13 March 2013; advance online publication 12 June 2013. doi:10.1038/psp.2013.23

degradation, absorption, active transport, and metabolism as the drug transits through the small intestine, allowing the incorporation of saturation effects and population variability. The ADAM model has been well described and used in the previous literature.[8,19]

In our previous work, a virtual "post-bariatric surgery" population was created using the ADAM model within a PBPK system containing characteristics of a morbidly obese population. Developed models for RYGB, BPD-DS, and JIB included specific anatomical and physiological parameters that are altered following surgery, namely: gastric capacity and fluid dynamics, gastric emptying time, small intestinal bypass, GI pH, bile flow, and alterations to regional abundance of drug-metabolizing enzymes (e.g. CYP3A) and efflux transporter P-glycoprotein. The model further incorporated whole body physiological changes, such as postsurgical recovery of renal function as a function of weight loss.[6]

Simulations predicted change in oral bioavailability of various drugs pre- to post-bariatric surgery, revealing the magnitude and direction of the effect to be surgery dependent, due to altered GI system parameters, and influenced by a complex interplay between drug characteristics, including: solubility, permeability, dissolution, gut wall metabolism, and dose level. However, no comparison so far has been made between the results of these simulations and existing clinical data.[6] In the current study, we report on the evaluation of previously developed post-bariatric surgery models by comparing the observed vs. predicted impact of bariatric surgery on oral exposure of cyclosporine and atorvastatin acid using virtual simulations.

RESULTS

Changes in oral drug bioavailability after bariatric surgery were demonstrated for cyclosporine and atorvastatin acid following RYGB, BPD-DS, and JIB.[10,11,20,21] Sex-, age-, height-, and weight-matched simulations were carried out based on the corresponding clinical studies using post-bariatric surgery models coupled to a full PBPK distribution model into the Simcyp Simulator (Simcyp Limited (a Certara Company), Sheffield, UK). The results from the comparison of observed vs. simulation studies are as follows:

Cyclosporine

Roux-en-Y gastric bypass. Following RYGB, Marterre and coworkers reported a 194% increase in the daily dose per kg body weight in kidney transplant patients ($n = 3$) of cyclosporin A (CsA) Sandimmune solution. CsA trough blood levels were monitored from 6 months before RYGB up to 12 months postoperatively, using an immunoassay technique (TDx, Abbott Laboratories). The observed reduction in exposure prompted an increase in the oral dose from 1.8 (±0.5) to 3.5

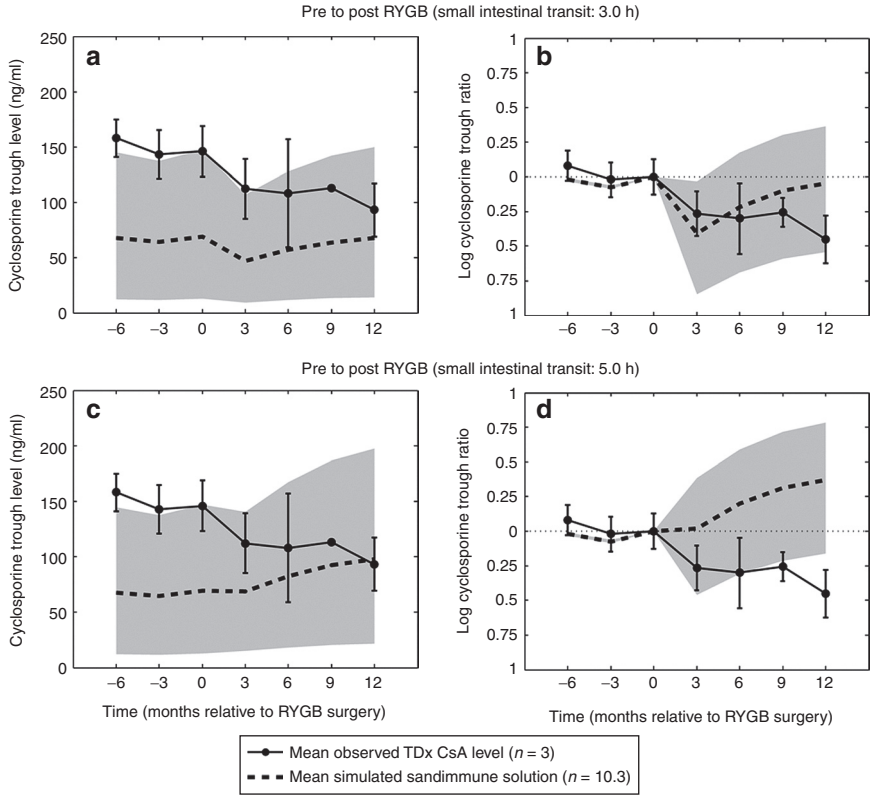

Figure 1 Mean and SD of observed cyclosporin A (CsA) TDx trough levels at steady state pre to post-Roux-en-Y gastric bypass (RYGB) at –6, –3, 0, 3, 6, 9, and 12 months relative to RYGB surgical event (0 months). Time points from –6 to 12 months correspond to dose levels of 1.7, 1.7, 1.8, 2.4, 2.8, 3.2, 3.5 mg/kg/day, respectively ($n = 3$) administered twice daily. Observed data are compared with simulated 50, 95, and 5% prediction interval, indicated by gray area, of CsA Sandimmune trough levels ($n = 10 \times 3$). (**a**) Simulated post-RYGB at a small intestinal transit time (SIT) of 3.0 h, (**b**) log-normalized simulated CsA trough ratio as compared with 0 months (RYGB SIT = 3.0 h), (**c**) simulated CsA trough levels at RYGB SIT of 5.0 h, (**d**) log-normalized simulated CsA trough ratio as compared with 0 months (RYGB SIT = 5.0 h).[20]

(±1.1) mg/kg/day in order to maintain pre-RYGB CsA trough levels (20) (**Figure 1a–d**). Owing to the reported overprediction of the TDx immunoassay, observed and simulated data were normalized for trough levels immediately before RYGB surgery, indicated by the time of 0 months (**Figure 1b,c**).[22]

In an age-, sex-, and weight-matched virtual population, oral drug exposure of Sandimmune CsA solution was simulated in 10 randomized trials consisting of 3 individuals in each trial (n = 10·3). Cyclosporine displayed a reduction in f_a from 0.40 (5–95% confidence interval (CI95): 0.24–0.59) to 0.19 (0.10–0.32) following RYGB, at a simulated SIT time of 3.0 h, whereas F_G remained unaltered at 0.86 (0.74–0.87). A 194% increase in dose level, resulted in a trough level ratio of 0.96 (0.58–1.44) as compared with the preoperative exposure at 0 months. Assuming a postsurgical SIT time of 5.0 h, cyclosporine displayed reduction in f_a to 0.26 (0.14–0.41), and F_G remained unaltered. A 194% increase in the dose level resulted in an overprediction in post-RYGB CsA trough levels, with a simulated post/presurgical ratio of 1.45 (0.85–2.19) as compared with preoperative exposure at 0 months (**Figure 1a–d**).

Simulations of the theoretical impact of RYGB on the solubilization enhanced cyclosporine Neoral microemulsion, at a postsurgical SIT of 3.0 h, produced an area under the concentration–time curve (AUC) ratio of 1.84 (1.26–2.37) at 12 months postsurgery as compared with the levels at 0 months relative to RYGB surgery. The observed increase in oral exposure of Neoral was due to a 194% dose increase, where f_a displayed an increase from 0.72 (0.47–0.92) to 0.82 (0.57–0.94), whereas F_G increased from 0.90 (0.81–0.96) to 0.94 (0.90–0.98) (**Supplementary Data** online).

Jejunoileal bypass. In a case study by Chenhsu *et al.*,[21] CsA blood levels at 2 h after administration at steady state (C2), administered as Neoral microemulsion in controls (n = 7) and post-JIB (n = 1), displayed a reduced exposure when comparing the mean C2 concentration over the administered dose range, reporting a reduction in C2 levels of ~59%.

Simulating demographically matched morbidly obese controls (n = 10·7) and post-JIB patients (SIT = 0.4 h; n = 10·1), cyclosporine displayed a reduction in C2 levels from 452 (153–776) to 357 (103–650) ng/ml at a dose level of 4 mg/kg/day and from 2,528 (388–6089) to 1,632 (571–2,811) ng/ml at a dose of 12 mg/kg/day. Simulated levels corresponded well with the linear regression of observed data as compared with the 5–95% prediction interval. The simulated reduction in oral drug exposure in the post-JIB population as compared with the controls was due to a reduction in f_a from 0.61 (0.35–0.86) to 0.12 (0.04–0.19), whereas F_G displayed a minor reduction from 0.90 (0.79–97) to 0.88 (0.75–0.96) at a therapeutic dose of 2 mg/kg/day. At a dose of 12 mg/kg/day, a major reduction in f_a was observed from 0.34 (0.16–0.53) to 0.08 (0.01–0.18), whereas F_G was reduced from 0.91 (0.81–0.93) to 0.90 (0.80–0.97) (**Figure 2**).

Assuming a SIT of 0.7 h after JIB, cyclosporine displayed a less apparent reduction in C2 levels due to a less apparent reduction in f_a to 0.19 (0.05–0.30) and 0.13 (0.02–0.26) at corresponding dose levels of 2 and 12 mg/kg/day, respectively. After JIB (SIT = 0.7 h), F_G was altered to 0.89 (0.79–0.96) and 0.92 (0.84–0.98) at a therapeutic dose level of 2 and 12 mg/kg/day, respectively (**Supplementary Data** online).

Atorvastatin

Roux-en-Y gastric bypass. In a clinical trial carried out on 12 morbidly obese patients, atorvastatin was administered as an immediate release tablet of 20–80 mg in fasted state where patients were allowed to eat 2 h after administration. Plasma concentration profiles were obtained from 0–8 h after drug administration before and 3–6 weeks after RYGB. The pre to postsurgical trend in oral exposure displayed a high variability where the overall reported trend displayed a median post/pre surgery AUC ratio of 1.12 (range: 0.34–2.33), albeit being statistically insignificant.[10]

Virtual simulations for oral drug exposure of atorvastatin acid pre- to post-RYGB were conducted in 10 randomized trials, each consisting of 12 age-, sex-, and BMI-matched individuals (n = 10 × 12). Assuming a reduction in SIT as function of the small intestinal bypass (SIT = 3.0 h) resulted in an overall increase in AUC with a simulated median post/presurgical AUC ratio of 1.13, capturing 100% of observed data within the simulated 95% prediction interval of 0.27–3.80 (**Figure 3a–j**). Alternatively, with an increase in SIT time post-RYGB (SIT = 5.0 h), atorvastatin acid displayed a median post/presurgical AUC ratio of 1.42 (0.34–4.91) (**Supplementary Data** online).

Simulated increase in exposure of atorvastatin following RYGB (SIT = 3.0 h) was due to a reduction in f_a from 0.58 (0.33–0.77) to 0.54 (0.29–0.74) counteracted by an increase in F_G from 0.69 (0.48–0.86) to 0.73 (0.53–0.88) (**Figure 4a,b**).

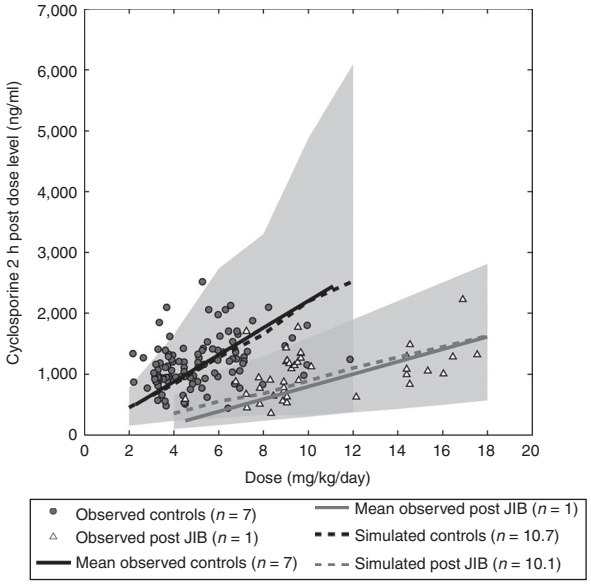

Figure 2 Observed mean blood concentration of cyclosporine microemulsion (Sandimmune Neoral; Novartis) at steady state 2 h postdosing in controls (n = 10 × 7) and one patient (n = 10 × 1) post-jejunoileal bypass (JIB) as compared with simulated sex- and age-matched controls (n = 300) and post-JIB (n = 800) at a small intestinal transit time of 0.4 h over dose range of 300–1,000 mg, where 5, 50, and 95% prediction intervals are indicated by gray areas.[21]

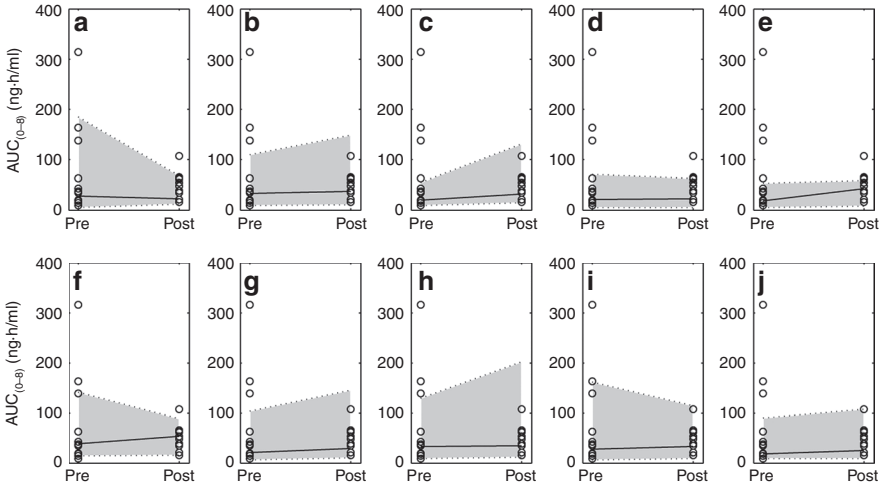

Figure 3 Simulated 50, 95, and 5% prediction interval (indicated by gray areas) of oral drug exposure of atorvastatin acid in randomized trials of age-, sex-, dose-, and BMI-matched patients pre- to post-Roux-en-Y gastric bypass surgery (small intestinal transit = 3.0 h) as compared with observed data. (**a**–**j**) Ten randomized simulated trials consisting of 12 individuals in each trial ($n = 10 \times 12$), as compared with observed ($n = 12$; open circles).[10] AUC, area under the concentration–time curve.

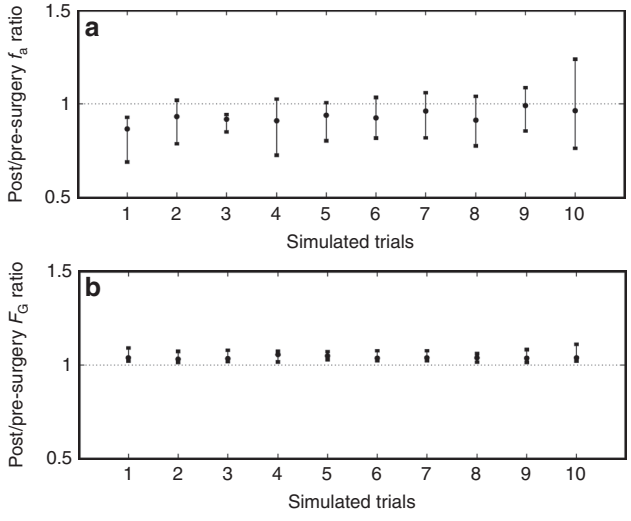

Figure 4 Simulated 50, 95, and 5% prediction intervals of the ratio of (**a**) fraction of dose absorbed in the intestine (f_a), and (**b**) fraction escaping gut wall metabolism (F_G) of atorvastatin acid pre- to post-Roux-en-Y gastric bypass surgery (small intestinal transit = 3.0 h) in 10 individually simulated randomized trials (1–10) consisting of 10 individuals in each pre- and postsurgery ($n = 10 \times 10$).

Assuming a reduced small intestinal motility (RYGB SIT = 5.0 h), the more apparent increase in AUC was the result of an extensive increase in f_a.

Biliopancreatic diversion with duodenal switch. Atorvastatin immediate release tablet 20–80 mg administered in the fasted state, allowing feeding at 2 h, displayed a significant increase in oral drug exposure following BPD-DS in 10 morbidly obese patients, with an observed mean AUC ratio of 2.0 (±1.0) and observed increase in the C_{max} from 20.0 ng/ml (±24.9) to 28.0 (±22.5), whereas t_{max} increased from 1.2h (±0.8) to 2.3h (±1.0) post-BPD-DS.[11]

Predicted plasma concentration–time profiles of atorvastatin acid were consistent with observed data before surgery in a morbidly obese population (**Supplementary Data** online).

However, simulated plasma concentration–time profiles following BPD-DS (SIT = 1.2 h) were unable to capture the observed increase in oral drug exposure. The predicted AUC ratio of 0.90 (0.16–2.24) was lower than expected due to a reduction in f_a from 0.61 (0.34–0.79) to 0.39 (0.06–0.72), which was counteracted by an increase in F_G from 0.69 (0.59–0.79) to 0.72 (0.63–0.81). C_{max} displayed a minor increase, with a post/pre-BPD-DS C_{max} ratio of 1.32 (0.31–2.38), whereas t_{max} displayed a post/pre-BPD-DS ratio of 0.62 (0.31–1.00). The simulated pre- to post-BPD-DS alterations in AUC, C_{max}, and t_{max} correspond to the central points of **Figure 5a–c**, respectively.

Sensitivity analysis was performed to assess the impact of potential physiological alterations postsurgery on the plasma exposure of atorvastatin acid, including the impact of: SIT, gastric emptying time, bile concentration in the terminal ileum, small intestinal enterocyte volume (V_{ent}), GI CYP3A content, and small intestinal permeability (P_{eff}). The AUC was insensitive to changes in the postsurgical bile concentration and V_{ent}. Following BPD-DS (SIT = 1.2 h), a fivefold increase in P_{eff} led to a post/presurgical AUC ratio of 1.93 (0.60–5.53), whereas C_{max} displayed a post/presurgical ratio of 4.36 (1.23–9.68). A fivefold increase in Q_{villi} resulted in a minor increase in AUC with a simulated post/pre-BPD-DS AUC ratio of 1.24 (0.22–3.24) and a C_{max} ratio of 1.86 (0.47–4.19). A reduction in GI CYP3A by fivefold gave a post/pre-BPD-DS AUC ratio of 1.13 (0.19–3.06) (**Figure 5**).

Pre to post-BPD-DS (SIT = 4.2 h) displayed an AUC ratio of 1.71 (0.74–5.79), C_{max} ratio of 1.56 (0.69–3.39), and a t_{max} ratio of 0.87 (0.51–1.31). In the sensitivity analysis, a twofold increase in Q_{villi} resulted in a post/presurgical AUC ratio of 2.07 (0.86–6.96) and a C_{max} ratio of 1.91 (0.84–4.22), whereas t_{max} remained unaltered. A twofold increase in P_{eff}

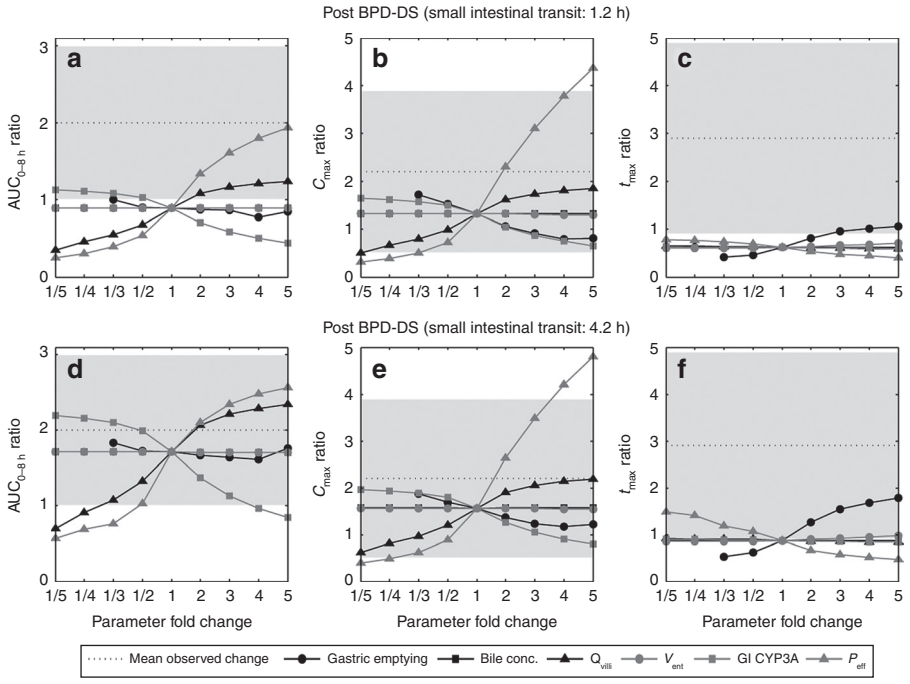

Figure 5 Spider plot of sensitivity analysis of simulated post/pre-biliopancreatic diversion with duodenal switch (BPD-DS) at a small intestinal transit time (SIT) of 1.2 h; (**a**) $AUC_{0-8\,h}$, (**b**) C_{max}, and (**c**) t_{max} ratio, BPD-DS (SIT = 4.2 h); (**d**) $AUC_{0-8\,h}$, (**e**) C_{max}, and (**f**) t_{max} ratio, examining the impact of the fold change in physiological parameters: gastric emptying, ileal bile concentration (bile conc.), villous blood flow (Q_{villi}), enterocytic volume (V_{ent}) in the remaining postsurgical small intestine, post-BPD-DS gastrointestinal CYP3A content, small intestinal permeability (P_{eff}), as compared with mean observed ratio pre- to post-BPD-DS.[11] AUC, area under the concentration–time curve; C_{max}, maximum plasma drug concentration; t_{max}, time of maximum plasma drug concentration.

displayed a post/pre-BPD-DS AUC ratio of 2.11 (0.90–6.91), a C_{max} ratio of 2.64 (1.17–5.66), and a minor reduction in t_{max}. A twofold reduction in GI CYP3A gave a post/presurgical AUC ratio of 1.99 (0.83–6.76), whereas C_{max} increased to a minor extent, displaying an AUC ratio of 1.80 (0.79–4.00). Gastric emptying had the most apparent impact on t_{max}, where a fivefold increase resulted in a post/pre-BPD-DS ratio of 1.78 (1.11–2.58) (**Figure 5**).

DISCUSSION

Cyclosporine

The immunosuppressant cyclosporine (molecular weight: 1202.61 g/mol) displays poor aqueous solubility and a relatively low permeability due to its lipophilic and bulky character making the compound dependent on bile-mediated solubility to facilitate absorption.[23,24] The drug is mainly metabolized by CYP3A4 in the intestine and liver and is subject to P-glycoprotein efflux.[25,26] The oral bioavailability displays a high interindividual variability, ranging from 5 to 89% for Sandimmune formulation, whereas Neoral displays improved absorption properties and an oral bioavailability of 21–73%.[27]

The simulated underprediction of Sandimmune TDx trough levels before RYGB surgery was expected and is most likely due to the unspecificity of the immunoassay displaying a high cross-reactivity between the parent compound and metabolites resulting in a significantly higher variability in the trough levels as compared with peak concentrations.[20,22]

Normalizing simulated cyclosporine trough levels to pre-RYGB levels produced a reduction in exposure comparable to observed data. Furthermore, a simulated 194% increase in Sandimmune dose levels recovered presurgical trough levels as stated in the publication.[20]

In the simulation study of cyclosporine Neoral, microemulsion pre to post-JIB observed data of the control population was well described within the 95% prediction interval of the simulated data, whereas the observed exposure post-JIB was well described within the 95% prediction interval of simulated data assuming a reduction in SIT time equivalent to the bypass (SIT = 0.4 h). An alternative "what-if" scenario simulating a longer transit time (SIT = 0.7 h) over predicted the observed mean blood concentration post-JIB as reported by Chenhsu *et al*. (**Figure 2**). The overprediction could suggest small intestinal motility to remain unaltered following JIB or be a result of a small postsurgical study population (n = 1), displaying a low study power, albeit the simulated magnitude of reduction in C2 levels post-JIB (SIT = 0.4 h) closely matched the estimated reduction in cyclosporine exposure following JIB in another case study where a patient was subject to a surgical reversal of the procedure. The reversed JIB produced an observed 2.78-fold increase in exposure in the case study.[21,28]

The simulated discrepancy in oral drug exposure of Sandimmune and Neoral pre to post-RYGB, where bariatric surgery had the highest effect on the oral bioavailability of Sandimmune, highlights the importance of formulation characteristics and its impact on oral drug bioavailability

pre- to post-bariatric surgery. The choice of a solubilized biopharmaceutical formulation such as a self-microemulsifying drug delivery system, solution, or dispersible tablet may be considered as a first-hand choice for patients undergoing bariatric surgery and are treated with limited solubility drugs with a narrow therapeutic index. This suggestion supports earlier observations in clinical practice, where alterations in pharmacotherapy post-bariatric surgery aim at switching to formulations displaying improved dissolution properties.[5]

Atorvastatin

The HMG-CoA reductase inhibitor atorvastatin, which is administered in the acid form, displays a high solubility and permeability. The compound is extensively metabolized in the small intestine and liver, namely by CYP3A4 but also via the UGT1A1 and UGT1A3 route. Atorvastatin acid and the lactone metabolite are also subject to interconversion by the UGTs and another minor chemical pathway. Atorvastatin acid is a substrate of P-glycoprotein efflux and OATP1B1-mediated active hepatic uptake.[29]

Trends in simulated oral drug exposure of atorvastatin pre to post-RYGB were consistent with observed data, where simulated trends in f_a and F_G suggested an interplay between reduced absorption area and bypass of regions highly abundant in CYP3A to be of high importance when considering the overall effect on oral bioavailability. Simulated RYGB (SIT = 3.0 h) produced the closest agreement with observed data of atorvastatin exposure following RYGB, again suggesting a reduction in SIT time to be the most likely consequence of surgery.[10]

The inability to recover the observed twofold increase in atorvastatin AUC pre to post-BPD-DS at a simulated SIT of 1.2 h may suggest additional postsurgical physiological parameters to be governing the trend in oral drug bioavailability post-BPD-DS. The exploratory sensitivity analysis identified a number of potential parameters leading to a comparable increase in oral drug exposure pre to post-BPD-DS. An increase in SIT following BPD-DS, corresponding to the linear regression relationship between mouth to cecum transit time and plasma levels of peptide YY, resulted in an AUC ratio of 1.71 (0.74–5.79). Furthermore, a simulated twofold increase in P_{eff} and Q_{villi}, or a twofold reduction in the GI content of CYP3A post-BPD-DS (SIT = 4.2 h) recovered the observed AUC of atorvastatin. The reoccurring underprediction of t_{max} following surgery may be explained by an altered postprandial response causing a delayed absorption.

These findings suggest that additional physiological parameters, such as impairment in permeability or redistribution of intestinal blood flow, may play an important role in governing trends in oral drug exposure pre to immediately post-BPD-DS. The results highlight the surgery-specific trends observed post-bariatric surgery due to the intricate interplay between fluid dynamics, absorption area, transporters, metabolism, and GI physiology.

Current limitations in simulating the impact of oral drug bioavailability following bariatric surgery include the lack of clinical and postsurgical physiological data. Nonetheless, the models integrate all available knowledge on changes known to occur in the GI tract following bariatric surgery and can assist with dosage recommendation when there is an absence of clinical observations.

Table 1 Summary of alterations to population template in order to mimic and simulate postsurgical condition as per Darwich *et al.*[6]

	Bariatric surgical procedures			
Parameters	**JIB**	**RYGB**	**BPD-DS**	**References**
Gastric emptying: liquids (minutes)	24,[a] CV: 38%	7, CV: 45%	24,[a] CV: 38%	39,40
Gastric capacity (ml)	250[a]	30	150	6,41
Q_{sec} stomach (l/h)	0.108	0.059	0.295	6
Initial volume of stomach fluid (ml)	50[a]	9.9	32.6	6
Gastric pH	1.5[a]	6.5	1.5[a]	42–44
Small intestinal bypass (centimeters and/or segments)	Retaining the duodenum, 20% of jejunum I and 23% of ileum IV[b]	100 cm (duodenum and jejunum I)[b]	Retaining 2.5 cm of duodenum and 250 cm of the distal ileum[c]	6,41
Bile exclusion (centimeters and segments)	Not applicable (jejunum II – ileum III)	110 cm (stomach – jejunum I)	252 cm (stomach – ileum III)	6,41
CYP3A4 abundance (nmol/total gut)	32.3, CV: 60%	48.3, CV: 60%	12.6,[d] CV: 38%	6
CYP3A5 abundance (nmol/total gut)	12.1, CV: 60%	18.0, CV: 60%	10.1,[d] CV: 38%	6
Mean small intestinal transit time (hours) – Scenario 1	0.4; $\alpha = 0.5$, $\beta = 0.4$	3.0; $\alpha = 2.6$, $\beta = 3.7$	1.2; $\alpha = 1.3$, $\beta = 1.9$	6,41
Mean small intestinal transit time (hours) – Scenario 2	0.7; $\alpha = 0.6$, $\beta = 0.4$	5.0; $\alpha = 4.0$, $\beta = 5.3$	4.2;[e] $\alpha = 3.7$, $\beta = 5.0$	6,12,13,16
Renal equation	MDRD	MDRD	MDRD	6,45–48

ADAM, advanced dissolution absorption, and metabolism; BPD-DS, biliopancreatic diversion with duodenal switch; CV, coefficient of variation; JIB, jejunoileal bypass; MDRD, modification of diet renal disease equation; Q_{sec}, secretion flow; RYGB, Roux-en-Y gastric bypass; α and β, Weibull scaling factors utilizing assuming a variance of 1.8 h.

[a]Unaltered parameter as compared with morbidly obese controls. [b]Setting human effective permeability (P_{eff}) of compounds close to zero in bypassed segments. [c]Altering small intestinal parameters in the ADAM model to conform to remaining segments. [d]Based on intestinal biopsy in the study population.[11] [e]Derived based on a pre- to postsurgical peptide YY level of 413% utilizing linear relation between peptide YY and small intestinal transit time as reported by Savage and coworkers.[16,18]

Conclusions

In this work, we demonstrated the potential of a PBPK and simulation to predict oral drug bioavailability post-bariatric surgery by evaluating earlier developed models using observed data for cyclosporine and atorvastatin. Trends in oral drug exposure of atorvastatin and cyclosporine were predicted well within the 95% prediction interval following RYGB using the previously developed model at a SIT time of 3.0 h. The results suggest a reduction in SIT time to be the most likely scenario following RYGB. The observed increase in atorvastatin exposure following BPD-DS could not be captured using the developed BPD-DS model incorporating all known physiological alterations.

A mechanistic PBPK modeling approach has the potential to serve as a tool in examining the impact of physiological alterations on oral drug bioavailability in the absence of clinical data. The demonstrated approach may allow a framework for optimization of oral drug therapy post-bariatric surgery.

METHODS

Bariatric surgery model. Sex-, age-, height-, and weight-matched simulations were carried out corresponding to identified clinical studies[10,11,20,21] using the ADAM model coupled to a full PBPK distribution model, incorporated into the Simcyp Simulator (Simcyp, Sheffield, UK) (Eqs. 2–4).[8,30] Detailed specification for the demographics and physiological parameters of the morbidly obese population have been published previously.[7] Similarly, surgical changes to the anatomy and physiology of GI tract following bariatric surgeries, including: RYGB, BPD-DS, and JIB are defined in an earlier publication.[6] Study population–specific surgical alterations are summarized in **Table 1**.

$$\text{Height} = C0 + C1 \cdot \text{Age} + C2 \cdot \text{Age}^2 \quad (2)$$

$$\text{Weight} = e^{(C0\ +\ C1 \cdot \text{Height})} \quad (3)$$

$$\text{BSA} = \text{Weight}^{\text{Weight exponent}} \cdot \text{Height}^{\text{Height exponent}} \quad (4)$$

Cyclosporine. The cyclosporine compound file, available in the Simcyp Simulator compound library, was adapted to account for formulation properties corresponding to Sandimmune solution and Sandimmune Neoral microemulsion (Novartis, East Hanover, NJ), using an aqueous solubility of 0.01 mg/ml and particle sizes of 3.73 and 0.03 μm, respectively, further allowing Neoral to supersaturate freely without precipitation assuming a linear dose–concentration relationship.[31] A full PBPK model was used to describe the cyclosporine distribution, where tissue to plasma partition coefficients (Kps) were obtained from *in vivo* tissue to plasma concentrations at steady state following intravenous infusion in rat.[32]

Atorvastatin acid. Physicochemical parameters for atorvastatin acid were taken from the publication by Lennernäs.[29] Metabolic data were obtained from the *in vitro* study reported by Jacobsen *et al.*;[33] CYP3A4 was found to be the main enzyme involved in the formation of the two primary metabolites ortho- and para-hydroxyatorvastatin acid with a minor contribution from CYP2C8. Intersystem extrapolation factors, which correct for differences in intrinsic activity per unit CYP enzyme relative to its native environment, were applied to the kinetic data for recombinantly expressed CYP3A4 and CYP2C8, respectively. Acyl glucuronidation of atorvastatin acid to the lactone and UDPGA-dependent metabolism of atorvastatin acid mainly via UGT1A1 to a minor ether glucuronide was also considered.[34,35] The resultant intrinsic clearance data were scaled to whole-organ values according to Eqs. 5 and 6.[36] The uptake of atorvastatin acid has been demonstrated in an OATP1B1-transfected cell system (HEK293 cells).[37,38] Although these *in vitro* data support the involvement of OATP1B1 in the hepatic uptake of atorvastatin acid, it was found that when used in combination with the metabolic data, the clearance was significantly underpredicted. To recover the plasma concentration time profile of atorvastatin acid before BPD-DS, $J_{\text{max,OATP1B1}}$ and $\text{Kp}_{\text{muscle}}$ were reestimated to 532.4 pmol/min/million cells and 4.0, using weighted least-square Nelder–Mead minimization method in the parameter estimation toolbox within the Simcyp Simulator.[11]

$$CLu_{H,\text{int}} = \frac{\text{ISEF} \cdot V_{\text{max-rhCYP}} \cdot \text{Abundance} \cdot \text{MPPGL} \cdot \text{Liver Weight}}{K_{m,u}} \quad (5)$$

$$CLu_{G,\text{int}} = \frac{\text{ISEF} \cdot V_{\text{max-rhCYP}} \cdot \text{Abundance}}{K_{m,u}} \quad (6)$$

Sensitivity analysis was carried out with regard to potential GI physiological parameters subject to potential alterations following surgery due to hormonal alterations, including: SIT time, villous blood flow (Q_{villi}), gastric emptying, small intestinal bile concentration, the enterocyte volume in the remaining small intestine (V_{ent}), postsurgical abundance of GI CYP3A (GI CYP3A), and small intestinal effective permeability (P_{eff}).

Analysis. Simulated data were visually inspected against observed data. In addition, the potential mechanism of changes to oral drug absorption was examined through the simulations in terms of assessing the effects on plasma drug concentration–time profile, maximum plasma drug concentration (C_{max}), time of maximum plasma drug concentration (t_{max}), f_a, and F_G.

Acknowledgments. The authors thank Basil Ammori, Salford Royal Hospital NHS Foundation Trust and David Turner, Simcyp (a Certara company) for discussions leading up to this work and James Kay for his assistance with the manuscript. Associate editor, A.R.-H. was not involved in the review or decision process for this paper. Simcyp's research is funded by a consortium of pharma companies.

Author contributions. A.R.-H., A.S.D., D.P., K.R.-Y., M.J., A.Å., H.C., and D.M.A. wrote the manuscript. A.R.-H., A.S.D., D.P., and D.M.A. designed research. A.R.-H., A.S.D., D.P., and D.M.A. performed research. A.S.D. analyzed data.

Conflict of interest. D.P., K.R.-Y., and M.J. are employees in Simcyp Limited (a Certara Company). A.R.-H. is an employee of the University of Manchester and part-time secondee to Simcyp Limited (a Certara Company). The other authors declared no conflict of interest.

Study Highlights

WHAT IS THE CURRENT KNOWLEDGE?

✓ Patients undergoing bariatric surgery receive various therapeutic drugs. A limited number of studies have investigated oral drug exposure postoperatively. Bariatric surgery models were previously developed using the ADAM model within the PBPK simulator, Simcyp.

WHAT QUESTION THIS STUDY ADDRESSED?

✓ We report on the evaluation of previously developed bariatric surgery PBPK models by comparing observed vs. predicted impact of surgery on oral exposure of cyclosporine and atorvastatin.

WHAT THIS STUDY ADDS TO OUR KNOWLEDGE

✓ Trends in oral exposure of atorvastatin and cyclosporine were well predicted following RYGB. Observed increase in atorvastatin exposure following BPD-DS could not be captured using the current model.

HOW THIS MIGHT CHANGE CLINICAL PHARMACOLOGY AND THERAPEUTICS

✓ The potential of a PBPK modeling approach was demonstrated, allowing a framework for optimizing oral drug therapy post-bariatric surgery. Developed models integrated available knowledge on physiological changes. The study highlights areas of further research, where models are not predictive due to the lack of information on systems parameters.

1. Flegal, K.M., Carroll, M.D., Ogden, C.L. & Curtin, L.R. Prevalence and trends in obesity among US adults, 1999-2008. *JAMA* **303**, 235–241 (2010).
2. Organisation for Economics Co-Operation and Development (OECD). Obesity and the Economics of Prevention: Fit not Fat - United Kingdom (England) Key Facts. <http://www.oecd.org/document/58/0,3746,en_2649_33929_46039034_1_1_1_1,00.html#Further_Reading> (2011). Accessed December 2012.
3. Buchwald, H. & Oien, D.M. Metabolic/bariatric surgery Worldwide 2008. *Obes. Surg.* **19**, 1605–1611 (2009).
4. Picot, J. *et al.* The clinical effectiveness and costeffectiveness of bariatric (weight loss) surgery for obesity: a systematic review and economic evaluation. *Health Technol. Assess.* **13**, 215–357 (2009).
5. Darwich, A.S. *et al.* Trends in oral drug bioavailability following bariatric surgery: examining the variable extent of impact on exposure of different drug classes. *Br. J. Clin. Pharmacol.* **74**, 774–787 (2012).
6. Darwich, A.S., Pade, D., Ammori, B.J., Jamei, M., Ashcroft, D.M. & Rostami-Hodjegan, A. A mechanistic pharmacokinetic model to assess modified oral drug bioavailability post bariatric surgery in morbidly obese patients: interplay between CYP3A gut wall metabolism, permeability and dissolution. *J. Pharm. Pharmacol.* **64**, 1008–1024 (2012).
7. Ghobadi, C. *et al.* Application of a systems approach to the bottom-up assessment of pharmacokinetics in obese patients: expected variations in clearance. *Clin. Pharmacokinet.* **50**, 809–822 (2011).
8. Jamei, M. *et al.* Population-based mechanistic prediction of oral drug absorption. *AAPS J.* **11**, 225–237 (2009).
9. Malone, M. & Alger-Mayer, S.A. Medication use patterns after gastric bypass surgery for weight management. *Ann. Pharmacother.* **39**, 637–642 (2005).
10. Skottheim, I.B. *et al.* Significantly altered systemic exposure to atorvastatin acid following gastric bypass surgery in morbidly obese patients. *Clin. Pharmacol. Ther.* **86**, 311–318 (2009).
11. Skottheim, I.B. *et al.* Significant increase in systemic exposure of atorvastatin after biliopancreatic diversion with duodenal switch. *Clin. Pharmacol. Ther.* **87**, 699–705 (2010).
12. Pellegrini, C.A., Deveney, C.W., Patti, M.G., Lewin, M. & Way, L.W. Intestinal transit of food after total gastrectomy and Roux-Y esophagojejunostomy. *Am. J. Surg.* **151**, 117–125 (1986).
13. Suzuki, S., Ramos, E.J., Goncalves, C.G., Chen, C. & Meguid, M.M. Changes in GI hormones and their effect on gastric emptying and transit times after Roux-en-Y gastric bypass in rat model. *Surgery* **138**, 283–290 (2005).
14. Gaggiotti, G. *et al.* Modifications of intestinal permeability test induced by biliopancreatic diversion: preliminary results. *Obes. Surg.* **5**, 424–426 (1995).
15. Mendieta-Zerón, H. *et al.* Biliopancreatic diversion induces villi elongation and cholecystokinin and ghrelin increase. *Diabetes Metab. Syndr.* **5**, 66–70 (2011).
16. Savage, A.P., Adrian, T.E., Carolan, G., Chatterjee, V.K. & Bloom, S.R. Effects of peptide YY (PYY) on mouth to caecum intestinal transit time and on the rate of gastric emptying in healthy volunteers. *Gut* **28**, 166–170 (1987).
17. Buell, M.G. & Harding, R.K. Effects of peptide YY on intestinal blood flow distribution and motility in the dog. *Regul. Pept.* **24**, 195–208 (1989).
18. Garcia-Fuentes, E. *et al.* Different effect of laparoscopic Roux-en-Y gastric bypass and open biliopancreatic diversion of Scopinaro on serum PYY and ghrelin levels. *Obes. Surg.* **18**, 1424–1429 (2008).
19. Darwich, A.S., Neuhoff, S., Jamei, M. & Rostami-Hodjegan, A. Interplay of metabolism and transport in determining oral drug absorption and gut wall metabolism: a simulation assessment using the "Advanced Dissolution, Absorption, Metabolism (ADAM)" model. *Curr. Drug Metab.* **11**, 716–729 (2010).
20. Marterre, W.F., Hariharan, S., First, M.R. & Alexander, J.W. Gastric bypass in morbidly obese kidney transplant recipients. *Clin. Transplant.* **10**, 414–419 (1996).
21. Chenhsu, R.Y., Wu, Y., Katz, D. & Rayhill, S. Dose-adjusted cyclosporine c2 in a patient with jejunoileal bypass as compared to seven other liver transplant recipients. *Ther. Drug Monit.* **25**, 665–670 (2003).
22. Steimer, W. Performance and specificity of monoclonal immunoassays for cyclosporine monitoring: how specific is specific? *Clin. Chem.* **45**, 371–381 (1999).
23. Venkataramanan, R. *et al.* Biliary excretion of cyclosporine in liver transplant patients. *Transplant. Proc.* **17**, 286–289 (1985).
24. Mehta, M.U. *et al.* Effect of bile on cyclosporin absorption in liver transplant patients. *Br. J. Clin. Pharmacol.* **25**, 579–584 (1988).
25. Wójcikowski, J., Pichard-Garcia, L., Maurel, P. & Daniel, W.A. Contribution of human cytochrome p-450 isoforms to the metabolism of the simplest phenothiazine neuroleptic promazine. *Br. J. Pharmacol.* **138**, 1465–1474 (2003).
26. Lown, K.S. *et al.* Role of intestinal P-glycoprotein (mdr1) in interpatient variation in the oral bioavailability of cyclosporine. *Clin. Pharmacol. Ther.* **62**, 248–260 (1997).
27. Paine, M.F., Davis, C.L., Shen, D.D., Marsh, C.L., Raisys, V.A. & Thummel, K.E. Can oral midazolam predict oral cyclosporine disposition? *Eur. J. Pharm. Sci.* **12**, 51–62 (2000).
28. Knight, G.C., Macris, M.P., Peric, M., Duncan, J.M., Frazier, O.H. & Cooley, D.A. Cyclosporine A pharmacokinetics in a cardiac allograft recipient with a jejuno-ileal bypass. *Transplant. Proc.* **20**, 351–355 (1988).
29. Lennernäs, H. Clinical pharmacokinetics of atorvastatin. *Clin. Pharmacokinet.* **42**, 1141–1160 (2003).
30. Jamei, M., Marciniak, S., Feng, K., Barnett, A., Tucker, G. & Rostami-Hodjegan, A. The Simcyp population-based ADME simulator. *Expert Opin. Drug Metab. Toxicol.* **5**, 211–223 (2009).
31. Mueller, E.A., Kovarik, J.M., van Bree, J.B., Tetzloff, W., Grevel, J. & Kutz, K. Improved dose linearity of cyclosporine pharmacokinetics from a microemulsion formulation. *Pharm. Res.* **11**, 301–304 (1994).
32. Bernareggi, A. & Rowland, M. Physiologic modeling of cyclosporin kinetics in rat and man. *J. Pharmacokinet. Biopharm.* **19**, 21–50 (1991).
33. Jacobsen, W. *et al.* Lactonization is the critical first step in the disposition of the 3-hydroxy-3-methylglutaryl-CoA reductase inhibitor atorvastatin. *Drug Metab. Dispos.* **28**, 1369–1378 (2000).
34. Goosen, T.C. *et al.* Atorvastatin glucuronidation is minimally and nonselectively inhibited by the fibrates gemfibrozil, fenofibrate, and fenofibric acid. *Drug Metab. Dispos.* **35**, 1315–1324 (2007).
35. Prueksaritanont, T., Tang, C., Qiu, Y., Mu, L., Subramanian, R. & Lin, J.H. Effects of fibrates on metabolism of statins in human hepatocytes. *Drug Metab. Dispos.* **30**, 1280–1287 (2002).
36. Howgate, E.M., Rowland Yeo, K., Proctor, N.J., Tucker, G.T. & Rostami-Hodjegan, A. Prediction of *in vivo* drug clearance from *in vitro* data. I: impact of inter-individual variability. *Xenobiotica.* **36**, 473–497 (2006).
37. Lau, Y.Y., Huang, Y., Frassetto, L. & Benet, L.Z. effect of OATP1B transporter inhibition on the pharmacokinetics of atorvastatin in healthy volunteers. *Clin. Pharmacol. Ther.* **81**, 194–204 (2007).
38. Amundsen, R., Christensen, H., Zabihyan, B. & Asberg, A. Cyclosporine A, but not tacrolimus, shows relevant inhibition of organic anion-transporting protein 1B1-mediated transport of atorvastatin. *Drug Metab. Dispos.* **38**, 1499–1504 (2010).
39. Hedberg, J., Hedenström, H., Karlsson, F.A., Edén-Engström, B. & Sundbom, M. Gastric emptying and postprandial PYY response after biliopancreatic diversion with duodenal switch. *Obes. Surg.* **21**, 609–615 (2011).

40. Horowitz, M. *et al.* Measurement of gastric emptying after gastric bypass surgery using radionuclides. *Br. J. Surg.* **69**, 655–657 (1982).
41. Wittgrove, A.C. & Clark, G.W. Laparoscopic gastric bypass, Roux-en-Y- 500 patients: technique and results, with 3-60 month follow-up. *Obes. Surg.* **10**, 233–239 (2000).
42. Smith, C.D., Herkes, S.B., Behrns, K.E., Fairbanks, V.F., Kelly, K.A. & Sarr, M.G. Gastric acid secretion and vitamin B12 absorption after vertical Roux-en-Y gastric bypass for morbid obesity. *Ann. Surg.* **218**, 91–96 (1993).
43. Behrns, K.E., Smith, C.D. & Sarr, M.G. Prospective evaluation of gastric acid secretion and cobalamin absorption following gastric bypass for clinically severe obesity. *Dig. Dis. Sci.* **39**, 315–320 (1994).
44. Hedberg, J., Hedenstrom, H. & Sundbom, M. Wireless pH-metry at the gastrojejunostomy after Roux-en-Y gastric bypass: a novel use of the BRAVO system. *Surg. Endosc.* **25**, 2302–2307 (2005).
45. Saliba, J. *et al.* Roux-en-Y gastric bypass reverses renal glomerular but not tubular abnormalities in excessively obese diabetics. *Surgery* **147**, 282–287 (2010).
46. Chagnac, A., Weinstein, T., Herman, M., Hirsh, J., Gafter, U. & Ori, Y. The effects of weight loss on renal function in patients with severe obesity. *J. Am. Soc. Nephrol.* **14**, 1480–1486 (2003).
47. Navarro-Díaz, M. *et al.* Effect of drastic weight loss after bariatric surgery on renal parameters in extremely obese patients: long-term follow-up. *J. Am. Soc. Nephrol.* **17**, S213–S217 (2006).
48. Serra, A. *et al.* The effect of bariatric surgery on adipocytokines, renal parameters and other cardiovascular risk factors in severe and very severe obesity: 1-year follow-up. *Clin. Nutr.* **25**, 400–408 (2006).

Supplementary information accompanies this paper on the *Pharmacometrics & Systems Pharmacology* website (http://www.nature.com/psp)

8.3.2 Compound Simcyp Simulator template input properties

Table 8.4. Drug specific parameters for atorvastatin acid.

Parameters	Value	References
PhysChem		
MW (g/mol)	546	(NCBI, 2011)
$LogP_{o:w}$	4.47	(Lennernas, 2003)
Acid-base nature	Acid	
pKa	4.46	
Blood binding		
BP	0.61	(Watanabe *et al.*)
fu_p	0.02	(Gibson, 1997)
Dissolution		
Solubility input	Measured	(Lennernas, 2003)
Aqueous solubility, pH 6 (mg/mL)	1.23	
Particle size (µm)	10	
Absorption		
Caco-2 pH7.4:7.4 (10^{-4} cm/s)	P_{app}: 7.9 ($P_{eff,man}$: 4.9)	(Wu *et al.*, 2000)
Distribution		
V_{ss} (L/kg)	4.76	(Gibson, 1997)
Distribution model	Full PBPK	
Prediction method	Rodgers *et al*.	(Rodgers *et al.*, 2005; Rodgers and Rowland, 2006)
Metabolism		
rCYP2C8: Para-OH		(Jacobsen *et al.*, 2000)
CL_{int} (µL/min/mg protein)	4.5	
V_{max} (pmol/min/pmol CYP)	0.29	
K_m (µM)	35.9	
ISEF	0.98	
rCYP3A4: Para-OH		
CL_{int} (uL/min/mg protein)	219	
V_{max} (pmol/min/pmol CYP)	29.8	
K_m (µM)	25.6	
ISEF	0.24	
rCYP3A4: Ortho-OH		
CL_{int} (µL/min/mg protein)	184	
V_{max} (pmol/min/pmol CYP)	29.3	
K_m (µM)	29.7	
ISEF	0.24	
UGT1A1		
CL_{int} (µL/min/mg protein)	5.23	
Acyl glucuronidation (Lactonisation)		
CL_{int} (µL/min/mg protein)	7.22	
Non-UGT (Lactonisation)		
CL_{int} (µL/min/mg protein)	200	
Transport		
P-glycoprotein (ABCB1; Apical efflux, intestine)		(Wu *et al.*, 2000)
J_{max} (pmol/min)	141[B]	
K_m (µM)	115	
OATP1B1 (SLCO1B1; Sinusoidal uptake, liver)		(Lau *et al.*, 2007; Amundsen *et al.*, 2010)
Jmax (pmol/min/10^6 hepatocytes)	1612[B]	
K_m (µM)	0.93	

BP =Blood to plasma ratio, fu_p=fraction unbound in plasma, ISEF=Inter System Extrapolation Factor, CLpd=Passive diffusion clearance.
[A]Predicted from Caco-2 permeability data.
[B]Derived utilising the parameter estimation toolbox within the Simcyp Simulator based on 12 healthy volunteers receiving atorvastatin acid 40 mg (Lilja *et al.*, 1999).

Table 8.5. Drug specific parameters for cyclosporine.

Parameters	Value	References
PhysChem		
MW (g/mol)	1202	(Turner, 2008; NCBI, 2011)
$LogP_{o:w}$	4.3	
Acid-base nature	Neutral	
pKa	NA	
Blood binding		
BP	1.36	(Turner, 2008)
fu_p	0.037	
Dissolution		
Sandimmune		(Andrysek, 2003; Persson *et al.*, 2005)
Solubility method	Human intestinal fluids	
Solubility (mg/mL)	0.011	
Particle Size (um)	1.84	
Supersaturation ratio	10	
Neoral		
Solubility method	Human intestinal fluids	
Solubility (mg/mL)	0.011	
Particle Size (um)	0.018	
Supersaturation ratio	1000	
Absorption		
$P_{eff,man}$	1.65	(Turner, 2008)
Distribution		
V_{ss} (L/kg)	5.6	(Bernareggi and Rowland, 1991)
Distribution model	Full PBPK	
Prediction method	Rat Kp's, measured.	
Metabolism		
CYP3A4		(Turner, 2008)
CL_{int} (uL/min/mg protein)	219	
V_{max} (pmol/min/mg microsomal protein)	29.8	
K_m (μM)	25.6	

BP =Blood to plasma ratio, fu_p=fraction unbound in plasma, $P_{eff,man}$=effective human jejunal permeability, V_{ss}=Volume of distribution at steady state following intravenous infusion.

8.3.3 Supplementary results

Simulated oral drug bioavailability of cyclosporine (Neoral®) post Roux-en-Y gastric bypass (Figure 8.1).

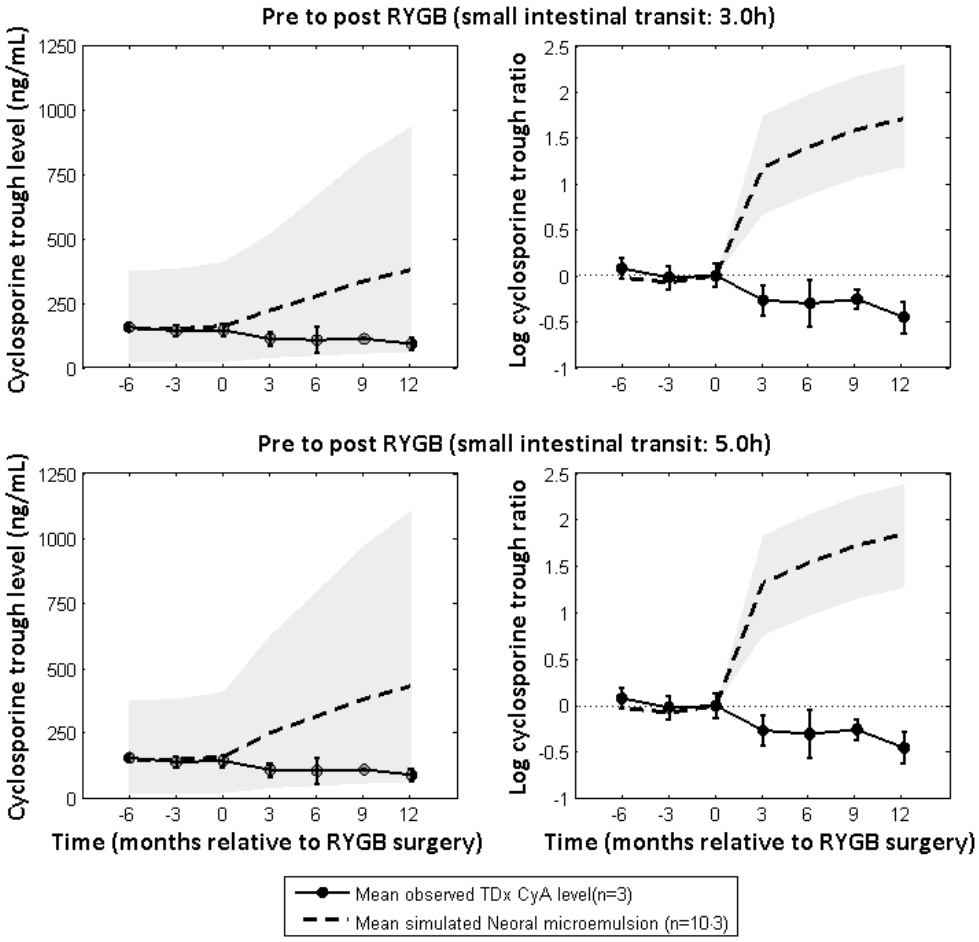

Figure 8.1. Mean and standard deviation of observed cyclosporine (CsA) TDx trough levels at steady state pre to post Roux-en-Y gastric bypass (RYGB) at -6, -3, 0, 3, 6, 9 and 12 months relative to RYGB surgical event (0 months). Time points from -6 to 12 months correspond to dose levels of: 1.7, 1.7, 1.8, 2.4, 2.8, 3.2, 3.5 mg/kg/day respectively (n patients=3) administered twice daily. Observed data is compared to simulated 50, 95 and 5% prediction interval, indicated by grey area, of cyclosporine Neoral® trough levels (n patients=10·3), A: Simulated post RYGB at a small intestinal transit time (SIT) of 3.0h, B: Log normalised simulated CsA trough ratio as compared to 0 months (RYGB SIT=3.0h), C: Simulated CsA trough levels at RYGB SIT of 5.0h, D: Log normalised simulated CsA trough ratio as compared to 0 months (RYGB SIT=5.0h) (Marterre *et al.*, 1996).

Simulated oral drug bioavailability of cyclosporine (Neoral®) post jejunoileal bypass at a small intestinal transit time of 0.7h (Figure 8.2).

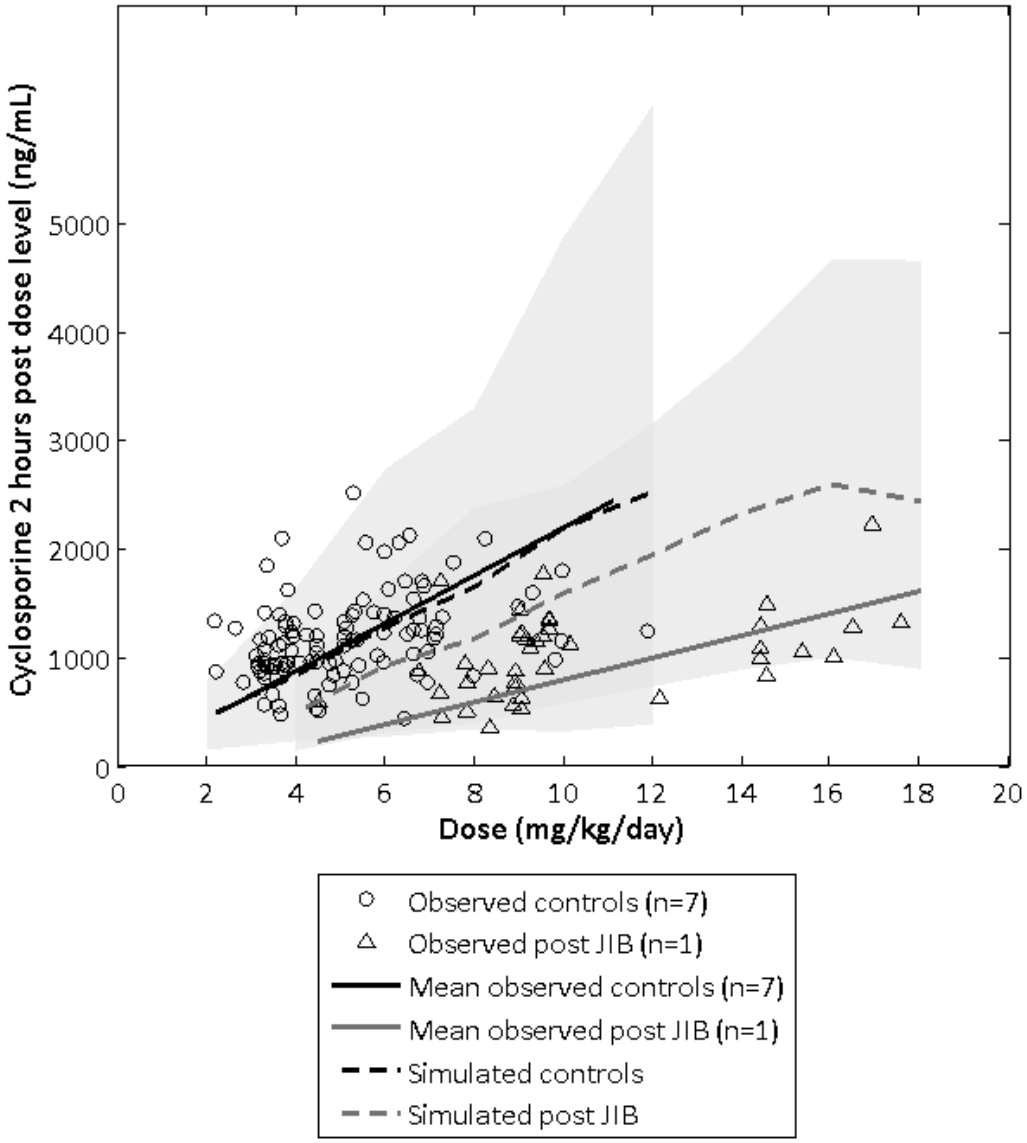

Figure 8.2. Observed mean blood concentration of cyclosporine microemulsion (Sandimmune® Neoral®, Novartis) at steady state 2 hours post dosing in controls (n=7) and one patient (n=1) post jejunoileal bypass (JIB) as compared to simulated sex and age matched controls (n=300) and post JIB (n patients=800) at a small intestinal transit time of 0.7 hours over dose range of 300 to 1,000 mg including, where 5, 50 and 95% prediction intervals are indicated by grey areas (Chenhsu *et al.*, 2003).

Simulated oral drug bioavailability of atorvastatin post Roux-en-Y gastric bypass at a small intestinal transit time of 5.0h (Figure 8.3).

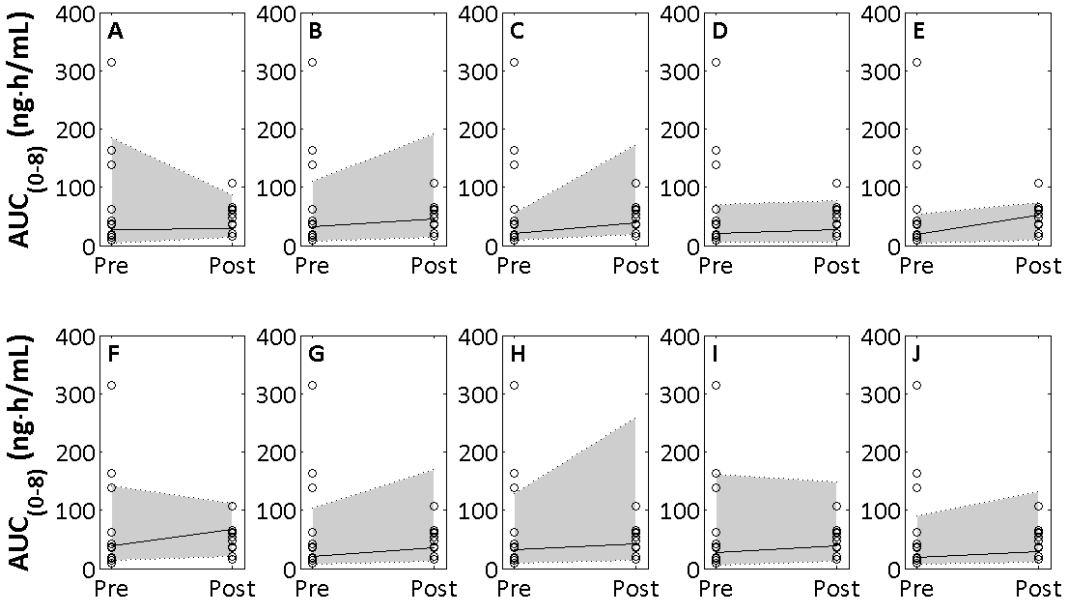

Figure 8.3. Simulated 50, 95 and 5% prediction interval (indicated by grey areas) of oral drug exposure of atorvastatin acid in randomised trials of age, sex, dose and BMI (Body Mass Index) matched patients pre to post Roux-en-Y gastric bypass surgery (small intestinal transit=5.0h) as compared to observed data A-J: Ten randomised simulated trials consisting of 10 individuals in each trial (n individuals=10·12), as compared to observed (n=12; ○) (Skottheim *et al.*, 2009).

Simulated oral drug bioavailability of atorvastatin acid in morbidly obese prior to biliopancreatic diversion with duodenal switch as compared to observed, utilising visual predictive check (VPC) (Skottheim *et al.*, 2010).

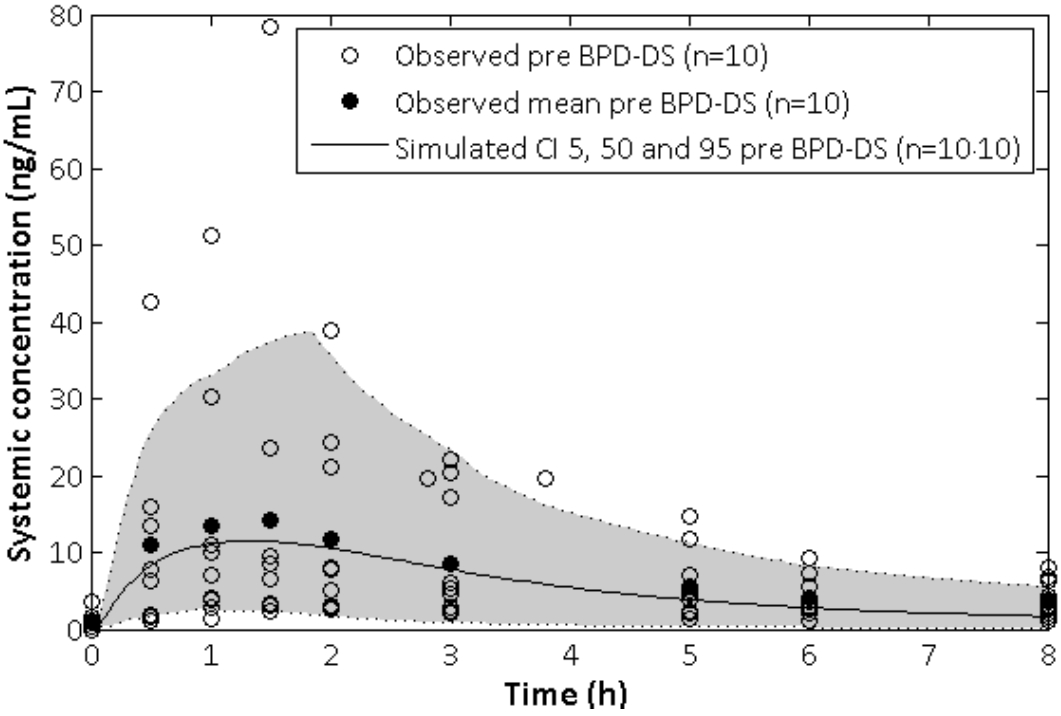

Figure 8.4. Age, sex, weight and dose matched simulated mean, 95th and 5th percentile of systemic plasma concentration of atorvastatin acid following orally administered atorvastatin acid immediate release (IR) 20-80 mg (n individuals=10·10) as compared to observed data (n=10) (Skottheim *et al.*, 2010).

8.3.4 References

Amundsen R, Christensen H, Zabihyan B, and Asberg A (2010) Cyclosporine A, but not tacrolimus, shows relevant inhibition of organic anion-transporting protein 1B1-mediated transport of atorvastatin. *Drug Metab Dispos* **38:**1499-1504.

Andrysek T (2003) Impact of physical properties of formulations on bioavailability of active substance: current and novel drugs with cyclosporine. *Molecular immunology* **39:**1061-1065.

Bernareggi A and Rowland M (1991) Physiologic modeling of cyclosporin kinetics in rat and man. *J Pharmacokinet Biopharm* **19:**21-50.

Chenhsu RY, Wu Y, Katz D, and Rayhill S (2003) Dose-adjusted cyclosporine c2 in a patient with jejunoileal bypass as compared to seven other liver transplant recipients. *Ther Drug Monit* **25:**665-670.

Gibson DM, Stern, R.H., and Whitfield, L.R. (1997) Absolute bioavailability of atorvastatin in man. *Pharm Res* **14:**S-253.

Jacobsen W, Kuhn B, Soldner A, Kirchner G, Sewing KF, Kollman PA, Benet LZ, and Christians U (2000) Lactonization is the critical first step in the disposition of the 3-hydroxy-3-methylglutaryl-CoA reductase inhibitor atorvastatin. *Drug Metab Dispos* **28:**1369-1378.

Lau YY, Huang Y, Frassetto L, and Benet LZ (2007) effect of OATP1B transporter inhibition on the pharmacokinetics of atorvastatin in healthy volunteers. *Clin Pharmacol Ther* **81:**194-204.

Lennernas H (2003) Clinical pharmacokinetics of atorvastatin. *Clin Pharmacokinet* **42:**1141-1160.

Lilja JJ, Kivisto KT, and Neuvonen PJ (1999) Grapefruit juice increases serum concentrations of atorvastatin and has no effect on pravastatin. *Clin Pharmacol Ther* **66:**118-127.

Marterre WF, Hariharan S, First MR, and Alexander JW (1996) Gastric bypass in morbidly obese kidney transplant recipients. *Clin Transplant* **10:**414-419.

NCBI (2011) PubChem Public Chemical Database, National Center of Biotechnology Information, USA.

Persson EM, Gustafsson AS, Carlsson AS, Nilsson RG, Knutson L, Forsell P, Hanisch G, Lennernas H, and Abrahamsson B (2005) The effects of food on the dissolution of poorly soluble drugs in human and in model small intestinal fluids. *Pharm Res* **22:**2141-2151.

Rodgers T, Leahy D, and Rowland M (2005) Physiologically based pharmacokinetic modeling 1: predicting the tissue distribution of moderate-to-strong bases. *J Pharm Sci* **94:**1259-1276.

Rodgers T and Rowland M (2006) Physiologically based pharmacokinetic modelling 2: predicting the tissue distribution of acids, very weak bases, neutrals and zwitterions. *J Pharm Sci* **95:**1238-1257.

Skottheim IB, Jakobsen GS, Stormark K, Christensen H, Hjelmesaeth J, Jenssen T, Asberg A, and Sandbu R (2010) Significant increase in systemic exposure of atorvastatin after biliopancreatic diversion with duodenal switch. *Clin Pharmacol Ther* **87:**699-705.

Skottheim IB, Stormark K, Christensen H, Jakobsen GS, Hjelmesaeth J, Jenssen T, Reubsaet JL, Sandbu R, and Asberg A (2009) Significantly altered systemic exposure to atorvastatin acid following gastric bypass surgery in morbidly obese patients. *Clin Pharmacol Ther* **86:**311-318.

Turner D (2008) Simcyp® User Manual Version 8.

Watanabe T, Kusuhara H, Maeda K, Kanamaru H, Saito Y, Hu Z, and Sugiyama Y Investigation of the rate-determining process in the hepatic elimination of HMG-CoA reductase inhibitors in rats and humans. *Drug Metab Dispos* **38:**215-222.

Wu X, Whitfield LR, and Stewart BH (2000) Atorvastatin transport in the Caco-2 cell model: contributions of P-glycoprotein and the proton-monocarboxylic acid co-transporter. *Pharm Res* **17:**209-215.

8.4 Assessing the turnover of the intestinal epithelia in pre-clinical species and human

8.4.1 Supplementary enterocyte turnover data in pre-clinical species and human

Table 8.6. Enterocyte turnover in the small intestine of the mouse.

Segment	Turnover (days)	SD	N	Method	References
Duodenum	2.81	0.23	16	H-Thymidine, *in vivo*	(Ferraris *et al.*, 1992)
Duodenum	3.09	0.31	16	H-Thymidine, *in vivo*	(Ferraris *et al.*, 1992)
Duodenum	2.43	0.13	NA	H-Thymidine, *in vivo*	(Cheng and Bjerknes, 1982)
Duodenum	2.35	0.56	5	H-Thymidine, *in vivo*	(Merzel and Leblond, 1969)
Duodenum	3.3	NA	8	H-Thymidine, *in vivo*	(Cheng and Leblond, 1974)
Duodenum	2	NA	1	H-Thymidine, *in vivo*	(Walker and Leblond, 1958)
Duodenum	2.08	NA	6	H-Thymidine, *in vivo*	(Grey, 1968)
Duodenum	1.71	NA	20	H-Thymidine, *in vivo*	(Lesher *et al.*, 1961)
Duodenum	2	NA	20	H-Thymidine, *in vivo*	(Lesher *et al.*, 1961)
Duodenum	2.21	NA	20	H-Thymidine, *in vivo*	(Lesher *et al.*, 1961)
Jejunum	3.17	0.33	16	H-Thymidine, *in vivo*	(Ferraris *et al.*, 1992)
Jejunum	2.85	0.31	16	H-Thymidine, *in vivo*	(Ferraris *et al.*, 1992)
Jejunum	2.59	0.18	NA	H-Thymidine, *in vivo*	(Cheng and Bjerknes, 1982)
Jejunum	3.4	NA	8	H-Thymidine, *in vivo*	(Cheng and Leblond, 1974)
Jejunum	4	NA	20	H-Thymidine, *in vivo*	(Thompson *et al.*, 1990)
Jejunum	1.83	NA	34	H-Thymidine, *in vivo*	(Fry *et al.*, 1961)
Jejunum	2.17	NA	34	H-Thymidine, *in vivo*	(Fry *et al.*, 1961)
Jejunum	2.21	NA	52	H-Thymidine, *in vivo*	(Fry *et al.*, 1961)
Ileum	2.6	0.38	16	H-Thymidine, *in vivo*	(Ferraris *et al.*, 1992)
Ileum	2.56	0.35	16	H-Thymidine, *in vivo*	(Ferraris *et al.*, 1992)
Ileum	2.43	0.12	NA	H-Thymidine, *in vivo*	(Cheng and Bjerknes, 1982)
Ileum	2	NA	NA	H-Thymidine, *in vivo*	(Quastler and Sherman, 1959)
Ileum	1.29	NA	10	H-Thymidine, *in vivo*	(Fry *et al.*, 1962)
Ileum	1.38	NA	8	H-Thymidine, *in vivo*	(Fry *et al.*, 1962)
Ileum	1.29	NA	10	H-Thymidine, *in vivo*	(Fry *et al.*, 1962)
Jejunum and ileum	3	NA	NA	H-Thymidine, *in vivo*	(Leblond and Messier, 1958)
NA	2.67	NA	7	H-Thymidine, *in vivo*	(Smith *et al.*, 1984)

NA=Not applicable.

Table 8.7. Enterocyte turnover in the small intestine of the rat.

Segment	Turnover (days)	SD	N	Method	References
Proximal SI	1.24	NA	2	H-Thymidine, *in vivo*	(Menge *et al.*, 1982)
Proximal SI	1.97	NA	2	H-Thymidine, *in vivo*	(Menge *et al.*, 1982)
Proximal SI	1.71	NA	2	H-Thymidine, *in vivo*	(Menge *et al.*, 1982)
Proximal SI	2.01	NA	2	H-Thymidine, *in vivo*	(Menge *et al.*, 1982)
Proximal SI	1.86	NA	2	H-Thymidine, *in vivo*	(Menge *et al.*, 1982)
Duodenum	1.57	NA	4	Histological study	(Leblond and Stevens, 1948)
Duodenum	1.2	0.2	4	C-glycoside, *in vivo*	(Macallan *et al.*, 1998)
Duodenum	1.59	NA	5	BrdUrd, *in vivo*	(Qi *et al.*, 2009)
Duodenum	1.78	NA	12	H-Thymidine, *in vivo*	(Holt *et al.*, 1983)
Duodenum	1.98	NA	12	H-Thymidine, *in vivo*	(Holt *et al.*, 1983)
Duodenum	2.5	NA	8	H-Thymidine, *in vivo*	(Loran and Althausen, 1960)
Duodenum	2.22	NA	6	H-Thymidine, *in vivo*	(Koldovsky *et al.*, 1966)
Median SI	2.07	NA	2	H-Thymidine, *in vivo*	(Menge *et al.*, 1982)
Median SI	2.3	NA	2	H-Thymidine, *in vivo*	(Menge *et al.*, 1982)
Median SI	1.88	NA	2	H-Thymidine, *in vivo*	(Menge *et al.*, 1982)
Median SI	1.68	NA	2	H-Thymidine, *in vivo*	(Menge *et al.*, 1982)
Median SI	1.44	NA	2	H-Thymidine, *in vivo*	(Menge *et al.*, 1982)
Proximal jejunum	1.5	NA	5	BrdUrd, *in vivo*	(Qi *et al.*, 2009)
Jejunum	2.29	NA	6	H-Thymidine, *in vivo*	(Thomson *et al.*, 1994)
Jejunum	2.21	NA	8	H-Thymidine, *in vivo*	(Thomson *et al.*, 1994)
Jejunum	1.54	NA	6	H-Thymidine, *in vivo*	(Thomson *et al.*, 1994)
Jejunum	2.33	NA	6	H-Thymidine, *in vivo*	(Thomson *et al.*, 1994)
Jejunum	2.25	NA	7	H-Thymidine, *in vivo*	(King *et al.*, 1983)
Jejunum	2.38	NA	7	H-Thymidine, *in vivo*	(King *et al.*, 1983)
Jejunum	2.04	NA	3	H-Thymidine, *in vivo*	(Cheeseman, 1986)
Jejunum	1.3	NA	NA	NA	(Bertalanffy and Lau, 1962)
Jejunum	2.06	NA	12	H-Thymidine, *in vivo*	(Holt *et al.*, 1983)
Jejunum	2.2	NA	12	H-Thymidine, *in vivo*	(Holt *et al.*, 1983)
Jejunum	2.08	NA	8	H-Thymidine, *in vivo*	(Loran and Althausen, 1960)
Jejunum	2.22	NA	6	H-Thymidine, *in vivo*	(Koldovsky *et al.*, 1966)
Jejunum	3.94	0.54	10	H-Thymidine, *in vivo*	(Shambaugh *et al.*, 1967)

Jejunum	1.3	NaN	16	Colchine technique, *in vivo*	(Bertalanffy, 1960)
Distal jejunum	1.64	NA	5	BrdUrd, *in vivo*	(Qi *et al.*, 2009)
Distal SI	2.5	NA	2	H-Thymidine, *in vivo*	(Menge *et al.*, 1982)
Distal SI	3.05	NA	2	H-Thymidine, *in vivo*	(Menge *et al.*, 1982)
Distal SI	2.7	NA	2	H-Thymidine, *in vivo*	(Menge *et al.*, 1982)
Distal SI	2.48	NA	2	H-Thymidine, *in vivo*	(Menge *et al.*, 1982)
Distal SI	1.45	NA	2	H-Thymidine, *in vivo*	(Menge *et al.*, 1982)
Proximal ileum	1.62	NA	5	BrdUrd, *in vivo*	(Qi *et al.*, 2009)
Ileum	1.88	NA	6	H-Alanine and lysine uptake	(Menge *et al.*, 1983)
Ileum	1.35	NA	4	Histological study	(Leblond and Stevens, 1948)
Ileum	1.64	NA	12	H-Thymidine, *in vivo*	(Holt *et al.*, 1983)
Ileum	1.37	NA	12	H-Thymidine, *in vivo*	(Holt *et al.*, 1983)
Ileum	1.6	NA	25	Vincristine, *in vivo*	(Alam *et al.*, 1994)
Ileum	2.82	NA	8	H-Thymidine, *in vivo*	(Loran and Althausen, 1960)
Ileum	2.5	NA	6	H-Thymidine, *in vivo*	(Koldovsky *et al.*, 1966)
Distal ileum	1.43	NA	5	BrdUrd, *in vivo*	(Qi *et al.*, 2009)
NA	2.1	NA	5	Colchine technique, *in vivo*	(Altmann and Enesco, 1967)

NA=Not applicable, SI=Small intestine.

Table 8.8. Enterocyte turnover in the human gastrointestinal tract.

Segment	Turnover (Days)	SD	N	Method	References
Oesophagus	6.35	2.08	1	H-Thymidine, *in vivo*	(Bell *et al.*, 1967)
Stomach	5	1	2	H-Thymidine, *in vivo*	(Macdonald *et al.*, 1964)
Stomach	3.5	0.5	3	H-Thymidine, *in vivo*	(Lipkin *et al.*, 1963b)
Stomach	3.46	1.21	16	BrdUrd, *in vivo*	(Patel *et al.*, 1993)
Stomach	2.58	1.17	10	BrdUrd, *in vivo*	(Patel *et al.*, 1993)
Stomach	3.43	1.14	4	H-Thymidine, *in vivo*	(Wright *et al.*, 1977)
Duodenum	5.42	NA	1	H-Thymidine, *in vivo*	(Macdonald *et al.*, 1964)
Duodenum	5.5	0.5	1	H-Thymidine, *in vivo*	(Macdonald *et al.*, 1964)
Duodenum	2	NA	56	Histological study	(Bertalanffy and Nagy, 1961)
Duodenum	1.26	0.17	2	H-Thymidine, *in vivo*	(Weinstein, 1974)
Jejunum	5	NA	3	H-Thymidine, *in vivo*	(Shorter *et al.*, 1964)
Ileum	1.4	NA	6	Histological study	(Bullen *et al.*, 2006)
Ileum	3	NA	3	H-Thymidine, *in vivo*	(Lipkin *et al.*, 1963b)
Colon	1	NA	2	H-Thymidine, *in vivo*	(Lipkin *et al.*, 1963a)
Colon	0.83	NA	3	H-Thymidine, *in vivo*	(Lipkin *et al.*, 1963b)
Colon	3.41	NA	66	BrdUrd, *in vivo*	(Potten *et al.*, 1992)
Colon	1.63	NA	1	H-Thymidine, *in vivo*	(Lipkin, 1969)
Colon	3.04	0.25	8	H-Thymidine, *in vitro*	(Bleiberg and Galand, 1976)
Rectum	5.5	0.5	2	H-Thymidine, *in vivo*	(Macdonald *et al.*, 1964)
Rectum	7	1	1	H-Thymidine, *in vivo*	(Cole and Mc, 1961)
Rectum	3.66	0.42	18	Histological study	(Shorter *et al.*, 1966)
Rectum	4.73	0.59	9	Histological study	(Shorter *et al.*, 1966)
Rectum	5.45	0.61	17	Histological study	(Shorter *et al.*, 1966)
Rectum	0.83	NA	3	H-Thymidine, *in vivo*	(Lipkin *et al.*, 1963b)
Rectum	3	NA	3	H-Thymidine, *in vivo*	(Shorter *et al.*, 1964)
Rectum	3.5	0.5	16	H-Thymidine, *in vitro*	(Deschner *et al.*, 1963)
Rectum	3.75	NA	8	H-Thymidine, *in vitro*	(Bleiberg *et al.*, 1970)

NA=Not applicable

8.4.2 References

Alam M, Midtvedt T, and Uribe A (1994) Differential cell kinetics in the ileum and colon of germfree rats. *Scand J Gastroenterol* **29:**445-451.

Altmann GG and Enesco M (1967) Cell number as a measure of distribution and renewal of epithelial cells in the small intestine of growing and adult rats. *Am J Anat* **121:**319-336.

Bell B, Almy TP, and Lipkin M (1967) Cell proliferation kinetics in the gastrointestinal tract of man. 3. Cell renewal in esophagus, stomach, and jejunum of a patient with treated pernicious anemia. *Journal of the National Cancer Institute* **38:**615-628.

Bertalanffy FD (1960) Mitotic rates and renewal times of the digestive tract epithelia in the rat. *Acta anatomica* **40:**130-148.

Bertalanffy FD and Lau C (1962) Cell Renewal. *International Journal of Cytology* **13:**357-366.
Bertalanffy FD and Nagy KP (1961) Mitotic activity and renewal rate of the epithelial cells of human duodenum. *Acta anatomica* **45:**362-370.
Bleiberg H and Galand P (1976) In vitro autoradiographic determination of cell kinetic parameters in adenocarcinomas and adjacent healthy mucosa of the human colon and rectum. *Cancer Res* **36:**325-328.
Bleiberg H, Mainguet P, Galand P, Chretien J, and Dupont-Mairesse N (1970) Cell renewal in the human rectum. In vitro autoradiographic study on active ulcerative colitis. *Gastroenterology* **58:**851-855.
Bullen TF, Forrest S, Campbell F, Dodson AR, Hershman MJ, Pritchard DM, Turner JR, Montrose MH, and Watson AJ (2006) Characterization of epithelial cell shedding from human small intestine. *Lab Invest* **86:**1052-1063.
Cheeseman CI (1986) Expression of amino acid and peptide transport systems in rat small intestine. *Am J Physiol* **251:**G636-641.
Cheng H and Bjerknes M (1982) Whole population cell kinetics of mouse duodenal, jejunal, ileal, and colonic epithelia as determined by radioautography and flow cytometry. *Anat Rec* **203:**251-264.
Cheng H and Leblond CP (1974) Origin, differentiation and renewal of the four main epithelial cell types in the mouse small intestine. V. Unitarian Theory of the origin of the four epithelial cell types. *Am J Anat* **141:**537-561.
Cole JW and Mc KA (1961) Observations of cell renewal in human rectal mucosa in vivo with thymidine-H3. *Gastroenterology* **41:**122-125.
Deschner E, Lewis CM, and Lipkin M (1963) In Vitro Study of Human Rectal Epithelial Cells. I. Atypical Zone of H3 Thymidine Incorporation in Mucosa of Multiple Polyposis. *J Clin Invest* **42:**1922-1928.
Ferraris RP, Villenas SA, and Diamond J (1992) Regulation of brush-border enzyme activities and enterocyte migration rates in mouse small intestine. *Am J Physiol* **262:**G1047-1059.
Fry RJ, Lesher S, and Kohn HI (1961) Age effect on cell-transit time in mouse jejunal epithelium. *Am J Physiol* **201:**213-216.
Fry RJ, Lesher S, and Kohn HI (1962) Influence of age on the transit time of cells of the mouse intestinal epithelium. III. Ileum. *Lab Invest* **11:**289-293.
Grey RD (1968) Epithelial cell migration in the intestine of the young mouse. *Developmental biology* **18:**501-504.
Holt PR, Kotler DP, and Pascal RR (1983) A simple method for determining epithelial cell turnover in small intestine. Studies in young and aging rat gut. *Gastroenterology* **84:**69-74.
King IS, Paterson JY, Peacock MA, Smith MW, and Syme G (1983) Effect of diet upon enterocyte differentiation in the rat jejunum. *J Physiol* **344:**465-481.
Koldovsky O, Sunshine P, and Kretchmer N (1966) Cellular migration of intestinal epithelia in suckling and weaned rats. *Nature* **212:**1389-1390.
Leblond CP and Messier B (1958) Renewal of chief cells and goblet cells in the small intestine as shown by radioautography after injection of thymidine-H3 into mice. *Anat Rec* **132:**247-259.
Leblond CP and Stevens CE (1948) The constant renewal of the intestinal epithelium in the albino rat. *Anat Rec* **100:**357-377.
Lesher S, Fry RJ, and Kohn HI (1961) Influence of age on transit time of cells of mouse intestinal epithelium. I. Duodenum. *Lab Invest* **10:**291-300.
Lipkin M (1969) Cell proliferation in gastrointestinal disease. *National Cancer Institute monograph* **30:**199-207.

Lipkin M, Bell B, and Sherlock P (1963a) Cell Proliferation Kinetics in the Gastrointestinal Tract of Man. I. Cell Renewal in Colon and Rectum. *J Clin Invest* **42:**767-776.

Lipkin M, Sherlock P, and Bell B (1963b) Cell Proliferation Kinetics in the Gastrointestinal Tract of Man. II. Cell Renewal in Stomach, Ileum, Colon, and Rectum. *Gastroenterology* **45:**721-729.

Loran MR and Althausen TL (1960) Cellular proliferation of intestinal epithelia in the rat two months after partial resection of the ileum. *The Journal of biophysical and biochemical cytology* **7:**667-672.

Macallan DC, Fullerton CA, Neese RA, Haddock K, Park SS, and Hellerstein MK (1998) Measurement of cell proliferation by labeling of DNA with stable isotope-labeled glucose: studies in vitro, in animals, and in humans. *Proc Natl Acad Sci U S A* **95:**708-713.

Macdonald WC, Trier JS, and Everett NB (1964) Cell Proliferation and Migration in the Stomach, Duodenum, and Rectum of Man: Radioautographic Studies. *Gastroenterology* **46:**405-417.

Menge H, Hopert R, Alexopoulos T, and Riecken EO (1982) Three-dimensional structure and cell kinetics at different sites of rat intestinal remnants during the early adaptive response to resection. *Research in experimental medicine Zeitschrift fur die gesamte experimentelle Medizin einschliesslich experimenteller Chirurgie* **181:**77-94.

Menge H, Sepulveda FV, and Smith MW (1983) Cellular adaptation of amino acid transport following intestinal resection in the rat. *J Physiol* **334:**213-223.

Merzel J and Leblond CP (1969) Origin and renewal of goblet cells in the epithelium of the mouse small intestine. *Am J Anat* **124:**281-305.

Patel S, Rew DA, Taylor I, Potten CS, Owen C, and Roberts SA (1993) Study of the proliferation in human gastric mucosa after in vivo bromodeoxyuridine labelling. *Gut* **34:**893-896.

Potten CS, Kellett M, Rew DA, and Roberts SA (1992) Proliferation in human gastrointestinal epithelium using bromodeoxyuridine in vivo: data for different sites, proximity to a tumour, and polyposis coli. *Gut* **33:**524-529.

Qi WM, Yamamoto K, Yokoo Y, Miyata H, Inamoto T, Udayanga KG, Kawano J, Yokoyama T, Hoshi N, and Kitagawa H (2009) Histoplanimetrical study on the relationship between the cell kinetics of villous columnar epithelial cells and the proliferation of indigenous bacteria in rat small intestine. *The Journal of veterinary medical science / the Japanese Society of Veterinary Science* **71:**463-470.

Quastler H and Sherman FG (1959) Cell population kinetics in the intestinal epithelium of the mouse. *Experimental cell research* **17:**420-438.

Shambaugh GE, MacNair DS, and Beisel WR (1967) Small-bowel epithelial migration during a generalized nonenteric infection in the rat. *Am J Dig Dis* **12:**403-408.

Shorter RG, Moertel CG, Titus JL, and Reitemeier RJ (1964) Cell Kinetics in the Jejunum and Rectum of Man. *Am J Dig Dis* **9:**760-763.

Shorter RG, Spencer RJ, and Hallenbeck GA (1966) Kinetic studies of the epithelial cells of the rectal mucosa in normal subjects and patients with ulcerative colitis. *Gut* **7:**593-596.

Smith MW, Patterson JY, and Peacock MA (1984) A comprehensive description of brush border membrane development applying to enterocytes taken from a wide variety of mammalian species. *Comparative biochemistry and physiology A, Comparative physiology* **77:**655-662.

Thompson EM, Price YE, and Wright NA (1990) Kinetics of enteroendocrine cells with implications for their origin: a study of the cholecystokinin and gastrin subpopulations combining tritiated thymidine labelling with immunocytochemistry in the mouse. *Gut* **31:**406-411.

Thomson AB, Cheeseman CI, Keelan M, Fedorak R, and Clandinin MT (1994) Crypt cell production rate, enterocyte turnover time and appearance of transport along the jejunal villus of the rat. *Biochimica et biophysica acta* **1191:**197-204.

Walker BE and Leblond CP (1958) Sites of nucleic acid synthesis in the mouse visualized by radioautography after administration of C14-labelled adenine and thymidine. *Experimental cell research* **14:**510-531.

Weinstein WM (1974) Epithelial cell renewal of the small intestinal mucosa. *The Medical clinics of North America* **58:**1375-1386.

Wright NA, Britton DC, Bone G, and Appleton DR (1977) An in vivo stathmokinetic study of cell proliferation in human gastric carcinoma and gastric mucosa. *Cell and tissue kinetics* **10:**429-436.

8.5 Development and assessment of a nested enzyme-within-enterocyte turnover model for mechanism-based inhibition in the small intestine

8.5.1 Supplementary data for sensitivity analysis

Table 8.10. Dose levels and observed absorption rate constants (k_a) of drugs included in the 17th WHO model list of Essential Medicines.

Drugs	Low dose (µmoles)*	Medium dose (µmoles)*	High dose (µmoles)*	(h^{-1})	References
Abacavir		1047.73		1.65	(Weller *et al.*, 2000)
Acetazolamide		1124.88		0.82	(Yano *et al.*, 1998)
Acetylsalicylic acid	555.07		2775.35	0.85	(Iiaz *et al.*, 2003)
Albendazole		1507.55		1.41	(Cotting *et al.*, 1990)
Allopurinol	734.69		2204.08	1.64	(Turnheim *et al.*,
Amiloride		21.77		1.77	(Savic *et al.*, 2007)
Amiodarone	154.96	309.93	619.86		
Amitriptyline		90.12		0.41	(Kukes *et al.*, 2009)
Amlodipine		12.23		0.79	(Flynn *et al.*, 2006)
Amodiaquine	189.68	379.36	758.72	1.41	(Jullien *et al.*, 2010)
Amoxicillin	684.17		1368.35	0.79	(Arancibia *et al.*,
Artemether		67.03		1.41	(Ezzet *et al.*, 1998)
Atazanavir	141.87	212.81	425.62	1.02	(Solas *et al.*, 2008)
Azathioprine		180.33			
Benznidazole		384.25			
Biperiden	6.42	6.42	6.42		
Bisoprolol	3.84		15.36		
Caffeine				2.36	(Kamimori *et al.*,
Carbamazepine	423.25		846.49	0.29	(Ismail and Rahman,
Cefixime		882.13		0.35	(Brittain *et al.*, 1985)

Additional references: (BNF, 2011; PubChem, 2011; WHO, 2011)

Table 8.10. Dose levels and observed absorption rate constants (ka) of drugs included in the 17th WHO model list of Essential Medicines.

Drugs	Low dose (µmoles)*	Medium dose (µmoles)*	High dose (µmoles)*	k_a (h^{-1})	References
Chloramphenicol		773.68			
Chloroquine	312.62		468.94	1.40	(Karunajeewa *et al.*, 2010)
Chlorpromazine	31.36	117.60	313.61	0.53	(Whitfield *et al.*, 1978)
Ciprofloxacin		754.51		2.70	(Sanchez Navarro *et al.*,
Clarithromycin		668.49		0.56	(Abduljalil *et al.*, 2009)
Clofazimine	105.62		211.24	0.99	(Nix *et al.*, 2004)
Clomipramine	31.76		79.40		
Cloxacillin	1147.10		2294.20		
Codeine		100.21			
Cyclizine		187.70		1.54	(Walker, 1995)
Cyclophosphamide		95.75			
Dapsone	100.68	201.37	402.74	0.93	(Simpson *et al.*, 2006)
Dexamethasone		5.10			
Diazepam	7.02	17.56	35.12		
Didanosine	105.83	423.32	846.64	1.51	(Velasque *et al.*, 2007)
Diethylcarbamazine	25.09		50.18	2.23	(Bolla *et al.*, 2002)
Digoxin	0.01		0.32		
Diloxanide		2136.03			
Doxycycline	112.50		225.01		
Efavirenz	1900.69	1900.69	1900.69	1.39	(Pfister *et al.*, 2003)

Additional references: (BNF, 2011; PubChem, 2011; WHO, 2011)

Table 8.10. Dose levels and observed absorption rate constants (ka) of drugs included in the 17th WHO model list of Essential Medicines.

Drugs	Low dose (µmoles)*	Medium dose (µmoles)*	High dose (µmoles)*	k_a (h^{-1})	References
Emitricitabine		808.91		0.54	(Hirt *et al.*, 2009)
Enalapril	6.64		13.28		
Erythromycin		340.63			
Ethambutol	489.45	1346.00	1957.81	0.47	(Jonsson *et al.*, 2011)
Ethinyl	0.10		0.12		
Ethosuximide		1770.94			
Ferrous		394.98		1.29	(Farheen *et al.*, 2002)
Fluconazole		163.25			
Fludrocortisone		0.26			
Fluoxetine		64.66			
Folic acid	0.91	2.27	11.33		
Furosemide	30.23	60.47	120.94		
Glibenclamide	5.06		10.12		
Griseofulvin	354.34		708.68		
Haloperidol	5.32		13.30		
Hydralazine	156.08		312.16		
Hydroxycarbamide	2629.69	4766.31	13148.44	3.29	(Paule *et al.*, 2011)
Hydrochlorothiazide	41.98		83.97	0.31	(Beermann and
Ibuprofen	969.55	1939.10	2908.66		
Indinavir		651.69		1.50	(Pfister *et al.*, 2003)

Additional references: (BNF, 2011; PubChem, 2011; WHO, 2011)

Table 8.10. Dose levels and observed absorption rate constants (ka) of drugs included in the 17th WHO model list of Essential Medicines.

Drugs	Low dose (µmoles)*	Medium dose (µmoles)*	High dose (µmoles)*	k_a (h^{-1})	References
Isoniazid	364.59	729.19	2187.56	1.85	(Wilkins *et al.*, 2011)
Ivermectin	3.43		6.86	0.24	(El-Tahtawy *et al.*,
Lactulose	135.85		540.47		
Lamivudine	130.86		654.29	4.65	(Moore *et al.*, 1999)
Levamisole	244.75		734.25		
Levodopa	507.13		1267.83	3.38	(Triggs *et al.*, 1996)
Levonorgestrel	0.10	2.40	4.80		
Levothyroxine	0.03	0.06	0.13		
Lithium		4060.04			
Lopinavir	159.03	211.99	318.07	0.26	(Dickinson *et al.*,
Lumefantrine		226.87		0.13	(Ezzet *et al.*, 1998)
Mebendazole	338.65		1693.24		
Medroxyprogestrone		12.94			
Mefloquine		660.83			
Mesna	2436.36		3654.55		
Metformin		3871.06		0.51	(Bardin *et al.*, 2012)
Methadone	16.16		32.32	0.39	(Rostami-Hodjegan *et*
Methotrexate		5.50		1.11	(Hoekstra *et al.*, 2006)
Mehtyldopa		1183.63			
Metoclopramide		33.36			

Additional references: (BNF, 2011; PubChem, 2011; WHO, 2011)

Table 8.10. Dose levels and observed absorption rate constants (ka) of drugs included in the 17th WHO model list of Essential Medicines.

Drugs	Low dose (µmoles)*	Medium dose (µmoles)*	High dose (µmoles)*	k_a (h^{-1})	References
Metronidazole	1168.54		2921.35		
Midazolam	23.02		46.05	2.20	(Gertz *et al.*, 2011)
Mifepristone		465.56			
Miltefosine	24.54		122.68	0.42	(Dorlo *et al.*, 2012)
Misoprostol	0.52	0.52	0.52		
Neostigmine		67.18			
Nevirapine	187.76	375.52	751.04	1.68	(de Maat *et al.*, 2002)
Niclosamide		1528.49			
Nicotine	12.33	409.42		3.79	(Stratford *et al.*, 1996)
Nifedipine			24.66		
Nitrofurtimox	104.42	28.87		2.22	(Ahmad *et al.*, 2009)
Nitrofurantoin		417.69	870.19	0.97	(Garcia-Bournissen *et*
Omeprazole	28.95	419.89			
Ondansetron	13.63	57.90	115.80		
Paracetamol	661.54	27.27	81.81		
Penicillamine		1984.62	3307.70	5.12	(Ogungbenro *et al.*,
Penicillin		1675.48			
Phenobarbital		713.49			
Phenytoin	64.59		430.60		
	99.10	198.20	396.40		

Additional references: (BNF, 2011; PubChem, 2011; WHO, 2011)

Table 8.10. Dose levels and observed absorption rate constants (ka) of drugs included in the 17th WHO model list of Essential Medicines.

Drugs	Low dose (µmoles)*	Medium dose (µmoles)*	High dose (µmoles)*	k_a (h^{-1})	References
Praziquantel	480.14		1920.58		
Prednisolone	13.87		69.36		
Primaquine	28.92		57.84		
Proguaril		394.12		0.51	(Hussein *et al.*, 1996)
Propranolol	77.12		154.24	0.97	(Parsons *et al.*, 1976)
Propylthiouracil		293.72		1.44	(Kampmann *et al.*,
Pyrantel		1211.78			
Pyrazinamide	1218.40	3249.06	4061.32	2.58	(Peloquin *et al.*, 1997)
Pyridostigmine		229.78		0.32	(Marino *et al.*, 1998)
Pyridoxine		147.77			
Pyrimethamine		100.52		1.31	(Trenque *et al.*, 2004)
Quinine		924.74		0.68	(Supanaranond *et al.*,
Ranitidine		477.09		1.31	(Hawwa *et al.*, 2012)
Ribavirin	818.99	1637.97	2456.96	1.45	(Wade *et al.*, 2006)
Rifabutin		177.09		0.20	(Gatti *et al.*, 1998)
Rifampicin	182.27		364.55	0.72	(Peloquin *et al.*, 1997)
Ritonavir	46.19	34.68	69.35	0.18	(Dickinson *et al.*,
Saquinavir	298.13		745.33	0.58	(Lavielle and Mentre,
Simvastatin	11.95	35.84	95.56	2.00	(Gertz *et al.*, 2011)
Senna		8.69			

Additional references: (BNF, 2011; PubChem, 2011; WHO, 2011)

Table 8.10. Dose levels and observed absorption rate constants (ka) of drugs included in the 17th WHO model list of Essential Medicines.

Drugs	Low dose (µmoles)*	Medium dose (µmoles)*	High dose (µmoles)*	k_a (h^{-1})	References
Spirionolactone		60.01			
Stavudine	66.90	89.20	133.80	0.45	(Panhard *et al.*, 2007)
Succimer		548.79			
Sulfadiazine		1997.79			
Sulfamethoxazole	394.82	1579.29	3158.59	2.61	(Li *et al.*, 2009)
Sulfasalazine		1255.04			
Tenofovir		853.03		1.06	(Baheti *et al.*, 2011)
Thioguanine		239.25			
Triclabendazole		695.10			
Trimethoprim	68.89	275.56	551.12	1.60	(Jelliffe *et al.*, 1997)
Valproic acid	693.43	1386.85	3467.13	4.10	(Williams *et al.*,
Verapamil	87.99		175.98	1.72	(Gupta *et al.*, 2002)
Warfarin	1.62	4.86	16.22	1.66	(Lane *et al.*, 2011)
Zidovudine	224.52	654.84	1122.58	2.86	(Panhard *et al.*, 2007)
Zinc sulphate		123.88			

Additional references: (BNF, 2011; PubChem, 2011; WHO, 2011)

8.5.2 Mechanism-based inhibitor parameters

Table 8.11. Mechanism-based inhibitors with corresponding inhibitory parameters based on review by Zhou, and co-workers, 2005.

Drug	$LogP_{o:w}$	$LogD_{o:w}$	C_{mic} (mg/mL)	fu_{mic}	$K_{I,u}$ (μM)	k_{inact} (h^{-1})	References
Fluoxetine	3.798	3.76	0.1	0.99	5.19	1.02	(Mayhew *et al.*, 2000)
K11002	3.896	3.896	0.2	0.97	0.49	1.56	(Jacobsen *et al.*, 2000)
N-desmethyl diltiazem	3.866	1.7	0.1	0.93	0.72	1.62	(Mayhew *et al.*, 2000)
17α-ethynylestradiol	4.106	4.11	0.1	0.99	17.75	2.40	(Lin *et al.*, 2002)
Dihydralazine	0.739	0.74	0.25	0.97	33.81	3.00	(Masubuchi and Horie, 1999)
Tamoxifen	5.133	3.45	0.05	0.99	0.20	3.06	(Zhao *et al.*, 2002)
K11777	3.962	3.81	0.2	0.97	0.06	3.24	(Jacobsen *et al.*, 2000)
Irinotecan	3.726	1.7	0.1	0.94	22.52	3.60	(Zhou *et al.*, 2005)
Silybin	4.232	3.97	0.1	0.98	31.52	3.60	(Sridar *et al.*, 2004)
Clarithromycin	2.805	1.71	0.1	0.97	5.32	4.32	(Mayhew *et al.*, 2000)
Amprenavir	2.678	2.68	0.1	0.99	1.38	4.38	(von Moltke *et al.*, 2000)
Ritonavir	2.333	2.33	1.025	0.87	0.06	4.68	(Koudriakova *et al.*, 1998)
N-desmethyl-tamoxifen	5.149	2.84	0.05	0.98	2.55	4.80	(Zhao *et al.*, 2002)
Tabimorelin	4.043	1.71	0.1	0.92	4.34	4.80	(Zdravkovic *et al.*, 2003)
Erythromycin	1.909	0.81	0.1	0.92	43.10	4.80	(Zhou *et al.*, 2005)
Isoniazid	-0.766	-0.77	0.1	0.99	224.85	4.80	(Wen *et al.*, 2002)
Mifepristone	6.193	6.18	0.1	0.99	4.63	5.34	(He *et al.*, 1999)
Verapamil	4.024	2.08	0.5	0.81	1.38	5.40	(Yeo and Yeo, 2001)
Oleuropein	-0.865	-0.87	0.1	0.99	21.89	5.40	(Zhou *et al.*, 2005)
SN-38	1.895	1.87	0.1	0.99	25.63	6.00	(Zhou *et al.*, 2005)

References: (Zhou *et al.*, 2005)

$LogP_{o:w}$=Octanol-water partition coefficient, $LogD_{o:w}$=Octanol-water distribution coefficient, $_{Cmic}$=Concentration of microsomes in assay, fu_{mic}=fraction unbound

Inhibitor in microsomal assay, $K_{I,u}$=Inhibitor concentration producing half of the maximal rate of inactivation, k_{inact}=Maximal rate of enzyme inactivation.

Table 8.11. (Continued) Mechanism-based inhibitors with corresponding inhibitory parameters based on review by Zhou, and co-workers, 2005.

Drug	$LogP_{o:w}$	$LogD_{o:w}$	C_{mic} (mg/mL)	fu_{mic}	$K_{I,u}$ (μM)	k_{inact} (h^{-1})	References
Diltiazem	4.727	2.98	0.075	0.98	1.96	6.60	(Jones *et al.*, 1999)
Glabridin	4.105	4.1	0.1	0.99	6.90	8.40	(Kent *et al.*, 2002)
Troleandomycin	3.46	2.56	0.1	0.98	0.18	9.00	(Zhou *et al.*, 2005)
Midazolam	3.798	3.76	0.1	0.99	5.72	9.00	(Khan *et al.*, 2002)
Raloxifene	4.569	3.05	0.1	0.97	9.64	9.60	(Chen *et al.*, 2002)
6',7'-dihydroxy-bergamottin	2.261	2.26	0.5	0.93	55.11	9.60	(Schmiedlin-Ren *et al.*, 1997)
Nelfinavir	7.278	7.25	1	0.88	4.90	10.80	(Lillibridge *et al.*, 1998)
Resveratrol	3.024	3.02	1	0.88	17.52	12.00	(Chan and Delucchi, 2000)
DPC 681	4.856	4.57	0.01	1.00	0.24	13.20	(Luo *et al.*, 2003)
(-)-Hydrastine	2.458	2.28	0.5	0.93	102.03	13.80	(Chatterjee and Franklin, 2003)
Diclofenac	4.548	1.77	0.5	0.65	1068.81	14.76	(Masubuchi *et al.*, 2002)
Bergamottin	5.382	5.38	0.5	0.93	3.92	18.00	(Schmiedlin-Ren *et al.*, 1997)
Mibefradil	6.213	3.9	0.1	0.97	2.23	24.00	(Prueksaritanont *et al.*, 1999)
Gestodene	2.022	2.02	0.1	0.99	45.36	24.00	(Guengerich, 1990)
Delavirdine	3.534	1.48	0.75	0.61	5.81	26.40	(Voorman *et al.*, 1998)
L-754,394	4.105	3.87	0.1	0.98	7.39	97.20	(Lightning *et al.*, 2000)
Nicardipine	4.893	4.41	1	0.86	0.52	120.00	(Ma *et al.*, 2000)

References: (Zhou *et al.*, 2005)

$LogP_{o:w}$=Octanol-water partition coefficient, $LogD_{o:w}$=Octanol-water distribution coefficient, $_{Cmic}$=Concentration of microsomes in assay, fu_{mic}=fraction unbound Inhibitor in microsomal assay, $K_{I,u}$=Inhibitor concentration producing half of the maximal rate of inactivation, k_{inact}=Maximal rate of enzyme inactivation.

8.5.3 Nested enzyme-within-enterocyte model code

The following script was developed by Adam S. Darwich, University of Manchester. Code optimisation was carried out with the assistance of Mr. Mike Croucher, University of Manchester.

Run file

```
%% NEWE model: Developed by Adam Darwich, University of
% Manchester
clear
%% MAIN INPUT PARAMS
dose_i=100000;                                  % umol
n_cells=10;
cell_cycles=5*n_cells;

%% PARAMS
dlmwrite('n_cells_b.txt',n_cells,'delimiter','D');
cellzero=0+(1-0).*rand(1,n_cells);
dose_i_sim=dose_i;
m=0;
a_cyp3a_gi=(90.8*(10^(-3)));
% nmol/total gut -> umol/total gut
a_cyp3a_gi_zero=repmat(a_cyp3a_gi,1,n_cells);
mppgl=39.7907;
% mg protein/g liver
v_hep=1.591;                          % L
d_hep=1080;                           % g/L
a_cyp3a_hep=240*mppgl*v_hep*d_hep*(10^(-6));
% pmol/mg protein -> umol/liver
ycell=zeros(2000,n_cells);
tcell=zeros(2000,n_cells);
ycycle=zeros(2000,n_cells);
tcycle=zeros(2000,n_cells);

%% ODE-SOLVER
```

```
tstart = 0;
tfinal = 200;
yzero=[ cellzero'; a_cyp3a_gi_zero'; dose_i_sim;
zeros(2,1); a_cyp3a_hep; zeros(4,1)];

refine = 4;
options=odeset('Events',@a_cyp3a_MBI_eventfun_B,…
'Refine',refine);
tout = tstart;
yout = yzero.';
teout = [];
yeout = [];
ieout = [];

tic
    for i = 1:cell_cycles
        [t y te ye
ie]=ode15s(@a_cyp3a_MBI_model_INHIB_ONLY_B,(tstart:0.01:tfi
nal),yzero,options);
        % Accumulate output: cell,intra.
        nt = length(t);
        tout = [tout; t(2:nt)];
        yout = [yout; y(2:nt,:)];
        teout = [teout; te];
        yeout = [yeout; ye];

        [num idx] = max(t(:));

        % Set new inicon.
        for i = 1:n_cells
            if y(idx,i) >= 1
                yzero(i) = 0;
                yzero(i+n_cells) = a_cyp3a_gi;
            elseif y(idx,i) < 1
                yzero(i) = y(idx,i);
```

```
                yzero(i+n_cells) = y(idx,i+n_cells);
            end
        end

        yzero(1+n_cells*2) = y(idx,1+n_cells*2);
        yzero(2+n_cells*2) = y(idx,2+n_cells*2);
        yzero(3+n_cells*2) = y(idx,3+n_cells*2);
        yzero(4+n_cells*2) = y(idx,4+n_cells*2);
        yzero(5+n_cells*2) = y(idx,5+n_cells*2);
        yzero(6+n_cells*2) = y(idx,6+n_cells*2);
        yzero(7+n_cells*2) = y(idx,7+n_cells*2);
        yzero(8+n_cells*2) = y(idx,8+n_cells*2);

        tstart = t(nt);
    end
toc
```

Model

```
%% FUNCTION: A_Enterocyte,CYP3A
function dY=a_cyp3a_MBI_model_INHIB_ONLY_B(t,y,te,ye,ie)

%% MODELPARAM
n_cells=load('n_cells_b.txt');
dY=zeros(8+n_cells*2,1);

%% PHYSPARAM
bw=75;                              % kg
v_sit=(126+44+31+24+18+12)/1000;    % L
v_ent=0.517;
v_pv=0.07;
v_hep=1.591;

d_hep=1080;                         % g/L

q_villi=19;                         % L/h
```

```
q_pv=74.1;
q_ha=23.35;

k_sit=0.21;                          % 1/h


kdeg_ent=0.042;
kdeg_hep=0.02;
kdeg_cyp3a=0.001;                    % 1/h


mppgl=39.7907;
% mg microsomal protein/g liver

mppi=2978;
% mg microsomal protein/total gut

a_cyp3a_gi=90.8*(10^(-3));
% nmolP450/total gut -> umolP450/total gut

a_cyp3a_hep=240*mppgl*v_hep*d_hep*(10^(-6));
% pmolP450/mg protein -> umolP450/liver

%% DRUGPARAM1 (Inhibitor)
ka_i=10;
clu_int1_i=0.01*60*10^(-6);
% uL/min/mg microsomal protein -> L/h/mg microsomal protein
k_inact_3a_i=2000;
% 1/h

k_i_i=2;
% umol/L

fu_i=0.25;
bp_i=0.96;
```

```
fu_b_i=fu_i/bp_i;
fu_gut_i=1;

v_i=1*bw - 3.6*v_hep*(d_hep/1000);
% L/kg -> L

% Inhibitor
clu_int1_gut_i=clu_int1_i*mppi;
clu_int1_hep_i=clu_int1_i*mppgl*v_hep*d_hep;

%% ODE MODEL
%% Inhibitor:
for a = 1:n_cells

    dY(a)=0 + kdeg_ent;

    % y(2; n_cells:n_cells*2)-Enterocytes: Inhib.
    dY(a+n_cells)=(a_cyp3a_gi)*kdeg_cyp3a - …
kdeg_cyp3a*y(a+n_cells) - y(a+n_cells)* …
(((k_inact_3a_i*fu_gut_i*y(2+n_cells*2))/ …
(k_i_i+fu_gut_i*y(2+n_cells*2))) );
end

% A_CYP3A-GIT: Mean and sum
x_a_cyp3a_gi=mean(y((n_cells+1):(n_cells*2)));
% x_a_cyp3a_gi=sum(y(1:n_cells));

% y(3)-Inhib: Conc_(gut lumen).
dY(1+n_cells*2)=-y(1+n_cells*2)*(ka_i + k_sit);

% y(4)-Inhib: Conc_ent.
dY(2+n_cells*2)=(y(1+n_cells*2)*ka_i -
y(2+n_cells*2)*q_villi -
clu_int1_gut_i*fu_gut_i*y(2+n_cells*2))/v_ent;
```

```
% y(5)-Inhib: Conc_pv.
dY(3+n_cells*2)=(y(2+n_cells*2)*q_villi +
y(7+n_cells*2)*q_pv - y(3+n_cells*2)*q_pv)/v_pv;

% y(6)-Hepatocytes: Inhib.
dY(4+n_cells*2)=a_cyp3a_hep*( kdeg_hep + kdeg_cyp3a ) -
y(4+n_cells*2)*((kdeg_hep + kdeg_cyp3a) +
((k_inact_3a_i*fu_b_i*y(6+n_cells*2))/(k_i_i+fu_b_i*y(6+n_c
ells*2))));

% y(7)-Hepatocytes: Cell cycle.
dY(5+n_cells*2)=0;

% y(8)-Inhib: Conc_hep.
dY(6+n_cells*2)=(y(3+n_cells*2)*q_pv + y(7+n_cells*2)…
*q_ha - y(6+n_cells*2)*(q_pv + q_ha)…
- clu_int1_hep_i*fu_b_i*y(6+n_cells*2))/v_hep;

% y(9)-Inhib: Conc_sys.
dY(7+n_cells*2)=(y(6+n_cells*2)*(q_pv + q_ha)…
- y(7+n_cells*2)*(q_pv + q_ha))/v_i;

% y(10)-Inhib: Conc_RoB.
dY(8+n_cells*2)=0;
```

Mex function in C++ programming language

```
#include<mex.h>

void mexFunction( int nlhs, mxArray *plhs[], int
nrhs, const mxArray *prhs[]) {

    double *n_cellsP;
    double *DYP;
    double *a_cyp3a_giP;
    double *kdeg_cyp3aP;
    double *yP;
    double *k_inact_3a_iP;
    double *fu_gut_iP;
    double *k_i_iP;
    double *kdeg_entP;
    int a, n_cells;
    double temp_prod1,temp_prod2;

     /* create pointers to the inputs */
    n_cellsP = mxGetPr(prhs[0]);
    DYP = mxGetPr(prhs[1]);
    a_cyp3a_giP = mxGetPr(prhs[2]);
    kdeg_cyp3aP = mxGetPr(prhs[3]);
    yP = mxGetPr(prhs[4]);
    k_inact_3a_iP =mxGetPr(prhs[5]);
    fu_gut_iP = mxGetPr(prhs[6]);
    k_i_iP = mxGetPr(prhs[7]);
    kdeg_entP = mxGetPr(prhs[8]);

    n_cells= (int) n_cellsP[0];
```

```
            temp_prod1 = a_cyp3a_giP[0]*kdeg_cyp3aP[0];
        /*in the  original, this was calculated every
        loop iteration despite the fact that they are
        constants.*/
            temp_prod2 = k_inact_3a_iP[0]*fu_gut_iP[0];
            for (a=0; a<n_cells; a++){

                DYP[a] = kdeg_entP[0];
                DYP[a+n_cells]= temp_prod1 -
        kdeg_cyp3aP[0]*yP[a+n_cells] -
        yP[a+n_cells]*(((temp_prod2*yP[1+n_cells*2])/(k_i
        _iP[0]+fu_gut_iP[0]*yP[1+n_cells*2])) );

             }
        }
```

Event function

```
function [value,isterminal,direction] =
a_cyp3a_MBI_eventfun_B(t,y)

% Param
n_cells=load('n_cells_b.txt');
cell_v=1:1:n_cells;
value = y(cell_v') - 1; % value = 1, event is triggered
isterminal(1:n_cells') = 1; % terminate after the first
event
direction = 0;  % get all the matrix of zeros
```

8.5.4 References

Abduljalil K, Kinzig M, Bulitta J, Horkovics-Kovats S, Sorgel F, Rodamer M, and Fuhr U (2009) Modeling the autoinhibition of clarithromycin metabolism during repeated oral administration. *Antimicrob Agents Chemother* **53:**2892-2901.

Ahmad M, Ahmad T, Sultan RA, and Murtaza G (2009) Pharmacokinetic study of nifedipine in healthy adult male human volunteers. *Tropical Journal of Pharmaceutical Research* **8:**385-391.

Arancibia A, Guttmann J, Gonzalez G, and Gonzalez C (1980) Absorption and disposition kinetics of amoxicillin in normal human subjects. *Antimicrob Agents Chemother* **17:**199-202.

Baheti G, Kiser JJ, Havens PL, and Fletcher CV (2011) Plasma and intracellular population pharmacokinetic analysis of tenofovir in HIV-1-infected patients. *Antimicrob Agents Chemother* **55:**5294-5299.

Bardin C, Nobecourt E, Larger E, Chast F, Treluyer JM, and Urien S (2012) Population pharmacokinetics of metformin in obese and non-obese patients with type 2 diabetes mellitus. *Eur J Clin Pharmacol* **68:**961-968.

Beermann B and Groschinsky-Grind M (1977) Pharmacokinetics of hydrochlorothiazide in man. *Eur J Clin Pharmacol* **12:**297-303.

BNF (2011) British National Formulary.

Bolla S, Boinpally RR, Poondru S, Devaraj R, and Jasti BR (2002) Pharmacokinetics of diethylcarbamazine after single oral dose at two different times of day in human subjects. *J Clin Pharmacol* **42:**327-331.

Brittain DC, Scully BE, Hirose T, and Neu HC (1985) The pharmacokinetic and bactericidal characteristics of oral cefixime. *Clin Pharmacol Ther* **38:**590-594.

Chan WK and Delucchi AB (2000) Resveratrol, a red wine constituent, is a mechanism-based inactivator of cytochrome P450 3A4. *Life Sci* **67:**3103-3112.

Chatterjee P and Franklin MR (2003) Human cytochrome p450 inhibition and metabolic-intermediate complex formation by goldenseal extract and its methylenedioxyphenyl components. *Drug Metab Dispos* **31:**1391-1397.

Chen Q, Ngui JS, Doss GA, Wang RW, Cai X, DiNinno FP, Blizzard TA, Hammond ML, Stearns RA, Evans DC, Baillie TA, and Tang W (2002) Cytochrome P450 3A4-mediated bioactivation of raloxifene: irreversible enzyme inhibition and thiol adduct formation. *Chemical research in toxicology* **15:**907-914.

Cotting J, Zeugin T, Steiger U, and Reichen J (1990) Albendazole kinetics in patients with echinococcosis: delayed absorption and impaired elimination in cholestasis. *Eur J Clin Pharmacol* **38:**605-608.

de Maat MM, Huitema AD, Mulder JW, Meenhorst PL, van Gorp EC, and Beijnen JH (2002) Population pharmacokinetics of nevirapine in an unselected cohort of HIV-1-infected individuals. *Br J Clin Pharmacol* **54:**378-385.

Dickinson L, Boffito M, Back D, Else L, von Hentig N, Davies G, Khoo S, Pozniak A, Moyle G, and Aarons L (2011) Sequential population pharmacokinetic modeling of lopinavir and ritonavir in healthy volunteers and assessment of different dosing strategies. *Antimicrob Agents Chemother* **55:**2775-2782.

Dorlo TP, Huitema AD, Beijnen JH, and de Vries PJ (2012) Optimal dosing of miltefosine in children and adults with visceral leishmaniasis. *Antimicrob Agents Chemother* **56:**3864-3872.

El-Tahtawy A, Glue P, Andrews EN, Mardekian J, Amsden GW, and Knirsch CA (2008) The effect of azithromycin on ivermectin pharmacokinetics--a population pharmacokinetic model analysis. *PLoS Negl Trop Dis* **2:**e236.

Ezzet F, Mull R, and Karbwang J (1998) Population pharmacokinetics and therapeutic response of CGP 56697 (artemether + benflumetol) in malaria patients. *Br J Clin Pharmacol* **46:**553-561.

Farheen A, Aslam T, Almas K, Bhatty N, and Nawaz M (2002) Biokinetics of inorganic iron in female volunteers. *Pakistan J Med Res* **41:**32-35.

Flynn JT, Nahata MC, Mahan JD, Jr., and Portman RJ (2006) Population pharmacokinetics of amlodipine in hypertensive children and adolescents. *J Clin Pharmacol* **46:**905-916.

Garcia-Bournissen F, Altcheh J, Panchaud A, and Ito S (2009) Is use of nifurtimox for the treatment of Chagas disease compatible with breast feeding? A population pharmacokinetics analysis. *Arch Dis Child* **95:**224-228.

Gatti G, Papa P, Torre D, Andreoni M, Poggio A, Bassetti M, and Marone P (1998) Population pharmacokinetics of rifabutin in human immunodeficiency virus-infected patients. *Antimicrob Agents Chemother* **42:**2017-2023.

Gertz M, Houston JB, and Galetin A (2011) Physiologically based pharmacokinetic modeling of intestinal first-pass metabolism of CYP3A substrates with high intestinal extraction. *Drug Metab Dispos* **39:**1633-1642.

Guengerich FP (1990) Mechanism-based inactivation of human liver microsomal cytochrome P-450 IIIA4 by gestodene. *Chemical research in toxicology* **3:**363-371.

Gupta S, Modi NB, Sathyan G, Ho Pl PL, and Aarons L (2002) Pharmacokinetics of controlled-release verapamil in healthy volunteers and patients with hypertension or angina. *Biopharm Drug Dispos* **23:**17-31.

Hawwa AF, Westwood PM, Collier PS, Millership JS, Yakkundi S, Thurley G, Shields MD, Nunn AJ, Halliday HL, and McElnay JC (2012) Prophylactic ranitidine treatment in critically ill children - a population pharmacokinetic study. *Br J Clin Pharmacol*.

He K, Woolf TF, and Hollenberg PF (1999) Mechanism-based inactivation of cytochrome P-450-3A4 by mifepristone (RU486). *J Pharmacol Exp Ther* **288:**791-797.

Hirt D, Urien S, Rey E, Arrive E, Ekouevi DK, Coffie P, Leang SK, Lalsab S, Avit D, Nerrienet E, McIntyre J, Blanche S, Dabis F, and Treluyer JM (2009) Population pharmacokinetics of emtricitabine in human immunodeficiency virus type 1-infected pregnant women and their neonates. *Antimicrob Agents Chemother* **53:**1067-1073.

Hoekstra M, Haagsma C, Neef C, Proost J, Knuif A, and van de Laar M (2006) Splitting high-dose oral methotrexate improves bioavailability: a pharmacokinetic study in patients with rheumatoid arthritis. *J Rheumatol* **33:**481-485.

Hussein Z, Eaves CJ, Hutchinson DB, and Canfield CJ (1996) Population pharmacokinetics of proguanil in patients with acute P. falciparum malaria after combined therapy with atovaquone. *Br J Clin Pharmacol* **42:**589-597.

Ijaz A, Bhatti NH, Rasheed S, Sadaf B, and Nawaz R (2003) Pharmacokinetic study of aspirin in healthy female volunteers. *Pakistan Journal of Biological Sciences* **6:**1404-1407.

Ismail R and Rahman AF (1993) Estimation of population pharmacokinetics for carbamazepine in Malaysian patients using the OPT computer program. *J Clin Pharm Ther* **18:**55-58.

Jacobsen W, Christians U, and Benet LZ (2000) In vitro evaluation of the disposition of A novel cysteine protease inhibitor. *Drug Metab Dispos* **28:**1343-1351.

Jelliffe RW, Gomis P, Tahani B, Ruskin J, and Sattler FR (1997) A population pharmacokinetic model of trimethoprim in patients with pneumocystis

pneumonia, made with parametric and nonparametric methods. *Ther Drug Monit* **19:**450-459.

Jones DR, Gorski JC, Hamman MA, Mayhew BS, Rider S, and Hall SD (1999) Diltiazem inhibition of cytochrome P-450 3A activity is due to metabolite intermediate complex formation. *J Pharmacol Exp Ther* **290:**1116-1125.

Jonsson S, Davidse A, Wilkins J, Van der Walt JS, Simonsson US, Karlsson MO, Smith P, and McIlleron H (2011) Population pharmacokinetics of ethambutol in South African tuberculosis patients. *Antimicrob Agents Chemother* **55:**4230-4237.

Jullien V, Ogutu B, Juma E, Carn G, Obonyo C, and Kiechel JR (2010) Population pharmacokinetics and pharmacodynamic considerations of amodiaquine and desethylamodiaquine in Kenyan adults with uncomplicated malaria receiving artesunate-amodiaquine combination therapy. *Antimicrob Agents Chemother* **54:**2611-2617.

Kamimori GH, Karyekar CS, Otterstetter R, Cox DS, Balkin TJ, Belenky GL, and Eddington ND (2002) The rate of absorption and relative bioavailability of caffeine administered in chewing gum versus capsules to normal healthy volunteers. *Int J Pharm* **234:**159-167.

Kampmann JP, Mortensen HB, Bach B, Waldorff S, Kristensen MB, and Hansen JM (1979) Kinetics of propylthiouracil in the elderly. *Acta Med Scand Suppl* **624:**93-98.

Karunajeewa HA, Salman S, Mueller I, Baiwog F, Gomorrai S, Law I, Page-Sharp M, Rogerson S, Siba P, Ilett KF, and Davis TM (2010) Pharmacokinetics of chloroquine and monodesethylchloroquine in pregnancy. *Antimicrob Agents Chemother* **54:**1186-1192.

Kent UM, Aviram M, Rosenblat M, and Hollenberg PF (2002) The licorice root derived isoflavan glabridin inhibits the activities of human cytochrome P450S 3A4, 2B6, and 2C9. *Drug Metab Dispos* **30:**709-715.

Khan KK, He YQ, Domanski TL, and Halpert JR (2002) Midazolam oxidation by cytochrome P450 3A4 and active-site mutants: an evaluation of multiple binding sites and of the metabolic pathway that leads to enzyme inactivation. *Mol Pharmacol* **61:**495-506.

Koudriakova T, Iatsimirskaia E, Utkin I, Gangl E, Vouros P, Storozhuk E, Orza D, Marinina J, and Gerber N (1998) Metabolism of the human immunodeficiency virus protease inhibitors indinavir and ritonavir by human intestinal microsomes and expressed cytochrome P4503A4/3A5: mechanism-based inactivation of cytochrome P4503A by ritonavir. *Drug Metab Dispos* **26:**552-561.

Kukes VG, Kondratenko SN, Savelyeva MI, Starodubtsev AK, and Gneushev ET (2009) Experimental and clinical pharmacokinetics of amitryptiline: comparative analysis. *Bull Exp Biol Med* **147:**434-437.

Lane S, Al-Zubiedi S, Hatch E, Matthews I, Jorgensen AL, Deloukas P, Daly AK, Park BK, Aarons L, Ogungbenro K, Kamali F, Hughes D, and Pirmohamed M (2011) The population pharmacokinetics of R- and S-warfarin: effect of genetic and clinical factors. *Br J Clin Pharmacol* **73:**66-76.

Lavielle M and Mentre F (2007) Estimation of population pharmacokinetic parameters of saquinavir in HIV patients with the MONOLIX software. *J Pharmacokinet Pharmacodyn* **34:**229-249.

Li XY, Gao F, Li ZQ, Guan W, Feng WL, and Ge RL (2009) Comparison of the pharmacokinetics of sulfamethoxazole in male chinese volunteers at low altitude and acute exposure to high altitude versus subjects living chronically at high altitude: an open-label, controlled, prospective study. *Clin Ther* **31:**2744-2754.

Lightning LK, Jones JP, Friedberg T, Pritchard MP, Shou M, Rushmore TH, and Trager WF (2000) Mechanism-based inactivation of cytochrome P450 3A4 by L-754,394. *Biochemistry* **39:**4276-4287.

Lillibridge JH, Liang BH, Kerr BM, Webber S, Quart B, Shetty BV, and Lee CA (1998) Characterization of the selectivity and mechanism of human cytochrome P450 inhibition by the human immunodeficiency virus-protease inhibitor nelfinavir mesylate. *Drug Metab Dispos* **26:**609-616.

Lin HL, Kent UM, and Hollenberg PF (2002) Mechanism-based inactivation of cytochrome P450 3A4 by 17 alpha-ethynylestradiol: evidence for heme destruction and covalent binding to protein. *J Pharmacol Exp Ther* **301:**160-167.

Luo G, Lin J, Fiske WD, Dai R, Yang TJ, Kim S, Sinz M, LeCluyse E, Solon E, Brennan JM, Benedek IH, Jolley S, Gilbert D, Wang L, Lee FW, and Gan LS (2003) Concurrent induction and mechanism-based inactivation of CYP3A4 by an L-valinamide derivative. *Drug Metab Dispos* **31:**1170-1175.

Ma B, Prueksaritanont T, and Lin JH (2000) Drug interactions with calcium channel blockers: possible involvement of metabolite-intermediate complexation with CYP3A. *Drug Metab Dispos* **28:**125-130.

Marino MT, Schuster BG, Brueckner RP, Lin E, Kaminskis A, and Lasseter KC (1998) Population pharmacokinetics and pharmacodynamics of pyridostigmine bromide for prophylaxis against nerve agents in humans. *J Clin Pharmacol* **38:**227-235.

Masubuchi Y and Horie T (1999) Mechanism-based inactivation of cytochrome P450s 1A2 and 3A4 by dihydralazine in human liver microsomes. *Chemical research in toxicology* **12:**1028-1032.

Masubuchi Y, Ose A, and Horie T (2002) Diclofenac-induced inactivation of CYP3A4 and its stimulation by quinidine. *Drug Metab Dispos* **30:**1143-1148.

Mayhew BS, Jones DR, and Hall SD (2000) An in vitro model for predicting in vivo inhibition of cytochrome P450 3A4 by metabolic intermediate complex formation. *Drug Metab Dispos* **28:**1031-1037.

Moore KH, Yuen GJ, Hussey EK, Pakes GE, Eron JJ, Jr., and Bartlett JA (1999) Population pharmacokinetics of lamivudine in adult human immunodeficiency virus-infected patients enrolled in two phase III clinical trials. *Antimicrob Agents Chemother* **43:**3025-3029.

Nix DE, Adam RD, Auclair B, Krueger TS, Godo PG, and Peloquin CA (2004) Pharmacokinetics and relative bioavailability of clofazimine in relation to food, orange juice and antacid. *Tuberculosis (Edinb)* **84:**365-373.

Ogungbenro K, Vasist L, Maclaren R, Dukes G, Young M, and Aarons L (2011) A semi-mechanistic gastric emptying model for the population pharmacokinetic analysis of orally administered acetaminophen in critically ill patients. *Pharm Res* **28:**394-404.

Panhard X, Legrand M, Taburet AM, Diquet B, Goujard C, and Mentre F (2007) Population pharmacokinetic analysis of lamivudine, stavudine and zidovudine in controlled HIV-infected patients on HAART. *Eur J Clin Pharmacol* **63:**1019-1029.

Parsons RL, Kaye CM, Raymond K, Trounce JR, and Turner P (1976) Absorption of propranolol and practolol in Coeliac disease. *Gut* **17:**139-143.

Paule I, Sassi H, Habibi A, Pham KP, Bachir D, Galacteros F, Girard P, Hulin A, and Tod M (2011) Population pharmacokinetics and pharmacodynamics of hydroxyurea in sickle cell anemia patients, a basis for optimizing the dosing regimen. *Orphanet J Rare Dis* **6:**30.

Peloquin CA, Jaresko GS, Yong CL, Keung AC, Bulpitt AE, and Jelliffe RW (1997) Population pharmacokinetic modeling of isoniazid, rifampin, and pyrazinamide. *Antimicrob Agents Chemother* **41:**2670-2679.

Pfister M, Labbe L, Hammer SM, Mellors J, Bennett KK, Rosenkranz S, and Sheiner LB (2003) Population pharmacokinetics and pharmacodynamics of efavirenz, nelfinavir, and indinavir: Adult AIDS Clinical Trial Group Study 398. *Antimicrob Agents Chemother* **47:**130-137.

Prueksaritanont T, Ma B, Tang C, Meng Y, Assang C, Lu P, Reider PJ, Lin JH, and Baillie TA (1999) Metabolic interactions between mibefradil and HMG-CoA reductase inhibitors: an in vitro investigation with human liver preparations. *Br J Clin Pharmacol* **47:**291-298.

PubChem (2011), National Center for Biotechnology Information.

Rostami-Hodjegan A, Wolff K, Hay AW, Raistrick D, Calvert R, and Tucker GT (1999) Population pharmacokinetics of methadone in opiate users: characterization of time-dependent changes. *Br J Clin Pharmacol* **48:**43-52.

Sanchez Navarro MD, Sayalero Marinero ML, and Sanchez Navarro A (2002) Pharmacokinetic/pharmacodynamic modelling of ciprofloxacin 250 mg/12 h versus 500 mg/24 h for urinary infections. *J Antimicrob Chemother* **50:**67-72.

Savic RM, Jonker DM, Kerbusch T, and Karlsson MO (2007) Implementation of a transit compartment model for describing drug absorption in pharmacokinetic studies. *J Pharmacokinet Pharmacodyn* **34:**711-726.

Schmiedlin-Ren P, Edwards DJ, Fitzsimmons ME, He K, Lown KS, Woster PM, Rahman A, Thummel KE, Fisher JM, Hollenberg PF, and Watkins PB (1997) Mechanisms of enhanced oral availability of CYP3A4 substrates by grapefruit constituents. Decreased enterocyte CYP3A4 concentration and mechanism-based inactivation by furanocoumarins. *Drug Metab Dispos* **25:**1228-1233.

Simpson JA, Hughes D, Manyando C, Bojang K, Aarons L, Winstanley P, Edwards G, Watkins WA, and Ward S (2006) Population pharmacokinetic and pharmacodynamic modelling of the antimalarial chemotherapy chlorproguanil/dapsone. *Br J Clin Pharmacol* **61:**289-300.

Solas C, Gagnieu MC, Ravaux I, Drogoul MP, Lafeuillade A, Mokhtari S, Lacarelle B, and Simon N (2008) Population pharmacokinetics of atazanavir in human immunodeficiency virus-infected patients. *Ther Drug Monit* **30:**670-673.

Sridar C, Goosen TC, Kent UM, Williams JA, and Hollenberg PF (2004) Silybin inactivates cytochromes P450 3A4 and 2C9 and inhibits major hepatic glucuronosyltransferases. *Drug Metab Dispos* **32:**587-594.

Stratford MR, Dennis MF, Hoskin PJ, Saunders MI, Hodgkiss RJ, and Rojas A (1996) Nicotinamide pharmacokinetics in normal volunteers and patients undergoing palliative radiotherapy. *Acta Oncol* **35:**213-219.

Supanaranond W, Davis TM, Pukrittayakamee S, Silamut K, Karbwang J, Molunto P, Chanond L, and White NJ (1991) Disposition of oral quinine in acute falciparum malaria. *Eur J Clin Pharmacol* **40:**49-52.

Trenque T, Simon N, Villena I, Chemla C, Quereux C, Leroux B, Jaussaud R, Remy G, Dupouy D, Millart H, Pinon JM, and Urien S (2004) Population pharmacokinetics of pyrimethamine and sulfadoxine in children with congenital toxoplasmosis. *Br J Clin Pharmacol* **57:**735-741.

Triggs EJ, Charles BG, Contin M, Martinelli P, Cortelli P, Riva R, Albani F, and Baruzzi A (1996) Population pharmacokinetics and pharmacodynamics of oral levodopa in parkinsonian patients. *Eur J Clin Pharmacol* **51:**59-67.

Turnheim K, Krivanek P, and Oberbauer R (1999) Pharmacokinetics and pharmacodynamics of allopurinol in elderly and young subjects. *Br J Clin Pharmacol* **48:**501-509.

Velasque LS, Estrela RC, Suarez-Kurtz G, and Struchiner CJ (2007) A new model for the population pharmacokinetics of didanosine in healthy subjects. *Braz J Med Biol Res* **40:**97-104.

von Moltke LL, Durol AL, Duan SX, and Greenblatt DJ (2000) Potent mechanism-based inhibition of human CYP3A in vitro by amprenavir and ritonavir: comparison with ketoconazole. *Eur J Clin Pharmacol* **56:**259-261.

Voorman RL, Maio SM, Hauer MJ, Sanders PE, Payne NA, and Ackland MJ (1998) Metabolism of delavirdine, a human immunodeficiency virus type-1 reverse transcriptase inhibitor, by microsomal cytochrome P450 in humans, rats, and other species: probable involvement of CYP2D6 and CYP3A. *Drug Metab Dispos* **26:**631-639.

Wade JR, Snoeck E, Duff F, Lamb M, and Jorga K (2006) Pharmacokinetics of ribavirin in patients with hepatitis C virus. *Br J Clin Pharmacol* **62:**710-714.

Walker RB (1995) HPLC analysis and pharmacokinetics of cyclizine, in: *School of Pharmaceutical Sciences*, pp 190, Rhodes University, Grahamstown.

Weller S, Radomski KM, Lou Y, and Stein DS (2000) Population pharmacokinetics and pharmacodynamic modeling of abacavir (1592U89) from a dose-ranging, double-blind, randomized monotherapy trial with human immunodeficiency virus-infected subjects. *Antimicrob Agents Chemother* **44:**2052-2060.

Wen X, Wang JS, Neuvonen PJ, and Backman JT (2002) Isoniazid is a mechanism-based inhibitor of cytochrome P450 1A2, 2A6, 2C19 and 3A4 isoforms in human liver microsomes. *Eur J Clin Pharmacol* **57:**799-804.

Whitfield LR, Kaul PN, and Clark ML (1978) Chlorpromazine metabolism. IX. Pharmacokinetics of chlorpromazine following oral administration in man. *J Pharmacokinet Biopharm* **6:**187-196.

WHO (2011) WHO Model List of Esssential Medicines, 17th Edition, WHO.

Wilkins JJ, Langdon G, McIlleron H, Pillai G, Smith PJ, and Simonsson US (2011) Variability in the population pharmacokinetics of isoniazid in South African tuberculosis patients. *Br J Clin Pharmacol* **72:**51-62.

Williams JH, Jayaraman B, Swoboda KJ, and Barrett JS (2012) Population pharmacokinetics of valproic Acid in pediatric patients with epilepsy: considerations for dosing spinal muscular atrophy patients. *J Clin Pharmacol* **52:**1676-1688.

Yano I, Takayama A, Takano M, Inatani M, Tanihara H, Ogura Y, Honda Y, and Inui K (1998) Pharmacokinetics and pharmacodynamics of acetazolamide in patients with transient intraocular pressure elevation. *Eur J Clin Pharmacol* **54:**63-68.

Yeo KR and Yeo WW (2001) Inhibitory effects of verapamil and diltiazem on simvastatin metabolism in human liver microsomes. *Br J Clin Pharmacol* **51:**461-470.

Zdravkovic M, Olsen AK, Christiansen T, Schulz R, Taub ME, Thomsen MS, Rasmussen MH, and Ilondo MM (2003) A clinical study investigating the pharmacokinetic interaction between NN703 (tabimorelin), a potential inhibitor of CYP3A4 activity, and midazolam, a CYP3A4 substrate. *Eur J Clin Pharmacol* **58:**683-688.

Zhao XJ, Jones DR, Wang YH, Grimm SW, and Hall SD (2002) Reversible and irreversible inhibition of CYP3A enzymes by tamoxifen and metabolites. *Xenobiotica* **32:**863-878.

Zhou S, Chan E, Li X, and Huang M (2005) Clinical outcomes and management of mechanism-based inhibition of cytochrome P450 3A4. *Ther Clin Risk Manag* **1:**3-13.

8.6 Discussion and conclusions

8.6.1 Midazolam following Roux-en-Y gastric bypass

The compound file for midazolam in Simcyp Simulator was adapted for immediate release formulation using the ADAM model (Table 8.12) (Turner, 2008; Jamei *et al.*, 2009).

Table 8.12. Simcyp Simulator midazolam compound file parameters.

Parameters	Value	References
PhysChem		
MW (g/mol)	325.8	(Turner, 2008; NCBI, 2011)
$LogP_{o:w}$	3.53	
Acid-base nature	Ampholyte	
pKa	10.95, 6.2	
Blood binding		
BP	0.603	(Turner, 2008)
fu_p	0.035	
Dissolution		
Solubility method	Intrinsic solubility estimation toolbox	(Turner, 2008)
Solubility (mg/mL)	0.015	
Particle Size (um)	10	
Supersaturation ratio	4	
Absorption		
$P_{eff,man}$	6.045	(Turner, 2008)
Distribution		
V_{ss} (L/kg)	1	(Turner, 2008)
Distribution model	Minimal PBPK	
Metabolism		
CYP3A4: 1-0H		(Turner, 2008)
V_{max} (pmol/min/pmol P450)	5.23	
K_m (μM)	2.16	
CYP3A4: 4-OH		
V_{max} (pmol/min/pmol P450)	5.2	
K_m (μM)	31.8	
CYP3A5: 1-0H		
V_{max} (pmol/min/pmol P450)	19.7	
K_m (μM)	4.16	
CYP3A5: 4-OH		
V_{max} (pmol/min/pmol P450)	4.03	
K_m (μM)	34.8	
Additional clearance		
CL_R (L/h)	0.085	

BP =Blood to plasma ratio, fu_p=fraction unbound in plasma, $P_{eff,man}$=effective human jejunal permeability, V_{ss}=Volume of distribution at steady state following intravenous infusion.

Midazolam IR using the ADAM model was validated against a semisimultaneous p.o. dose of 5 mg followed by a 2 mg intravenous infusion over 30 minutes at 6 hours post oral dosing in healthy volunteers (n=12) weighing 66.1±15.2 kg and aged between 19 and 42 years (Lee *et al.*, 2002). Performance was evaluated using visual predictive check (Figure 8.5).

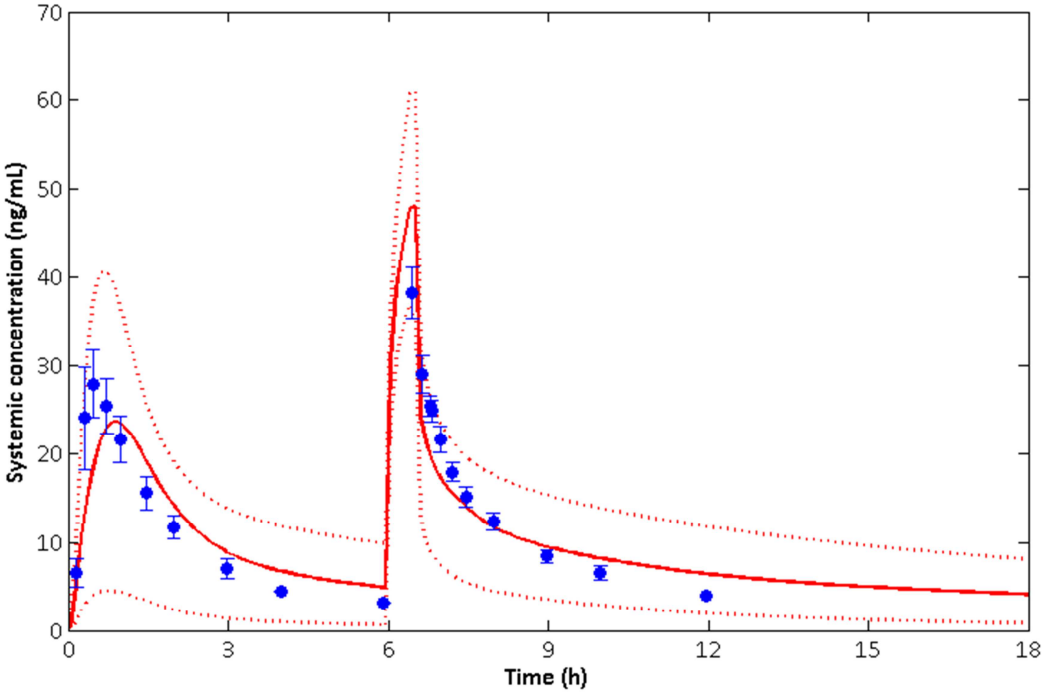

Figure 8.5. Simulated midazolam in healthy volunteers administered as an immediate-release 5 mg oral dose using the Advanced Dissolution Absorption and Metabolism (ADAM) model followed by a 30 minute intravenous infusion of 2 mg midazolam 6 hours post oral dosing as compared to observed data in 12 individuals. Observed data digitised using GetData Graph Digitiser (Lee *et al.*, 2002).

Midazolam IR 7.5 mg followed by an intravenous bolus of 5 mg at 150 minutes after the oral dose was simulated in morbidly obese pre to post Roux-en-Y gastric bypass utilising developed models (Darwich *et al.*, 2012). Oral midazolam displayed a 1.13-fold increase in exposure following Roux-en-Y gastric bypass (small intestinal transit=2.5h) mainly due to an increase in F_G (Figure 8.6).

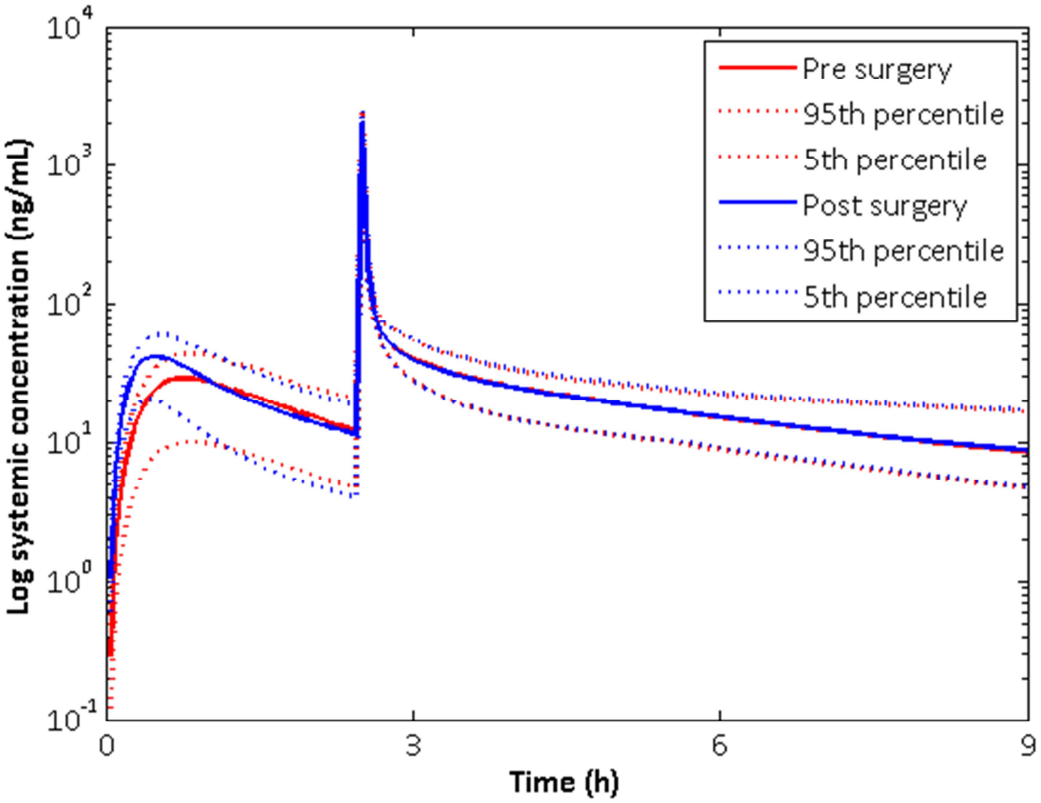

Figure 8.6. Simulated midazolam pre to post Roux-en-Y gastric bypass in morbidly obese administered as an immediate-release 7.5 mg followed by a 30 minute infusion of 5 mg over 150 minutes post oral dosing.

8.6.2 References

Darwich AS, Pade D, Ammori BJ, Jamei M, Ashcroft DM, and Rostami-Hodjegan A (2012) A mechanistic pharmacokinetic model to assess modified oral drug bioavailability post bariatric surgery in morbidly obese patients: interplay between CYP3A gut wall metabolism, permeability and dissolution. *J Pharm Pharmacol* **64:**1008-1024.

Jamei M, Turner D, Yang J, Neuhoff S, Polak S, Rostami-Hodjegan A, and Tucker G (2009) Population-based mechanistic prediction of oral drug absorption. *AAPS J* **11:**225-237.

Lee JI, Chaves-Gnecco D, Amico JA, Kroboth PD, Wilson JW, and Frye RF (2002) Application of semisimultaneous midazolam administration for hepatic and intestinal cytochrome P450 3A phenotyping. *Clin Pharmacol Ther* **72:**718-728.

NCBI (2011) PubChem Public Chemical Database, National Center of Biotechnology Information, USA.

Turner D (2008) Simcyp® User Manual Version 8.